

INVESTIGATING THE USE OF SMALL- DIAMETER SOFTWOOD AS GUARDRAIL POSTS (DYNAMIC TEST RESULTS)

Submitted by

Jason A. Hascall, M.S.C.E., E.I.T.
Research Engineer

Ronald K. Faller, Ph.D., P.E.
Research Assistant Professor

John D. Reid, Ph.D.
Professor

Dean L. Sicking, Ph.D., P.E.
Professor and MwRSF Director

MIDWEST ROADSIDE SAFETY FACILITY
University of Nebraska-Lincoln
527 Nebraska Hall
Lincoln, Nebraska 68588-0529
(402) 472-0965

and

David E. Kretschmann
Research Engineer

FOREST PRODUCTS LABORATORY
U.S. Department of Agriculture – Forest Service
One Gifford Pinchot Drive
Madison, Wisconsin 53726
(608) 231-9307

MwRSF Research Report No. TRP-03-179-07

March 28, 2007

TECHNICAL REPORT DOCUMENTATION PAGE

1. Report No. TRP-03-179-07	2.	3. Recipient's Accession No.	
4. Title and Subtitle Investigating the Use of Small-Diameter Softwood as Guardrail Posts (Dynamic Test Results)		5. Report Date Final: March 28, 2007 Draft: January 30, 2007	
		6.	
7. Author(s) Hascall, J.A., Faller, R.K., Reid, J.D., Sicking, D.L., and Kretschmann, D.E.		8. Performing Organization Report No. TRP-03-179-07	
9. Performing Organization Name and Address Midwest Roadside Safety Facility (MwRSF) University of Nebraska-Lincoln 527 Nebraska Hall Lincoln, Nebraska 68588-0529		10. Project/Task/Work Unit No.	
		11. Contract © or Grant (G) No. UNL: 25-1112-0024-001 FPL: 03-DG-11111133-121	
12. Sponsoring Organization Name and Address Forest Products Laboratory U.S. Department of Agriculture – Forest Service One Gifford Pinchot Drive Madison, Wisconsin 53726		13. Type of Report and Period Covered Draft Report: August 2003 – March 2007	
		14. Sponsoring Agency Code FPL 10-664	
15. Supplementary Notes Prepared in cooperation with U.S. Department of Transportation, Federal Highway Administration.			
16. Abstract (Limit: 200 words) A modified version of the Midwest Guardrail System (MGS), utilizing small-diameter round wood posts, was developed, tested, and evaluated. Three systems were developed using different species of timber, Douglas Fir, Ponderosa Pine, and Southern Yellow Pine. A combination of Barrier VII computer simulation modeling and several series of cantilever bogie tests, conducted in both a rigid sleeve and soil, were used to determine the required diameter of post for each species in order to serve as an equivalent substitute for the standard steel post used in the barrier system. The final recommended nominal sizes were determined to be 184 mm (7 ¼ in.) for Douglas Fir, 203 mm (8 in.) for Ponderosa Pine, and 190 mm (7 ½ in.) for Southern Pine. In addition, a grading criteria limiting knot size and ring density was established for each species. The final recommended knot sizes were limited to 51 mm (2 in.) and smaller for Douglas Fir, 102 mm (4 in.) or smaller for Ponderosa Pine, and 62 mm (2.5 in.) or smaller for Southern Yellow Pine. The minimum ring density for each post species was to exceed or equal 6 rings-per-inch for Douglas Fir, 6 rings-per-inch for Ponderosa Pine, and 4 rings-per-inch for Southern Yellow Pine. Two of the guardrail systems, one using Douglas Fir posts and another using Ponderosa Pine posts, were full-scale vehicle crash tested and reported in accordance to the Test Level 3 (TL-3) requirements specified in the National Cooperative Highway Research Program (NCHRP) Report No. 350, Recommended Procedures for the Safety Performance Evaluation of Highway Features. Testing of the third system, using Southern Pine posts, was not conducted based on the adequacy of previous testing on 184-mm (7 ¼-in.) diameter Southern Yellow Pine posts on the standard W-beam guardrail system as well as a comparable post design strength to that of the other two species. The two full-scale crash tests showed that the modified Midwest Guardrail System functioned adequately for both wood species. Therefore, the three round wood post alternatives will serve as an acceptable substitute to the standard W152x13.4 (W6x9) steel post utilized in the MGS.			
17. Document Analysis/Descriptors Highway Safety, Wood Posts, Round Posts, MGS, Longitudinal Barrier, W-Beam Guardrail, Douglas Fir, Ponderosa Pine, Southern Yellow Pine, Crash Testing		18. Availability Statement No restrictions. Document available from: National Technical Information Services, Springfield, Virginia 22161	
19. Security Class (this report) Unclassified	20. Security Class (this page) Unclassified	21. No. of Pages 436	22. Price

DISCLAIMER STATEMENT

The contents of this report reflect the views of the authors who are responsible for the facts and the accuracy of the data presented herein. The contents do not necessarily reflect the official views nor policies of the U.S. Department of Agriculture, Forest Service, Forest Products Laboratory nor the Federal Highway Administration. This report does not constitute a standard, specification, or regulation.

ACKNOWLEDGMENTS

The authors wish to acknowledge several sources that made a contribution to this project: (1) the United States Department of Agriculture, Forest Service, Forest Products Laboratory for sponsoring this project; (2) Interstate Timber Products Co., Arnold Forest Products Corporation, The Burke-Parsons-Bowlby Corporation, Hills Products Group, JH Baxter and Co., and All-Weather Wood Products for donating the round wood posts; and (3) MwRSF personnel for constructing the barriers and conducting the crash tests.

Acknowledgment is also given to the following individuals who made a contribution to the completion of this research project.

Midwest Roadside Safety Facility

J.R. Rohde, Ph.D., P.E., Associate Professor
R.W. Bielenberg, M.S.M.E., E.I.T., Research Associate Engineer
J.C. Holloway, M.S.C.E., E.I.T., Research Manager
K.A. Polivka, M.S.M.E., E.I.T., Research Associate Engineer
C.L. Meyer, B.S.M.E., E.I.T., Research Engineer II
A.T. Russell, B.S.B.A., Laboratory Mechanic II
K.L. Krenk, B.S.M.A, Field Operations Manager
Tom McMaster, Laboratory Mechanic I
Undergraduate and Graduate Assistants

Forest Products Laboratory

Dick Shilts, Technician
Tim Nelson, Technician
Sara Fishwild, Technician
Evan Parks, Summer Student
Robert Hall, Summer Student

Timber Products Inspection

Cliff Eddington, Douglas Fir and Ponderosa Pine Grader
Jerry Koontz, Douglas Fir Grader
Dave Whipple, Ponderosa Pine and Southern Pine Grader

The Burke-Parsons-Bowlby Corporation

Richard E. Bowlby, President
Buddy Downing

Arnold Forest Products Co.

Doug Arnold, President

Interstate Timber Products Co.

Daniel J. Mushett, Owner

Hills Products Group

Jody Parker

Rogue Valley Fuels

Allen Surgeon

Goshen Forest Products

Mike Babcock

All-Weather Wood Products

Rick Danielson
Justin Wilson

JH Baxter and Co.

Randy Baileys

Dunlap Photography

James Dunlap, President and Owner

TABLE OF CONTENTS

	Page
Disclaimer Statement.....	iii
Acknowledgments.....	iv
Table of Contents.....	vi
List of Figures.....	x
List of Tables.....	xvii
1 Introduction.....	19
1.1 Background.....	19
1.2 Objective.....	20
1.3 Research Approach.....	21
2 Literature Review.....	24
2.1 Prior Wood Post Testing.....	24
2.1.1 Static and Dynamic Post Testing.....	24
2.1.2 Full-Scale Crash Testing.....	33
2.1.3 Summary of Wood Post Testing.....	36
2.2 Grading.....	37
3 Sampling.....	42
3.1 Sample Collection.....	42
3.2 Sample Documentation.....	44
4 Physical Testing - Round One.....	49
4.1 Purpose.....	49
4.2 Scope.....	49
4.3 Round Wood Post.....	52
4.4 Equipment and Instrumentation.....	52
4.4.1 Bogie.....	53
4.4.2 Accelerometer.....	54
4.4.3 Pressure Tape Switches.....	54
4.4.4 Photography Cameras.....	55
4.5 Data Processing.....	55
4.6 End of Test Determination.....	55
5 Round 1 Cantilever Test Results.....	57
5.1 Introduction.....	57
5.2 MOR Results.....	57
5.2.1 Douglas Fir.....	57
5.2.2 Ponderosa Pine.....	58
5.2.3 Southern Yellow Pine.....	58
6 Preliminary Post Size Determination.....	63
6.1 Probability Method.....	63
6.1.1 BARRIER VII Modeling.....	64
6.1.2 MGS Model.....	64
6.1.3 BARRIER VII Results.....	65
6.1.4 Post Reliability.....	68
6.2 Static Method.....	71
6.3 Dynamic Method.....	73

6.4 Post Size Conclusion and Summary	75
7 Inertial Effects.....	76
7.1 Introduction.....	76
7.2 Fracture Time Investigation.....	78
7.3 Possible Explanation – The Inertial Spike Theory	94
7.3.1 Explanation and Physical Description	94
7.3.2 Impulse and Analysis.....	95
7.3.3 Distinction between Real and Inertial Forces	99
7.4 Effects of the Inertial Spike Theory.....	99
7.4.1 Predicted Impulse and Angular Momentum.....	101
7.4.2 Supplemental Testing.....	102
7.4.3 Effects of Inertial Spike on Post Size	106
7.4.4 Effects on Future Testing.....	106
8 Physical Testing – Round Two	107
8.1 Purpose.....	107
8.2 Pretest Documentation and Preparation.....	107
8.3 Scope.....	112
9 System Details – Round Two	114
9.1 Round Wood Posts.....	114
9.2 Equipment and Instrumentation.....	115
10 Round 2 Cantilever Test Results.....	116
10.1 MOR Results.....	116
10.1.1 Douglas Fir.....	116
10.1.2 Ponderosa Pine.....	117
10.1.3 Southern Yellow Pine	117
10.2 Adjusted Peak Force	122
10.2.1 Douglas Fir.....	124
10.2.2 Ponderosa Pine.....	124
10.2.3 Southern Yellow Pine	124
11 Intermediate Post Size Determination	125
11.1 Overview.....	125
11.2 Probability Method for Determining Size.....	125
11.2.1 Strength Distribution Model	125
11.2.2 Minimum Size Determination.....	132
12 Physical Testing – Soil Bogie Testing	135
12.1 Scope.....	135
12.2 Results.....	135
12.2.1 Ponderosa Pine.....	137
12.2.2 Douglas Fir.....	140
12.3 Re-Evaluation of Post Size	142
12.4 Results – Additional Soil Tests.....	145
12.4.1 Douglas Fir.....	146
12.4.2 Ponderosa Pine.....	146
12.4.3 Southern Yellow Pine	148
12.4.4 Testing Conclusion	148
13 Barrier VII Modeling - System Evaluation.....	150

13.1 Round Post Properties – BARRIER VII Model	150
13.2 BARRIER VII Results	153
14 Summary and Full-Scale Test Recommendation	156
14.1 Summary	156
14.2 Full-Scale Crash Test Recommendation	160
14.2.1 Douglas Fir	161
14.2.2 Ponderosa Pine	161
14.2.3 Southern Yellow Pine	162
14.2.4 System Details	162
15 Test Requirements and Evaluation Criteria	163
15.1 Test Requirements	163
15.2 Evaluation Criteria	163
16 Design Details	165
17 Test Conditions	203
17.1 Test Facility	203
17.2 Vehicle Tow and Guidance System	203
17.3 Test Vehicles	203
17.4 Data Acquisition Systems	210
17.4.1 Accelerometers	210
17.4.2 Angular Rate Transducers	211
17.4.3 High-Speed Photography	211
17.4.4 Pressure Tape Switches	214
18 Crash Test No. MGSDF-1	215
18.1 Test No. MGSDF-1	215
18.2 Test Description	215
18.3 System and Component Damage	217
18.4 Vehicle Damage	219
18.5 Occupant Risk Values	220
18.6 Discussion	220
19 Crash Test No. MGSPP-1	237
19.1 Test No. MGSPP-1	237
19.2 Test Description	237
19.3 System and Component Damage	238
19.4 Vehicle Damage	241
19.5 Occupant Risk Values	242
19.6 Discussion	242
20 Summary, Conclusions, and Recommendations	260
21 References	266
22 Appendices	271
APPENDIX A - General Post Grading Criteria	272
APPENDIX B - Round 1 Cantilever Bogie Test Results	276
APPENDIX C - Barrier VII Simulation Deck	322
APPENDIX D - Supplemental Inertia Cantilever Bogie Test Results	335
APPENDIX E - Round 2 Cantilever Bogie Test Results	339
APPENDIX F - MGSDF System Details – English Units	386
APPENDIX G - MGSPP System Details – English Units	396

APPENDIX H - MGSSP System Details – English Units	406
APPENDIX I - Test Nos. MGSDF-1 and MGSP-1 Summary Sheets – English Units.....	416
APPENDIX J - Occupant Compartment Deformation, Test Nos. MGSDF-1 and MGSP-1	419
APPENDIX K - Accelerometer and Rate Transducer Data Analysis	424

List of Figures

	Page
Figure 1. NPGB-4, 9, and 10 Bogie Testing Results	32
Figure 2. Major Dimensions of Round Wood Posts	42
Figure 3. Bogie Testing Matrix.....	50
Figure 4. Bogie Testing Setup	51
Figure 5. Bending Stress Distribution.....	52
Figure 6. Rigid Frame Bogie on Guidance Track.....	54
Figure 7. Rail Slope Diagram	66
Figure 8. Wheel Snag Diagram.....	66
Figure 9. Force vs. Deflection NPGB - 4, 9, and 10.....	69
Figure 10. Bogie Test DF-1 Non-Filtered Acceleration	76
Figure 11. Bogie-Post Impact – Frame 102	78
Figure 12. Post Bending Prior to Fracture - Frame 107.....	79
Figure 13. Post After Fracture - Frame 108	79
Figure 14. DF-1 Raw Acceleration with Fracture Interval	80
Figure 15. DF-2 Raw Acceleration with Fracture Intervals	81
Figure 16. DF-3 Raw Acceleration with Fracture Interval	82
Figure 17. DF-4 Raw Acceleration with Fracture Interval	82
Figure 18. DF-5 Raw Acceleration with Fracture Interval	83
Figure 19. DF-7 Raw Acceleration with Fracture Interval	83
Figure 20. DF-8 Raw Acceleration with Fracture Interval	84
Figure 21. DF-10 Raw Acceleration with Fracture Intervals	84
Figure 22. DF-11 Raw Acceleration with Fracture Intervals	85
Figure 23. DF-15 Raw Acceleration with Fracture Interval	85
Figure 24. PP-5 Raw Acceleration with Fracture Intervals	86
Figure 25. PP-8 Raw Acceleration with Fracture Intervals	86
Figure 26. PP-9 Raw Acceleration with Fracture Interval.....	87
Figure 27. PP-11 Raw Acceleration with Fracture Interval.....	87
Figure 28. PP-13 Raw Acceleration with Fracture Interval.....	88
Figure 29. PP-14 Raw Acceleration with Fracture Intervals	88
Figure 30. SY-2 Raw Acceleration with Fracture Interval	89
Figure 31. SY-3 Raw Acceleration with Fracture Interval	89
Figure 32. SY-4 Raw Acceleration with Fracture Interval	90
Figure 33. SY-5 Raw Acceleration with Fracture Interval	90
Figure 34. SY-7 Raw Acceleration with Fracture Interval	91
Figure 35. SY-8 Raw Acceleration with Fracture Interval	91
Figure 36. SY-9 Raw Acceleration with Fracture Intervals	92
Figure 37. SY-10 Raw Acceleration with Fracture Interval	92
Figure 38. SY-11 Raw Acceleration with Fracture Intervals	93
Figure 39. SY-13 Raw Acceleration with Fracture Interval	93
Figure 40. Setup and Results - Test PT-1	99
Figure 41. Acceleration vs. Time - Test No. SY-3	104
Figure 42. Acceleration vs. Time - Test No. SYPI-3.....	104
Figure 43. Round Two Bogie Testing Matrix.....	113

Figure 44. Major Dimensions of Round Wood Posts - Round Two Testing.....	114
Figure 45. Douglas Fir Population and Target Population Strength Distribution	130
Figure 46. Ponderosa Pine Population and Target Population Strength Distribution.....	130
Figure 47. Southern Yellow Pine Population and Target Population Strength Distribution	131
Figure 48. Soil Bogie Test Setup	136
Figure 49. Initial Soil Pressure Distribution [22].....	143
Figure 50. Soil Force Distribution	143
Figure 51. Post Free-Body Diagram	144
Figure 52. Post Shear Force Diagram	144
Figure 53. Post Bending Moment Diagram	144
Figure 54. Barrier VII Post Strength Model	151
Figure 55. Lateral Capacity BARRIER VII Model	153
Figure 56. MGS Round Post Douglas Fir Details – System Layout	166
Figure 57. MGS Round Post Douglas Fir Details – End Rail and Splice Detail	167
Figure 58. MGS Round Post Douglas Fir Details – Post Detail.....	168
Figure 59. MGS Round Post Douglas Fir Details – Segmented blockout Detail	169
Figure 60. MGS Round Post Douglas Fir Details – Anchor Post Detail	170
Figure 61. MGS Round Post Douglas Fir Details – BCT Anchor Cable Detail.....	171
Figure 62. MGS Round Post Douglas Fir Details – Ground Strut and Anchor Bracket Detail.....	172
Figure 63. MGS Round Post Douglas Fir Details – Rail Section Detail	173
Figure 64. MGS Round Post Douglas Fir Details – Grading Specifications.....	174
Figure 65. MGS Round Post Douglas Fir Photographs.....	175
Figure 66. MGS Round Post Douglas Fir Photographs.....	176
Figure 67. MGS Round Post Douglas Fir Photographs.....	177
Figure 68. MGS Round Post Douglas Fir Photographs.....	178
Figure 69. MGS Round Post Ponderosa Pine Details – System Layout.....	179
Figure 70. MGS Round Post Ponderosa Pine Details – End Rail and Splice Detail	180
Figure 71. MGS Round Post Ponderosa Pine Details – Post Detail	181
Figure 72. MGS Round Post Ponderosa Pine Details – Segmented Blockout Detail.....	182
Figure 73. MGS Round Post Ponderosa Pine Details – Anchor Post Detail	183
Figure 74. MGS Round Post Ponderosa Pine Details – BCT Anchor Cable Detail.....	184
Figure 75. MGS Round Post Ponderosa Pine Details – Ground Strut and Anchor Bracket Detail.....	185
Figure 76. MGS Round Post Ponderosa Pine Details – Rail Section Detail	186
Figure 77. MGS Round Post Ponderosa Pine Details – Grading Specifications	187
Figure 78. MGS Round Post Ponderosa Pine Photographs	188
Figure 79. MGS Round Post Ponderosa Pine Photographs	189
Figure 80. MGS Round Post Ponderosa Pine Photographs	190
Figure 81. MGS Round Post Ponderosa Pine Photographs	191
Figure 82. MGS Round Post Ponderosa Pine Photographs	192
Figure 83. MGS Round Post Ponderosa Pine Photographs	193
Figure 84. MGS Round Post Southern Yellow Pine Details – System Layout	194
Figure 85. MGS Round Post Southern Yellow Pine Details – End Rail and Splice Detail.....	195
Figure 86. MGS Round Post Southern Yellow Pine Details – Post Detail.....	196
Figure 87. MGS Round Post Southern Yellow Pine Details – Segmented Blockout Detail	197
Figure 88. MGS Round Post Southern Yellow Pine Details – Anchor Post Detail.....	198

Figure 89. MGS Round Post Southern Yellow Pine Details – BCT Anchor Cable Detail	199
Figure 90. MGS Round Post Southern Yellow Pine Details – Ground Strut and Anchor Bracket Detail	200
Figure 91. MGS Round Post Southern Yellow Pine Details – Rail Section Detail	201
Figure 92. MGS Round Post Southern Yellow Pine Details – Grading Specifications	202
Figure 93. Test Vehicle, Test MGSDF-1	204
Figure 94. Vehicle Dimensions, Test MGSDF-1	205
Figure 95. Test Vehicle, MGSPP-1	206
Figure 96. Vehicle Dimensions, Test MGSPP-1	207
Figure 97. Vehicle Target Locations, Test MGSDF-1	208
Figure 98. Vehicle Target Locations, Test MGSPP-1	209
Figure 99. Locations of High-Speed Cameras, Test MGSDF-1	212
Figure 100. Locations of High-Speed Cameras, Test MGSPP-1	213
Figure 101. Impact Location, Test MGSDF-1	222
Figure 102. Summary of Test Results and Sequential Photographs, Test MGSDF-1	223
Figure 103. Additional Sequential Photographs, Test MGSDF-1	224
Figure 104. Additional Sequential Photographs, Test MGSDF-1	225
Figure 105. Documentary Photographs, Test MGSDF-1	226
Figure 106. Documentary Photographs, Test MGSDF-1	227
Figure 107. Vehicle Final Position and Trajectory, Test MGSDF-1	228
Figure 108. System Damage, Test MGSDF-1	229
Figure 109. System Damage, Test MGSDF-1	230
Figure 110. System Damage, Test MGSDF-1	231
Figure 111. System Damage, Test MGSDF-1	232
Figure 112. System Damage, Test MGSDF-1	233
Figure 113. Vehicle Damage, Test MGSDF-1	234
Figure 114. Vehicle Damage, Test MGSDF-1	235
Figure 115. Occupant Compartment Damage, Test MGSDF-1	236
Figure 116. Impact Location, Test MGSwww.mapquest.com	244
PP-1	244
Figure 117. Summary of Test Results and Sequential Photographs, Test MGSPP-1	245
Figure 118. Additional Sequential Photographs, Test MGSPP-1	246
Figure 119. Additional Sequential Photographs, Test MGSPP-1	247
Figure 120. Additional Sequential Photographs, Test MGSPP-1	248
Figure 121. Documentary Photographs, Test MGSPP-1	249
Figure 122. Vehicle Final Position and Trajectory Marks, Test MGSPP-1	250
Figure 123. System Damage, Test MGSPP-1	251
Figure 124. System Damage, Test MGSPP-1	252
Figure 125. System Damage, Test MGSPP-1	253
Figure 126. System Damage, Test MGSPP-1	254
Figure 127. System Damage, Test MGSPP-1	255
Figure 128. System Damage, Test MGSPP-1	256
Figure 129. Vehicle Damage, MGSPP-1	257
Figure 130. Vehicle Damage, MGSPP-1	258
Figure 131. Occupant Compartment Damage, Test MGSPP-1	259
Figure B-1. Results of Test No. DF-1	277

Figure B-2. Results of Test No. DF-2.....	278
Figure B-3. Results of Test No. DF-3.....	279
Figure B-4. Results of Test No. DF-4.....	280
Figure B-5. Results of Test No. DF-5.....	281
Figure B-6. Results of Test No. DF-6.....	282
Figure B-7. Results of Test No. DF-7.....	283
Figure B-8. Results of Test No. DF-8.....	284
Figure B-9. Results of Test No. DF-9.....	285
Figure B-10. Results of Test No. DF-10.....	286
Figure B-11. Results of Test No. DF-11.....	287
Figure B-12. Results of Test No. DF-12.....	288
Figure B-13. Results of Test No. DF-13.....	289
Figure B-14. Results of Test No. DF-14.....	290
Figure B-15. Results of Test No. DF-15.....	291
Figure B-16. Results of Test No. PP-1	292
Figure B-17. Results of Test No. PP-2	293
Figure B-18. Results of Test No. PP-3	294
Figure B-19. Results of Test No. PP-4	295
Figure B-20. Results of Test No. PP-5	296
Figure B-21. Results of Test No. PP-6	297
Figure B-22. Results of Test No. PP-7	298
Figure B-23. Results of Test No. PP-8	299
Figure B-24. Results of Test No. PP-9	300
Figure B-25. Results of Test No. PP-10	301
Figure B-26. Results of Test No. PP-11	302
Figure B-27. Results of Test No. PP-12	303
Figure B-28. Results of Test No. PP-13	304
Figure B-29. Results of Test No. PP-14	305
Figure B-30. Results of Test No. PP-15	306
Figure B-31. Results of Test No. SY-1.....	307
Figure B-32. Results of Test No. SY-2.....	308
Figure B-33. Results of Test No. SY-3.....	309
Figure B-34. Results of Test No. SY-4.....	310
Figure B-35. Results of Test No. SY-5.....	311
Figure B-36. Results of Test No. SY-6.....	312
Figure B-37. Results of Test No. SY-7.....	313
Figure B-38. Results of Test No. SY-8.....	314
Figure B-39. Results of Test No. SY-9.....	315
Figure B-40. Results of Test No. SY-10.....	316
Figure B-41. Results of Test No. SY-11.....	317
Figure B-42. Results of Test No. SY-12.....	318
Figure B-43. Results of Test No. SY-13.....	319
Figure B-44. Results of Test No. SY-14.....	320
Figure B-45. Results of Test No. SY-15.....	321
Figure D-1. Results of Test No. SYPI-1	336
Figure D-2. Results of Test No. SYPI-2.....	337

Figure D-3. Results of Test No. SYPI-3.....	338
Figure E-1. Results of Test No. DF-16.....	341
Figure E-2. Results of Test No. DF-17.....	342
Figure E-3. Results of Test No. DF-18.....	343
Figure E-4. Results of Test No. DF-19.....	344
Figure E-5. Results of Test No. DF-20.....	345
Figure E-6. Results of Test No. DF-21.....	346
Figure E-7. Results of Test No. DF-22.....	347
Figure E-8. Results of Test No. DF-23.....	348
Figure E-9. Results of Test No. DF-24.....	349
Figure E-10. Results of Test No. DF-25.....	350
Figure E-11. Results of Test No. DF-26.....	351
Figure E-12. Results of Test No. DF-27.....	352
Figure E-13. Results of Test No. DF-28.....	353
Figure E-14. Results of Test No. DF-29.....	354
Figure E-15. Results of Test No. DF-30.....	355
Figure E-16. Results of Test No. PP-16.....	356
Figure E-17. Results of Test No. PP-17.....	357
Figure E-18. Results of Test No. PP-18.....	358
Figure E-19. Results of Test No. PP-19.....	359
Figure E-20. Results of Test No. PP-20.....	360
Figure E-21. Results of Test No. PP-21.....	361
Figure E-22. Results of Test No. PP-22.....	362
Figure E-23. Results of Test No. PP-23.....	363
Figure E-24. Results of Test No. PP-24.....	364
Figure E-25. Results of Test No. PP-25.....	365
Figure E-26. Results of Test No. PP-26.....	366
Figure E-27. Results of Test No. PP-27.....	367
Figure E-28. Results of Test No. PP-28.....	368
Figure E-29. Results of Test No. PP-29.....	369
Figure E-30. Results of Test No. PP-30.....	370
Figure E-31. Results of Test No. SY-16.....	371
Figure E-32. Results of Test No. SY-17.....	372
Figure E-33. Results of Test No. SY-18.....	373
Figure E-34. Results of Test No. SY-19.....	374
Figure E-35. Results of Test No. SY-20.....	375
Figure E-36. Results of Test No. SY-21.....	376
Figure E-37. Results of Test No. SY-22.....	377
Figure E-38. Results of Test No. SY-23.....	378
Figure E-39. Results of Test No. SY-24.....	379
Figure E-40. Results of Test No. SY-25.....	380
Figure E-41. Results of Test No. SY-26.....	381
Figure E-42. Results of Test No. SY-27.....	382
Figure E-43. Results of Test No. SY-28.....	383
Figure E-44. Results of Test No. SY-29.....	384
Figure E-45. Results of Test No. SY-30.....	385

Figure F-1. MGS Round Post Douglas Fir English Details – System Layout.....	387
Figure F-2. MGS Round Post Douglas Fir English Details – End Rail and Splice Detail	388
Figure F-3. MGS Round Post Douglas Fir English Details – Post Detail	389
Figure F-4. MGS Round Post Douglas Fir English Details – Segmented Block Detail.....	390
Figure F-5. MGS Round Post Douglas Fir English Details – Anchor Post Detail	391
Figure F-6. MGS Round Post Douglas Fir English Details – BCT Anchor Cable Detail	392
Figure F-7. MGS Round Post Douglas Fir English Details – Ground Strut and Anchor Bracket Detail	393
Figure F-8. MGS Round Post Douglas Fir English Details – Rail Section Detail	394
Figure F-9. MGS Round Post Douglas Fir English Details – Grading Specifications	395
Figure G-1. MGS Round Post Ponderosa Pine English Details – System Layout	397
Figure G-2. MGS Round Post Ponderosa Pine English Details – End Rail and Splice Detail..	398
Figure G-3. MGS Round Post Ponderosa Pine English Details – Post Detail.....	399
Figure G-4. MGS Round Post Ponderosa Pine English Details – Segmented Blockout Detail	400
Figure G-5. MGS Round Post Ponderosa Pine English Details – Anchor Post Detail.....	401
Figure G-6. MGS Round Post Ponderosa Pine English Details – BCT Anchor Cable Detail ..	402
Figure G-7. MGS Round Post Ponderosa Pine English Details – Ground Strut and Anchor Bracket Detail	403
Figure G-8. MGS Round Post Ponderosa Pine English Details – Rail Section Detail.....	404
Figure G-9. MGS Round Post Ponderosa Pine English Details – Grading Specifications.....	405
Figure H-1. MGS Round Post Southern Pine English Details – System Layout	407
Figure H-2. MGS Round Post Southern Pine English Details – End Rail and Splice Detail....	408
Figure H-3. MGS Round Post Southern Pine English Details – Post Detail	409
Figure H-4. MGS Round Post Southern Pine English Details – Segmented Blockout Detail ..	410
Figure H-5. MGS Round Post Southern Pine English Details – Anchor Post Detail.....	411
Figure H-6. MGS Round Post Southern Pine English Details – BCT Anchor Cable Detail.....	412
Figure H-7. MGS Round Post Southern Pine English Details – Ground Strut and Anchor Bracket Detail	413
Figure H-8. MGS Round Post Southern Pine English Details – Rail Section Detail	414
Figure H-9. MGS Round Post Southern Pine English Details – Grading Specifications.....	415
Figure I-1. Summary of Test Results and Sequential Photographs, Test MGSDF-1	417
Figure I-2. Summary of Test Results and Sequential Photographs, Test MGSPP-1	418
Figure J-1. Occupant Compartment Deformation Data, Test MGSDF-1	420
Figure J-2. Occupant Compartment Deformation Index (OCDI), Test MGSDF-1	421
Figure J-3. Occupant Compartment Deformation Data, Test MGSPP-1.....	422
Figure J-4. Occupant Compartment Deformation Index (OCDI), Test MGSPP-1.....	423
Figure K-1. Graph of Longitudinal Deceleration – Filtered Data, Test MGSDF-1	425
Figure K-2. Graph of Longitudinal Occupant Impact Velocity – Filtered Data, Test MGSDF-1	426
Figure K-3. Graph of Longitudinal Occupant Displacement – Filtered Data, Test MGSDF-1.	427
Figure K-4. Graph of Lateral Deceleration – Filtered Data, Test MGSDF-1	428
Figure K-5. Graph of Lateral Occupant Impact Velocity – Filtered Data, Test MGSDF-1	429
Figure K-6. Graph of Lateral Occupant Displacement – Filtered Data, Test MGSDF-1	430
Figure K-7. Graph of Longitudinal Deceleration – Filtered Data, Test MGSPP-1	431
Figure K-8. Graph of Longitudinal Occupant Impact Velocity – Filtered Data, Test MGSPP-1	432

Figure K-9. Graph of Longitudinal Occupant Displacement – Filtered Data, Test MGSPP-1 .	433
Figure K-10. Graph of Lateral Deceleration – Filtered Data, Test MGSPP-1	434
Figure K-11. Graph of Lateral Occupant Impact Velocity – Filtered Data, Test MGSPP-1	435
Figure K-12. Graph of Lateral Occupant Displacement – Filtered Data, Test MGSPP-.....	436

List of Tables

	Page
Table 1. Dynamic Post Strength	24
Table 2. Static Post Breaking Strength	25
Table 3. Dynamic Post Testing Results by Michie.....	26
Table 4. Dynamic Post Testing Results for Red and Southern Yellow Pine Species.....	26
Table 5. Southwest Research Institute Pendulum Test Results	29
Table 6. Post Testing Matrix and Test Results Summary.....	31
Table 7. Summary of 1971 Southwest Research Institute Testing	33
Table 8. Rosson, Bierman and Rohde Post Test Summary	35
Table 9. SPIB Timber Grading Summary.....	38
Table 10. Knot Grading Criteria for Select Structural Timbers [40]	39
Table 11. Knot Grading Criteria for No. 1 Timbers [40].....	39
Table 12. Knot Grading Criteria for No. 2 Timbers [40].....	39
Table 13. WWPA Timber Grading Summary	40
Table 14. Knot Grading Criteria for Select Structural Timbers [41]	40
Table 15. Douglas Fir Pre-Test Documentation	45
Table 16. Ponderosa Pine Pre-Test Documentation	46
Table 17. Southern Yellow Pine Pre-Test Documentation.....	47
Table 18. Douglas Fir Test Day Measurements.....	48
Table 19. Ponderosa Pine Test Day Measurements.....	48
Table 20. Southern Yellow Pine Test Day Measurements	48
Table 21. Dynamic Douglas Fir Round Wood Post Test Results.....	60
Table 22. Dynamic Ponderosa Pine Round Wood Post Test Results	61
Table 23. Dynamic Southern Yellow Pine Round Wood Post Test Results	62
Table 24. FPL BARRIER VII Results Summary	67
Table 25. Probability Method Calculation Summary	70
Table 26. Static Method Calculation Summary	72
Table 27. Dynamic Method Calculation Summary	73
Table 28. Post Diameter Calculation Summary.....	75
Table 29. Douglas Fir Impulse-Momentum Comparison.....	97
Table 30. Ponderosa Pine Impulse-Momentum Comparison	97
Table 31. Southern Yellow Pine Impulse-Momentum Comparison.....	98
Table 32. Supplemental Bogie Testing Predictions.....	101
Table 33. Supplemental Bogie Test Results Comparison.....	102
Table 34. Supplemental Bogie Test Results Summary.....	105
Table 35. Douglas Fir Round Two Pre-Test Documentation	108
Table 36. Ponderosa Pine Round Two Pre-Test Documentation	109
Table 37. Southern Yellow Pine Round Two Pre-Test Documentation.....	110
Table 38. Douglas Fir Round Two Test Day Measurements.....	111
Table 39. Ponderosa Pine Round Two Test Day Measurements.....	111
Table 40. Southern Yellow Pine Round Two Test Day Measurements	111
Table 41. Douglas Fir Round Wood Post Test Results - Round Two Testing	119
Table 42. Ponderosa Pine Round Wood Post Test Results - Round Two Testing	120
Table 43. Southern Yellow Pine Round Wood Post Test Results - Round Two Testing.....	121

Table 44. Douglas Fir - Adjusted Peak Force.....	122
Table 45. Ponderosa Pine – Adjusted Peak Force	123
Table 46. Southern Yellow Pine – Adjusted Peak Force.....	123
Table 47. Dynamic Magnification Factor - Round 1 Bogie Testing	127
Table 48. Dynamic Magnification Factor - Round 2 Bogie Testing	127
Table 49. Dynamic Magnification Factor Excluding Inertial Effects.....	128
Table 50. Douglas Fir Random Sample Testing Results	131
Table 51. Ponderosa Pine Random Sample Testing Results	132
Table 52. Southern Yellow Pine Random Sample Testing Results.....	132
Table 53. Minimum Diameter Calculation	133
Table 54. Soil Bogie Test Overview.....	138
Table 55. Soil Bogie Test Results Summary	139
Table 56. BARRIER VII Round Wooden Post Lateral Properties Summary	152
Table 57. FPL BARRIER VII Results Summary	154
Table 58. Critical Impact Point Determination.....	155
Table 59. NCHRP Report No. 350 Test Level 3 Crash Test Conditions [26]	164
Table 60. NCHRP Report No. 350 Evaluation Criteria for Crash Tests [26].....	164
Table 61. Soil Gap Dimensions	219
Table 62. Permanent Rail Deflection.....	219
Table 63. Soil Gap Dimensions and Rail Height Measurements.....	240
Table 64. Ponderosa Pine Permanent Rail Deflection	241
Table 65. Summary of Safety Performance Evaluation.....	265

1 INTRODUCTION

1.1 Background

Prompted by the devastating forest fire season of 2000, President Bill Clinton initiated the development of what would become the National Fire Plan. The plan established four main goals: to improve prevention and suppression, reduce hazardous fuels, restore fire adapted ecosystems, and to promote community assistance [1].

One of the most commonly used prevention techniques is fuel management, an idea that has been around for many years. In the 1960's, the U.S. Department of Agriculture (USDA) - Forest Service began managing fuels by using controlled burn techniques [2]. Using these techniques, fires were initiated in areas where they could be contained in order to consume the small-diameter forest thinnings (SDT's) that might serve as fuel for fires in the future. These thinnings were most commonly made up of various pine and fir species. Although this method is generally effective, it offers no economic benefits and has high risks.

Today, there are many uses for the small diameter trees that make up the majority of the forest thinnings consumed during controlled burns. Uses for the thinnings include lumber, structural roundwood, wood composites, wood fiber products, compost, mulch, energy, and fuels [3]. The idea is to remove the fuel and sell it for use in various products, hopefully recovering the cost of removing the material. The more products there are, the more likely the cost of removing the SDT's will be recovered. Therefore, more uses for small diameter trees must be developed [4].

Guardrail post production is one possible application for SDT's that is under consideration. Using SDT's in guardrail systems would provide a new application for thinnings while also reducing the cost of the barrier system.

Guardrail systems constructed on today's roadsides have two main functions. First, they safely redirect vehicles that impact the barrier systems. Second, they dissipate much of the vehicle's kinetic energy during the impact event. Safe redirection prevents the impacting vehicle from contacting the hazard behind the system and also prevents secondary collisions with vehicles sharing the roadway. Energy dissipation reduces the forces applied to the vehicle during the redirection process and thereby reduces the risk of injury to the vehicle's occupants.

The Midwest Guardrail System (MGS) is a specific type of W-beam guardrail that will be used in the study [5-7]. MGS was specifically designed for the high center of gravity vehicles found on today's roadways. The system uses a higher rail mounting height, a shallower post embedment depth, deeper blockouts, and a modified post placement scheme than previous guardrail systems which often fail to perform adequately for the larger and higher vehicles. As with all strong-post, W-beam guardrail systems, MGS dissipates energy through the deflection and deformation of the rail and the rotation of the posts in the soil. If the wood posts have insufficient bending strength, the bulk of the impacting vehicle's energy will be absorbed by the W-beam element, thus increasing the tensile force in the rail. If the force increases beyond the capacity of the rail, it will fail, allowing the impacting vehicle to pass through. Therefore, the posts must have sufficient structural capacity to displace founding soils and absorb energy.

1.2 Objective

The objective of the research project was to determine the properties of the Douglas Fir, Ponderosa Pine, and Southern Yellow Pine wood species when used as round posts under impact loading conditions. The primary goal of this research was to determine an acceptable diameter and grading specification for the three species in order to allow these species to serve as

substitutes for the rectangular Southern Yellow Pine and wide-flange steel posts currently used in guardrail applications, more specifically the Midwest Guardrail System.

1.3 Research Approach

As discussed in Section 1.1, historical testing has shown that wood posts should generally have sufficient strength to rotate in the soil without fracturing. Hence, the most important task of the research described herein was identifying the necessary size and wood grading criteria to assure such behavior, yet maintain the low costs and high availability that is required in a competitive industry.

BARRIER VII [8], a computer simulation program was utilized to establish failure criteria for the MGS system, and an acceptable level of risk for that failure was defined. Once an acceptable level of risk had been established, the results of physical testing could be compared with results from soil bogie tests conducted on the standard steel post used in the MGS system. Based on those comparisons, the diameter of the wood posts could be selected to be capable of developing the capacity that was required to meet the established level of reliability.

A series of dynamic and static cantilever tests was conducted to develop a preliminary post diameter. In order to complete the testing, a sample of posts was collected for each species. Each specimen in the sample was required to meet a general grading criterion that is presented in Appendix A.

The general grading criteria pertain mostly to the manufacturing methods and manufacturing defects. The criteria were specified to prevent damaged or poorly processed products from being used in a guardrail system based on those parameters established for wood poles by the American National Standards Institute (ANSI) in ANSI 05.1 [9]. Specific changes

were made to the limits on manufacturing methods, scars, shape, straightness, splits, shakes, decay, holes, slope of grain, and compression wood.

The total sample was composed of two sub-samples, sample A and sample B. Sample A was made up of posts falling into three categories based on variation in knot locations and sizes, and ring density. Sample B was randomly selected. Dynamic and static testing was conducted on sample A, and static testing was conducted on sample B.

When an approximate diameter had been determined from the first set of tests, a second set of cantilever tests was conducted on a sample of posts that were selected in the same manner as before. The second set of cantilever tests was conducted to evaluate and verify the capacity of posts with the adjusted diameter. Based on the results of the second set of tests, the required post diameter and wood grading specifications were adjusted as needed to develop the desired capacity.

When the post diameter had been finalized, dynamic soil bogie tests were conducted to verify that the diameter was large enough to give the posts sufficient capacity to rotate in the soil rather than fracture. Since this was not the case, the diameter of the posts was increased based on the results, and a second set of soil bogie tests was conducted. The second set of tests verified that the new diameter was large enough, and the results of the soil tests were used in BARRIER VII computer simulations to evaluate the effectiveness of the barrier system. The simulations showed that the posts should be adequate, and a full-scale test was recommended for two of the three species.

This report is divided into 20 chapters plus references and appendices. The first chapter serves as an introduction and overview of the project. Chapter 2 contains a comprehensive literature review and overview of the grading criteria for wood posts. Chapter 3 contains a

thorough explanation of the sampling and documentation procedures used for the testing specimen. It also includes summaries of properties recorded for each post.

Chapters 4 and 5 contain information from the first round of dynamic testing. Chapter 4 describes the physical testing setup, includes the round 1 bogie testing matrix, and presents the details of the testing, including information on the devices used to record impact events, data processing methods, and wood post details. Chapter 5 presents the results of the first round of tests.

In Chapter 6, the diameter for the second round of testing is selected based on the results of the first round of testing and some initial computer simulation modeling. Chapter 7 describes the flaws discovered in the bogie testing methods, the effects they can have, and the possible solutions to remedy the problem. Chapters 8, 9, and 10 describe the second set of cantilever sleeve testing and results.

Chapter 11 discusses modifications in the diameter requirements based on the results from the second round of testing. The process of testing the candidate post sizes in soil is described in Chapter 12, and Chapter 13 presents computer simulation findings with the final post size recommendations. Chapter 14 contains the full scale crash test recommendations, and Chapter 15 describes the test requirements and evaluation criteria for those recommendations. Design details and photographs for all three systems are shown in Chapter 16. Chapter 17 presents the full-scale crash test site conditions, and Chapters 18 and 19 describe the Douglas Fir and Ponderosa Pine tests, respectively. Finally, Chapter 20 contains a summary of the research project and conclusions made from the results.

2 LITERATURE REVIEW

2.1 Prior Wood Post Testing

A limited amount of research has been conducted on round wooden posts. This section is a summary of those studies and associated results that are relevant to this project.

2.1.1 Static and Dynamic Post Testing

Beginning in 1960, Graham et al. [10] conducted a six-year program to develop revised standards for New York's traffic barriers. Both bogie and full-scale tests were conducted to identify the capacity and safety performance of various guardrail posts in rigid foundations and soils. The bogie test results are presented in Table 1.

Table 1. Dynamic Post Strength

Post	Force	Maximum Resistance									
		Fine Sand		Speed		Glacial Till		Speed		Concrete	
		kg	(lbs)	m/s	(mph)	kg	(lbs)	m/s	(mph)	kg	(lbs)
Steel S76x8.5 (S3x5.7)	Lateral									2631 (5800)	8.9 (20)
	Longitudinal									2449 (5400)	4.5 (10)
76.2 mm x 50.8 mm x 4.76 mm (3 in. x 2 in. x 3/16 in.) Steel Tube	Lateral									680 (1500)	8.9 (20)
	Longitudinal									907 (2000)	4.5 (10)
57.2 mm x 50.8 mm x 6.1 kg/m (2 1/4 in. x 2 in. x 4.1 lbs/ft) Steel Right of Way Fence Posts	Lateral									1678 (3700)	8.9 (20)
	Longitudinal									1860 (4100)	8.9 (20)
	Lateral									1134 (2500)	8.9 (20)
	Longitudinal									1315 (2900)	8.9 (20)
	Lateral									2132 (4700)	4.5 (10)
	Longitudinal									953 (2100)	13.4 (30)
	Lateral									1089 (2400)	13.4 (30)
	Lateral	2495 (5500)	8.9 (20)	5942 (13100)	8.9 (20)						
	Lateral	1724 (3800)	4.5 (10)	4627 (10200)	8.9 (20)						
	Lateral	2812 (6200)	4.5 (10)	3538 (7800)	4.5 (10)						
	Longitudinal	1724 (3800)	8.9 (20)	2041 (4500)	8.9 (20)						
	Longitudinal	1361 (3000)	8.9 (20)	2041 (4500)	8.9 (20)						
	Longitudinal	1724 (3800)	8.9 (20)	2087 (4600)	8.9 (20)						
	Longitudinal	1633 (3600)	4.5 (10)	1724 (3800)	4.5 (10)						
	Lateral	2631 (5800)	8.9 (20)	4717 (10400)	8.9 (20)						
	Lateral	2177 (4800)	4.5 (10)	3221 (7100)	8.9 (20)						
	Lateral			3810 (8400)	4.5 (10)						
	Longitudinal	2631 (5800)	8.9 (20)	4309 (9500)	4.5 (10)						
	Longitudinal	2994 (6600)	8.9 (20)	3175 (7000)	4.5 (10)						
	Longitudinal	2359 (5200)	4.5 (10)	3039 (6700)	8.9 (20)						

In 1961, Cichowski et al. [11] conducted several static post tests and full-scale crash tests at the General Motors Proving Ground. Static post tests were conducted on both the weak axis (side impact) and the strong axis (front impact) of concrete, steel, and rectangular wood posts. The maximum measured breaking strength for each type of post is listed in Table 2. A 457-mm (18-in.) load height was used for all of the tests.

Table 2. Static Post Breaking Strength

Post Type	Size	Treatment/Details	Details	Side Impact		Front Impact	
				kN	(lbs)	kN	(lbs)
Wood	152 mm x 203 mm (6 in. x 8 in.)	No Treatment		104.5	(23500)	106.3	(23900)
		4 Yrs. Pressure		95.6	(21500)	107.2	(24100)
		5 Yrs. Pressure		94.3	(21200)	114.3	(25700)
		6 Yrs. Dipped		57.8	(13000)	71.2	(16000)
Steel	152 mm x 102 mm (6 x 4 in.) - I Beam			16.5	(3700)	5.8	(1300)
Concrete	152 mm x 203 mm (6 in. x 8 in.)	13 mm (1/2 in.) Vertical Rebar	6 mm (1/4 in.) Horizontal Rebar	25.8	(5800)	36.5	(8200)
			10 mm (3/8 in.) Horizontal Rebar	25.8	(5800)	34.7	(7800)
		16 mm (5/8 in.) Vertical Rebar	6 mm (1/4 in.) Horizontal Rebar	19.1	(4300)	43.1	(9700)
			10 mm (3/8 in.) Horizontal Rebar	20.5	(4600)	46.7	(10500)

In a study conducted by Michie and Gatchell in 1974 [12], southern pine, red oak, and steel posts were tested with a pendulum. The testing showed that 152 mm x 152 mm (6 in. x 6 in.) and 152 mm x 203 mm (6 in. x 8 in.) wood posts have qualities equal or superior to those of W6x8.5 and S3x5.7 steel posts. They also concluded that the performance of wood posts greatly depends on the location of knots. In their report, Michie and Gatchell suggested selecting posts based on the grain distortion caused by knots, avoiding knots that distort the grain in the tension face for more than a third of the width of the face.

Also in 1974, Michie, Gatchell, and Duke [13] performed dynamic tests on both round and rectangular wood posts of varying species and sizes fixed in a sleeve with an impact height of 610 mm (24 in.). Sizes ranged from 102-mm x 102-mm (4-in. x 4-in.) to 203-mm x 203-mm (8-in x 8-in.), and included both rectangular and round cross-sections. The species tested consisted of Douglas Fir, Red Pine, Red Oak, and Southern Pine. Although no soil interaction was taken into account, the researchers concluded that the specific shape has little influence on results stating, "...the engineer can use sawed or round material and expect equal performance for equal moments of inertia." Results from the experiment are shown in Tables 3 and 4 for round and rectangular post data, respectively.

Table 3. Dynamic Post Testing Results by Michie

	Nominal Width		Nominal Depth		Peak Force		Avg. Force		Fracture Energy	
	mm	(in.)	mm	(in.)	kN	(kips)	kN	(kips)	kN-mm	(kip-ft)
Red Oak	101.6	4.0	101.6	4.0	24.5	5.5	11.7	2.6	3.0	2.18
	101.6	4.0	152.4	6.0	48.5	10.9	24.6	5.5	5.5	4.05
	152.4	6.0	152.4	6.0	51.6	11.6	22.7	5.1	4.8	3.54
	152.4	6.0	203.2	8.0	97.9	22.0	35.2	7.9	10.1	7.42
Southern Pine	101.6	4.0	152.4	6.0	36.5	8.2	16.0	3.6	3.2	2.35
	152.4	6.0	152.4	6.0	44.5	10.0	16.9	3.8	3.8	2.80
	203.2	8.0	203.2	8.0	116.1	26.1	44.8	10.1	16.0	11.80
Douglas Fir	101.6	4.0	101.6	4.0	24.5	5.5	11.7	2.6	3.0	2.18
	101.6	4.0	152.4	6.0	48.5	10.9	24.6	5.5	5.5	4.05
	152.4	6.0	203.2	8.0	51.6	11.6	22.7	5.1	4.8	3.54
	203.2	8.0	203.2	8.0	97.9	22.0	35.2	7.9	10.1	7.42

Table 4. Dynamic Post Testing Results for Red and Southern Yellow Pine Species

Species	Diameter		Peak Force		Average Force		Fracture Energy	
	mm	(in.)	kN	(kips)	kN	(kips)	kN-m	(kip-ft)
Southern Yellow Pine	229	(9.0)	74.7	(16.8)	32.0	(7.2)	7.4	(5.46)
Red Pine	155	(6.1)	18.2	(4.1)	9.8	(2.2)	1.2	(.92)
	165	(6.5)	35.1	(7.9)	17.3	(3.9)	2.7	(1.99)
	168	(6.6)	25.4	(5.7)	12.5	(2.8)	1.7	(1.28)
	171	(6.8)	35.6	(8.0)	16.9	(3.8)	2.7	(1.99)
	184	(7.3)	53.4	(12.0)	28.9	(6.5)	4.7	(3.50)
	218	(8.6)	71.2	(16.0)	40.5	(9.1)	6.0	(4.45)
	231	(9.1)	76.1	(17.1)	45.8	(10.3)	7.7	(5.66)
	236	(9.3)	95.2	(21.4)	43.6	(9.8)	10.4	(7.65)
	165	(6.5)	36.0	(8.1)	16.0	(3.6)	2.5	(1.81)
	178	(7.0)	49.4	(11.1)	28.0	(6.3)	4.7	(3.50)
	178	(7.0)	28.9	(6.5)	12.0	(2.7)	2.5	(1.81)
	184	(7.3)	32.9	(7.4)	12.9	(2.9)	2.9	(2.16)
	197	(7.8)	74.7	(16.8)	52.0	(11.7)	8.8	(6.50)
	207	(8.2)	58.7	(13.2)	33.8	(7.6)	5.4	(3.99)
	216	(8.5)	94.7	(21.3)	91.2	(20.5)	14.3	(10.57)
	248	(9.8)	88.1	(19.8)	55.2	(12.4)	8.4	(6.23)

In 1978, Calcote et al. [14] studied the effects of soil on the performance of guardrail posts. Eighty pendulum tests were conducted on steel and wood posts in four different types of soil. As a control value, the tests were also conducted with posts in a fixed support. For this experiment, 152-mm x 203 mm (6-in. x 8 in.) Douglas Fir posts were used with an 889-mm (35-in.) embedment depth. The mode of failure for all strong axis tests was soil yielding. For the

weak-axis tests, the failure mode was generally post fracture with the exception of the saturated clay test in which the soil failed first.

Another study by Jeyapalan et al. [15] in 1984 compared 178-mm (7-in.) round Southern Yellow Pine (SYP) posts to W152x12.6 (W6x8.5) steel posts. In the study, three static tests were conducted for each of two types of soil, cohesive and cohesionless. Of the three tests in each soil type, two were steel posts embedded at depths of 1,118 mm (44 in.) and 965 mm (38 in.), and one test consisted of a round wood post embedded at 965 mm (38 in.), all with a load height of 533 mm (21 in.). From these tests, the researchers concluded that round wood posts and steel posts perform very similarly. In the cohesive soil test, the 1,118-mm (44-in.) deep steel post had nearly identical results to the 965-mm (38-in.) deep wooden post. The peak force and energy dissipated by the wood post were 16.5 kN (3.7 kips) and 5.7 kJ (50.4 kip-in.), respectively, while the equivalent values for the steel post were 16.9 kN (3.8 kips) and 5.8 kJ (51.6 kip-in.), respectively. The 965-mm (38-in.) deep steel post test resulted in 14.7 kN (3.3 kips) and 5.2 kJ (45.6 kip-in.) respectively, approximately 10 percent less than that observed for the round wooden post. In the cohesionless soil, the 1,118-mm (44-in.) deep post surpassed the round post in both peak force and energy by about 20 percent, with a peak force of 17.3 kN (3.9 kips) and an energy value of 7.0 kJ (62.4 kip-in.). The 965-mm (38-in.) deep steel post, however, showed a higher peak force, 14.7 kN (3.3 kips), but a lower amount of absorbed energy, 5.7 kJ (50.4 kip-in.), than the round post.

In the dynamic tests in cohesive soil, the steel post's performance exceeded that of the wooden post in both peak force and total energy absorbed. Peak force for the steel post was 76 kN (17 kips) while the wood post's peak force was 73 kN (16 kips). The energy absorbed was

40.5 kJ (359 kip-in.) for the steel post and 36.9 kJ (326 kip-in.) for the wood post. A comparison for the cohesionless soil was not available due to the wood post fracturing almost immediately.

Based upon these static and dynamic tests, the researchers concluded that steel posts are sufficient substitutes for round posts used in guardrail systems found in Texas. The authors did caution that more tests should be completed in the future.

Bronstad et al. [16] conducted a study in 1988 on bridge rail transitions. A total of twelve pendulum tests were performed on both wood and steel posts. The impact height was 533 mm (21 in.) with a 1,814-kg (4,000-lb) pendulum. The different types of steel posts were tested at an embedment depth of 1,118 mm (44 in.), with and without a 460 mm x 610 mm (18 in. x 24 in.) soil paddle, while the various sizes of wood posts used a 914-mm (36-in.) embedment depth. The results, presented in Table 5, showed two important findings: (1) the soil paddle does not make a significant difference in the stiffness or maximum force and (2) the W6x15.5 posts are nearly as stiff as the 254-mm x 254-mm (10-in x 10-in.) wood posts.

Table 5. Southwest Research Institute Pendulum Test Results

	Post Type	Max. Force		Avg. Stiffness		Total Impulse		Failure Type
		kN	(kips)	kN/mm	(kips/in.)	kN-sec	(kip-sec)	
Square	305 mm x 305 mm (12 in. x 12 in.) Wood	92.08	(20.7)	0.597	(3.41)	10.12	(2.274)	Soil Yield
	305 mm x 305 mm (12 in. x 12 in.) Wood	105.87	(23.8)			10.10	(2.271)	Soil Yield
	254 mm x 254 mm (10 in. x 10 in.) Wood	72.51	(16.3)	0.447	(2.55)	6.87	(1.544)	Soil Yield
	254 mm x 254 mm (10 in. x 10 in.) Wood	72.95	(16.4)			NA	NA	Post Fracture
	203 mm x 203 mm (8 in. x 8 in.) Wood	58.72	(13.2)	0.292	(1.67)	5.72	(1.287)	Soil Yield
	203 mm x 203 mm (8 in. x 8 in.) Wood	51.60	(11.6)			4.85	(1.091)	Soil Yield
Strong Axis	W152x23.0 (W6x15.5) With paddles	90.74	(20.4)	0.420	(2.40)	11.01	(2.475)	Soil Yield
	W152x23.0 (W6x15.5) With paddles	81.40	(18.3)			10.90	(2.450)	Soil Yield
	W152x23.0 (W6x15.5)	85.41	(19.2)	0.399	(2.28)	11.73	(2.637)	Soil Yield
	W152x23.0 (W6x15.5)	76.95	(17.3)			9.85	(2.215)	Soil Yield
	W152x13.4 (W6x8.5)	56.49	(12.7)	0.431	(2.46)	2.54	(0.572)	Soil Yield
	W152x13.4 (W6x8.5)	56.49	(12.7)			3.91	(0.879)	Soil Yield
	W152x13.4 (W6x8.5)	45.37	(10.2)			2.22	(0.500)	Soil Yield
	W152x13.4 (W6x8.5)	36.92	(8.3)			2.97	(0.667)	Soil Yield
	152 mm x 203 mm (6 in. x 8 in.) Wood	52.04	(11.7)	0.273	(1.56)	3.11	(0.699)	Soil Yield
	153 mm x 203 mm (6 in. x 8 in.) Wood	28.47	(6.4)			2.29	(0.514)	Soil Yield
	154 mm x 203 mm (6 in. x 8 in.) Wood	32.47	(7.3)			2.35	(0.529)	Soil Yield
	155 mm x 203 mm (6 in. x 8 in.) Wood	32.03	(7.2)			1.94	(0.437)	Soil Yield
Weak Axis	W152x23.0 (W6x15.5)	48.04	(10.8)	0.228	(1.30)	7.74	(1.740)	Post Yield
	W152x23.0 (W6x15.5)	46.71	(10.5)			7.64	(1.717)	Post Yield
	W152x13.4 (W6x8.5)	21.35	(4.8)	0.201	(1.15)	1.25	(0.280)	Post Yield
	W152x13.4 (W6x8.5)	18.24	(4.1)			1.08	(0.243)	Post Yield
	W152x13.4 (W6x8.5)	22.69	(5.1)			1.28	(0.287)	Post Yield
	W152x13.4 (W6x8.5)	19.13	(4.3)			1.26	(0.284)	Post Yield
	152 mm x 203 mm (6 in. x 8 in.) Wood	49.82	(11.2)	0.341	(1.95)	0.69	(0.154)	Post Fracture
	153 mm x 203 mm (6 in. x 8 in.) Wood	28.91	(6.5)			0.46	(0.103)	Post Fracture
	154 mm x 203 mm (6 in. x 8 in.) Wood	35.59	(8.0)			NA	NA	Soil Yield
	155 mm x 203 mm (6 in. x 8 in.) Wood	49.38	(11.1)			0.83	(0.186)	Post Fracture

In 1995, Rohde and Reid [17-19] studied grading specifications and requirements for wood posts in W-beam guardrail. The authors noted that the grade of a post was significantly influenced by wane, missing wood on the corners of the post, even when it was located at the ends of the posts where it has little or no influence on performance. To deal with this problem, the posts were graded twice, once according to the Southern Pine Inspection Bureau (SPIB) standards [20] and a second time without considering wane on the ends of the posts. This re-grading significantly altered the grade of many posts.

After completing static and dynamic tests, the researchers concluded that there was no significant benefit achieved by requiring Grade 1 SPIB posts and suggested lowering the requirement to Grade 2 with the wane and knot criteria relaxed at the ends of the posts. The

results were believed to effectively lower the costs of guardrail installations without adversely impacting its safety performance.

In 1996, Holloway et al. [21] conducted a study to evaluate a deeper post embedment. In this study, the researchers examined the use of a 1,270-mm (50-in.) embedment depth as opposed to the standard 1,118-mm (44-in.) depth for both 152-mm x 203-mm (6-in. x 8-in.) grade 2 Southern Yellow Pine timber posts and W152x13.4 (W6x9) steel posts. Five dynamic tests were conducted for each, with one of the five utilizing the extended embedment depth. The researchers noted that timber posts performed better than steel in all cases. The test results also suggested that the additional 152 mm (6 in.) of embedment depth made little difference in the stiffness or the dynamic performance of the posts. This conclusion is contradictory to most other studies concerning post embedment depth and may be attributed to the very small sample size used in the tests or other variables not considered during the testing.

Goeller et al. [22], also completed post testing in 1997 for a project studying the soil-post interaction forces during a guardrail impact. Twenty-nine post tests were conducted in soil, eleven of which were 152-mm x 203-mm (6-in. x 8-in.) wood posts, twelve of which were W6x9 steel posts, and the remainder of which were W6x16 steel posts. The results showed that the wood posts produced a lower force than the steel posts and that a triangular soil pressure distribution most closely approximated the test data.

Also in 1997, Smith et al. [23] studied the interaction of posts and guardrail. Smith concluded that the reaction of the post during vehicular collisions significantly changes depending on the soil moisture content, stating that the higher the moisture content, the lower the load capacity. Results from the ten timber tests are shown in Table 6. An impact height of 544 mm (21.4 in.) was used for all tests.

Table 6. Post Testing Matrix and Test Results Summary

Post				Soil		Peak Force		Residual Force	
Length		Embedment Depth		Material	Moisture Content				
mm	(in.)	mm	(in.)		%	kN	(kips)	kN	(kips)
1829	(72)	1118	(44)	Cohesive	17.5	62.3	(14.00)	60.6	(13.63)
1829	(72)	1118	(44)	Cohesive	21.7	28.9	(6.50)	21.2	(4.77)
1829	(72)	1118	(44)	Cohesive	23	21.4	(4.80)	21.5	(4.84)
1829	(72)	1118	(44)	Cohesive	20.6	30.9	(6.95)	24.7	(5.56)
1829	(72)	1118	(44)	Cohesive	12.1	66.7	(15.00)	52.6	(11.82)
1829	(72)	1118	(44)	Cohesive	12.7	48.9	(11.00)	48.1	(10.82)
1981	(78)	1321	(52)	Cohesive	12.7	47.6	(10.70)	0.0	(0.00)
1981	(78)	1321	(52)	Cohesive	13.1	62.3	(14.00)	60.3	(13.56)
1829	(72)	1118	(44)	Noncohesive	2.9	41.1	(9.25)	22.2	(5.00)
1829	(72)	1118	(44)	Noncohesive	4.1	18.3	(4.11)	7.8	(1.75)

Another study of the interaction of guardrail posts and soil was conducted by Coon et al. [24]. The study examined W152x13.5 (W6x9) and W152x23.8 (W6x16) steel posts and 152-mm x 203-mm (6-in. x 8-in.) wood posts with a 549-mm (21.6-in.) impact height as well as a 1,092-mm (43-in.) embedment depth. The researchers found that the energy absorbed when a wood post fractured was significantly lower than when a post rotated in the soil.

Also in 1998, Denman and Welch [25] developed the REGENT System, a flared-end terminal created to meet the Test Level 3 requirements of NCHRP Report 350 [26]. During their research, they noticed several problems that were attributed to the variation in the posts. For instance, in a system constructed with several Grade 2 posts followed by a Dense Select Structural post, the vehicle had a tendency to snag on the stronger post causing it to spin or rollover. After investigating the availability and the cost of stronger posts, it was decided to utilize a dual grading system, where the area 305 mm (12 in.) above and below the ground line was required to meet the select structural requirements and the remainder of the post length was allowed to fall into Grade 2.

A project completed by Kuipers and Reid [27] in 2003 studied the embedment depth for the steel posts used in the Midwest Guardrail System (MGS). In the post study, ten dynamic bogie tests were completed using standard W152x23.8 (W6x16) posts with an impact height of

630 mm (24.8 in.). W152x23.8 (W6x16) posts were used instead of the W152x13.4 (W6x9) posts typically used in the MGS system to avoid significant yielding of the posts during the tests, allowing researchers to focus on the influence of the soil behavior on the system.

Results from three tests, tests NPGB-4, 9, and 10, are shown in Figure 1. The forces from the tests averaged 29.0 kN (6.52 kips) and 29.6 kN (6.66 kips) at a deflections of 381 mm (15 in.) and 597 mm (23.5 in.), respectively, with local force peaks exceeding that level.

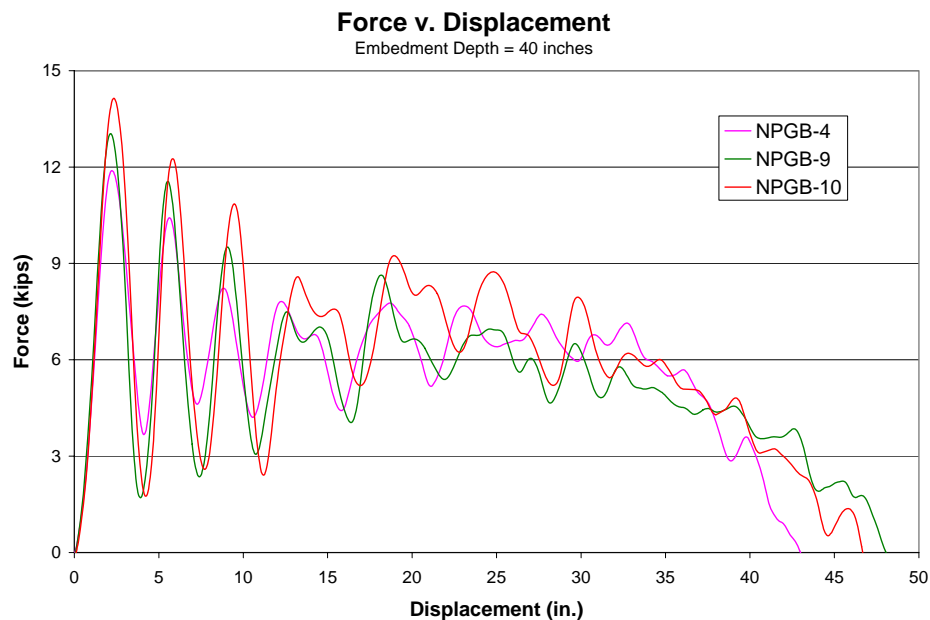


Figure 1. NPGB-4, 9, and 10 Bogie Testing Results

In the tests, it was noted that the shallow posts with a 940-mm (37-in.) embedment depth pulled out of the soil while the majority simply rotated in the soil. The report also showed that more energy was absorbed by the system when the posts rotated in the soil rather than being pulled out of the ground. The total energy absorbed by the rotating posts with a 1,016-mm (40-in.) embedment depth averaged 29.8 kJ (263.8 kip-in.), while that of the posts utilizing a 940-mm (37-in.) embedment depth averaged only 24.9 kJ (220.4 kip-in.), resulting in a 16 percent decrease.

2.1.2 Full-Scale Crash Testing

In 1967, the federal government required that all guardrail systems pass dynamic testing. With this requirement, the cost of guardrail increased by more than one dollar per foot. Bronstad [28] of SwRI and Burket of the Ohio Department of Highways looked for a way to reduce the cost. In order to verify compliance with the new regulations, six full-scale sedan crash tests were performed on several variations of the existing Ohio W-beam guardrail system. Each test examined an inexpensive modification that could be made on in-place guardrail systems, therefore avoiding the cost of replacement. Results are shown in Table 7.

Table 7. Summary of 1971 Southwest Research Institute Testing

Test No.	Post Size	Weight		Speed		Impact Angle	Results
		kN	(kips)	m/s	(mph)	degrees	
ODH-1	102 mm x 102 mm (4 in. x 4 in.)	20.41	(4.589)	30.0	(67.0)	25	Vehicle Rolled
ODH-2	102 mm x 152 mm (4 in. x 6 in.)	19.59	(4.404)	27.7	(62.0)	25.3	Good Redirection
ODH-3	178 mm (7 in.) diameter	19.77	(4.445)	27.9	(62.5)	28.7	Vehicle Rolled
ODH-4	152 mm (6 in.) diameter	18.87	(4.242)	28.2	(63.1)	28.3	Good Redirection (High Roll Angle)
ODH-5	152 mm x 152 mm (6 in. x 6 in.) Notched	19.60	(4.407)	31.7	(70.8)	26.7	Good Redirection

Test nos. ODH-2, 4, and 5 were considered successful tests, and all three would be able to be used in roadside applications. Test nos. ODH-1 and 3 failed due to the vehicle rolling.

In 1988, Sicking et al. [29] conducted a study to optimize strong-post, W-beam guardrail systems to lower the costs of installation and maintenance. Several full-scale sedan crash tests were completed, including tests on W-beam guardrail systems using round, 178-mm (7-in.) diameter wood posts and W152x12.6 (W6x8.5) steel posts with both 965-mm (38-in.) and 1,219-mm (48-in.) embedment depths. It was found that the designs utilizing wood posts carried a much lower cost than systems using the equivalent steel counterparts. The study also found that by using an increased post spacing of 2,540 mm (100 in.) and a new 965-mm (38-in.) embedment depth, the cost for both steel and wood systems could be drastically reduced. Lastly, the report added that blockouts could be used if desired, but they were not found to be cost

beneficial. The blockouts would only help to alleviate wheel snag that proved to be only a minor issue in the tests conducted.

Also in 1988, Sicking et al. [30] developed two new end treatments for the standard guardrail system that met the NCHRP 230 [31] requirements. This research effort included full-scale vehicle crash tests of a guardrail system with round, wood posts. Domed 178-mm (7-in.) diameter by 1,905-mm (75-in.) long posts were used in the system with a 965-mm (38-in.) embedment depth and a top of rail height of 686 mm (27 in.). The tests included both head-on and rail-face impacts, and proved that terminals utilizing round wood posts met impact performance guidelines.

In 1995, Sicking, Bligh, Bullard, and Ross [32-34] conducted a full-scale crash test of W-beam guardrail with round, Southern Pine posts. This particular test followed NCHRP Report 350 test designation 3-11, using a 2,000-kg (4,409-lb) pickup truck impacting at 100 km/h (62.14 mph) and 25 degrees. The Southern Pine posts were 184 mm (7.25 in.) in diameter by 1,905 mm (75 in.) long and spaced at 1905 mm (75 in.). The embedment depth was 1,118 mm (44 in.). The blockouts were fabricated with one concave side to meet flush with the round posts. The test was successful since the vehicle was safely contained and redirected with little damage or intrusion into the occupant compartment. The researchers determined the most critical concern with the test to be the high exit angle of 26.1 degrees. However, upon review of the vehicle trajectory after leaving the rail, the possible problems derived from this high exit angle were considered to be minimal. Therefore, TTI researchers suggested that the round post system was nearly equivalent to the standard G4(2W) system and was an acceptable substitute.

In another research project, Rosson, Bierman, and Rohde [35-36] looked at methods to reduce the deflection of guardrail placed directly in front of roadside hazards. Four full-scale

crash tests were conducted using steel posts, and computer simulations using BARRIER VII were used in place of four additional tests with timber posts. To complete the simulations, twenty dynamic post tests were completed, with the results presented in Table 8. The researchers found that the best option was to reduce the post spacing to half the normal spacing.

Table 8. Rosson, Bierman and Rohde Post Test Summary

Soil Type	Moisture Content	Embedment Depth	Post Type	Average Force		Peak Force		Fracture Energy	
				kN	(kips)	kN	(kips)	kN-m	(kip-in.)
Clay	Low (12%)	Extended	Steel	47.86	(10.76)	59.83	(13.45)	25.53	(225.96)
		1270 mm (50 in.)	Timber	47.68	(10.72)	59.61	(13.40)	25.44	(225.12)
				60.32	(13.56)	75.40	(16.95)	32.17	(284.76)
		Standard	Steel	43.81	(9.85)	54.76	(12.31)	23.37	(206.85)
		1118 mm (44 in.)	Timber	38.03	(8.55)	47.55	(10.69)	20.29	(179.55)
				52.58	(11.82)	65.74	(14.78)	28.05	(248.22)
	Optimum (17%)			48.13	(10.82)	60.18	(13.53)	25.67	(227.22)
		Standard	Steel	50.22	(11.29)	62.76	(14.11)	26.79	(237.09)
				36.96	(8.31)	46.22	(10.39)	19.72	(174.51)
		1118 mm (44 in.)	Timber	60.63	(13.63)	75.80	(17.04)	32.34	(286.23)
				24.73	(5.56)	30.92	(6.95)	13.19	(116.76)
		Standard	Steel	19.75	(4.44)	24.69	(5.55)	10.53	(93.24)
Sand	Unsaturated	1118 mm (44 in.)	Timber	21.71	(4.88)	27.13	(6.10)	11.58	(102.48)
				21.22	(4.77)	26.51	(5.96)	11.48	(101.64)
				21.66	(4.87)	26.91	(6.05)	15.28	(135.24)
		Standard	Steel	26.56	(5.97)	31.85	(7.16)	14.16	(125.37)
				19.71	(4.43)	24.64	(5.54)	10.51	(93.03)
		1118 mm (44 in.)	Timber	28.65	(6.44)	35.81	(8.05)	15.28	(135.24)
				11.08	(2.49)	13.83	(3.11)	5.91	(52.29)

An additional project utilizing round wooden posts in a guardrail transition to concrete bridge rail was completed in 1999 by Buth et al. [37]. The Southern Pine posts used were 178 mm (7 in.) in diameter and 1,905 mm (75 in.) long with a 1,118-mm (44-in.) embedment depth. Once again, blockouts with a concave side were used to make a flush connection between the post and the blockout. The first test failed to meet NCHRP Report 350 requirements. But, with the insertion of two 3,200-mm (126-in.) long pieces of 89-mm (3.5-in.) diameter pipe into the tubular rail element, the system proved to be adequate.

In 2004, Seckinger et al. [38-39] issued a report on a study of guardrail systems encased in pavement mow strips. In the study, steel and 178-mm (7-in.) diameter round, Southern Pine posts were tested in mow strips constructed of concrete or asphalt with various types of fill,

including grout, asphalt, and rubber mats. After both bogie and full-scale testing, the recommendation was to assure a minimum 457-mm x 457-mm (18-in. x 18-in.) leave-out, or gap in the mow strip, and to fill the leave-out with a standard two-sack grout. Systems using both W152x13.4 (W6x9) steel and 178-mm (7-in.) diameter, round wood posts were successfully tested. The results showed the importance of post rotation in the success of guardrail systems. If rotation was not important, no leave-out would be required.

2.1.3 Summary of Wood Post Testing

In summary, numerous bogie tests have been conducted on steel, rectangular wood, and round wood guardrail posts in both soil and a cantilever sleeve. Cantilever tests on round posts were conducted for Red Pine on posts with diameters ranging from 155 mm (6.1 in.) to 248 mm (9.75 in.), and led to the conclusion that for an equivalent moment of inertia, rectangular and round wood posts behaved the same.

Soil bogie tests were also conducted for a variety of posts. Round wood tests included a test on a 178 mm (7 in.) diameter SYP post embedded at 965 mm (38 in.), which showed behavior similar to steel posts embedded at 1,118 mm (44 in.). Other soil tests largely concentrated on steel posts and 152-mm x 203-mm (6-in. x 8-in.) rectangular wood posts. The general trend was that the two behaved very similarly, with some tests suggesting steel posts were better and others suggesting wood posts were better. Another conclusion that was made from the testing was that increased soil moisture content lowered the capacity of the soil, and therefore the energy absorbed by a given type of post.

Full-scale crash tests were also conducted to meet NCHRP Report 230 requirements. These tests include those conducted at TTI on a standard guardrail system built with 178-mm (7-in.) diameter SYP posts embedded at both 965 mm (38 in.) and 1219 mm (48 in.). NCHRP

Report 230 tests were also conducted on end treatments for the system using the same 178-mm (7-in.) diameter posts. The results suggested that utilizing round wood posts lowered the cost of the system.

Those full-scale tests meeting the requirements of NCHRP Report 350 include tests conducted on a guardrail system and a bridge rail transition section, respectively utilizing 184-mm (7.25-in.) diameter and 178-mm (7-in.) diameter SYP posts, both of which were embedded at 1,118 mm (44 in.), respectively. The success of these systems formed the foundation for the work in this study.

The effects of concrete or asphalt mow strips were also investigated under NCHRP Report 350 for a system using 178-mm (7-in.) diameter SYP posts. The findings specified a minimum leave out section of 457 mm x 457 mm (18 in. x 18 in.).

2.2 Grading

In the United States, six associations are responsible for establishing and publishing grading rules. Since this study was limited to the Southern Yellow Pine, Douglas Fir, and Ponderosa Pine species, only three were determined to be applicable, the Southern Pine Inspection Bureau [40], the Western Wood Products Association (WWPA) [41], and the West Coast Lumber Inspection Bureau [42].

The SPIB is responsible for the grading rules for all Southern Pine species found below the Mason-Dixon line. This includes the four main species, longleaf, slash, shortleaf, and loblolly, and several other less prominent species.

Although not an exact science, grading lumber is a means of separating the lumber by its quality, strength, and appearance. For timbers, defined by the SPIB as all lumber with a cross-section larger than 127-mm x 127-mm (5-in. x 5 in.), there are four distinct grades, Select

Structural, No. 1, No. 2, and No. 3. Grade No. 3 is not suggested for applications where strength or appearance are important and will not be considered in this report. The remaining three grades can be further subdivided into dense and not dense categories simply based on the ring density of the lumber. Table 9 lists the three grades and several grading criteria. Other grading criteria are also used, but make little or no difference in the grade separation and are not shown. Dense grades follow the same guidelines but have 6 or more annual rings per inch with 1/3 or more of the ring being summerwood. Lumber can also classify as dense if it has 4 or more annual rings per inch with 1/2 or more being summerwood.

Table 9. SPIB Timber Grading Summary

Defect	Select Structural	No. 1	No. 2
Decay	Allowed in Knots	Allowed in Knots	Decay Limited to 10% of Cross-section if Wholly Enclosed within 4 Surfaces of Each Piece. 5% Otherwise.
Firm Red Heart	Up to 10%	No Limit	No Limit
Slope of Grain	1 in 14	1 in 11	1 in 6
Holes	Scattered <1/4" Diameter	Scattered <1/4" Diameter	<1-1/2" Diameter
Splits	Less than Thickness	Less than Thickness	Less than 1-1/4 Times the Thickness
Wane	1/8 of Width, 1/4 of Length	1/6 of Width, 1/3 of Length	1/4 of Face on One Edge, 1/3 of Face on Both Edges
Knots	As Per Table Below		

The grading rules concerning knots vary widely depending on the size of the timber. SPIB has created three tables defining the allowable standards for knots. They are presented below in Tables 10, 11, and 12.

Table 10. Knot Grading Criteria for Select Structural Timbers [40]

Select Structural Timbers			
Nominal Width of Face	Narrow Face And At Edge of Wide Face	Centerline Wide Face	Unsound Knots
5"	1-3/8"		1"
6"	1-5/8"	1-5/8"	1-1/4"
8"	1-7/8"	2-1/4"	1-1/2"
10"	2-1/8"	2-3/4"	2"
12"	2-3/8"	3-1/4"	2-1/8"
14"	2-1/2"	3-5/8"	2-1/4"
16"	2-3/4"	3-7/8"	2-1/2"
18"	3-7/8"	4-1/8"	2-1/2"
20"	3"	4-3/8"	3"

Table 11. Knot Grading Criteria for No. 1 Timbers [40]

No. 1 Timbers			
Nominal Width of Face	Narrow Face And At Edge of Wide Face	Centerline Wide Face	Unsound Knots
5"	1-3/4"		1-3/8"
6"	2-1/8"	2-1/8"	1-5/8"
8"	2-1/2"	2-3/4"	2"
10"	2-3/4"	3-1/2"	2-1/2"
12"	3-1/8"	4-1/4"	2-7/8"
14"	3-3/8"	4-3/4"	3-1/8"
16"	3-1/2"	5"	3-3/8"
18"	3-1/2"	5-1/4"	3-1/2"
20"	3-1/2"	5-1/2"	3-1/2"

Table 12. Knot Grading Criteria for No. 2 Timbers [40]

No. 2 Timbers		
Nominal Width of Face	Narrow Face, Edge of Wide Face, Centerline Wide Face	Unsound Knots
5"	2-1/2"	1-3/8"
6"	3"	1-5/8"
8"	4-1/2"	2"
10"	5-1/2"	2-1/2"
12"	6-1/2"	2-7/8"
14"	7-1/2"	3-1/8"
16"	8"	3-3/8"
18"	8-1/2"	3-1/2"
20"	9"	3-1/2"

As mentioned, a second set of grading rules, published by the WWP, pertains to the Ponderosa Pine and Douglas Fir species. These rules also separate timbers into four categories, Select Structural, No. 1, No. 2, and No. 3. The grading criteria are listed in Table 13 below. Lumber qualifying as dense follows the same guidelines as the SPIB criteria, with the exception that dense lumber can have less than 4 rings per inch as long as 1/2 is summerwood.

Table 13. WWP Timber Grading Summary

Defect	Select Structural	No. 1	No. 2	No. 3
Checks	Seasoning checks - single or opposite with sum less than half the thickness of a piece	Seasoning checks - single or opposite with sum less than half the thickness of a piece	Seasoning Checks	Seasoning Checks
Pockets	Medium Pitch Pockets	Medium Pitch Pockets	Pitch or Bark Pockets	Pitch or Bark Pockets
Slope of Grain	1 in 12	1 in 10	1 in 6	No Limit
Shakes	1/3 Thickness on end	1/3 Thickness on end	1/2 length, 1/2 thickness, limited as splits if through ends	Full length if not continuous
Splits	Equal in length to 3/4 thickness of the piece or equivalent end checks	Equal in length to width of the piece or equivalent end checks	Medium or equivalent end checks	1/4 length
Wane	1/8 width of any face or equivalent slightly more for short distances	1/4 width of any face or equivalent slightly more for short distances	1/3 width of any face or equivalent slightly more for short distances	1/3 width of any face or equivalent slightly more for short distances
Skips	Occasional 1/16 in deep, 2' long	Occasional 1/8 in deep, 2' long	1/8" deep, 2' long, 1/16" deep if full length	1/8" in both width and thickness if surfaced, 1/2" scant if rough
Knots	As Per Table Below			

Table 14. Knot Grading Criteria for Select Structural Timbers [41]

Wide Face Width	Knot Size Permitted		
	Select Structural Timbers	Grade No. 1	Grade No. 2
5"	1"	1-1/2"	2-1/4"
6"	1-1/4"	1-7/8"	2-3/4"
8"	1-5/8"	2-1/2"	3-3/4"
10"	2"	3-1/8"	4-3/4"
12"	2-3/8"	3-3/4"	5-3/4"
14"	2-1/2"	4"	6-3/4"
16"	2-3/4"	4-1/4"	7-3/4"
18"	3"	4-1/2"	8-3/4"

Similar to the SPIB grading rules, the WWPA rules contain many different criteria for knots depending on the grade. Table 14 shows the acceptable knot sizes for three grades. Knots for Grade No. 3 are simply limited to $\frac{3}{4}$ the width of the face. In the WWPA rules, the knot size permitted on the widest face is permitted on all faces.

The third set of grading rules is Standard No. 17, written by the WCLB. The standard pertains to the Douglas Fir species and specifies grading rules identical to those of the WWPA with two exceptions. First, Standard No. 17 does not separate mining grades from post and timber grades as the WWPA does. Second, there is no No. 3 grading category. Since, mining grades are not assigned stress values, they will not be relevant to the study. The remaining grades are Select Structural, equivalent to WWPA Select Structural, No. 1 Structural, equivalent to WWPA No. 1, and No. 2 Structural, equivalent to WWPA No. 2.

3 SAMPLING

3.1 Sample Collection

Initially, a post diameter was selected for the three species based on the success of 184-mm (7.25-in.) diameter Southern Pine guardrail posts from full-scale crash tests conducted by Sicking, Bligh, Bullard, and Ross [32-34]. Sizes for the two alternate species were determined using tabulated strength values for Douglas Fir and Ponderosa Pine to carry a bending moment equivalent to that of the Southern Pine posts. These sizes were 216 mm (8.5 in.) for Ponderosa Pine and 191 mm (7.5 in.) for Douglas Fir, as shown in Figure 2. The diameter for Southern Pine was held at 184 mm (7.25 in.), as shown in Figure 2. The 1,981-mm (78-in.) length was arbitrarily selected to assure sufficient length to increase the post embedment depth if needed.

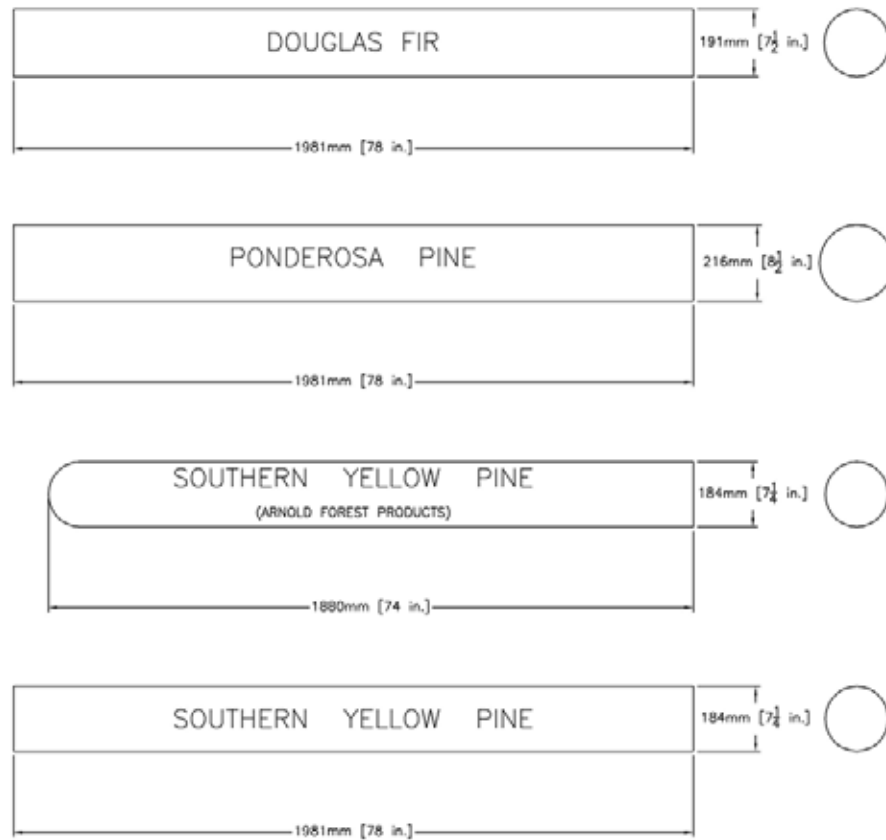


Figure 2. Major Dimensions of Round Wood Posts

Unlike some materials, wood is highly variable. Its strength can drastically change with variation in species, ring density, knot size and density, moisture content, and even region of origin. Ponderosa Pine is simply not as strong as Douglas Fir or Southern Yellow Pine.

Attempting to investigate the effects of the two most influential variables, knots and ring density, three categories of posts were defined. The categories were low ring density without knots (BASELINE), low ring density with knots (KNOTS), and high ring density without knots (HRD). Posts were categorized based on ring density, knot frequency, and knot density. Posts with 4 or fewer rings-per-inch were defined as low ring density and 6 or more rings-per-inch were defined as high ring density. Posts with any knots larger than 63.5 mm (2.5 in.) in diameter were placed in the knots category, while posts with knots that were less than 38.1 mm (1.5 in.) in diameter were considered to be without knots and could be placed in the baseline or HRD categories. A portion of the testing was intended to isolate the properties of posts in these three categories, and a portion was intended to determine the properties of the random population.

For the Douglas Fir and Ponderosa Pine species, categorized posts were selected first to assure that each category had a sample of 10 posts. When those 30 posts were selected, another 40 posts were randomly pulled from the production line to establish a random population sample for static testing. Ponderosa Pine samples were donated by Hills Products Group, and Douglas Fir samples were donated by All-Weather Wood Products.

For the Southern Yellow Pine species, a total of 90 posts were shipped to the outdoor testing facility at MwRSF. From this sample, 30 were selected for the three specific categories and another 40 were selected from the remainder for the population sample. The Southern Yellow Pine posts were donated by Arnold Forest Products Corporation, Burke-Parsons-Bowlby Corporation, and Interstate Timber Products Co.

When the sample arrived at the test site, researchers estimated the Modulus of Elasticity (MOE) for each post using a stress wave technique [43]. Using this technique, each post was tapped once with a hammer, sending a stress wave through the post. At the same time, a sensor determined the time the stress wave took to travel to the other end of the post and return. Knowing this time and the length of the post, the wave velocity could be calculated and used with the mass density to determine the MOE. Posts were then ranked within each category by the estimated MOE values. Once the order was determined, the posts were paired in order, making a total of five pairs per category. With both posts in a pair having similar MOE values, one was randomly chosen to be sent to the Forest Products Laboratory for static testing and the other remained in Lincoln for dynamic testing.

3.2 Sample Documentation

The posts were extensively documented. Moisture contents were measured at three locations: 533 mm (21 in.), 991 mm (39 in.), and 1,448 mm (57 in.) from the bottom of the post using a pin-type moisture meter. The area within this region was defined as the critical zone, the zone where fracture was likely to occur. Circumference was also measured in the three locations of the critical zone and additionally at both the top and bottom of the post. Weights and lengths were measured to determine an approximate density. Ring counts were taken over a three-inch length, and knots were carefully documented. Photographs of each post were also taken during documentation.

To record the knots on the round posts, a unique procedure had to be adopted. A circular template with a radial mark at every 5th degree, similar to a protractor, was created to sit on top of the post. An arrow was randomly drawn on the top of the posts, defining the front of each post, and the zero-degree mark was aligned with the arrow. Each knot was given an angle and a

distance from the top of the post down to the center of the knot. Additionally, dimensions were recorded for the size of each knot. The same procedure was used for gouges and other defects in the posts. Summaries of the documentation are presented in Tables 15, 16, and 17. Tables containing all of the post properties are presented in Appendix A.

Table 15. Douglas Fir Pre-Test Documentation

Post Number	Weight		Avg. Length		Circumference						Volume		Density		Moisture Content (%)			Ring Density
	kg	(lbs)	mm	(in.)	Critical Zone Average		Top		Bottom		cm³	(in.³)	kg/m³	(lbs/ft³)	21" From Top	21" From Bottom	Center	(rings/in.)
					mm	(in.)	mm	(in.)	mm	(in.)								
2	25	(55)	1988	(78.250)	586	(23.083)	575	(22.625)	597	(23.500)	54202	(3308)	460	(28.73)	30	25	43	9.67
3	29	(63)	1980	(77.958)	573	(22.542)	581	(22.875)	578	(22.750)	52036	(3175)	549	(34.28)	26	28	30	25.67
6	26	(58)	1958	(77.083)	583	(22.958)	584	(23.000)	568	(22.375)	53285	(3252)	494	(30.82)	23	22	24	8.00
9	27	(59)	1981	(78.000)	582	(22.917)	575	(22.625)	594	(23.375)	53544	(3267)	500	(31.20)	26	26	24	14.33
10	27	(60)	1982	(78.042)	585	(23.042)	572	(22.500)	578	(22.750)	53487	(3264)	509	(31.76)	21	20	31	7.00
11	25	(55)	1982	(78.042)	586	(23.083)	575	(22.625)	584	(23.000)	53866	(3287)	463	(28.91)	22	33	22	19.33
13	28	(62)	1969	(77.521)	583	(22.958)	578	(22.750)	584	(23.000)	53543	(3267)	525	(32.79)	43	30	51	8.33
15	32	(71)	1981	(78.000)	580	(22.833)	581	(22.875)	587	(23.125)	53248	(3249)	605	(37.76)	45	39	50	11.00
18	23	(50)	1981	(78.000)	576	(22.667)	565	(22.250)	568	(22.375)	51839	(3163)	437	(27.31)	27	26	31	10.00
20	25	(56)	1981	(78.000)	580	(22.833)	578	(22.750)	581	(22.875)	53026	(3236)	479	(29.90)	21	23	25	13.00
22	21	(46)	1979	(77.917)	589	(23.208)	597	(23.500)	584	(23.000)	54862	(3348)	380	(23.74)	30	26	32	5.33
24	29	(63)	1967	(77.438)	573	(22.542)	587	(23.125)	572	(22.500)	52054	(3177)	549	(34.27)	34	28	32	5.33
25	29	(63)	1975	(77.750)	599	(23.583)	597	(23.500)	597	(23.500)	56485	(3447)	506	(31.58)	50	53	45	7.33
26	25	(56)	1965	(77.375)	584	(23.000)	584	(23.000)	565	(22.250)	53356	(3256)	476	(29.72)	55	27	48	6.33
27	22	(49)	1969	(77.500)	587	(23.125)	587	(23.125)	581	(22.875)	54240	(3310)	410	(25.58)	22	30	25	6.00

Table 16. Ponderosa Pine Pre-Test Documentation

	Post Number	Weight		Avg. Length		Circumference						Volume		Density		Moisture Content (%)			Ring Density (rings/in.)
		kg	(lbs)	mm	(in.)	Critical Zone Average		Top		Bottom		cm ³	(in. ³)	kg/m ³	(lbs/ft ³)	21" From Top	21" From Bottom	Center	
						mm	(in.)	mm	(in.)	mm	(in.)								
Ponderosa Pine	101	35	(77)	1981	(77.979)	659	(25.958)	664	(26.125)	660	(26.000)	68685	(4191)	509	(31.74)	20	19	19	6.00
	104	54	(120)	1982	(78.042)	718	(28.250)	705	(27.750)	714	(28.125)	80677	(4923)	672	(41.94)	22	19	23	5.67
	105	52	(115)	1982	(78.042)	704	(27.708)	695	(27.375)	699	(27.500)	77700	(4742)	671	(41.91)	19	16	26	7.33
	106	33	(73)	1978	(77.875)	709	(27.917)	714	(28.125)	695	(27.375)	79015	(4822)	419	(26.16)	21	19	18	5.67
	109	37	(81)	1981	(78.000)	669	(26.333)	651	(25.625)	714	(28.125)	71371	(4355)	515	(32.14)	20	18	17	5.00
	111	48	(105)	1981	(78.000)	706	(27.792)	705	(27.750)	705	(27.750)	78493	(4790)	607	(37.88)	19	19	22	14.00
	112	51	(112)	1981	(78.000)	713	(28.083)	686	(27.000)	714	(28.125)	79436	(4847)	640	(39.93)	23	19	19	25.00
	117	35	(77)	1983	(78.083)	709	(27.917)	702	(27.625)	699	(27.500)	78739	(4805)	444	(27.69)	20	22	18	18.33
	118	46	(102)	1980	(77.938)	714	(28.125)	699	(27.500)	711	(28.000)	79886	(4875)	579	(36.16)	19	20	19	9.33
	120	58	(128)	1982	(78.021)	704	(27.708)	699	(27.500)	705	(27.750)	77967	(4758)	745	(46.49)	20	19	22	12.67
	122	50	(110)	1983	(78.063)	722	(28.417)	772	(30.375)	705	(27.750)	83209	(5078)	600	(37.43)	21	19	23	11.00
	123	34	(75)	1981	(78.000)	643	(25.333)	689	(27.125)	667	(26.250)	67245	(4104)	506	(31.58)	23	20	16	11.67
	124	45	(99)	1982	(78.042)	707	(27.833)	708	(27.875)	718	(28.250)	79184	(4832)	567	(35.40)	22	23	19	16.67
	127	53	(116)	1982	(78.021)	705	(27.750)	699	(27.500)	711	(28.000)	78348	(4781)	672	(41.93)	25	22	28	13.00
	128	38	(83)	1981	(78.000)	656	(25.833)	695	(27.375)	645	(25.375)	68698	(4192)	548	(34.21)	16	15	16	10.67

Table 17. Southern Yellow Pine Pre-Test Documentation

	Post Number	Weight		Avg. Length		Circumference						Volume		Density		Moisture Content (%)			Ring Density (rings/in.)
		kg	(lbs)	mm	(in.)	Critical Zone Average		Top		Bottom		cm ³	(in. ³)	kg/m ³	(lbs/ft ³)	21" From Top	21" From Bottom	Center	
						mm	(in.)	mm	(in.)	mm	(in.)								
Southern Yellow Pine	303	32	(70)	1960	(77.146)	594	(23.375)	616	(24.250)	591	(23.250)	56038	(3420)	567	(35.37)	28	19	20	2.67
	304	25	(56)	1962	(77.250)	566	(22.292)	518	(20.375)	584	(23.000)	49846	(3042)	510	(31.81)	27	22	23	2.50
	305	23	(50)	1973	(77.688)	591	(23.250)	587	(23.125)	603	(23.750)	55227	(3370)	411	(25.64)	29	29	24	6.00
	306	28	(61)	1968	(77.479)	579	(22.792)	584	(23.000)	562	(22.125)	52570	(3208)	526	(32.86)	19	26	24	6.33
	309	35	(77)	1985	(78.167)	594	(23.375)	581	(22.875)	562	(22.125)	54463	(3324)	641	(40.03)	19	21	22	3.33
	314	29	(65)	1986	(78.188)	592	(23.292)	575	(22.625)	610	(24.000)	55268	(3373)	533	(33.30)	23	27	23	3.00
	316	30	(66)	1954	(76.917)	597	(23.500)	584	(23.000)	587	(23.125)	55627	(3395)	538	(33.60)	29	22	31	3.00
	317	27	(59)	1960	(77.146)	599	(23.583)	581	(22.875)	597	(23.500)	56065	(3421)	477	(29.80)	23	24	25	3.00
	318	27	(59)	1974	(77.729)	600	(23.625)	587	(23.125)	597	(23.500)	56385	(3441)	475	(29.63)	22	21	20	3.00
	320	29	(64)	1976	(77.792)	593	(23.333)	578	(22.750)	581	(22.875)	54709	(3339)	531	(33.13)	20	19	21	2.33
	322	38	(84)	1869	(73.583)	581	(22.875)	575	(22.625)	572	(22.500)	52024	(3175)	732	(45.72)	19	20	19	7.33
	323	34	(76)	1879	(73.958)	582	(22.917)	597	(23.500)	581	(22.875)	52859	(3226)	652	(40.71)	33	21	23	4.67
	327	26	(58)	1999	(78.708)	568	(22.375)	562	(22.125)	559	(22.000)	50532	(3084)	521	(32.50)	16	16	16	9.50
	328	32	(70)	1976	(77.813)	596	(23.458)	594	(23.375)	610	(24.000)	56268	(3434)	564	(35.23)	16	20	18	8.00
	330	31	(69)	1973	(77.688)	577	(22.708)	568	(22.375)	594	(23.375)	52677	(3215)	594	(37.09)	15	15	14	11.00

As the moisture content of a wood post increases up to 23 percent, the strength of the wood fibers within the post decreases. Beyond 23 percent, the wood strength is fairly constant. In their actual use, the moisture content may exceed 23 percent, and therefore the posts would be saturated. Upon completion of documentation, the posts were placed in a 1,219-mm (48-in.) deep tank of water in an effort to saturate the critical zone of the posts, replicating the worst case scenario the posts may encounter when used in an actual guardrail system.

The moisture content and weight of the posts were measured again on test day to give a more accurate representation of the posts after they had been soaked in water. The results of those measurements are shown in Tables 18, 19, and 20. Note that all of the posts were saturated in the critical region.

Table 18. Douglas Fir Test Day Measurements

Test No.	Post No.	Weight (lbs)	Moisture Content (%)			Circumference at Bottom (in.)
			21 in. from Top	Mid-Length	21 in. from Bottom	
DF-1	2	76	10	37	59	23 5/8
DF-2	3	76	16	40	56	22 7/8
DF-3	6	64	16	50	65	22 3/4
DF-4	9	64	15	30	64	23 1/2
DF-5	10	67	16	67	64	23
DF-6	11	74	15	41	63	23 1/4
DF-7	13	73	17	62	59	23 1/8
DF-8	15	82	16	55	59	23 3/8
DF-9	18	70	18	31	61	23
DF-10	20	73	15	51	57	23 1/4
DF-11	22	61	24	29	37	23 1/4
DF-12	24	61	17	28	31	22 3/4
DF-13	25	75	40	31	32	23 5/8
DF-14	26	68	18	26	45	22 1/2
DF-15	27	64	22	51	61	23 1/2

Table 19. Ponderosa Pine Test Day Measurements

Test No.	Post No.	Weight (lbs)	Moisture Content (%)			Circumference at Bottom (in.)
			21 in. from Top	Mid-Length	21 in. from Bottom	
PP-1	101	113	17	39	43	26
PP-2	104	130	16	27	26	28
PP-3	105	131	16	28	31	27 1/2
PP-4	106	97	15	39	38	27 1/2
PP-5	109	90	13	18	38	29 1/4
PP-6	111	120	15	35	38	28 3/4
PP-7	112	128	19	26	27	29 1/4
PP-8	117	101	15	33	38	28 3/4
PP-9	118	112	15	23	36	28
PP-10	120	130	17	29	30	28
PP-11	122	149	19	51	49	27 3/4
PP-12	123	103	31	48	41	27 1/4
PP-13	124	133	17	43	52	29 3/8
PP-14	127	125	21	32	36	28
PP-15	128	93	26	42	47	25 1/2

Table 20. Southern Yellow Pine Test Day Measurements

Test No.	Post No.	Weight (lbs)	Moisture Content (%)			Circumference at Bottom (in.)
			21 in. from Top	Center	21 in. from Bottom	
SY-1	303	89	45	52	50	23 3/4
SY-2	304	71	21	46	41	23 1/8
SY-3	305	81	42	70	68	23 3/4
SY-4	306	72	17	37	43	22 3/4
SY-5	309	89	10	25	31	22 3/8
SY-6	314	87	9	34	37	23 3/4
SY-7	316	88	10	39	32	23 1/4
SY-8	317	82	9	54	40	23 5/8
SY-9	318	90	7	36	35	22 7/8
SY-10	320	89	14	31	31	23
SY-11	322	90	13	29	25	22 7/8
SY-12	323	83	12	28	27	22 3/4
SY-13	327	67	13	25	27	22 1/2
SY-14	328	90	12	48	31	24
SY-15	330	81	12	30	27	27 7/8

4 PHYSICAL TESTING - ROUND ONE

4.1 Purpose

In previous research, there has been no dynamic testing of round Ponderosa Pine or Douglas Fir posts, and therefore bogie tests were undertaken on both species to determine their dynamic properties. In addition, dynamic testing of Southern Yellow Pine posts was also conducted to serve as a standard for comparison.

4.2 Scope

Initial bogie tests were conducted with the round posts installed in a rigid steel sleeve embedded in concrete. Fifteen tests were conducted for each of the three species. The target impact condition for the tests was 32 km/h (20 mph), with the impact occurring at the centerline of the bogie, 632 mm (24.875 in.) above the ground. The angle of impact was irrelevant since a round cross-section does not have a strong or weak axis. Therefore, the arrow randomly drawn on the top of the post during documentation was used as the impact side. The testing matrix for the thirty initial tests is shown in Figure 3 below, and the test setup and impact conditions are shown in Figure 4.

Test No.	Post No.	Wooden Post Type		Post Length (in.)	Post Diameter (in.)
DF-1	2	Round	Douglas Fir	78.3	7.35
DF-2	3	Round	Douglas Fir	78.0	7.18
DF-3	6	Round	Douglas Fir	77.1	7.31
DF-4	9	Round	Douglas Fir	78.0	7.29
DF-5	10	Round	Douglas Fir	78.0	7.33
DF-6	11	Round	Douglas Fir	78.0	7.35
DF-7	13	Round	Douglas Fir	77.5	7.31
DF-8	15	Round	Douglas Fir	78.0	7.27
DF-9	18	Round	Douglas Fir	78.0	7.22
DF-10	20	Round	Douglas Fir	78.0	7.27
DF-11	22	Round	Douglas Fir	77.9	7.39
DF-12	24	Round	Douglas Fir	77.4	7.18
DF-13	25	Round	Douglas Fir	77.8	7.51
DF-14	26	Round	Douglas Fir	77.4	7.32
DF-15	27	Round	Douglas Fir	77.5	7.36
PP-1	101	Round	Ponderosa Pine	78.0	8.26
PP-2	104	Round	Ponderosa Pine	78.0	8.99
PP-3	105	Round	Ponderosa Pine	78.0	8.82
PP-4	106	Round	Ponderosa Pine	77.9	8.89
PP-5	109	Round	Ponderosa Pine	78.0	8.38
PP-6	111	Round	Ponderosa Pine	78.0	8.85
PP-7	112	Round	Ponderosa Pine	78.0	8.94
PP-8	117	Round	Ponderosa Pine	78.1	8.89
PP-9	118	Round	Ponderosa Pine	77.9	8.95
PP-10	120	Round	Ponderosa Pine	78.0	8.82
PP-11	122	Round	Ponderosa Pine	78.1	9.05
PP-12	123	Round	Ponderosa Pine	78.0	8.06
PP-13	124	Round	Ponderosa Pine	78.0	8.86
PP-14	127	Round	Ponderosa Pine	78.0	8.83
PP-15	128	Round	Ponderosa Pine	78.0	8.22
SY-1	303	Round	Southern Yellow Pine	77.1	7.44
SY-2	304	Round	Southern Yellow Pine	77.3	7.1
SY-3	305	Round	Southern Yellow Pine	77.7	7.4
SY-4	306	Round	Southern Yellow Pine	77.5	7.25
SY-5	309	Round	Southern Yellow Pine	78.2	7.44
SY-6	314	Round	Southern Yellow Pine	78.2	7.41
SY-7	316	Round	Southern Yellow Pine	76.9	7.84
SY-8	317	Round	Southern Yellow Pine	77.1	7.51
SY-9	318	Round	Southern Yellow Pine	77.7	7.52
SY-10	320	Round	Southern Yellow Pine	77.8	7.43
SY-11	322	Round	Southern Yellow Pine	73.6	7.28
SY-12	323	Round	Southern Yellow Pine	74.0	7.29
SY-13	327	Round	Southern Yellow Pine	78.7	7.12
SY-14	328	Round	Southern Yellow Pine	77.8	7.47
SY-15	330	Round	Southern Yellow Pine	77.7	7.23

NOTES:

- (1) TARGET SPEED = 20 MPH
- (2) IMPACT ORIENTATION: CENTERLINE OF POST (W/ARROW POINTING TOWARD BOGIE) AND CENTERLINE OF BOGIE
- (3) SOUTHERN PINE HAVE DOMED TOPS



**FOREST PRODUCTS LAB
ROUND POST TESTING
BOGIE SETUP
TEST MATRIX**

Drawing Name:
FPL Bogie Testing Matrix

Scale:
None

Sheet:
4 of 4
Date:
11/2/04
By:
JAH
Rev:
KAP

Figure 3. Bogie Testing Matrix

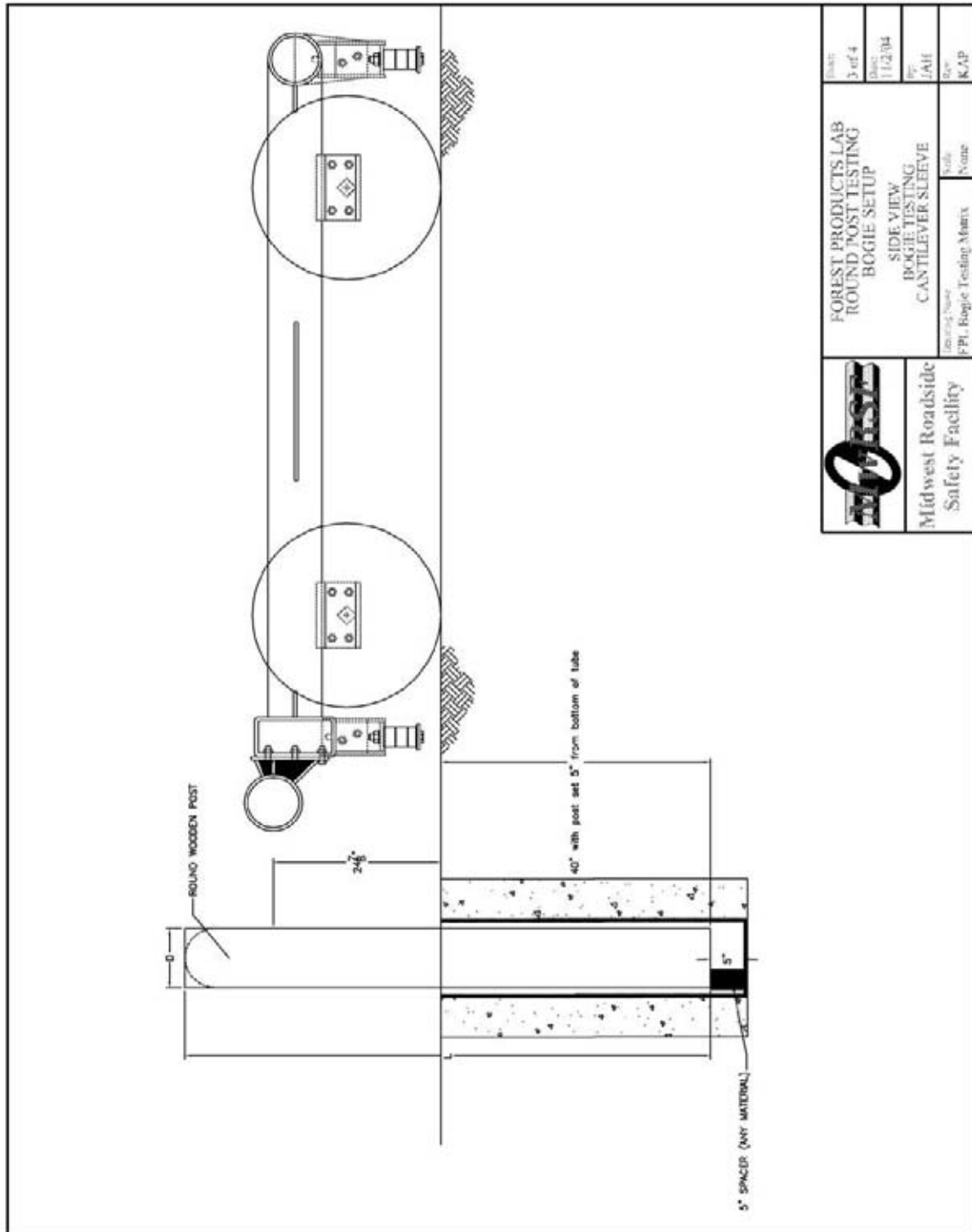


Figure 4. Bogie Testing Setup

4.3 Round Wood Post

Compared to steel sections, wood posts have highly variable sizes. Although two posts may have the same nominal diameter, it is not likely that the actual diameters will be the same. Because of this, it is incorrect to compare the resistive moments or resistive forces of the posts directly. Instead, a factor must be introduced that allows comparisons to be made between posts with different sizes. This factor is the Modulus of Rupture.

The Modulus of Rupture (MOR) is the maximum stress felt in the outer fibers of the post. The MOR is calculated by dividing the maximum bogie impact moment, M_{MAX} , by the section modulus, S , of the post. Because it is a stress value, the cross-section and the applied moment have already been taken into account, making it possible to compare post strengths without consideration of the cross-section or loading condition.

$$MOR = \frac{M_{MAX}}{S} \quad S = \frac{(\pi)(r)^3}{4}$$

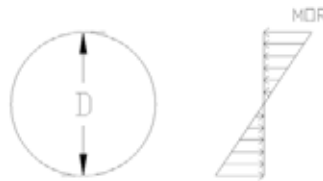


Figure 5. Bending Stress Distribution

4.4 Equipment and Instrumentation

A variety of equipment and instrumentation was used to record and collect data. It was important to gather correct data using affordable instrumentation in order to understand and derive meaningful conclusions of the physical tests. Equipment and instruments utilized in this testing included:

- Bogie
- Accelerometer

- Pressure Tape Switches
- Photography Cameras
- Digital Video Cameras

4.4.1 Bogie

A rigid-frame bogie was used to impact the posts. A variable height, detachable impact head was constructed and used in the testing. The bogie head was constructed of 203-mm (8-in.) diameter, 12.5-mm (0.5-in.) thick standard steel pipe, with 19-mm (0.75-in.) neoprene belting wrapped around the pipe to prevent local damage to the post from the impact. The impact head was bolted to the bogie vehicle, creating a rigid frame. The bogie with the impact head is shown on the guidance track in Figure 6. Use of this impact head allowed a 632-mm (24.875-in.) impact height, corresponding to the MGS mounting height. The weight of the bogie with the addition of the mountable impact head was 728 kg (1,605 lbs). The speed chosen for the first set of impact tests, 32 km/h (20 mph), approximated the lateral velocity of the posts in a full scale system impact.

A pickup truck with a reverse cable tow system was used to propel the bogie. When the bogie reached the end of the guidance system, it was released from the tow cable, allowing it to be free rolling when it impacted the post. A remote braking system was installed on the bogie allowing it to be safely brought to rest after the test.



Figure 6. Rigid Frame Bogie on Guidance Track

4.4.2 Accelerometer

One triaxial piezoresistive accelerometer system with a range of ± 200 G's was mounted on the bogie vehicle near its center of gravity, and used to measure the acceleration in the longitudinal, lateral, and vertical directions at a sample rate of 3,200 Hz. The accelerometer, Model EDR-3, was developed by Instrumental Sensor Technology (IST) of Okemos, Michigan. The EDR-3 was configured with 256 Kb of RAM memory and a 1,120 Hz lowpass filter. Computer software, "DynaMax 1 (DM-1)" and "DADiSP", were used to analyze and plot the accelerometer data.

4.4.3 Pressure Tape Switches

Three pressure tape switches, spaced at 1-m (3.3-ft) intervals and placed near the end of the bogie track, were used to determine the speed of the bogie before the impact. As the left-front tire of the bogie passed over each tape switch, a strobe light was fired sending an electronic timing signal to the data acquisition system. The system recorded the signals and the time each occurred. The speed was then calculated using the spacing between the sensors and the time between the signals.

4.4.4 Photography Cameras

One high-speed Photron digital video camera or one high-speed VITcam digital video camera, both with speeds of 500 frames per second, was used to document each test. One Canon digital video camera with a speed of 29.97 frames per second was also employed to document each test. Both cameras were placed approximately 25 ft from the centerline of the posts, with a field of view perpendicular to the bogie's direction of travel. Flood lights were used to light the base of the posts, allowing the fracture and fracture surface to be clearly examined in the videos. A Nikon Coolpix 8700 digital camera was used to document pre- and post-test conditions of each post.

4.5 Data Processing

Initially, the data was filtered using a SAE Class 60 Butterworth filter conforming to the SAE J211/1 specifications [44-45]. The processed acceleration data was then multiplied by the mass of the bogie to get the impact force using Newton's Second Law. Next, the acceleration trace was integrated to find the change in velocity. Initial velocity of the bogie, calculated using the data from the pressure tape switches, was then used to determine the bogie velocity throughout the test. The calculated bogie's velocity trace was then integrated to find the displacement. Subsequently, the force-deflection curve was plotted for each test. Finally, integration of the force-deflection curve provided the energy-displacement curve for each test.

4.6 End of Test Determination

During an impact, the accelerometer records the accelerations the bogie feels from all sources, not just the post. Because of this, vibrations in the bogie vehicle, impact head, and accelerometer mounting assembly are also recorded and result in a high frequency acceleration trace. Since the bogie vehicle may still be vibrating after the impact event, the data may extend

well beyond the failure of the post. For this reason, the end of the test needed to be defined in some manner.

In general, this event time was identified as the third time the filtered acceleration trace crossed the X-axis from positive to negative. However, in many cases this resulted in unreasonably long test durations, so two limits were established. First, all tests were limited to a 20 in. maximum deflection because it was decided that no post would have the capacity to deflect more than 508 mm (20 in.) in a cantilever sleeve without complete fracture. Second, each test was limited by the bogie-post contact time. For each test, the high-speed video was used to establish the length of time the bogie was actually in contact with the post. This time was then used to define the end of the test.

5 ROUND 1 CANTILEVER TEST RESULTS

5.1 Introduction

Accelerometer data was processed for each test in order to obtain acceleration, velocity, and displacement curves, as well as force-deflection curves. Individual test results are provided in Appendix B. A summary for the round one testing program is provided in Table 21 for the Douglas Fir species, Table 22 for the Ponderosa Pine species, and Table 23 for the Southern Yellow Pine species.

5.2 MOR Results

The MOR was calculated for each test and is shown in the mentioned tables. Southern Yellow Pine resulted in the highest average MOR value of 61.1 MPa (8.9 ksi), and Douglas Fir and Ponderosa Pine resulted in MOR values of 59.4 MPa (8.6 ksi) and 49.0 MPa (7.1 ksi), respectively. As expected and due to the dynamic nature of the testing and the benefits of the round cross-section, all three MOR averages were higher than the tabulated values of 52 MPa (7.5 ksi) for Douglas Fir, 35 MPa (5.1 ksi) for Ponderosa Pine, and 55 MPa (8.0 ksi) for Southern Yellow Pine found in the Wood Handbook [46].

5.2.1 Douglas Fir

The baseline category for the Douglas Fir tests had an average MOR of 51.7 MPa (7.50 ksi); the knots category had an average of 60.9 MPa (8.83 ksi), and the HRD category had an average MOR of 65.5 MPa (9.50 ksi). The difference between the highest and lowest categories was more than 25 percent, a significant variation for posts of the same species from the same region. The average ring density for the knots category was more than twice that of the baseline category, likely resulting in a large influence on strength.

5.2.2 Ponderosa Pine

The 48.0 MPa (7.1 ksi) average MOR for Ponderosa Pine can be broken down into three categories. The baseline category, low ring density without knots, showed the lowest MOR with a value of 39.0 MPa (5.66 ksi). The HRD category showed the highest MOR with a value of 63.3 MPa (9.18 ksi), while the knots category fell in between with an MOR of 44.8 MPa (6.50 ksi). Although the results may seem alarming since the knots category fell above the baseline category, special attention should be given to the ring density of the posts within the knots category as it was, on average, more than twice as high as the ring density of the posts within the baseline category. This is likely the reason the knots category was stronger than the baseline category.

5.2.3 Southern Yellow Pine

For Southern Yellow Pine, the knots category MOR ranked the lowest followed by the baseline and HRD categories with 48.3 MPa (7.01 ksi), 50.6 MPa (7.34 ksi), and 84.4 MPa (12.24 ksi), respectively. Again, the three categories varied significantly with the largest discrepancy between the HRD category and the others. This also shows that a post's ring density greatly influences its strength.

These results demonstrate that there may be some correlation between the presence of knots and a higher ring density. The random sample, however, does not strongly support this, since posts with small knots also have a high ring density. Instead, it suggests that the average ring density for the baseline category was abnormally low. For Ponderosa Pine, the average ring density for the baseline category was 5.9 rings-per-inch, while the random population average was 11.6 rings-per-inch. The same is true for Douglas Fir in which case the average ring density

for the baseline category was 6.1 rings-per-inch, and the random population average was 10 rings-per-inch.

Table 21. Dynamic Douglas Fir Round Wood Post Test Results

Post Test No.	Post No.	Category	Ring Density rings/in.	Average Diameter mm (in.)	Peak Force				Rupture			Moisture Content (%)	Modulus of Rupture Mpa (kips/in. ²)	Impact Velocity m/s (mph)	
					Time ms	Force kN (kips)	Deflection mm (in.)	Energy kJ (kip-in.)	Time ms	Deflection mm (in.)	Energy kJ (kip-in.)				
DF-11	22	BASELINE	5.33	187 (7.4)	5	39.8 (9.0)	45 (1.8)	0.88 (7.8)	40.6 (23.8)	359 (14.1)	2.69 (23.8)	37	38.8 (5.63)	9.1 (20.4)	
DF-12	24		5.33	182 (7.2)	12.5	65.1 (14.6)	113 (4.5)	3.04 (26.9)	28.8 (32.5)	254 (10.0)	3.67 (32.5)	31	69.2 (10.04)	9.2 (20.7)	
DF-13	25		7.33	191 (7.5)	5.6	56.6 (12.7)	52 (2.0)	1.29 (11.4)	36.9 (33.1)	326 (12.8)	3.74 (33.1)	32	52.6 (7.62)	9.2 (20.7)	
DF-14	26		6.33	186 (7.3)	11.9	47.1 (10.6)	106 (4.2)	2.81 (24.8)	60.6 (59.8)	506 (19.9)	6.76 (59.8)	45	47.2 (6.84)	9.1 (20.3)	
DF-15	27		6.00	187 (7.4)	11.6	51.5 (11.6)	105 (4.1)	2.75 (24.3)	37.2 (37.2)	326 (12.9)	4.63 (41.0)	61	50.7 (7.36)	9.2 (20.6)	
BASELINE Average			6.07	187 (7.4)	9.32	52.0 (11.7)	84 (3.3)	2.15 (19.1)	40.82	354 (13.9)	4.30 (38.0)	41	51.7 (7.50)	9.2 (20.5)	
DF-6	11	KNOTS	19.33	186 (7.3)	11.9	53.8 (12.1)	108 (4.3)	3.24 (28.7)	50.9 (50.9)	446 (17.5)	5.24 (46.4)	63	53.3 (7.73)	9.3 (20.9)	
DF-7	13		8.33	185 (7.3)	5.3	44.1 (9.9)	47 (1.9)	0.94 (8.3)	20.3 (20.3)	177 (7.0)	2.50 (22.1)	59	44.4 (6.44)	9.0 (20.1)	
DF-8	15		11.00	184 (7.3)	11.9	76.9 (17.3)	100 (3.9)	3.39 (30.0)	64.7 (64.7)	506 (19.9)	6.58 (58.2)	59	78.7 (11.42)	8.6 (19.3)	
DF-9	18		10.00	183 (7.2)	12.5	68.0 (15.3)	110 (4.3)	3.27 (28.9)	40.6 (40.6)	345 (13.6)	5.08 (45.0)	61	71.1 (10.32)	9.0 (20.2)	
DF-10	20		13.00	184 (7.3)	12.5	55.7 (12.5)	113 (4.4)	3.24 (28.7)	39.7 (39.7)	348 (13.7)	4.02 (35.6)	57	57.0 (8.26)	9.2 (20.7)	
KNOTS Average			12.33	185 (7.3)	10.82	59.7 (13.4)	96 (3.8)	2.82 (24.9)	43.24	364 (14.3)	4.68 (41.5)	60	60.9 (8.83)	9.0 (20.2)	
DF-1	2	HRD	9.67	186 (7.3)	11.9	73.1 (16.4)	107 (4.2)	3.39 (30.0)	45.9 (45.9)	392 (15.4)	5.86 (51.9)	59	72.4 (10.50)	9.2 (20.5)	
DF-2	3		25.67	182 (7.2)	12.5	83.5 (18.8)	112 (4.4)	3.78 (33.5)	62.5 (62.5)	508 (20.0)	8.64 (76.5)	56	88.7 (12.87)	9.1 (20.4)	
DF-3	6		8.00	185 (7.3)	12.2	60.0 (13.5)	110 (4.3)	2.89 (25.6)	39.7 (39.7)	345 (13.6)	4.44 (39.3)	65	60.3 (8.75)	9.2 (20.5)	
DF-4	9		14.33	185 (7.3)	12.5	60.0 (13.5)	105 (4.1)	2.71 (24.0)	63.4 (63.4)	504 (19.8)	4.87 (43.1)	64	60.7 (8.81)	8.6 (19.2)	
DF-5	10		7.00	186 (7.3)	5.6	45.6 (10.3)	51 (2.0)	1.08 (9.5)	36.9 (36.9)	324 (12.7)	3.57 (31.6)	64	45.4 (6.59)	9.2 (20.5)	
HRD Average			12.93	185 (7.3)	10.94	64.4 (14.5)	97 (3.8)	2.77 (24.5)	49.68	414 (16.3)	5.47 (48.5)	62	65.5 (9.50)	9.1 (20.2)	
Overall Average			10.44	185 (7.3)	10.36	58.7 (13.2)	92 (3.6)	2.58 (22.8)	44.6 (44.6)	378 (14.9)	4.82 (42.6)	54	59.37 (8.6)	9.1 (20.3)	
Standard Deviation			5.70	2.14 (0.1)	3.12771	12.7 (2.8)	27 (1.1)	1.00 (8.9)	13.3 (13.3)	99 (3.9)	1.64 (14.5)	12	14.14 (2.1)	0.2 (0.5)	
Douglas Fir															

*Data Filtered According to SAE J211/1 Requirements
Limited by Maximum Deflection Criterion (20 in.)
Limited by Time of Contact

Table 22. Dynamic Ponderosa Pine Round Wood Post Test Results

Post Test No.		Post No.	Category	Ring Density rings/in.	Average Diameter mm (in.)	Peak Force				Rupture			Moisture Content (%)	Modulus of Rupture Mpa (kips/in. ²)	Impact Velocity m/s (mph)
						Time ms	Force kN (kips)	Deflection mm (in.)	Energy kJ (kip-in.)	Time ms	Deflection mm (in.)	Energy kJ (kip-in.)			
PP-1	101	BASELINE	6.00	210 (8.3)	5.3	57.1 (12.8)	49 (1.9)	1.24 (10.9)	46.6	410 (16.2)	3.80 (33.7)	43	39.8 (5.77)	9.2 (20.6)	
PP-2	104		5.67	228 (9.0)	5.6	66.5 (15.0)	50 (2.0)	1.51 (13.3)	60.6	509 (19.9)	4.65 (41.1)	26	35.9 (5.21)	8.9 (20.0)	
PP-3	105		7.33	224 (8.8)	5.6	75.1 (16.9)	50 (2.0)	1.76 (15.6)	15.3	132 (5.2)	5.11 (45.3)	31	43.0 (6.24)	9.0 (20.2)	
PP-4	106		5.67	226 (8.9)	5.3	61.5 (13.8)	49 (1.9)	1.42 (12.6)	35	317 (12.5)	2.59 (22.9)	38	34.4 (4.99)	9.4 (21.0)	
PP-5	109		5.00	213 (8.4)	12.2	63.2 (14.2)	108 (4.3)	3.26 (28.9)	53.1	451 (17.7)	5.26 (46.6)	38	42.1 (6.11)	9.1 (20.4)	
BASELINE Average			5.93	220 (8.7)	6.8	64.7 (14.5)	61 (2.4)	1.84 (16.3)	42.12	364 (14.3)	4.28 (37.9)	35	39.0 (5.66)	9.1 (20.4)	
PP-11	122	KNOTS	11.00	230 (9.0)	6.6	83.4 (18.8)	61 (2.4)	1.98 (17.6)	16.3	145 (5.7)	5.56 (49.2)	49	44.3 (6.42)	9.3 (20.9)	
PP-12	123		11.67	205 (8.1)	5.6	56.8 (12.8)	52 (2.0)	1.32 (11.7)	45.9	410 (16.1)	3.10 (27.5)	41	42.5 (6.17)	9.3 (20.8)	
PP-13	124		16.67	225 (8.9)	5.9	70.7 (15.9)	54 (2.1)	1.63 (14.4)	12.2	109 (4.3)	3.46 (30.7)	52	39.9 (5.79)	9.2 (20.5)	
PP-14	127		13.00	224 (8.8)	13.1	92.9 (20.9)	115 (4.5)	4.89 (43.3)	16.3	141 (5.5)	6.53 (57.8)	36	52.9 (7.68)	9.1 (20.3)	
PP-15	128		12.67	209 (8.2)	5.3	62.9 (14.1)	46 (1.8)	1.27 (11.3)	24.1	199 (7.8)	4.14 (36.7)	47	44.4 (6.44)	8.7 (19.5)	
KNOTS Average			13.00	218 (8.6)	7.3	73.3 (16.5)	66 (2.6)	2.22 (19.6)	22.96	201 (7.9)	4.56 (40.4)	45	44.8 (6.50)	9.1 (20.4)	
PP-6	111	HRD	14.00	225 (8.8)	12.5	137.0 (30.8)	114 (4.5)	6.23 (55.1)	53.4	438 (17.2)	10.32 (91.4)	38	77.7 (11.28)	9.4 (21.1)	
PP-7	112		25.00	227 (8.9)	12.5	144.3 (32.4)	111 (4.4)	6.33 (56.0)	67.5	507 (20.0)	14.26 (126.2)	27	79.3 (11.51)	9.2 (20.7)	
PP-8	117		18.33	226 (8.9)	12.2	96.7 (21.7)	111 (4.4)	4.72 (41.8)	16.6	147 (5.8)	6.58 (58.3)	38	54.1 (7.85)	9.3 (20.9)	
PP-9	118		9.33	227 (9.0)	5.6	67.8 (15.2)	52 (2.0)	1.52 (13.4)	35.6	314 (12.3)	4.37 (38.6)	36	37.1 (5.38)	9.3 (20.8)	
PP-10	120		12.67	224 (8.8)	11.6	118.9 (26.7)	101 (4.0)	5.41 (47.9)	65.6	508 (20.0)	9.81 (86.8)	30	68.1 (9.87)	9.0 (20.2)	
HRD Average			15.87	226 (8.9)	10.88	112.9 (25.4)	98 (3.8)	4.84 (42.8)	47.74	383 (15.1)	9.07 (80.3)	34	63.3 (9.18)	9.3 (20.7)	
Avg.			11.60	221 (8.7)	8.326667	83.6 (18.8)	75 (2.9)	2.97 (26.2)	37.6	316 (12.4)	5.97 (52.8)	38	49.04 (7.1)	9.2 (20.5)	
St. Dev.			5.54	8.04 (0.3)	3.427091	28.8 (6.5)	30 (1.2)	1.97 (17.4)	19.9	156 (6.1)	3.19 (28.3)	8	14.67 (2.1)	0.2 (0.4)	

*Data Filtered According to SAE J211/1 Requirements

Limited by Maximum Deflection Criterion (20 in.)

Limited by Time of Contact

Table 23. Dynamic Southern Yellow Pine Round Wood Post Test Results

Post Test No.	Post No.	Category	Ring Density rings/in.	Average Diameter mm (in.)	Peak Force				Rupture			Moisture Content (%)	Modulus of Rupture Mpa (kips/in. ²)	Impact Velocity m/s (mph)	
					Time ms	Force kN (kips)	Deflection mm (in.)	Energy kJ (kip-in.)	Time ms	Deflection mm (in.)	Energy kJ (kip-in.)				
Southern Yellow Pine															
SY-1	303	KNOTS	2.67	189 (7.4)	5.3	52.3 (11.8)	45 (1.8)	1.06 (9.4)	46.3	368 (14.5)	4.17 (36.9)	50	49.9 (7.23)	8.4 (18.9)	
SY-2	304		2.50	180 (7.1)	11.6	39.2 (8.8)	104 (4.1)	2.27 (20.1)	14.7	132 (5.2)	2.89 (25.6)	41	43.1 (6.25)	8.9 (20.5)	
SY-3	305		6.00	188 (7.4)	5	38.7 (8.7)	44 (1.8)	0.81 (7.2)	20.6	179 (7.0)	2.58 (22.9)	68	37.5 (5.44)	8.9 (20.0)	
SY-4	306		6.33	184 (7.3)	13.1	60.9 (13.7)	110 (4.3)	2.71 (24.0)	65.3	509 (20.0)	6.68 (59.1)	43	62.6 (9.08)	8.6 (19.2)	
SY-5	309		3.33	189 (7.4)	12.5	50.8 (11.4)	105 (4.1)	2.78 (24.6)	30.3	246 (9.7)	4.53 (40.1)	31	48.5 (7.03)	8.6 (19.2)	
KNOTS Average			4.17	186 (7.3)	9.5	48.4 (10.9)	82 (3.2)	1.93 (17.0)	35.44	287 (11.3)	4.17 (36.9)	47	48.3 (7.01)	8.7 (19.6)	
SY-6	314	BASELINE	3.00	188 (7.4)	5.3	47.6 (10.7)	48 (1.9)	1.10 (9.7)	39.4	343 (13.5)	4.63 (40.9)	37	45.8 (6.65)	9.2 (20.5)	
SY-7	316		3.00	190 (7.5)	5.9	53.2 (11.9)	53 (2.1)	1.23 (10.9)	36.3	314 (12.4)	3.14 (27.8)	32	49.9 (7.23)	9.0 (20.2)	
SY-8	317		3.00	191 (7.5)	12.5	54.4 (12.2)	113 (4.4)	2.75 (24.3)	15.3	137 (5.4)	3.44 (30.4)	40	50.5 (7.32)	9.2 (20.6)	
SY-9	318		3.00	191 (7.5)	5.6	51.1 (11.5)	49 (1.9)	1.16 (10.2)	16.3	139 (5.5)	3.73 (33.0)	35	47.2 (6.85)	8.8 (19.7)	
SY-10	320		2.33	189 (7.4)	13.4	62.4 (14.0)	114 (4.5)	2.86 (25.3)	22.8	188 (7.4)	6.07 (53.8)	31	59.8 (8.67)	8.7 (19.4)	
BASELINE Average			2.87	190 (7.5)	8.54	53.7 (12.1)	76 (3.0)	1.82 (16.1)	26.02	224 (8.8)	4.20 (37.2)	35	50.6 (7.34)	9.0 (20.1)	
SY-11	322	HRD	7.33	185 (7.3)	11.3	102.6 (23.1)	98 (3.8)	4.48 (39.6)	65.3	507 (20.0)	9.15 (81.0)	25	104.4 (15.14)	8.9 (19.9)	
SY-12	323		4.67	185 (7.3)	11.9	81.4 (18.3)	103 (4.0)	3.42 (30.3)	15.9	136 (5.3)	4.90 (43.3)	27	82.3 (11.94)	8.8 (19.8)	
SY-13	327		9.50	181 (7.1)	12.2	73.3 (16.5)	103 (4.1)	3.17 (28.1)	16.9	140 (5.5)	4.46 (39.5)	27	79.7 (11.56)	8.6 (19.3)	
SY-14	328		8.00	190 (7.5)	11.3	62.0 (13.9)	96 (3.8)	2.99 (26.5)	20	168 (6.6)	3.83 (33.9)	31	58.5 (8.48)	8.8 (19.6)	
SY-15	330		11.00	183 (7.2)	11.9	93.3 (21.0)	103 (4.1)	4.00 (35.4)	58.1	470 (18.5)	6.86 (60.7)	27	97.0 (14.07)	8.9 (19.9)	
HRD Average			8.10	185 (7.3)	11.72	82.5 (18.5)	101 (4.0)	3.61 (32.0)	35.24	284 (11.2)	5.84 (51.7)	27	84.4 (12.24)	8.8 (19.7)	
Avg.			5.04	187 (7.4)	9.92	61.5 (13.8)	86 (3.4)	2.45 (21.7)	32.2	265 (10.4)	4.74 (41.9)	36	61.10 (8.9)	8.8 (19.8)	
St. Dev.			2.82	3.46 (0.1)	3.347963	18.7 (4.2)	28 (1.1)	1.14 (10.1)	18.6	143 (5.6)	1.78 (15.7)	11	20.35 (3.0)	0.2 (0.5)	

*Data Filtered According to SAE J211/1 Requirements

Limited by Maximum Deflection Criterion (20 in.)

Limited by Time of Contact

6 PRELIMINARY POST SIZE DETERMINATION

When the preliminary bogie tests were completed, it was necessary to adjust the post sizes for each species. The selected sizes needed to be large enough to give the post sufficient strength to rotate through the soil rather than fracture, but also be as small as possible to save on material costs. To determine this size, a statistical analysis of post strength was used along with two secondary methods, the static and the dynamic methods. The statistical analysis, called the probability method, was structured to limit the probability of failure of a guardrail system during a design limit impact to a defined level. The static method was designed to equate the capacity of the Douglas Fir and Ponderosa Pine posts to that of Southern Yellow Pine posts which had previously been accepted for use in guardrail systems. The dynamic method was based on allowable stress design, using the MOR from the knots category, historically the lowest, to assure that posts were large enough to endure the soil forces. The last two methods were used to verify the results of the first, and all three methods are presented below.

6.1 Probability Method

Initially, an acceptable level of risk was established. That level of risk was selected as a three percent chance that the structure would fail when a design limit impact occurred on a guardrail installed in strong soils, at any given location. Three percent may seem high, but the strong soil and extreme impact conditions that will be used in the full-scale and bogie testing have an impact on the failure level. The vast majority of soils across the nation would not be capable of developing resistive forces equivalent to those of the strong soil used in the tests. In addition, the impact conditions represent a worst case scenario of ran-off-road crashes. Those two factors considered, the risk of post failure would be dramatically lower for most roadside installations.

The next decision to be made was the determination of failure. One study, completed by Reid and Rohde [17-19], suggested that a standard guardrail system should meet the NCHRP Report 350 Test 3-11 requirements even after three consecutive posts failed. BARRIER VII was used to investigate the effects of weak posts on the MGS system in order to determine the appropriate failure criteria.

6.1.1 BARRIER VII Modeling

Barrier VII is a non-linear, 2-dimensional (2-D) computer simulation program that was used to model the guardrail system. The program was used in lieu of other vehicle-barrier impact simulation programs because of its extensive use and validation in previous impacts. The program has been used to model longitudinal barriers since its inception and has been validated on a wide variety of systems including guardrail, guardrail transitions, flexible barriers, box beams, and timber railings. In addition, the use of BARRIER VII has been recommended in NCHRP Report 350, and, in some cases, has been accepted as a sufficient substitute for full-scale testing by the Federal Highway Administration [47].

6.1.2 MGS Model

The baseline MGS BARRIER VII model was taken from a previous model developed and validated by Kuipers [48]. The model had 173 nodes and 201 members, including 172 beam elements and 29 post elements. A typical model is presented in Appendix C along with an AutoCAD schematic of the model. Properties for the rectangular wood anchor posts, which differed from the steel posts found throughout the system, were not adjusted because the same anchors will be utilized in the new system.

The properties for the steel posts used throughout the remainder of the system were also left alone since bogie-soil behavior was unknown for the round posts. Initially, a modification

was considered to adjust the longitudinal properties of the post to match the lateral properties since the soil behavior of a round post would be independent of the direction of impact. However, unlike steel posts, the round posts are able to rotate fairly easily around their vertical axis, greatly reducing their longitudinal force capacity. Since that magnitude of this reduction was not quantifiable, their longitudinal properties were also approximated based on the model's steel post definition. This seemed to be a reasonable assumption since the target behavior for the round posts was to be equivalent to a W152x13.4 (W6x9) steel post.

6.1.3 BARRIER VII Results

Simulations were completed on the system for models with 0, 1, 2, 3, and 4 consecutive weak posts. The weak post model was defined with the same parameters as a strong post except for its failure deflection. The weak post failure deflection was defined at 61 mm (2.4 in.) to assure that the posts failed. This deflection was based on soil bogie testing in which wood posts fractured at a very low deflection. Impact points were at 283 mm (9.375 in.) increments, beginning 953 mm (37.5 in.) upstream of the first weak post and ending 953 mm (37.5 in.) downstream of the last weak post.

The parameters collected from the simulations include maximum dynamic deflection, maximum rail tension, rail slope, and wheel snag. The rail slope is the maximum slope of the rail in the horizontal plane, as shown in Figure 7, with the lateral direction being the y-axis and the longitudinal direction being the x-axis. The values were determined to give an estimate of the potential for pocketing. The steeper the rail, the greater the chance the vehicle will pocket. Since rail slope varies with the number of nodes used in its approximation, both 3 node and 5 node analyses were completed.

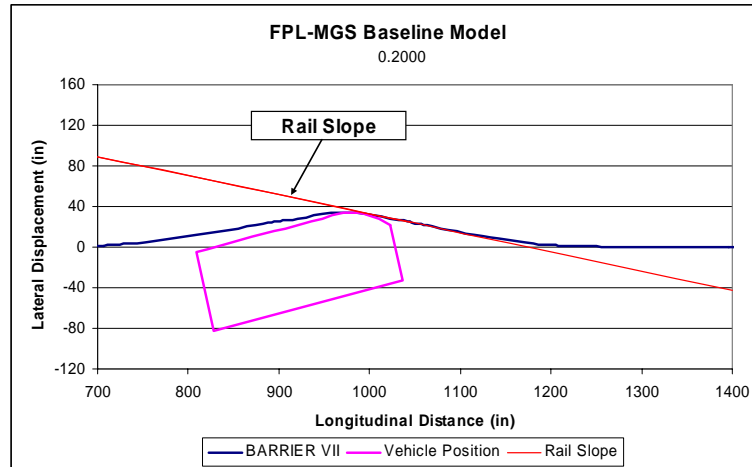


Figure 7. Rail Slope Diagram

Wheel snag parameters consist of two important values, snag and d_y . Snag is the amount of overlap between the vehicle tire and the post transverse to the system at the ground level. The variable d_y is simply the deflection of the post at the center height of the rail, which is used to determine the deflection of the post at the height of the snag calculation. Both are illustrated in Figure 8.

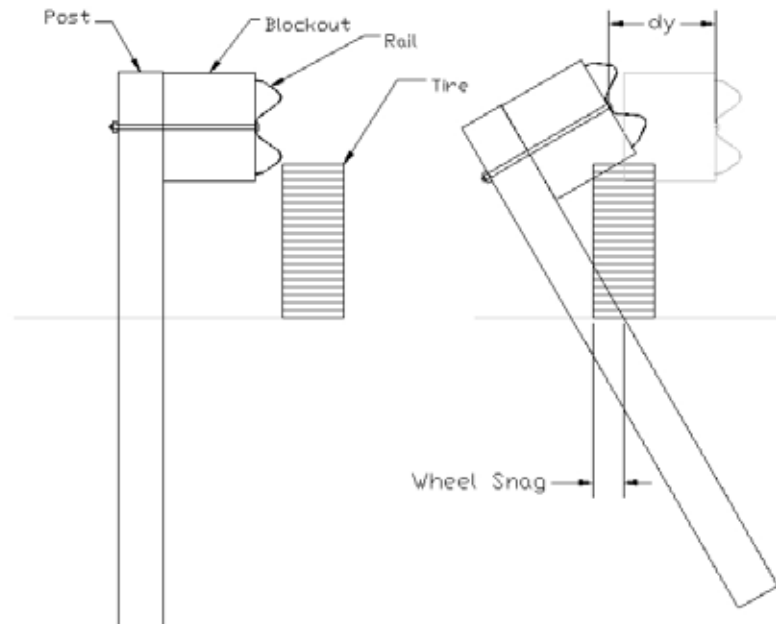


Figure 8. Wheel Snag Diagram

The maximum results are summarized in Table 24. These peak results shown below for a varying number of weak posts are not necessarily from the same simulation run. Instead, they may have been obtained from multiple runs performed at different impact points within the same system.

Table 24. FPL BARRIER VII Results Summary

No. Weak Posts	Maximum Deflection		Maximum Rail Tension		Pocketing Analysis		Snag Analysis **			
					3 Node	5 Node	Snag		dy	
	mm	(in.)	kN	(kips)	(Rail Slope)		mm	(in.)	mm	(in.)
0	1024	(40.3)	301	(67.6)	0.292	0.286	147	(5.78)	373	(14.68)
1	1181	(46.5)	291	(65.5)	0.345	0.317	139	(5.47)	380	(14.98)
2	1257	(49.5)	299	(67.3)	0.345	0.320	141	(5.54)	379	(14.93)
3	1310	(51.6)	299	(67.3)	0.345	0.325	137	(5.39)	369	(14.51)
4	1371	(54.0)	307	(68.9)	0.345	0.324	141	(5.54)	377	(14.83)

** Wheel snag was not reported when dy exceeded 15 in. because the post was considered to be broken.

The results from the FPL simulations show that there is no distinct point at which one additional failed post will cause the system to drastically fail. However, the general trend in the data shows that the more consecutive weak posts the system contains, the more severe the impact criteria. Maximum deflection, maximum rail tension, and maximum rail slope all show a general increase as the number of failed posts increased.

One interesting phenomenon was the decrease in rail tension from the baseline model to that with one, two, and three weak posts. This decrease was attributed to the longitudinal strength of the posts. When one post failed, the restraint on the rail was reduced, lowering the maximum rail tension. However, as more posts failed, the increased deflection caused the tension to increase once again.

Although the simulation did not identify a specific failure criterion, one still needed to be determined. Clearly the case with four weak posts was the worst. It exceeded the MGS baseline model in deflection by nearly 356 mm (14 in.), with the total deflection as high as 1372 mm (54 in.).

At some level, the maximum deflection will be so high that the system will need to be placed too far from the obstacle it is shielding to be feasible for use in many locations. Median widths, right-of-way distances, and bridge span lengths restrict the amount of deflection a guardrail system is allowed. Therefore, a maximum allowable deflection for the system was established at 1321 mm (52 in.). A larger maximum deflection could have been chosen, but the clearance needed for installation would also have increased. As such, a deflection of 1,321 mm (52 in.) seemed to be a reasonable limit.

The conclusion from the previous study by Rohde and Reid was that three consecutive failed posts would constitute an acceptable system, but four consecutive failed posts would not. This conclusion was based on engineering judgment and the results of BARRIER VII computer simulation completed in their study. This four post limit was also the result found by enforcing the 1321-mm (52-in.) maximum deflection criterion. Therefore, the probability that four consecutive posts would fracture prematurely needed to be less than three percent.

6.1.4 Post Reliability

If the probability of a single post failing is represented as P_f , it can be shown that the probability of four consecutive posts failing is $(P_f)^4$, which must be less than 0.03. Therefore, the probability of a single post failing, P_f , must be less than $(0.03)^{1/4} = 0.42$. For the purposes of the project, a maximum allowable P_f value of 0.4 was chosen.

The next step in the post size selection was to determine a minimum required force, or the minimum force that a post needed to resist if it were to rotate in the soil rather than fracture. Historical bogie testing results were examined and are presented in Figure 9. Bogie test nos. NPGB-4, 9, and 10 were conducted on W152x23.8 (W6x16) steel posts using a 1,016-mm (40-in.) embedment depth [27]. For these tests, the resisting force averaged 29.0 kN (6.52 kips) and

29.6 kN (6.66 kips) at a deflections of 381 mm (15 in.) and 597 mm (23.5 in.), respectively, with local force peaks exceeding that level. To account for the local peaks exceeding these average values, as shown in Figure 9, a minimum force of 42 kN (9.5 kips) was selected.

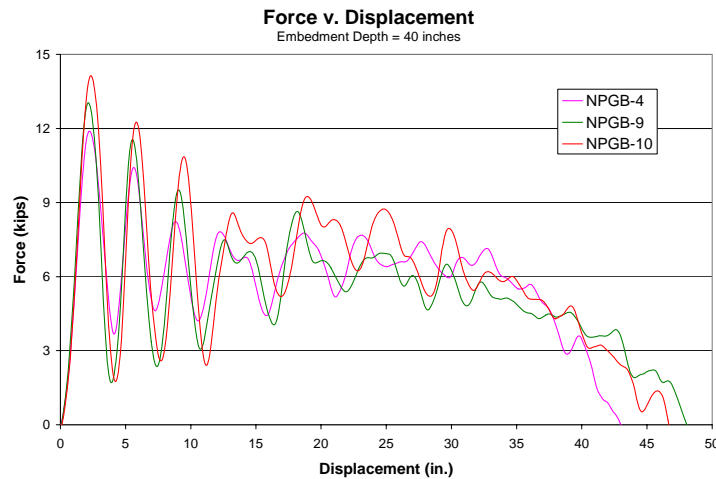


Figure 9. Force vs. Deflection NPGB - 4, 9, and 10

To meet the established probability requirements, 60 percent of the posts must exceed the 42-kN (9.5-kip) force limit. Using the average standard deviation and mean from the 15 dynamic bogie tests and assuming a normal distribution, the required mean peak force level that would return a 40 percent probability value of 42 kN (9.5 kips) was calculated for each species as follows.

$$X = \mu_x + Z \sigma_x$$

$$\mu_x = X - Z \sigma_x$$

$$Z = \Phi^{-1}(P) = -0.25$$

Φ = Standard Normal Distribution Function

P = Required Probability (0.4)

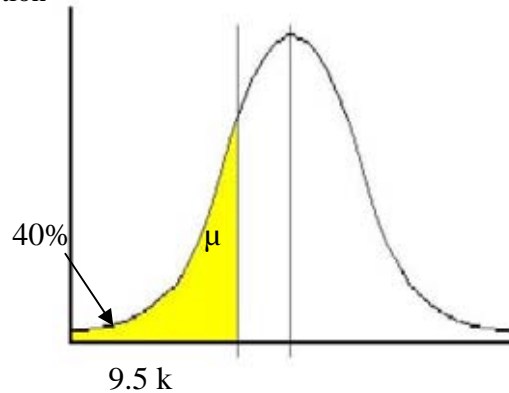
μ_x = Required Sample Mean

σ_x = Sample Standard Deviation

X = 40% Probability Force \geq 9.5 kips

$$\sigma_x = \begin{cases} 2.8 \text{ kips (Douglas Fir)} \\ 6.5 \text{ kips (Ponderosa Pine)} \\ 4.0 \text{ kips (Southern Yellow Pine)} \end{cases}$$

$$\mu_x = \begin{cases} 10.2 \text{ kips (Douglas Fir)} \\ 11.2 \text{ kips (Ponderosa Pine)} \\ 10.6 \text{ kips (Southern Yellow Pine)} \end{cases}$$



This required mean peak force was then used to calculate a required diameter of the posts based on the average dynamic modulus of rupture (MOR) values for each species. The equations used for the calculations are presented below followed by the results which are summarized in Table 25.

$$M = (L)(P)$$

L = Impact Height

μ_x = Impact Force

σ_x = MOR

$$d = \sqrt[3]{\frac{32 M}{\pi \sigma_x}}$$

Table 25. Probability Method Calculation Summary

	L		μ_x		σ_x		M		d	
	mm	(in.)	kN	(kips)	MPa	(kips/in. ²)	kN-m	(kip-in.)	mm	(in.)
Douglas Fir	632	24.875	45.4	10.2	59.3	8.6	28.7	253.7	170	6.69
Ponderosa Pine	632	24.875	49.8	11.2	49.0	7.1	31.5	278.6	187	7.36
Southern Yellow Pine	632	24.875	47.2	10.6	61.4	8.9	29.8	263.7	170	6.71

According to the probability method, 60 percent of 169.9-mm (6.69-in.) diameter Douglas Fir, 186.9-mm (7.36-in.) diameter Ponderosa Pine, and 170.4-mm (6.71-in.) diameter Southern Yellow Pine posts should reach or exceed 42 kN (9.5 kips) when impacted at 632 mm (24.875 in.) in a cantilever sleeve. This being stated, it should also be noted that the method used to determine these values has several limitations. First, the sample only included 15 posts, a very small sample considering the variability of wood. Second, the properties from the three categories were not weighted, but rather lumped together equally without consideration of their respective representation in the total post population. This meant that the mean determined from the testing may not have been an accurate representation of the total population. Third, lumping the data together also made it difficult to say how grading criteria affect the results.

6.2 Static Method

The second method used in determining post size was based on the results of the 40 static tests. This method began with the preliminary assumption that a 184-mm (7.25-in.) diameter Southern Yellow Pine (SYP) post was more than sufficiently strong for use in the W-beam guardrail system. This fact was based on successful full-scale crash tests conducted at TTI where 178-mm (7.0-in.) diameter and 184-mm (7.25-in.) diameter SYP posts were used in two barrier systems which met the NCHRP Report No. 230 and NCHRP Report No. 350 requirements, respectively [32-34].

An alternate species was believed to have sufficient capacity if its static strength was found to be equal to that of a 178-mm (7.0-in.) diameter SYP post. The smaller diameter was selected because it passed the test. The 15 static SYP tests were used to generate a criteria for comparison. The 5th percentile, SYP capacity was found to be 24 kN (5.4 kips) based on a 5th percentile overall MOR of 27.5 MPa (3.993 ksi) and the 178 mm (7.0-in.) diameter. The 5th

percentile value implied that 95 percent of 178 mm (7.0-in.) diameter SYP posts would reach a resisting force of 24 kN (5.4 kips) or higher. It should be noted that the 5th percentile was selected because it is commonly used in the timber industry. Although the results would differ, any percentile could have been chosen to complete the calculations.

The same standard was established for the other two species. In both Ponderosa Pine and Douglas Fir, 95 percent of the posts were required to reach or exceed a resisting force of 24 kN (5.4 kips). Using the 5th percentile MOR value determined for each of the two species, the diameter required to meet the force criteria was determined. Equations used in this method are provided below, followed by a summary of the calculations in Table 26.

$$M = (L)(P)$$

$$L = \text{Impact Height}$$

$$P = \text{SYP Impact Force (5.4 kips)}$$

$$\sigma_{\text{Static}} = \text{MOR}_{5\%}$$

$$d = \sqrt[3]{\frac{32 M}{\pi \sigma_{\text{Static}}}}$$

Table 26. Static Method Calculation Summary

	L		P		σ_b		M		d	
	mm	(in.)	kN	(kips)	Mpa	(kips/in. ²)	kN-m	(kip-in.)	mm	(in.)
Douglas Fir	631.83	24.875	24.0	5.4	38.0	55.516	15.2	134.3	160	6.28
Ponderosa Pine	631.83	24.875	24.0	5.4	24.1	3.497	15.2	134.3	186	7.31
Southern Yellow Pine	Not Applicable								184	7.25

The method suggests that 95 percent of the posts with a diameter of 160 mm (6.28 in.) for Douglas Fir or 186 mm (7.31 in.) for Ponderosa Pine will reach or exceed a static load of 24 kN (5.4 kips) at the 632 mm (24.875-in.) load height. As with the probability method, some limitations exist. Again, the properties for the three categories were lumped together with the same consequences as before. Although a normal distribution was assumed, the parameters used to develop the distribution may not have been thoroughly representative of the population.

6.3 Dynamic Method

The third and final calculation method combined parts of each of the previous calculation methods. In this method, the average MOR value, determined for the knots category for both species, was used to determine a diameter that would be capable of carrying a 44.5-kN (10-kip) applied load.

The increased load was determined from the results of tests NPGB 4, 9, and 10 as before, but was selected to be high enough to exceed the majority of the local peaks in the force data. Previously, the estimated soil force was based on a 20 percent increase from the average rather than the magnitudes of individual peaks.

Although the baseline posts showed the lowest MOR for both species, the knots category was selected as the critical category. This was done because it was believed that the baseline results were misleadingly low due to the relatively low ring density of the posts within the category. It was suspected that for a more similar average ring density, the MOR for the knots category would fall well below that for the baseline category. The equations used for the dynamic method are shown below, followed by a summary of the calculations in Table 27.

$$M = (L)(P)$$

$$L = \text{Impact Height}$$

$$P = \text{Impact Force}$$

$$\sigma_b = \text{MOR}_{\text{Dynamic Knots}}$$

$$d = \text{diameter}$$

$$d = \sqrt[3]{\frac{32 M}{\pi \sigma_b}}$$

Table 27. Dynamic Method Calculation Summary

	L		P		σ_b		M		d	
	mm	(in.)	kN	(kips)	MPa	(kips/in. ²)	kN-m	(kip-in.)	mm	(in.)
Douglas Fir	631.83	24.875	44.5	10	60.9	8.83	28.1	248.8	168	6.6
Ponderosa Pine	631.83	24.875	44.5	10	44.8	6.5	28.1	248.8	185	7.3
Southern Yellow Pine	631.83	24.875	44.5	10	48.3	7.01	28.1	248.8	180	7.1

The dynamic method was based on allowable stress design, unlike the other two methods that were founded on probability. This method concluded that the critical knots category, with an average diameter of 168 mm (6.6 in.) for Douglas Fir, 185 mm (7.3 in.) for Ponderosa Pine, and 180 mm (7.1 in.), will have an average dynamic capacity of 44.5 kN (10 kips) at 632 mm (24.875 in.). Again, the method has several drawbacks, the first of which is the unknown population strength distribution. The knots category may represent 90 percent of the population, in which case 45 percent of the posts would not reach the suggested capacity. In turn this would result in a 4.1 percent chance of failure in the full system due to four consecutive posts failing. On a similar note, the distribution of the other two categories was not considered. A portion of the posts in those categories may also fall below the required capacity, depending on the average and magnitude of the standard deviation within the category.

6.4 Post Size Conclusion and Summary

After considering the results from all three methods, a final size was determined for each of the wood species. Final suggested diameters were rounded up to the nearest quarter of an inch for manufacturing purposes. Similarities between the results of the three methods offered assurance that diameters determined using the probability method were reasonable and accurate. The sizes determined with each method and the suggested sizes are presented in Table 28 below. These suggested sizes should be used in a second round of cantilever testing to assure that the MOR does not vary with post diameter.

Table 28. Post Diameter Calculation Summary

Species	Suggested Diameter							
	Probability Method		Static Method		Dynamic Method		Suggested	
	mm	(in.)	mm	(in.)	mm	(in.)	mm	(in.)
Douglas Fir	170	6.69	160	6.28	168	6.60	171	6.75
Ponderosa Pine	187	7.36	186	7.31	185	7.30	191	7.50
Southern Yellow Pine	170	6.71	178	7.00	180	7.10	178	7.00

7 INERTIAL EFFECTS

7.1 Introduction

As stated previously in Section 6.2, the most important parameter of the bogie testing was the peak force generated by the post before fracture. If the peak post capacity exceeds the peak resisting force of the soil, the posts should be capable of rotating rather than fracturing. Preliminarily, this force was selected as the highest peak of the filtered force verses time plot, but after the data was processed, analyzed, and preliminary post sizes selected, questions arose with regard to its appropriateness.

A sample raw acceleration plot is presented in Figure 10. The bogie acceleration trace exhibits two large distinct and separate acceleration peaks. The question was, is wood capable of behaving like this plot suggests?

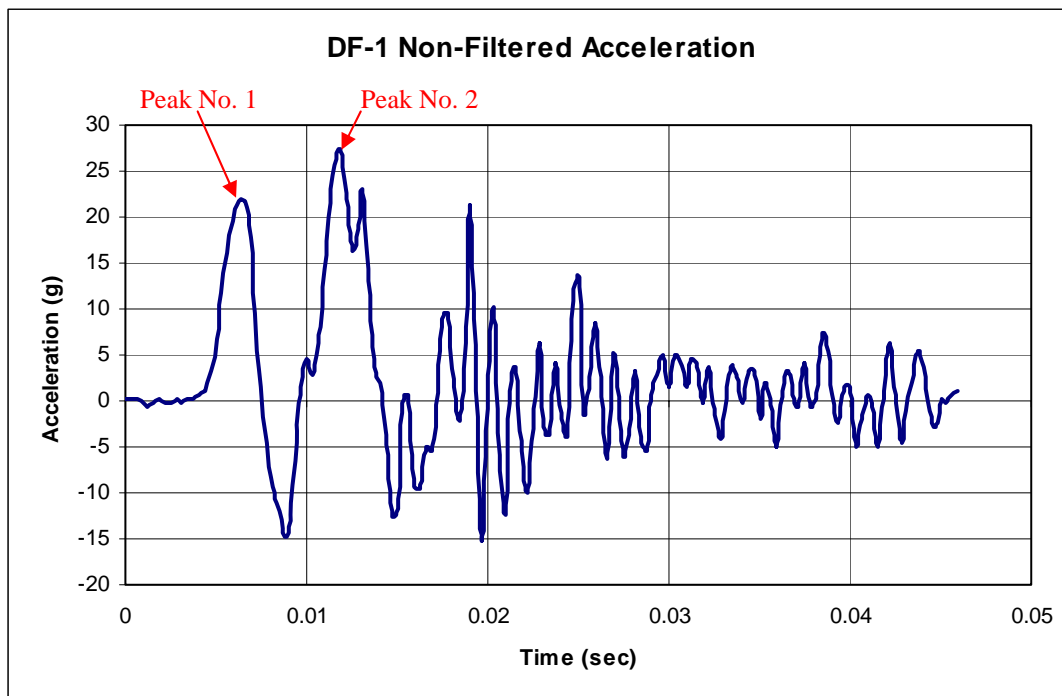


Figure 10. Bogie Test DF-1 Non-Filtered Acceleration

The data shown in Figure 10 suggested that the wood post reached a peak force, relaxed, and then reached a second peak force, sometimes higher and sometimes lower than the first. The cases in which the second peak was lower than the first suggests that the fibers reached some maximum stress value, relaxed, and then failed at some stress value lower than the maximum reached previously.

Another possible explanation of this behavior was a sequential failure in which the outer fibers fractured, allowing increased deflection in the post. As the post deflected farther, the layers failed sequentially at lower and lower peak force values. If this was indeed the case, a clear failure should have been evident as the peak force was reached. In this explanation, as a wood specimen begins to bend, tensile and compressive stresses develop in the wood fibers, with the maximum stress occurring at the extreme edges of the cross section. When the fibers within the wood reach their ultimate strength or stress, those fibers will fracture and carry no load at all. This behavior is much different than that observed in ductile materials, such as mild steel. As the fibers fracture, the effective cross section is reduced ring by ring, and the bending moment capacity gets smaller and smaller. This suggests that the posts should reach some peak force value, at which the outer fibers begin to fail, and then the force should drop off rapidly as the cross section shrinks. Such behavior cannot explain the phenomenon shown in Figure 10, especially if the first peak exceeded the second.

Although the second explanation is a clear possibility, typical wood behavior suggested a much different performance than the first explanation. Wood typically behaves in a very brittle manner, with a near linear stress-strain relationship. This means that the stress in the wood fibers should increase until failure at their ultimate stress. If the applied stress never exceeds the ultimate capacity of the wood, the fibers should not break. If the applied stress was removed and

reapplied, the stress in the fibers should decrease, and then increase until the failure stress or the maximum applied stress was reached. They should never fail at a stress below that already reached since it in turn must have been below the ultimate strength if the fibers did not fracture.

7.2 Fracture Time Investigation

To investigate this phenomenon further, the high-speed digital video footage from the post bogie tests was studied. The videos were used to identify the point at which the outer fibers in the posts clearly failed. In many tests, this failure point was very apparent and took place between two consecutive frames. For those tests, the numbers of the two consecutive frames were recorded along with the number of the impact frame or the frame in which the bogie first contacted the post. Examples of all three frames are shown in Figures 11, 12, and 13 for a post with the critical region painted white to show the fracture very clearly. Figure 11 depicts the frame at impact, Figure 12 shows the frame prior to post fracture, and Figure 13 shows the frame immediately after post fracture.

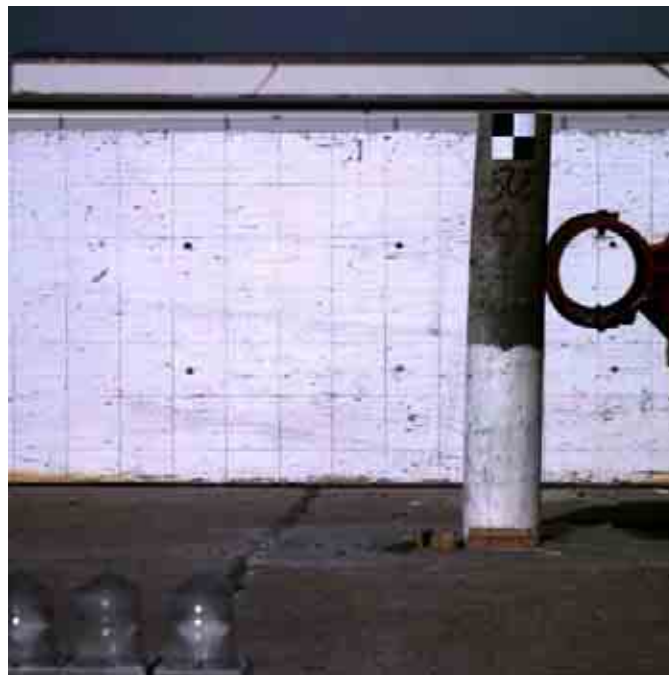


Figure 11. Bogie-Post Impact – Frame 102



Figure 12. Post Bending Prior to Fracture - Frame 107

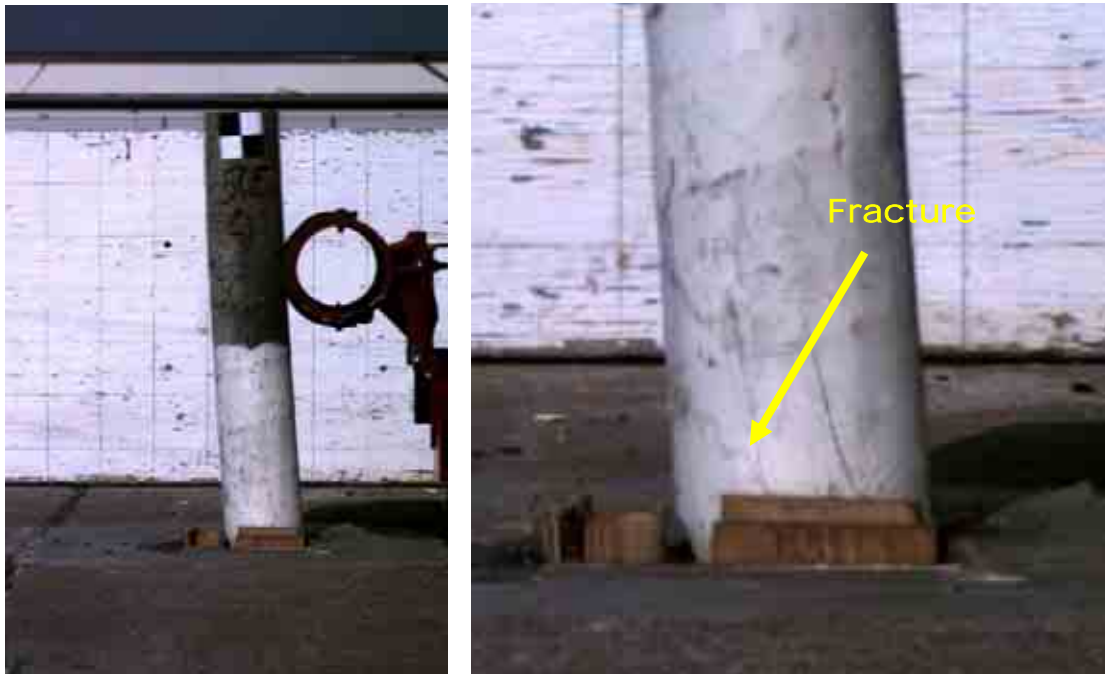


Figure 13. Post After Fracture - Frame 108

The frame numbers from the three figures were also used to calculate the time between them. For instance, since the camera recorded at a rate of 500 frames per second, the time

between consecutive frames is approximately 0.002 seconds. For test no. DF-1, the three frame nos. were 144, 147, and 148. Therefore, the time between impact and frame no. 147 was 0.006 seconds and the time between frame nos. 147 and 148 was 0.002 seconds. Plotting these times on the longitudinal acceleration plots, with the first rise in acceleration considered as the impact, will show where the fractures occurred relative to the acceleration peaks. A plot of this comparison for test no. DF-1 is shown in Figure 14.

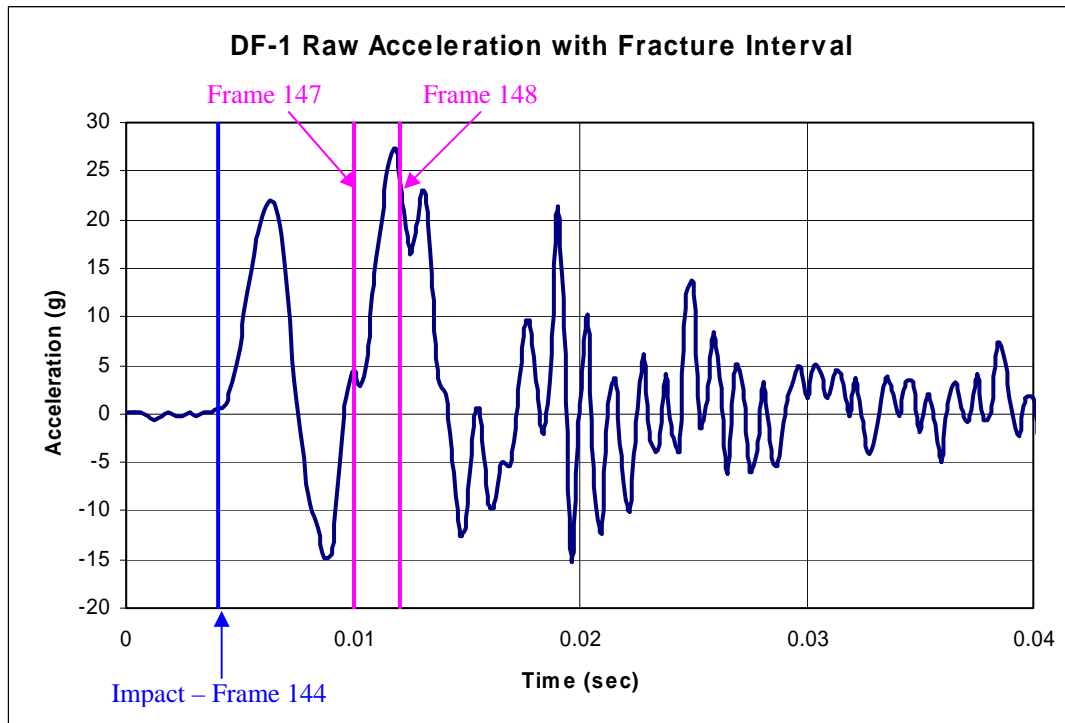


Figure 14. DF-1 Raw Acceleration with Fracture Interval

Similar plots are shown below in Figures 15 through 39 for the remainder of the round one post tests in which a visible fracture was present. Impact is not labeled on these plots, but is always taken as the first rise in acceleration, similar to the plot of test no. DF-1. Plots containing more than two frame lines displayed more than one distinct fracture with a fracture occurring between each pair of lines.

Before considering the plots in detail, attention should be drawn to two inaccuracies that may affect the analysis. The first was the inaccuracy in determining the impact time. Although the frame selected as the impact frame was the first frame showing contact between the post and the bogie, it did not mean that the time associated with that frame was the time of the first contact. In fact, the initial impact could have occurred up to 0.002 seconds prior to that frame. This meant that the fracture window could shift up to 0.002 seconds to the right, in some cases shifting to encompass the maximum acceleration peak. This is shown by the additional shading in Figure 18. The second inaccuracy was the visibility of the fracture. As stated, several tests did not exhibit a visible fracture. Hence, the first fracture may not have been visible initially, and the broken fibers only became visible after the second or third fracture event. This may explain some cases such as that of Figures 20, 23, 25, 29, 33, 38, and 39 in which the fracture interval as shown did not make sense even including a 0.002 second shift.

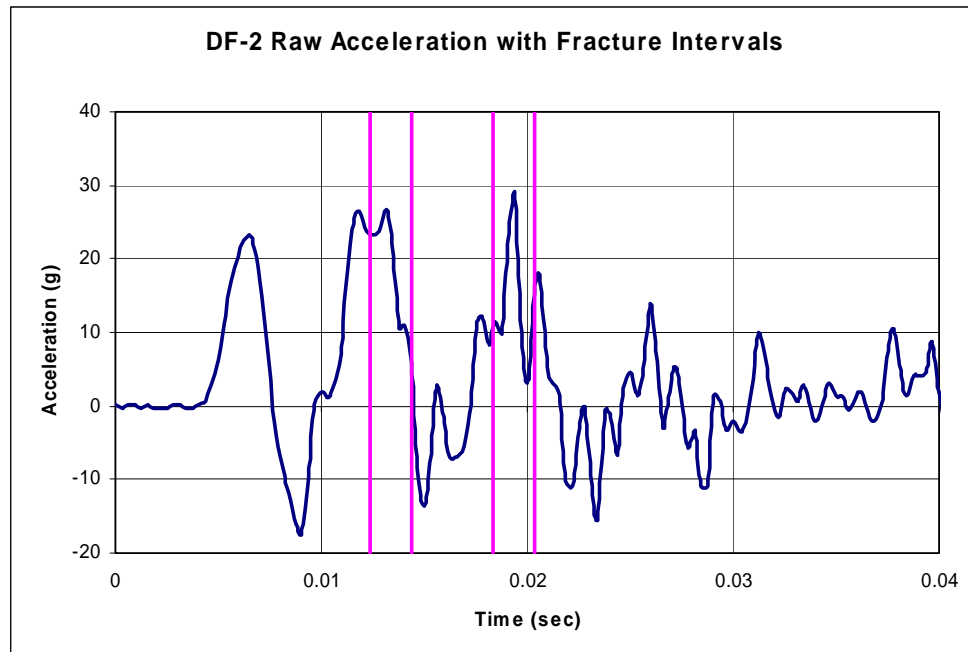


Figure 15. DF-2 Raw Acceleration with Fracture Intervals

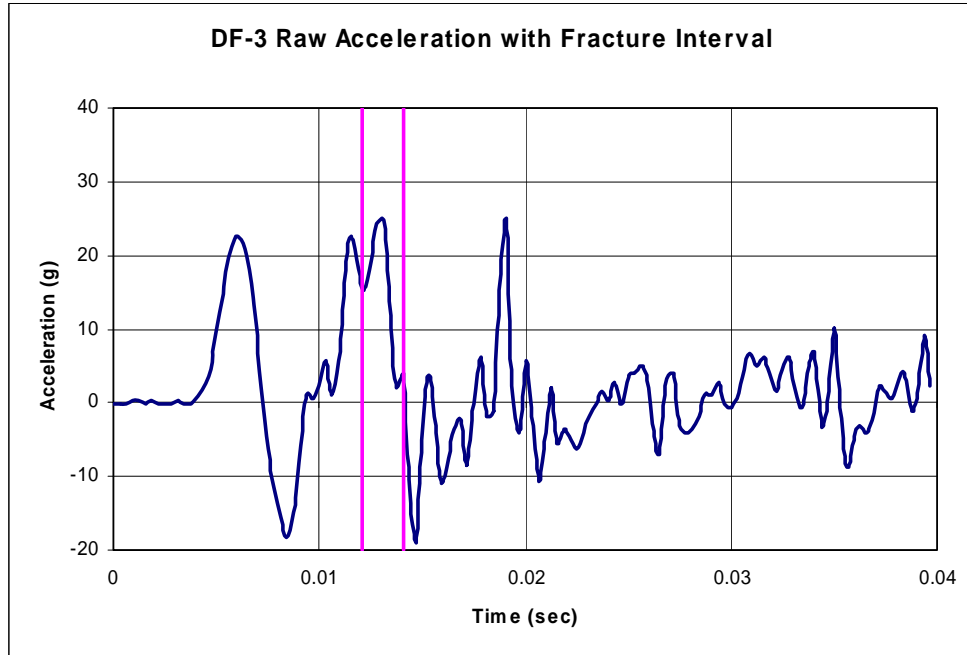


Figure 16. DF-3 Raw Acceleration with Fracture Interval

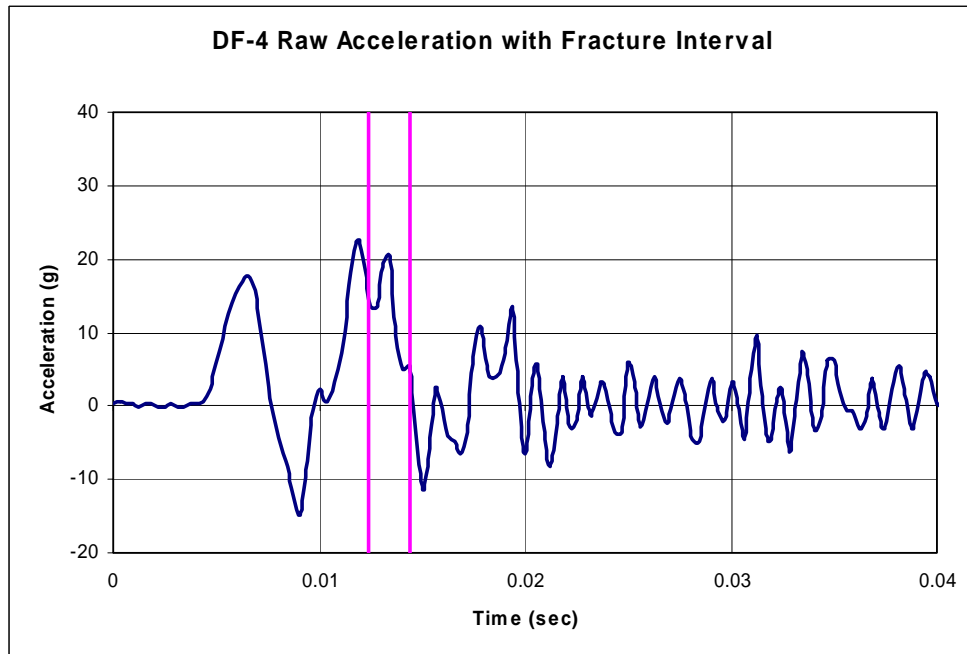


Figure 17. DF-4 Raw Acceleration with Fracture Interval

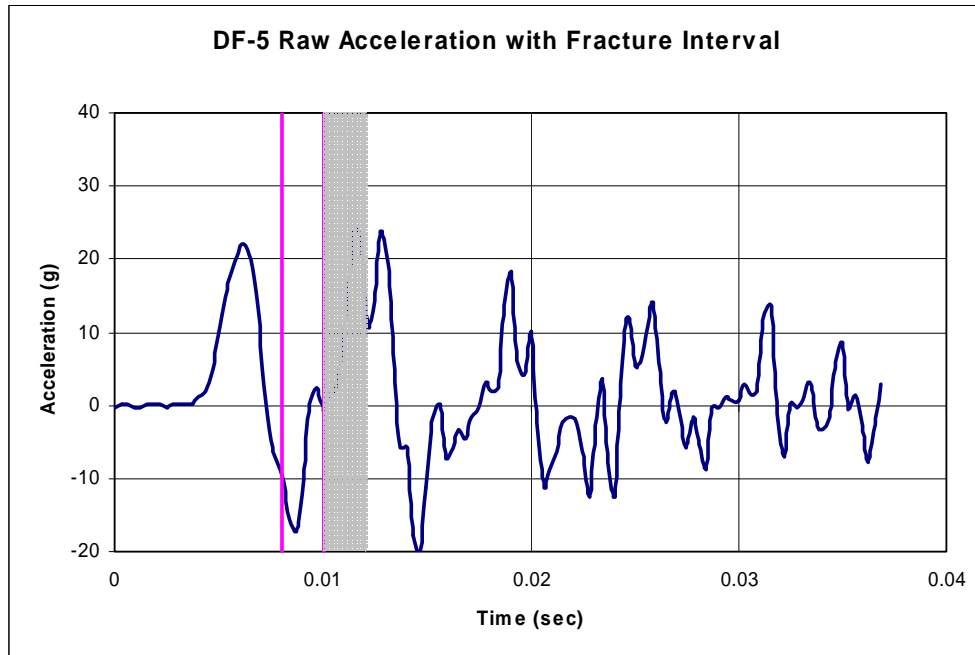


Figure 18. DF-5 Raw Acceleration with Fracture Interval

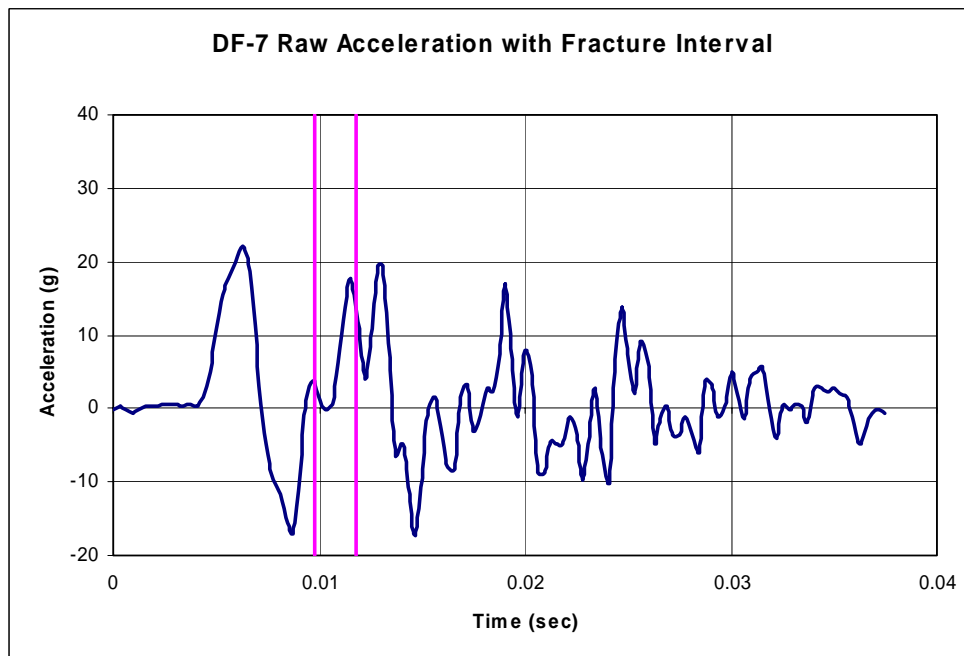


Figure 19. DF-7 Raw Acceleration with Fracture Interval

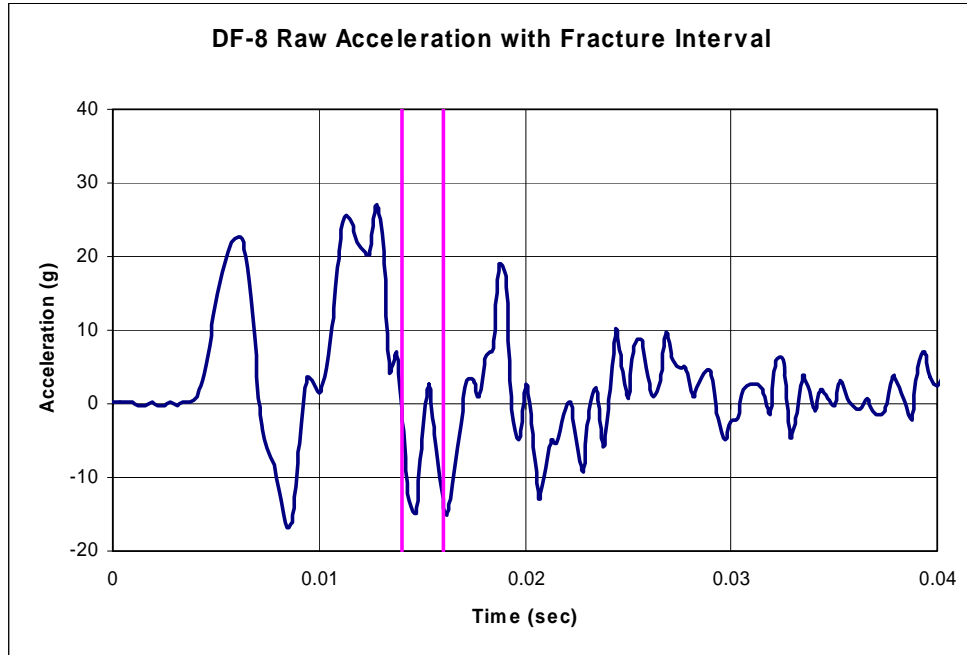


Figure 20. DF-8 Raw Acceleration with Fracture Interval

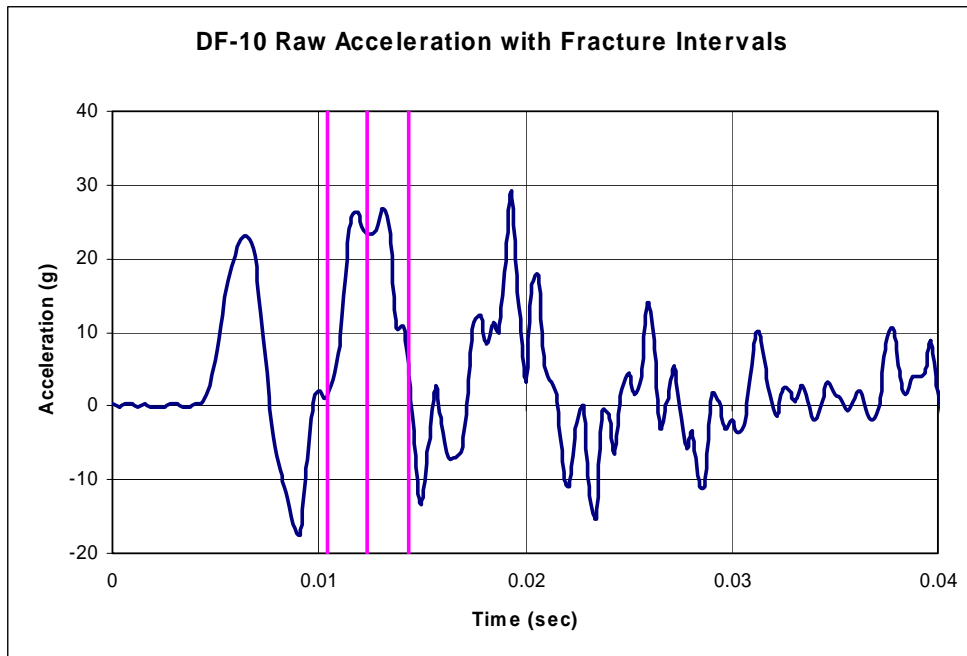


Figure 21. DF-10 Raw Acceleration with Fracture Intervals

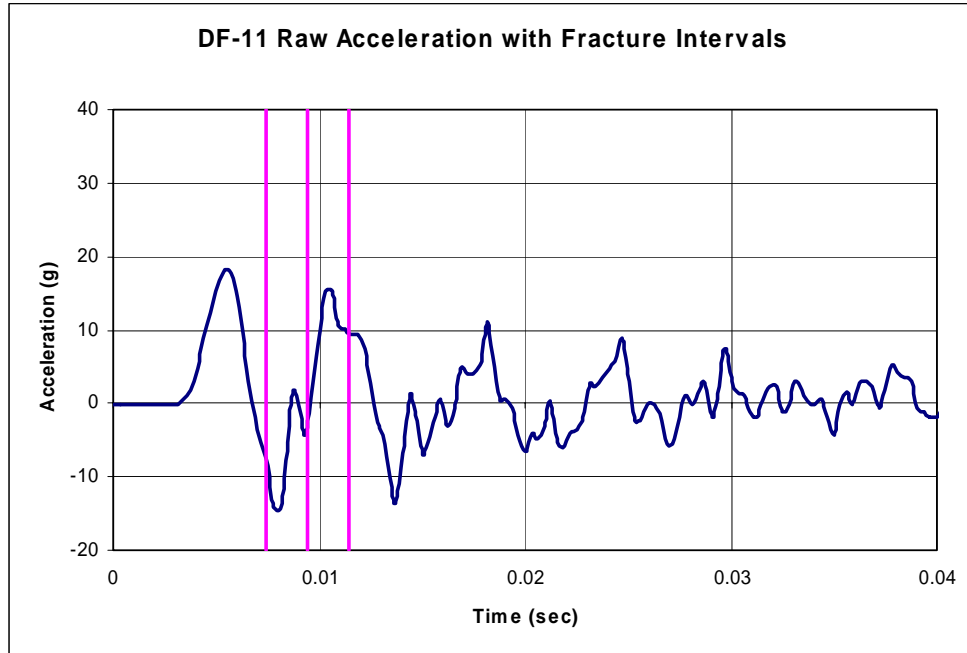


Figure 22. DF-11 Raw Acceleration with Fracture Intervals

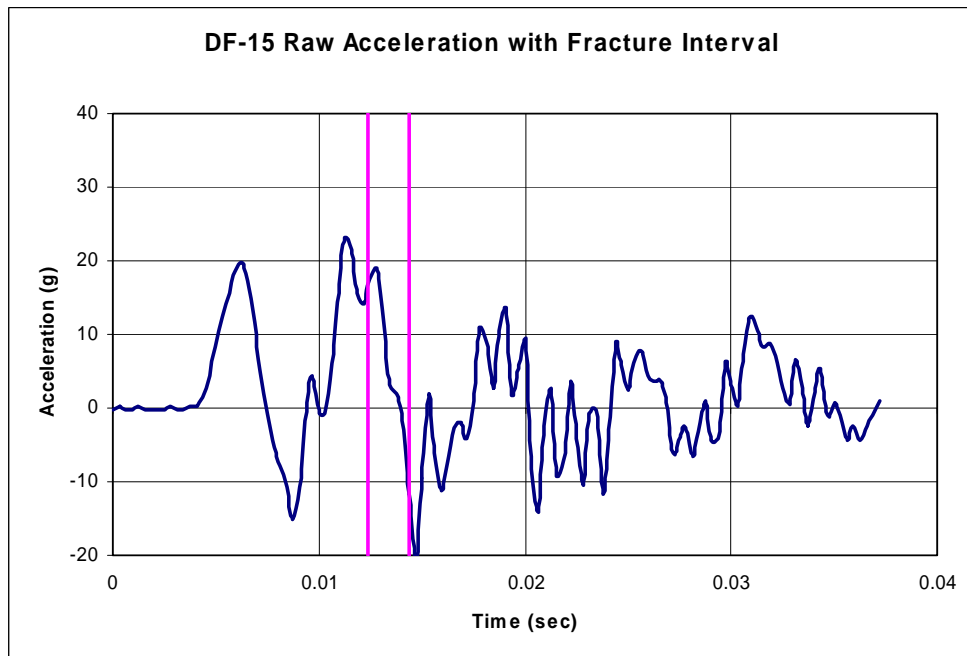


Figure 23. DF-15 Raw Acceleration with Fracture Interval

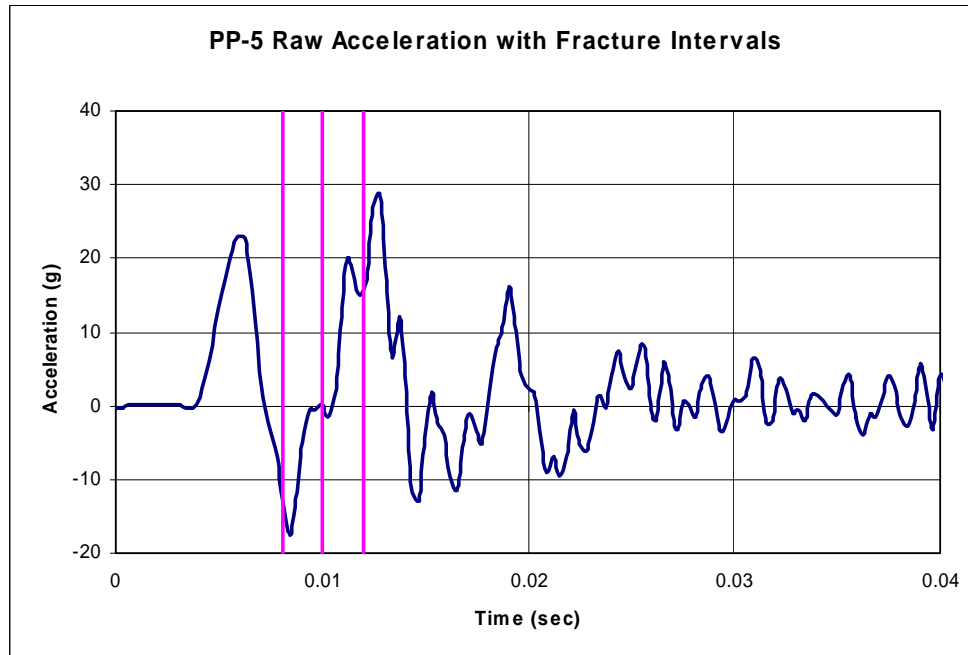


Figure 24. PP-5 Raw Acceleration with Fracture Intervals

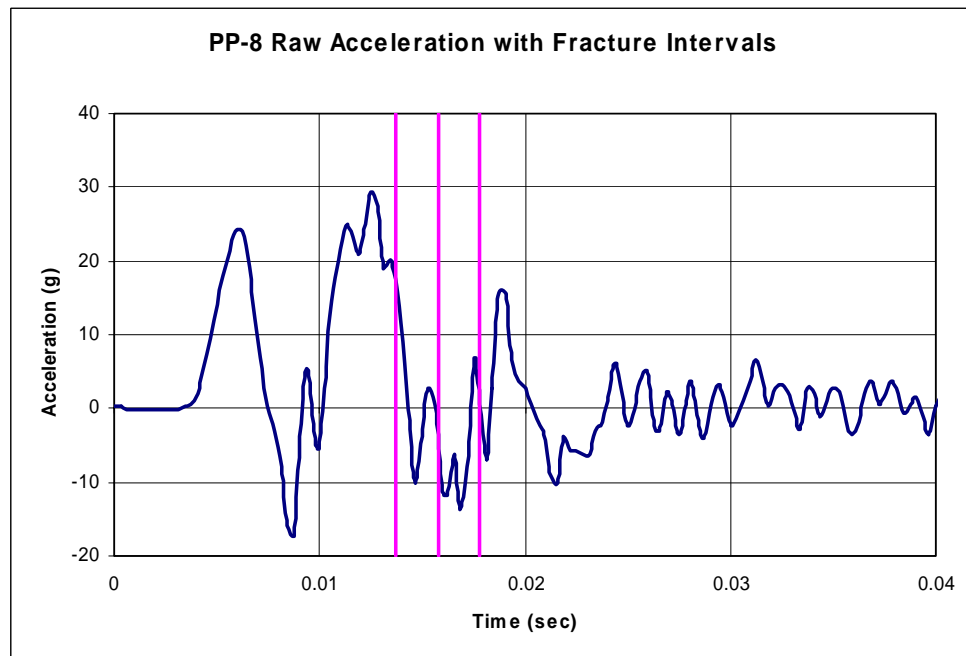


Figure 25. PP-8 Raw Acceleration with Fracture Intervals

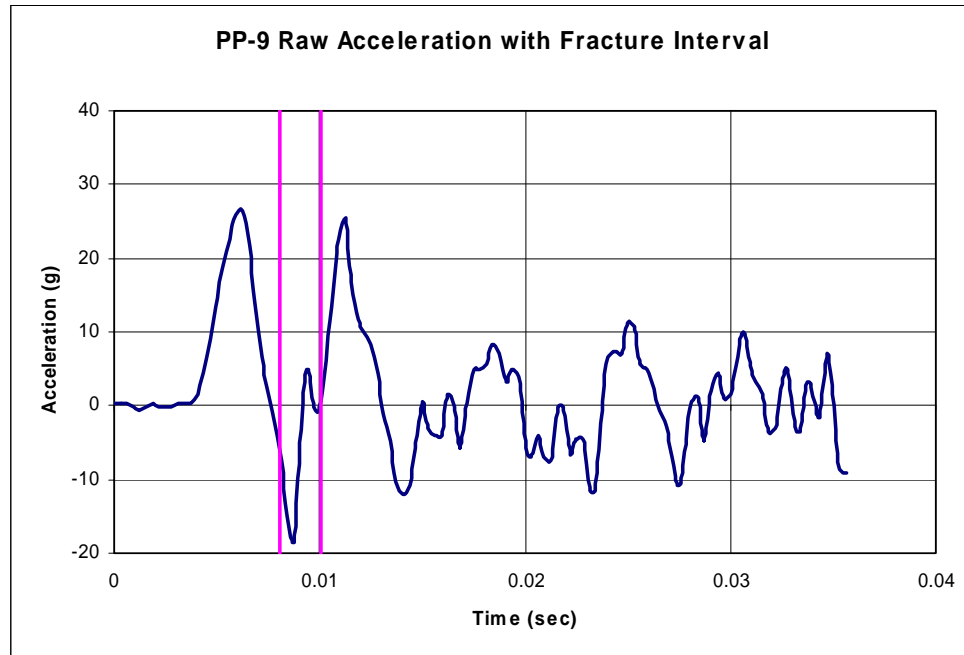


Figure 26. PP-9 Raw Acceleration with Fracture Interval

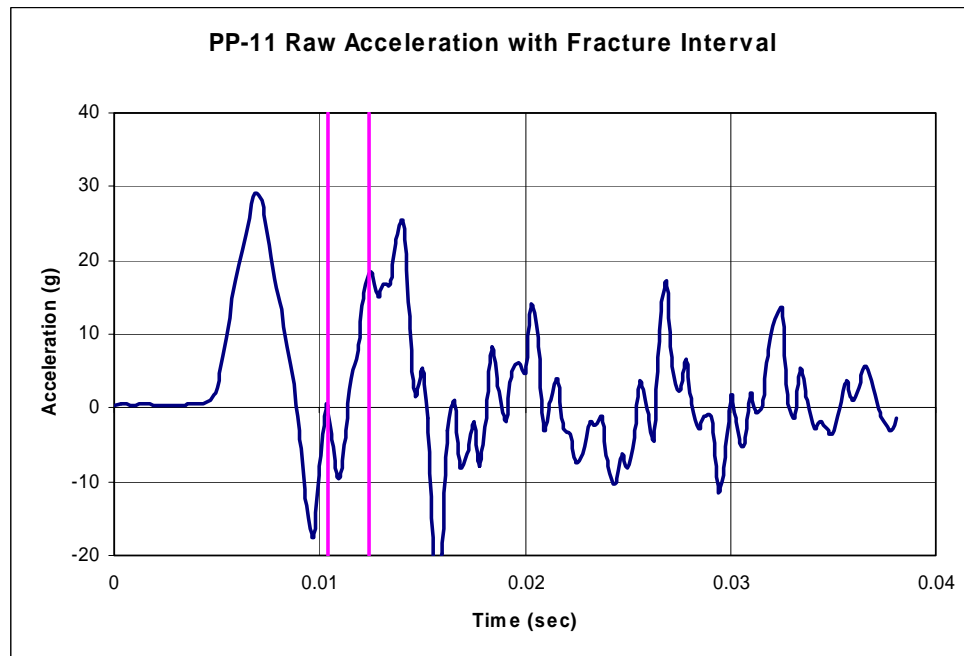


Figure 27. PP-11 Raw Acceleration with Fracture Interval

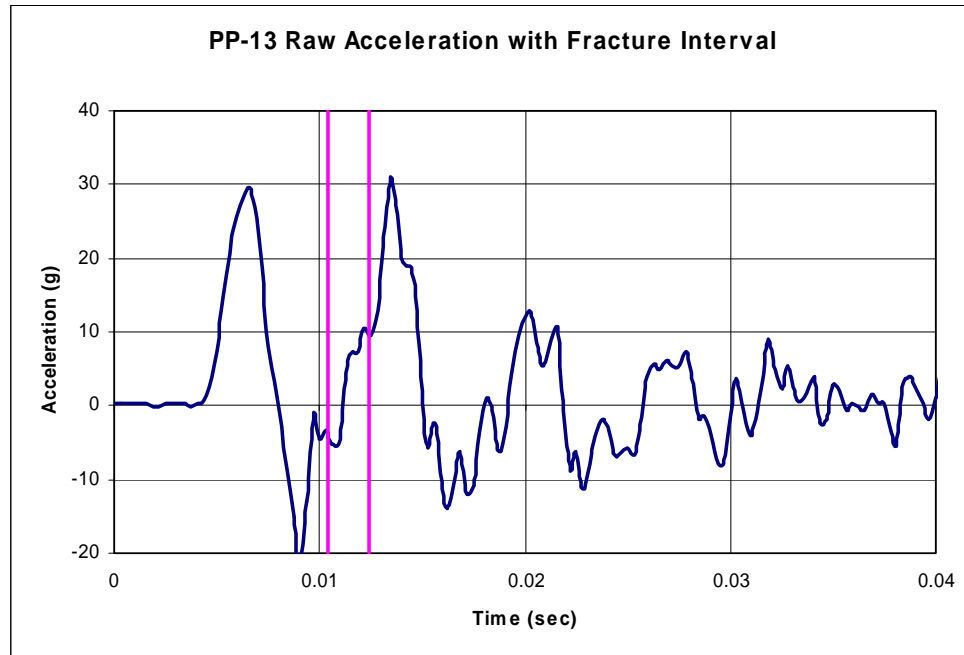


Figure 28. PP-13 Raw Acceleration with Fracture Interval

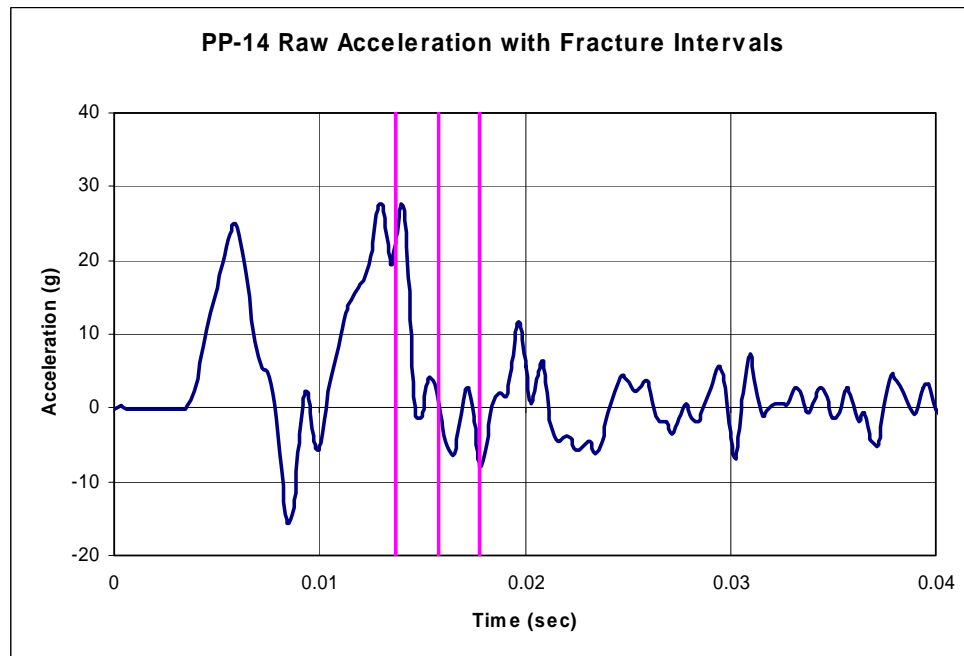


Figure 29. PP-14 Raw Acceleration with Fracture Intervals

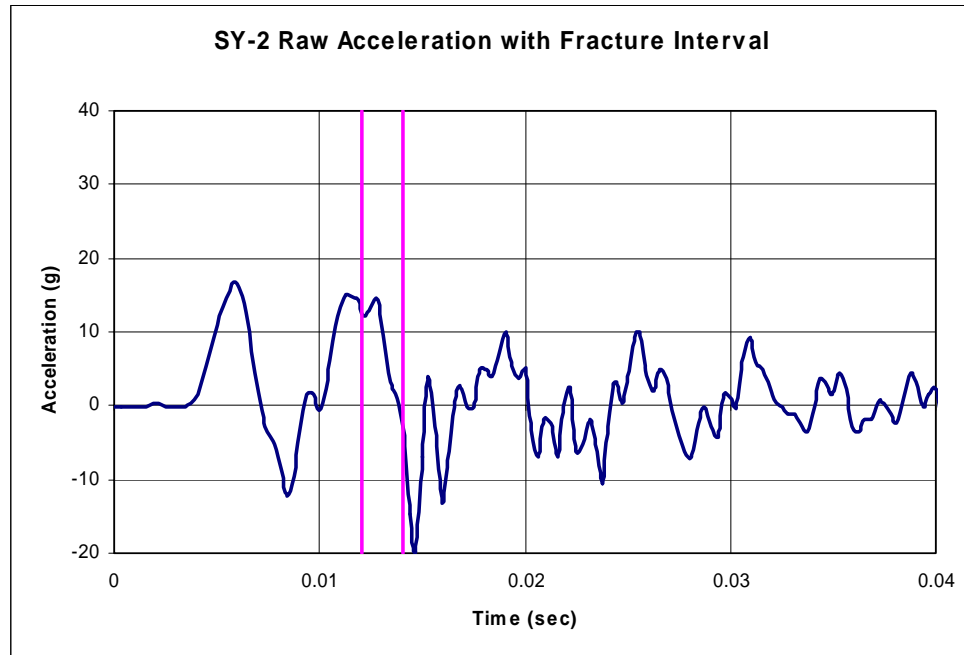


Figure 30. SY-2 Raw Acceleration with Fracture Interval

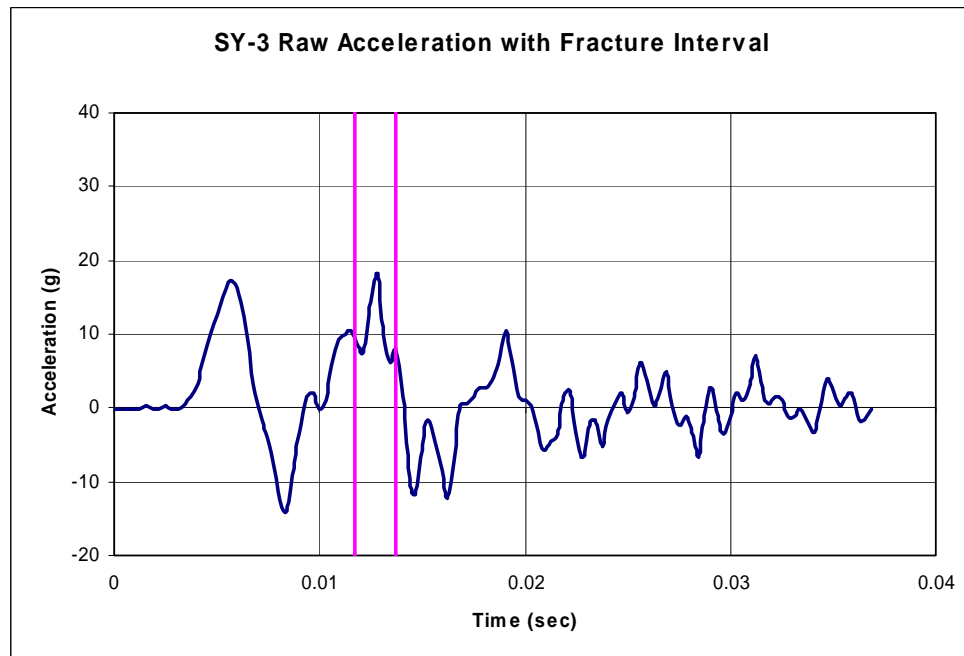


Figure 31. SY-3 Raw Acceleration with Fracture Interval

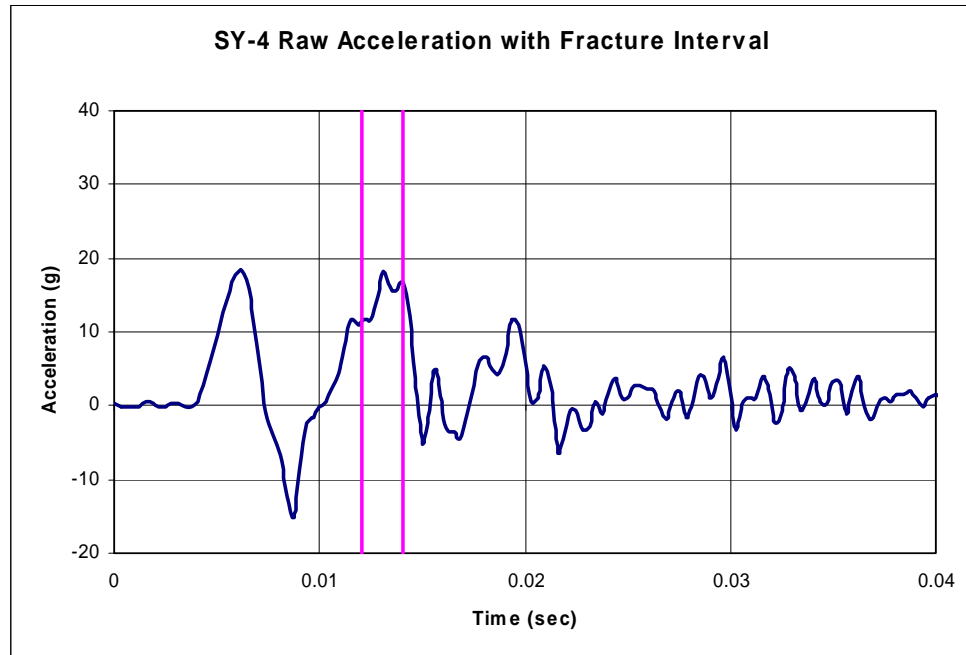


Figure 32. SY-4 Raw Acceleration with Fracture Interval

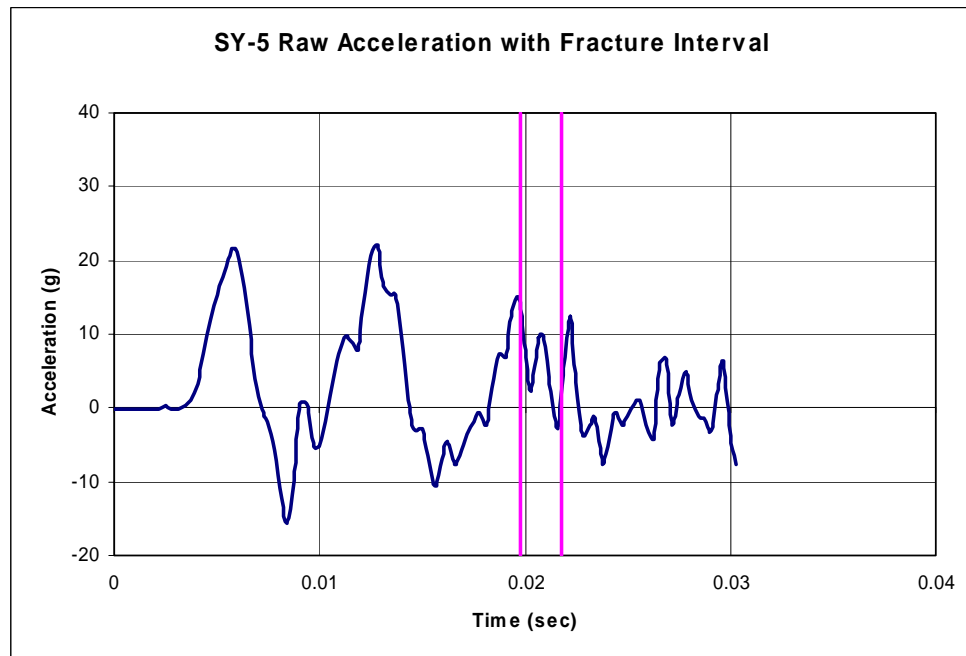


Figure 33. SY-5 Raw Acceleration with Fracture Interval

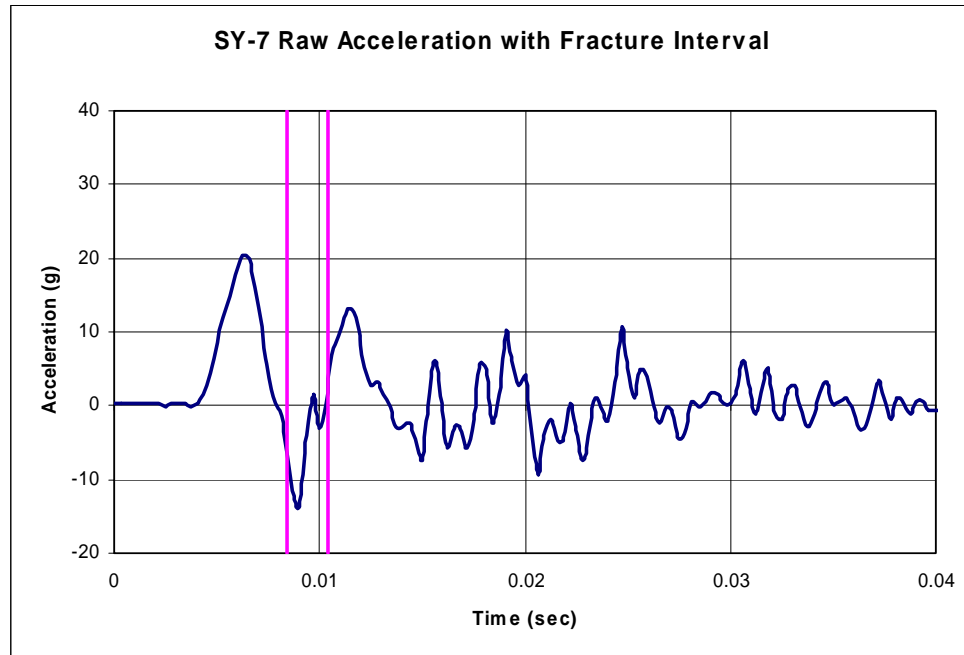


Figure 34. SY-7 Raw Acceleration with Fracture Interval

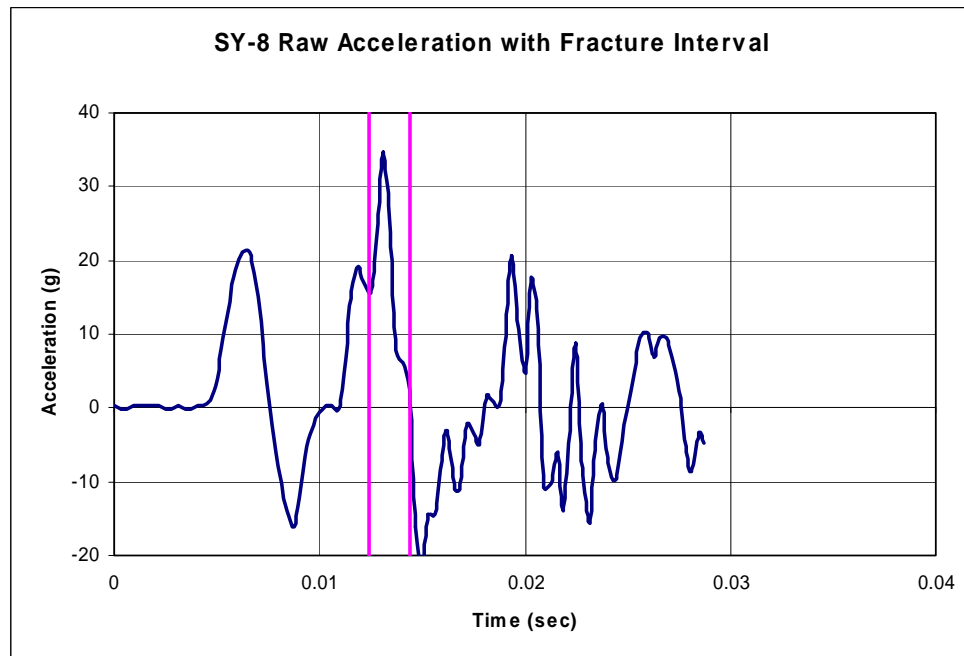


Figure 35. SY-8 Raw Acceleration with Fracture Interval

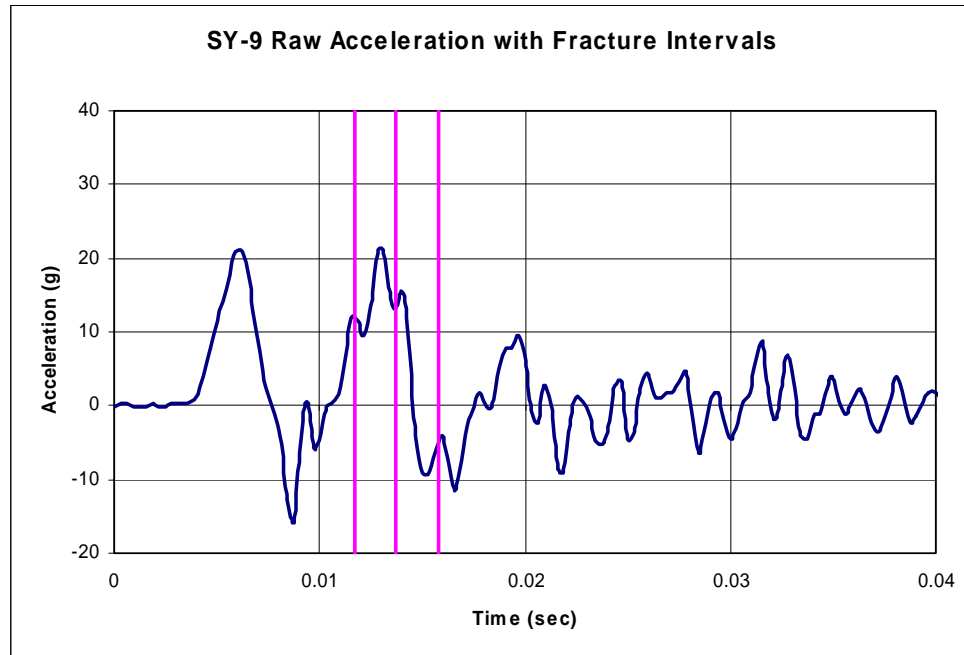


Figure 36. SY-9 Raw Acceleration with Fracture Intervals

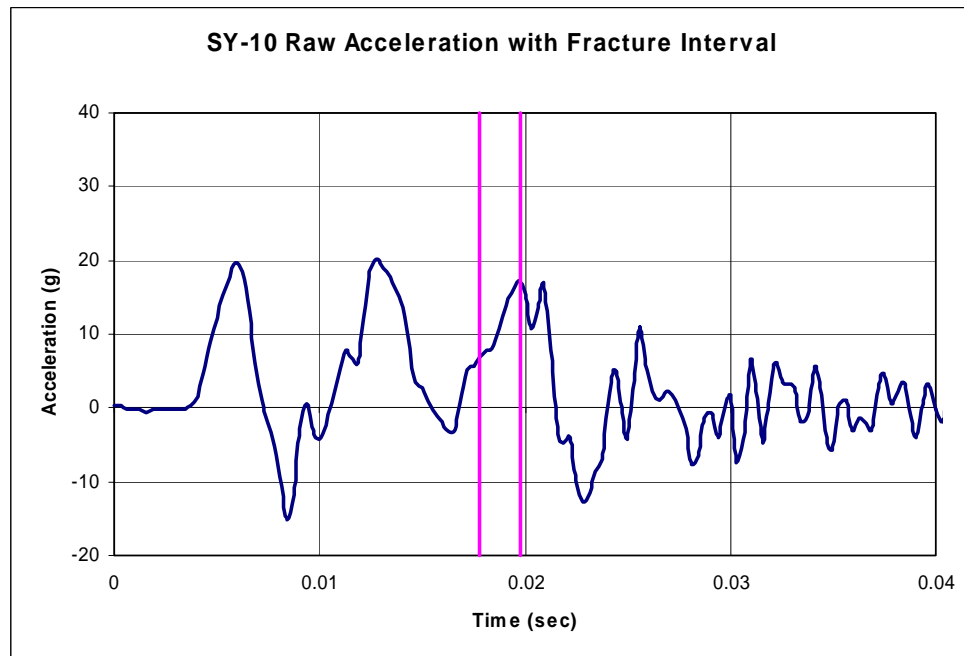


Figure 37. SY-10 Raw Acceleration with Fracture Interval

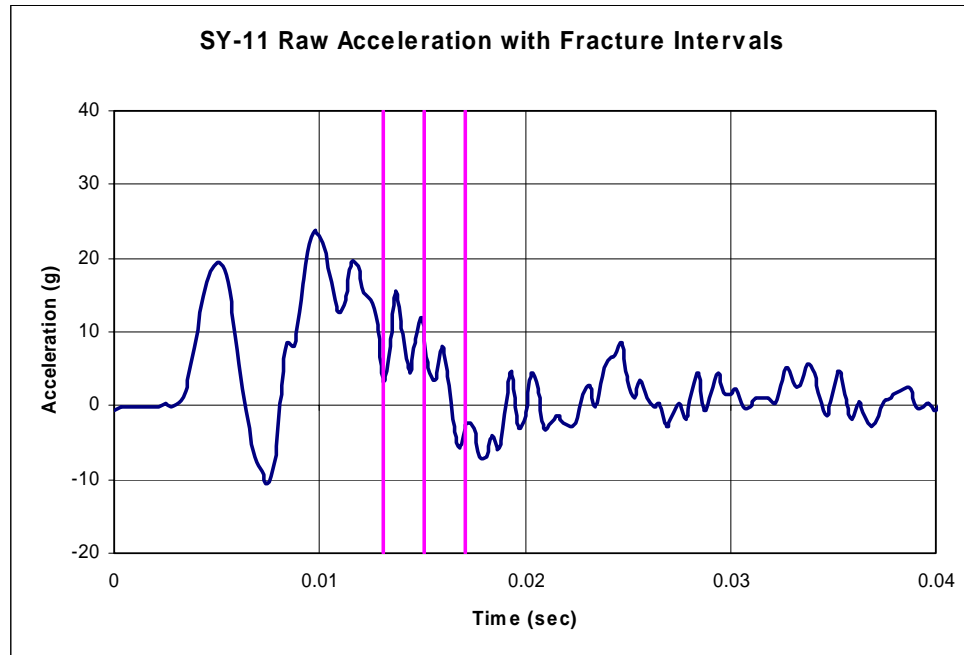


Figure 38. SY-11 Raw Acceleration with Fracture Intervals

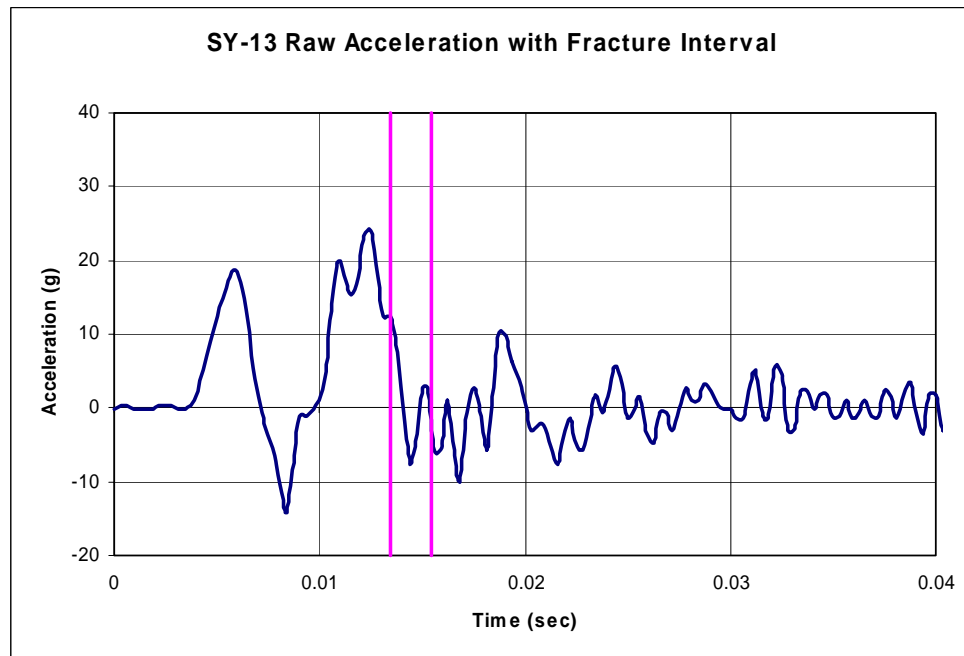


Figure 39. SY-13 Raw Acceleration with Fracture Interval

If the initial peak force was the maximum, and the post was indeed bending during that time, it should have failed during that spike rather than at a subsequent lower spike. However, none of the tests exhibited this behavior. This will be discussed in Section 7.3.

7.3 Possible Explanation – The Inertial Spike Theory

After learning that all of the posts failed at some time after the initial peak force, concern was raised that the initial acceleration spike may not have been caused by the bending of the post, but rather by the impulse of the impact.

7.3.1 Explanation and Physical Description

When completing the bogie tests with the posts inserted in a fixed sleeve, some compliance must have existed between the post and the sleeve. This compliance occurred as a result of the shimming methods used to more rigidly fix the post in the foundation as well as from the variability in the cross section and straightness of the post. If the posts were perfect cylinders, the compliance in the system might have been negligible. However, when using wood posts, it was not possible to shim the post so every inch of its length was rigidly fixed.

Assuming this compliance exists, it would allow some, initial, free rotation and translation of the post as it was impacted by the bogie. Since the post was at rest, some initial force would be required to cause this motion, and the impulse of such a force should be equal to the change in momentum of the post, or its total momentum since the post began at rest.

If, during this initial rotation and translation, the posts were not bending, but rather just moving, the wood fibers in the posts would not be under any significant stress. In this case, the entire initial impulse force from the bogie was causing the post to move but not bend. Therefore, the initial impulse magnitude would have no meaning in relation to the shear bending strength of the posts.

7.3.2 Impulse and Analysis

The first pieces of supporting evidence were the acceleration trace vs. fracture time plots, which strongly supported the inertial spike theory. As shown in the plots, none of the failures occurred during the initial acceleration spike. Rather, the failures generally took place at a global or local peak sometime after the initial spike.

The next piece of supporting evidence was a simple impulse-momentum calculation. If the first spike was indeed caused by the inertia of the post, the impulse from the spike should have been equal to the change in momentum of the post. To investigate this comparison, the angular momentum of each post was calculated, converted to linear momentum, and compared to the impulse of the initial force spike from the acceleration trace. The momentum calculations were made assuming that: (1) each post rotated at the ground level with the impact height of each post moving at the initial velocity of the bogie head and (2) the mass of each post was distributed evenly throughout its length. The momentum calculation is shown below. The calculated values and the comparisons for each test are presented in Tables 29 through 31.

The momentum to impulse ratio clearly shows that the two values are very close for each test. The Douglas Fir tests appear to be the most different, with the change in momentum averaging 83 percent of the impulse. For the Ponderosa Pine and Southern Yellow Pine species, the average difference is much smaller. Change in momentum averaged 107 percent of the impulse for Ponderosa Pine, and 100 percent for the Southern Yellow Pine. The similarity of the results strongly supports the inertial spike theory.

$$\omega = \frac{V}{H_I}$$

V = Initial Bogie Velocity

H_I = Impact Height

ω = Angular Velocity

* Note that the post was divided in two for simplicity.

$$I_{Cylinder} = \frac{mr^2}{4} + \frac{mL^2}{3}$$

$I_{Cylinder}$ = Moment of inertia of a solid cylinder about one end

$$I_{Total} = I_1 + I_2$$

I_1 = Moment of inertia of the above ground portion

I_2 = Moment of inertia of the below ground portion

L = Length of the upper or lower portions of the post

r = Radius of the post

$$m_1 = \left(\frac{W}{32.174 \frac{ft}{s^2}} \right) \left(\frac{L_T - 40 in.}{L_T} \right)$$

$$m_2 = \left(\frac{W}{32.174 \frac{ft}{s^2}} \right) \left(\frac{40 in.}{L_T} \right)$$

W = Weight of the post

L_T = Total length of the post

$$H_G = I_{Total} \omega$$

H_G = Angular momentum of the post

$$M = \frac{H_G}{H_I}$$

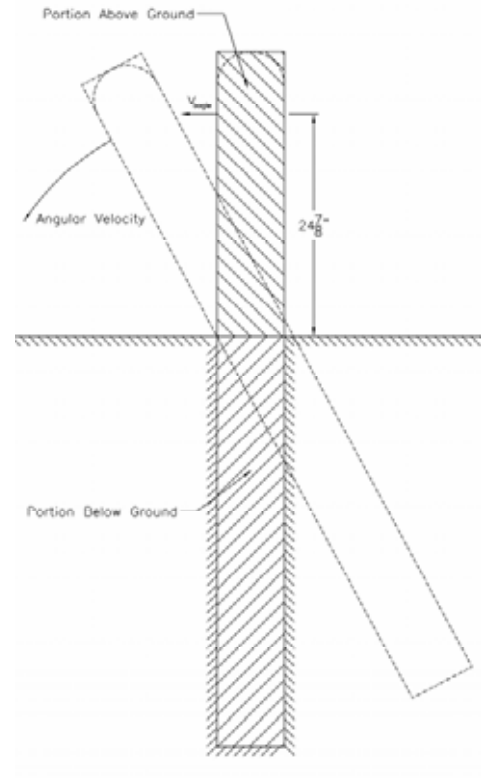
M = Linear Momentum

$$I = \int F dt$$

F = Bogie force

I = Impulse

$$I = \Delta M = M_{Final} - M_{Initial} = M_{Final} = M$$



*Velocity of the post at MGS height just after impact was assumed to be equal to the initial velocity of the bogie. This assumption was supported by: (1) film analysis that showed no separation between the post and the impact head, and (2) no significant amount of bogie velocity reduction during the initial portion of the impact.

Table 29. Douglas Fir Impulse-Momentum Comparison

Test No.	Angular Momentum (H _G)		Linear Momentum (M)		*Impulse (I)		Ratio	Ratio
	J-s	(ft-lbs-sec)	N-sec	(lb-sec)	N-s	(lb-sec)	I / M	M / I
DF-1	166.11	(122.52)	262.90	(59.10)	289.45	(65.07)	1.10	0.91
DF-2	164.28	(121.17)	260.00	(58.45)	315.20	(70.86)	1.21	0.82
DF-3	135.86	(100.20)	215.02	(48.34)	285.30	(64.14)	1.33	0.75
DF-4	130.09	(95.95)	205.89	(46.29)	245.37	(55.16)	1.19	0.84
DF-5	145.72	(107.48)	230.62	(51.85)	288.07	(64.76)	1.25	0.80
DF-6	163.57	(120.64)	258.87	(58.20)	299.55	(67.34)	1.16	0.86
DF-7	153.41	(113.15)	242.79	(54.58)	277.71	(62.43)	1.14	0.87
DF-8	167.38	(123.45)	264.91	(59.55)	306.70	(68.95)	1.16	0.86
DF-9	149.39	(110.19)	236.43	(53.15)	281.27	(63.23)	1.19	0.84
DF-10	159.76	(117.83)	252.84	(56.84)	316.76	(71.21)	1.25	0.80
DF-11	131.68	(97.12)	208.40	(46.85)	240.61	(54.09)	1.15	0.87
DF-12	131.71	(97.14)	208.44	(46.86)	282.77	(63.57)	1.36	0.74
DF-13	163.20	(120.37)	258.28	(58.06)	323.82	(72.80)	1.25	0.80
DF-14	143.99	(106.20)	227.89	(51.23)	278.46	(62.60)	1.22	0.82
DF-15	138.10	(101.86)	218.56	(49.13)	254.83	(57.29)	1.17	0.86
Average	149.62	(110.35)	236.79	(53.23)	285.72	(64.23)	1.21	0.83

*Calculation based on $\int Fdt$.

Table 30. Ponderosa Pine Impulse-Momentum Comparison

Test No.	Angular Momentum (H _G)		Linear Momentum (M)		*Impulse (I)		Ratio	Ratio
	J-s	(ft-lbs-sec)	N-sec	(lb-sec)	N-s	(lb-sec)	I / M	M / I
PP-1	247.02	(182.19)	390.94	(87.89)	325.64	(73.21)	0.83	1.20
PP-2	276.11	(203.65)	436.99	(98.24)	369.11	(82.98)	0.84	1.18
PP-3	281.85	(207.88)	446.08	(100.28)	432.56	(97.24)	0.97	1.03
PP-4	215.32	(158.81)	340.77	(76.61)	353.78	(79.53)	1.04	0.96
PP-5	194.30	(143.31)	307.51	(69.13)	306.66	(68.94)	1.00	1.00
PP-6	268.92	(198.34)	425.60	(95.68)	465.33	(104.61)	1.09	0.91
PP-7	281.15	(207.37)	444.97	(100.03)	425.69	(95.70)	0.96	1.05
PP-8	224.17	(165.34)	354.79	(79.76)	348.19	(78.28)	0.98	1.02
PP-9	247.21	(182.33)	391.25	(87.96)	374.23	(84.13)	0.96	1.05
PP-10	278.34	(205.29)	440.51	(99.03)	392.66	(88.27)	0.89	1.12
PP-11	331.15	(244.25)	524.10	(117.82)	472.98	(106.33)	0.90	1.11
PP-12	227.25	(167.61)	359.65	(80.85)	318.13	(71.52)	0.88	1.13
PP-13	290.09	(213.96)	459.12	(103.21)	417.85	(93.94)	0.91	1.10
PP-14	269.45	(198.73)	426.44	(95.87)	373.21	(83.90)	0.88	1.14
PP-15	233.09	(171.92)	368.90	(82.93)	380.34	(85.50)	1.03	0.97
Average	257.70	(190.07)	407.84	(91.69)	383.76	(86.27)	0.94	1.07

*Calculation based on $\int Fdt$.

Table 31. Southern Yellow Pine Impulse-Momentum Comparison

Test No.	Angular Momentum (H _G)		Linear Momentum (M)		*Impulse (I)		Ratio	Ratio
	J-s	(ft-lbs-sec)	N-sec	(lb-sec)	N-s	(lb-sec)	I / M	M / I
SY-1	174.43	(128.65)	276.06	(62.06)	307.01	(69.02)	1.11	0.90
SY-2	151.58	(111.80)	239.89	(53.93)	221.13	(49.71)	0.92	1.08
SY-3	170.06	(125.43)	269.15	(60.51)	238.29	(53.57)	0.89	1.13
SY-4	144.59	(106.64)	228.83	(51.44)	249.89	(56.18)	1.09	0.92
SY-5	181.68	(134.00)	287.54	(64.64)	294.00	(66.09)	1.02	0.98
SY-6	189.49	(139.76)	299.89	(67.42)	290.26	(65.25)	0.97	1.03
SY-7	183.62	(135.43)	290.60	(65.33)	293.53	(65.99)	1.01	0.99
SY-8	175.17	(129.20)	277.23	(62.32)	271.42	(61.02)	0.98	1.02
SY-9	186.69	(137.70)	295.47	(66.42)	300.33	(67.52)	1.02	0.98
SY-10	181.63	(133.96)	287.46	(64.62)	265.29	(59.64)	0.92	1.08
SY-11	172.62	(127.32)	273.20	(61.42)	259.56	(58.35)	0.95	1.05
SY-12	158.93	(117.22)	251.54	(56.55)	243.57	(54.76)	0.97	1.03
SY-13	139.40	(102.81)	220.62	(49.60)	246.49	(55.41)	1.12	0.90
SY-14	185.79	(137.03)	294.04	(66.10)	272.03	(61.15)	0.93	1.08
SY-15	169.66	(125.14)	268.52	(60.37)	307.06	(69.03)	1.14	0.87
Average	171.02	(126.14)	270.67	(60.85)	270.66	(60.85)	1.00	1.00

*Calculation based on JFdt.

The final piece of supporting evidence was a bogie test completed at MwRSF in December of 2004. The test was conducted in soil on a 1,778-mm (70-in.) long W152x23.8 (W6x16) steel post with a 1,016-mm (40-in.) embedment depth. For the test, the post was cut into two pieces at 102 mm (4 in.) above the ground line and re-connected with a hinge on the back side, as shown in Figure 40. This allowed the post to rotate freely as it bent backwards. To measure the actual load in the post, a load cell was placed on the front side of the post, connecting the top and bottom sections. With the exception of the soil, the post was impacted using the same conditions as those used in the round post study. The data from the load cell was compared to that from the accelerometer, and the results are presented in Figure 40.

The graph clearly shows that the data from the accelerometer contained an initial spike that was not present in the data from the load cell. This suggested that there was indeed an additional force felt by the bogie that was not due to the bending of the post but rather due to the

acceleration of the post and the soil. Although this test was completed in soil, it suggests that there is indeed an inertial spike at the front end of the accelerometer data.

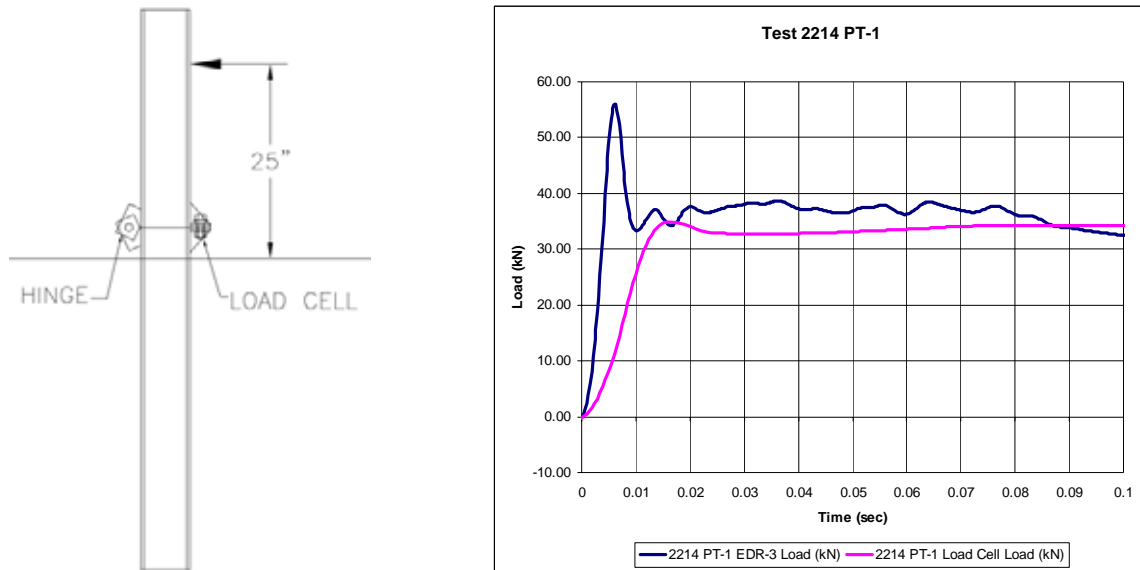


Figure 40. Setup and Results - Test PT-1

7.3.3 Distinction between Real and Inertial Forces

If the inertial spike theory is true, the inertial force and the real resistive force need to be separated to determine the actual strength of the posts. When the post tests were conducted with some amount of compliance in the sleeve, the inertial force was very distinct. However, the less compliance that exists, the more vague the distinction will become. For example, in a fully fixed test where the posts were embedded in concrete, the inertial and real forces would be combined into a single spike and distinguishing between the two would be impossible.

7.4 Effects of the Inertial Spike Theory

Consideration of the inertial spike theory may have a significant effect on some of the post tests while having little or no effect on others. In the cases in which the inertial spike was lower than a subsequent spike, very little change will occur. Several of these tests were filtered without the inertial spike, but only very slight changes were noted in the peak force levels.

For the cases in which the inertial spike was also the maximum spike, the theory may have significant effects. The first problem was that excluding the inertial spike severely reduced the calculated strength of the posts because the maximum force was significantly lowered. However, considering the inertial spike theory in more detail, the strength of the post may not be as low as this new analysis suggests.

If the bogie impacts a post and causes it to rotate, the fixed sleeve must eventually bring the base of the post to a stop, or it would never fracture. If the inertia of the post is great enough, the sleeve's slowing force may cause bending in the post or even failure. If this occurs, the additional force from the bogie, required to fracture the post, may only be responsible for a small portion of the ultimate stress in the fibers since the two opposing forces act simultaneously. When this occurs, determining the force that was required to fracture the post is very difficult. In the other scenario, when the inertial force is great enough that the sleeve's slowing force can fail the fibers by itself, the bogie may not even apply additional force to fracture the post. This potential scenario greatly complicates efforts to eliminate the effects of the inertial spike from the analysis.

Because the theory had a potentially significant effect on the future tests within the project, three additional bogie tests were conducted at half the impact speed to prove or disprove that inertia caused the initial spike in the dynamic data. If inertia did cause the initial spike, the impulse should also be cut in half because the momentum of the post would also be cut in half.

7.4.1 Predicted Impulse and Angular Momentum

Using the same procedures as before, the angular momentum, linear momentum, and impulse were predicted for the tests and are shown in Table 32. It was assumed that the impulse would be the same as the calculated momentum, as it was for the previous Southern Yellow Pine post tests.

Table 32. Supplemental Bogie Testing Predictions

Post No.	Dry Weight		Wet Weight		Angular Momentum (H _G)		Linear Momentum (M)		Predicted Impulse (I)		Predicted Peak Force		Peak Force (Test Results)	
	kg	(lb)	kg	(lb)	J-s	(ft-lbs-sec)	N-sec	(lb-sec)	N-s	(lb-sec)	kN	(k)	kN	(k)
SYPI-1	30.4	(67)	33.1	(73)	70.67	(52.12)	111.85	(25.14)	111.85	(25.14)	52.30	(11.76)	79.71	(17.92)
SYPI-2	34.0	(75)	36.3	(80)	86.31	(63.66)	136.59	(30.71)	136.59	(30.71)	63.87	(14.36)	89.99	(20.23)
SYPI-3	29.0	(64)	31.3	(69)	98.26	(72.47)	155.51	(34.96)	155.51	(34.96)	72.71	(16.35)	99.37	(22.34)

A significant assumption was made to calculate the peak force. This assumption was the period, or duration, of the impulse. If the period of the impulse was the same as the previous tests at 32 km/hr (20 mph), the peak force would be half of what it was previously. If the duration of the impulse was twice the previous duration, the peak force would be a quarter of its previous value.

Based on prior experience, the duration of an impact is often fairly independent of the impact velocity. This meant that the duration of the impact event would be approximately the same as before, and for the purposes of the project, it will be assumed to be exactly the same. Therefore, an impulse duration of 0.003208 sec, which was the average duration for the previous tests, was chosen.

A semi-parabolic impulse spike approximation was used to calculate the peak force because it more closely approximated the physical test data as compared to a triangular or parabolic distribution. The impulse was approximated as:

$$I = \frac{2(\Delta t)(F_{Peak})}{3}$$

Rearranging the equation for peak load resulted in the expression shown below, which was then used to determine the force values for each post. These results are also shown in Table 32.

$$F_{Peak} = \frac{3(I)}{2(\Delta t)}$$

7.4.2 Supplemental Testing

Three supplemental bogie tests were conducted on round Southern Yellow Pine posts from the same lot as those tested previously. In this set of tests, the impact speed was reduced, and all other factors were held consistent with the previous tests. Note that test no. SYPI-3 was conducted at 6.1 m/s (13.6 mph) rather than the anticipated 4.5 m/s (10 mph.).

When the tests were completed, the accelerometer data was analyzed and investigated as before. The test results for peak acceleration, peak force, impulse, linear momentum, as calculated previously, and impact speed are presented and compared to the prior tests in Table 33. Complete results for the three tests are provided in Appendix D, and a summary of the test results is provided in Table 34. A ratio of the results from the supplemental tests to the results from the original tests is also calculated to show its similarity to the ratio of the impact speeds.

Table 33. Supplemental Bogie Test Results Comparison

Test No.	Peak Acceleration	Peak Force		Predicted Peak Force		Impulse (I)		Linear Momentum (M)		Impact Speed	
	(G's)	kN	(Kips)	kN	(Kips)	N-sec	(lb-sec)	N-sec	(lb-sec)	m/s	(ft/s)
SYPI-1	11.17	79.71	17.92	52.31	11.76	139.45	31.35	111.83	25.14	4.47	14.67
SYPI-2	12.61	90.00	20.23	63.88	14.36	170.20	38.26	136.60	30.71	4.54	14.90
SYPI 1-2 Average	11.89	84.86	19.08	58.09	13.06	154.83	34.81	124.22	27.93	4.51	14.78
SY 1-15 Average	19.99	142.71	32.08			270.66	60.85	270.67	60.85	8.84	29.00
Ratio	0.595	0.595	0.595			0.572	0.572	0.459	0.459	0.510	0.510
SYPI-3	13.92	99.39	22.34	72.73	16.35	178.69	40.17	155.51	34.96	6.06	19.88
SY 1-15 Average	19.99	142.71	32.08			270.66	60.85	270.67	60.85	8.84	29.00
Ratio	0.696	0.696	0.696			0.660	0.660	0.575	0.575	0.686	0.686

The results shown in Table 33 were very close to those shown in Table 32, which were predicted by the inertial spike theory. For the first two supplemental tests, conducted at approximately 4.5 m/s (10.0 mph), the peak acceleration, peak force, and impulse of the initial acceleration spike should have been approximately half of the values determined for tests conducted at 8.9 m/s (20 mph). As shown in Table 33, the new values ranged from 57 percent to 60 percent of the old, very close to what was expected. The third test, conducted at approximately 5.8 m/s (13 mph), should have reached peak acceleration, peak force, and impulse values for the initial acceleration spike that were about 65 percent of the values determined for the previous tests. Again, the results support this with values ranging from 66 percent to 70 percent of the previous results. These comparisons offer significant support for the inertial spike theory.

A comparison of the acceleration vs. time plots is shown in Figures 41 and 42. In test no. SY-3, shown in Figure 41, the initial spike of the filtered acceleration exceeded the second peak. However, the initial spike in the filtered data was just slightly over half of the second spike when the velocity was decreased for test no. SYPI-3, as shown in Figure 42. Clearly, the impact velocity has a large effect on the magnitude of the initial filtered acceleration spike.

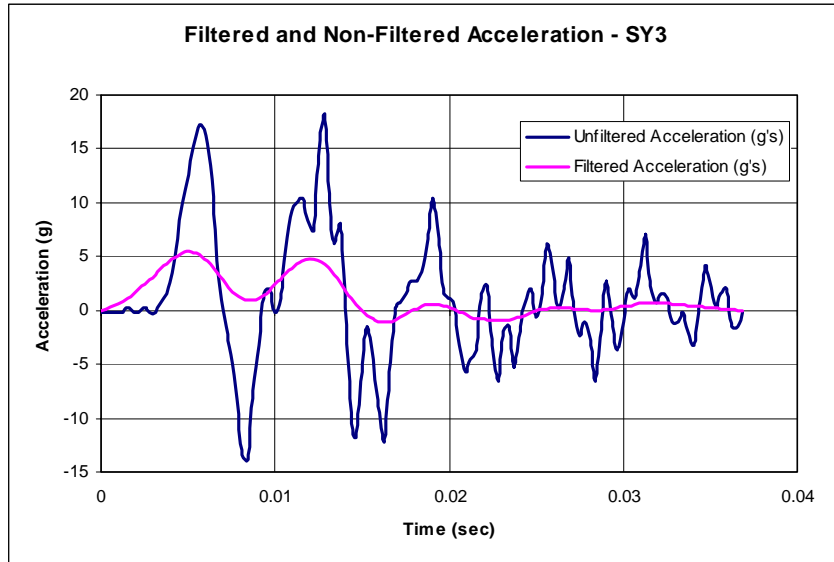


Figure 41. Acceleration vs. Time - Test No. SY-3

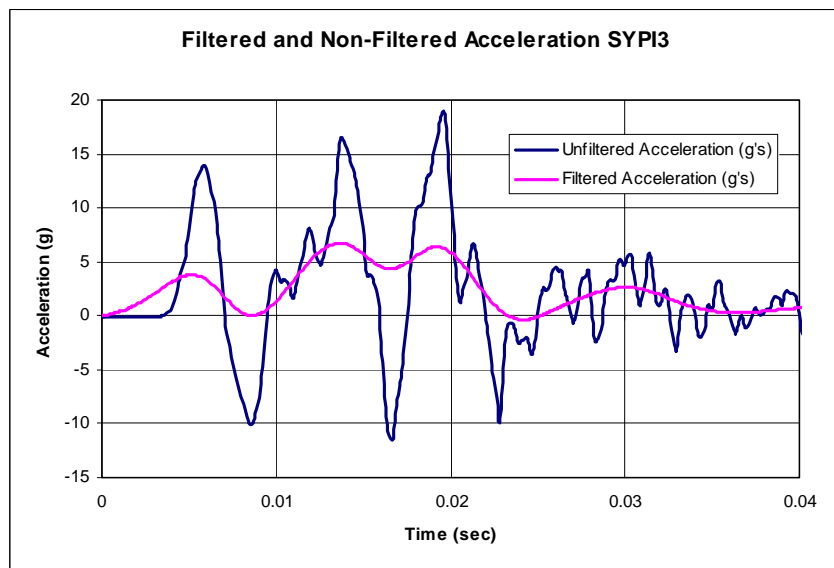


Figure 42. Acceleration vs. Time - Test No. SYPI-3

Table 34. Supplemental Bogie Test Results Summary

Post Test No.	Post Number	Post Category	Ring Density rings/in.	Average Diameter mm (in.)	Peak Force				Rupture			Moisture Content (%)	Modulus of Rupture Mpa (k/in. ²)	Impact Velocity m/s (mph)
					Time ms	Force kN (kips)	Deflection mm (in.)	Energy kJ (kip-in.)	Time ms	Deflection mm (in.)	Energy kJ (kip-in.)			
Inertial SYP	SYPI-1	C	4.00	177 (6.9)	19.2	57.1 (12.8)	81 (3.2)	2.27 (20.1)	197.6	457 (18.0)	6.23 (55.4)	26	54.4 (7.89)	4.5 (10.0)
	SYPI-2	B	10.33	186 (7.3)	26.2	63.9 (14.4)	106 (4.2)	3.87 (34.3)	155.9	216 (8.5)	7.50 (66.4)	22	70.2 (10.18)	4.5 (10.2)
	SYPI-3	A	2.67	185 (7.3)	13.6	48.1 (10.8)	81 (3.2)	1.39 (12.3)	88.2	463 (18.2)	4.40 (39.0)	28	46.6 (6.75)	6.1 (13.6)
Overall Average			5.67	182 (7.2)	19.66667	56.3 (12.7)	89 (3.5)	2.51 (22.2)	147.2	378 (14.9)	6.05 (53.6)	25	57.05 (8.3)	5.0 (11.2)
Standard Deviation			4.09	5.16 (0.2)	6.31295	7.9 (1.8)	15 (0.6)	1.26 (11.2)	55.2	141 (5.5)	1.56 (13.8)	3	12.05 (1.7)	0.9 (2.0)

*Data Filtered According to SAE J2111/1 Requirements

Limited by Maximum Deflection Criterion (20 in.)

Limited by Time of Contact

*Peak forces included in Table 34 are filtered as previous test results, and therefore differ from those shown in Table 32 and Table 33, which are unfiltered.

7.4.3 Effects of Inertial Spike on Post Size

The cases in which the inertial spike was not the maximum overall force will have no effect on the post size determination. However, for the other cases, the MOR for the individual tests would decrease, reducing the overall average MOR for the species. This in turn would increase the recommended diameter for the posts. Unfortunately, the second set of posts was ordered before the inertial effects were fully investigated. Therefore, no diameter modification could be made prior to the second round of testing.

Instead, some modifications were made to the impact conditions. As shown in tests SYPI 1 through 3, the initial spike could be significantly reduced by lowering the impact velocity of the bogie. In fact, if the velocity of the bogie was halved, the initial impulse should also be halved. Although the modification will not eliminate the inertia problem, it will significantly reduce it and should help in determining the actual fracturing force for each post.

7.4.4 Effects on Future Testing

In future tests, similar adjustments should be made. Although changing the restraint conditions would also modify the results, the alteration could make the peak force determination more difficult as alluded to previously. Therefore, the only change that is suggested is the reduction of the impact speed.

The new theory offers further understanding into the physics of cantilever post impacts and will likely help fine tune bogie testing procedures used in the future. Clearly the historic methods of testing cannot produce accurate results and should be abandoned.

8 PHYSICAL TESTING – ROUND TWO

8.1 Purpose

After determining that the original post diameter chosen for each of the species was too large, an additional 15 dynamic bogie tests of each species were conducted on posts of the smaller diameters determined in Chapter 6. Again, the posts were divided into three categories, knots, baseline, and high ring density, and again the purpose of the testing was to evaluate the strength of the posts in bending.

8.2 Pretest Documentation and Preparation

Prior to post testing, the samples were extensively documented using all of the same techniques that were used in the first round. In addition, the critical region for each of the posts was painted white. This painted region greatly increased the visibility of the post fracture because it caused the cracks in the surface to appear very dark against the white background. The test documentation summaries are presented below in Tables 36, 35, and 37. In addition, the posts were soaked in tanks of water to increase the moisture content as in the first round of testing. Tables 39, 38, and 40 show the recorded test day values for moisture content, weight, and base circumference.

Table 35. Douglas Fir Round Two Pre-Test Documentation

	Post Number	Weight		Avg. Length		Circumference						Volume		Density		Moisture Content (%)			Ring Density (rings/in.)
		kg	(lbs)	mm	(in.)	Critical Zone Average		Top		Bottom		cm ³	(in. ³)	kg/m ³	(lbs/ft ³)	21" From Top	21" From Bottom	Center	
						mm	(in.)	mm	(in.)	mm	(in.)								
Douglas Fir	401	29	(63)	1984	(78.125)	506	(19.917)	486	(19.125)	521	(20.500)	40274	(2458)	710	(0.03)	65	58	71	3.67
	403	25	(55)	1986	(78.188)	573	(22.542)	540	(21.250)	610	(24.000)	51873	(3165)	481	(0.02)	67	65	63	4.33
	404	35	(78)	1985	(78.167)	561	(22.083)	508	(20.000)	572	(22.500)	48685	(2971)	727	(0.03)	53	49	39	4.33
	405	29	(63)	1984	(78.125)	543	(21.375)	521	(20.500)	575	(22.625)	46744	(2852)	611	(0.02)	65	67	71	4.00
	410	27	(59)	1985	(78.167)	566	(22.292)	552	(21.750)	587	(23.125)	50750	(3097)	527	(0.02)	66	65	69	3.67
	414	24	(52)	1984	(78.125)	549	(21.625)	527	(20.750)	565	(22.250)	47431	(2894)	497	(0.02)	47	56	51	4.00
	415	27	(59)	1985	(78.146)	554	(21.792)	527	(20.750)	575	(22.625)	48230	(2943)	555	(0.02)	74	71	74	3.67
	417	26	(58)	1983	(78.083)	527	(20.750)	530	(20.875)	587	(23.125)	45287	(2764)	581	(0.02)	60	63	61	3.67
	418	29	(65)	1984	(78.125)	586	(23.083)	565	(22.250)	613	(24.125)	54390	(3319)	542	(0.02)	22	30	29	5.67
	419	29	(65)	1985	(78.167)	564	(22.208)	546	(21.500)	581	(22.875)	50182	(3062)	588	(0.02)	32	48	48	5.67
	421	31	(68)	1985	(78.146)	557	(21.917)	549	(21.625)	568	(22.375)	48967	(2988)	630	(0.02)	60	66	63	12.33
	422	32	(71)	1984	(78.125)	545	(21.458)	521	(20.500)	527	(20.750)	45876	(2799)	702	(0.03)	21	21	22	7.67
	425	28	(62)	1985	(78.167)	536	(21.083)	521	(20.500)	540	(21.250)	44988	(2745)	625	(0.02)	36	32	26	9.33
	426	29	(63)	1984	(78.125)	560	(22.042)	559	(22.000)	575	(22.625)	49754	(3036)	574	(0.02)	67	65	70	8.33
	429	31	(69)	1984	(78.125)	579	(22.792)	575	(22.625)	591	(23.250)	53056	(3238)	590	(0.02)	59	39	70	5.67

Table 36. Ponderosa Pine Round Two Pre-Test Documentation

	Post Number	Weight		Avg. Length		Circumference						Volume		Density		Moisture Content (%)			Ring Density (rings/in.)
		kg	(lbs)	mm	(in.)	Critical Zone Average		Top		Bottom		cm ³	(in. ³)	kg/m ³	(lbs/ft ³)	21" From Top	21" From Bottom	Center	
						mm	(in.)	mm	(in.)	mm	(in.)								
Ponderosa Pine	502	26	(58)	1984	(78.125)	564	(22.208)	575	(22.625)	581	(22.875)	50882	(3105)	517	(0.02)	15	17	17	5.67
	505	27	(59)	1982	(78.042)	570	(22.458)	540	(21.250)	622	(24.500)	51894	(3167)	516	(0.02)	15	17	15	6.33
	506	22	(48)	1983	(78.083)	564	(22.208)	578	(22.750)	638	(25.125)	52448	(3201)	415	(0.01)	17	15	17	4.67
	508	25	(55)	1981	(78.000)	576	(22.667)	559	(22.000)	635	(25.000)	53475	(3263)	467	(0.02)	10	9	10	4.33
	510	24	(53)	1981	(78.000)	510	(20.083)	527	(20.750)	549	(21.625)	42370	(2586)	567	(0.02)	14	13	12	3.33
	515	22	(48)	1982	(78.042)	506	(19.917)	521	(20.500)	559	(22.000)	41900	(2557)	520	(0.02)	36	30	44	5.33
	516	21	(47)	1981	(78.000)	529	(20.833)	559	(22.000)	552	(21.750)	45374	(2769)	470	(0.02)	17	16	17	7.00
	517	20	(45)	1980	(77.958)	548	(21.583)	540	(21.250)	546	(21.500)	47110	(2875)	433	(0.02)	13	13	13	5.33
	518	26	(57)	1984	(78.125)	539	(21.208)	552	(21.750)	565	(22.250)	46735	(2852)	553	(0.02)	30	31	27	6.67
	519	20	(43)	1985	(78.167)	514	(20.250)	495	(19.500)	527	(20.750)	41582	(2537)	469	(0.02)	14	15	19	7.67
	521	30	(66)	1982	(78.042)	605	(23.833)	610	(24.000)	622	(24.500)	58391	(3563)	513	(0.02)	14	14	15	15.00
	526	24	(54)	1984	(78.125)	602	(23.708)	606	(23.875)	610	(24.000)	57538	(3511)	426	(0.02)	16	16	17	19.33
	527	25	(56)	1983	(78.083)	568	(22.375)	565	(22.250)	603	(23.750)	51742	(3157)	491	(0.02)	18	16	22	13.33
	528	30	(67)	1984	(78.125)	592	(23.292)	594	(23.375)	606	(23.875)	55593	(3393)	547	(0.02)	11	13	11	26.33
	530	33	(73)	1985	(78.146)	586	(23.083)	600	(23.625)	610	(24.000)	55177	(3367)	600	(0.02)	33	43	31	15.00

Table 37. Southern Yellow Pine Round Two Pre-Test Documentation

	Post Number	Weight		Avg. Length		Circumference						Volume		Density		Moisture Content (%)			Ring Density (rings/in.)
		kg	(lbs)	mm	(in.)	Critical Zone Average		Top		Bottom		cm ³	(in. ³)	kg/m ³	(lbs/ft ³)	21" From Top	21" From Bottom	Center	
						mm	(in.)	mm	(in.)	mm	(in.)								
Southern Yellow Pine	602	24	(54)	1880	(74.000)	572	(22.500)	568	(22.375)	552	(21.750)	50962	(3110)	481	(0.02)	19	18	18	2.67
	604	24	(52)	1871	(73.667)	572	(22.500)	556	(21.875)	565	(22.250)	50960	(3110)	463	(0.02)	16	16	16	2.67
	605	23	(51)	1875	(73.833)	570	(22.458)	565	(22.250)	568	(22.375)	51121	(3120)	453	(0.02)	18	19	18	2.67
	606	29	(63)	1886	(74.250)	575	(22.625)	575	(22.625)	559	(22.000)	51675	(3153)	553	(0.02)	34	42	39	2.67
	610	25	(56)	1969	(77.500)	526	(20.708)	521	(20.500)	543	(21.375)	43896	(2679)	579	(0.02)	15	12	15	2.67
	612	27	(59)	1870	(73.625)	572	(22.500)	572	(22.500)	575	(22.625)	51571	(3147)	519	(0.02)	29	43	37	2.67
	613	26	(57)	1879	(73.958)	572	(22.500)	565	(22.250)	565	(22.250)	51178	(3123)	505	(0.02)	17	18	16	2.67
	615	24	(53)	1890	(74.417)	575	(22.625)	565	(22.250)	572	(22.500)	51773	(3159)	464	(0.02)	29	19	27	2.00
	618	34	(74)	1892	(74.500)	572	(22.500)	565	(22.250)	565	(22.250)	51187	(3124)	656	(0.02)	32	29	24	4.33
	619	31	(69)	1868	(73.542)	581	(22.875)	572	(22.500)	572	(22.500)	52759	(3220)	593	(0.02)	47	32	39	1.67
	621	33	(73)	1990	(78.333)	568	(22.375)	562	(22.125)	578	(22.750)	51009	(3113)	649	(0.02)	13	12	11	4.00
	622	34	(76)	1986	(78.208)	580	(22.833)	581	(22.875)	606	(23.875)	53692	(3277)	642	(0.02)	13	14	14	12.67
	625	29	(63)	1901	(74.833)	565	(22.250)	559	(22.000)	565	(22.250)	50204	(3064)	569	(0.02)	12	11	10	8.00
	626	30	(67)	1885	(74.208)	569	(22.417)	562	(22.125)	565	(22.250)	50837	(3102)	598	(0.02)	20	19	19	5.00
	627	34	(75)	1881	(74.042)	573	(22.542)	572	(22.500)	572	(22.500)	51626	(3150)	659	(0.02)	30	34	27	9.00

Table 38. Douglas Fir Round Two Test Day Measurements

Test No.	Post No.	Weight (lbs)	Moisture Content (%)			Circumference at Bottom (in.)
			21 in. from Top	Center	21 in. from Bottom	
DF-16	401	59	25	58	70	22 1/8
DF-17	403	56	23	59	61	23 7/8
DF-18	404	79	30	45	54	22 3/4
DF-19	405	59	28	46	70	22 1/2
DF-20	410	60	21	35	66	23 1/4
DF-21	414	51	23	41	65	22 1/2
DF-22	415	60	49	59	72	22 3/4
DF-23	417	59	52	62	64	23 1/4
DF-24	418	69	21	46	61	24 1/2
DF-25	419	64	23	66	63	23 1/8
DF-26	421	64	21	67	60	22 3/8
DF-27	422	68	19	51	60	23 1/4
DF-28	425	65	20	27	63	21 1/2
DF-29	426	62	19	29	71	22 3/4
DF-30	429	69	25	54	59	23 3/8

Table 39. Ponderosa Pine Round Two Test Day Measurements

Test No.	Post No.	Weight (lbs)	Moisture Content (%)			Circumference at Bottom (in.)
			21 in. from Top	Center	21 in. from Bottom	
PP-16	502	66	15	15	42	23 1/4
PP-17	505	69	14	29	48	24 7/8
PP-18	506	63	15	26	46	25 1/2
PP-19	508	68	16	23	48	25 1/4
PP-20	510	55	15	45	48	22
PP-21	515	54	14	44	46	22 1/4
PP-22	516	52	15	15	49	22 1/2
PP-23	517	51	13	15	46	22 1/4
PP-24	518	62	18	25	34	22 1/4
PP-25	519	46	14	16	38	21
PP-26	521	77	11	21	40	25 1/8
PP-27	526	71	19	34	46	24 1/2
PP-28	527	77	58	64	58	23 7/8
PP-29	528	75	17	41	39	24 1/4
PP-30	530	87	34	46	43	24

Table 40. Southern Yellow Pine Round Two Test Day Measurements

Test No.	Post No.	Weight (lbs)	Moisture Content (%)			Circumference at Bottom (in.)
			21 in. from Top	Center	21 in. from Bottom	
SY-16	602	57	18	28	45	22 1/2
SY-17	604	56	16	38	57	22 3/8
SY-18	605	59	16	38	53	22 3/8
SY-19	606	62	19	34	40	22 3/8
SY-20	610	68	17	46	60	23 1/4
SY-21	612	65	18	50	56	22 3/4
SY-22	613	69	18	44	48	22 1/2
SY-23	615	62	19	41	44	22 1/2
SY-24	618	77	17	41	51	22 5/8
SY-25	619	74	18	45	48	22 1/2
SY-26	621	85	16	50	50	22 5/8
SY-27	622	85	16	46	50	23 5/8
SY-28	625	83	16	55	59	22 7/8
SY-29	626	73	16	31	38	22 5/8
SY-30	627	80	16	29	37	22 1/2

8.3 Scope

The second series of bogie tests was conducted with the round posts installed in a rigid steel sleeve that was embedded in concrete. Fifteen tests were conducted for each species with a centerline impact at approximately 20.9 km/h (13 mph), 632 mm (24.875 in.) above the ground. The speed was reduced from the first round of testing in order to reduce the inertial spike discussed previously. It should also be noted that in the second round of tests, the posts were arranged so the most knotty face was oriented toward the impacting bogie (i.e., placing the critical knots in the tension face). This arrangement was not followed in the first round of tests. The testing matrix for the second round of tests is shown in Figure 43 below. The test setup was identical to the previous setup.

Test No.	Post No.	Wooden Post Type		Post Length (in.)	Post Diameter (in.)
DF-16	401	Round	Douglas Fir	78.1	6.34
DF-17	403	Round	Douglas Fir	78.2	7.18
DF-18	404	Round	Douglas Fir	78.2	7.03
DF-19	405	Round	Douglas Fir	78.1	6.80
DF-20	410	Round	Douglas Fir	78.2	7.10
DF-21	414	Round	Douglas Fir	78.1	7.88
DF-22	415	Round	Douglas Fir	78.1	6.94
DF-23	417	Round	Douglas Fir	78.1	6.60
DF-24	418	Round	Douglas Fir	78.1	7.35
DF-25	419	Round	Douglas Fir	78.2	7.07
DF-26	421	Round	Douglas Fir	78.1	6.98
DF-27	422	Round	Douglas Fir	78.1	6.83
DF-28	425	Round	Douglas Fir	78.2	6.71
DF-29	426	Round	Douglas Fir	78.1	7.02
DF-30	429	Round	Douglas Fir	78.1	7.25
PP-16	502	Round	Ponderosa Pine	78.1	7.07
PP-17	505	Round	Ponderosa Pine	78.0	7.15
PP-18	506	Round	Ponderosa Pine	78.1	7.07
PP-19	508	Round	Ponderosa Pine	78.0	7.22
PP-20	510	Round	Ponderosa Pine	78.0	6.39
PP-21	515	Round	Ponderosa Pine	78.0	6.34
PP-22	516	Round	Ponderosa Pine	78.0	6.63
PP-23	517	Round	Ponderosa Pine	78.0	6.87
PP-24	518	Round	Ponderosa Pine	78.1	6.75
PP-25	519	Round	Ponderosa Pine	78.2	6.45
PP-26	521	Round	Ponderosa Pine	78.0	7.59
PP-27	526	Round	Ponderosa Pine	78.1	7.55
PP-28	527	Round	Ponderosa Pine	78.1	7.12
PP-29	528	Round	Ponderosa Pine	78.1	7.41
PP-30	530	Round	Ponderosa Pine	78.1	7.35
SY-16	602	Round	Southern Yellow Pine	74.0	7.16
SY-17	604	Round	Southern Yellow Pine	73.7	7.16
SY-18	605	Round	Southern Yellow Pine	73.8	7.15
SY-19	606	Round	Southern Yellow Pine	74.3	7.20
SY-20	610	Round	Southern Yellow Pine	77.5	6.59
SY-21	612	Round	Southern Yellow Pine	73.6	7.16
SY-22	613	Round	Southern Yellow Pine	74.0	7.16
SY-23	615	Round	Southern Yellow Pine	74.4	7.20
SY-24	618	Round	Southern Yellow Pine	74.5	7.16
SY-25	619	Round	Southern Yellow Pine	73.5	7.28
SY-26	621	Round	Southern Yellow Pine	78.3	7.12
SY-27	622	Round	Southern Yellow Pine	78.2	7.27
SY-28	625	Round	Southern Yellow Pine	74.8	7.08
SY-29	626	Round	Southern Yellow Pine	74.2	7.14
SY-30	627	Round	Southern Yellow Pine	74.0	7.18

NOTES:

- (1) TARGET SPEED = 13 MPH (NOT LOWER)
- (2) IMPACT ORIENTATION: CENTERLINE OF POST (W/ARROW POINTING TOWARD BOGIE) AND CENTERLINE OF BOGIE
- (3) SOME SOUTHERN PINE HAVE DOMED TOPS


	FOREST PRODUCTS LAB ROUND POST TESTING ROUND TWO BOGIE SETUP TEST MATRIX		Sheet: 4 of 4
	Drawing Name: FPL Bogie Testing Matrix		Date: 7/27/05
Midwest Roadside Safety Facility	Scale: None	By: JAH	Rev: KAP

Figure 43. Round Two Bogie Testing Matrix

9 SYSTEM DETAILS – ROUND TWO

9.1 Round Wood Posts

All of the round post samples were again donated by companies in the forestry industry. Ponderosa Pine samples were donated by Hills Products Group, Douglas Fir samples were donated by All-Weather Wood Products, and Southern Yellow Pine samples were donated by Arnold Forest Products Corporation, The Burke-Parsons-Bowlby Corporation, and Interstate Timber Products Co.

The nominal length of the posts was again 1,981 mm (78 in.). The nominal target diameter of the posts was 171 mm (6.75 in.) for Douglas Fir, 191 mm (7.5 in.) for Ponderosa Pine, and 178 mm (7.0 in.) for Southern Yellow Pine. Figure 44 shows the dimensions for each of the selected posts.

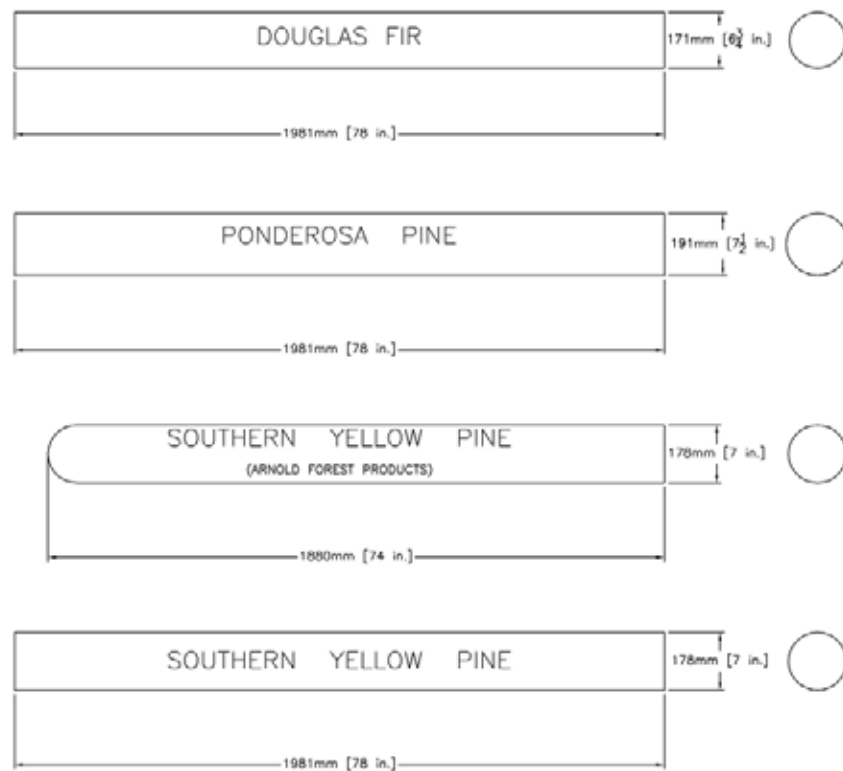


Figure 44. Major Dimensions of Round Wood Posts - Round Two Testing

9.2 Equipment and Instrumentation

The equipment and instrumentation used in the second round of tests was largely the same as that used in the first round. The only exception was the use of two additional high-speed digital video cameras. During the second round of tests, one high-speed Photron digital video camera and two high-speed VITcam digital video cameras, all with speeds of 500 frames per second, were used to record the events. One of the high-speed cameras was focused on the base of the post, clearly displaying the fracture as it occurred. A second camera was focused on the impact location, which was used to investigate any interaction between the bogie impact head and the posts.

Once again, the cameras were placed approximately 25 ft from the centerline of the posts, with a field of view perpendicular to the bogie's direction of travel. When needed, flood lights were used to light the base of the posts. The recorded acceleration data was processed in the same manner as that recorded in the first round of bogie tests. The end of the test was also determined in the same manner as before.

10 ROUND 2 CANTILEVER TEST RESULTS

Bogie vehicle acceleration traces were processed for each of the tests in order to determine acceleration, velocity, and displacement curves, as well as force vs. deflection curves using the procedure described previously. Results for individual tests can be found in Appendix E, and test results and summary data can be found in Tables 42, 41, and 43 for Douglas Fir, Ponderosa Pine, and Southern Yellow Pine, respectively.

10.1 MOR Results

Similar to the first round of tests, an MOR value was calculated for each of the 45 tests and is shown in the mentioned tables. The highest average MOR was 57 MPa (8.3 ksi) for the Douglas Fir posts, the lowest average MOR was 48.1 MPa (7.0 ksi) for the Southern Yellow Pine posts, and the Ponderosa Pine posts had an MOR of 49 MPa (7.2 ksi). With the exception of Southern Yellow Pine, which dropped in average MOR by more than 20 percent, the average MOR values were very similar to those from the previous round of testing. The average for Ponderosa Pine increased by 1 percent, and that for Douglas Fir decreased by 3 percent.

10.1.1 Douglas Fir

The Douglas Fir tests showed an overall decrease in MOR of 3 percent. This drop corresponded to an average MOR value of 57 MPa (8.3 ksi). The lowest average MOR for the individual categories was 49 MPa (7.2 ksi) for the knots category, a 16 percent decrease from the previous round of tests, and the highest was 69 MPa (10 ksi) for the HRD category, a 6 percent increase. The baseline category fell in the middle with an average MOR of 53 MPa (7.6 ksi), a 1 percent increase from the previous testing. The highest MOR for an individual test was 77 MPa (11 ksi) for test DF-28 in the HRD category, and the lowest MOR was 26 MPa (3.7 ksi) for test DF-17 in the knots category. Again, the difference could be attributed to the presence of knots

and a decreased ring density of 4.33 rings-per-inch for DF-17 as compared to 9.33 rings-per-inch for DF-28.

10.1.2 Ponderosa Pine

Ponderosa Pine had an average MOR of 49 MPa (7.2 ksi). The knots category showed an MOR of 46 MPa (6.7 ksi), a 2 percent increase, the baseline category showed an MOR of 50 MPa (7.3 ksi), a 29 percent increase, and the HRD category showed an MOR of 52 MPa (7.6 ksi), an 18 percent decrease. The highest MOR was 71.0 MPa (10.30 ksi) for test PP-26 in the HRD category, and the lowest was 31.9 MPa (4.62 ksi) for test PP-19 in the knots category. Clearly, there was a significant difference between the two extremes. In addition to the presence of knots, a likely explanation was the difference in ring density from 15.0 rings-per-inch for PP-26 to 4.33 rings-per-inch for PP-19.

10.1.3 Southern Yellow Pine

Southern Yellow Pine had an average MOR of 48.1 MPa (7.0 ksi). The knots category had the lowest MOR of 38.5 MPa (5.6 ksi), a 20 percent decrease from the first round. The HRD category MOR was the highest at 61.6 MPa (8.94 ksi), but decreased by 27 percent from the first round. Finally, the baseline category had an average MOR of 44.2 MPa (6.42 ksi), a 12 percent decrease from round 1.

The differences in the average MOR between the two rounds of testing have significant effects on the suggested diameter for both species. For instance, the 6 percent increase noticed in the Douglas Fir HRD category would constitute a 3-mm (0.125-in.) decrease in diameter. As this percentage increases, it begins to make significant differences in the amount of material in a post. Placing the knots in the tension face clearly lowered the MOR for the knots category, which may have significant effects on the final size of the posts. Orienting the knots may not

have been completely warranted since posts installed in the field will be placed randomly rather than in the worst-case orientation.

Table 41. Douglas Fir Round Wood Post Test Results - Round Two Testing

Post Test No.	Post No.	Category	Ring Density rings/in.	Average Diameter		Peak Force					Rupture			Moisture Content (%)	Modulus of Rupture Mpa (kips/in. ²)	Impact Velocity m/s (mph)
						Time ms	Force kN (kips)	Deflection mm (in.)	Energy kJ (kip-in.)	Time ms	Deflection mm (in.)	Energy kJ (kip-in.)				
DF-16	401	KNOTS	3.67	161 (6.3)	12.2	38.9 (8.8)	74 (2.9)	1.20 (10.6)	90.9	510 (20.1)	3.52 (31.2)	70	60.0 (8.70)	6.2 (13.8)		
DF-17	403		4.33	182 (7.2)	13.1	23.9 (5.4)	78 (3.1)	0.99 (8.8)	52.2	302 (11.9)	1.45 (12.8)	61	25.5 (3.69)	6.1 (13.5)		
DF-18	404		4.33	178 (7.0)	14.4	58.4 (13.1)	83 (3.3)	1.93 (17.1)	105.3	509 (20.0)	5.80 (51.3)	54	66.1 (9.58)	5.9 (13.2)		
DF-19	405		4.00	173 (6.8)	14.4	45.4 (10.2)	83 (3.3)	1.44 (12.7)	68.4	371 (14.6)	2.78 (24.6)	70	56.5 (8.20)	5.9 (13.2)		
DF-20	410		3.67	180 (7.1)	12.5	37.1 (8.3)	74 (2.9)	1.26 (11.1)	65.6	368 (14.5)	2.59 (22.9)	66	40.8 (5.91)	6.1 (13.6)		
KNOTS Average			4.00	175 (6.9)	13.3	40.7 (9.2)	78 (3.1)	1.36 (12.1)	76.5	412 (16.2)	3.23 (28.6)	64	49.8 (7.22)	6.0 (13.5)		
DF-21	414	BASELINE	4.00	175 (6.9)	12.5	40.8 (9.2)	75 (3.0)	1.39 (12.3)	56.3	323 (12.7)	2.29 (20.2)	65	49.1 (7.12)	6.1 (13.8)		
DF-22	415		3.67	176 (6.9)	13.8	31.5 (7.1)	80 (3.1)	1.17 (10.4)	43.8	247 (9.7)	1.78 (15.7)	72	37.1 (5.38)	5.9 (13.3)		
DF-23	417		3.67	168 (6.6)	12.2	40.6 (9.1)	75 (3.0)	1.46 (12.9)	54.4	322 (12.7)	2.30 (20.4)	64	55.3 (8.02)	6.3 (14.1)		
DF-24	418		5.67	186 (7.3)	14.1	60.5 (13.6)	88 (3.5)	2.02 (17.8)	90.6	510 (20.1)	4.66 (41.2)	61	59.9 (8.68)	6.4 (14.3)		
DF-25	419		5.67	179 (7.1)	13.8	54.8 (12.3)	78 (3.1)	1.54 (13.6)	101.6	509 (20.0)	4.01 (35.5)	63	60.9 (8.83)	5.8 (13.0)		
BASELINE Average			4.53	177 (7.0)	13.3	45.6 (10.3)	79 (3.1)	1.52 (13.4)	69.3	382 (15.0)	3.01 (26.6)	65	52.5 (7.61)	6.1 (13.7)		
DF-26	421	HRD	12.33	177 (7.0)	20.3	60.4 (13.6)	118 (4.6)	3.66 (32.4)	63.1	319 (12.6)	6.11 (54.1)	60	69.8 (10.13)	6.1 (13.7)		
DF-27	422		7.67	173 (6.8)	20.6	59.3 (13.3)	121 (4.8)	3.79 (33.6)	184.1	508 (20.0)	13.74 (121.6)	60	73.1 (10.60)	6.2 (13.9)		
DF-28	425		9.33	170 (6.7)	13.4	59.1 (13.3)	82 (3.2)	1.85 (16.4)	110.3	509 (20.0)	8.39 (74.2)	63	76.8 (11.13)	6.2 (14.0)		
DF-29	426		8.33	178 (7.0)	21.6	58.2 (13.1)	128 (5.1)	3.71 (32.8)	68.7	365 (14.4)	5.47 (48.4)	71	66.2 (9.60)	6.2 (14.0)		
DF-30	429		5.67	184 (7.3)	14.7	58.6 (13.2)	85 (3.3)	1.67 (14.8)	104.1	509 (20.0)	5.24 (46.4)	59	60.3 (8.75)	5.9 (13.2)		
HRD Average			8.67	177 (7.0)	18.1	59.1 (13.3)	107 (4.2)	2.94 (26.0)	106.1	442 (17.4)	7.79 (68.9)	63	69.2 (10.04)	6.1 (13.7)		
Avg.			5.73	176 (6.9)	14.9	48.5 (10.9)	88 (3.5)	1.94 (17.2)	84.0	412 (16.2)	4.67 (41.4)	64	57.15 (8.3)	6.1 (13.6)		
St. Dev.			2.59	6.56 (0.3)	3.2	12.2 (2.7)	18 (0.7)	0.97 (8.6)	35.3	99 (3.9)	3.16 (28.0)	5	13.99 (2.0)	0.2 (0.4)		

*Data Filtered According to SAE J2117 Requirements

Limited by Maximum Deflection Criterion (20 in.)

Limited by Time of Contact

Table 42. Ponderosa Pine Round Wood Post Test Results - Round Two Testing

Ponderosa Pine														
Post Test No.	Post No.	Category	Ring Density rings/in.	Average Diameter mm (in.)	Peak Force				Rupture			Moisture Content (%)	Modulus of Rupture Mpa (kips/in. ²)	Impact Velocity m/s (mph)
					Time ms	Force kN (kips)	Deflection mm (in.)	Energy kJ (kip-in.)	Time ms	Deflection mm (in.)	Energy kJ (kip-in.)			
PP-16	502	KNOTS	5.67	179 (7.1)	15.0	41.6 (9.3)	82 (3.2)	1.20 (10.6)	56.6	291 (11.5)	2.78 (24.6)	42	46.2 (6.70)	6.2 (13.8)
PP-17	505		6.33	181 (7.1)	14.1	44.9 (10.1)	80 (3.2)	1.21 (10.7)	22.5	126 (5.0)	1.63 (14.4)	48	48.2 (7.00)	6.1 (13.5)
PP-18	506		4.67	179 (7.1)	15.0	41.7 (9.4)	92 (3.6)	1.32 (11.7)	22.8	137 (5.4)	1.74 (15.4)	46	46.4 (6.73)	5.9 (13.2)
PP-19	508		4.33	183 (7.2)	13.4	30.5 (6.9)	81 (3.2)	1.06 (9.4)	22.5	134 (5.3)	1.36 (12.0)	48	31.9 (4.62)	5.9 (13.2)
PP-20	510		3.33	162 (6.4)	25.0	37.6 (8.5)	153 (6.0)	1.26 (11.1)	33.1	200 (7.9)	1.70 (15.0)	48	56.5 (8.20)	6.1 (13.6)
KNOTS Average			4.87	177 (7.0)	16.5	39.2 (8.8)	97 (3.8)	1.21 (10.7)	31.5	178 (7.0)	1.84 (16.3)	46	45.8 (6.65)	6.0 (13.5)
PP-21	515	BASELINE	5.33	161 (6.3)	15.9	31.6 (7.1)	97 (3.8)	1.12 (9.9)	89.7	510 (20.1)	3.35 (29.7)	46	48.6 (7.05)	6.1 (13.8)
PP-22	516		7.00	168 (6.6)	13.8	42.6 (9.6)	86 (3.4)	1.22 (10.8)	26.3	159 (6.3)	2.33 (20.6)	49	57.3 (8.31)	5.9 (13.3)
PP-23	517		5.33	174 (6.9)	15.6	32.5 (7.3)	94 (3.7)	1.12 (9.9)	45.6	266 (10.5)	2.12 (18.8)	46	39.4 (5.71)	6.3 (14.1)
PP-24	518		6.67	171 (6.8)	15.9	46.1 (10.4)	100 (3.9)	1.65 (14.6)	88.4	508 (20.0)	3.73 (33.0)	34	58.8 (8.53)	6.4 (14.3)
PP-25	519		7.67	164 (6.4)	13.8	32.8 (7.4)	87 (3.4)	1.03 (9.1)	55.3	327 (12.9)	3.87 (34.3)	38	48.1 (6.98)	5.8 (13.0)
BASELINE Average			6.40	168 (6.6)	15.0	37.1 (8.3)	93 (3.7)	1.23 (10.9)	61.1	354 (13.9)	3.08 (27.3)	43	50.4 (7.32)	6.1 (13.7)
PP-26	521	HRD	15.00	193 (7.6)	20.6	79.0 (17.8)	122 (4.8)	4.50 (39.8)	75.9	384 (15.1)	6.66 (59.0)	40	71.0 (10.30)	6.1 (13.7)
PP-27	526		19.33	192 (7.5)	20.9	65.1 (14.6)	116 (4.6)	2.85 (25.2)	55.3	278 (10.9)	4.46 (39.5)	46	59.5 (8.63)	6.2 (13.9)
PP-28	527		13.33	181 (7.1)	15.3	40.3 (9.1)	93 (3.7)	1.51 (13.4)	89.7	493 (19.4)	4.18 (37.0)	58	43.8 (6.36)	6.2 (14.0)
PP-29	528		26.33	188 (7.4)	20.0	50.3 (11.3)	114 (4.5)	3.24 (28.7)	122.8	508 (20.0)	9.85 (87.2)	39	48.5 (7.03)	6.2 (14.0)
PP-30	530		15.00	186 (7.3)	15.3	37.9 (8.5)	92 (3.6)	1.47 (13.0)	50.0	282 (11.1)	3.43 (30.3)	43	37.6 (5.45)	5.9 (13.2)
HRD Average			17.80	188 (7.4)	18.4	54.5 (12.3)	108 (4.2)	2.72 (24.0)	78.7	389 (15.3)	5.72 (50.6)	45	52.1 (7.55)	6.1 (13.7)
Avg.			9.69	178 (7.0)	16.6	43.6 (9.8)	99 (3.9)	1.72 (15.2)	57.1	307 (12.1)	3.55 (31.4)	45	49.46 (7.2)	6.1 (13.6)
St. Dev.			6.65	10.4 (0.4)	3.4	13.1 (3.0)	20 (0.8)	1.01 (8.9)	30.5	144 (5.7)	2.24 (19.8)	6	9.91 (1.4)	0.2 (0.4)

*Data Filtered According to SAE J211/1 Requirements

Limited by Maximum Deflection Criterion (20 in.)

Limited by Time of Contact

Table 43. Southern Yellow Pine Round Wood Post Test Results - Round Two Testing

Post Test No.	Post Number	Post Category	Ring Density rings/in.	Average Diameter		Peak Force					Rupture			Moisture Content (%)	Modulus of Rupture Mpa (kips/in. ²)	Impact Velocity m/s (mph)	
				mm	in.	Time ms	Force kN (kips)	Deflection mm (in.)	Energy kJ (kip-in.)	Time ms	Deflection mm (in.)	Energy kJ (kip-in.)					
Southern Yellow Pine																	
KNOTS Average																	
SY-16	602	KNOTS	2.67	182	(7.2)	62.5	40.0 (9.0)	365 (14.4)	1.62 (14.4)	90.0	509 (20.0)	3.54 (31.4)	45	42.7 (6.20)	5.9 (13.2)		
SY-17	604	KNOTS	2.67	182	(7.2)	14.7	33.3 (7.5)	83 (3.3)	0.94 (8.3)	58.4	312 (12.3)	2.35 (20.8)	57	35.6 (5.17)	5.7 (12.8)		
SY-18	605	KNOTS	2.67	181	(7.1)	12.5	25.2 (5.7)	69 (2.7)	0.87 (7.7)	84.4	443 (17.4)	1.86 (16.5)	53	27.1 (3.93)	5.6 (12.6)		
SY-19	606	KNOTS	2.67	183	(7.2)	11.9	27.0 (6.1)	73 (2.9)	1.01 (9.0)	88.1	508 (20.0)	2.95 (26.1)	40	28.4 (4.12)	6.2 (14.0)		
SY-20	610	KNOTS	2.67	167	(6.6)	12.5	42.7 (9.6)	75 (3.0)	1.38 (12.2)	30.6	180 (7.1)	1.88 (16.6)	60	58.5 (8.49)	6.2 (13.8)		
KNOTS Average																	
SY-21	612	BASELINE	2.67	182	(7.2)	5.0	21.6 (4.9)	32 (1.2)	0.31 (2.7)	85.9	509 (20.1)	2.64 (23.3)	56	23.1 (3.35)	6.3 (14.2)		
SY-22	613	BASELINE	2.67	182	(7.2)	12.2	48.3 (10.9)	77 (3.0)	1.54 (13.6)	95.9	509 (20.0)	6.17 (54.6)	48	51.6 (7.48)	6.4 (14.4)		
SY-23	615	BASELINE	2.00	183	(7.2)	19.1	44.0 (9.9)	114 (4.5)	2.47 (21.9)	48.8	274 (10.8)	3.77 (33.3)	44	46.3 (6.71)	6.2 (13.8)		
SY-24	618	BASELINE	4.33	182	(7.2)	18.4	52.1 (11.7)	107 (4.2)	2.94 (26.0)	107.8	508 (20.0)	7.03 (62.2)	51	55.7 (8.08)	6.0 (13.5)		
SY-25	619	BASELINE	1.67	185	(7.3)	20.3	43.7 (9.8)	116 (4.6)	2.33 (20.6)	64.4	344 (13.5)	3.41 (30.2)	48	44.5 (6.45)	5.9 (13.3)		
BASELINE Average																	
SY-26	621	HRD	4.00	181	(7.1)	19.7	67.0 (15.1)	113 (4.5)	4.04 (35.8)	332.5	453 (17.8)	13.43 (118.9)	50	72.9 (10.57)	6.1 (13.6)		
SY-27	622	HRD	12.67	184	(7.3)	5.6	41.4 (9.3)	35 (1.4)	0.67 (5.9)	88.7	508 (20.0)	2.91 (25.7)	50	42.3 (6.14)	6.2 (13.9)		
SY-28	625	HRD	8.00	180	(7.1)	15.0	54.3 (12.2)	91 (3.6)	1.69 (15.0)	97.2	508 (20.0)	5.83 (51.6)	59	60.0 (8.71)	6.2 (13.8)		
SY-29	626	HRD	5.00	181	(7.1)	19.1	61.3 (13.8)	106 (4.2)	3.06 (27.1)	152.5	509 (20.0)	10.41 (92.2)	38	66.3 (9.62)	5.8 (13.0)		
SY-30	627	HRD	9.00	182	(7.2)	19.1	62.7 (14.1)	113 (4.5)	3.64 (32.2)	104.7	508 (20.0)	7.08 (62.7)	37	66.6 (9.67)	6.2 (13.9)		
HRD Average																	
			7.73	182	(7.2)	15.7	57.3 (12.9)	92 (3.6)	2.62 (23.2)	155.1	497 (19.6)	7.93 (70.2)	47	61.6 (8.94)	6.1 (13.7)		
	Avg.		4.36	181	(7.1)	17.8	44.3 (10.0)	105 (4.1)	1.90 (16.8)	102.0	439 (17.3)	5.02 (44.4)	49	48.11 (7.0)	6.1 (13.6)		
	St. Dev.		3.13	4.02	(0.2)	13.3	13.8 (3.1)	77 (3.0)	1.13 (10.0)	69.7	108 (4.3)	3.36 (29.7)	7	15.35 (2.2)	0.2 (0.5)		

*Data Filtered According to SAE J211/1 Requirements

Limited by Maximum Deflection Criterion (20 in.)

Limited by Time of Contact

10.2 Adjusted Peak Force

It is difficult to compare peak forces between posts that varied in size. As such, an adjusted peak force was calculated based on a post's MOR and nominal diameter. This adjusted peak force was simply a prediction of the peak force for the specified diameter that could be used to make comparisons between individual categories and individual posts.

To calculate such a predicted force, the method presented in Chapter 6 was used. Once again, this assumed a linear stress distribution and standard elastic bending theory. The adjusted force values were calculated for each of the posts at their nominal size for round 2 and are shown in Tables 45, 44, and 46 below.

Table 44. Douglas Fir - Adjusted Peak Force

	Post Test No.	Post Number	Post Category	6.75 in. Diameter Adjusted Peak Force	
				kN	(kips)
Douglas Fir	DF-16	401	KNOTS	47.0	(10.56)
	DF-17	403	KNOTS	19.9	(4.48)
	DF-18	404	KNOTS	51.7	(11.63)
	DF-19	405	KNOTS	44.3	(9.96)
	DF-20	410	KNOTS	31.9	(7.18)
	KNOTS Average			39.0	(8.76)
	DF-21	414	BASELINE	38.5	(8.65)
	DF-22	415	BASELINE	29.1	(6.53)
	DF-23	417	BASELINE	43.3	(9.73)
	DF-24	418	BASELINE	46.9	(10.54)
	DF-25	419	BASELINE	47.7	(10.72)
	BASELINE Average			41.1	(9.23)
	DF-26	421	HRD	54.7	(12.29)
	DF-27	422	HRD	57.2	(12.86)
	DF-28	425	HRD	60.1	(13.51)
	DF-29	426	HRD	51.8	(11.65)
	DF-30	429	HRD	47.2	(10.62)
	HRD Average			54.2	(12.19)
	Avg.			44.75	(10.1)
	St. Dev.			10.96	(2.5)

Table 45. Ponderosa Pine – Adjusted Peak Force

	Post Test No.	Post Number	Post Category	7.5 in. Diameter Adjusted Peak Force	
				kN	(kips)
Ponderosa Pine	PP-16	502	KNOTS	49.6	(11.16)
	PP-17	505	KNOTS	51.8	(11.65)
	PP-18	506	KNOTS	49.8	(11.20)
	PP-19	508	KNOTS	34.2	(7.69)
	PP-20	510	KNOTS	60.7	(13.65)
	KNOTS Average			49.2	(11.07)
	PP-21	515	BASELINE	52.2	(11.74)
	PP-22	516	BASELINE	61.6	(13.84)
	PP-23	517	BASELINE	42.3	(9.51)
	PP-24	518	BASELINE	63.2	(14.20)
	PP-25	519	BASELINE	51.7	(11.62)
	BASELINE Average			54.2	(12.18)
	PP-26	521	HRD	76.3	(17.16)
	PP-27	526	HRD	63.9	(14.36)
	PP-28	527	HRD	47.1	(10.58)
	PP-29	528	HRD	52.1	(11.71)
	PP-30	530	HRD	40.3	(9.07)
	HRD Average			55.9	(12.58)
	Avg.			53.13	(11.9)
	St. Dev.			10.65	(2.4)

Table 46. Southern Yellow Pine – Adjusted Peak Force

	Post Test No.	Post Number	Post Category	7.0 in. Diameter Adjusted Peak Force	
				kN	(kips)
Southern Yellow Pine	SY-16	602	KNOTS	37.3	(8.39)
	SY-17	604	KNOTS	31.1	(7.00)
	SY-18	605	KNOTS	23.7	(5.32)
	SY-19	606	KNOTS	24.8	(5.57)
	SY-20	610	KNOTS	51.1	(11.49)
	KNOTS Average			33.6	(7.55)
	SY-21	612	BASELINE	20.2	(4.54)
	SY-22	613	BASELINE	45.1	(10.13)
	SY-23	615	BASELINE	40.4	(9.08)
	SY-24	618	BASELINE	48.7	(10.94)
	SY-25	619	BASELINE	38.8	(8.73)
	BASELINE Average			38.6	(8.69)
	SY-26	621	HRD	63.6	(14.30)
	SY-27	622	HRD	36.9	(8.31)
	SY-28	625	HRD	52.4	(11.79)
	SY-29	626	HRD	57.9	(13.02)
	SY-30	627	HRD	58.2	(13.08)
	HRD Average			53.8	(12.10)
	Avg.			42.02	(9.4)
	St. Dev.			13.40	(3.0)

10.2.1 Douglas Fir

The adjusted peak forces for the Douglas Fir tests are shown in Table 44. Once again, the trend continued with the knots category being the weakest and the high ring density category being the strongest.

10.2.2 Ponderosa Pine

Adjusted peak forces for the Ponderosa Pine tests are shown in Table 45. As anticipated, for this species, the category trend is shown with knots as the weakest and high ring density as the strongest.

10.2.3 Southern Yellow Pine

The adjusted peak forces calculated for the Southern Yellow Pine tests are shown in Table 46, and again, the categories rank as anticipated.

11 INTERMEDIATE POST SIZE DETERMINATION

11.1 Overview

After completing the second round of cantilever bogie tests, it was necessary to determine a post diameter in order to proceed with soil bogie tests. The method used to determine this size was a more refined version of the probability method presented previously. Similar to the former method, the new method established a required minimum force capacity of 9.5 kips, which was based on previous post testing. Also similar to the previous method, a 3 percent failure rate was established as an acceptable level of risk for the system to fail due to the failure of four consecutive posts when the system is subjected to the NCHRP Report 350 Test Level-3 criteria.

11.2 Probability Method for Determining Size

A post size had to be determined for each species that would allow each post to have a probability of fracture less than 40 percent. That is, a probability that the post will break, rather than rotate through the soil. Therefore, a strength distribution was needed for each species in order to determine the 40th percentile MOR.

11.2.1 Strength Distribution Model

To develop such a model, a random sample was needed. In the study, the only truly random population sample was tested statically. All the dynamic tests were conducted on posts in subcategories of the population, and the percentage of the population that each category represented was unknown. Therefore, the only data that could be used to construct a population distribution was the random static testing.

The problem with using the static data to construct a distribution was that the strength values that needed to be considered were dynamic strength values, not static strength values. The dynamic strength exceeded the static strength. To account for this, a dynamic magnification

factor was estimated and applied to the random static test results. The dynamic magnification factor was determined based on the testing in the individual subcategories of Baseline, High Ring Density, and Knots. The static and dynamic tests were compared and the ratio between them was determined for each category within each species, as shown in Tables 47 and 48. This adjustment was made for both the first and second round cantilever tests, and the overall average for each species was used as the final magnification factor.

Looking carefully at the data, one will notice that there are some apparent shortcomings in this determination. Clearly, there is a large variability in the dynamic magnification factor and the average MOR values. In some cases such as the round 1 Ponderosa Pine tests, the MOR trend between categories is different for the static and dynamic tests. Another weakness is the arrangement of knots. In the second round, the dynamic tests were completed with the most knotty face as the impact face. This was not the case for the static tests, and likely resulted in a misleadingly low dynamic magnification factor. If this is the case, the shortcoming will result in a low dynamic MOR and hence a high suggested diameter.

The magnification factor was then applied to the static MOR, generating a random sample of dynamic test results that could be used to determine the size of post necessary to resist the soil forces.

Table 47. Dynamic Magnification Factor - Round 1 Bogie Testing

Round 1 Tests			Knots	Baseline	HRD	Average
Ponderosa Pine	Average MOR (ksi)	Static Testing	3.9	4.7	6.65	
		Dynamic Testing	6.5	5.66	9.18	
	Dynamic Magnification Factor		1.67	1.20	1.38	1.42
Douglas Fir	Average MOR (ksi)	Static Testing	6.16	7.04	7.29	
		Dynamic Testing	8.83	7.5	9.5	
	Dynamic Magnification Factor		1.43	1.07	1.30	1.27
Southern Yellow Pine	Average MOR (ksi)	Static Testing	4.995	7.845	10.9154	
		Dynamic Testing	7.01	7.34	12.24	
	Dynamic Magnification Factor		1.40	0.94	1.12	1.15

Table 48. Dynamic Magnification Factor - Round 2 Bogie Testing

Round 2 Tests			Knots	Baseline	HRD	Average	Overall Average
Ponderosa Pine	Average MOR (ksi)	Static Testing	5.069	5.069	6.607		
		Dynamic Testing	6.65	7.32	7.55		
	Dynamic Magnification Factor		1.31	1.44	1.14	1.30	1.36
Douglas Fir	Average MOR (ksi)	Static Testing	5.775	6.047	9.112		
		Dynamic Testing	7.22	7.61	10.04		
	Dynamic Magnification Factor		1.25	1.26	1.10	1.20	1.24
Southern Yellow Pine	Average MOR (ksi)	Static Testing	5.086	5.628	10.274		
		Dynamic Testing	5.58	6.42	8.94		
	Dynamic Magnification Factor		1.10	1.14	0.87	1.04	1.09

Values presented in Table 47 include the inertial effects found in the first round of testing which may overestimate the dynamic magnification factors. To account for this, the inertial spikes were removed from the data and the dynamic magnification factors were re-calculated and are presented in Table 49.

Table 49. Dynamic Magnification Factor Excluding Inertial Effects

Round 1 Tests			Knots	Baseline	HRD	Average	Overall Average
Ponderosa Pine	Average MOR (ksi)	Static Testing	3.9	4.7	6.65		
		Dynamic Testing	5.6	5.4	8.8		
	Dynamic Magnification Factor		1.44	1.15	1.32	1.30	1.30
Douglas Fir	Average MOR (ksi)	Static Testing	6.16	7.04	7.29		
		Dynamic Testing	8.4	6.3	9.5		
	Dynamic Magnification Factor		1.36	0.89	1.30	1.19	1.20
Southern Yellow Pine	Average MOR (ksi)	Static Testing	4.995	7.845	10.9154		
		Dynamic Testing	6.32	7.18	12.24		
	Dynamic Magnification Factor		1.27	0.92	1.12	1.10	1.07

With the unknown effects of the inertia spike on the fracture of the post discussed in Chapter 7, the lower dynamic magnification factors may predict dynamic strengths that are below the actual capacity of the posts. However, actual dynamic strengths may be overestimated by the inclusion of the inertial effects. In addition, the dynamic magnification factors calculated from the second round of testing may also underestimate actual dynamic strengths, as discussed previously.

Therefore, both sets of dynamic magnification factors were used in the subsequent calculations. Since the two effects likely offset one another, the results based on the original magnification factors, including inertial effects, are presented within the text. The results based on the modified magnification factors, excluding inertial effects, are presented in Appendix F. The final size recommendation, excluding inertial effects, increased the target diameter for Ponderosa Pine by 6.35 mm (0.25 in.), but did not change the Douglas Fir results.

With this dynamic adjustment completed, there was still one stipulation that was unaccounted for, the grading criteria. Clearly, if all grades of posts were eligible to be used in the system, the average MOR would be lowered significantly. This in turn would increase the required post diameter. Therefore, it was decided that a grading criteria should be established to

specify the minimum post quality that was acceptable for use in the system. The grading criteria needed to be strict enough to assure a high quality, and therefore a relatively small post size, but lax enough to include a large enough percentage of the population that it remained economical to produce the posts.

The final grading criteria were determined by investigating the effects on the average MOR of removing a portion of the posts within each species that failed to meet a certain grading criteria. For instance, within the Ponderosa Pine species, removing the posts with knots exceeding 102 mm (4 in.) in diameter and ring densities less than or equal to 6 rings-per-inch, raised the average MOR by 2 percent, increased its standard deviation by 6 percent, and only eliminated 8 percent of the population. For Douglas Fir, the criteria raised the MOR by 3 percent, decreased the standard deviation by 8 percent, and eliminated 17 percent of the population. The final criteria are presented below.

Douglas Fir:

- Maximum 2 in. diameter knot size.
- Ring density of 6 rings-per-inch or more.

Ponderosa Pine:

- Maximum 4 in. diameter knot size.
- Ring density of 6 rings-per-inch or more.

Southern Yellow Pine:

- Maximum 2 ½ in. diameter knot size.
- Rings density of 4 rings-per-inch or more.

After the grading criteria were specified, the random samples were sorted to exclude those posts that would not have fallen into the acceptable range. The remaining acceptable

samples made up the target population and were used to develop a strength distribution that was in turn used to determine the acceptable diameters. Distribution plots for both the random population sample and the target population sample are shown in Figures 45, 46, and 47 for a generated sample of 1000 posts each. Static MOR, dynamic MOR, and the respective standard deviations are shown in Tables 50 and 51 for the random and target populations of each species.

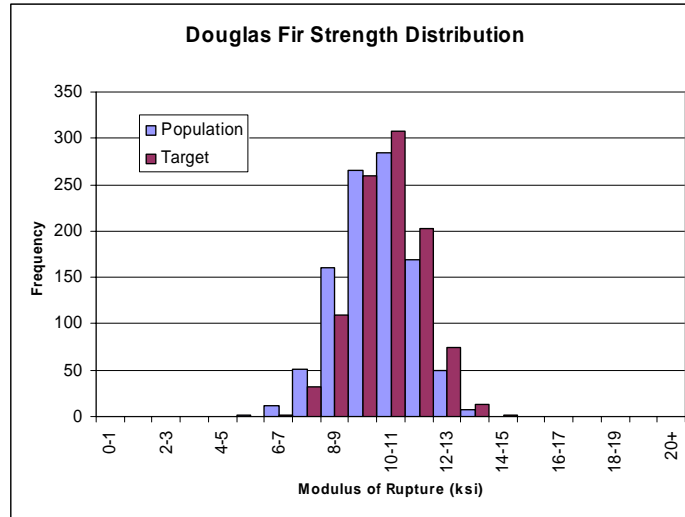


Figure 45. Douglas Fir Population and Target Population Strength Distribution

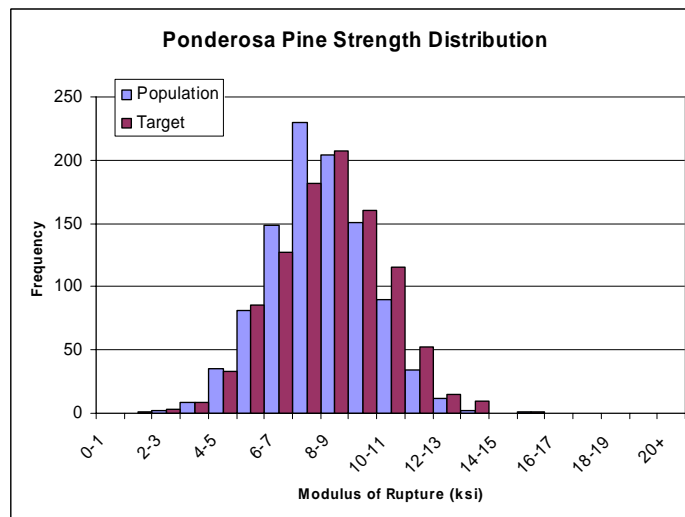


Figure 46. Ponderosa Pine Population and Target Population Strength Distribution

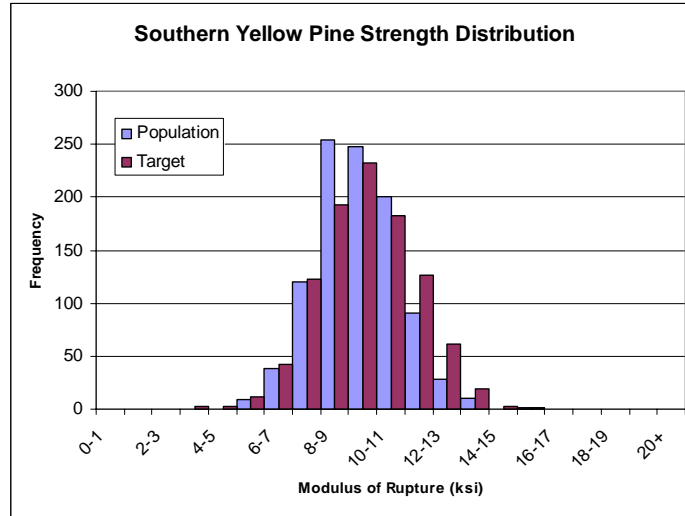


Figure 47. Southern Yellow Pine Population and Target Population Strength Distribution

It is clear from the two figures and tables that the target population has a higher mean MOR than the general population. This is reasonable since the target population excludes some posts which fall at the lower end of the population distribution in terms of quality. From Tables 50, 51, and 52, it is apparent that the target category for Ponderosa Pine was less of an improvement than that for Douglas Fir. With the MOR increasing by only 0.9 MPa (0.13 ksi), and the standard deviation increasing, the minimum diameter calculated for the population and the target population may be very similar, as will be discussed in Section 11.2.2. However, it is important to maintain some minimum grading criteria so that timber producers will not allow poorer and poorer material into the manufacturing process.

Table 50. Douglas Fir Random Sample Testing Results

Douglas Fir				
Sample	Static Testing Results		Adjusted Dynamic Results	
	Mean MOR (ksi)	Standard Deviation (ksi)	Mean MOR (ksi)	Standard Deviation (ksi)
Random Population Sample	8.10	1.07	10.00	1.33
Target Population Sample			10.34	1.22

Table 51. Ponderosa Pine Random Sample Testing Results

Ponderosa Pine				
Sample	Static Testing Results		Adjusted Dynamic Results	
	Mean MOR (ksi)	Standard Deviation (ksi)	Mean MOR (ksi)	Standard Deviation (ksi)
Random Population Sample	5.95	1.33	8.09	1.81
Target Population Sample			8.22	1.93

Table 52. Southern Yellow Pine Random Sample Testing Results

Southern Yellow Pine				
Sample	Static Testing Results		Adjusted Dynamic Results	
	Mean MOR (ksi)	Standard Deviation (ksi)	Mean MOR (ksi)	Standard Deviation (ksi)
Random Population Sample	8.57	1.40	9.30	1.50
Target Population Sample			9.64	1.70

11.2.2 Minimum Size Determination

The proper minimum size was then determined using elastic bending equations and the estimated MOR. As stated previously, 60 percent of the posts must withstand an impact force of 42 kN (9.5 kips) at a height of 632 mm (24.875 in.), or a bending moment capacity of 26.7 kN-m (236 kip-in.). This meant that the post diameter needed to be selected so a post with an ultimate strength equal to the 40 percent MOR value would have a moment capacity of 26.7 kN-m (236 kip-in.). The equation used to determine the diameter was a form of the simple elastic bending stress equation and is shown below.

$$d = \sqrt[3]{\frac{(32)(L)(P)}{(\pi)(40\% \text{ MOR})}}$$

where L = Impact Height, 632 mm (24.875 in.)
P = Minimum Impact Force, 42 kN (9.5 kips)
d = Required Diameter

Mean MOR, standard deviation, 40 percent MOR, and the calculated minimum diameter are shown in Table 53 for the three species graded populations. Final minimum diameter values

were rounded up from the values shown to the nearest quarter of an inch for manufacturing purposes.

Table 53. Minimum Diameter Calculation

	Douglas Fir		Ponderosa Pine		Southern Yellow Pine	
	MPa	(ksi)	MPa	(ksi)	MPa	(ksi)
Mean MOR	71.29	(10.34)	56.67	(8.22)	66.47	(9.64)
Standard Deviation	8.41	(1.22)	13.31	(1.93)	11.72	(1.70)
40% MOR	69.15	(10.03)	53.3	(7.73)	63.50	(9.21)
Minimum Diameter	158 mm	(6.21 in.)	172 mm	(6.78 in.)	162 mm	(6.39 in.)

As alluded to, the minimum calculated diameter for the Ponderosa Pine population was 173 mm (6.8 in.), only 0.5 mm (0.02 in.) larger than the target population. Although this is the case, the minimum grading criteria needs to remain for quality assurance purposes as discussed in Section 11.2.1.

The minimum diameter was determined, and an acceptable range and target diameter needed to be established. The range of acceptable post diameters was set at 1 in. to allow some tolerance in the manufacturing process. The lower bound of the range was set at the minimum diameter, and the target diameter was set 6.4 mm (0.25 in.) above the lower bound. The calculated diameters are shown below. The minimum diameter for each species was 12.7 mm (0.5 in.) less than the diameter recommended previously.

Douglas Fir:

$$165 \text{ mm} \begin{matrix} +19 \text{ mm} \\ -6 \text{ mm} \end{matrix} \left(\begin{matrix} 6.5 \text{ in.} + 0.75 \text{ in.} \\ -0.25 \text{ in.} \end{matrix} \right)$$

Ponderosa Pine:

$$184 \text{ mm} \begin{matrix} +19 \text{ mm} \\ -6 \text{ mm} \end{matrix} \left(\begin{matrix} 7.25 \text{ in.} + 0.75 \text{ in.} \\ -0.25 \text{ in.} \end{matrix} \right)$$

Southern Yellow Pine

$$171 \text{ mm} \begin{matrix} +19 \text{ mm} \\ -6 \text{ mm} \end{matrix} \left(\begin{matrix} 6.75 \text{ in.} + 0.75 \text{ in.} \\ -0.25 \text{ in.} \end{matrix} \right)$$

Target values were specified simply to give producers a size that was above the minimum requirement. The actual target diameter could have been selected as any value within the range and was much less important than the range itself. Although post producers will attempt to find posts meeting the target diameter, when few are available, they will inevitably select posts from their stockpile that fall anywhere within the specified range.

Rounding the minimum diameter up to the nearest ¼ in. resulted in a probability of failure for each post that was lower than originally suggested. For 159-mm (6.25-in.) Douglas Fir posts, the probability of failure was just over 35 percent, 5 percent lower than desired. For Ponderosa Pine, the increase to 178 mm (7 in.) lowered the probability of failure to 27 percent, 13 percent lower than what was needed. The probability of failure for Southern Yellow Pine was between the two at 30 percent. These adjustments also increase the reliability of the guardrail system. For a Douglas Fir system, the probability of failure, due to four consecutive failed posts, with 159-mm (6.25-in.) diameter posts was about 1.5 percent. For guardrail systems using either 178-mm (7-in.) diameter Ponderosa Pine posts or 165-mm (6.5-in.) diameter Southern Yellow Pine posts, the probability of failure was less than 1 percent.

Finally, allowing posts with diameters larger than the target values significantly reduces the probability of failure for each post and the system. For instance, the probability that a 178-mm (7-in.) diameter Douglas Fir post will fail is 0.4 percent, leading to a very small probability that the system will fail due to the failure of the posts. The same is true for Ponderosa Pine in which a 197-mm (7.75-in.) diameter post has a probability of failure just under 6 percent. This also corresponds to a very small system failure probability.

12 PHYSICAL TESTING – SOIL BOGIE TESTING

12.1 Scope

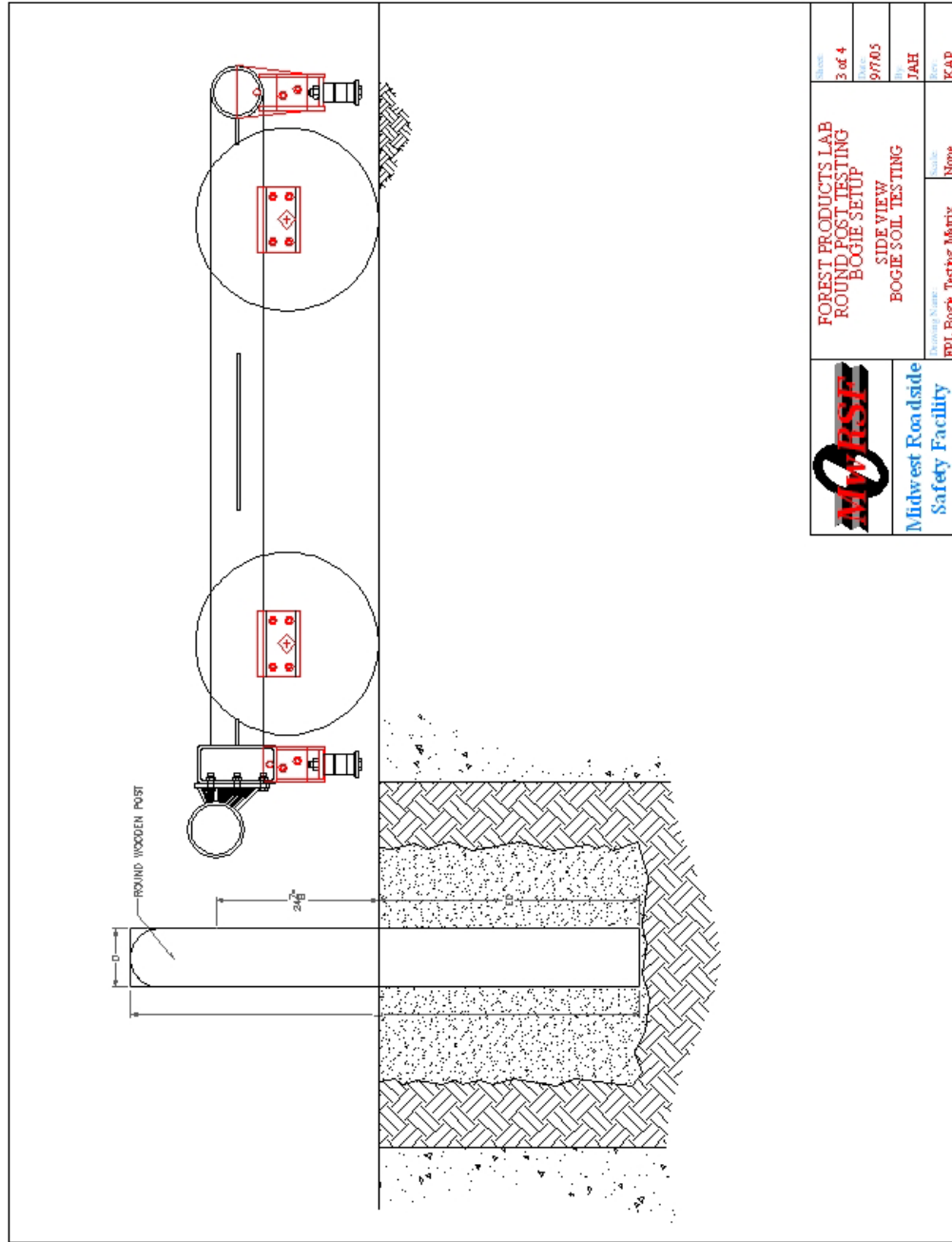
After determining the minimum diameter required for the posts to rotate in soil rather than fracture, soil bogie tests were completed to verify the results. Initially, a total of six soil tests were completed for Douglas Fir and Ponderosa Pine, three for each species. A 1,016-mm (40-in.) embedment depth, the standard embedment depth for the MGS system, was used as the starting point for the first two tests of each species. The tests were conducted at approximately 11.2 m/s (25 mph). This velocity was chosen so the kinetic energy of the bogie exceeded the energy absorbed in the previous soil-post tests which were used to determine the approximate peak load. Prior to testing, the moisture content and diameter of each post was measured and recorded. The soil bogie test setup is shown in Figure 48.

For the preliminary soil tests, the species of the posts was ignored, assuming that the behavior of a 203-mm (8-in.) diameter Ponderosa Pine post and a 203-mm (8-in.) Southern Yellow Pine post will be the same as long as neither post fractures. Therefore, the species of the post did not always correspond to the test name. Based on the same reasoning, the posts were not soaked in water as soaking the wood material should not have affected the soil response.

12.2 Results

The raw data was once again acquired using a triaxial piezoresistive accelerometer system recording at 3,200 Hz, three pressure tape switches, and a series of cameras including two high speed VITcam digital video cameras, and a JVC digital video camera.

The data was processed using the same methods used in the cantilever sleeve tests. The end of the test was determined as the most appropriate of the first, second, or third time the acceleration trace crossed the X-axis from positive to negative. Summaries of the results for all




	FOREST PRODUCTS LAB		3 of 4
	ROUND POST TESTING		97765
	BOGIE SETUP		IAH
	SIDE VIEW		KAP
Midwest Roadside Safety Facility		BOGIE SOIL TESTING	
FPL Bogie Testing Matrix		None	

Figure 48. Soil Bogie Test Setup

of the soil tests are presented in Table 54 and Table 55, with complete results for each test presented in Appendix G.

The energy and deflection quantities were estimated at three times throughout the tests, the time corresponding to the peak force, the time corresponding to 381 mm (15 in.) of deflection, and at the end of the test. Data was provided at 381 mm (15 in.) deflection because previous studies have shown that the rail typically separates from the post at this deflection, thus making the post largely ineffective beyond this point.

12.2.1 Ponderosa Pine

As shown in Table 54, the first two Ponderosa Pine tests, PP-31 and 32, ended in post fracture and absorbed a very small amount of energy as compared with previous soil tests. When this occurred, the embedment depth for the third test, PP-33, was reduced to 940 mm (37 in.), but the post still fractured.

Analyzing the data showed that the peak force averaged 48.7 kN (11.0 kips), with the highest peak reaching 52.2 kN (11.7 kips). This average peak force would produce a maximum stress of 53 MPa (7.7 ksi), which was still less than the average MOR for the species. However, 41 percent of the post population was weaker than this, which implied that all three posts were in the lower 41 percent of the distribution.

The 48.7 kN (11.0 kips) average was 15 percent higher than the anticipated 42 kN (9.5 kips), suggesting that the posts were undersized. This high force peak may have been due to the differences in the cross-sections of the round wooden posts and the NPGb tests used to estimate the force. Although their round cross-section should more easily cut through the soil, the wooden posts were wider than the steel posts, counter acting the effects of the shape. The wooden posts likely also had different surface interactions with the soil as compared to steel

Table 54. Soil Bogie Test Overview

	Post Test No.	Test Date	Species	In Soil Diameter mm (in.)	Embedment Depth mm (in.)	Moisture Content (%)	Impact Velocity m/s (mph)	Final Post Status
Ponderosa Pine	PP-31	9/16/2005	PP	183.76 (7.24)	1016 (40.00)	29	11.7 (26.2)	Fractured
	PP-32	9/19/2005	PP	184.77 (7.28)	1016 (40.00)	48	10.9 (24.5)	Fractured
	PP-33	9/29/2005	SYP	185.93 (7.32)	940 (37.00)	10	11.5 (25.7)	Fractured
			Avg.	184.82 (7.28)		29	11.4 (25.5)	
			St. Dev.	1.09 (0.04)		19	0.4 (0.9)	
	PP-34	11/7/2005	PP	202.44 (7.97)	940 (37.00)	25	10.9 (24.3)	Rotated
	PP-35	11/7/2005	PP	200.66 (7.90)	940 (37.00)	24	11.3 (25.3)	Rotated
	PP-36	11/7/2005	PP	199.14 (7.84)	940 (37.00)	20	10.6 (23.8)	Rotated
	PP-37	11/7/2005	PP	194.06 (7.64)	940 (37.00)	23	11.2 (25.1)	Rotated
			Avg.	199.07 (7.84)		23	11.0 (24.6)	
Douglas Fir			St. Dev.	3.61 (0.14)		2	0.3 (0.7)	
	DF-31	9/19/2005	SYP	165.48 (6.52)	1016 (40.00)	17	11.1 (24.8)	Rotated
	DF-32	9/19/2005	PP	165.48 (6.52)	1016 (40.00)	15	10.9 (24.4)	Fractured
	DF-33	9/23/2005	SYP	168.28 (6.63)	940 (37.00)	17	10.8 (24.2)	Fractured
			Avg.	166.41 (6.56)		16	10.9 (24.4)	
			St. Dev.	1.61 (0.06)		1	0.1 (0.3)	
	DF-34	10/4/2005	DF	181.86 (7.16)	940 (37.00)	15	11.2 (25.1)	Rotated
	DF-35	10/5/2005	DF	180.34 (7.10)	940 (37.00)	19	11.5 (25.7)	Rotated
	DF-36	10/5/2005	DF	175.26 (6.90)	940 (37.00)	18	11.1 (24.8)	Fractured
			Avg.	179.15 (7.05)		17	11.3 (25.2)	
Southern Yellow Pine			St. Dev.	3.46 (0.14)		2	0.2 (0.4)	
	SY-31	12/16/2005	SYP	186.44 (7.34)	940 (37.00)	21	10.9 (24.3)	Fractured
	SY-32	12/16/2005	SYP	185.17 (7.29)	940 (37.00)	30	11.4 (25.4)	Rotated
	SY-33	12/16/2005	SYP	183.90 (7.24)	940 (37.00)	25	11.6 (26.0)	Rotated
			Avg.	185.17 (7.29)		25	11.3 (25.3)	
			St. Dev.	1.27 (0.05)		5	0.4 (0.9)	
	RWP-1	9/29/2005	SYP	152 x 203 (6 x 8)	940 (37.00)	NA	11.6 (25.9)	Rotated
	RWP-2	9/29/2005	SYP	152 x 203 (6 x 8)	1016 (40.00)	NA	11.2 (25.2)	Rotated
			Avg.	152 x 203 (6 x 8)	(38.50)	NA	7.7 (17.3)	
			St. Dev.		(2.12)	NA	6.4 (14.3)	

Table 55. Soil Bogie Test Results Summary

	Post Test No.	Peak Force						381 mm (15 in.) Deflection			Final					
		Time ms	Force kN	Force (kips)	Deflection mm	Deflection (in.)	Energy kJ	Energy (kip-in.)	Time ms	Energy kJ	Energy (kip-in.)	Time ms	Deflection mm	Deflection (in.)	Energy kJ	Energy (kip-in.)
Ponderosa Pine	PP-31	11.9	50.5	(11.3)	137	(5.4)	4.22	(37.4)	34.7	9.63	(85.3)	57.2	618	(24.3)	10.17	(90.0)
	PP-32	6.3	43.6	(9.8)	68	(2.7)	1.20	(10.6)	N/A	N/A	N/A	29.4	312	(12.3)	3.34	(29.6)
	PP-33	5.6	52.2	(11.7)	64	(2.5)	1.44	(12.8)	35.3	11.20	(99.2)	102.8	969	(38.1)	24.34	(215.4)
	Avg.	7.9	48.7	(11.0)	90	(3.5)	2.29	(20.3)	35.0	10.42	(92.2)	63.1	633	(24.9)	12.62	(111.7)
	St. Dev.	3.5	4.6	(1.0)	41	(1.6)	1.68	(14.9)	0.4	1.11	(9.8)	37.1	329	(12.9)	10.71	(94.8)
	PP-34	5.6	93.6	(21.0)	61	(2.4)	2.60	(23.0)	38.8	14.39	(127.3)	136.6	1059	(41.7)	29.37	(259.9)
	PP-35	5.3	76.0	(17.1)	60	(2.3)	2.00	(17.7)	35.9	9.65	(85.4)	147.8	1322	(52.0)	26.41	(233.8)
Douglas Fir	PP-36	5.3	88.4	(19.9)	56	(2.2)	2.28	(20.2)	38.1	7.52	(66.6)	130.0	1179	(46.4)	17.88	(158.2)
	PP-37	5.3	62.2	(14.0)	59	(2.3)	1.74	(15.4)	35.6	6.69	(59.2)	149.1	1401	(55.2)	21.44	(189.7)
	Avg.	5.4	80.0	(18.0)	59	(2.3)	2.16	(19.1)	37.1	9.56	(84.6)	140.9	1240	(48.8)	23.77	(210.4)
	St. Dev.	0.1	14.0	(3.1)	2	(0.1)	0.37	(3.3)	1.6	3.45	(30.5)	9.2	152	(6.0)	5.12	(45.3)
	DF-31	5.9	40.9	(9.2)	65	(2.6)	1.21	(10.7)	36.6	10.62	(94.0)	177.5	1346	(53.0)	33.25	(294.3)
	DF-32	5.9	57.1	(12.8)	64	(2.5)	1.62	(14.3)	N/A	N/A	N/A	35.6	376	(14.8)	3.60	(31.9)
	DF-33	6.3	57.1	(12.8)	67	(2.6)	1.64	(14.5)	36.9	6.53	(57.8)	60.0	608	(23.9)	7.75	(68.6)
Southern Yellow Pine	Avg.	6.0	51.7	(11.6)	66	(2.6)	1.49	(13.2)	36.8	8.58	(75.9)	91.0	777	(30.6)	14.87	(131.6)
	St. Dev.	0.2	9.3	(2.1)	1	(0.1)	0.24	(2.1)	0.2	2.89	(25.6)	75.9	506	(19.9)	16.05	(142.1)
	DF-34	6.3	81.9	(18.4)	70	(2.7)	2.49	(22.0)	36.3	9.43	(83.5)	151.9	1344	(52.9)	25.56	(226.3)
	DF-35	5.6	52.8	(11.9)	64	(2.5)	1.59	(14.1)	35.9	14.25	(126.1)	144.7	1202	(47.3)	32.14	(284.5)
	DF-36	5.3	50.1	(11.3)	59	(2.3)	1.34	(11.8)	36.9	12.64	(111.9)	69.1	682	(26.8)	14.01	(124.0)
	Avg.	5.7	61.6	(13.9)	64	(2.5)	1.80	(16.0)	36.4	12.11	(107.2)	121.9	1076	(42.4)	23.90	(211.6)
	St. Dev.	0.5	17.6	(4.0)	5	(0.2)	0.61	(5.4)	0.5	2.45	(21.7)	45.9	349	(13.7)	9.18	(81.2)
Southern Yellow Pine	SY-31	5.3	53.6	(12.1)	57	(2.3)	1.48	(13.1)	36.6	6.32	(55.9)	91.2	898	(35.3)	13.95	(123.4)
	SY-32	5.6	68.2	(15.3)	64	(2.5)	1.94	(17.2)	35.0	6.86	(60.7)	143.3	1417	(55.8)	18.84	(166.8)
	SY-33	5.6	69.4	(15.6)	65	(2.6)	1.99	(17.6)	34.4	7.86	(69.6)	139.1	1338	(52.7)	24.80	(219.5)
	Avg.	5.5	63.7	(14.3)	62	(2.4)	1.80	(16.0)	35.3	7.01	(62.1)	124.5	1218	(47.9)	19.20	(169.9)
	St. Dev.	0.2	8.8	(2.0)	4	(0.2)	0.28	(2.5)	1.1	0.78	(6.9)	28.9	280	(11.0)	5.44	(48.1)
	RWP-1	5.3	69.7	(15.7)	61	(2.4)	2.03	(17.9)	35.6	13.86	(122.7)	119.7	1076	(42.4)	27.95	(247.3)
	RWP-2	40.3	62.7	(14.1)	405	(15.9)	19.57	(173.2)	37.5	18.07	(160.0)	145.9	975	(38.4)	40.57	(359.0)
Southern Yellow Pine	Avg.	15.3	66.2	(14.9)	157	(6.2)	7.29	(95.6)	36.6	15.97	(141.3)	98.2	777	(30.6)	24.65	(218.2)
	St. Dev.	21.8	5.0	(1.1)	217	(8.5)	10.67	(94.4)	1.3	2.98	(26.3)	61.4	433	(17.1)	17.80	(157.5)

posts due to the roughness of the wood grain. Finally, differences in the soil gradation, amount of soil compaction, and methods used to compact the soil could have had some effect on the results.

12.2.2 Douglas Fir

Unlike the Ponderosa Pine tests, one of the first two Douglas Fir tests ended in soil failure, with the rotation of the post absorbing 33.25 kJ (294.3 kip-in.) of energy, as shown in Table 55. Since one of the posts did fail, a reduced embedment depth of 940 mm (37 in.) was also tried for the Douglas Fir posts, and as in the Ponderosa Pine test, this shallower post fractured rather than rotating.

With a 51.7 kN (11.6 kips) average peak load for the first three tests, the data analysis again suggested that the peak forces in the soil tests were higher than anticipated. Unlike Ponderosa Pine, the average peak force for Douglas Fir corresponded to a maximum bending stress that exceeded the average MOR, suggesting that over half of the post population should have failed.

The average peak force exceeded the predicted load by 22 percent, and the highest of the peaks reached 57.1 kN (12.8 kips), exceeding the prediction by nearly 35 percent. The results suggested the Douglas Fir posts were also too small. Again, the increased force was likely due to differences in cross-section, surface friction, and soil compaction between the NPGB and round wooden post tests.

In order for the posts to rotate through the soil, one of two changes needed to be made. The first option was to decrease the force required for the post to move through the soil. The second option was to increase the force required to break the post. A decreased soil force could be reached by reducing the post embedment depth from 940 mm (37 in.) to 864 mm (34 in.) or

less, but doing so might have caused the posts to be pulled out of the soil before they were allowed to rotate through the soil. This behavior was observed by Kuipers and Reid in their NPGb post study, in which the W152x23.8 (W6x16) steel posts began pulling out of the soil at an embedment depth of 940 mm (37 in.). The study showed that the posts which had pulled out of the soil absorbed less energy than those that did not. The pullout phenomenon was not observed in the round wood post testing, but reducing the embedment depth further, may well have led to the same problem.

To increase the post breaking force, the grading criteria could be tightened, allowing only top quality posts to be installed in the system, or the diameter of the posts could be increased. Tightening the grading criteria would eliminate a larger percentage of the posts, making the system more and more expensive to construct. Increasing the diameter would increase the soil resistance and also the post rotation force which already exceeded the optimal force level of 42.3 kN (9.5 kips) for MGS.

Although a reduced post embedment depth could have been tested, the results of such testing would not have been conclusive. In the strong soil used for the testing, post pull-out may not have occurred even at the reduced embedment depth. In the weaker soils that are found in the majority of the guardrail installation locations, the posts may pull-out of the soil with a much lower resistance. Therefore, testing at a reduced embedment depth might not have accurately predicted the potential for post pull-out.

Of the two remaining options, adjusting the grading criteria was avoided to keep the cost of the guardrail system as low as possible and allow the highest percentage of forest thinning material to be used. The final option, increasing the post diameter, was selected although the

impact force exceeded the optimum level. Choosing this option, the system would still function adequately.

12.3 Re-Evaluation of Post Size

After the initial soil bogie tests showed that the selected diameter for the two species was too small, the size was re-evaluated. Once again, the refined probability method was employed. The anticipated peak force was increased to 53 kN (12 kips) for the Douglas Fir and Southern Yellow Pine samples, and 58 kN (13 kips) for the Ponderosa Pine samples. The anticipated force level was higher for the Ponderosa Pine species to account for the larger diameter. The larger diameter would require greater force to move more soil, thus creating a flatter cross-section that was more resistant to soil rotation. In addition, a more realistic soil pressure distribution was used to determine the maximum moment in the post. The assumed soil distribution was based on a study conducted by Goeller at MwRSF [22]. Goeller found that the soil distribution shown in Figure 49 was the most accurate. However, it did not exactly match the results of the round post testing.

In the initial soil testing, the fracture surface ranged from 51 mm (2 in.) to 203 mm (8 in.) lower than those found in the cantilever tests, and averaged about 102 mm (4 in.) below the ground. Assuming this would also be the location of the maximum moment, the soil pressure distribution needed to be adjusted to reflect this. The second check that was made was to determine the rotation point of a round post during a soil test. Similar to Goeller's results, the rotation point was approximately 305 mm (12 in.) below the ground. Therefore, the soil pressure switched directions at 305 mm (12 in.) below the ground as before. The pressure distribution was adjusted so that the maximum moment was approximately 102 mm (4 in.) below the surface, which corresponded to the fracture surface. The adjusted distribution is shown in Figure 50.

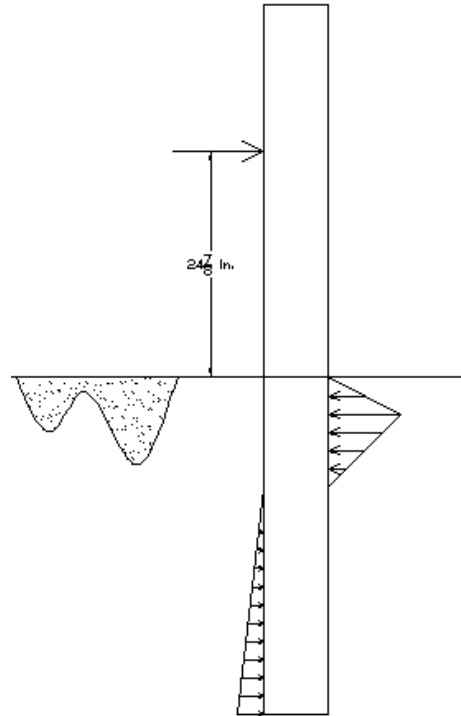


Figure 49. Initial Soil Pressure Distribution [22]

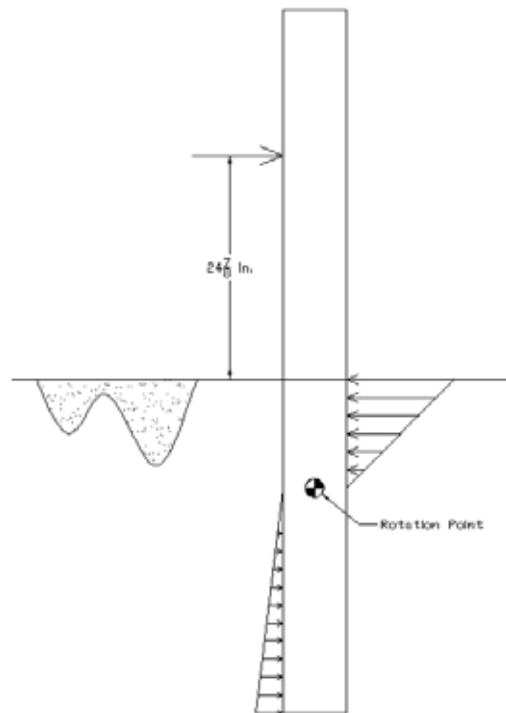


Figure 50. Soil Force Distribution

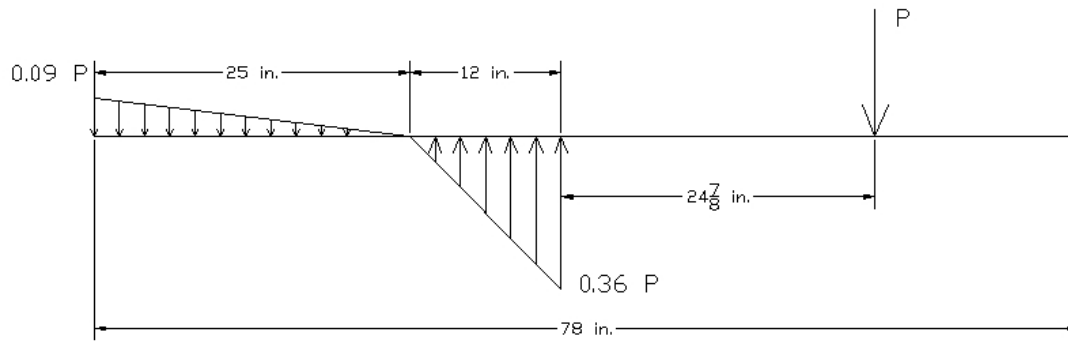


Figure 51. Post Free-Body Diagram

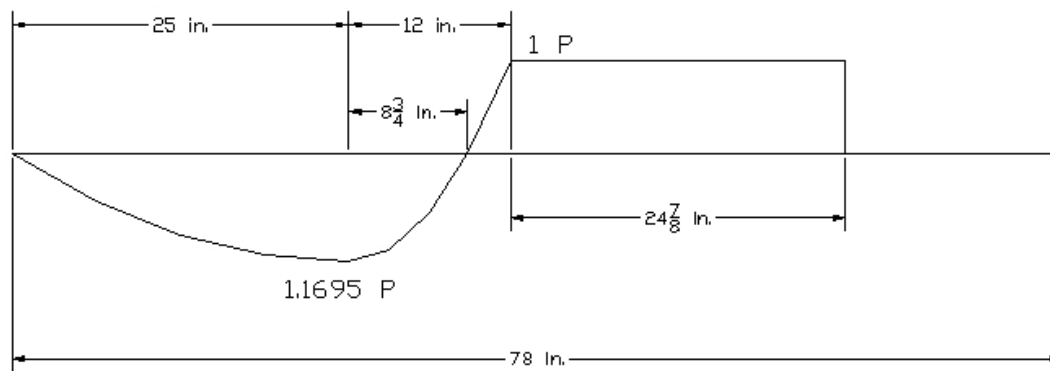


Figure 52. Post Shear Force Diagram

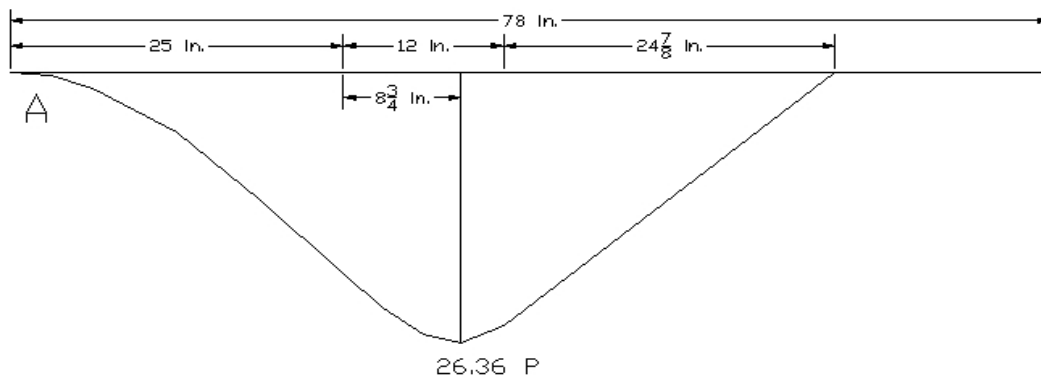


Figure 53. Post Bending Moment Diagram

The modified pressure distribution effectively increased the maximum moment by 6 percent from (24.875)(P) kip-in. to (26.387)(P) kip-in., as shown in Figure 53, where P was the peak load in kips at the impact height. It should be noted that the actual soil pressure distribution and rotation point vary with each individual test and depend on numerous factors such as soil compaction, soil moisture content, and embedment depth. Many soil pressure distribution models have been developed, but the distribution shown in Figure 50 seemed to fit the post fracture results the most closely.

With the increased peak force and modified pressure distribution, the probability method returned minimum diameter values of 174 mm (6.85 in.) for Douglas Fir, 195 mm (7.67 in.) for Ponderosa Pine, and 179 mm (7.04 in.) for Southern Yellow Pine. Rounding to the next highest quarter inch, the acceptable ranges of post sizes were determined as follows.

Douglas Fir:

$$184 \text{ mm} \begin{matrix} +19 \text{ mm} \\ -6 \text{ mm} \end{matrix} \left(\begin{matrix} 7.25 \text{ in.} + 0.75 \text{ in.} \\ -0.25 \text{ in.} \end{matrix} \right)$$

Ponderosa Pine:

$$203 \text{ mm} \begin{matrix} +19 \text{ mm} \\ -6 \text{ mm} \end{matrix} \left(\begin{matrix} 8.00 \text{ in.} + 0.75 \text{ in.} \\ -0.25 \text{ in.} \end{matrix} \right)$$

Southern Yellow Pine

$$190 \text{ mm} \begin{matrix} +19 \text{ mm} \\ -6 \text{ mm} \end{matrix} \left(\begin{matrix} 7.5 \text{ in.} + 0.75 \text{ in.} \\ -0.25 \text{ in.} \end{matrix} \right)$$

12.4 Results – Additional Soil Tests

As shown in Table 54, additional tests were conducted on posts with diameters exceeding the new minimum calculated diameter. An embedment depth of 940 mm (37 in.) was chosen for the tests, and the impact speed of 11.2 m/s (25 mph) remained the same. Since the majority of

the posts fractured in the previous tests, the decision was made to use the species of wood corresponding to the test name, unlike the initial soil tests.

12.4.1 Douglas Fir

Three additional tests were conducted for Douglas Fir, with Table 55 showing the results. The diameters for the three posts were 182 mm (7.16 in.), 180 mm (7.10 in.), and 175 mm (6.9 in.). Both tests conducted on posts with diameters within the acceptable range ended successfully with soil failure. However, test DF-36 did not result in soil failure, but rather post fracture. Although 175 mm (6.9 in.) did exceed the minimum suggested diameter of 174 mm (6.85 in.), the failure should not be alarming. The probability that such a post would fail under a 50.1 kN (11.3 kip) peak load was 19 percent. It seems reasonable that this specific post could have fallen within the 19 percent that should fail.

The energy absorbed by the post rotation at 381 mm (15 in.) ranged from 9.43 kJ (83.5 kip-in.) to 14.25 kJ (126.1 kip-in.), and averaged 12.11 kJ (107.2 kip-in.). In comparison, these values were lower than the energy absorbed by standard 152 mm x 203 mm (6 in. x 8 in.) rectangular wood posts, shown in Table 55, but higher than the standard W152x13.4 (W6x9) steel posts used in the MGS system [27]. Similar to Ponderosa Pine, this suggests that the dynamic deflection of the Midwest Guardrail System with Douglas Fir posts would be less than the same system utilizing standard steel posts, but more than a system utilizing rectangular wood posts of the same length.

12.4.2 Ponderosa Pine

Four additional soil tests were conducted for the Ponderosa Pine species. Post specifications are shown in Table 54, and results are shown in Table 55. Clearly for this series of tests, the energy absorbed was found to increase for barrier deflections through 381 mm (15 in.)

and with increasing post diameter. The smallest post, 194 mm (7.64 in.) diameter, fell outside the acceptable range, but still ended in soil failure.

The absorbed energy after 381 mm (15 in.) of deflection was as small as 6.69 kJ (59.2 kip-in.) and as high as 14.39 kJ (127.3 kip-in.), higher than any of the other soil tests. The average energy was 9.56 kJ (84.6 kip-in.), which was lower than the 13.9 kJ (122 kip-in.) absorbed by a standard 152 mm x 203 mm (6 in. x 8 in.) rectangular wood post embedded at 940 mm (37 in.), tested at MwRSF in September 2005. The average was also lower than the 10.5 kJ (92.5 kip-in.) of energy absorbed by standard W152x13.4 (W6x9) steel posts embedded at 940 mm (37 in.) [27]. This suggests that an MGS system utilizing round Ponderosa Pine posts would deflect more than a system constructed with steel posts or rectangular wood posts.

Clearly, there were significant differences in energy absorption between the Douglas Fir and Ponderosa Pine samples, with the average energy absorbed by the Ponderosa Pine posts less than 80 percent of that by Douglas Fir posts. There was also a large amount of variation between tests within the Ponderosa Pine species. At 381 mm (15 in.) of deflection, test no. PP-34 had absorbed more than twice the energy absorbed in test no. PP-37.

The differences in the testing were not consistent, nor entirely explainable by theory. Larger diameter posts should generate larger soil forces, but this was not always the case. Therefore, the differences must be attributed to other testing variables such as soil variation. The soil gradation, soil moisture content, amount of soil compaction, and method of soil compaction could all have made significant differences in the post-soil interaction, and therefore effect the post-soil forces.

12.4.3 Southern Yellow Pine

Three Southern Yellow Pine tests were conducted on posts of 186-mm (7.34-in.), 185-mm (7.29-in.), and 184-mm (7.24-in.) diameters. The two smaller diameter posts rotated through the soil, while the larger diameter post fractured. Although this may seem alarming, the larger post may have fallen in the lower spectrum of post strength causing it to fail at a lower stress value.

The energy absorbed by the post rotation through 381 mm (15 in.) ranged from 6.32 kJ (55.9 kip-in.) to 7.86 kJ (69.6 kip-in.), with an average of 7.01 kJ (62.1 kip-in.). Comparing these values to those of the other two species shows that Southern Yellow Pine resulted in the lowest average energy absorption even though the diameters of the posts were larger than those for Douglas Fir. These results suggest that there may be significant variation in the soil compaction techniques and procedures; however, this variability is also likely to exist in installed systems.

12.4.4 Testing Conclusion

Unlike the first set of soil tests, less than 40 percent of the posts within each species failed in the second round. Even though the number of tests conducted was small, the results supported the conclusion that the suggested minimum diameter was adequate.

While this is true, one should notice that in several of the tests, the peak soil forces exceeded the target failure capacity. For instance, in test no. PP-34, the peak load of 93.6 kN (21.0 kips) exceeded the predicted 57.8-kN (13.0-kip) load by over 60 percent. For Douglas Fir, peak forces for test no. DF-34 exceeded the predicted 53.4-kN (12.0-kip) load by more than 50 percent.

This known, one might wonder why such a small percentage of the posts actually fractured. There are several possible explanations, the first of which is inertial effects. As discussed in Chapter 7, some of the force felt by the bogie vehicle was required to initiate movement in the post, not causing the post to bend. The inertial effects must have also existed in soil testing, and may have been even greater than the cantilever tests since the bogie not only had to move the post, but also the soil. Therefore, peak forces felt by the bogie could have been much higher than those felt by the post, possibly over-estimating the required diameter.

A second explanation may relate to the quality of the posts. With a small number of tests, the quality of the samples could have been higher or lower than average. If the sample was higher than average, the posts could have easily carried the higher load without fracture. However, it is impossible to know whether or not this was the case since the strength of the sample was unknown.

13 BARRIER VII MODELING - SYSTEM EVALUATION

Prior to full-scale vehicle crash testing, Barrier VII [8] computer modeling was utilized to predict the behavior of the MGS system constructed with the recommended round wooden post sizes.

13.1 Round Post Properties – BARRIER VII Model

Representative round post models were developed to generate more accurate simulations with BARRIER VII. Since the results from the testing varied extensively and inconsistently, the seven tests were combined to determine a single BARRIER VII round post model. This action was reasonable because the target properties for the posts were independent of their species, and no adjustments were made to the system to account for these differences.

In the BARRIER VII model, post load curves were approximated using a perfectly plastic model similar to that shown in Figure 54. The post's force-deflection curve was defined using the stiffness, yield force, yield moment, and maximum deflection.

Although the model is not a perfect representation of the test results, it does offer a very simple and somewhat accurate representation of a post rotating through soil. In the initial portion of the curve, the force resistance increases as the post begins to move and compress the soil. Eventually, the force reaches its yield point, P_y , and the stress on the soil is great enough that the soil fails and allows the post to rotate through with a constant force. At some point, the post reaches a maximum deflection, Δ_{fail} , at which it separates from the rail making it ineffective, with no resistive capacity.

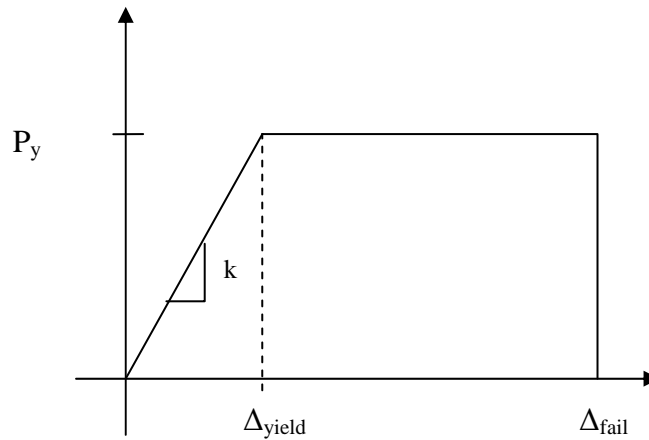
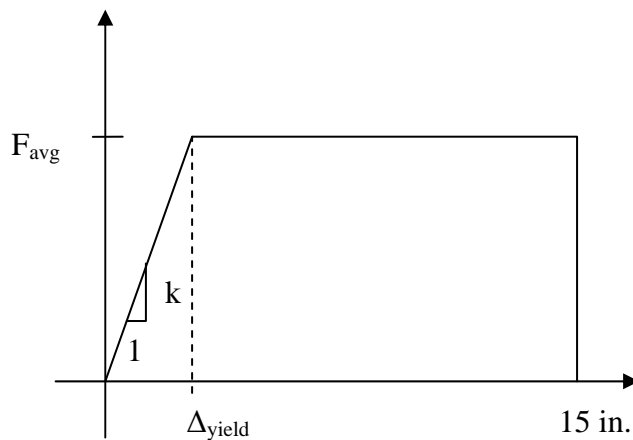


Figure 54. Barrier VII Post Strength Model

Knowing that in a typical impact, the posts and the rail separate after approximately 381 mm (15 in.) of deflection, the parameters of the post model were based on the behavior of the post up to that point. Therefore, the maximum post deflection was set at 381 mm (15 in.).

To determine the yield moment, M_y , the average force, P_y , through the 381 mm (15 in.) deflection was multiplied by the impact height, h . The average force was determined by equating the average energy dissipated in the actual tests to that in the BARRIER VII force model, as shown in the calculations below. A similar procedure, in which the average slope of the actual initial force spike was equated to the slope of the BARRIER VII model, was used to determine the stiffness. Calculations are also shown below.



$$AREA = F_{avg} \left(\left(\frac{\Delta_{yield}}{2} \right) + (15 - \Delta y) \right)$$

AREA = Average Energy at 15 in.

$$SLOPE = \frac{F_{avg}}{\Delta_{yield}}$$

SLOPE = Average Slope

Properties from the seven soil tests that were relevant to the BARRIER VII post model are summarized in Table 56 for the lateral direction. Since round Southern Yellow Pine posts have already been tested with the standard guardrail system, only the Douglas Fir and Ponderosa Pine species were considered. The average energy and average slope were used to determine F_{avg} equal to 28.9 kN (6.49 kips) and Δ_{yield} equal to 24 mm (0.96 in.). A plot of the seven soil tests with the BARRIER VII lateral post model is shown in Figure 55.

Table 56. BARRIER VII Round Wooden Post Lateral Properties Summary

Test No.	Energy at 381 mm (15 in.)		Peak Force		Deflection		Slope	
	kJ	(kip-in.)	kN	(kips)	mm	(in.)	kN/mm	(kips/in.)
DF-34	9.4	(83.5)	81.9	(18.4)	70	(2.7)	1.17	(6.72)
DF-35	14.3	(126.1)	52.8	(11.9)	64	(2.5)	0.83	(4.69)
DF-36	12.6	(111.9)	50.1	(11.3)	59	(2.3)	0.85	(4.86)
PP-34	14.4	(127.3)	93.6	(21.0)	61	(2.4)	1.54	(8.82)
PP-35	9.6	(85.4)	76.0	(17.1)	60	(2.3)	1.27	(7.27)
PP-36	7.5	(66.6)	88.4	(19.9)	56	(2.2)	1.58	(8.99)
PP-37	6.7	(59.2)	62.2	(14.0)	59	(2.3)	1.05	(6.00)
Overall Average	10.7	(94.3)	72.1	(16.2)	61	(2.4)	1.18	(6.75)

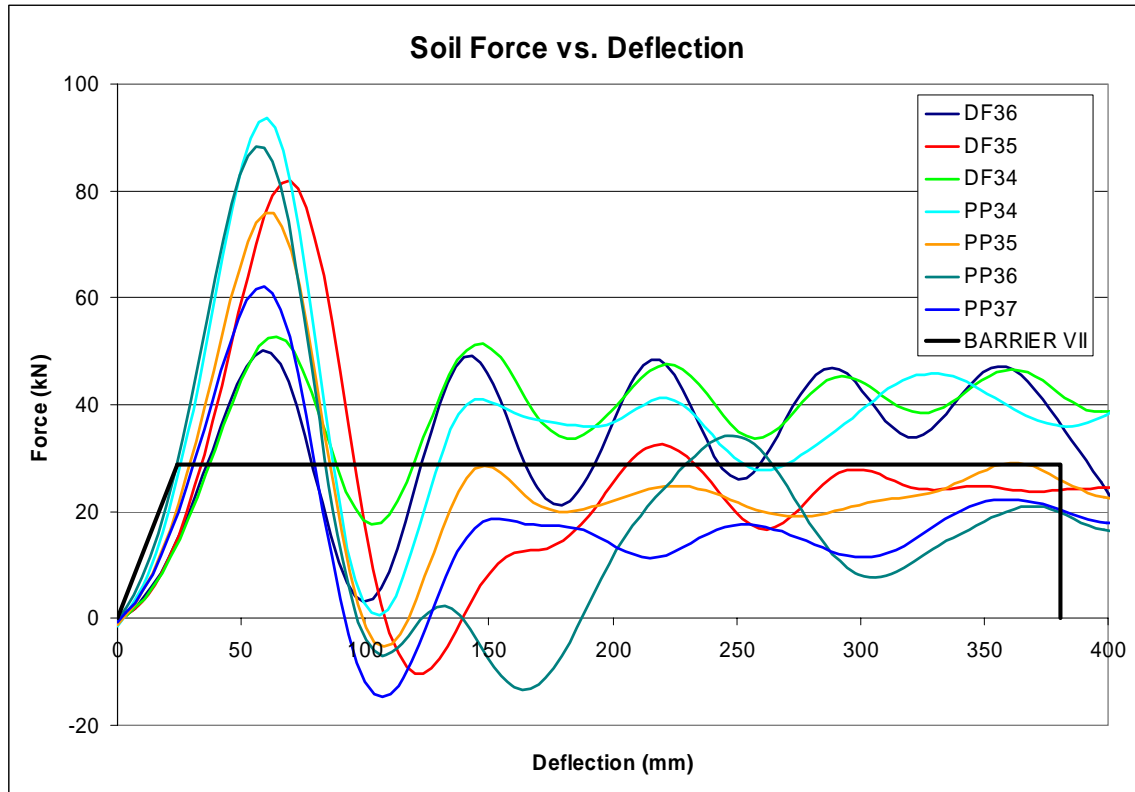


Figure 55. Lateral Capacity BARRIER VII Model

Since the longitudinal load on the posts is applied very slowly, the capacity in that direction was based on the results of static testing by Jeyapalan [15], previously discussed in Chapter 2. For this direction of loading, the BARRIER VII F_{avg} and Δ_{yield} properties were determined as 16.5 kN (3.7 kips) and 70 mm (2.76 in.), respectively. For comparison purposes, the BARRIER VII parameters used for the standard MGS model with W152x13.4 (W6x9) steel posts were $F_{avg} = 25.8$ kN (5.8 kips) and $\Delta_{yield} = 24$ mm (0.96 in.).

13.2 BARRIER VII Results

BARRIER VII simulations were completed for a baseline model and models with 1, 2, 3, and 4 consecutive weak posts. The simulations were conducted in same manner as before with the same weak post model. Once again, the parameters collected from the simulations included

maximum dynamic deflection, maximum rail tension, rail slope, and wheel snag. Results from the simulations are presented in Table 57.

Table 57. FPL BARRIER VII Results Summary

No. Weak	Maximum Deflection	Maximum Rail Tension	Pocketing Analysis		Snag Analysis **		
			3 Node	5 Node	Node	Snag	dy
	(in.)	(kips)	(Rail Slope)		(no.)	(in.)	(in.)
0	40.5	65.9	0.345	0.317	96	6.29	14.38
1	44.6	66.7	0.357	0.331	105	6.14	14.66
2	47.9	68.0	0.357	0.332	114	6.36	15.00
3	49.9	68.1	0.358	0.338	122	6.16	14.99
4	52.2	69.2	0.357	0.337	130	6.36	14.99

** Wheel snag was not reported when dy exceeded 15 in. because the post was considered to be broken.

The results compiled are the maximum quantity for each category for the given model. This implies that for each model, quantities in different categories are not necessarily from the same run within the model, but a combination of the most critical values from all the runs.

These results did not show a distinct point at which one additional failed post would cause the system to drastically fail. However, a four consecutive post failure matched the previous limit that a maximum deflection in excess of 1321 mm (52 in.) was too large, and therefore, system failure was determined to be caused by the fracture or failure of four consecutive posts. It should be noted that the 1,321-mm (52-in.) limit could be increased or reduced in the future. However, this deflection limit was selected based on reasonable engineering judgment.

In addition, a critical impact point (CIP) was selected based on the BARRIER VII results for the system with no weak posts. As shown in Table 58, impact simulations were conducted with an impact point every 238 mm (9.375 in.) beginning 953 mm (37.5 in.) upstream of post no. 12, and ending 953 mm (37.5 in.) downstream of post no. 12. The analysis showed that wheel snag was the most extreme when the vehicle impacted at the mid-span between two posts. It also showed that maximum rail tension and maximum deflection were well below their limiting

values. Although the rail slope was intended to help indicate the vehicle's propensity for pocketing, recent testing has shown that the rail slope can greatly exceed the values determined in the model without resulting in vehicle pocketing. Therefore, wheel snag was considered to be the critical factor in determining the CIP.

Table 58. Critical Impact Point Determination

Barrier VII Run ID (no.)	Impact Node (no.)	Impact Location (relative to post 12)	Parallel Time (sec)	Maximum Deflection (in.)	Maximum Rail Tension (kips)	Pocketing Analysis		Snag Analysis **		
						3 Node (Rail Slope)	5 Node	Node (no.)	Snag (in.)	dy (in.)
FPL-B-1	56	37.5 in. u.s.	0.3022	40.12	64.54	-0.3309	-0.3129	69	6.29	14.21
								87	5.52	14.38
FPL-B-2	57	28.125 in. u.s.	0.3006	40.47	63.73	-0.3267	-0.3093	69	5.15	13.05
FPL-B-3	58	18.75 in. u.s.	0.3006	40.15	62.69	-0.3264	-0.3172	69	4.12	11.48
FPL-B-4	59	9.375 in. u.s.	0.297	39.09	64.32	-0.3264	-0.314	69	2.64	10.46
FPL-B-5	60	0 in. u.s.	0.2884	37.9	65.48	-0.3264	-0.3137	69	1.28	9.32
FPL-B-6	61	9.375 in. d.s.	0.2856	38.3	65.85	-0.332	-0.3141	none	none	none
FPL-B-7	62	18.75 in. d.s.	0.2988	38.88	65.27	-0.3366	-0.3137	96	1.11	11.39
FPL-B-8	63	28.125 in. d.s.	0.2994	39.23	65.01	-0.3438	-0.3115	96	3.19	12.81
FPL-B-9	64	37.5 in. d.s.	0.2988	39.8	64.85	-0.3453	-0.3092	78	6.02	14.28
								96	4.69	14.01

As stated, the wheel snag was most severe when the impact occurred at the mid-span between two posts, and theoretically more severe in the upstream impact than the downstream impact. However, the CIP was not selected as the mid-span upstream of post 12, but rather as the mid-span downstream of post 12 due to the presence of a rail splice at this location, which made it the more critical of the two mid-spans.

14 SUMMARY AND FULL-SCALE TEST RECOMMENDATION

14.1 Summary

In the study, small-diameter Douglas Fir, Ponderosa Pine, and Southern Yellow Pine round wood posts were investigated for use in an MGS guardrail system. The introduction of round wood post MGS would open a new product market for the timber industry, help to facilitate the cost of removing dangerous forest fire fuels, and serve as an effective and economical alternative to other barrier systems used on today's roadways.

The study began with two rounds of cantilever bogie tests that isolated the behavior and strength of the posts. The objective of the testing was to optimize the diameter of the posts used in the new system, maintaining a careful balance between cost and effectiveness. The determination of the post diameter was based on the strength of the posts and estimated soil resistance from previous post testing. After the first round of testing, the diameter values of 171 mm (6.75 in.) for the Douglas Fir species, 191 mm (7.5 in.) for the Ponderosa Pine species, and 178 mm (7.0 in.) for the Southern Yellow Pine species were estimated to be sufficient.

However, following the first round of tests, significant flaws were found in the standard testing methods used in cantilever bogie tests. These flaws had the potential to overestimate post strength by as much as 50 percent due to the effects of inertia, leading to inaccurate and misleading diameter calculations. After identifying the problem, an alternate procedure was investigated with a series of three additional cantilever bogie tests. The tests confirmed the problem and showed that a reduction in bogie impact speed would significantly reduce the inertial effects, leading to a much more accurate prediction of ultimate fiber stress. Unfortunately, the flaws were not identified in time to modify the original diameter calculations

as the posts had already been ordered, but the adjustments were utilized in the second round of tests.

The second round of cantilever bogie tests was conducted with the reduced bogie impact speed. When the tests were completed, a diameter range was chosen for each species to proceed with soil tests. The target diameter values were 165 mm (6.5 in.) for Douglas Fir, 184 mm (7.25 in.) for Ponderosa Pine, and 171 mm (6.75 in.) for Southern Yellow Pine, all three with an acceptable range of 6 mm (0.25 in.) below and 19 mm (0.75 in.) above the target. The second round of cantilever tests was also used to develop a grading criterion for the two species. The grading criterion was based on the population distribution of knots and ring density. This new criterion needed to be tight enough to reduce the diameter of the posts as much as possible, but relaxed enough to allow a high percentage of the posts to qualify. Bogie soil tests were conducted to verify these results.

The initial soil bogie tests showed that the estimate made for the soil resistance force was 20 percent lower than the actual force determined from the testing. Because of this, five of the first six posts tested fractured rather than rotating as desired. Although the embedment of the posts could have been reduced to bring the peak force closer to the optimal 42.3 kN (9.5 kips), such a reduction could also lead to a reduced energy absorption capacity caused by the posts pulling out of the soil. Therefore, it was decided to increase the post diameter and accept a force level that exceeded the optimum level.

Based on the peak resisting force determined from the six initial tests, the target nominal diameter was adjusted to 184 mm (7.25 in.) for Douglas Fir, 203 mm (8.00 in.) for Ponderosa Pine, and 191 mm (7.50 in.) for Southern Yellow Pine. The acceptable ranges remained at 6 mm (0.25 in.) below the target and 19 mm (0.75 in.) above the target.

A second set of seven bogie tests – three for Douglas Fir and four for Ponderosa Pine – was conducted on posts of the new diameter, this time with six of the posts rotating through the soil and only one fracturing.

For Ponderosa Pine, the final target diameter was 203 mm (8.00 in.), with an acceptable range from 197 mm (7.75 in.) to 222 mm (8.75 in.). The standard deviation for the posts was determined as 8 mm (0.3 in.) from the random population sample. Using Monte Carlo simulation, a 1,000-sample population was developed from these parameters based on a normal distribution. Once the size distribution was developed, a second simulation was completed to develop an MOR for each of the generated post diameters. These two models were combined with elastic bending equations to determine the peak force capacity for each of the generated samples. Once this was determined, the average peak force and standard deviation was determined and used to determine the percentage of the posts falling below the 58-kN (13-kip) requirement.

For the target diameter, the average peak force was determined as 69.6 kN (15.64 kips) with a standard deviation of 18.2 kN (4.09 kips). This resulted in a 26 percent chance of post failure, falling below the desired limit. For the mid-range diameter of 210 mm (8.25 in.), the average was 76.3 kN (17.15 kips) with a standard deviation of 19.8 kN (4.45 kips), lowering the probability of failure to 18 percent. Based on these calculations, the probability that the entire system may fail due to four consecutive posts failing is somewhere between 0.1 and 0.5 percent.

It should be noted that this determination is not the probability that the system will fail, but the probability that four consecutive posts will fail when impacted under the NCHRP Report 350 Test Designation 3-11 criteria. This four post failure would in turn lead to a deflection exceeding the maximum allowable deflection of 1321 mm (52 in.).

The actual failure probability for the entire system under such impact conditions would depend on the probability of failure for the rail, the anchors, the bolts, and all other parts of the system. These parts were not considered in the failure calculations because the research focused on the behavior of the posts.

Additionally, the probability that the system would fail when installed along roadways across the country would depend on soil and impact severity variations. As stated previously, the criteria set forth in NCHRP Report 350 Test Designation 3-11 for soil and impact conditions represent a “worst practical condition.” In Report 350, the impact speed and angle have been selected near the 85th percentile of all ran-off-road passenger vehicle accidents, the test vehicles have been chosen as 5th and 95th percentile vehicle weights, and the impact location has been specified as the location most likely to result in failure. Combining these factors shows that the vast majority of actual vehicular impacts with the guardrail system will be less severe than the tested case.

The same Monte Carlo procedure was followed for Douglas Fir which had a final target diameter of 184 mm (7.25 in.), with an acceptable range from 178 mm (7.0 in.) to 203 mm (8.0 in.). The standard deviation for the Douglas Fir post diameter was 5 mm (0.2 in.). An average peak force of 65.2 kN (14.65 kips) with a standard deviation of 9.5 kN (2.14 kips) was determined for the target diameter, and an average of 72.1 kN (16.2 kips) with a standard deviation of 10.5 kN (2.36 kips) was determined for the mid-range diameter. The probability of a post falling below the 53.4 kN (12 kip) limit was 12.2 percent for the target diameter and 3.2 percent for the mid-range diameter.

For Southern Yellow Pine, the results were similar. The final target diameter was 190.5 mm (7.5 in.), with acceptable diameters falling between 184 mm (7.25 in.) and (8.25 in.). The

standard deviation for the diameter of the collected samples was 3 mm (0.1 in.). The average peak force for the target diameter was 71.6 kN (16.1 kips) with a standard deviation of 12.9 kN (2.9 kips), and the average peak force for the mid-range diameter was 78.8 kN (17.7 kips) with a standard deviation of 14.2 kN (3.2 kips). This resulted in a post failure probability of 7.7 percent for the target diameter and 3.7 percent for the mid-range diameter.

14.2 Full-Scale Crash Test Recommendation

Two full-scale crash tests were recommended, one for each of the Douglas Fir and Ponderosa Pine species. A Southern Yellow Pine test was not recommended, as the post type and size has been tested previously on a standard W-beam guardrail system. The full-scale crash tests were to be used to verify the results found herein and validate the system to the NCHRP Report No. 350 standards.

Two factors, target diameter and grading criteria, need to be considered in the final recommendation. The grading criteria for the posts used in the full-scale tests should meet the grading criteria established for each species. Since the grading criteria are based on the population of the production line, meaning that the vast majority of the posts leaving the manufacturing line will exceed these criteria, no effort should be made to select posts of the lowest possible quality. In selecting a target diameter and range, more care should be taken.

When producers fill a post order, they will select posts fitting the size range from a stock pile on site. Timber producers will attempt to find posts with diameters close to the established target, but will inevitably select any material that falls within the upper and lower bounds of the established range. Therefore, the average diameter of the selected posts will probably fall somewhere between the target and the mid-range of the limits. The standard deviation should be

fairly consistent. Knowing this, the probability of failure for a single post will fall between two extremes, that for the target diameter, and that for the mid-range diameter.

In full-scale testing, the more critical of the two cases should be tested, implying that the posts should be selected with a sample average near the target diameter rather than an average near the mid-range diameter.

The recommended grading criteria and diameter ranges for the full-scale tests are presented below for each species. In addition, posts of all three species must meet the general grading criteria discussed previously and presented in Appendix H.

14.2.1 Douglas Fir

Douglas Fir grading specifications include limits on knot size and ring density. For the Douglas Fir species, the allowable knot diameter shall not exceed 51 mm (2 in.). The ring density of the posts should not be less than 6 rings-per-inch as averaged over a 76-mm (3-in.) length. Based on the reduced-diameter probability calculations, the nominal diameter of the posts installed for the full-scale test should be approximately 184 mm (7.25 in.). Post diameters should range between 178 mm (7.00 in.) and 203 mm (8.00 in.).

14.2.2 Ponderosa Pine

Specific grading criteria for Ponderosa Pine also include limitations on knots and ring density. Any knots found on the surface of the post shall not exceed 102 mm (4 in.) in diameter. Ring density should not be less than 6 rings-per-inch as averaged over a 76-mm (3-in.) length. The nominal diameter for the posts installed for the full-scale test should be about 203 mm (8.00 in.), and all individual post diameters must fall between 197 mm (7.75 in.) and 222 mm (8.75 in.).

14.2.3 Southern Yellow Pine

Southern Yellow Pine grading specifications specify the allowable knot diameter shall not exceed 64 mm (2.5 in.), and the minimum ring density as 4 rings-per-inch as averaged over a 76-mm (3 in.) length. The nominal diameter for the posts should be about 190 mm (7.50 in.), and all individual post diameters must fall between 184 mm (7.25 in.) and 210 mm (8.25 in.).

14.2.4 System Details

The two full-scale crash tests should be conducted on a standard MGS installation, with the standard steel posts replaced by the round timber posts embedded 940 mm (37 in.) into the soil, and the rectangular blockouts replaced with special concave blockouts made to fit the round posts. All other aspects of the system should remain the same, including all anchor post details, rail mounting height, and post spacing.

15 TEST REQUIREMENTS AND EVALUATION CRITERIA

15.1 Test Requirements

Longitudinal barriers, such as W-beam guardrail systems, must satisfy the requirements provided in NCHRP Report No. 350 to be accepted for use on National Highway System (NHS) construction projects or as a replacement for existing systems not meeting current safety standards. According to NCHRP Report No. 350 TL-3 criteria, the barrier system must be subjected to two full-scale vehicle crash tests as follows:

1. Test Designation 3-10 consisting of an 820-kg (1,808-lb) small car impacting the guardrail system at a nominal speed and angle of 100.0 km/h (62.1 mph) and 20 degrees, respectively.
2. Test Designation 3-11 consisting of a 2,000-kg (4,409-lb) pickup truck impacting the guardrail system at a nominal speed and angle of 100.0 km/h (62.1 mph) and 25 degrees, respectively.

Based on the success of prior small car testing on the Midwest Guardrail System (7), the 820-kg (1,808-lb) small car crash test was deemed unnecessary for this project. In addition, full-scale vehicle crash testing on the MGS with Southern Yellow Pine posts was also deemed unnecessary based on: (1) the success of prior Southern Yellow Pine round post, W-beam guardrail systems and (2) the proposed crash testing of two Midwest Guardrail Systems using both Ponderosa Pine and Douglas Fir round posts. The test conditions for TL-3 longitudinal barriers are summarized in Table 59.

15.2 Evaluation Criteria

Evaluation criteria for full-scale vehicle crash testing are based on three appraisal areas: (1) structural adequacy; (2) occupant risk; and (3) vehicle trajectory after collision. Criteria for structural adequacy are intended to evaluate the ability of the barrier to contain and redirect the vehicle in a predictable manner. Occupant risk criteria evaluate the degree of hazard to

occupants in the impacting vehicle. Finally, vehicle trajectory after collision is a measure of the potential for the post-impact trajectory of the vehicle to cause subsequent multi-vehicle accidents. This criterion indicates the potential safety hazard for the occupants of other vehicles or the occupants of the impacting vehicle when subjected to secondary collisions with other fixed objects. These three evaluation criteria are defined in Table 60. The vehicle crash tests were conducted and reported in accordance with the procedures provided in NCHRP Report No. 350.

Table 59. NCHRP Report No. 350 Test Level 3 Crash Test Conditions [26]

Test Article	Test Level	Barrier Section	Test Designation	Impact Conditions				Evaluation Criteria *
				Test Vehicle	Speed		Angle	
					km/h	(mph)	degrees	
Longitudinal Barrier	3	Length of Need	3-10	820C	100	(62.1)	20	A,D,F,H,I,K,M
			S3-10 ^a	700C	100	(62.1)	20	A,D,F,H,I,K,M
			3-11	2000P	100	(62.1)	25	A,D,F,K,L,M
		Transition	3-20 ^d	820C	100	(62.1)	20	A,D,F,H,I,K,M
			S3-20 ^a	700C	100	(62.1)	20	A,D,F,H,I,K,M
			3-21	2000P	100	(62.1)	25	A,D,F,K,L,M

*Evaluation criteria explained in Table 60.

Table 60. NCHRP Report No. 350 Evaluation Criteria for Crash Tests [26]

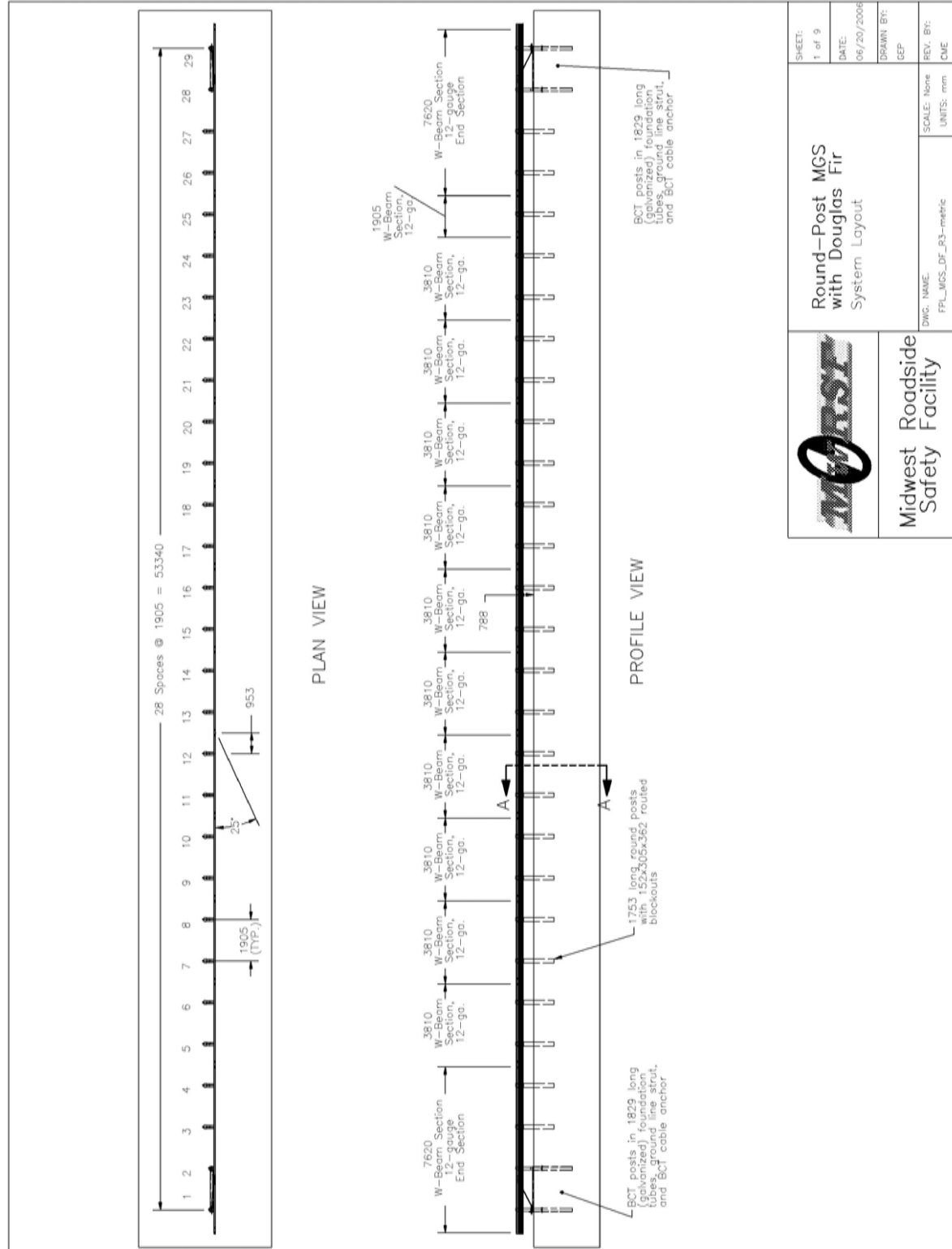
Evaluation Factors		Evaluation Criteria
Structural Adequacy	A.	Test article should contain and redirect the vehicle; the vehicle should not penetrate, underide, or override the installation although controlled lateral deflection of the test article is acceptable.
Occupant Risk	D.	Detached elements, fragments or other debris from the test article should not penetrate or show potential for penetrating the occupant compartment, or present an undue hazard to other traffic, pedestrians, or personnel in a work zone. Deformations of, or intrusions into, the occupant compartment that could cause serious injuries should not be permitted.
	F.	The vehicle should remain upright during and after collision although moderate roll, pitching, and yawing are acceptable.
	G.	It is preferable, although not essential, that the vehicle remain upright during and after collision
	H.	Longitudinal and lateral occupant impact velocities should fall below the preferred value of 9 m/s (29.53 ft/s), or at least below the maximum allowable value of 12 m/s (39.37 ft/s).
	I.	Longitudinal and lateral occupant ridedown accelerations should fall below the preferred value of 15 g's, or at least below the maximum allowable value of 20 g's.
Vehicle Trajectory	K.	After collision it is preferable that the vehicle's trajectory not intrude into adjacent traffic lanes.
	L.	The occupant impact velocity in the longitudinal direction should not exceed 12 m/s (39.37 ft/s), and the occupant ridedown acceleration in the longitudinal direction should not exceed 20 G's.
	M.	The exit angle from the test article preferably should be less than 60 percent of the test impact angle measured at the time of vehicle loss of contact with the test device.

16 DESIGN DETAILS

Design details are shown in Figures 56 through 64 for the Douglas Fir system, Figures 69 through 77 for the Ponderosa Pine system, and Figures 84 through 92 for the Southern Yellow Pine system. Photographs of the Douglas Fir system are shown in Figures 65 through 68, and photographs of the Ponderosa Pine system are shown in Figures 78 through 83.

The Douglas Fir and Ponderosa Pine test installations were configured with an anchor system consisting of rectangular timber posts placed in steel foundation tubes. The anchor system was designed to replicate the capacity of a tangent guardrail end terminal. No crashworthy end terminal was tested, and therefore, none was installed in either system.

The posts in both systems were placed in a compacted course, crushed limestone material meeting Grading B of AASHTO M 147-65 (1990) as found in NCHRP Report No. 350. In addition, all lap-splice connections between the W-beam guardrail segments were installed with the upstream segment overlapping the downstream segment to reduce vehicle snag at the splices.



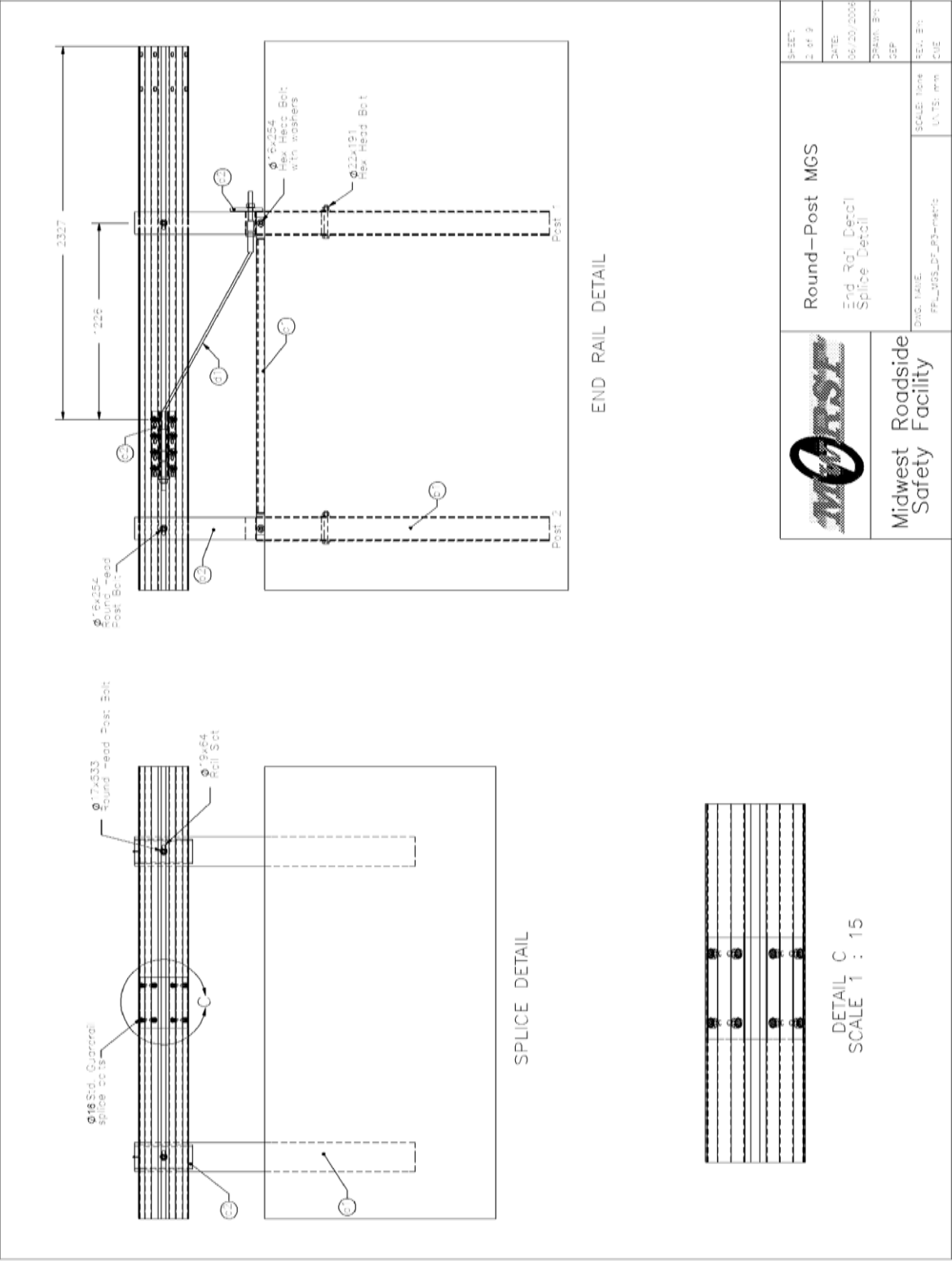


Figure 57. MGS Round Post Douglas Fir Details – End Rail and Splice Detail

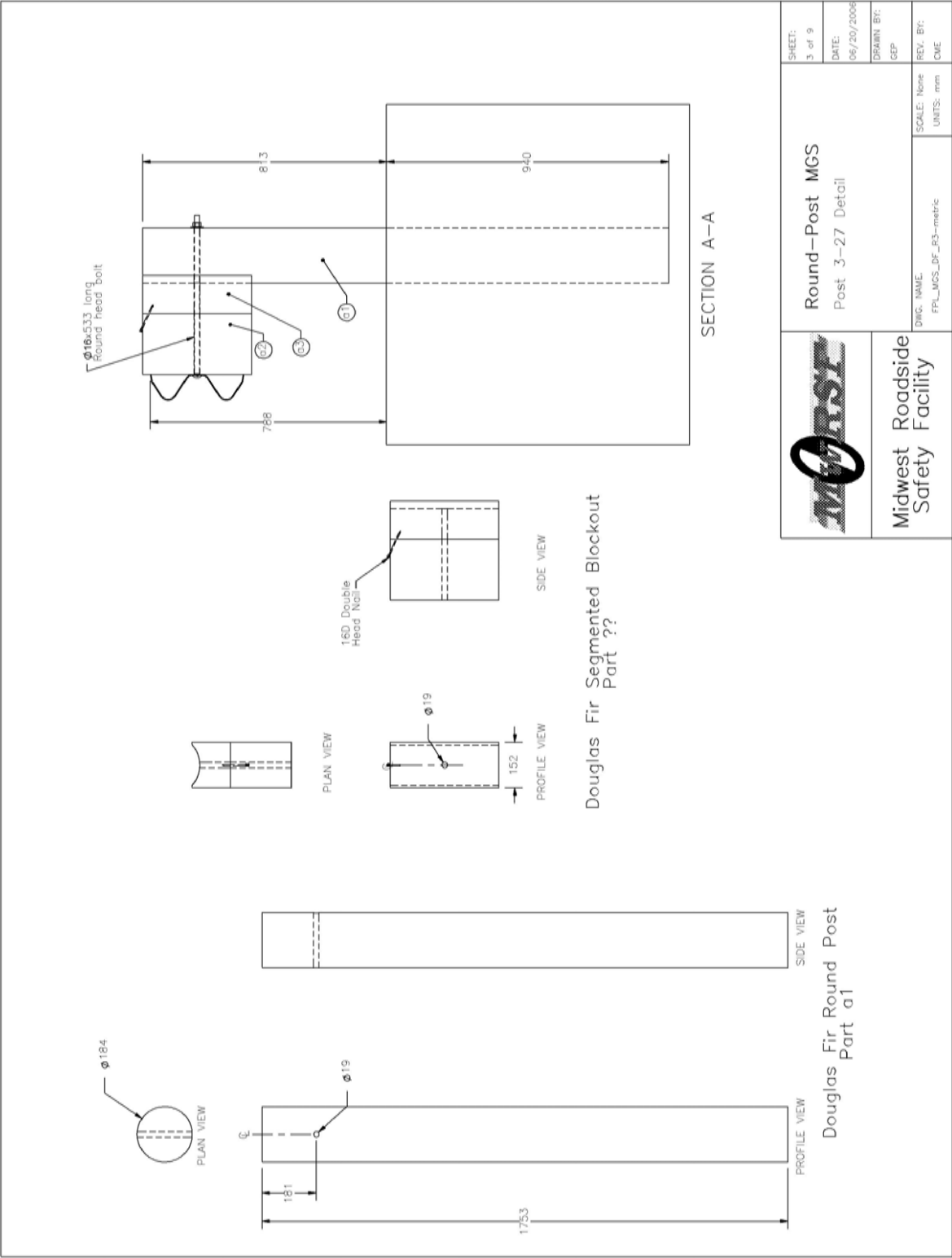


Figure 58. MGS Round Post Douglas Fir Details – Post Detail

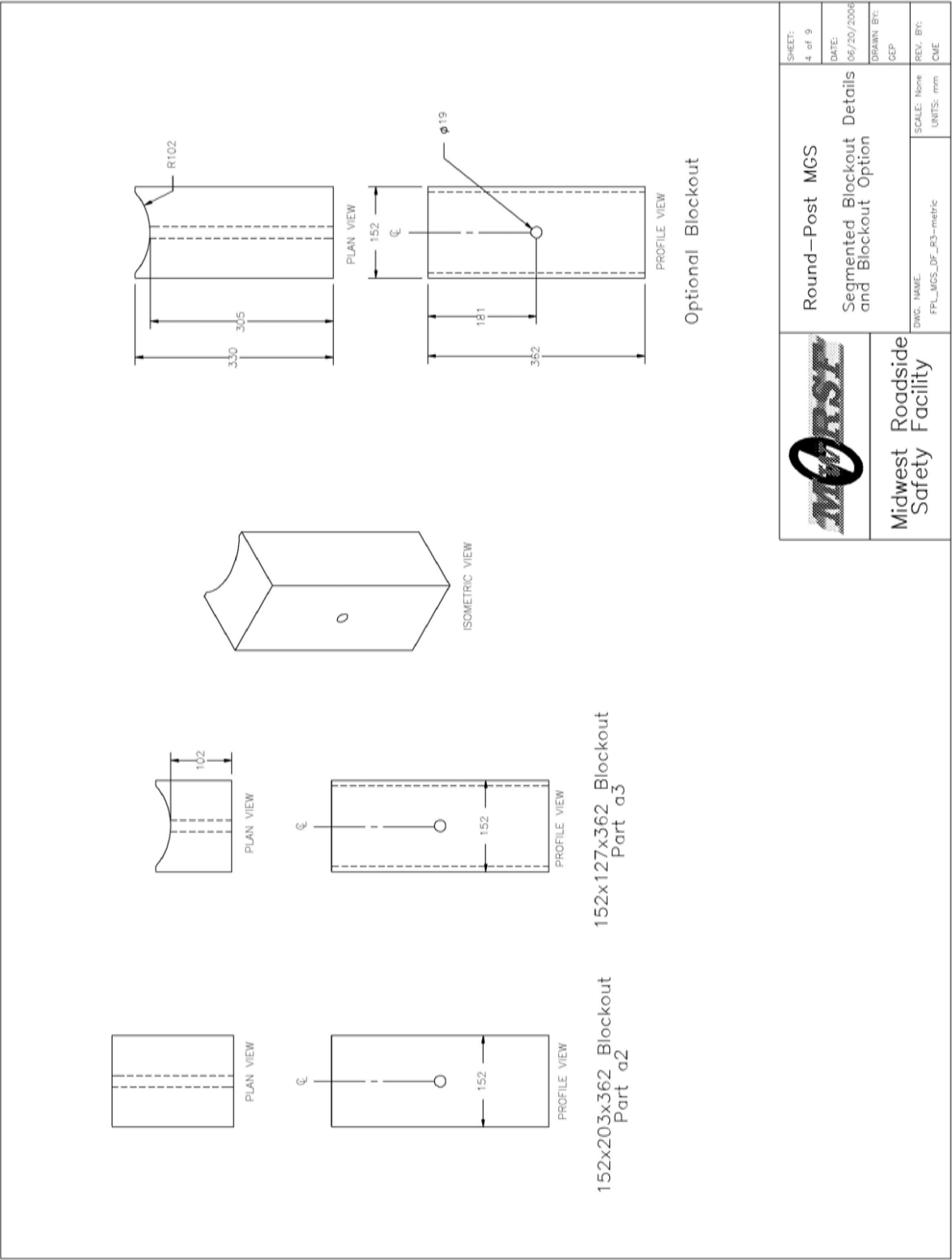


Figure 59. MGS Round Post Douglas Fir Details – Segmented blockout Detail

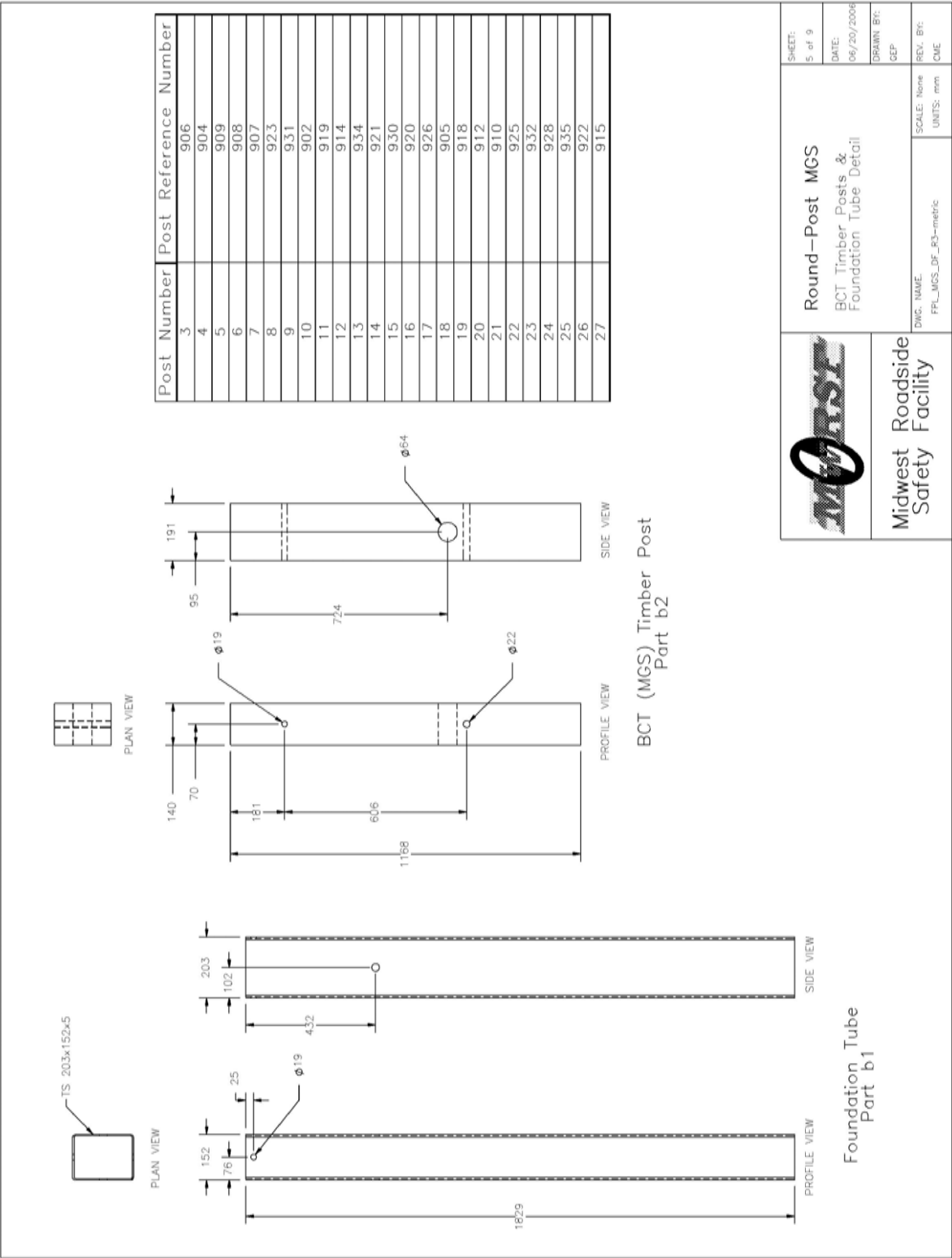


Figure 60. MGS Round Post Douglas Fir Details – Anchor Post Detail

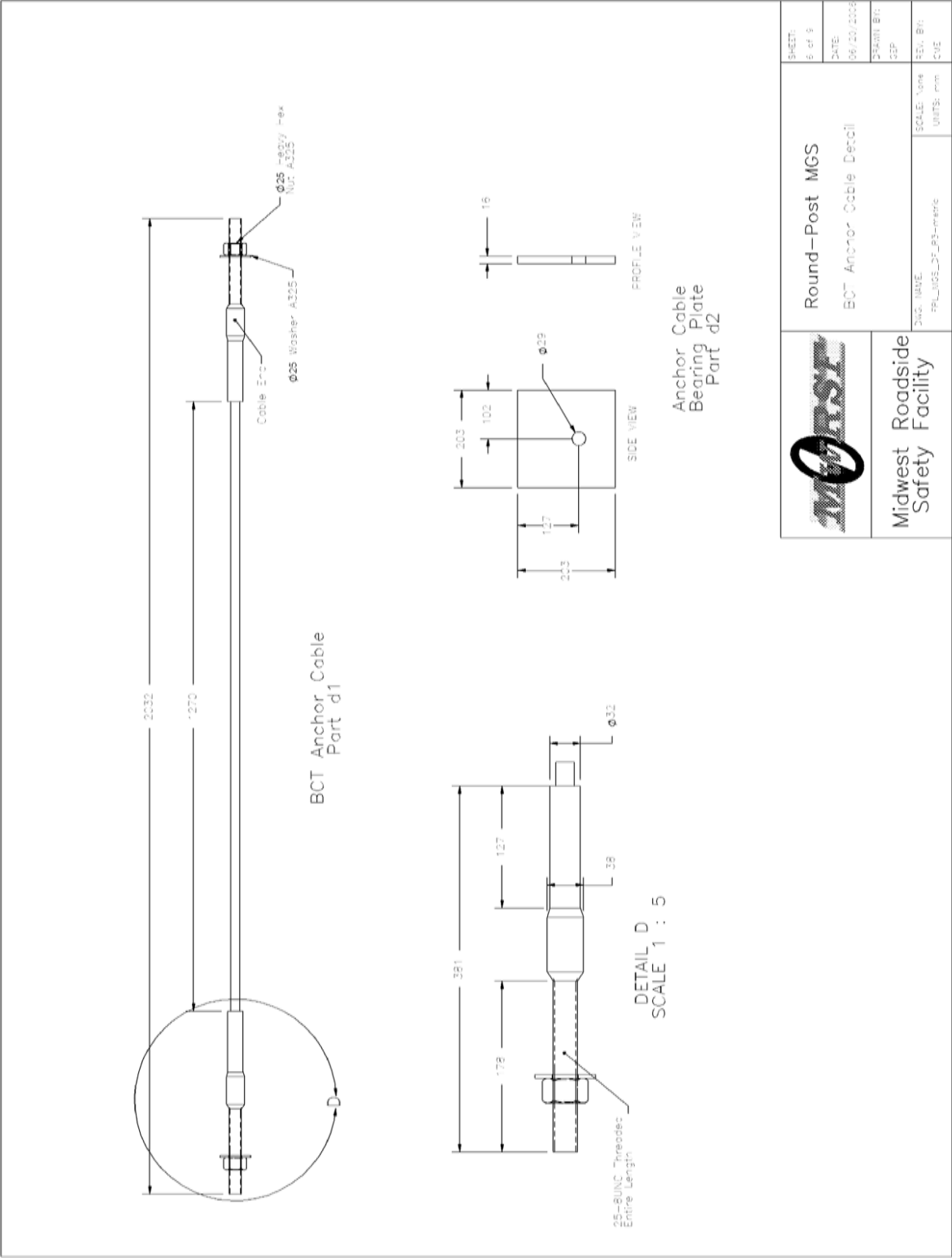


Figure 61. MGS Round Post Douglas Fir Details – BCT Anchor Cable Detail

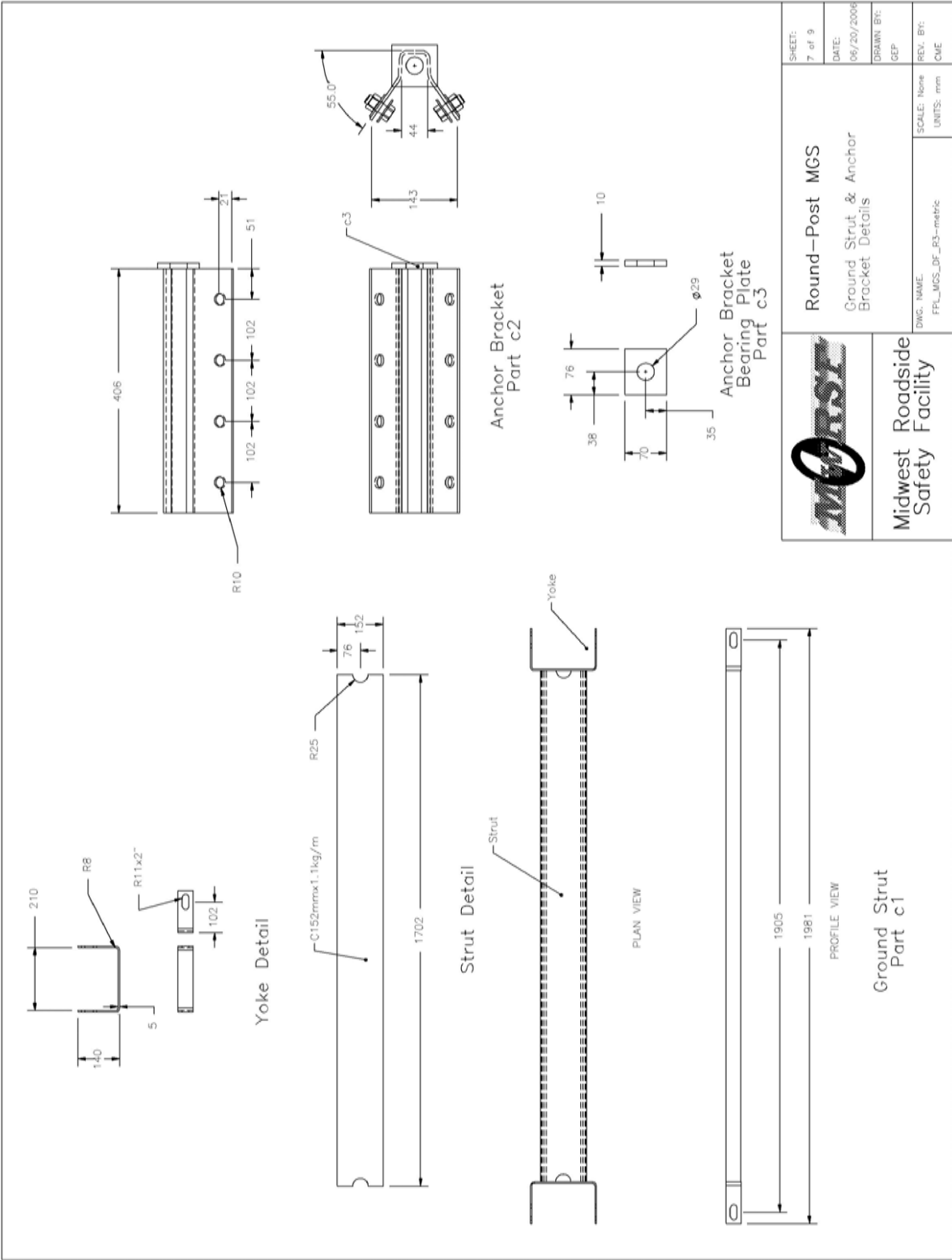


Figure 62. MGS Round Post Douglas Fir Details – Ground Strut and Anchor Bracket Detail

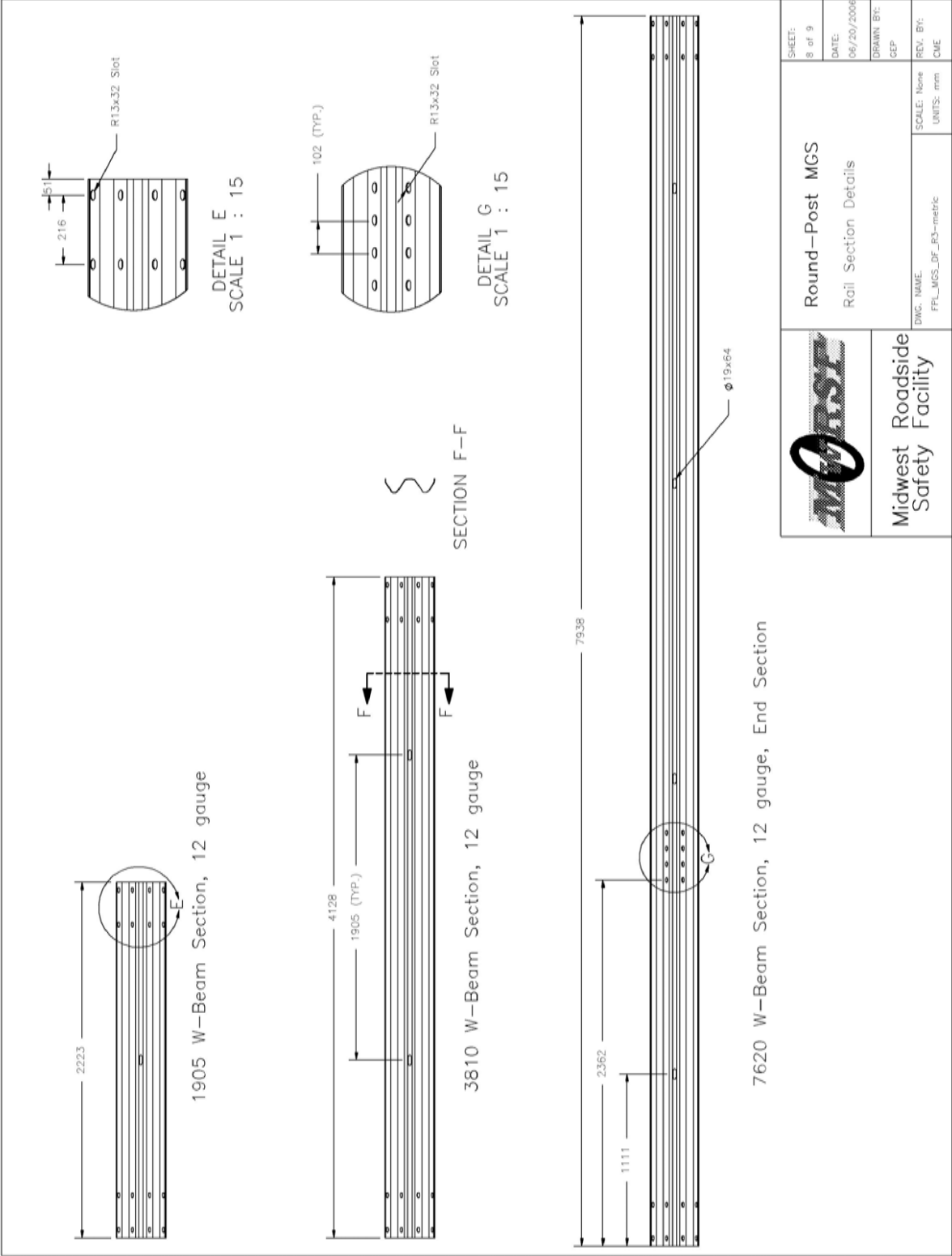


Figure 63. MGS Round Post Douglas Fir Details – Rail Section Detail

<p><i>General</i></p> <p>Guardrail Post Grading Criteria</p> <p>All posts shall meet the current quality requirements of the American National Standards Institute (ANSI) 05.1, "Wood Poles" except as supplemented herein:</p> <p>Manufacture: All posts shall be smooth shaved by machine. No "ringing" of the posts, as caused by improperly adjusted peeling machine, is permitted. All outer and inner bark shall be removed during the shaving process. All knots and knobs shall be trimmed smooth and flush with the surface of the posts. The guardrail posts will be a minimum of 1.75 m (69 in.) long. The use of peeler cores is prohibited.</p> <p>Ground-line: The ground-line, for the purpose of applying these restrictions of ANSI 05.1 that reference the ground-line, shall be defined as being located 914 mm (36 in.) from the butt end of each post.</p> <p>Size: The size of the posts shall be classified based on their diameter at the ground-line and their length and will be species specific. The ground-line diameter shall be specified by diameter in 6 mm ($\frac{1}{4}$ in.) breaks. The length shall be specified in 300 mm (1 ft) breaks. Dimension shall apply to fully seasoned posts. When measured between their extreme ends, the post shall be no shorter than the specified lengths but may be up to 75 mm (3 in.) longer.</p> <p>Scars: Scars are permitted in the middle third as defined in ANSI 05.1 provided that the depth of the trimmed scar is not more than (1 in.).</p> <p>Shape and Straightness: All timber posts shall be nominally round in cross section. A straight line drawn from the centerline of the top to the center of the butt of any post shall not deviate from the centerline of the post more than 32 mm ($1\frac{1}{4}$ in.) at any point. Posts shall be free from reverse bends.</p> <p>Splits and Shakes: Splits or ring shakes are not permitted in the top two thirds of the post. Splits not to exceed the diameter in length are permitted in the bottom third of the post. A single shake is permitted in the bottom third, provided it is not wider than one-half the butt diameter.</p> <p>Decay: Allowed in knots only.</p> <p>Holes: Pin holes 1 mm ($1/16$ in.) or less are not restricted.</p> <p>Slope of Grain: 1 in 10.</p> <p>Compression Wood: Not allowed, in the outer 25 mm (1 in.) or if exceeding $\frac{1}{4}$ of the radius.</p> <p>Timber Spacers: When timber spacers are required, the timber species shall be the same as those furnished for the timber posts. The size and hole location shall be as shown on the plans, with a tolerance of 6 mm ($\frac{1}{4}$ in.). Spacers shall be of medium grain, at least four (4) rings per inch on one end, and free from splits, shakes, compression wood or decay in any form. Individual knots, knot clusters or knots in the same cross section of a face are permitted, provided they are sound or firm, and are limited in cumulative width (when measured between lines parallel to the edges) to no more than one-half the width of the face. Wane or the absence of wood is limited to one-third of the face on no more than 10 percent of the lot. Slope of grain deviation is limited to one in six. The material may be rough sawn or surfaced, full size, hit or miss, with a tolerance of 6 mm ($\frac{1}{4}$ in.) for all dimensions.</p> <p>Treatment: Treating — American Wood-Preservers' Association (AWPA) — Book of Standards (BOS) U1-05 use category system UCS: user specification for treated wood; commodity specification B: Posts, Wood for Highway Construction must be met using the methods outlined in AWPA BOS T1-05 Section 8.2. Each post treated shall have a minimum sapwood depth of 19 mm ($\frac{3}{4}$ in.) as determined by examination of the tops and butts of each post. Material that has been air dried or kiln dried shall be inspected for moisture content in accordance with AWPA standard M2 prior to treatment. Tests of representative pieces shall be conducted. The lot shall be considered acceptable when the average moisture content does not exceed 25 percent. Pieces exceeding 29 percent moisture content shall be rejected and removed from the lot.</p>		<p>Species Specific Criteria</p> <p>Douglas Fir: Knot diameter for posts of Douglas Fir shall not exceed 51 mm (2 in.). Ring density for the species shall be at least 6 rings-per-inch as measured over a 76 mm (3 in.) distance. The diameter of the Douglas Fir posts shall be 184 mm (7$\frac{1}{4}$ in.) at the ground line with a upper limit of 203 mm (8 in.).</p>		<p>Midwest Roadside Safety Facility</p> <p>DWG. NAME: FPL_MGS_DF_R3-metric</p> <p>SCALE: None</p> <p>UNITS: mm</p>		<p>Round-Post MGS</p> <p>Grading Specifications</p>	<p>SHEET: 9 of 9</p> <p>DATE: 06/20/2006</p> <p>DRAWN BY: CEP</p> <p>REV. BY: CME</p>
---	--	---	--	---	--	--	---

Figure 64. MGS Round Post Douglas Fir Details – Grading Specifications



Figure 65. MGS Round Post Douglas Fir Photographs



Figure 66. MGS Round Post Douglas Fir Photographs



Figure 67. MGS Round Post Douglas Fir Photographs



Figure 68. MGS Round Post Douglas Fir Photographs



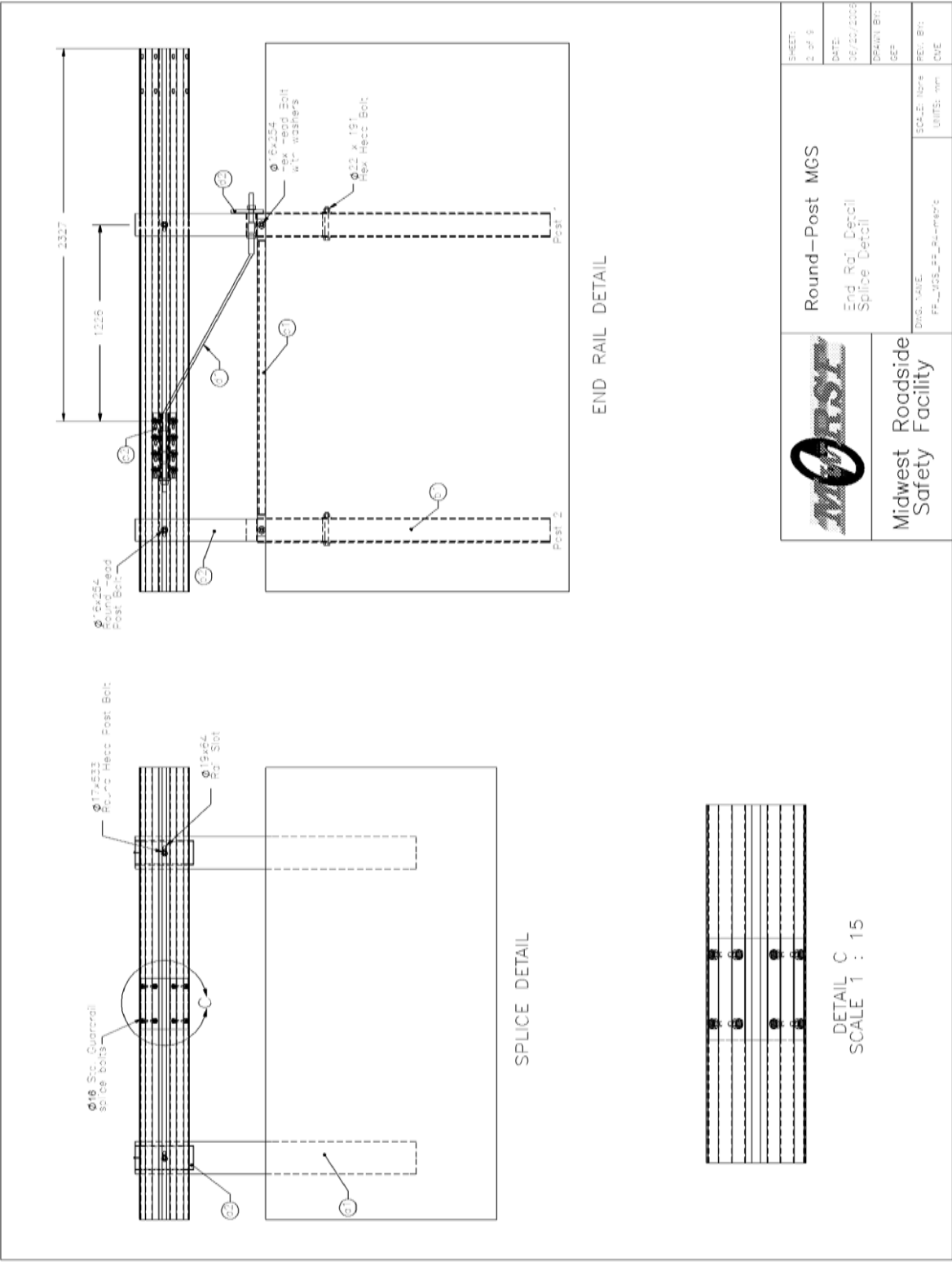


Figure 70. MGS Round Post Ponderosa Pine Details – End Rail and Splice Detail

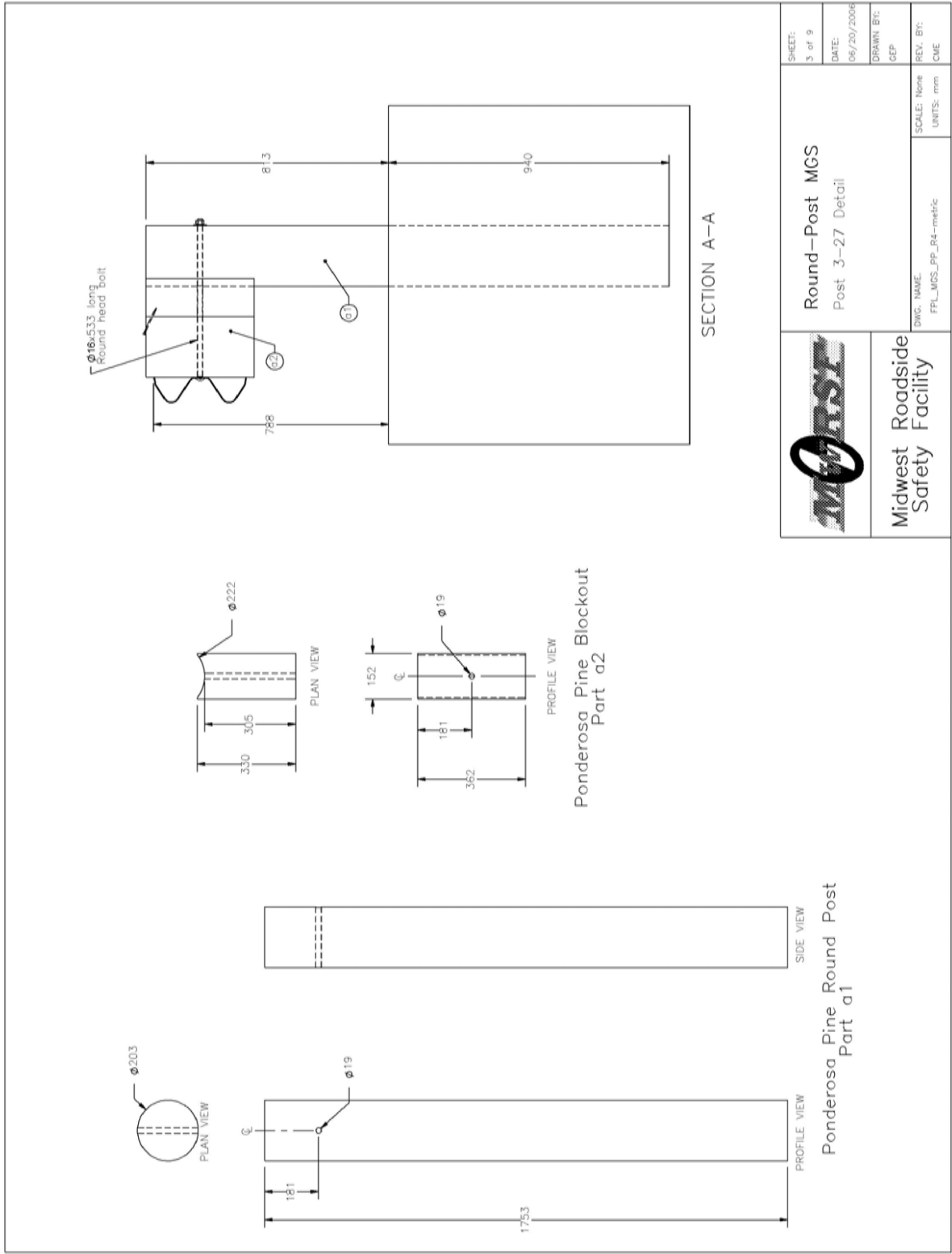


Figure 71. MGS Round Post Ponderosa Pine Details – Post Detail

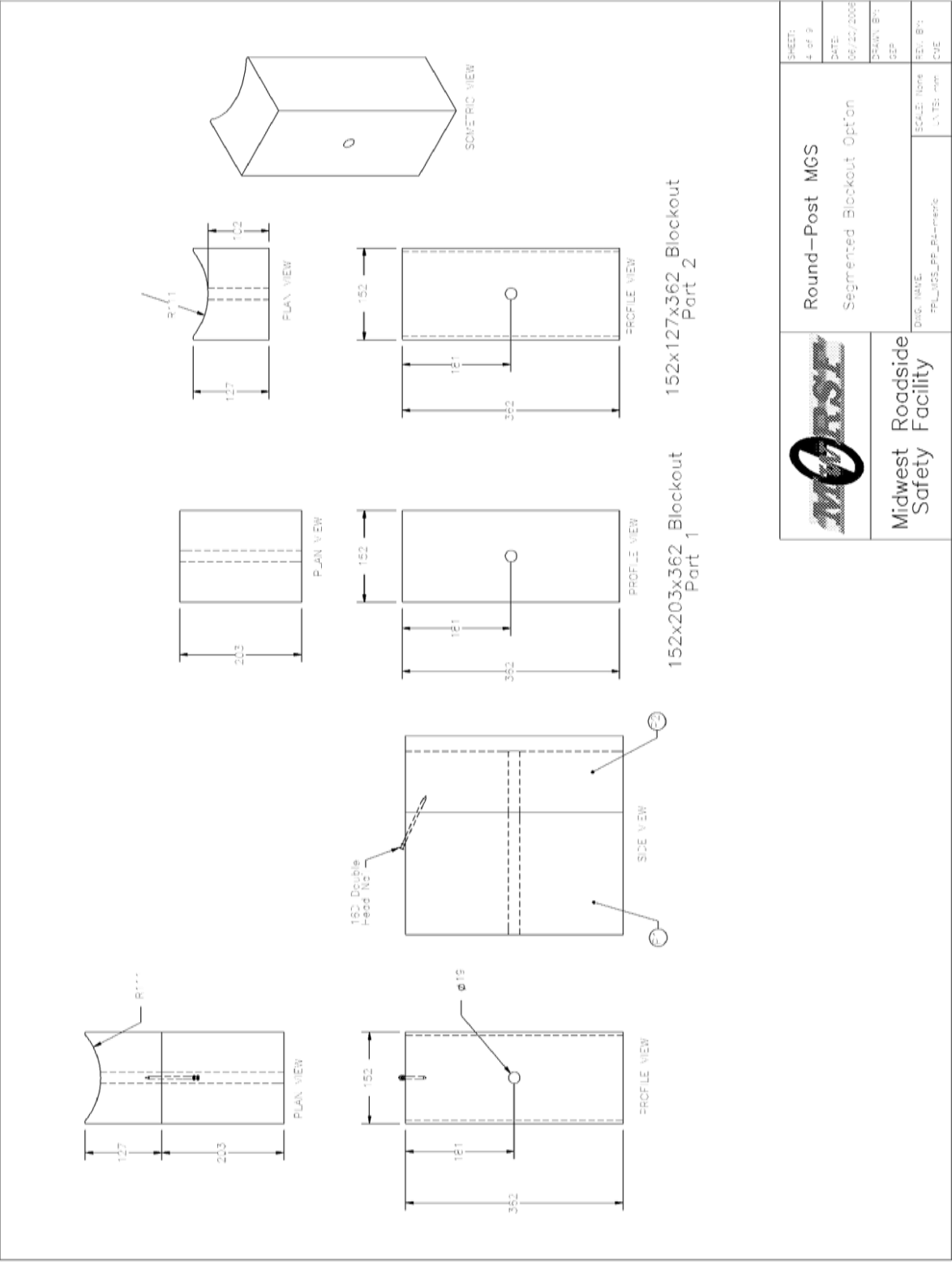
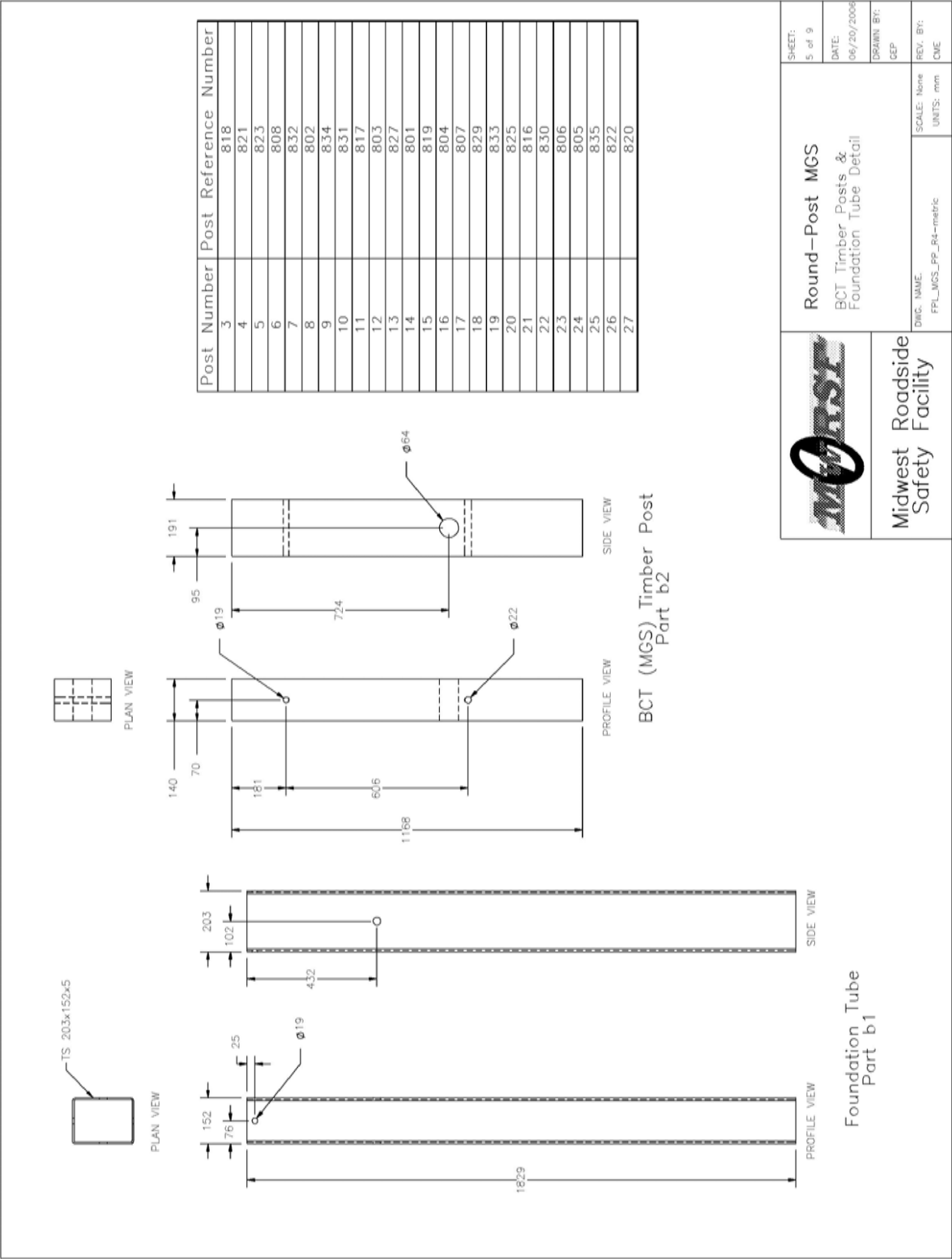



Figure 72. MGS Round Post Ponderosa Pine Details – Segmented Blockout Detail



Post Number	Post Reference Number
3	818
4	821
5	823
6	808
7	832
8	802
9	834
10	831
11	817
12	803
13	827
14	801
15	819
16	804
17	807
18	829
19	833
20	825
21	816
22	830
23	806
24	805
25	835
26	822
27	820



Midwest
Roadside
Safety
Facility

Round-Post MGS
BCT Timber Posts &
Foundation Tube Detail

SHEET:
5 of 9

DATE:
06/20/2008

DRAWN BY:
GEP

REV. BY:
ONE

SCALE: None
UNITS: mm

Doc. NAME:
FPL_MGS_PP_B4-metric

Figure 73. MGS Round Post Ponderosa Pine Details – Anchor Post Detail

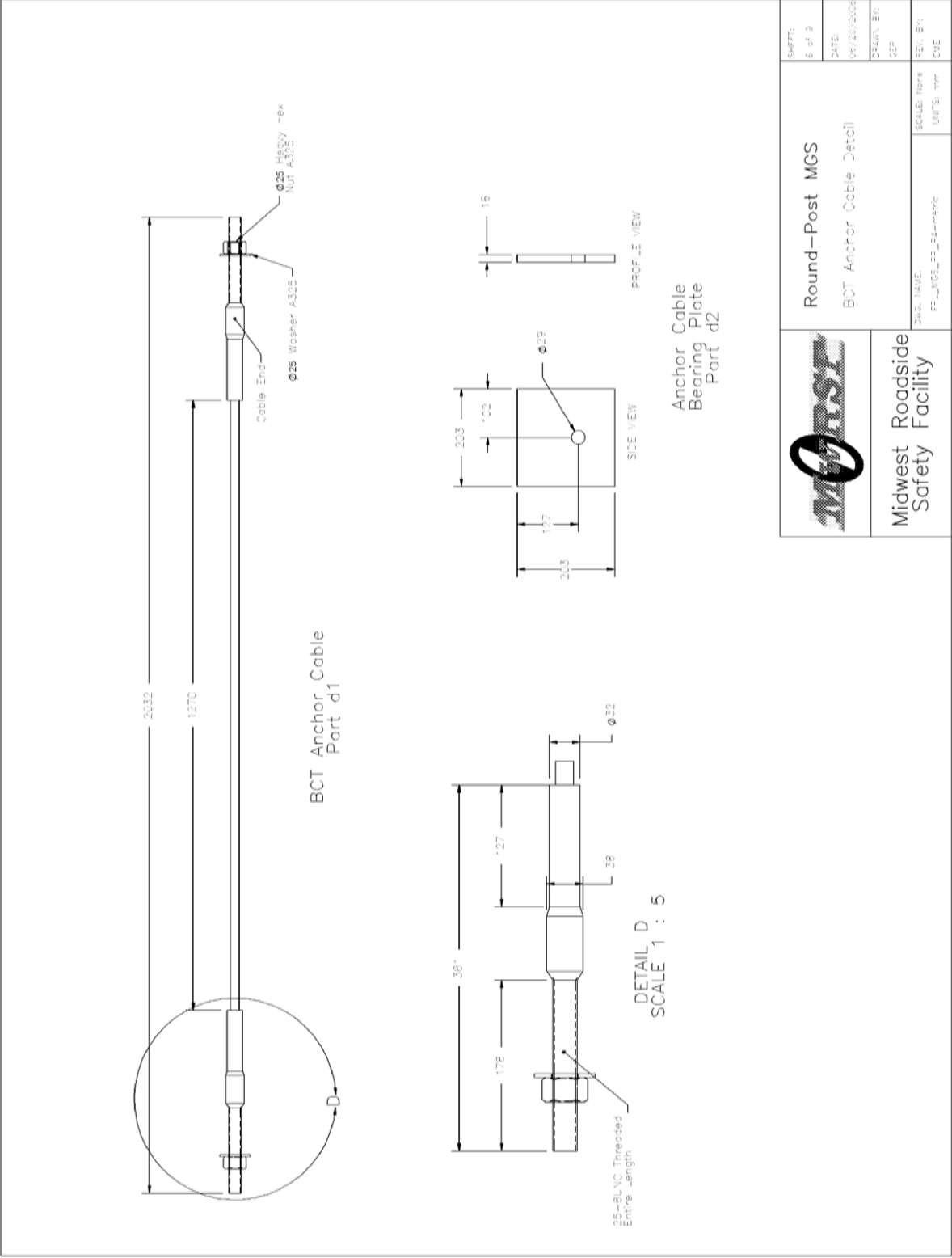
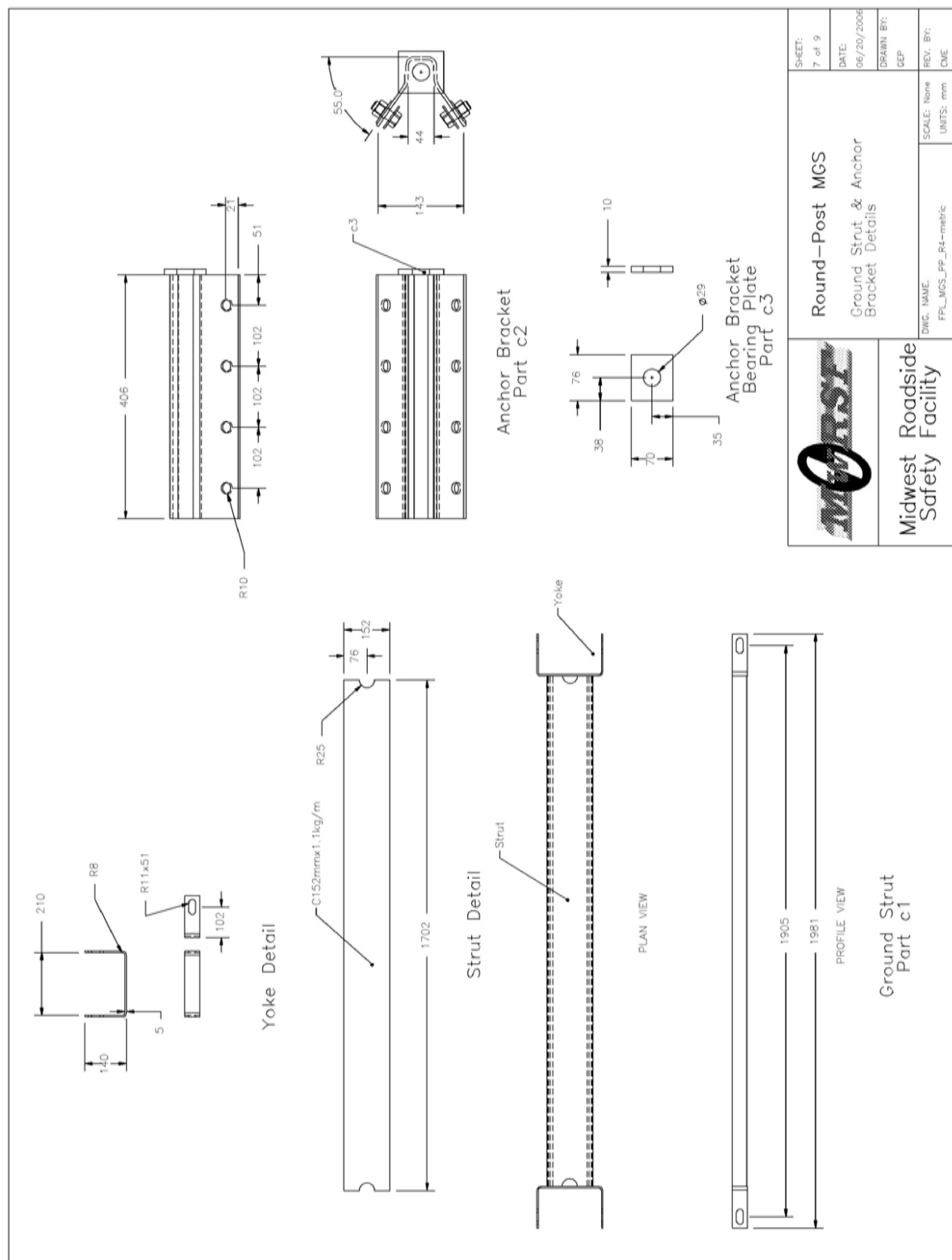


Figure 74. MGS Round Post Ponderosa Pine Details – BCT Anchor Cable Detail



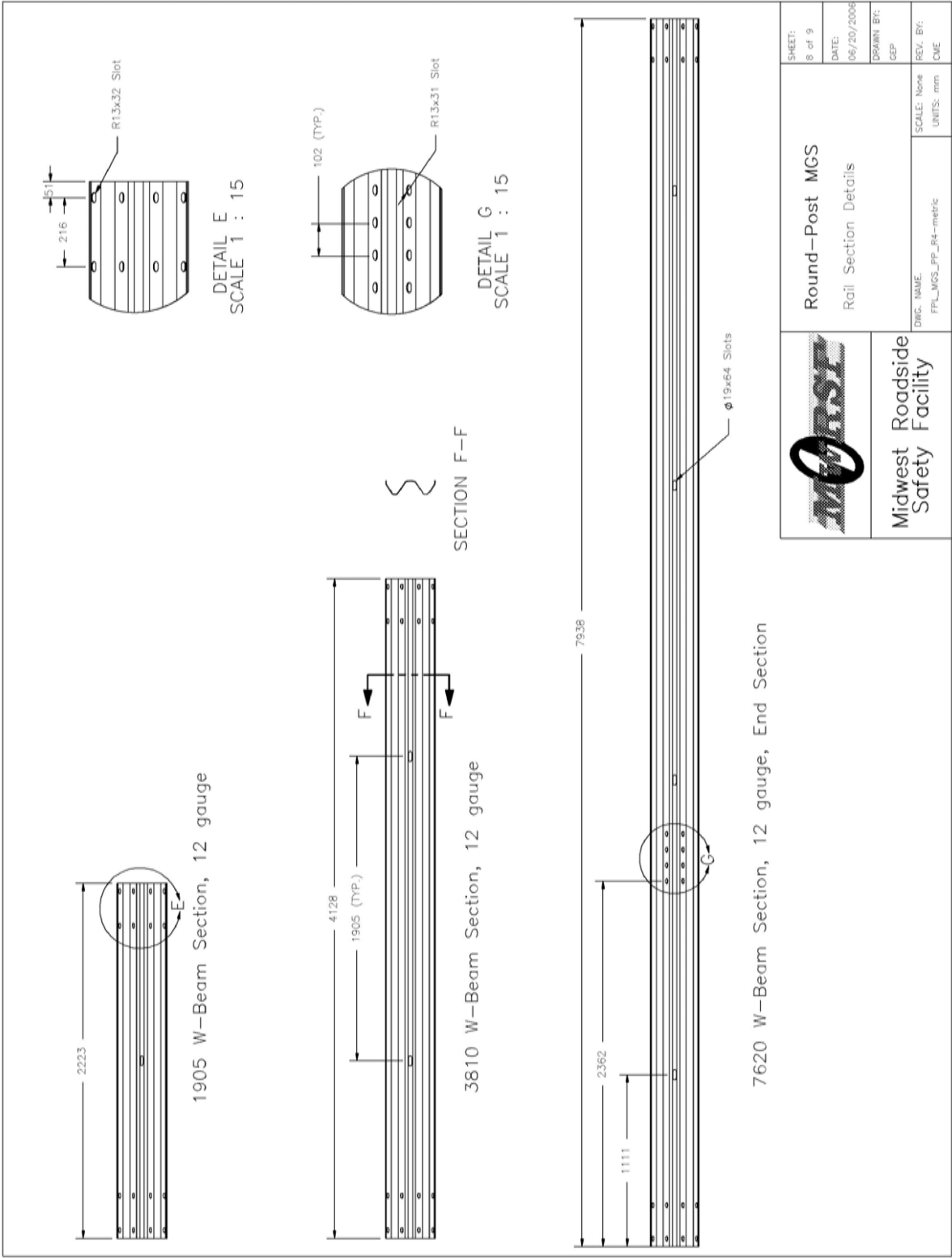


Figure 76. MGS Round Post Ponderosa Pine Details – Rail Section Detail

General		Guardrail Post Grading Criteria	
All posts shall meet the current quality requirements of the American National Standards Institute (ANSI) 05.1, "Wood Poles" except as supplemented herein:			
Manufacture:	All posts shall be smooth shayed by machine. No "ringing" of the posts, as caused by improperly adjusted peeling machine, is permitted. All outer and inner bark shall be removed during the shaving process. All knots and knobs shall be trimmed smooth and flush with the surface of the posts. The guardrail posts will be a minimum of 1.75 m (69 in.) long. The use of peeler cores is prohibited.		
Ground-line:	The ground-line, for the purpose of applying these restrictions of ANSI 05.1 that reference the ground-line, shall be defined as being located 914 mm (36 in.) from the butt end of each post.		
Size:	The size of the posts shall be classified based on their diameter at the ground-line and their length and will be species specific. The ground-line diameter shall be specified by diameter in 6 mm (¼ in.) breaks. The length shall be specified in 300 mm (1 ft) breaks. Dimension shall apply to fully seasoned posts. When measured between their extreme ends, the post shall be no shorter than the specified lengths but may be up to 75 mm (3 in.) longer.		
Scars:	Scars are permitted in the middle third as defined in ANSI 05.1 provided that the depth of the trimmed scar is not more than (1 in.).		
Shape and Straightness:	All timber posts shall be nominally round in cross section. A straight line drawn from the centerline of the top to the center of the butt of any post shall not deviate from the centerline of the post more than 32 mm (1¼ in.) at any point. Posts shall be free from reverse bends.		
Splits and Shakes:	Splits or ring shakes are not permitted in the top two thirds of the post. Splits not to exceed the diameter in length are permitted in the bottom third of the post. A single shake is permitted in the bottom third, provided it is not wider than one-half the butt diameter.		
Decay:	Allowed in knots only.		
Holes:	Pin holes 1 mm (1/16 in.) or less are not restricted.		
Slope of Grain:	1 in 10.		
Compression Wood:	Not allowed, in the outer 25 mm (1 in.) or if exceeding ¼ of the radius.		
Timber Spacers:	When timber spacers are required, the timber species shall be the same as those furnished for the timber posts. The size and hole location shall be as shown on the plans, with a tolerance of 6 mm (¼ in.). Spacers shall be of medium grain, at least four (4) rings per inch on one end, and free from splits, shakes, compression wood or decay in any form. Individual knots, knot clusters or knots in the same cross section of a face are permitted, provided they are sound or firm, and are limited in cumulative width (when measured between lines parallel to the edges) to no more than one-half the width of the face. Wane or the absence of wood is limited to one-third of the face on no more than 10 percent of the lot. Slope of grain deviation is limited to one in six. The material may be rough sawn or surfaced, full size, hit or miss, with a tolerance of 6 mm (¼ in.) for all dimensions.		
Treatment:	Treating – American Wood-Preservers' Association (AWPA) – Book of Standards (BOS) U1-05 use category system UCS: user specification for treated wood; commodity specification B; Posts; Wood for Highway Construction must be met using the methods outlined in AWPA BOS T1-05 Section 8.2. Each post treated shall have a minimum sapwood depth of 19 mm (¾ in.) as determined by examination of the tops and butts of each post. Material that has been air dried or kiln dried shall be inspected for moisture content in accordance with AWPA standard M2 prior to treatment. Tests of representative pieces shall be conducted. The lot shall be considered acceptable when the average moisture content does not exceed 25 percent. Pieces exceeding 29 percent moisture content shall be rejected and removed from the lot.		
Species Specific Criteria		 <div> <div>Round-Post MGS</div> <div>Grading Specifications</div> </div>	
Ponderosa Pine:		Knot diameter for posts of Ponderosa Pine shall not exceed 102 mm (4 in.). Ring density for the species shall be at least 6 rings-per-inch as measured over a 76 mm (3 in.) distance. The diameter of the Ponderosa Pine posts shall be 203 mm (8 in.) at the ground line with an upper limit of 222 mm (8¾ in.).	
		Dwg. Name: FPL_MGS_PP_R4-metric Scale: None Units: mm	Date: 06/20/2008 Drawn By: CEP Rev: B/C CME

Figure 77. MGS Round Post Ponderosa Pine Details – Grading Specifications



Figure 78. MGS Round Post Ponderosa Pine Photographs



Figure 79. MGS Round Post Ponderosa Pine Photographs



Figure 80. MGS Round Post Ponderosa Pine Photographs



Figure 81. MGS Round Post Ponderosa Pine Photographs

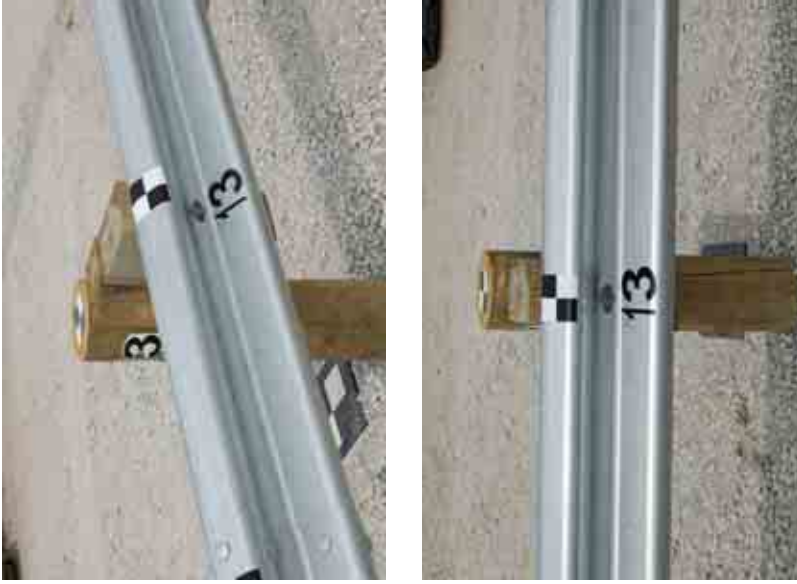
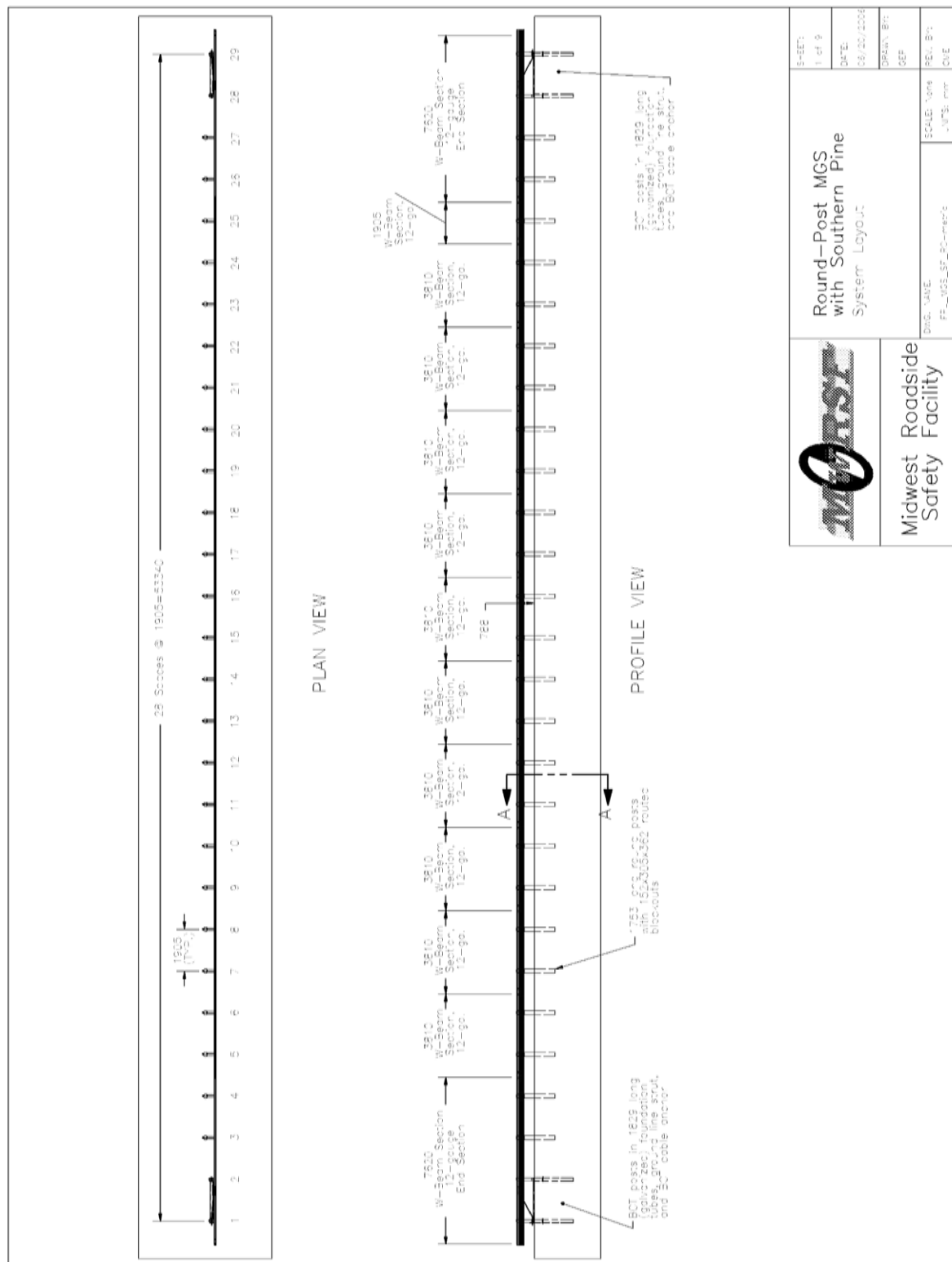


Figure 82. MGS Round Post Ponderosa Pine Photographs



Figure 83. MGS Round Post Ponderosa Pine Photographs



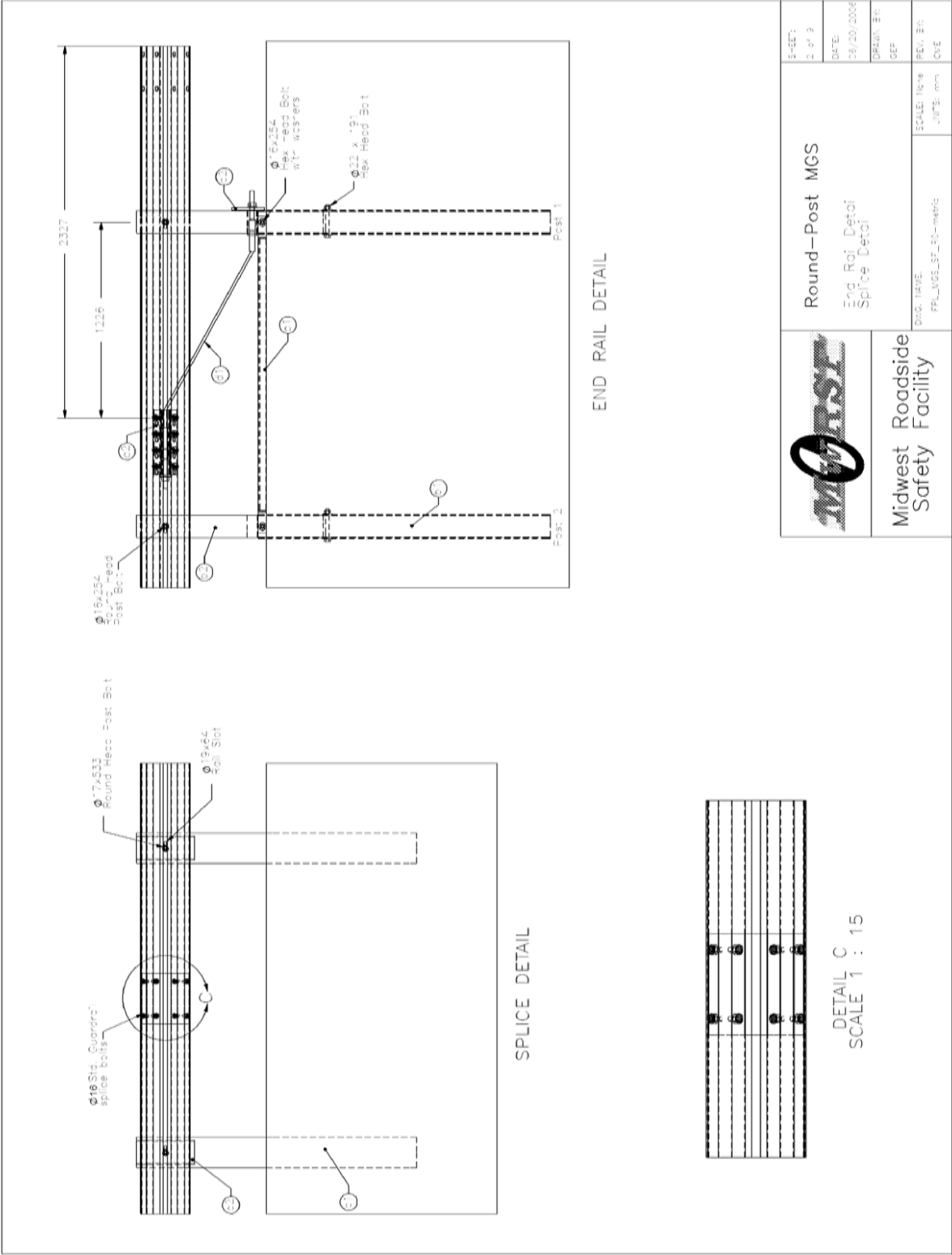


Figure 85. MGS Round Post Southern Yellow Pine Details – End Rail and Splice Detail

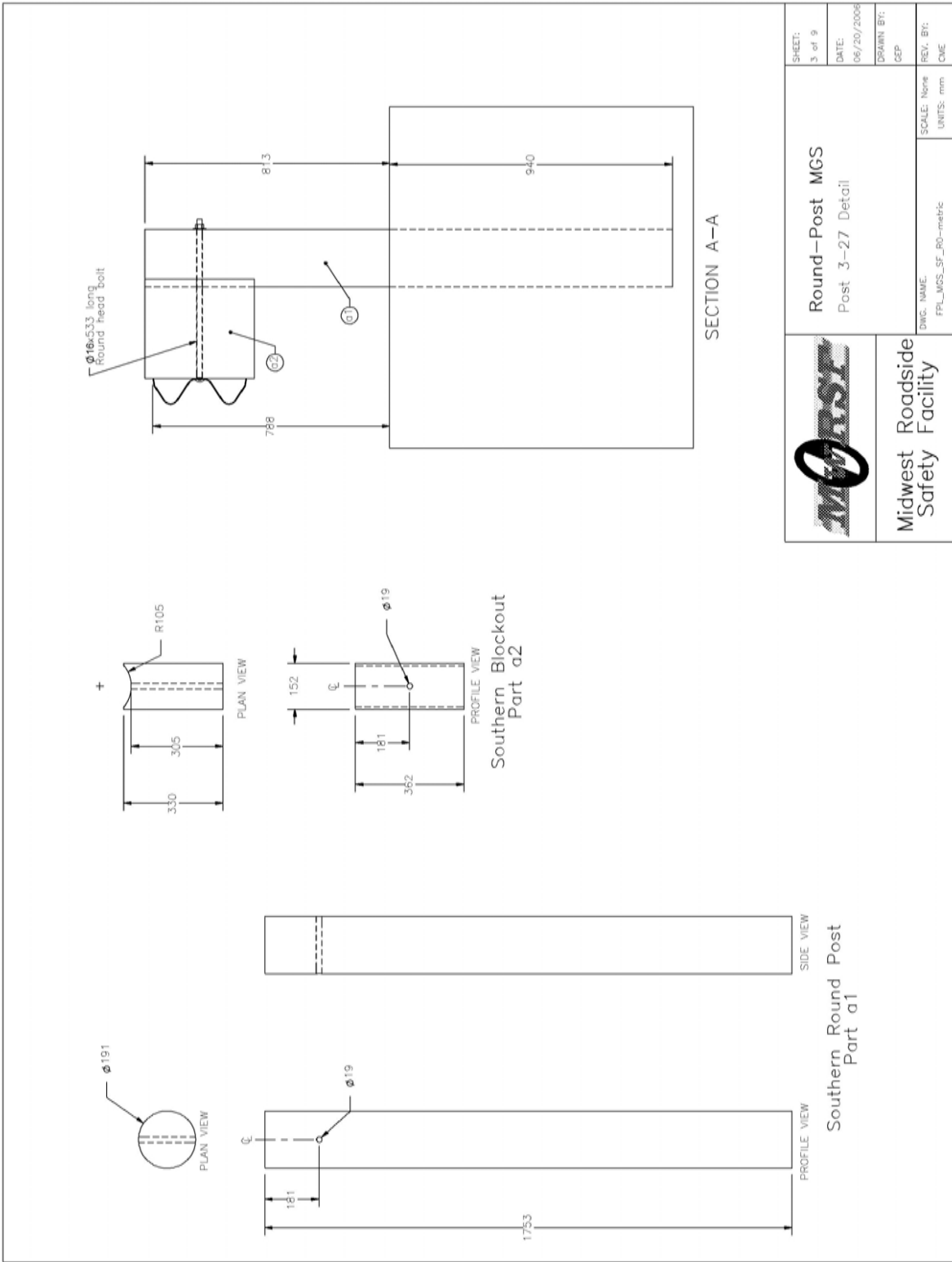


Figure 86. MGS Round Post Southern Yellow Pine Details – Post Detail

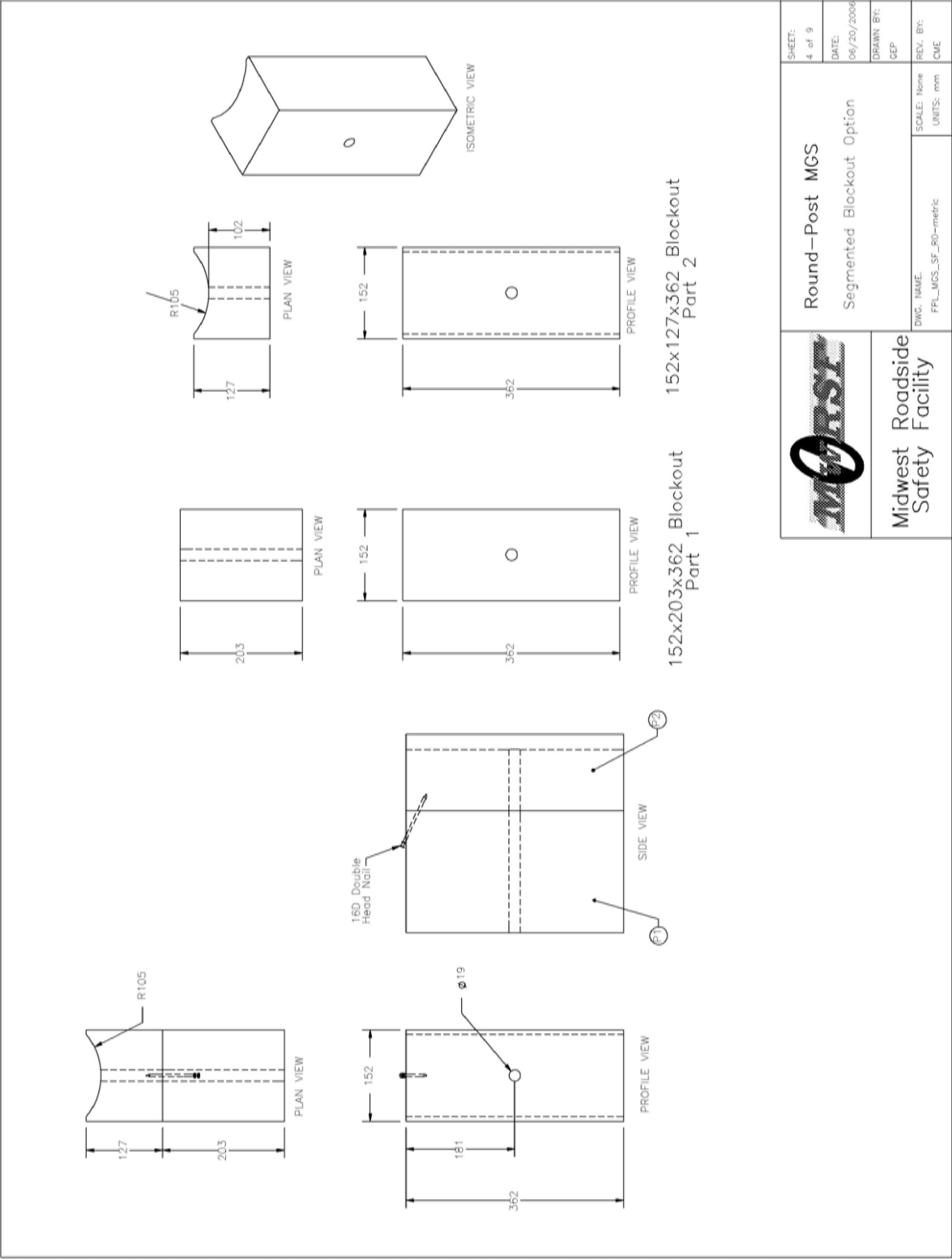


Figure 87. MGS Round Post Southern Yellow Pine Details – Segmented Blackout Detail

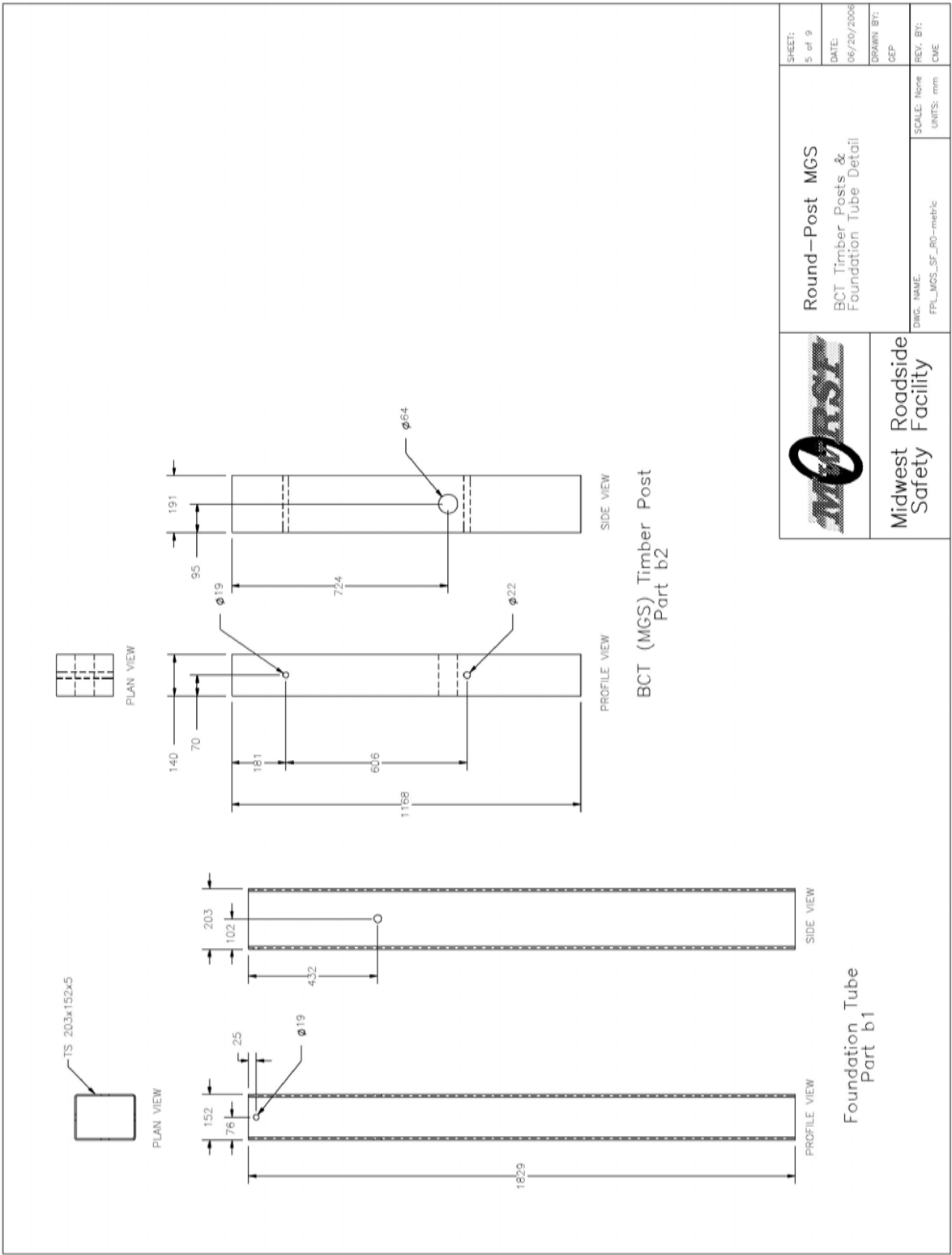


Figure 88. MGS Round Post Southern Yellow Pine Details – Anchor Post Detail

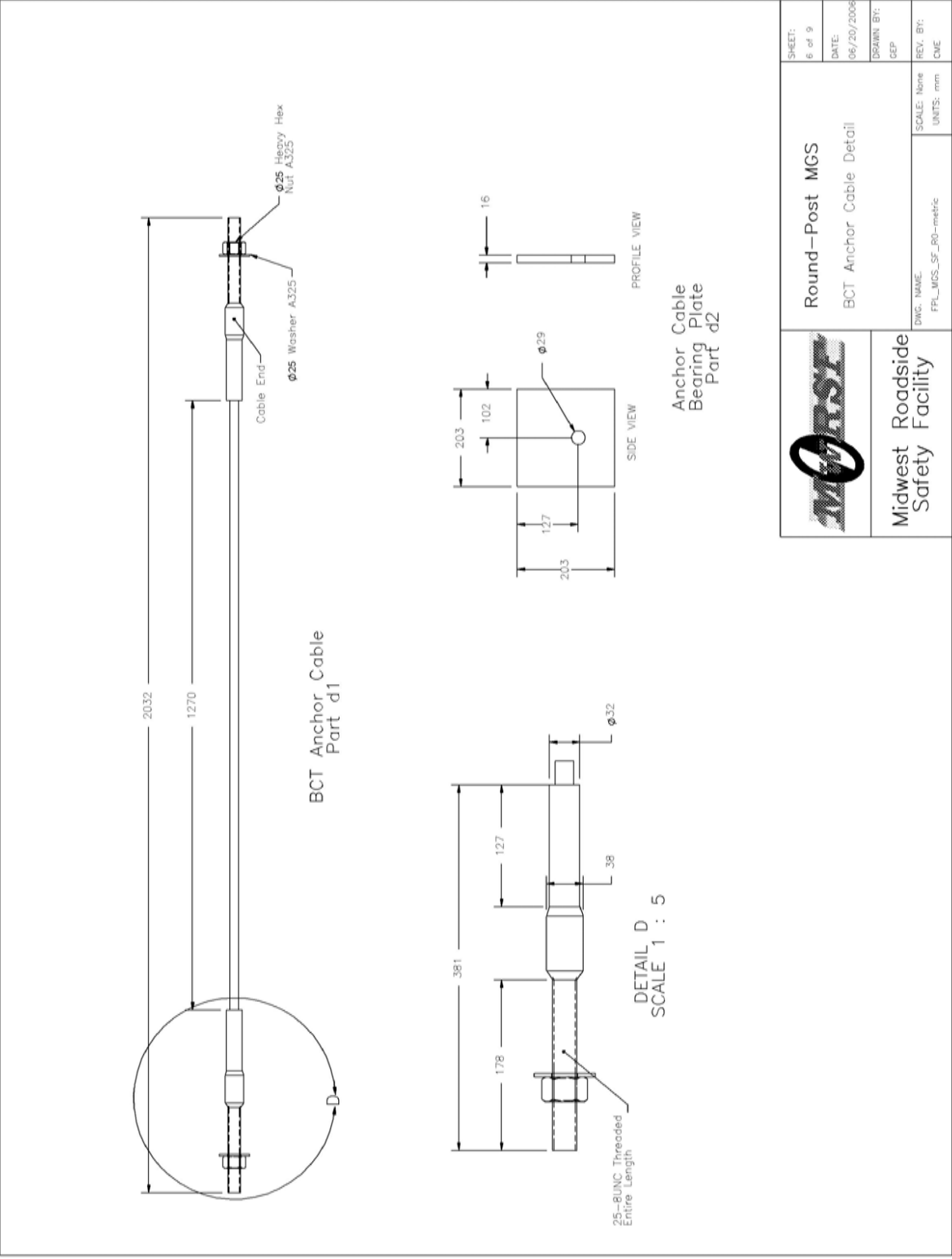


Figure 89. MGS Round Post Southern Yellow Pine Details – BCT Anchor Cable Detail

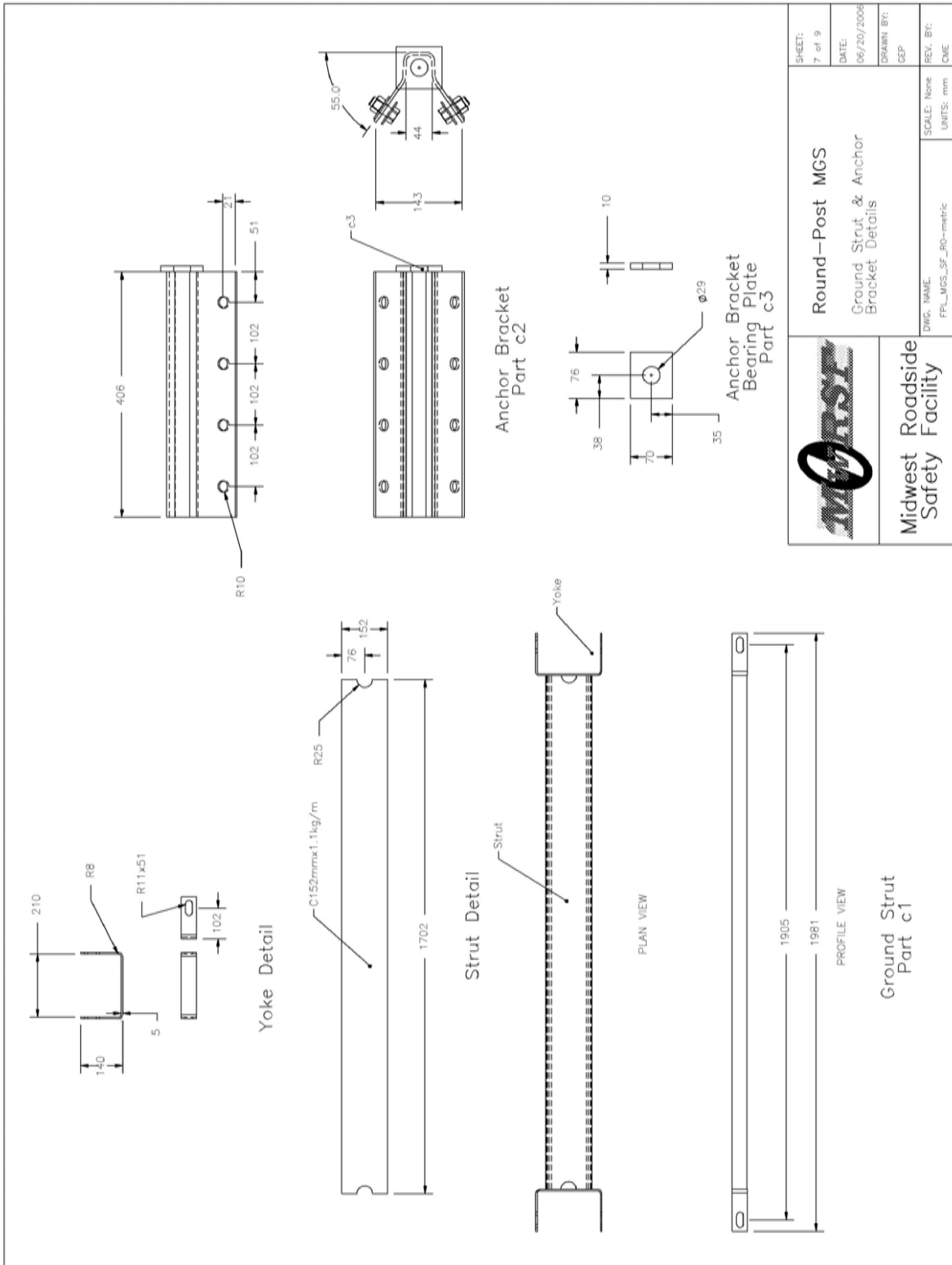


Figure 90. MGS Round Post Southern Yellow Pine Details – Ground Strut and Anchor Bracket Detail

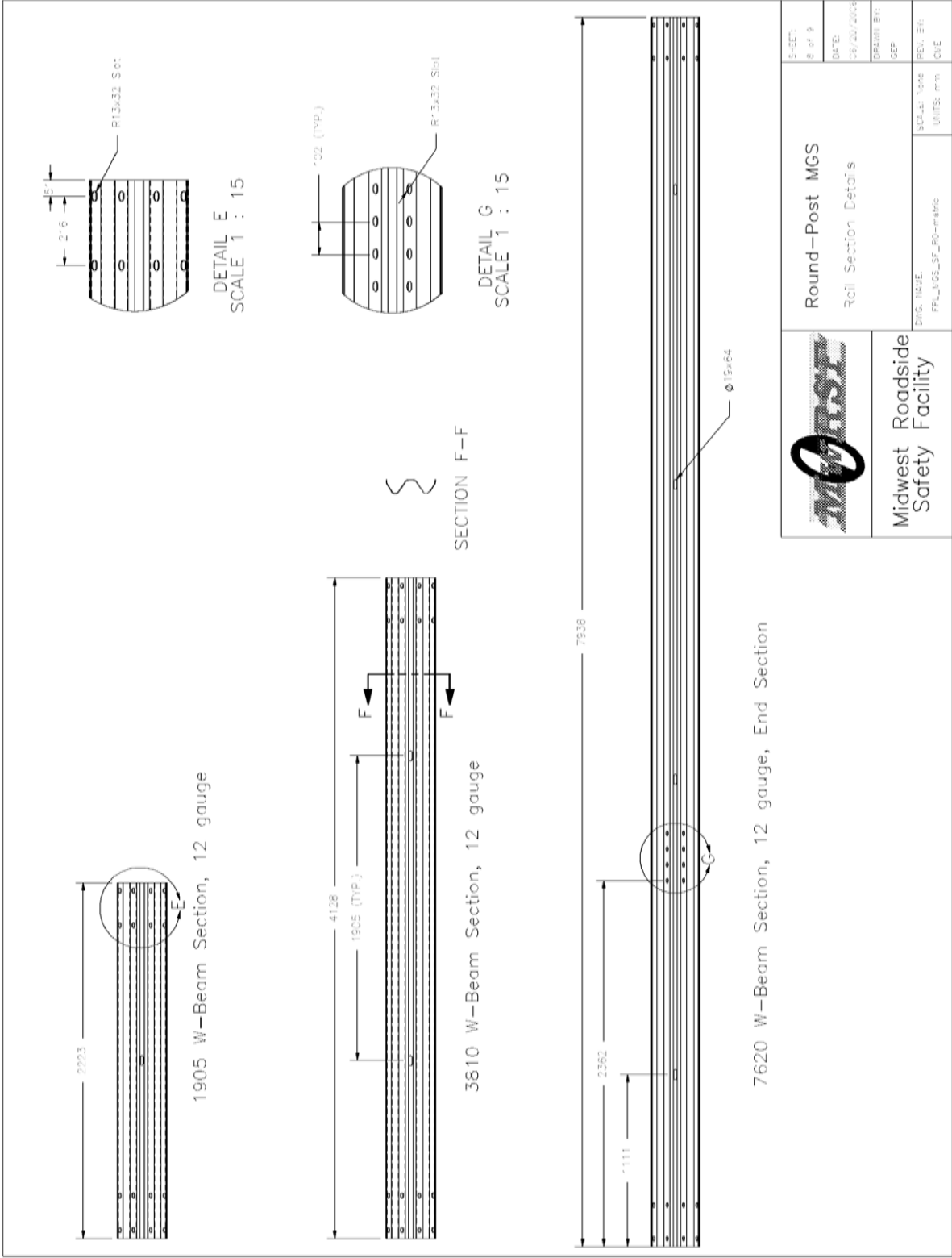


Figure 91. MGS Round Post Southern Yellow Pine Details – Rail Section Detail

<p><i>General</i></p>	<p align="center">Guardrail Post Grading Criteria</p> <p>All posts shall meet the current quality requirements of the American National Standards Institute (ANSI) 05.1, "Wood Poles" except as supplemented herein:</p> <p>Manufacture: All posts shall be smooth shaved by machine. No "ringing" of the posts, as caused by improperly adjusted peeling machine, is permitted. All outer and inner bark shall be removed during the shaving process. All knots and knolls shall be trimmed smooth and flush with the surface of the posts. The guardrail posts will be a minimum of 1.75 m (69 in.) long. The use of peeler cores is prohibited.</p> <p>Ground-line: The ground-line, for the purpose of applying these restrictions of ANSI 05.1 that reference the ground-line, shall be defined as being located 914 mm (36 in.) from the butt end of each post.</p> <p>Size: The size of the posts shall be classified based on their diameter at the ground-line and their length and will be species specific. The ground-line diameter shall be specified by diameter in 6 mm (¼ in.) breaks. The length shall be specified in 300 mm (1 ft) breaks. Dimension shall apply to fully seasoned posts. When measured between their extreme ends, the post shall be no shorter than the specified lengths but may be up to 75 mm (3 in.) longer.</p> <p>Scars: Scars are permitted in the middle third as defined in ANSI 05.1 provided that the depth of the trimmed scar is not more than (1 in.).</p> <p>Shape and Straightness: All timber posts shall be nominally round in cross section. A straight line drawn from the centerline of the top to the center of the butt of any post shall not deviate from the centerline of the post more than 32 mm (1¼ in.) at any point. Posts shall be free from reverse bends.</p> <p>Splits and Shakes: Splits or ring shakes are not permitted in the top two thirds of the post. Splits not to exceed the diameter in length are permitted in the bottom third of the post. A single shake is permitted in the bottom third, provided it is not wider than one-half the butt diameter.</p> <p>Decay: Allowed in knots only.</p> <p>Holes: Pin holes 1 mm (1/16 in.) or less are not restricted.</p> <p>Slope of Grain: 1 in 10.</p> <p>Compression Wood: Not allowed, in the outer 25 mm (1 in.) or if exceeding ¼ of the radius.</p> <p>Timber Spacers: When timber spacers are required, the timber species shall be the same as those furnished for the timber posts. The size and hole location shall be as shown on the plans, with a tolerance of 6 mm (¼ in.). Spacers shall be of medium grain, at least four (4) rings per inch on one end, and free from splits, shakes, compression wood or decay in any form. Individual knots, knot clusters or knots in the same cross section of a face are permitted, provided they are sound or firm, and are limited in cumulative width (when measured between lines parallel to the edges) to no more than one-half the width of the face. Wane or the absence of wood is limited to one-third of the face on no more than 10 percent of the lot. Slope of grain deviation is limited to one in six. The material may be rough sawn or surfaced, full size, hit or miss, with a tolerance of 6 mm (¼ in.) for all dimensions.</p> <p>Treatment: Treating – American Wood-Preservers' Association (AWPA) – Book of Standards (BOS) U1-05 use category system UCS: user specification for treated wood; commodity specification B; Posts; Wood for Highway Construction must be met using the methods outlined in AWPA BOS T1-05 Section 8.2. Each post treated shall have a minimum sapwood depth of 19 mm (¾ in.) as determined by examination of the tops and butts of each post. Material that has been air dried or kiln dried shall be inspected for moisture content in accordance with AWPA standard M2 prior to treatment. Tests of representative pieces shall be conducted. The lot shall be considered acceptable when the average moisture content does not exceed 25 percent. Pieces exceeding 29 percent moisture content shall be rejected and removed from the lot.</p>	<table border="1"> <tr> <td data-bbox="1161 222 1266 630">  <p>Midwest Safety Roadside Facility</p> </td><td data-bbox="1161 630 1266 1753"> <p align="center">Round-Post MGS</p> <p align="center">Grading Specifications</p> </td><td data-bbox="1266 222 1347 630"> <p>SHEET: 9 of 9</p> <p>DATE: 06/20/2006</p> <p>DRAWN BY: GEP</p> <p>REV. BY: CME</p> </td></tr> <tr> <td data-bbox="1161 630 1266 1753"> <p>DNIC NAME: FPL_MGS_SF_R0-metric</p> </td><td data-bbox="1266 630 1347 1753"> <p>SCALE: None UNITS: mm</p> </td><td data-bbox="1266 222 1347 630"></td></tr> </table> <p><i>Species Specific Criteria</i></p> <p>Southern Pine: Knot diameter for posts of Southern Pine shall not exceed 64 mm (2½ in.). Ring density for the species shall be at least 4 rings-per-inch as measured over a 76 mm (3 in.) distance. The diameter of the Southern Pine posts shall be 190 mm (7½ in.) at the ground line with a upper limit of 210 mm (8¼ in.).</p>	 <p>Midwest Safety Roadside Facility</p>	<p align="center">Round-Post MGS</p> <p align="center">Grading Specifications</p>	<p>SHEET: 9 of 9</p> <p>DATE: 06/20/2006</p> <p>DRAWN BY: GEP</p> <p>REV. BY: CME</p>	<p>DNIC NAME: FPL_MGS_SF_R0-metric</p>	<p>SCALE: None UNITS: mm</p>	
 <p>Midwest Safety Roadside Facility</p>	<p align="center">Round-Post MGS</p> <p align="center">Grading Specifications</p>	<p>SHEET: 9 of 9</p> <p>DATE: 06/20/2006</p> <p>DRAWN BY: GEP</p> <p>REV. BY: CME</p>						
<p>DNIC NAME: FPL_MGS_SF_R0-metric</p>	<p>SCALE: None UNITS: mm</p>							

Figure 92. MGS Round Post Southern Yellow Pine Details – Grading Specifications

17 TEST CONDITIONS

17.1 Test Facility

The testing facility is located at the Lincoln Air Park on the northwest side of the Lincoln Municipal Airport which is approximately 8.0 km (5 mi.) northwest from the University of Nebraska-Lincoln's city campus.

17.2 Vehicle Tow and Guidance System

A reverse cable tow system, utilizing a 1:2 mechanical advantage, was used to propel the test vehicle. The distance traveled as well as the speed of the tow vehicle were one-half of those measures observed in the actual test vehicle. The test vehicle was released from the tow cable before impact with the barrier system. A digital speedometer was located on the tow vehicle to increase the accuracy of the test vehicle impact speed.

A vehicle guidance system developed by Hinch [50] was used to steer the test vehicle. A guide-flag, attached to the front-right wheel and the guide cable, was sheared off before impact with the barrier system. The 9.5-mm (0.375-in.) diameter guide cable was tensioned to approximately 15.6 kN (3,500 lbs), and supported laterally and vertically every 30.48 m (100 ft) by hinged stanchions. The hinged stanchions stood upright while holding up the guide cable, but as the vehicle was towed down the line, the guide-flag struck and knocked each stanchion to the ground. For tests MGSDF-1 and MGSPP-1, the vehicle guidance systems were 301 m (988 ft) and 329 m (1080 ft) long, respectively.

17.3 Test Vehicles

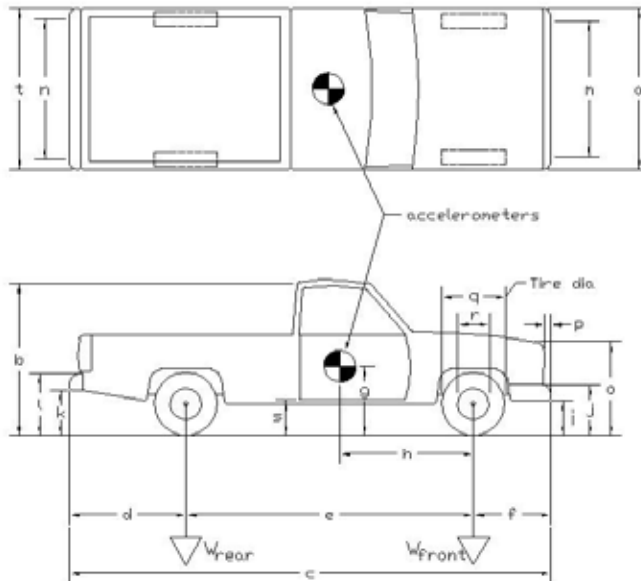
For test no. MGSDF-1, a 2000 GMC C2500 pickup truck was used as the test vehicle. The test inertial and gross static weights were 2,018 kg (4,450 lbs). The test vehicle is shown in Figure 93, with its dimensions shown in Figure 94.



Figure 93. Test Vehicle, Test MGSDF-1

Date: 6/16/06 Test Number: MGSDf-1 Model: 2000P/ 2500
 Make: GMC Vehicle I.D.#: 1GDGC24R3YF420768
 Tire Size: 247/75R16 Year: 2000 Odometer: 299666

*(All Measurements Refer to Impacting Side)



Vehicle Geometry - mm (in.)

a 1880 (74.0) b 1848 (72.75)
 c 5537 (218) d 1321 (52)
 e 3340 (131.5) f 876 (34.5)
 g 667 (26.25) h 899 (35.4)
 i 622 (24.5) j 800 (31.5)
 k 622 (24.5) l 800 (31.5)
 m 1600 (63) n 1626 (64)
 o 1041 (41) p 76 (3)
 q 768 (30.25) r 445 (17.5)
 s 483 (19) t 1867 (73.5)
 Wheel Center Height Front 368 (14.5)
 Wheel Center Height Rear 368 (14.5)
 Wheel Well Clearance (FR) 905 (35.625)
 Wheel Well Clearance (RR) 965 (38)

Frame Height (FR) 416 (16.375)

Frame Height (RR) 686 (27)

Engine Type 8 CYL. GAS

Engine Size 5.7 L 350 CID

Transmission Type:

Automatic or Manual

FWD or RWD or 4WD

Weights kg (lbs)	Curb	Test Inertial	Gross Static
W_{front}	<u>1211 (2669)</u>	<u>1171 (2581)</u>	<u>1171 (2581)</u>
W_{rear}	<u>868 (1914)</u>	<u>848 (1869)</u>	<u>848 (1869)</u>
W_{total}	<u>2079 (4583)</u>	<u>2018 (4450)</u>	<u>2018 (4450)</u>

GVWR Rating

front 4100

rear 6000

total 8600

Note any damage prior to test: None

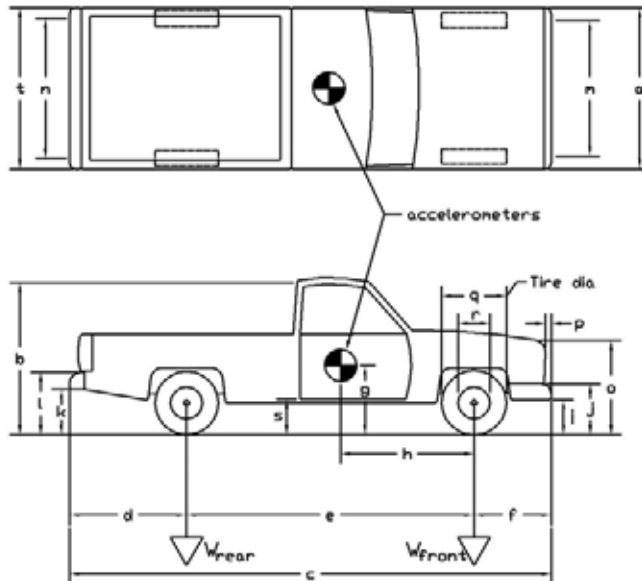
Figure 94. Vehicle Dimensions, Test MGSDf-1



Figure 95. Test Vehicle, MGSP-1

Date: 6/1/06 Test Number: MGSP-1 Model: 2000P/ 2500
 Make: GMC Vehicle I.D.#: 1GDGC24R4YF418396
 Tire Size: LT245/75 R16 Year: 2000 Odometer: 224500

*(All Measurements Refer to Impacting Side)



Vehicle Geometry - mm (in.)

a 1880 (74.0) b 1918 (75.5)
 c 5556 (218.75) d 1283 (50.5)
 e 3350 (131.875) f 924 (36.375)
 g 514 (20.25) h 1413 (55.625)
 i 451 (17.75) j 670 (26.375)
 k 629 (24.75) l 806 (31.75)
 m 1594 (62.75) n 1622 (63.875)
 o 1035 (40.75) p 89 (3.5)
 q 632 (24.875) r 445 (17.5)
 s 476 (18.75) t 1848 (72.75)
 Wheel Center Height Front 368 (14.5)
 Wheel Center Height Rear 378 (14.875)
 Wheel Well Clearance (FR) 908 (35.75)
 Wheel Well Clearance (RR) 972 (38.25)

Weights kg (lbs)	Curb	Test Inertial	Gross Static
W_{front}	<u>1131 (2493)</u>	<u>1168 (2576)</u>	<u>1168 (2576)</u>
W_{rear}	<u>828 (1826)</u>	<u>856 (1888)</u>	<u>856 (1888)</u>
W_{total}	<u>1959 (4319)</u>	<u>2025 (4464)</u>	<u>2025 (4464)</u>

GVWR Rating

front 8800
 rear 6000
 total 8600

Frame Height (FR) 410 (16.125)
 Frame Height (RR) 705 (27.75)

Engine Type 8 CYL. GAS

Engine Size 5.7 L 350 CID

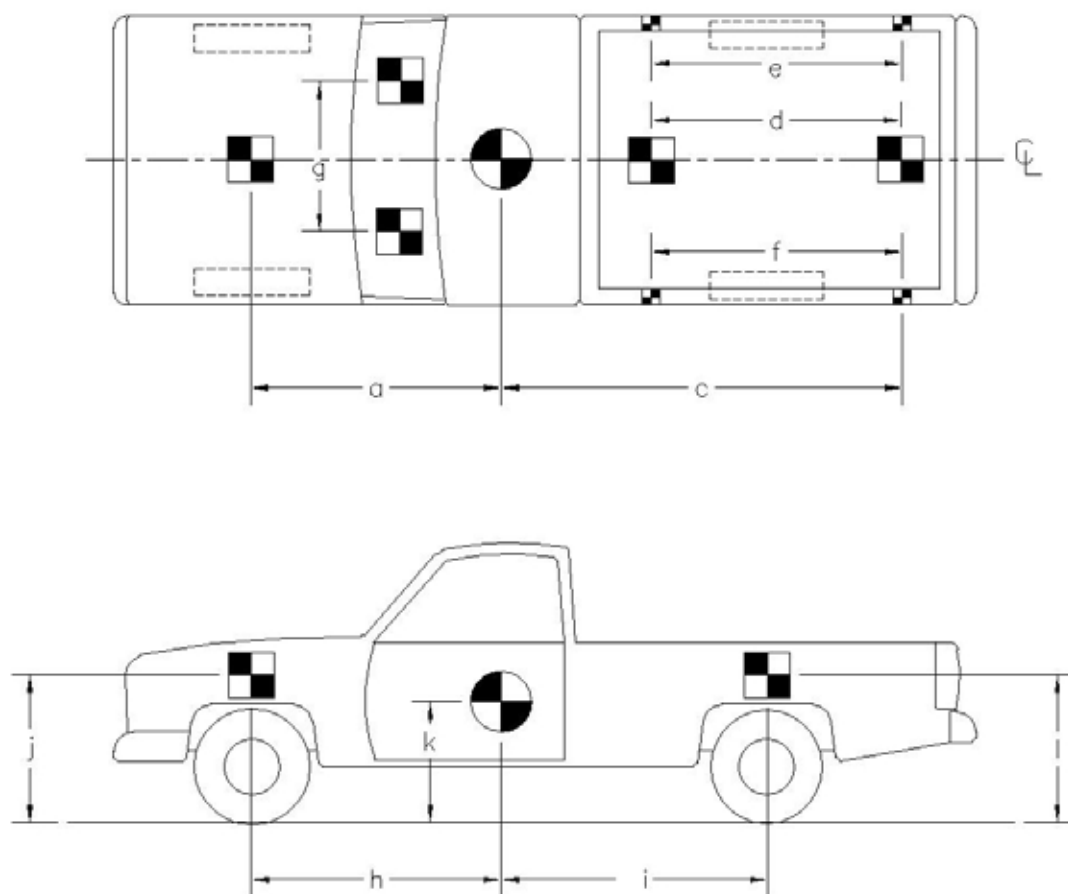
Transmission Type:

(Automatic) or Manual

FWD or (RWD) or 4WD

Note any damage prior to test: None

Figure 96. Vehicle Dimensions, Test MGSP-1

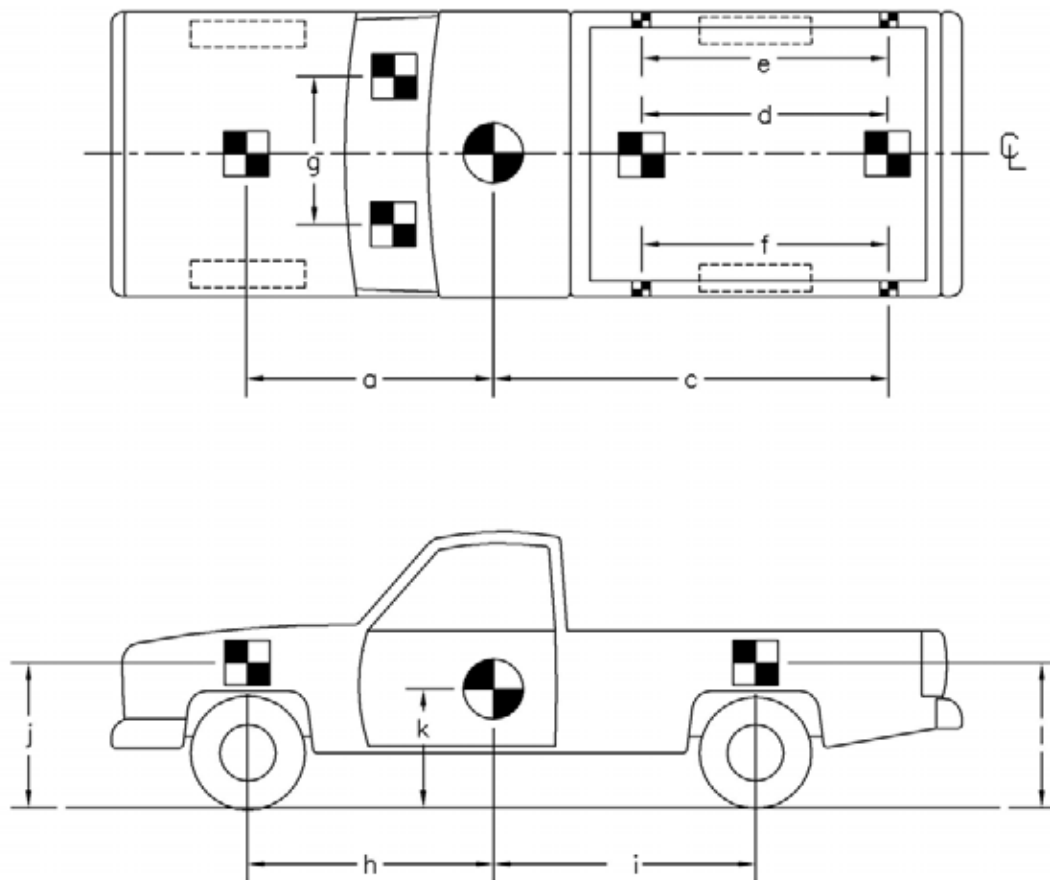


TEST #: mgsdf-1

TARGET GEOMETRY -- mm (in.)

a	<u>1610 (63.375)</u>	d	<u>1692 (66.625)</u>	g	<u>911 (35.875)</u>	j	<u>1006 (39.625)</u>
b	<u>—</u>	e	<u>2153 (84.75)</u>	h	<u>1407 (55.4)</u>	k	<u>667 (26.25)</u>
c	<u>2638 (103.875)</u>	f	<u>2153 (84.75)</u>	i	<u>1934 (76.125)</u>	l	<u>1067 (42)</u>

Figure 97. Vehicle Target Locations, Test MGSDF-1



TEST #: mgsp-1

TARGET GEOMETRY -- mm (in.)

a	<u>1610 (63.375)</u>	d	<u>1632 (64.25)</u>	g	<u>921 (36.25)</u>	j	<u>1006 (39.625)</u>
b	<u>—</u>	e	<u>2153 (84.75)</u>	h	<u>1413 (55.625)</u>	k	<u>667 (26.25)</u>
c	<u>2562 (100.875)</u>	f	<u>2153 (84.75)</u>	i	<u>1937 (76.25)</u>	l	<u>1064 (41.875)</u>

Figure 98. Vehicle Target Locations, Test MGSPP-1

For test MGSPP-1, a 2000 GMC C2500 pickup truck was used as the test vehicle. The test inertial and gross static weights were 2,025 kg (4,464 lbs). The test vehicle is shown in Figure 95, with its dimensions shown in Figure 96.

Black and white, checkered targets were placed on the vehicle, as shown in Figure 97 for test MGSDF-1 and Figure 98 for MGSPP-1, to aid in the analysis of the high-speed digital video. One target was placed directly above each of the wheels, and another was placed at the vehicle's center of gravity on both the driver and passenger sides. In addition, targets were placed on the top of the vehicle. One was placed at the vehicle's center of gravity, two were placed on the windshield, one was placed on the hood of the vehicle, two were placed in the pickup box, and four targets were placed on the side walls of the box, aligned with those placed in the box.

The front wheels of the test vehicle were aligned for camber, caster, and toe-in values of zero so the vehicle would track properly along the guide cable. A 5B flash bulb was mounted on the left quarter point of the vehicle's roof to pinpoint the time of impact with the test article on the high-speed video footage. The flash bulb was fired by a pressure tape switch mounted on the front-left corner of the bumper. A remote-controlled brake system was installed in the test vehicle so the vehicle could be brought safely to a stop after the test.

17.4 Data Acquisition Systems

Three data acquisition systems, two accelerometers and one rate transducer, were used to measure the motion of the vehicle. The output data from all three devices was analyzed and plotted using the "DynaMax 1 (DM-1)" and "DADiSP" computer software programs.

17.4.1 Accelerometers

Two triaxial piezoresistive accelerometer systems with a range of ± 200 G's were used to measure the acceleration in the longitudinal, lateral, and vertical directions. Both systems were

developed by Instrumented Sensor Technology (IST) of Okemos, Michigan. The first environmental shock and vibration sensor/recorder system, Model EDR-4M6, recorded at a sample rate of 10,000 Hz and includes three differential channels as well as three single-ended channels. The EDR-4 was configured with 6 MB of RAM memory and a 1,500 Hz lowpass filter.

The second environmental shock and vibration sensor/recorder system, Model EDR-3, recorded at a sample rate of 3,200 Hz and was configured with 256 kB of RAM memory and a 1,120 Hz lowpass filter.

17.4.2 Angular Rate Transducers

An Analog Devices, Inc. model ADXRS300 rate gyro with a range of ± 1200 degrees/sec in each of the three directions (pitch, roll, and yaw) was used to measure the rotational rates of motion of the test vehicle. The rate transducer was internally mounted on EDR-4M6, and therefore was also rigidly attached to the vehicle near its center of gravity. Rate transducer signals were stored in the internal memory of EDR-4M6.

17.4.3 High-Speed Photography

For test no. MGSDf-1, four high-speed VITcam digital video cameras, one high-speed 16-mm Red Lake E/cam video camera, and seven digital video cameras were used. Camera details, lens information, and camera operating speeds are shown along with a schematic of the camera locations in Figure 99.

For test no MGSP-1, four high-speed VITcam digital video cameras, and seven digital video cameras were used. Camera details, lens information, and camera operating speeds are shown along with a schematic of the camera locations in Figure 100.

MGSDF-1 Camera Summary

No.	Type	Operating Speed (frames/sec)	Lens	Lens Setting
1	Vitcam CTM	500	12 mm fixed	12 mm
2	Vitcam CTM	500	Sigma 24-135 mm	70 mm
3	Vitcam CTM	500	Sigma 24-70 mm	24 mm
4	Vitcam CTM	500	Sigma Ex 70-200 mm	70 mm
2	Canon-ZR10	29.97		
4	Canon-ZR30	29.97		
6	Canon-ZR25	29.97		
7	Canon-ZR90	29.97		
8	Canon-ZR90	29.97		
1	JVC - GZ-MC500 (Everio)	29.97		
2	JVC - GZ-MC40u (Everio)	29.97		

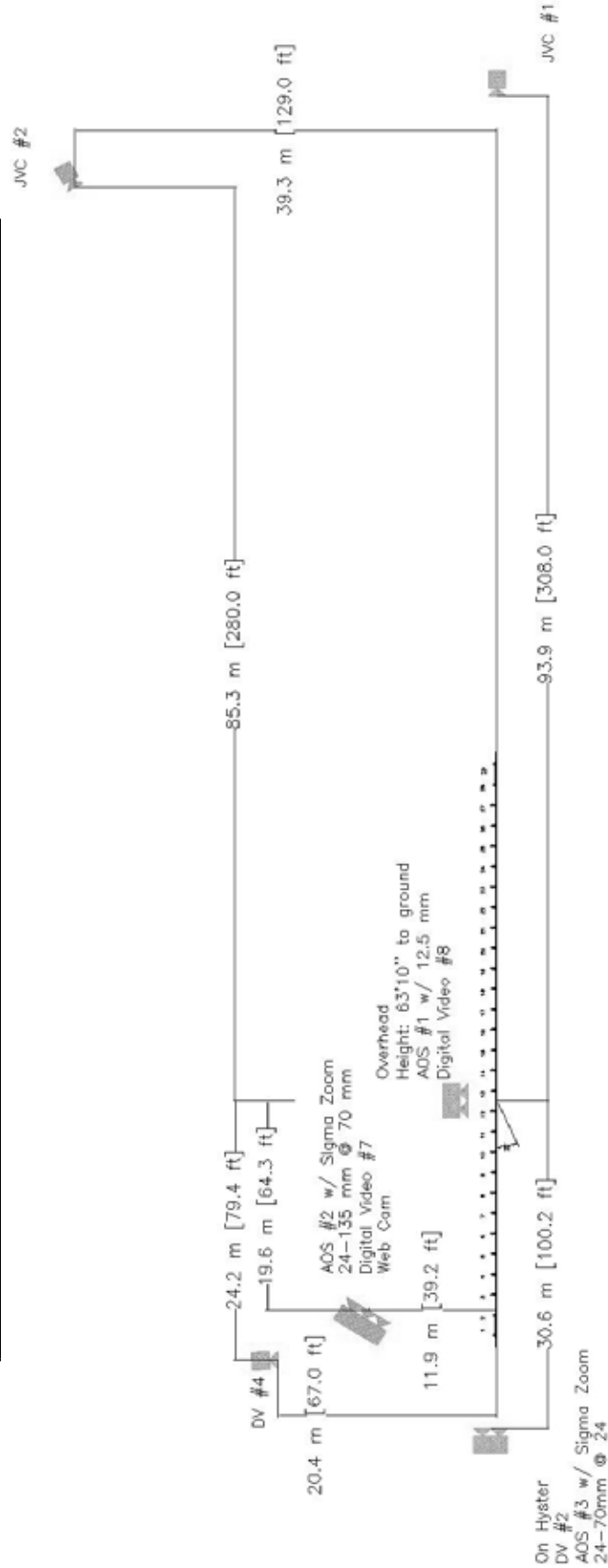


Figure 99. Locations of High-Speed Cameras, Test MGSDF-1

MGSP-1 Camera Summary

No.	Type	Operating Speed (frames/sec)	Lens	Lens Setting
1	Vitcam CTM	500	12 mm fixed	12 mm
2	Vitcam CTM	500	Sigma 24-135 mm	70 mm
3	Vitcam CTM	500	Sigma 24-70 mm	70 mm
4	Vitcam CTM	500	AP0 70-200 mm	200 mm
20	Redlake E/Cam Camera	500	TV Zoom Lens 8-48 mm	20 mm
2	Canon-ZR10	29.97		
4	Canon-ZR30	29.97		
6	Canon-ZR25	29.97		
7	Canon-ZR90	29.97		
8	Canon-ZR90	29.97		
1	JVC - GZ-MC500 (Everio)	29.97		
2	JVC - GZ-MC400 (Everio)	29.97		

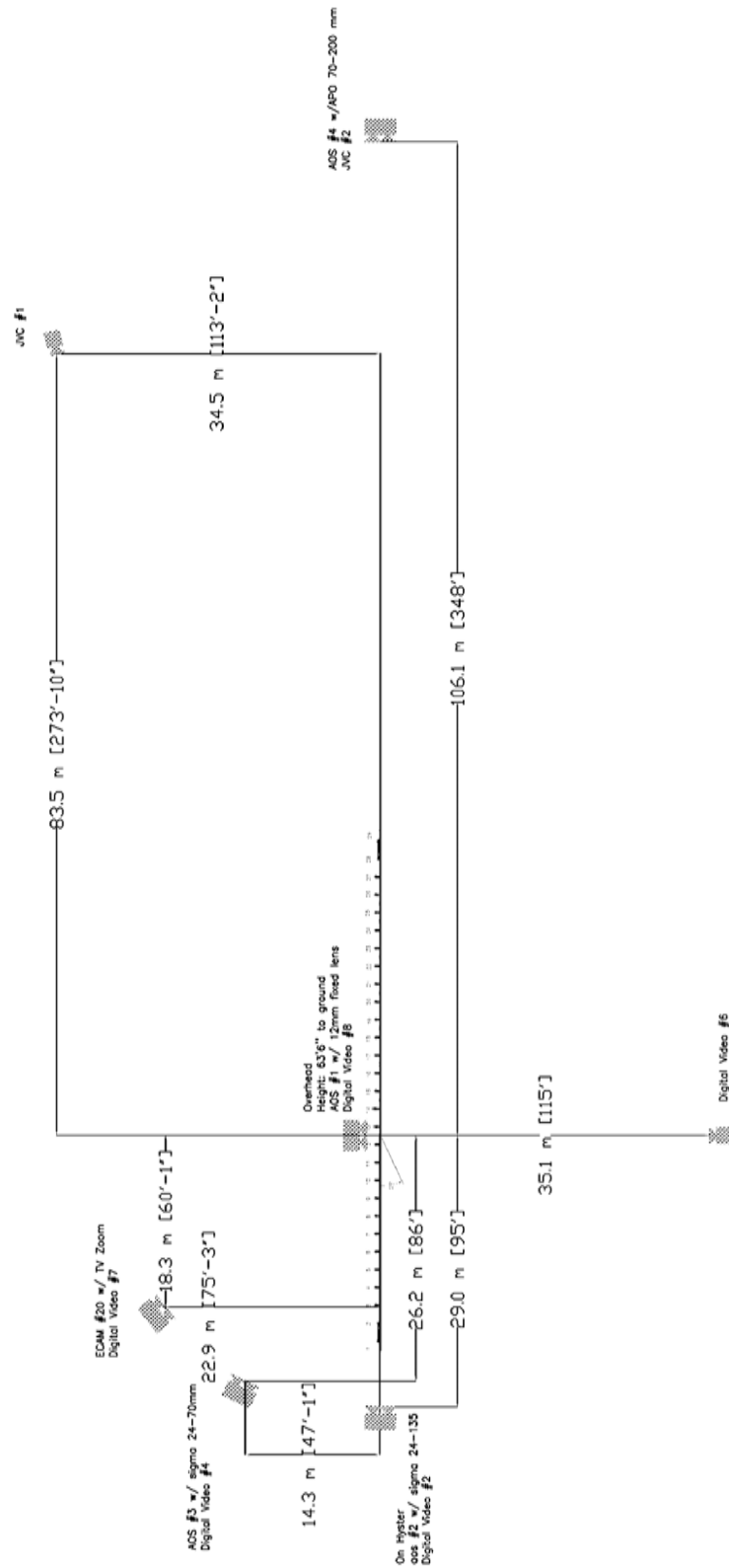


Figure 100. Locations of High-Speed Cameras, Test MGSP-1

The VITcam and E/cam videos were analyzed using Image Express MotionPlus and Redlake Motion Scope software, respectively. Camera speed and camera divergence factors were considered in the analysis of the high-speed videos.

17.4.4 Pressure Tape Switches

For both tests, five pressure-activated tape switches, spaced at 2-m (6.56-ft) intervals, were used to determine the speed of the vehicle before impact. Each tape switch fired a strobe light which sent an electronic timing signal to the data acquisition system as the left-front tire of the test vehicle passed over it. The test vehicle speed was then determined from the electronic timing mark data recorded using the “Test Point” software. Strobe lights and high-speed film analysis are used only as a backup in the event that vehicle speed cannot be determined from the electronic data.

18 CRASH TEST NO. MGSDF-1

18.1 Test No. MGSDF-1

Test no. MGSDF-1 was conducted according to NCHRP Report No. 350 Test Designation 3-11. The 2,018-kg (4,450-lb) pickup truck impacted the test article at a speed of 100.0 km/h (62.14 mph) and an angle of 25.5 degrees. The target critical impact point was 953 mm (37 ½ in.) downstream of the centerline of post no. 12. Actual vehicle impact with the barrier system occurred 152.4 mm (6 in.) downstream of the target. A summary of the test results and sequential photographs are shown in Figure 102. Additional sequential and documentary photographs are shown in Figures 103 through 106. An equivalent English-unit summary is shown in Appendix I.

18.2 Test Description

After 0.004 sec, the left-front bumper corner was crushing as post no. 13 deflected backward. At approximately 0.012 sec, post no. 12 began deflecting, and a bend developed in the rail between post nos. 12 and 13. After 0.024 sec, post no. 14 also deflected backward. At this same time, flattening of the rail was clearly evident in the impact region. Post no. 13 was the first post to fracture, breaking at 0.040 sec, at which time post no. 15 also deflected backward.

At 0.044 sec, post nos. 11 and 12 and their corresponding blockouts rotated downstream. At approximately 0.05 sec, a bend developed in the rail at post no. 15. Post no. 14 fractured after approximately 0.083 sec, the same time at which the posts and blockouts downstream of impact rotated toward the impact location. Approximately 0.104 sec after impact, post no. 16 deflected backward. At this same time, the left-front tire impacted the upstream face of post no. 14. The left-front tire slipped under the rail after 0.120 sec as the rail continued to crush the left-front corner of the test vehicle, and post no. 16 also deflected backward at this time.

At 0.148 sec, post no. 15 was impacted and pushed by the left-front tire, and post no. 17 began to deflect backward. After 0.154 sec, the damage being caused by the rail was largely concentrated to the left door panel. Post no. 15 fractured after 0.16 sec and continued to be pushed forward by the front of the truck and the left-front wheel. Post no. 17 began deflecting after 0.176 sec, followed by post no. 18 which began deflecting after 0.190 sec.

After 0.212 sec, post no.16 was impacted by the left-front wheel, causing it to fracture after 0.224 sec, the same time at which the rail developed a significant bend at post no. 17. The vehicle continued to push post no. 16 away from the system until 0.254 sec. The left-front corner of the vehicle was lifted slightly by the rail at 0.214 sec. At 0.270 sec, the left-front wheel impacted post no. 17 causing it to fracture. After 0.276 sec, a fold developed at post no. 18, which began to deflect at 0.286 sec and fractured after 0.322 sec. Upon the fracture of post no. 18, a bend developed in the rail at post no. 19.

At 0.340 sec, post no. 17 was being pushed forward by the left-front tire, post no.18 broke away from the system, and post no. 19 deflected backward. At approximately 0.385 sec, the entire left side of the pickup truck was in contact with the rail, with the vehicle becoming parallel to the system at approximately 0.527 sec. At 0.596 sec, the pickup truck was contacting and overhanging post no. 19. The back of the vehicle lost contact with the rail at approximately 0.671 sec as it began to yaw counterclockwise.

After 0.778 sec, the rail began to fall off the blockouts corresponding to the posts upstream of post no. 12. The separation of the rail from the blockouts continued at post no. 12 after 1.480 sec, and by 1.700 sec the rail had lost its connection with all the posts upstream of post no. 21. The front of the vehicle remained in contact with the system through the duration of the event.

18.3 System and Component Damage

The upstream anchor suffered fairly minimal damage. The guardrail tore from both post nos. 1 and 2. Post no. 1 was bent downstream approximately 5 to 10 degrees, and the steel anchor tubes were pulled downstream slightly. Post nos. 3 through 6 showed no signs of damage and no rotation. Post nos. 7 and 8 were twisted so their blockouts were rotated approximately 10 degrees downstream. Post nos. 9, 10, and 11 were also twisted downstream, but approximately 20 degrees.

Post no. 12 was rotated slightly downstream and backward. There was a small buckle in the rail at post no. 12, and the upstream corner of the blockout was crushed by the guardrail. Actual impact occurred 152 mm (6 in.) downstream of the impact target, with the contact marks continuing along the top rail through post no. 20. Post no. 13 was broken below the ground. There was a small buckle in the rail at the centerline of the post, three buckles in the top rail at 279 mm (11 in.), 914 mm (36 in.), and 1,448 mm (57 in.) downstream of the post, and two buckles in the bottom rail at 686 mm (27 in.) and 1,143 mm (45 in.) downstream of the post. A 660-mm (26-in.) long section of rail was severely flattened beginning 508 mm (20 in.) downstream of post no. 13. Contact marks on the bottom rail began at post no. 13 and continued through post no. 20.

Similar to post no. 13, post no. 14 broke off below the ground. Three buckles were present in the upper rail at 254 mm (10 in.), 813 mm (32 in.), and 1,321 mm (52 in.) downstream of post no. 14. Post no. 15 was also broken off at the ground. Another major buckle was located at the centerline of post no. 15, where the slot was torn by the post bolt pulling free from the rail. Two additional buckles in the top rail were located 406 mm (16 in.) and 1,092 mm (43 in.) downstream of post no. 15.

Post no. 16 was completely pulled from the ground without fracture or significant damage. The rail slot corresponding to post no. 16 was slightly torn, and there were buckles in the rail at the centerline of the post, 635 mm (25 in.) downstream of the post, and at the downstream end of the rail splice. Post nos. 17 through 19 were all broken off at the ground level. The rail slot corresponding to post 17 was torn where the bolt pulled from the rail, and there was a buckle in the rail located 483 mm (19 in.) downstream of the slot. There were also two very small buckles in the upper rail at 508 mm (20 in.) and 1,372 mm (54 in.) downstream of post no. 19.

Post no. 20 was split vertically with the fracture plane passing through the longitudinal axis of the bolt hole. The post was leaning downstream and backward between 5 and 15 degrees. The slot corresponding to post no. 20 was torn where the bolt pulled free from the rail, and there was a large buckle in the rail at the location of the slot. A second, smaller buckle was located in the top rail, 1,499 mm (59 in.) downstream of the post. In addition, the blockout was broken off the post. Post nos. 21 and 22 showed no damage. The rail pulled away from the bolt at post no. 21, and there was a buckle at the splice following post no. 22. White contact marks were identified on the upper rail beginning 152 mm (6 in.) upstream of post no. 22 and continuing to the pickup truck's final resting location.

Post no. 23 showed minimal damage, with the blockout rotated about 15 degrees downstream. Post nos. 24 through 29 showed no damage except soil gaps, as detailed in Table 61. Soil gap dimensions for other relevant posts, as measured at the ground line, are also shown in Table 61. Permanent set rail deflections are also provided in Table 62.

Table 61. Soil Gap Dimensions

Post No.	Soil Gap Dimensions							
	Upstream		Downstream		Back		Front	
	mm	(in.)	mm	(in.)	mm	(in.)	mm	(in.)
1	102	(4.00)	-	-	25	(1.00)	114	(4.50)
2	89	(3.50)	-	-	-	-	-	-
11	-	-	-	-	-	-	25	(1.00)
12	19	(0.75)	-	-	38	(1.50)	44	(1.75)
13	-	-	-	-	25	(1.00)	76	(3.00)
16	864-mm (34-in.) diameter soil cavity							
19	991-mm x 813-mm x 127-mm (39-in. x 32-in. x 5-in.) soil cavity							
24	-	-	13	(0.50)	-	-	-	-
29	Soil Heave		38	(1.50)	-	-	-	-

Table 62. Permanent Rail Deflection

Post No.	Permanent Set			
	Back of Post		Back of Rail	
	mm	(in.)	mm	(in.)
9	13	(0.50)	-25	-(1.00)
10	25	(1.00)	13	(0.50)
11	51	(2.00)	-25	-(1.00)
12	102	(4.00)	51	(2.00)
13	NA	NA	381	(15.00)
14	NA	NA	584	(23.00)
15	NA	NA	584	(23.00)
16	NA	NA	679	(26.75)
17	NA	NA	781	(30.75)
18	NA	NA	902	(35.50)
19	NA	NA	673	(26.50)
20	140	(5.50)	178	(7.00)

18.4 Vehicle Damage

Vehicle damage was fairly minimal with the extent of the damage limited to the left-front corner of the vehicle. The plastic grill was crushed into the front of the pickup truck and torn on the left side. The left-front headlight assembly was also crushed. The front bumper of the vehicle was crushed from the center region and toward the left side. The right-front side of the grill was also deformed inward, and the front frame was bent with a small tear.

The left-front quarter panel was crushed backward and inward. The left-front tire was separated from the rim. Severe rail indentations were located at the front of the left door, the fuel tank cover was torn off, and the left-rear taillight broke away from the pickup truck.

18.5 Occupant Risk Values

The longitudinal and lateral occupant impact velocities (OIV's) were both determined to be 4.03 m/s (13.2 ft/s). The maximum 0.010-sec average occupant ridedown decelerations (ORD's) in the longitudinal and lateral directions were 8.76 g's and 5.69 g's, respectively. It is noted that the OIV's and the ORD's were within the suggested limits provided in NCHRP Report No. 350. In addition, values for the Post-impact Head Deceleration (PHD) and Theoretical Head Impact Velocity (THIV) were calculated. PHD and THIV values are not required by NCHRP Report No. 350, but are listed as optional data for reporting. The PHD was determined to be 8.87 g's, and the THIV was determined to be 6.82 m/s (22.4 ft/s). The results of the occupant risk data are summarized in Figure 102. Results are shown graphically in Appendix K.

18.6 Discussion

An analysis of the test results for test no. MGSDF-1 showed that the MGS utilizing round Douglas Fir posts adequately contained and redirected the test vehicle with controlled lateral displacement of the guardrail system. Although seven of the posts fractured during the impact, none of the posts or other detached elements showed potential for penetrating the occupant compartment nor presented undue hazard to other traffic. Deformations of, or intrusions into, the occupant compartment, potentially injuring occupants did not occur. The pickup truck did not penetrate nor ride over the guardrail and remained upright for the duration of the collision. Vehicle roll, pitch, and yaw angular displacements were present and noted, but were within

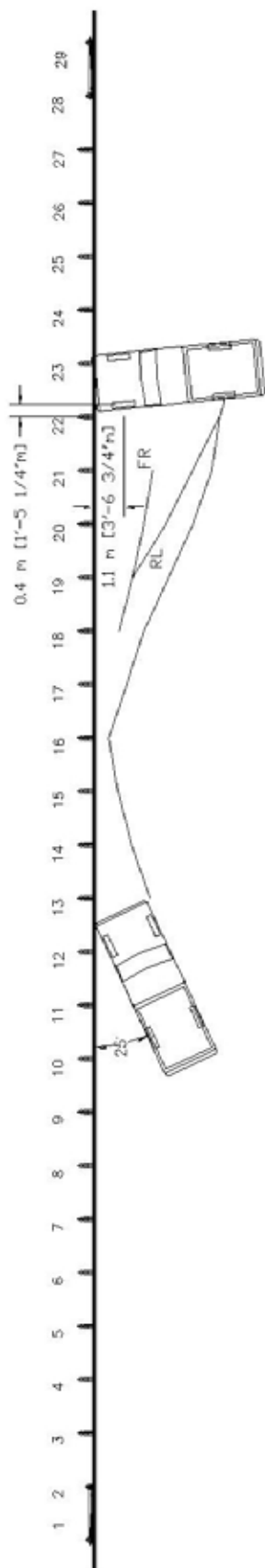
acceptable limits. The vehicle's trajectory revealed minimal intrusion into adjacent traffic lanes. The vehicle's exit angle was not recorded because the vehicle remained in contact with the system for the duration of the event. Therefore, test no. MGSDf-1, conducted on the MGS utilizing round Douglas Fir wood posts, was determined to be acceptable according to the TL-3 safety performance criteria found in NCHRP Report No. 350.



Figure 101. Impact Location, Test MGSDF-1



0.000 sec 0.134 sec 0.204 sec 0.372 sec 0.596 sec



- Test Number..... MGSDF-1 (3-11)
- Date 6/16/06
- Test Article..... Midwest Guardrail System
 - Key Elements.....Round Douglas Fir Posts
- Impact Location..... 953 mm Downstream of Post 12
- Soil Type Grading B AASHTO M147-65 (1990)
- Vehicle Model.....2000 GMC C2500
 - Curb 2,078 kg
 - Test Inertial..... 2,018 kg
 - Gross Static..... 2,018 kg
- Vehicle Speed
 - Impact..... 100.0 km/h
 - ExitNA
- Vehicle Angle
 - Impact (trajectory) 25.5 deg
 - Exit (trajectory).....NA
- Vehicle Stability Satisfactory
- Vehicle Snagging Minor
- Occupant Ridedown Deceleration (10 msec avg.)
 - Longitudinal 8.76 g's < 20 g's
 - Lateral 5.69 g's < 20 g's
- Occupant Impact Velocity
 - Longitudinal 4.03 m/s < 12 m/s
 - Lateral 4.03 m/s < 12 m/s
- THIV 6.84 m/s < 12 m/s (not req.)
- PHD 8.87 g's < 20 g's (not req.)
- Vehicle Damage.....Moderate
 - TAD 11-LFQ-4
 - SAE..... 10LFQ-4
 - OCDI LF0000000000
- Vehicle Stopping Distance..... 19.2 m downstream of impact
- Test Article DamageModerate
 - Maximum Deflection
 - Permanent Set.....902 mm
 - Dynamic 1,529 mm
 - Working Width 1,531 mm

Figure 102. Summary of Test Results and Sequential Photographs, Test MGSDF-1



0.000 sec



0.386 sec



0.064 sec



0.670 sec



0.148 sec



1.276 sec



0.212 sec



1.654 sec

Figure 103. Additional Sequential Photographs, Test MGSDF-1



0.000 sec



0.544 sec



0.084 sec



0.792 sec



0.214 sec



1.068 sec



0.398 sec



2.088 sec

Figure 104. Additional Sequential Photographs, Test MGSDF-1



Figure 105. Documentary Photographs, Test MGSDF-1



Figure 106. Documentary Photographs, Test MGSDF-1



Figure 107. Vehicle Final Position and Trajectory, Test MGSDF-1



Figure 108. System Damage, Test MGSDF-1



Figure 109. System Damage, Test MGSDf-1



Figure 110. System Damage, Test MGSDf-1



Figure 111. System Damage, Test MGSDf-1



Figure 112. System Damage, Test MGSDF-1



Figure 113. Vehicle Damage, Test MGSDF-1



Figure 114. Vehicle Damage, Test MGSDF-1



Figure 115. Occupant Compartment Damage, Test MGSDF-1

19 CRASH TEST NO. MGSPP-1

19.1 Test No. MGSPP-1

Test no. MGSPP-1 was conducted according to NCHRP Report No. 350 Test Designation 3-11. The 2,025-kg (4,464-lb) pickup truck impacted the test article at a speed of 100.2 km/h (62.27 mph) and an angle of 25.5 degrees. The target critical impact point was 953 mm (37 ½ in.) downstream of the centerline of post no. 12. Actual vehicle impact with the barrier system occurred 229 mm (9 in.) downstream of the target. A summary of the test results and sequential photographs are shown in Figure 117. Additional sequential and documentary photographs are shown in Figures 118 through 121. An equivalent English-unit summary is shown in Appendix I.

19.2 Test Description

At 0.008 sec after impact, the left-front bumper crushed inward, and at 0.016 sec after impact, post no. 13 began deflecting backward. After 0.024 sec, the W-beam guardrail began to flatten, and after 0.046 sec, post no. 13 broke.

Post no. 14 began to deflect about 0.054 sec after impact, the same time that a buckle formed in the guardrail at post nos. 12 and 14. At 0.064 sec after impact, the hood of the pickup truck extended over the rail, and at 0.082 sec, the hood was pushing post no. 14 back. After 0.116 sec, there was definite contact between post no. 14 and the left-front tire.

After 0.098 sec, another buckle formed in the guardrail at post no. 15. At 0.116 sec after impact, post no. 15 began deflecting, and broke off at 0.146 sec, at which time a buckle formed in the rail at post no. 16. The left door was in contact with the rail, and the left-front tire was underneath the rail at 0.136 sec. After 0.152 sec, the rail wrapped around the front of the bumper

to the middle of the grill and continued to crush it inward. Post no. 16 began to deflect at 0.156 sec and fractured at 0.172 sec. Post no. 17 began deflecting shortly after at 0.200 sec.

By 0.234 sec, the entire left side of the pickup truck was in contact with the rail. At 0.242 sec, another buckle formed in the guardrail at post no. 18. The left corner of the rear bumper was situated on top of the guardrail at 0.308 sec. After 0.326 sec, the rail between post nos. 7 and 11 was being pulled off the posts and was completely separated by 0.692 sec. At 0.400 sec, the truck became parallel to the system, with the rear of the truck losing contact at 0.426 sec. The rail buckled at post no. 19 after 0.564 sec. Finally, the pickup truck exited the system at 0.776 sec.

19.3 System and Component Damage

Post nos. 1 and 2 were unharmed with minor damage to the ground-line-strut connecting them. The rail popped free from post nos. 2 through 11 without tearing the slot. Post nos. 2 through 10 showed minor rotation downstream, and post no. 11 was rotated approximately 10 degrees downstream. Post no. 12 was still attached to the rail with a slight buckle on the top and bottom of the rail at the downstream end of blackout no. 12.

The first contact marks were tire, plastic, and paint marks noted on the upper rail 229 mm (9 in.) downstream of the target impact. The marks continued through post no. 18. Similar marks began on the bottom rail 305 mm (12 in.) upstream of post no. 13 and continued through post no. 19.

The rail was pulled from post no 13 without signs of slot tearing. The rail showed random buckles and kinks between post nos. 13 and 18, and was also flattened from post no. 13 through the next downstream splice. Post no. 13 was rotated back approximately 20 degrees and showed minor twisting downstream.

Post no.14 was broken and lying 1829 mm (72 in.) behind the back of the rail at the midspan between target nos. 17 and 18. The concave blockout broke off the bolt while the rectangular blockout remained attached. Post no. 15 was also broken and found 4,572 mm (180 in.) behind post no. 22 with both blockouts still attached. Post no. 16 was broken and lying just in front of post no. 14 with both blockouts still attached. Post no. 17 was the final post to fracture and was 1829 mm (72 in.) behind post no. 18 with both blockouts attached. The rail slots corresponding to post nos. 14, 16, and 17 had tears in the side walls, while the slot corresponding to post no. 15 showed no tearing.

There was a major buckle and bend in the rail at the upstream edge of blockout no. 18. The concave blockout was severely split and fractured, while only minor splitting was noted in the main rectangular blockout. Post no 18 was also rotated back about 30 degrees and downstream slightly. The rail popped free from the post bolt with no signs of tearing in the slot.

The final major buckle in the system was at the upstream edge of blockout no. 19. There was no damage to post no. 19, and the rail was still attached to the post bolt. Post nos. 20 – 24 showed no signs of damage. There was a slight buckle in the rail between post nos. 24 and 25, and post no. 25 was bent back slightly. Finally, post nos. 26 and 27 were rotated slightly upstream with no signs of additional damage. The soil gaps and rail height at each post are shown in Table 63. The system permanent deflection is shown in Table 64.

Table 63. Soil Gap Dimensions and Rail Height Measurements

Post No.	Soil Gap Dimensions								Rail Height	
	Upstream		Downstream		Back		Front			
	mm	(in.)	mm	(in.)	mm	(in.)	mm	(in.)	mm	(in.)
1	76	(3.00)	-	-	-	(1.00)	-	-	495	(19.50)
2	38	(1.50)	-	-	-	-	-	-	432	(17.00)
3	6	(0.25)	-	-	-	-	-	-	267	(10.50)
4	-	-	-	-	-	-	-	-	178	(7.00)
5	-	-	-	-	-	-	-	-	152	(6.00)
6	-	-	-	-	-	-	-	-	76	(3.00)
7	-	-	-	-	-	-	-	-	102	(4.00)
8	-	-	-	-	-	-	-	-	152	(6.00)
9	-	-	-	-	-	-	-	-	254	(10.00)
10	-	-	-	-	-	-	-	-	356	(14.00)
11	13	(0.50)	-	-	-	-	6	(0.25)	432	(17.00)
12	19	(0.75)	-	-	13	(0.50)	13	(0.50)	483	(19.00)
13	-	-	-	-	25	(1.00)	76	(3.00)	597	(23.50)
14	508-mm (20-in.) diameter soil cavity								470	(18.50)
15	432-mm (17-in.) diameter soil cavity								457	(18.00)
16	432-mm (17-in.) diameter soil cavity behind post						44	(1.75)	521	(20.50)
17	-	-	-	-	-	-	76	(3.00)	584	(23.00)
18	457-mm (18-in.) diameter soil cavity upstream of post								559	(22.00)
19	-	-	-	-	-	-	-	-	495	(19.50)
20	-	-	-	-	-	-	-	-	495	(19.50)
21	-	-	-	-	-	-	-	-	483	(19.00)
22	-	-	-	-	-	-	-	-	495	(19.50)
23	-	-	-	-	-	-	-	-	483	(19.00)
24	-	-	-	-	-	-	-	-	470	(18.50)
25	-	-	-	-	-	-	-	-	470	(18.50)
26	-	-	-	-	-	-	-	-	470	(18.50)
27	-	-	-	-	-	-	-	-	457	(18.00)
28	-	-	-	-	-	-	-	-	457	(18.00)
29	-	-	38	(1.50)	-	-	-	-	470	(18.50)

Table 64. Ponderosa Pine Permanent Rail Deflection

Post No.	Permanent Set			
	Back of Post		Back of Rail	
	mm	(in.)	mm	(in.)
9	0	(0.00)	44	(1.75)
Midspan	-	-	51	(2.00)
10	-25	-(1.00)	64	(2.50)
Midspan	-	-	70	(2.75)
11	13	(0.50)	51	(2.00)
Midspan	-	-	32	(1.25)
12	6	(0.25)	13	(0.50)
Midspan	-	-	95	(3.75)
13	184	(7.25)	191	(7.50)
Midspan	-	-	305	(12.00)
14	NA	NA	432	(17.00)
Midspan	-	-	565	(22.25)
15	NA	NA	660	(26.00)
Midspan	-	-	705	(27.75)
16	NA	NA	679	(26.75)
Midspan	-	-	699	(27.50)
17	NA	NA	654	(25.75)
Midspan	-	-	629	(24.75)
18	298	(11.75)	210	(8.25)
Midspan	-	-	64	(2.50)
19	-57	-(2.25)	-57	-(2.25)
Midspan	-	-	-57	-(2.25)
20	-76	-(3.00)	-64	-(2.50)

19.4 Vehicle Damage

The majority of the vehicle damage was concentrated to the left-front corner of the pickup truck. The left-front quarter panel, grill, and light housing were bent and crushed inward severely. Two longitudinal dents were present on the left side of the vehicle due to the sliding along the rail. In addition, the side of the box was scratched longitudinally. The left-front steel rim had significant bending and damage, and the left-rear tire had abrasions on the outer sidewall.

The front bumper was pulled away from the right-front corner of the vehicle and showed a major buckle in the center. The right-front headlight housing was intact, but shifted from its original location.

There was minor undercarriage damage including a buckled frame on the front-left corner, and a damaged front-left steering arm. The remainder of the pickup truck showed no sign of damage.

19.5 Occupant Risk Values

The longitudinal and lateral occupant impact velocities (OIV's) were determined to be 5.90 m/s (19.3 ft/s) and 4.09 m/s (13.4 ft/s), respectively. The maximum 0.010-sec average occupant ridedown decelerations (ORD's) in the longitudinal and lateral directions were 6.85 g's and 7.18 g's, respectively. It is noted that the OIV's and the ORD's were within the suggested limits provided in NCHRP Report No. 350. In addition, values for the Post-impact Head Deceleration (PHD) and Theoretical Head Impact Velocity (THIV) were calculated. PHD and THIV values are not required by NCHRP Report No. 350, but are listed as optional data for reporting. The PHD was determined to be 8.47 g's and the THIV was determined to be 6.12 m/s (22.4 ft/s). The results of the occupant risk data are summarized in Figure 117. Results are shown graphically in Appendix K.

19.6 Discussion

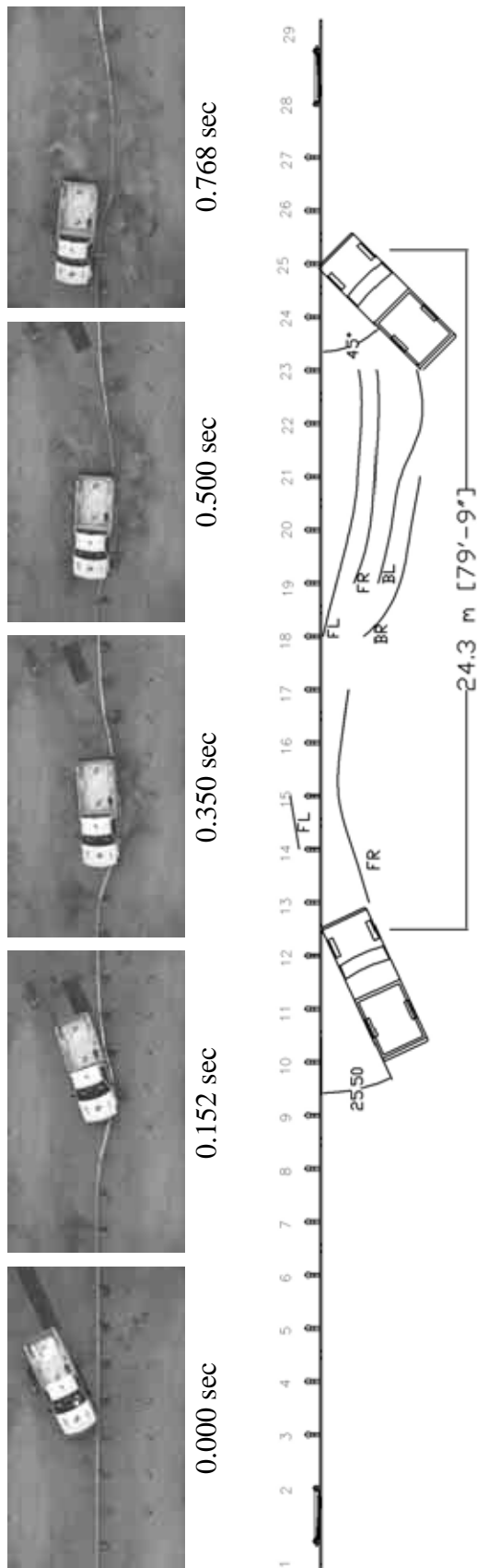
The analysis of the results for test no. MGSP-1 showed that the MGS utilizing round Ponderosa Pine posts adequately contained and redirected the test vehicle with controlled lateral displacements of the system. None of the detached elements, posts, or fragments showed potential for penetrating the occupant compartment nor presented undue hazard to traffic in adjacent lanes. No deformations of, or intrusions into the occupant compartment showed potential for causing serious injury. The test vehicle did not penetrate nor ride over the guardrail system and remained upright for the duration of the event. Vehicle roll, pitch, and yaw angular displacements were determined, but were deemed acceptable, not adversely influencing occupant

risk safety criteria. The vehicle's trajectory revealed minimum intrusion into adjacent traffic lanes. In addition, the vehicle's exit angle was less than 60 percent of the impact angle. Therefore, test no. MGSPP-1, conducted on the MGS utilizing round Ponderosa Pine posts was determined to be acceptable according to the TL-3 safety performance criteria found in NCHRP Report No. 350.



Figure 116. Impact Location, Test MGSww.mapquest.com

PP-1



• Test Number	MGSP-1 (3-11)	• Occupant Ridedown Deceleration (10 msec avg.)
• Date	6/1/06	Longitudinal 5.90 g's < 20 g's
• Test Article	Midwest Guardrail System	Lateral 4.09 g's < 20 g's
• Key Elements	Round Ponderosa Pine Posts	
• Impact Location	953 mm Downstream of Post 12	Occupant Impact Velocity
• Soil Type	Grading B AASHTO M147-65 (1990)	Longitudinal 6.85 m/s < 12 m/s
• Vehicle Model	2000 GMC C2500	Lateral 7.18 m/s < 12 m/s
• Curb	1,959 kg	THIV 6.12 m/s < 12 m/s (not req.)
• Test Inertial	2,025 kg	PHD 8.47 g's < 20 g's (not req.)
• Gross Static	2,025 kg	Vehicle Damage.....Moderate
• Vehicle Speed		TAD 11-LFQ-4
• Impact	100.2 km/h	SAE 10LFWE5
• Exit	37.4 km/h	OCDI LF000000000
• Vehicle Angle		Vehicle Stopping Distance..... 24.3 m downstream of impact
• Impact (trajectory)	25.5 deg	Test Article Damage.....Moderate
• Exit (trajectory)	19.9 deg	Maximum Deflection
• Vehicle Stability	Satisfactory	Permanent Set.....705 mm
• Vehicle Snagging	Minor	Dynamic 956 mm
		Working Width 1,234 mm

Figure 117. Summary of Test Results and Sequential Photographs, Test MGSP-1



0.000 sec



0.258 sec



0.040 sec



0.398 sec



0.082 sec



0.600 sec



0.148 sec



0.808 sec

Figure 118. Additional Sequential Photographs, Test MGSPP-1



0.000 sec



0.146 sec



0.068 sec



0.236 sec



0.102 sec



0.308 sec



0.122 sec



0.692 sec

Figure 119. Additional Sequential Photographs, Test MGSPP-1



0.000 sec



0.214 sec



0.106 sec



0.344 sec



0.136 sec



0.426 sec



0.172 sec



0.736 sec

Figure 120. Additional Sequential Photographs, Test MGSPP-1

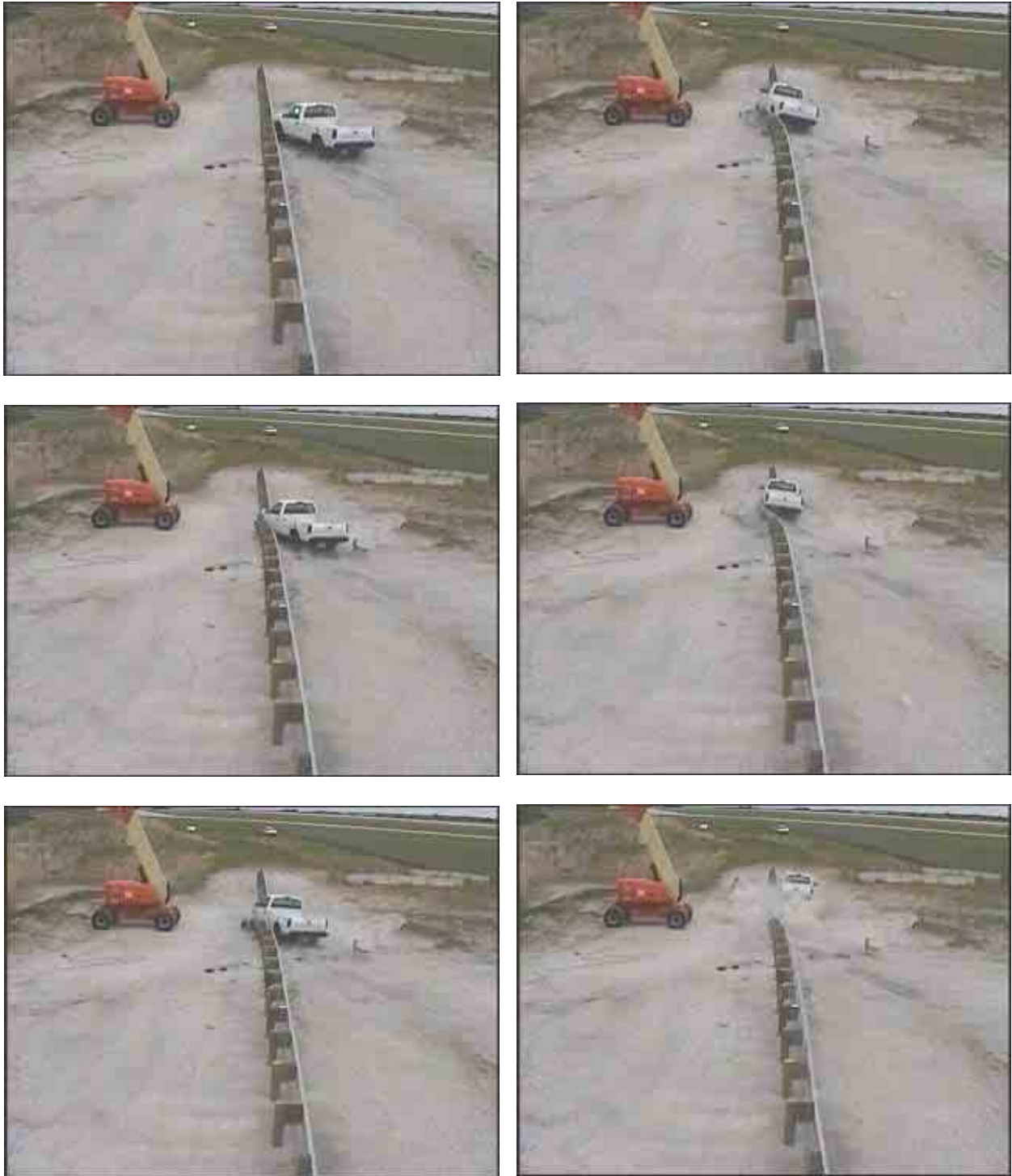


Figure 121. Documentary Photographs, Test MGSPP-1



Figure 122. Vehicle Final Position and Trajectory Marks, Test MGSP-1



Figure 123. System Damage, Test MGSPP-1



Figure 124. System Damage, Test MGSPP-1



Figure 125. System Damage, Test MGSPP-1



Figure 126. System Damage, Test MGSPP-1



Figure 127. System Damage, Test MGSPP-1



Figure 128. System Damage, Test MGSPP-1



Figure 129. Vehicle Damage, MGSPP-1



Figure 130. Vehicle Damage, MGSP-1



Figure 131. Occupant Compartment Damage, Test MGSPP-1

20 SUMMARY, CONCLUSIONS, AND RECOMMENDATIONS

The Midwest Guardrail System, utilizing round Douglas Fir, Ponderosa Pine, and Southern Yellow Pine posts, was developed in order to provide an additional market for small-diameter timber, while at the same time developing an economical guardrail system for State Departments of Transportation, the National Parks, and other local and county governments. The modified MGS was successfully crash tested according to the TL-3 criteria found in NCHRP Report No. 350. The test results from the full-scale vehicle tests indicate that the round post MGS designs are suitable for use on Federal-aid highways. However, any significant modifications made to the W-beam guardrail design would require additional analysis and could only be verified through the use of full-scale crash testing. A summary of the safety performance evaluations are provided in **Table 65**.

20.1 Component Testing

During the component testing phase, several conclusions were drawn concerning the effectiveness and accuracy of the testing methods. As described in Chapter 7, every type of impact testing is subject to some level of inertial effects. Using traditional methods of testing and analysis, these inertial effects can result in misleadingly high component strength values.

Although these effects will never be fully eliminated from cantilever sleeve testing, there are several ways to reduce their influence. First, the impact speed can be reduced. The transfer of momentum is directly related to the velocity of the impacting vehicle. Therefore, when the velocity is reduced, so are the inertial effects. The drawback to this method is that testing at reduced speeds reduces the material strength increase caused by the dynamic magnification.

The second modification that can help control inertial effects is the use of a crushable impact head. With a crushable impact head, the inertial forces from the impact are absorbed by

the deformation of the impact head rather than being recorded by the bogie's accelerometer. One drawback regarding the use of such an impact head is the increased cost of each component test. Not only does the cost increase due to the additional material used in each test, but it also increases due to the additional research that must be conducted to tune the deformable head to prevent it from being too soft or too stiff. Another drawback is that force versus deflection data cannot directly be acquired from an analysis of the bogie acceleration data due to the fact that the bogie nose also crushes as the post displaced under loading.

A third method to manage the inertial effects is to utilize computer simulation. This method, like the previous, significantly increases the cost of each test; not due to an increase in material, but rather due to an increase in analysis time. Using this method, each test would have to be replicated using computer simulation, significantly increasing the time required to determine the strength of the component being tested.

In post-soil component testing, the inertial effects are also present, although they have a reduced influence on the test results. This limited influence occurs because the strength of the post is not being measured, but rather the resistive capacity of the post-soil system. While the inertia of both the post and soil causes a measured increase in resistive capacity, the inertia will also be present in the actual system. Therefore, the resistive capacity of a post in soil, whether installed in a full system or installed as a single post, includes the portion of the force caused by inertia. Hence, no modifications should be made to the post-soil bogie testing methods.

20.2 MGS Performance

Although the initial research and post size determination were based on a system that was predicted to fail with the fracture of four consecutive posts, both full-scale crash tests indicated that the system failure criteria exceeds this prediction. In test no. MGSDF-1, seven consecutive

posts failed, yet the system effectively redirected the impacting vehicle. This result indicates that the MGS, installed with round posts, has the capability to perform in an acceptable manner when more than four consecutive posts fracture.

20.3 Viability of Alternate Posts for the MGS

The research results contained herein demonstrates the capability of the MGS to be installed with alternative posts. Although only three alternatives have been investigated, many more could be utilized with minimal research effort. Such alternatives may include posts with differences in size, shape, strength, or material. Of course, all of these alternatives would need to be tested and approved prior to installation.

The validation of an alternative post style should be done in three steps. First, cantilever sleeve testing should be used to verify that the post strength is of sufficient magnitude to ensure that it will be capable of rotating in the soil. The ease of rotation, is greatly influenced by both the shape and the size of the post and, for any post type, may be adjusted by varying the post's embedment depth. Second, cantilever soil testing must be utilized to verify that the resistive capacity of the post in the soil, in both the lateral and longitudinal directions, is equivalent or greater than the standard steel post used for the system. Again, the resistive capacity of a post is strongly dependent on both the shape and the size of the post and may be adjusted by changing the embedment depth. Finally, a full-scale vehicle crash test must be conducted to verify that the MGS with alternative posts performs in an acceptable manner.

As with the Southern Yellow Pine species, the full-scale vehicle crash test may be waived if similar full-scale crash testing adequately demonstrates that the MGS installed with the prospective replacement post will function effectively.

20.4 Future Research Needs

The Midwest Guardrail System (MGS) was modified using round wood posts and subjected to two full-scale vehicle crash tests. For these tests, successful barrier performance was obtained using either Douglas Fir or Ponderosa Pine posts. System details were also developed for a round-post, Southern Yellow Pine barrier system, even though an additional crash test was not performed. For the Douglas Fir and Ponderosa Pine post systems, dynamic barrier deflections were found to be 1,529 mm (60.2 in.) and 956 mm (37.6 in.), respectively. In comparison, the steel post MGS was evaluated in test no. NPG-4 under similar impact conditions and resulted in a dynamic deflection equal to 1,094 mm (43.1 in.). As such, it is apparent that the Ponderosa Pine post MGS has similar lateral barrier stiffness to that of the steel post MGS. Therefore, the Ponderosa Pine post MGS should be capable of being attached to existing thrie beam approach guardrail transition designs in a similar manner to that already used for the steel post MGS. However, the Douglas Fir post MGS resulted in a 435 mm (17.1 in.) increase in dynamic rail deflection to that observed for the steel post MGS. Therefore, if the Douglas Fir post MGS is to be attached to existing thrie beam approach guardrail transitions, it must be transitioned to a stiffened guardrail system well in advance of the thrie beam guardrail sections. Further research is needed to identify the specific nature of such a design.

Currently, several guardrail end terminals exist for use in treating the ends of longitudinal W-beam guardrail systems, such as the MGS. These end terminal systems were originally developed for standard-height, strong-post, W-beam guardrail systems, but they were later adapted to the MGS which utilized steel posts. As such, it is the researcher's opinion that the existing, crashworthy guardrail end terminals would be applicable for use as long as the round-post MGS is not significantly stiffer than the steel-post MGS. However, it should be noted that

the use of round, wood posts in the terminal itself would need to be verified through full-scale crash testing.

20.5 Installation of the Round-Post MGS

Full-scale vehicle crash testing, combined with dynamic component testing, of two different round post MGS systems has been used to determine the maximum dynamic barrier deflections and working widths for the systems using either round Douglas Fir and Ponderosa Pine posts. Dynamic component testing was used to determine comparable structural properties, grading, and size for Southern Yellow Pine posts for use as a substitute to the Douglas Fir and Ponderosa Pine posts previously evaluated in the MGS. The dynamic barrier deflection and working width results, along with the installation manual, which has yet to be prepared, should allow roadway designers to utilize the new round post guardrail systems with confidence when protecting roadside hazards.

Highway agencies are strongly encouraged to consider adopting the new barrier systems as soon as FHWA acceptance letters are issued. Installation of the modified barrier systems using round timber posts will: (1) continue to provide motorist safety along our nation's highways and roadways, (2) increase the U.S. and individual state timber industries, and (3) help to reduce the risk of devastating forest fires across the country.

Table 65. Summary of Safety Performance Evaluation

Evaluation Factors		Evaluation Criteria	Test MGSDf-1	Test MGSPF-1
Structural Adequacy	A.	Test article should contain and redirect the vehicle; the vehicle should not penetrate, underide, or override the installation although controlled lateral deflection of the test article is acceptable.	S	S
Occupant Risk	D.	Detached elements, fragments or other debris from the test article should not penetrate or show potential for penetrating the occupant compartment, or present an undue hazard to other traffic, pedestrians, or personnel in a work zone. Deformations of, or intrusions into, the occupant compartment that could cause serious injuries should not be permitted.	S	S
	F.	The vehicle should remain upright during and after collision although moderate roll, pitching, and yawing are acceptable.	S	S
	G.	It is preferable, although not essential, that the vehicle remain upright during and after collision	S	S
	H.	Longitudinal and lateral occupant impact velocities should fall below the preferred value of 9 m/s (29.53 ft/s), or at least below the maximum allowable value of 12 m/s (39.37 ft/s).	S	S
	I.	Longitudinal and lateral occupant ridedown accelerations should fall below the preferred value of 15 g's, or at least below the maximum allowable value of 20 g's.	S	S
Vehicle Trajectory	K.	After collision it is preferable that the vehicle's trajectory not intrude into adjacent traffic lanes.	S	S
	L.	The occupant impact velocity in the longitudinal direction should not exceed 12 m/s (39.37 ft/s), and the occupant ridedown acceleration in the longitudinal direction should not exceed 20 G's.	S	S
	M.	The exit angle from the test article preferably should be less than 60 percent of the test impact angle measured at the time of vehicle loss of contact with the test device.	S	S

21 REFERENCES

1. *Collaborative Approach for Reducing Wildland Fire Risks to Communities and the Environment*. U.S. Department of Interior and U.S. Department of Agriculture, August 2001.
2. Gorte, R.W., *Forest Fires and Forest Health*, CRS Report 95-511, CRS Report for Congress. 14 July 1995. National Council for Science and the Environment, July 21, 2003.
3. LeVan-Green, S.L., Livingston, J.M., *Uses for Small-Diameter and Low-Value Forest Thinnings*, Ecological Restoration March 2003: 34-38.
4. Paun, D. and Jackson, G., *Potential for Expanding Small-Diameter Timber Market Assessing Use of Wood Posts in Highway Applications*, General Technical Report FPL-GTR-120, Department of Agriculture, Forest Service, Forest Products Laboratory, Madison, Wisconsin, 2000.
5. Sicking, D.L., Reid, J.D., and Rohde, J.R., *Development of the Midwest Guardrail System*, Transportation Research Record 1797, Transportation Research Board, Washington, D.C., 2002.
6. Faller, R.K., Polivka, K.A., Kuipers, B.D., Bielenberg, R.W., Reid, J.D., and Rohde, J.R., *Midwest Guardrail System for Standard and Special Applications*, Transportation Research Record, No. 1890, Transportation Research Board, Washington D.C., 2004.
7. Polivka, K.A., Faller, R.K., Sicking, D.L., Reid, J.D., Rohde, J.R., Holloway, J.C., Bielenberg, R.W., and Kuipers, B.D., *Development of the Midwest Guardrail System (MGS) for Standard and Reduced Post Spacing and in Combination with Curbs*, MwRSF Research Report No. TRP-03-139-04, Final Report to the Midwest States Regional Pooled Fund Program, Midwest Roadside Safety Facility, University of Nebraska-Lincoln, Lincoln, Nebraska, September 1, 2004.
8. Powell, G. H., *Barrier VII - A Computer Program for Evaluation of Automobile Barrier Systems*, Report No. FHWA-RD-73-51, Prepared for the Federal Highway Administration, U.S. Department of Transportation, Washington, D.C., 1973.
9. American National Standards Institute, *Wood Poles*, ANSI 05.1, 1992.
10. Graham, M.D., Burnett, W.C., Gibson, J.L., and Freer, R.H., *New Highway Barriers: The Practical Application of Theoretical Design*, Highway Research Record Number 174, 1967.
11. Cichowski, W.G., Skeels, P.C., and Hawkins, W.R., *Guardrail Installations – Appraisal by Proving Ground Car Impact, and Laboratory Tests*, General Motors Proving Ground, Milford, Michigan, 1961.

12. Gatchell, C.J. and Michie, J.D., *Pendulum Impact Tests of Wooden and Steel Highway Guardrail Posts*, USDA Forest Service Research PAPER NE-311, Northeastern Forest Experiment Station, Upper Darby, Pennsylvania, 1974.
13. Michie, J.D, Gatchell, C.J., and Duke, T.J., *Dynamic Evaluation of Timber Posts for Highway Guardrails*, Highway Research Record 343, 1971.
14. Calcote, L.R. and Kimball, C.E., *Properties of Guardrail Posts for Various Soil Types*, Transportation Research Record 679, 1978.
15. Jeyapalan, J.K., Dewey, J.F., Hirsch, T.J., Ross, H.E., and Cooner, H., *Soil-Foundation Interaction Behavior of Highway Guardrail Posts*, Transportation Research Record 970, 1984.
16. Bronstad, M.E., Calcote, L.R., Ray, M.H., and Mayer, J.B., *Guardrail-Bridge Rail Transition Designs Volume 1*, Research Report. Publication No. FHWA/RD-86/178, 1988.
17. Rohde, J.R. and J.D. Reid, *Evaluation of the Performance Criteria for Wood Posts in Strong-Post W-Beam Guardrail*, TRB Paper 971206, Transportation Research Board 76th Annual Meeting, January 1997.
18. Rohde, J.R., Reid, J.D., and Sicking, D.L., *Evaluation of the Effect of Wood Quality on W-beam Guardrail Performance*, Transportation Research Report No. TRP-03-60-96, Midwest Roadside Safety Facility, University of Nebraska-Lincoln, Lincoln, Nebraska, November 1995.
19. Rohde, J.R. and Reid, J.D., *Evaluation of the Performance Criteria for Wood Posts in Strong-Post W-Beam Guardrail*, Research Report, Midwest Roadside Safety Facility, University of Nebraska-Lincoln, Lincoln, Nebraska, 1995.
20. Southern Pine Inspection Bureau, *Standard Grading Rules*, July, 2002.
21. Holloway, J.C., Bierman, M.G., Pfeifer, B.G., Rosson, B.T., and Sicking, D.L., *Performance Evaluation of KDOT W-Beam Systems Volume II: Component Testing and Computer Simulation*, Research Report TRP-03-39-96, Midwest Roadside Safety Facility, The University of Nebraska-Lincoln, Lincoln, May 1996.
22. Goeller, M.D. and Rohde, J.R., *Soil Behavior During a Guardrail Post Impact*, Thesis Report, Midwest Roadside Safety Facility, The University of Nebraska-Lincoln, Lincoln, Nebraska, May 2000.
23. Smith, R.P. and Rohde, J.R., *Quantification of Guardrail Post-Soil Interaction*, Thesis Report, Midwest Roadside Safety Facility, The University of Nebraska-Lincoln, Lincoln, Nebraska, August 1997.

24. Coon, B.A., Reid, J.D., and Rohde, J.R., *Dynamic Impact Testing of Guardrail Posts Embedded in Soil*, Research Report TRP-03-77-98, Midwest Roadside Safety Facility, The University of Nebraska-Lincoln, Lincoln, Nebraska, July 1999.
25. Denman and Welch, *Development of a Flared end Terminal to NCHRP Report 350*, E-TECH Testing Services, Inc., Rocklin, California, December 1998.
26. Ross, H.E., Sicking, D.L., Zimmer, R.A. and Michie, J.D., *Recommended Procedures for the Safety Performance Evaluation of Highway Features*, National Cooperative Research Program (NCHRP) Report No. 350, Transportation Research Board, Washington, D.C., 1993.
27. Kuipers, B.D. and Reid, J.D., *Testing of W152X23.8 (W6X16) Steel Posts-Soil Embedment Depth Study for the Midwest Guardrail System*, Research Report TRP-03-136-03, Midwest Roadside Safety Facility, The University of Nebraska-Lincoln, Lincoln, Nebraska, June 2003.
28. Bronstad, M.E. and Burket, R.B., *Evaluation of Timber Weak-Post Guardrail Systems*, Highway Research Record 343, 1971.
29. Sicking, D.L., Bligh, R.P., and Ross, Jr., H.E., *Optimization of Strong Post W-Beam Guardrail*, Research Report 1147-1F, Texas Transportation Institute, The Texas A & M University System, College Station, Texas, November, 1988.
30. Sicking, D.L., Qureshy, A.B., Bligh, R.P., Ross, H.E., and Buth C.E., *Development of New Guardrail End Treatments*, Research Report 404-1F, Texas Transportation Institute, The Texas A & M University System, College Station, Texas, October 1988.
31. Michie, J.D., *Recommended Procedures for the Safety Performance Evaluation of Highway Appurtenances*, National Cooperative Research Program (NCHRP) Report 230: Transportation Research Board, Washington, D.C., 1981.
32. Bligh, R.P., Sicking, D.L., and Ross Jr., H.E., *Development of a Strong Beam Guardrail-to-Bridge-Rail Transition*, Transportation Research Record 1198, 1988.
33. Bligh, R.P. and Sicking, D.L., *Applications of Barrier VII in Design of Flexible Barriers*, Transportation Research Record 1233, 1989.
34. Bligh, R.P. and Bullard, D.L., *Crash Testing and Evaluation of Round, Wood Post, W-Beam Guardrail System*, Research Study No. 405391, Texas Transportation Institute, The Texas A & M University System, College Station, Texas, October 1995.
35. Rosson, B.T., Bierman, M.G., and Rohde, J. R., *Assessment of Guardrail-Strengthening Techniques*, Transportation Research Record 1528, 1996.

36. Bierman, M.G., *Behavior of Guardrail Posts to Lateral Impact Loads*, Thesis Report, Midwest Roadside Safety Facility, The University of Nebraska-Lincoln, Lincoln, Nebraska, December 1995.
37. Buth, C.E., Williams, W.F., Bligh, R.P., and Menges, W.L., *Tests 9,10 and 11: NCHRP Report 350 Test 3-21 of the Texas Tubular W-Beam Transition*, Research Report 1804-9, Texas Transportation Institute, The Texas A & M University System, College Station, Texas, November 1999.
38. Seckinger, N.R., Abu-Odeh, A., Bligh, R.P., and Roschke, P.N., *Evaluation of Guardrail Systems Performance when Encased in Pavement Mow Strips*, TRB 2004 Annual Meeting CD-ROM, Texas Transportation Institute, The Texas A&M University, College Station, College Station, Texas, January 2004.
39. Seckinger, N.R., Abu-Odeh, A., Bligh, R.P., and Roschke, P.N., *Performance of Guardrail Systems Encased in Pavement Mow Strips*, ASCE Journal of Transportation Engineering, Vol. 131, No. 11, Nov. 2005, pp. 851-860.
40. Southern Pine Inspection Bureau, *Standard Grading Rules*. July 2002.
41. Western Wood Products Association, *Western Lumber Grading Rules 98*, March 1998.
42. West Coast Lumber Inspection Bureau, *Standard No. 17 Grading Rules for West Coast Lumber*, September 2004.
43. Ross, R.J. and Pellerin, R.F., *Nondestructive Testing for Assessing Wood Members in Structures: A Review*, General Technical Report FPL-GTR-70 (Rev.). Madison, WI: U.S. Department of Agriculture, Forest Service, Forest Products Laboratory, 1994.
44. Society of Automotive Engineers (SAE), *Instrumentation for Impact Test – Part 1 – Electronic Instrumentation – SAE J211/1 MAR95*, New York City, NY, 1999.
45. Coon, Brian A., *Methodology for Digital Filtering of Data Using DADiSP*, Research Report, Midwest Roadside Safety Facility, University of Nebraska-Lincoln, Lincoln Nebraska, 1999.
46. U.S. Department of Agriculture – Forest Products Laboratory, *Wood Handbook*, 1999.
47. Coon, B.A. and Reid, J.D., *Barrier VII – A Brief Overview*, General Report. Midwest Roadside Safety Facility, University of Nebraska-Lincoln, Lincoln Nebraska, 2003.
48. Kuipers, Beau D., *Identification of a Critical Flare Rate for W-Beam Guardrail in High-Speed Facilities Using Computer Simulation*, A Thesis, University of Nebraska-Lincoln, Lincoln Nebraska, 2004.

49. Beer, Ferdinand P. and E. Russell Johnston Jr., *Vector Mechanics for Engineers Dynamics*, Sixth Edition. Boston: WCB McGraw-Hill, 1996.
50. Hinch, J., Yang, T-L, and Owings, R., *Guidance Systems for Vehicle Testing*, ENSCO, Inc., Springfield, VA, 1986.
51. *Vehicle Damage Scale for Traffic Investigators*, Second Edition, Technical Bulletin No. 1, Traffic Accident Data (TAD) Project, National Safety Council, Chicago, Illinois, 1971.
52. *Collision Deformation Classification – Recommended Practice J224 March 1980*, Handbook Volume 4, Society of Automotive Engineers (SAE), Warrendale, Pennsylvania, 1985.

22 APPENDICES

APPENDIX A - General Post Grading Criteria

Guardrail Post Grading Criteria

General

All posts shall meet the current quality requirements of the American National Standards Institute (ANSI) 05.1, “Wood Poles” except as supplemented herein:

Manufacture:

All posts shall be smooth shaved by machine. No “ringing” of the posts, as caused by improperly adjusted peeling machine, is permitted. All outer and inner bark shall be removed during the shaving process. All knots and knobs shall be trimmed smooth and flush with the surface of the posts. The guardrail posts will be a minimum of 1.75 m (69 in.) long. The use of peeler cores is prohibited.

Ground-line:

The ground-line, for the purpose of applying these restrictions of ANSI 05.1 that reference the ground-line, shall be defined as being located 914 mm (36 in.) from the butt end of each post.

Size:

The size of the posts shall be classified based on their diameter at the ground-line and their length and will be species specific. The ground-line diameter shall be specified by diameter in 6 mm (¼ in.) breaks. The length shall be specified in 300 mm (1 ft) breaks. Dimension shall apply to fully seasoned posts. When measured between their extreme ends, the post shall be no shorter than the specified lengths but may be up to 75 mm (3 in.) longer.

Scars:

Scars are permitted in the middle third as defined in ANSI 05.1 provided that the depth of the trimmed scar is not more than (1 in.).

Shape and Straightness:

All timber posts shall be nominally round in cross section. A straight line drawn from the centerline of the top to the center of the butt of any post shall not deviate from the centerline of the post more than 32 mm (1¼ in.) at any point. Posts shall be free from reverse bends.

Splits and Shakes:

Splits or ring shakes are not permitted in the top two thirds of the post. Splits not to exceed the diameter in length are permitted in the bottom third of the post. A single shake is permitted in the bottom third, provided it is not wider than one-half the butt diameter.

Decay:

Allowed in knots only.

Holes:

Pin holes 1 mm (1/16 in.) or less are not restricted.

Slope of Grain:

1 in 10.

Compression Wood:

Not allowed, in the outer 25 mm (1 in.) or if exceeding $\frac{1}{4}$ of the radius.

Timber Spacers:

When timber spacers are required, the timber species shall be the same as those furnished for the timber posts. The size and hole location shall be as shown on the plans, with a tolerance of 6 mm ($\frac{1}{4}$ in.), Spacers shall be of medium grain, at least four (4) rings per inch on one end, and free from splits, shakes, compression wood or decay in any form. Individual knots, knot clusters or knots in the same cross section of a face are permitted, provided they are sound or firm, and are limited in cumulative width (when measured between lines parallel to the edges) to no more than one-half the width of the face. Wane or the absence of wood is limited to one-third of the face on no more than 10 percent of the lot. Slope of grain deviation is limited to one in six. The material may be rough sawn or surfaced, full size, hit or miss, with a tolerance of 6 mm ($\frac{1}{4}$ in.) for all dimensions.

Treatment:

Treating - American Wood-Preservers' Association (AWPA) – Book of Standards (BOS) U1-05 use category system UCS: user specification for treated wood; commodity specification B; Posts; Wood for Highway Construction must be met using the methods outlined in AWPA BOS T1-05 Section 8.2.

Each post treated shall have a minimum sapwood depth of 19 mm ($\frac{3}{4}$ in.) as determined by examination of the tops and butts of each post. Material that has been air dried or kiln dried shall be inspected for moisture content in accordance with AWPA standard M2 prior to treatment. Tests of representative pieces shall be conducted. The lot shall be considered acceptable when the average moisture content does not exceed 25 percent. Pieces exceeding 29 percent moisture content shall be rejected and removed from the lot.

Species Specific Criteria

Douglas Fir:

Knot diameter for posts of Douglas Fir shall not exceed 51 mm (2 in.). Ring density for the species shall be at least 6 rings-per-inch as measured over a 76 mm (3 in.) distance. The diameter of the Douglas Fir posts shall be 184 mm (7¼ in.) at the ground line with a upper limit of 203 mm (8 in.).

Ponderosa Pine:

Knot diameter for posts of Ponderosa Pine shall not exceed 102 mm (4 in.). Ring density for the species shall be at least 6 rings-per-inch as measured over a 76 mm (3 in.) distance. The diameter of the Ponderosa Pine posts shall be 203 mm (8 in.) at the ground line with an upper limit of 222 mm (8¾ in.).

Southern Pine:

Knot diameter for posts of Southern Pine shall not exceed 64 mm (2½ in.). Ring density for the species shall be at least 4 rings-per-inch as measured over a 76 mm (3 in.) distance. The diameter of the Southern Pine posts shall be 190 mm (7½ in.). at the ground line with a upper limit of 210 mm (8¼ in.).

APPENDIX B - Round 1 Cantilever Bogie Test Results

Figure B-1. Results of Test No. DF-1.....	277
Figure B-2. Results of Test No. DF-2.....	278
Figure B-3. Results of Test No. DF-3.....	279
Figure B-4. Results of Test No. DF-4.....	280
Figure B-5. Results of Test No. DF-5.....	281
Figure B-6. Results of Test No. DF-6.....	282
Figure B-7. Results of Test No. DF-7.....	283
Figure B-8. Results of Test No. DF-8.....	284
Figure B-9. Results of Test No. DF-9.....	285
Figure B-10. Results of Test No. DF-10.....	286
Figure B-11. Results of Test No. DF-11.....	287
Figure B-12. Results of Test No. DF-12.....	288
Figure B-13. Results of Test No. DF-13.....	289
Figure B-14. Results of Test No. DF-14.....	290
Figure B-15. Results of Test No. DF-15.....	291
Figure B-16. Results of Test No. PP-1	292
Figure B-17. Results of Test No. PP-2	293
Figure B-18. Results of Test No. PP-3	294
Figure B-19. Results of Test No. PP-4	295
Figure B-20. Results of Test No. PP-5	296
Figure B-21. Results of Test No. PP-6	297
Figure B-22. Results of Test No. PP-7	298
Figure B-23. Results of Test No. PP-8	299
Figure B-24. Results of Test No. PP-9	300
Figure B-25. Results of Test No. PP-10	301
Figure B-26. Results of Test No. PP-11	302
Figure B-27. Results of Test No. PP-12	303
Figure B-28. Results of Test No. PP-13	304
Figure B-29. Results of Test No. PP-14	305
Figure B-30. Results of Test No. PP-15	306
Figure B-31. Results of Test No. SY-1.....	307
Figure B-32. Results of Test No. SY-2.....	308
Figure B-33. Results of Test No. SY-3.....	309
Figure B-34. Results of Test No. SY-4.....	310
Figure B-35. Results of Test No. SY-5.....	311
Figure B-36. Results of Test No. SY-6.....	312
Figure B-37. Results of Test No. SY-7.....	313
Figure B-38. Results of Test No. SY-8.....	314
Figure B-39. Results of Test No. SY-9.....	315
Figure B-40. Results of Test No. SY-10.....	316
Figure B-41. Results of Test No. SY-11.....	317
Figure B-42. Results of Test No. SY-12.....	318
Figure B-43. Results of Test No. SY-13.....	319
Figure B-44. Results of Test No. SY-14.....	320
Figure B-45. Results of Test No. SY-15.....	321

Midwest Roadside Safety Facility

Bogie Test Summary		
Test Information		
Test Number:	CL Bogie MGS Height	
Test Date:	DF-1	
Failure Type:	9-Nov-2004	
	0	
Post Properties		
Post Type:	Douglas Fir - Round Wooden	
Post Size:	186.7 mm Dia. metric	7.35 in. Dia.
Post Length:	198.8 cm	(504.8 cm)
Embedment Depth:	101.6 cm	(258.1 cm)
Category:	HRD	
Soil Properties		
Gradation:	NA	
Moisture Content:	NA	
Compaction Method:	NA	
Soil Density, γ_d :	NA kg/m ³	NA
Bogie Properties		
Impact Velocity:	9.2 m/s	(20.5 mph) (30.1 fps)
Impact Location:	63.2 cm	(24.9 in) above groundline
Bogie Mass:	728 kg	(1605 lbf)
Data Acquired		
Accelerometer Data:	EDR-3	
Camera Data:	Side View-DV and Photon	

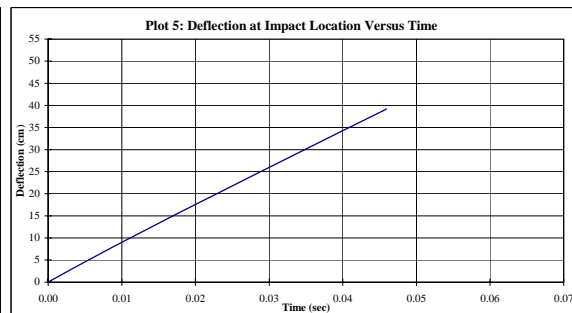
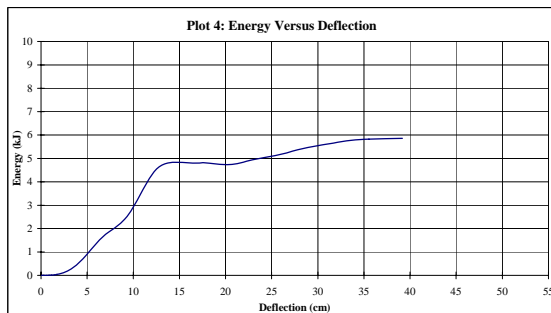
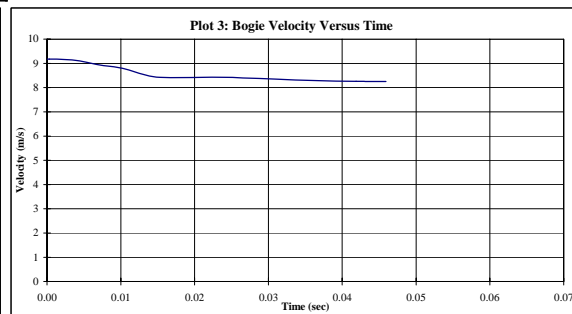
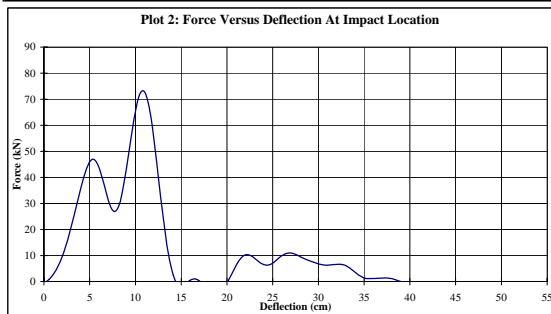
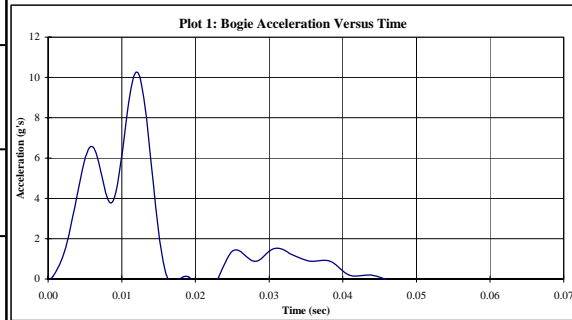


Figure B-1. Results of Test No. DF-1

Midwest Roadside Safety Facility

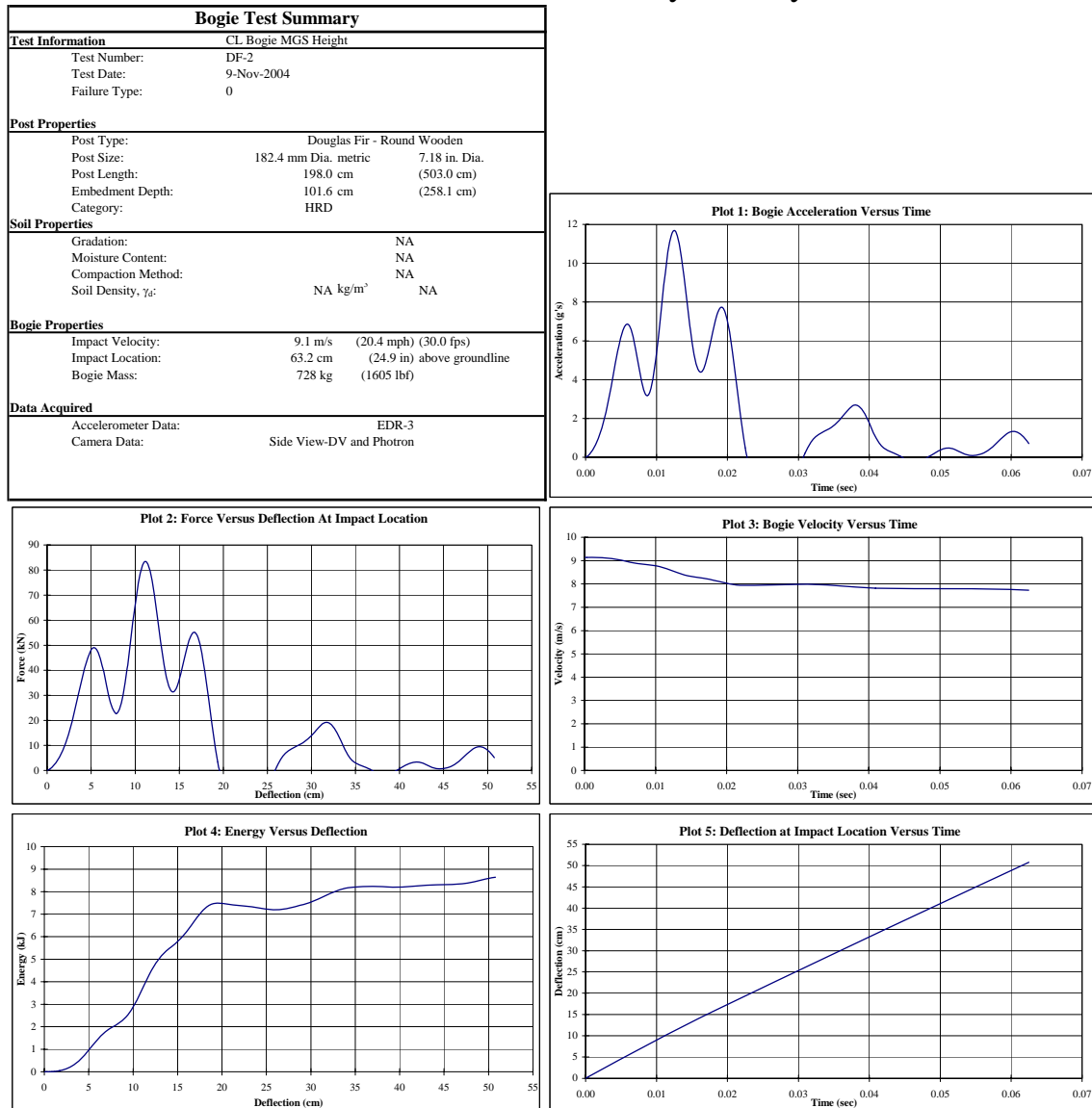


Figure B-2. Results of Test No. DF-2

Midwest Roadside Safety Facility

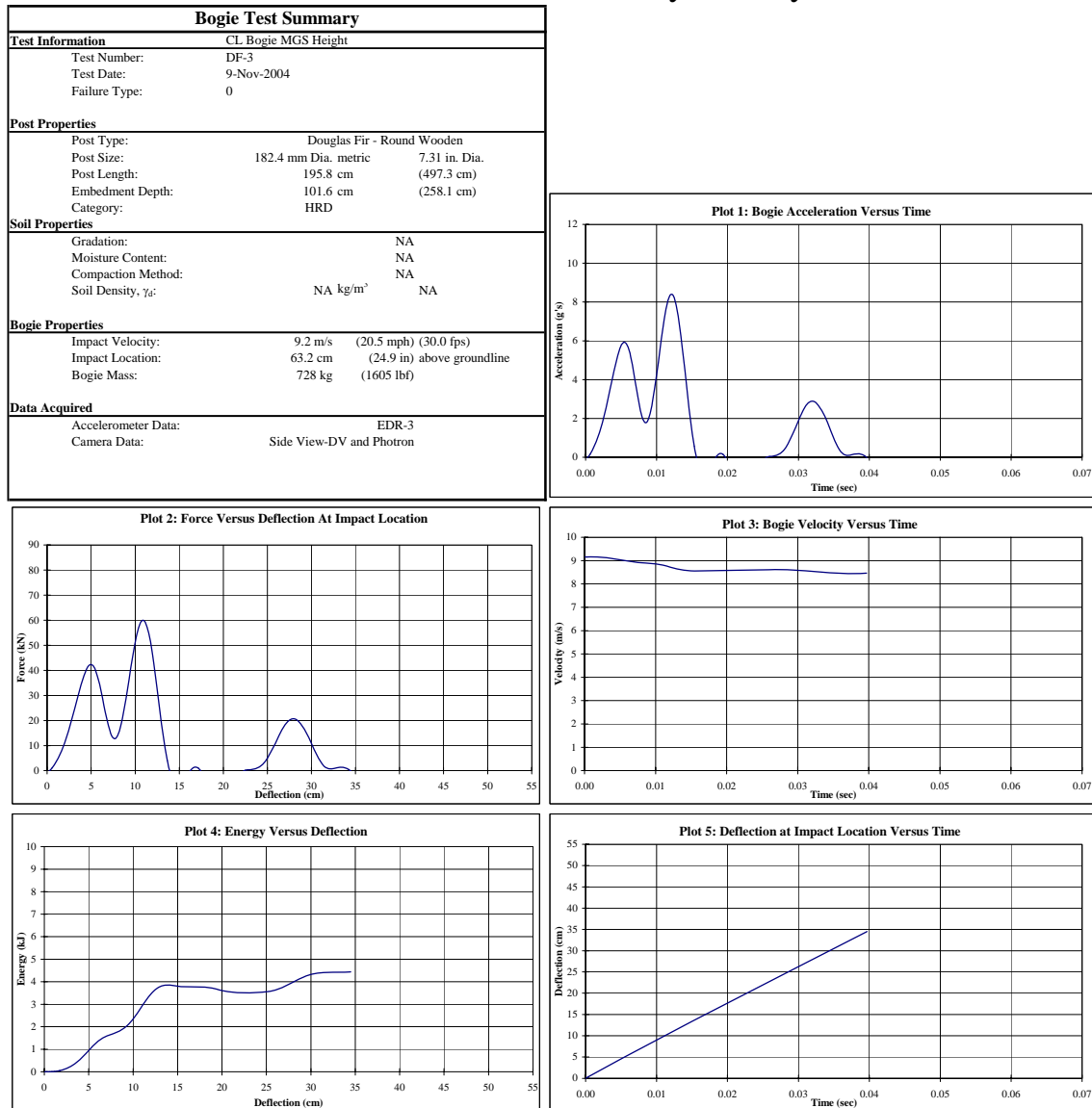


Figure B-3. Results of Test No. DF-3

Midwest Roadside Safety Facility

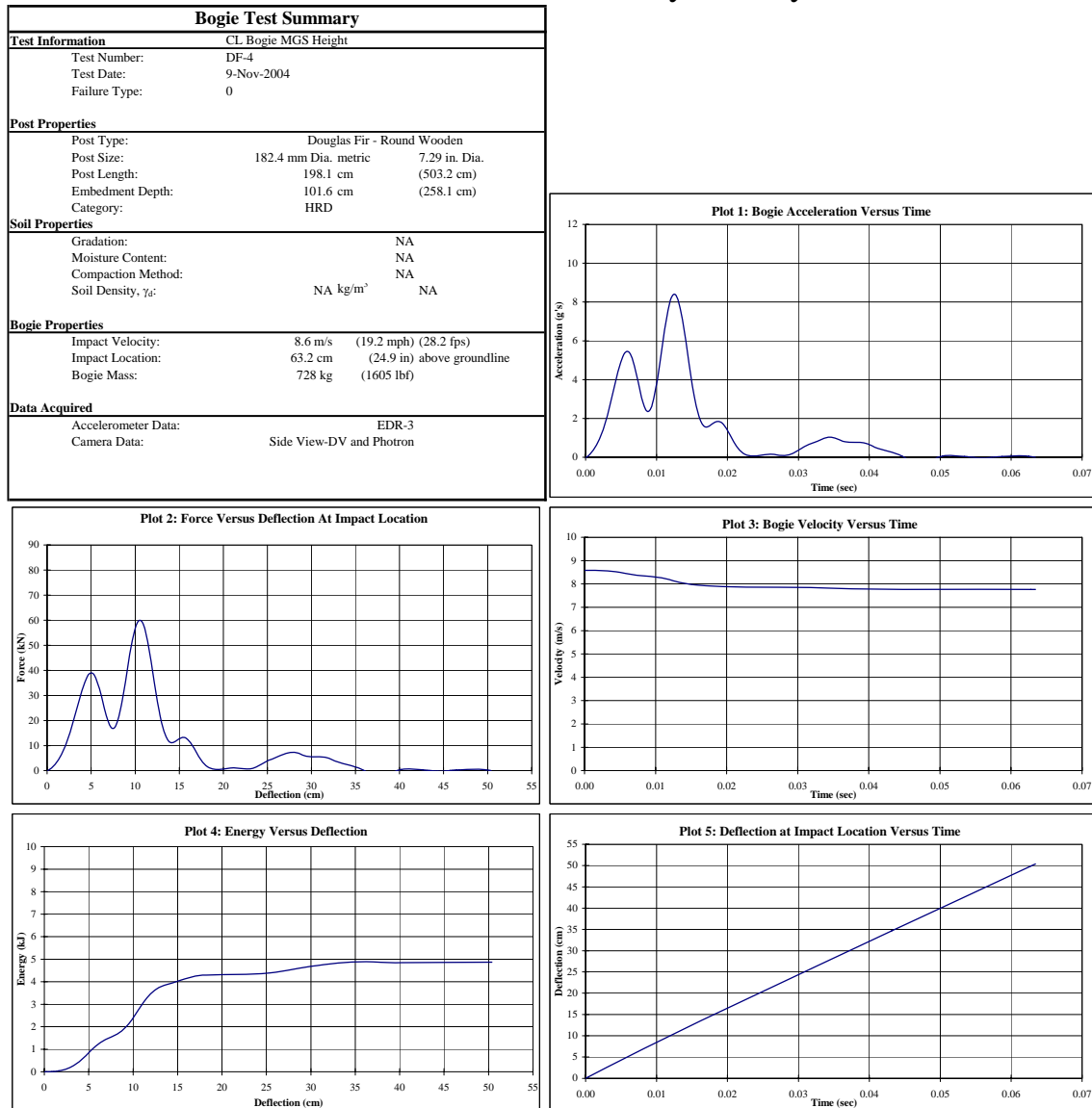


Figure B-4. Results of Test No. DF-4

Midwest Roadside Safety Facility

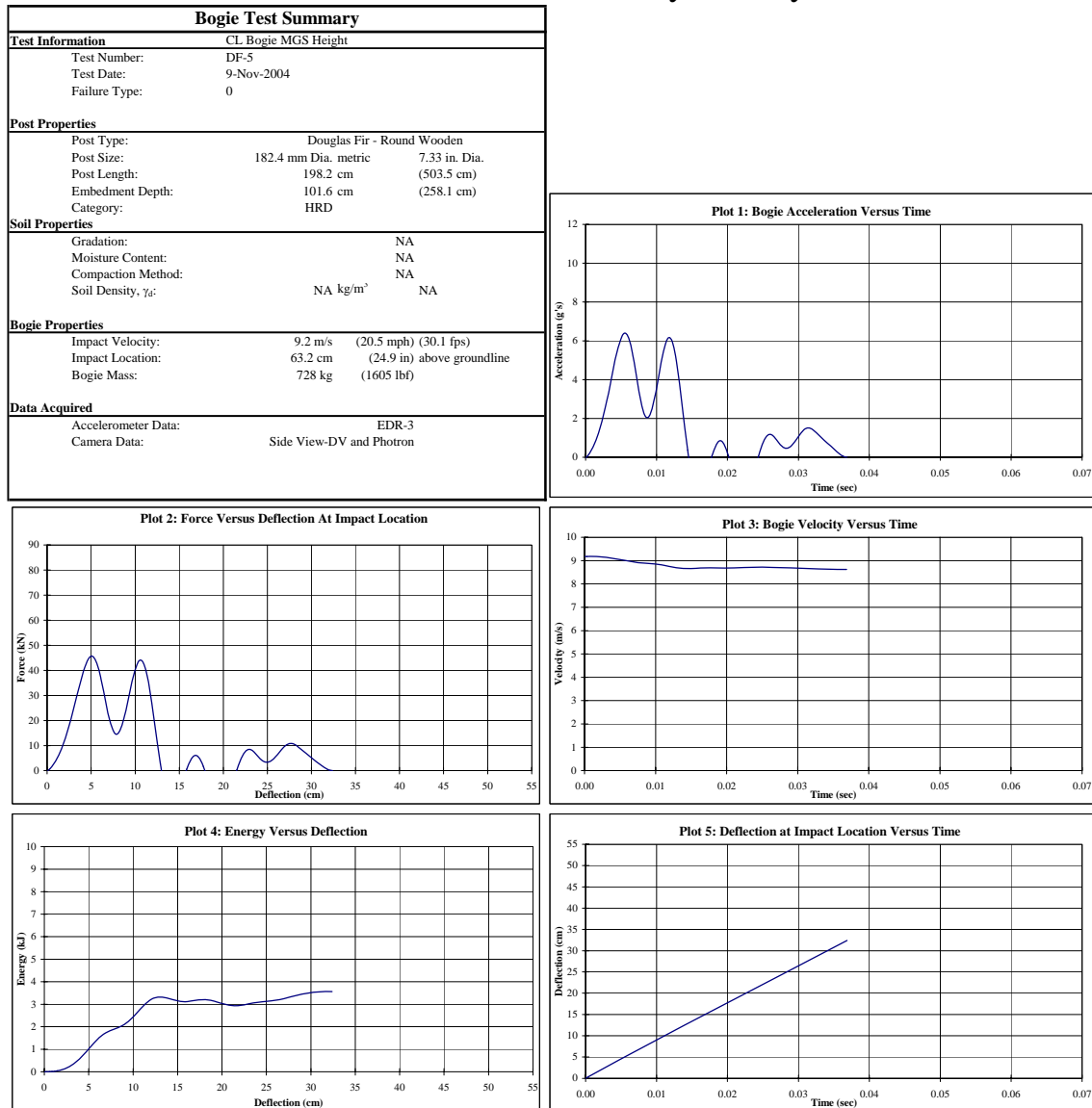


Figure B-5. Results of Test No. DF-5

Midwest Roadside Safety Facility

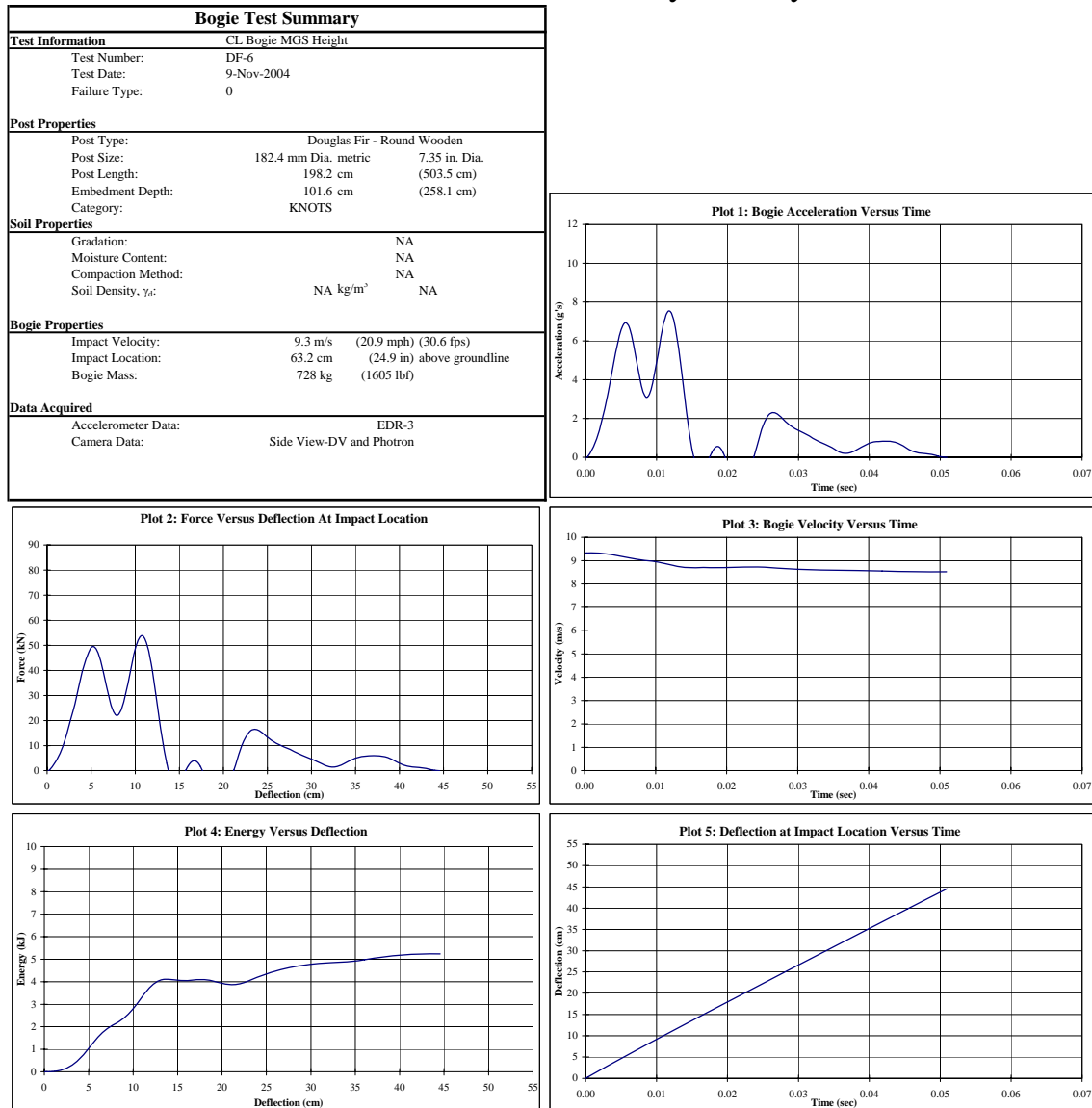


Figure B-6. Results of Test No. DF-6

Midwest Roadside Safety Facility

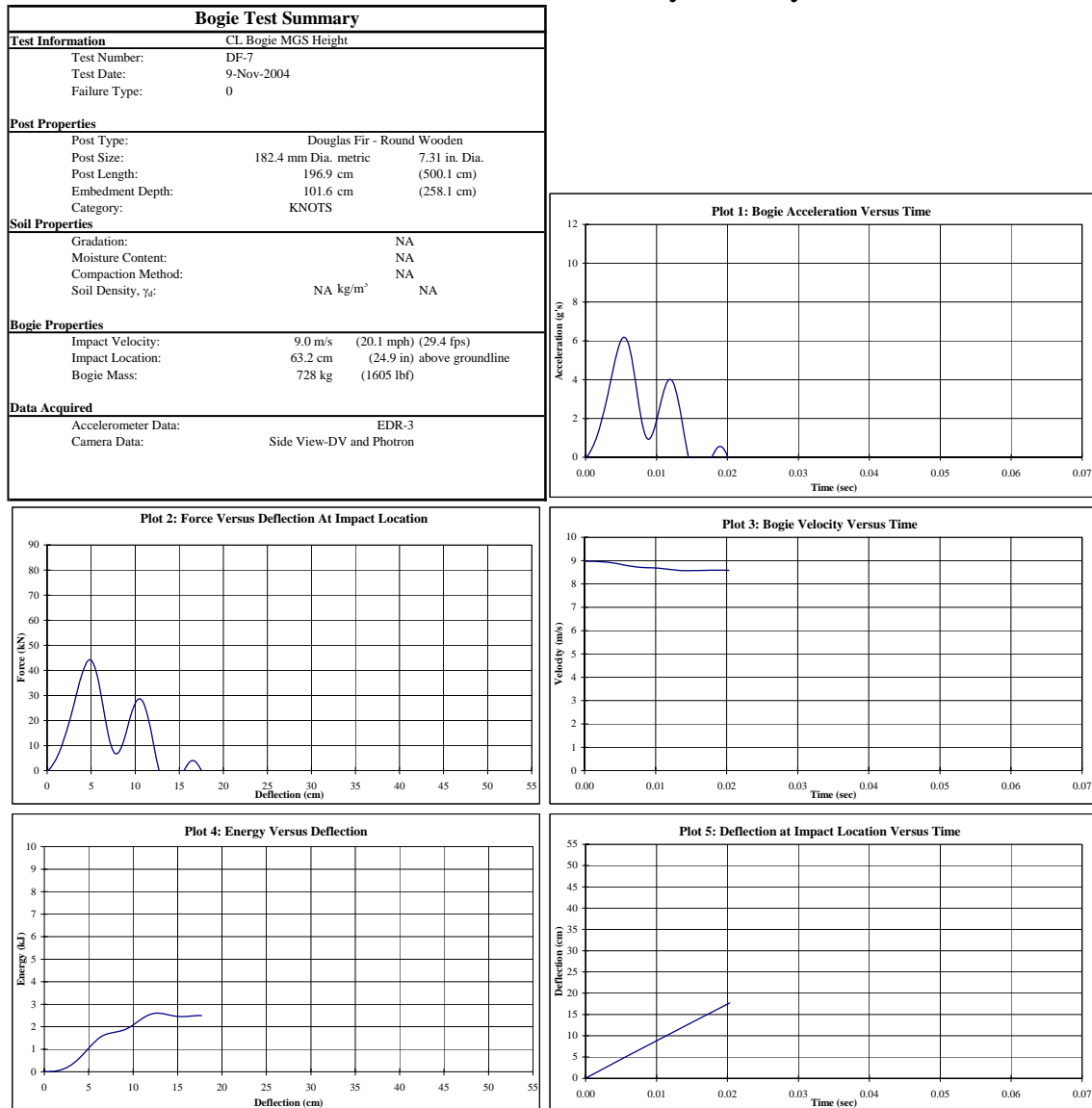


Figure B-7. Results of Test No. DF-7

Midwest Roadside Safety Facility

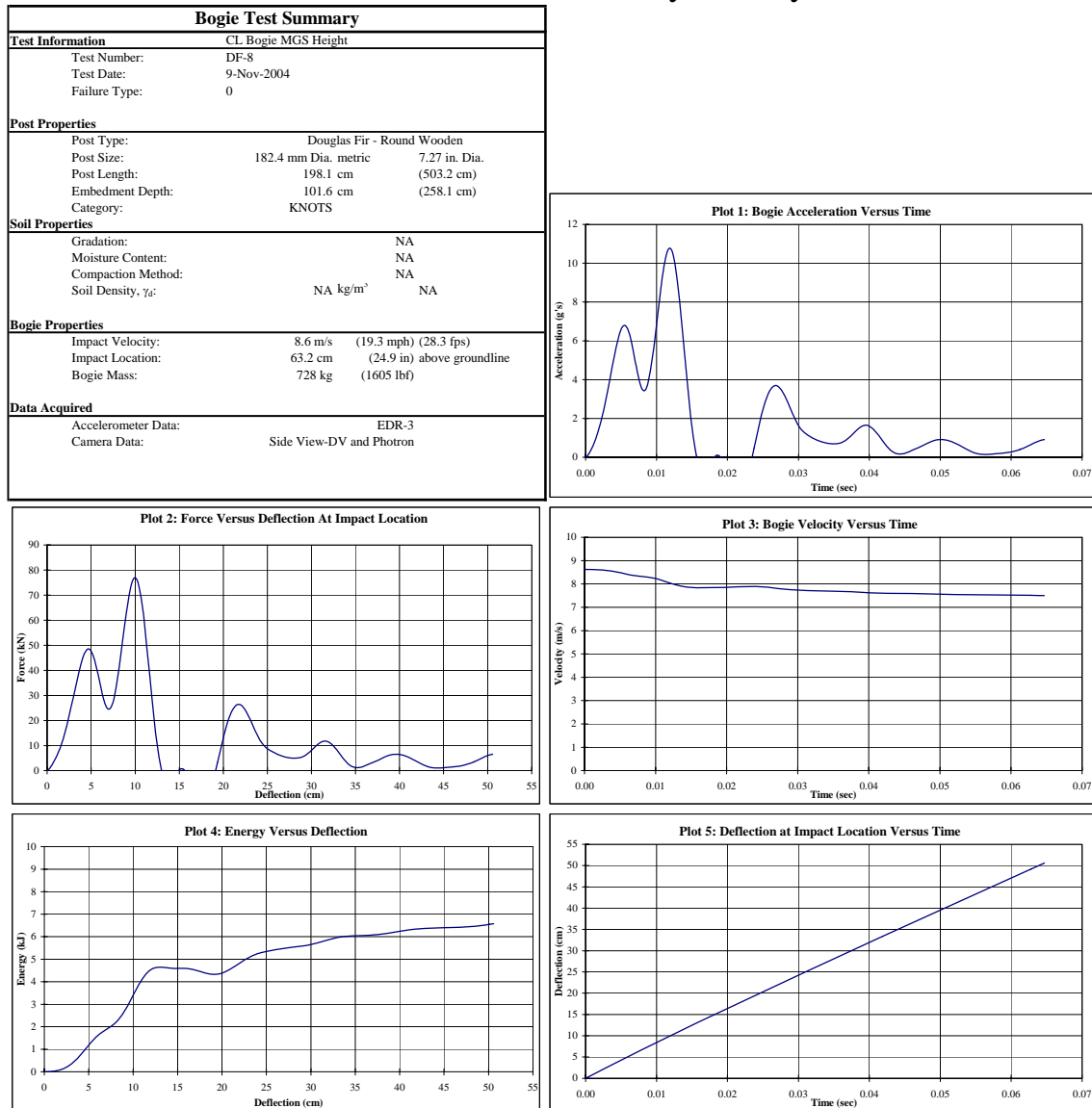


Figure B-8. Results of Test No. DF-8

Midwest Roadside Safety Facility

Bogie Test Summary		
Test Information	CL Bogie MGS Height	
Test Number:	DF-9	
Test Date:	9-Nov-2004	
Failure Type:	0	
Post Properties		
Post Type:	Douglas Fir - Round Wooden	
Post Size:	182.4 mm Dia. metric	7.22 in. Dia.
Post Length:	198.1 cm	(503.2 cm)
Embedment Depth:	101.6 cm	(258.1 cm)
Category:	KNOTS	
Soil Properties		
Gradation:	NA	
Moisture Content:	NA	
Compaction Method:	NA	
Soil Density, γ_d :	NA kg/m ³	NA
Bogie Properties		
Impact Velocity:	9.0 m/s	(20.2 mph) (29.6 fps)
Impact Location:	63.2 cm	(24.9 in) above groundline
Bogie Mass:	728 kg	(1605 lbf)
Data Acquired		
Accelerometer Data:	EDR-3	
Camera Data:	Side View-DV and Photon	

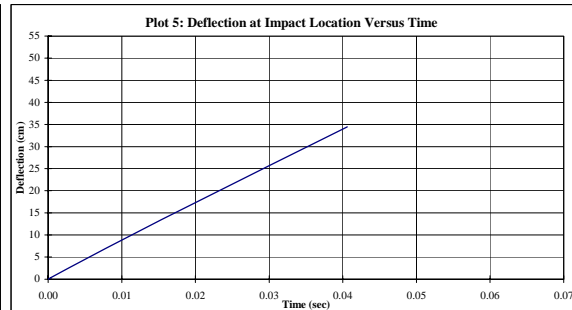
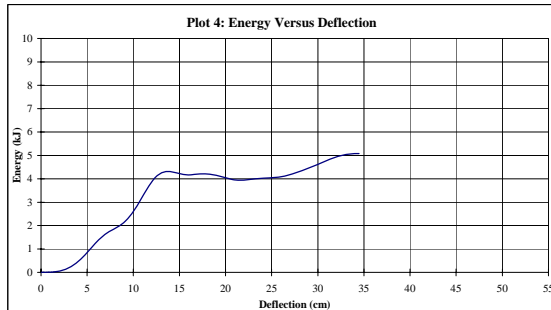
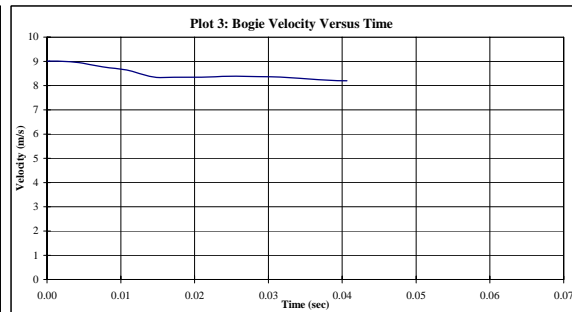
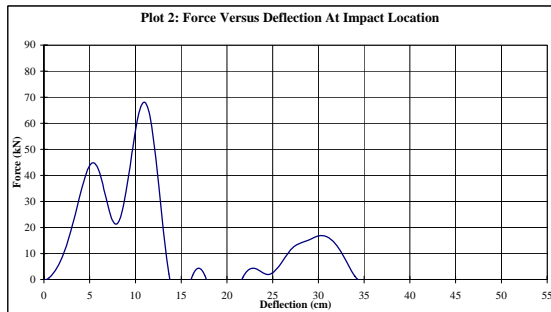
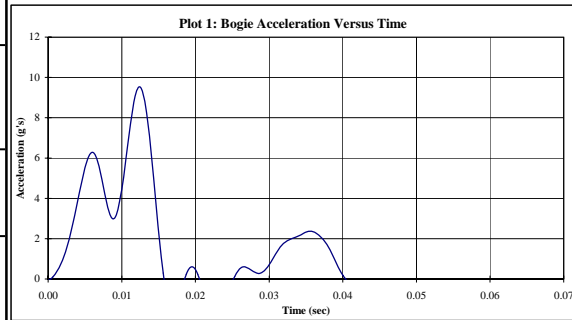


Figure B-9. Results of Test No. DF-9

Midwest Roadside Safety Facility

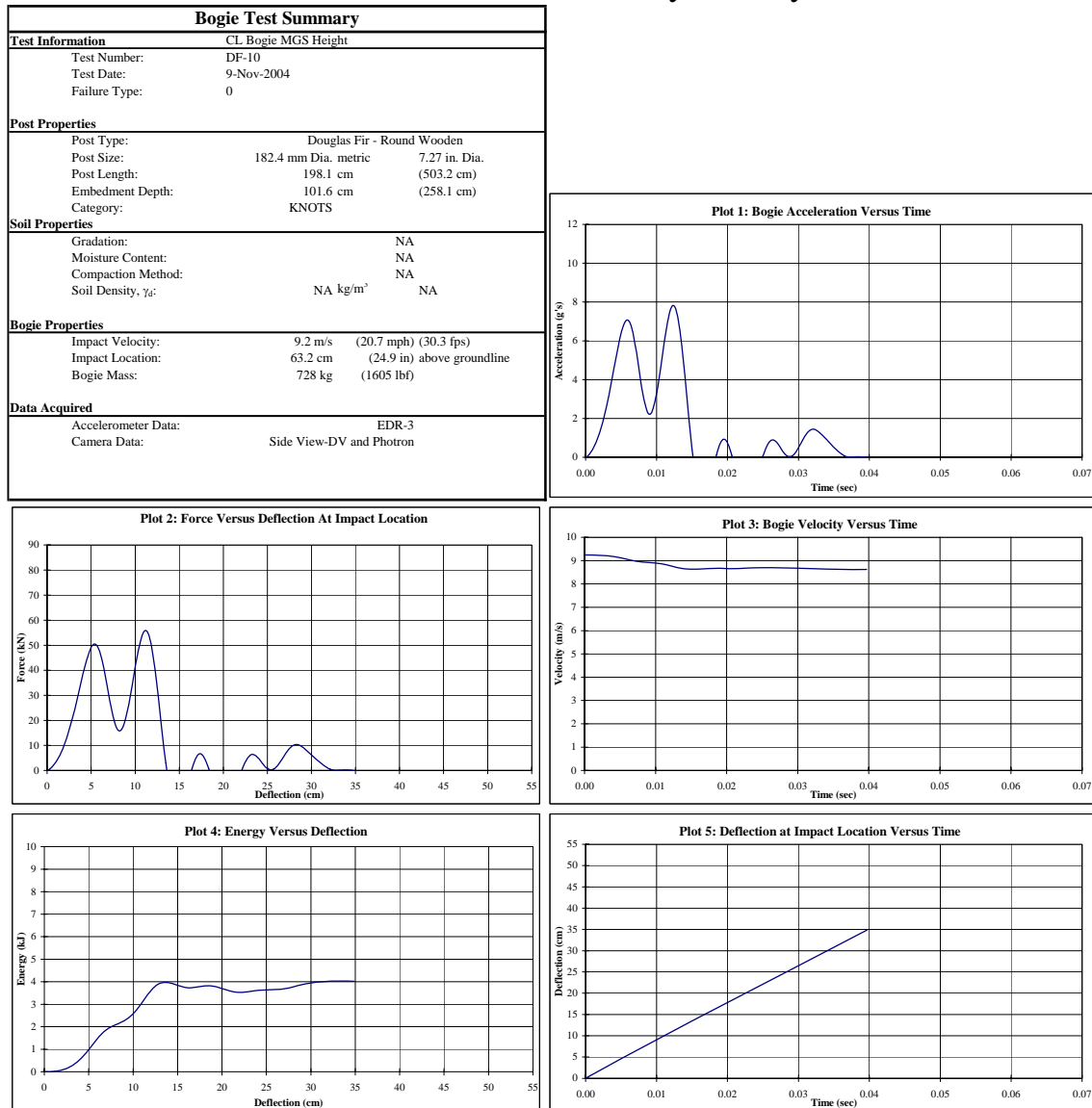


Figure B-10. Results of Test No. DF-10

Midwest Roadside Safety Facility

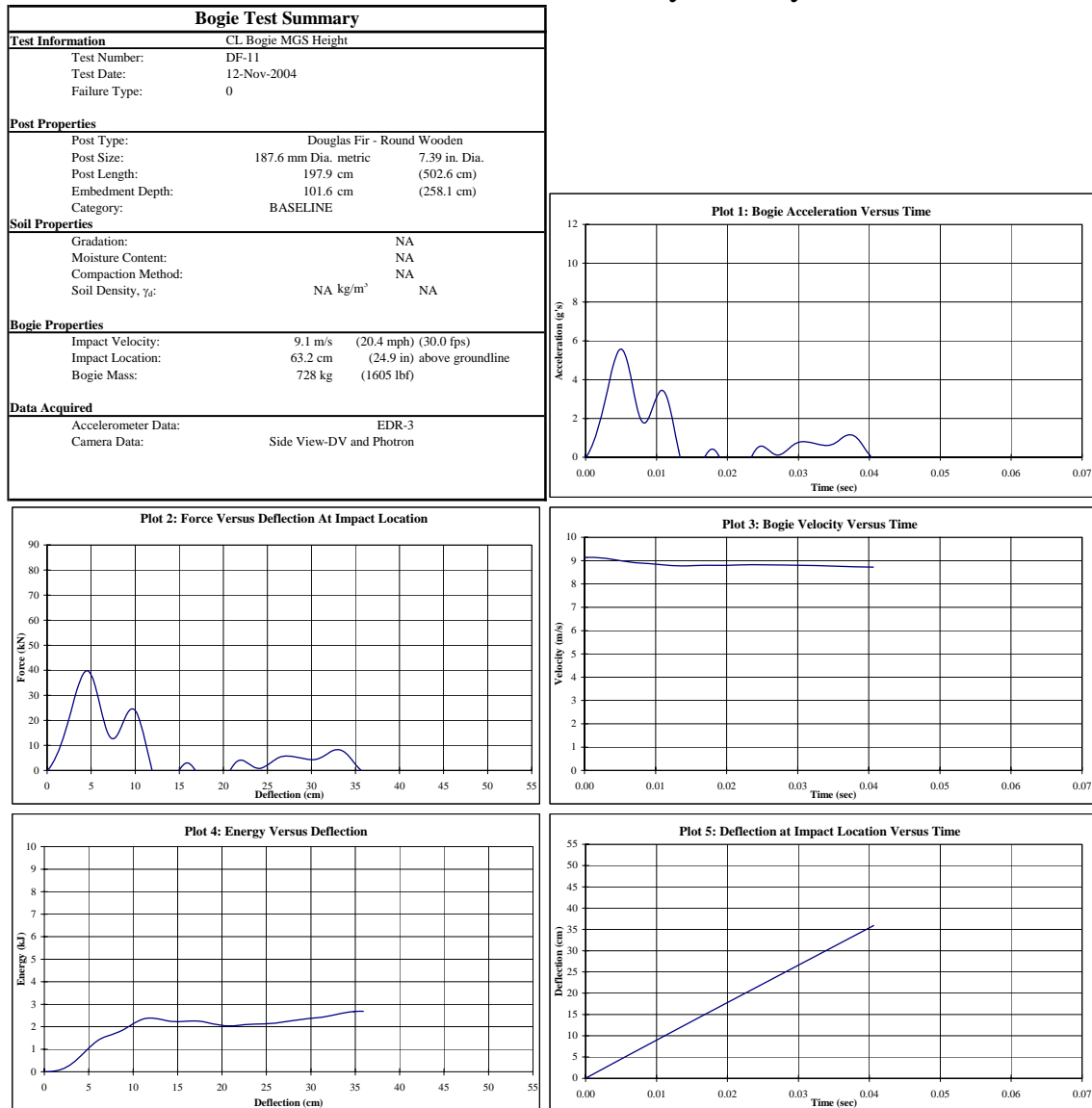


Figure B-11. Results of Test No. DF-11

Midwest Roadside Safety Facility

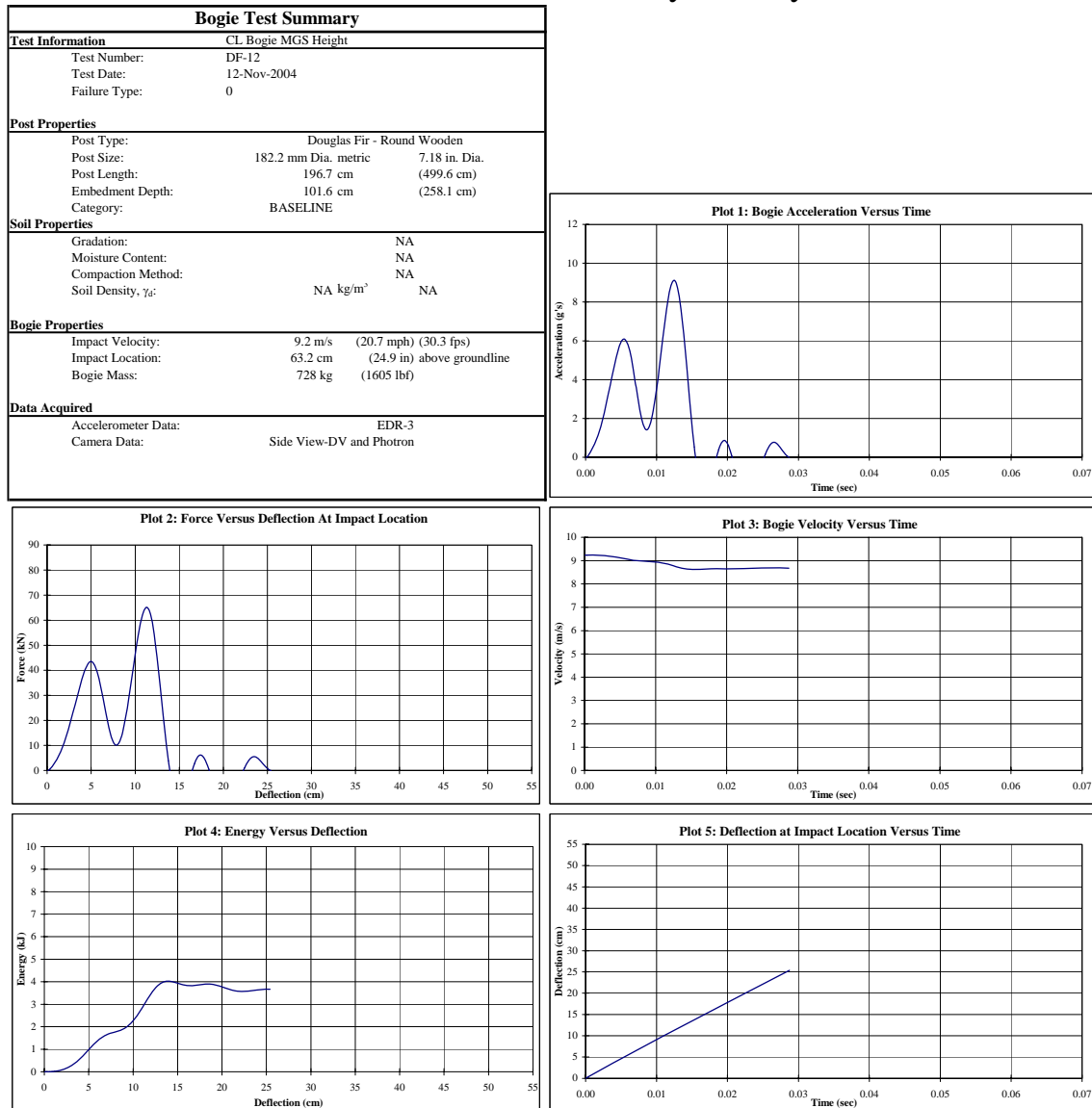


Figure B-12. Results of Test No. DF-12

Midwest Roadside Safety Facility

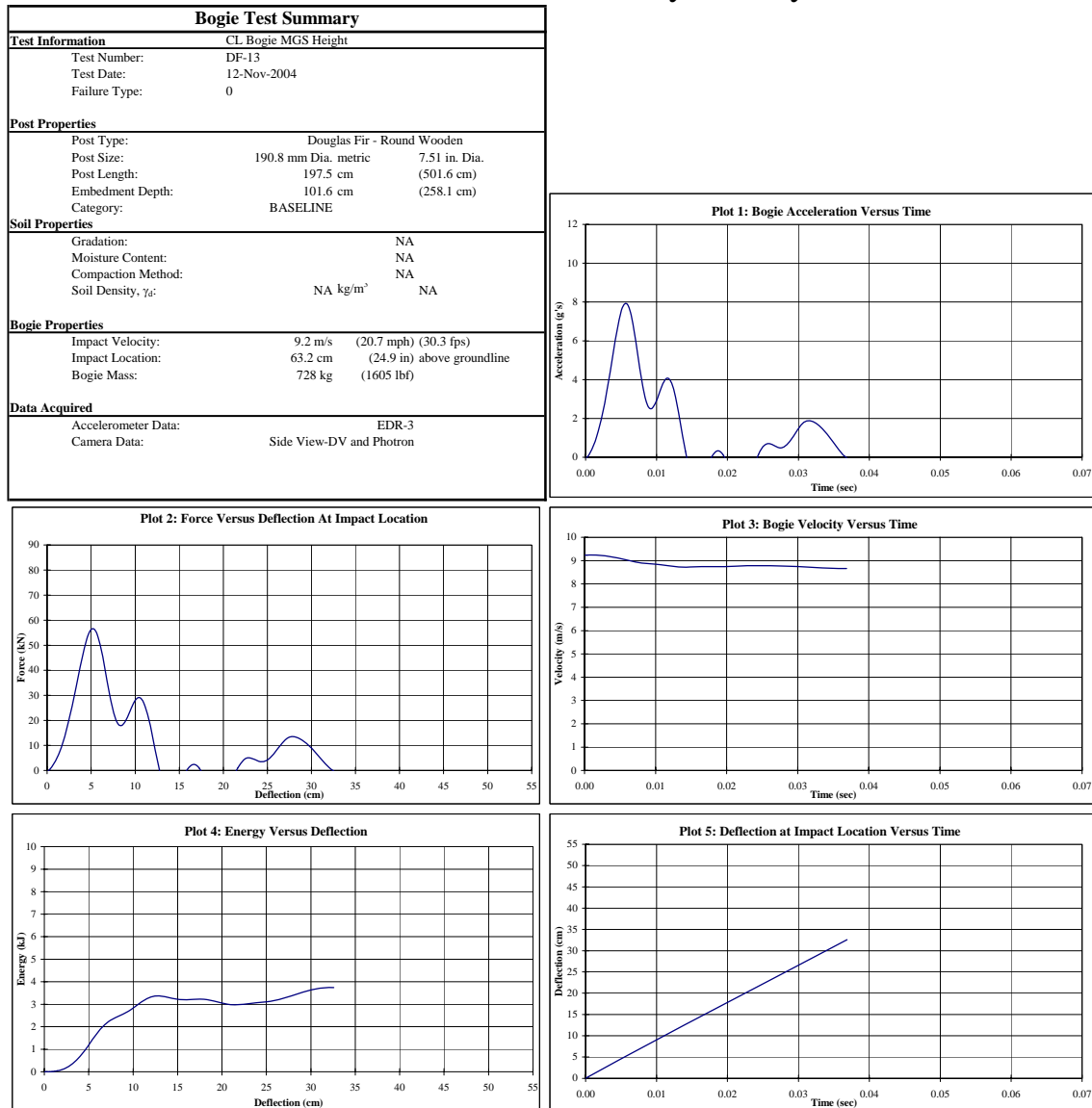


Figure B-13. Results of Test No. DF-13

Midwest Roadside Safety Facility

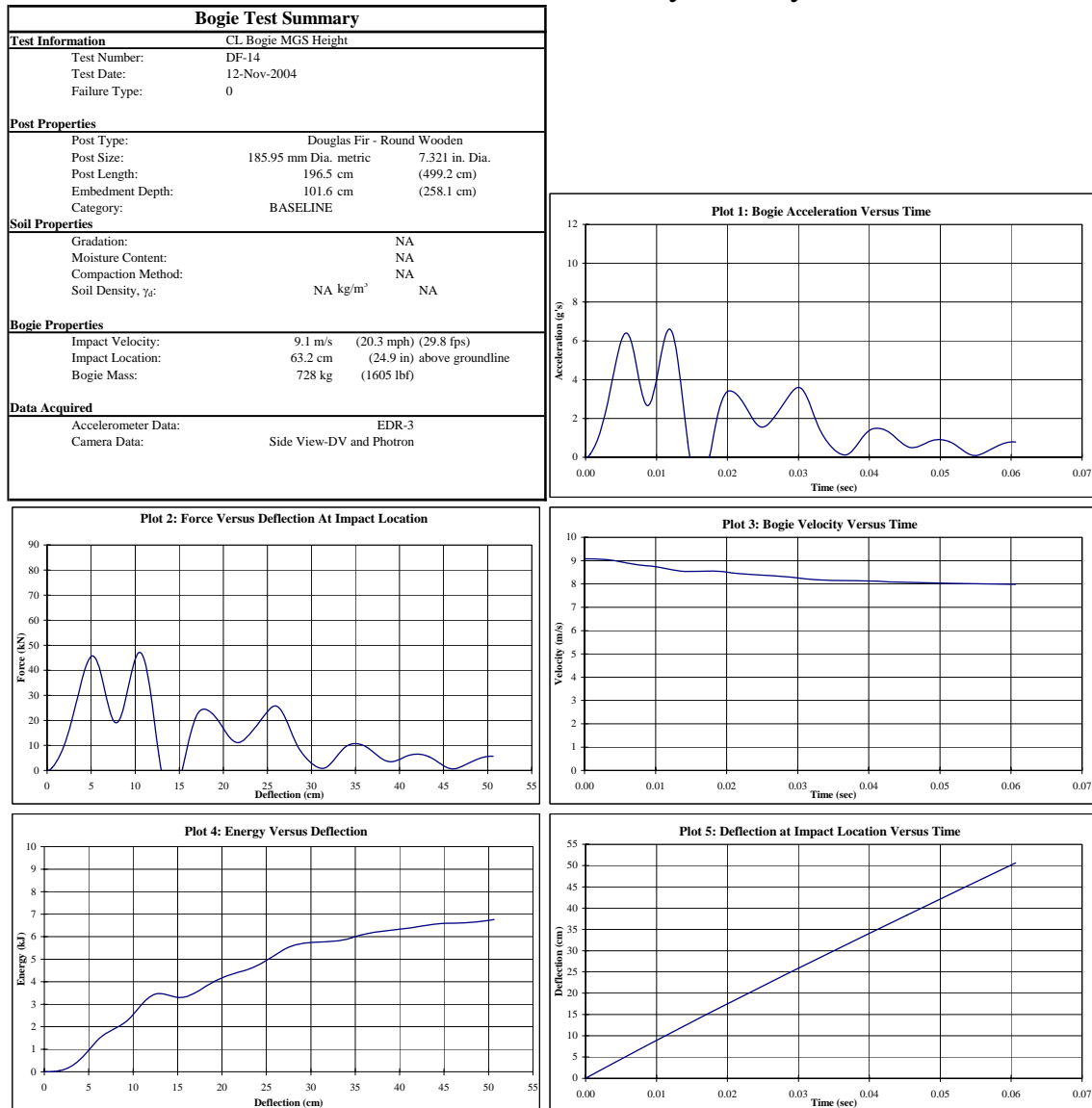


Figure B-14. Results of Test No. DF-14

Midwest Roadside Safety Facility

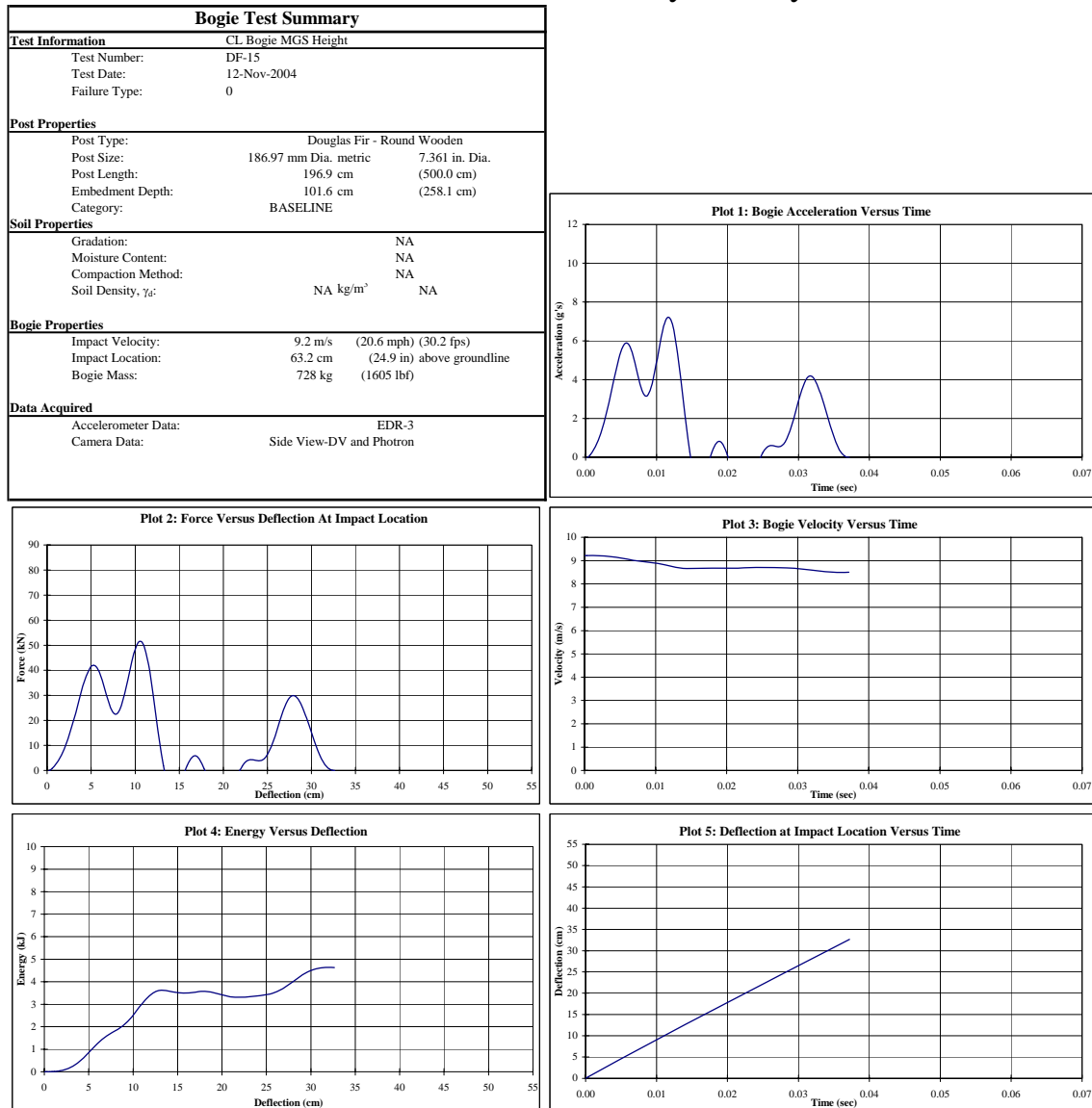


Figure B-15. Results of Test No. DF-15

Midwest Roadside Safety Facility

Bogie Test Summary		
Test Information	CL Bogie MGS Height	
Test Number:	PP-1	
Test Date:	12-Nov-2004	
Failure Type:	0	
Post Properties		
Post Type:	Ponderosa Pine - Round Wooden	
Post Size:	209.8 mm Dia. metric	8.26 in. Dia.
Post Length:	198.1 cm	(503.1 cm)
Embedment Depth:	101.6 cm	(258.1 cm)
Category:	BASELINE	
Soil Properties		
Gradation:	NA	
Moisture Content:	NA	
Compaction Method:	NA	
Soil Density, γ_d :	NA kg/m ³	NA
Bogie Properties		
Impact Velocity:	9.2 m/s	(20.6 mph) (30.2 fps)
Impact Location:	63.2 cm	(24.9 in) above groundline
Bogie Mass:	728 kg	(1605 lbf)
Data Acquired		
Accelerometer Data:	EDR-3	
Camera Data:	Side View-DV and Photon	

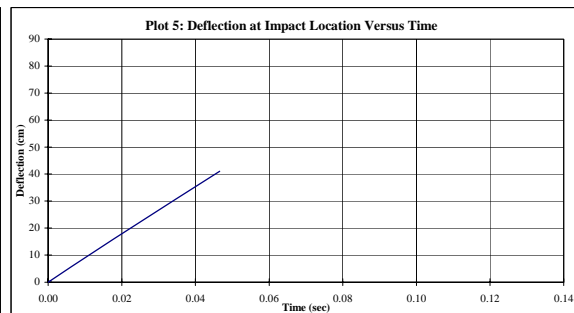
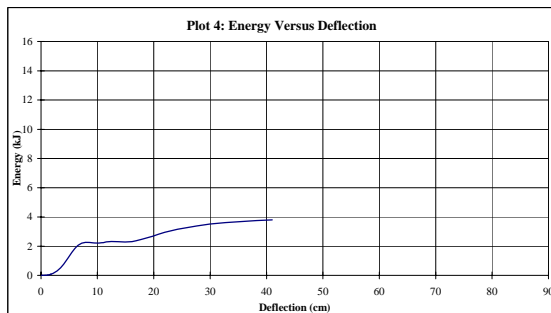
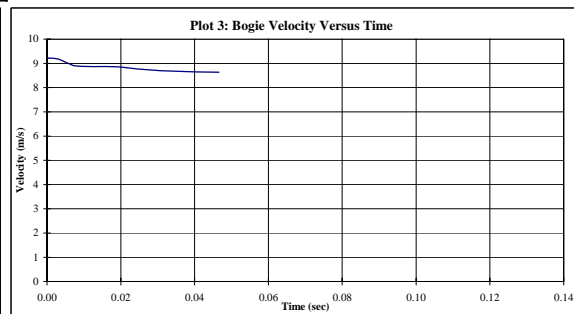
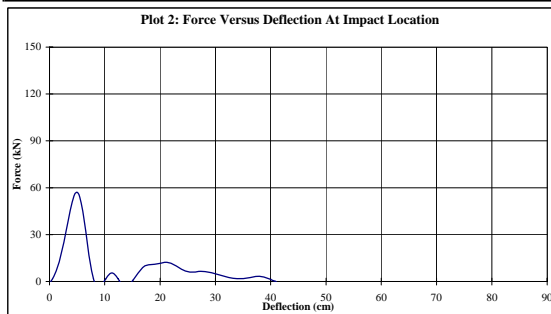
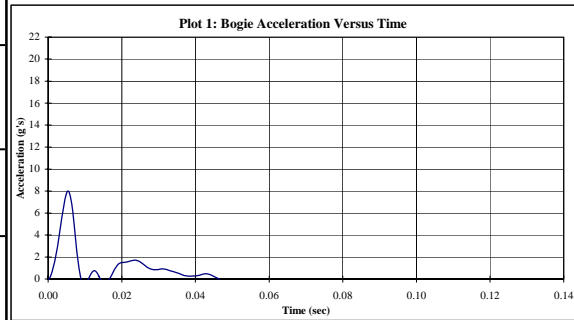


Figure B-16. Results of Test No. PP-1

Midwest Roadside Safety Facility

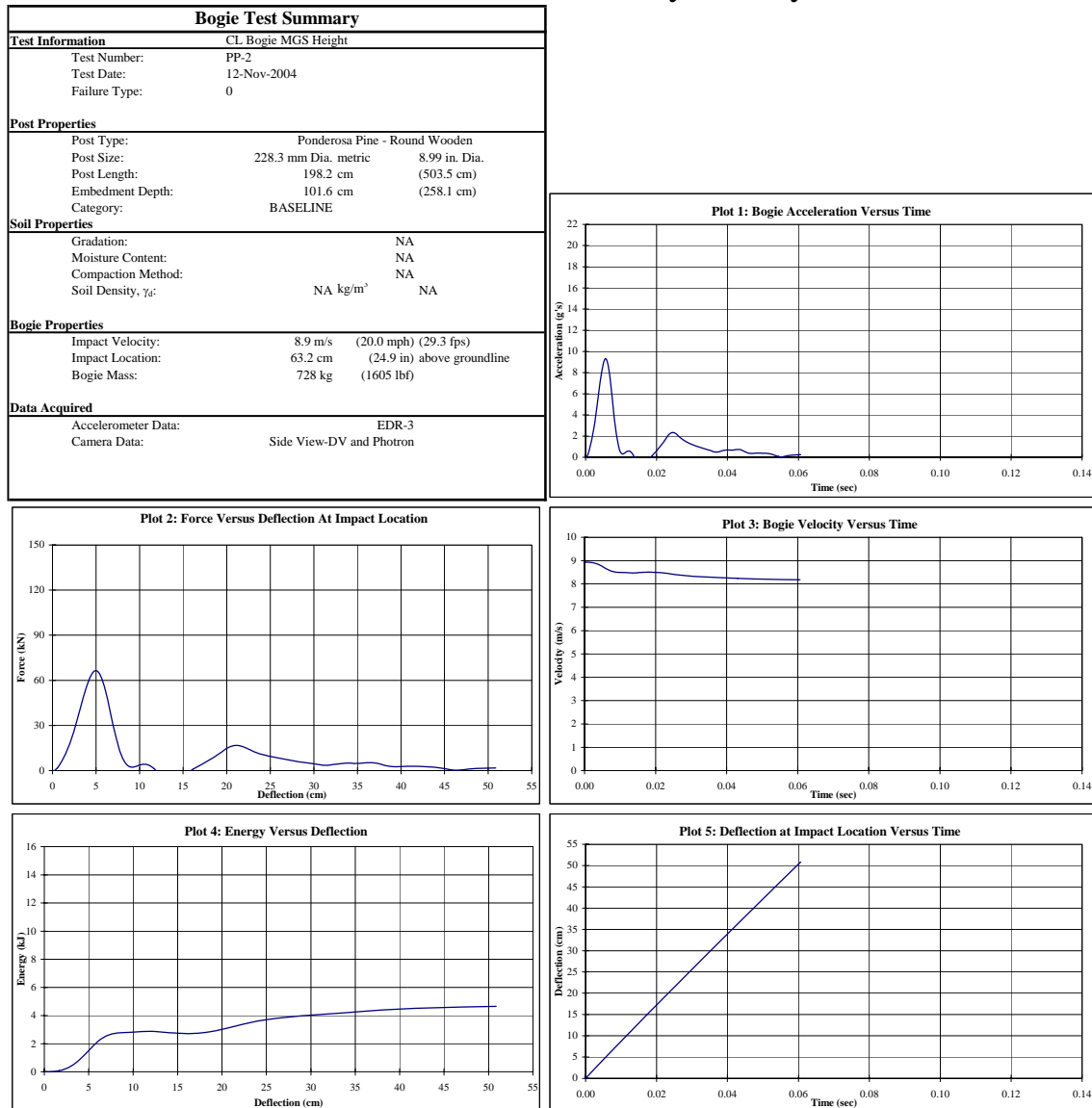


Figure B-17. Results of Test No. PP-2

Midwest Roadside Safety Facility

Bogie Test Summary		
Test Information	CL Bogie MGS Height	
Test Number:	PP-3	
Test Date:	12-Nov-2004	
Failure Type:	0	
Post Properties		
Post Type:	Ponderosa Pine - Round Wooden	
Post Size:	224.0 mm Dia. metric	8.82 in. Dia.
Post Length:	198.2 cm	(503.5 cm)
Embedment Depth:	101.6 cm	(258.1 cm)
Category:	BASELINE	
Soil Properties		
Gradation:	NA	
Moisture Content:	NA	
Compaction Method:	NA	
Soil Density, γ_d :	NA kg/m ³	NA
Bogie Properties		
Impact Velocity:	9.0 m/s	(20.2 mph) (29.7 fps)
Impact Location:	63.2 cm	(24.9 in) above groundline
Bogie Mass:	728 kg	(1605 lbf)
Data Acquired		
Accelerometer Data:	EDR-3	
Camera Data:	Side View-DV and Photon	

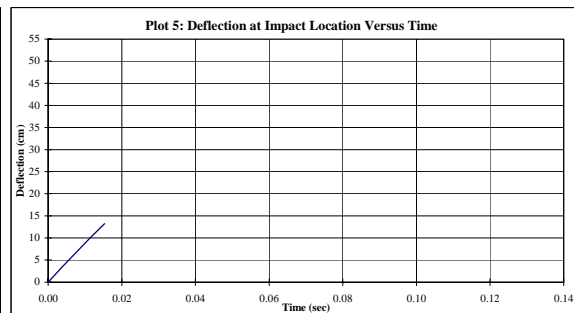
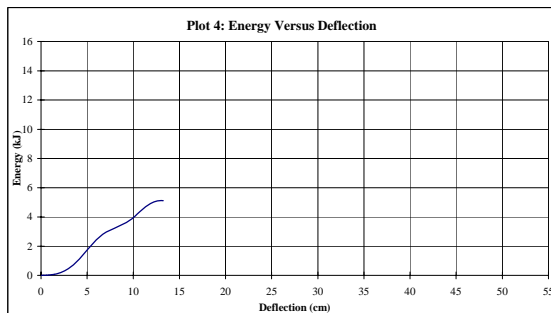
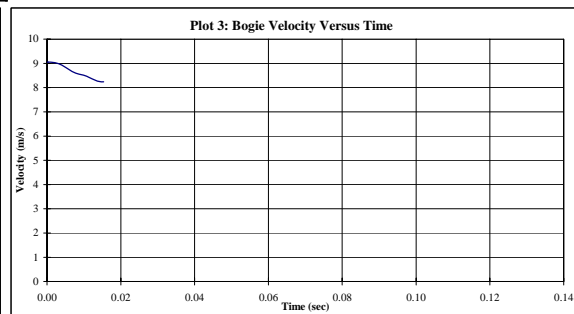
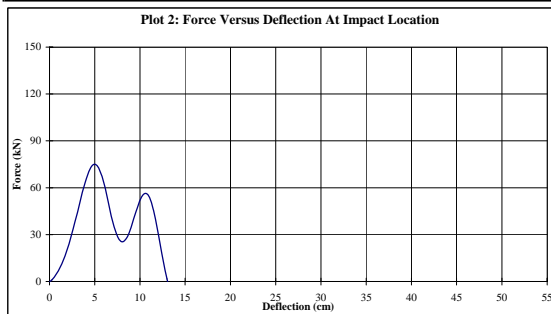
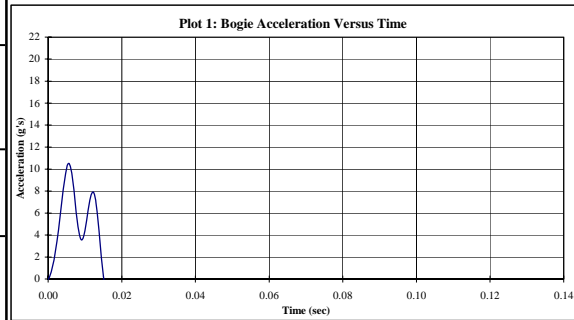


Figure B-18. Results of Test No. PP-3

Midwest Roadside Safety Facility

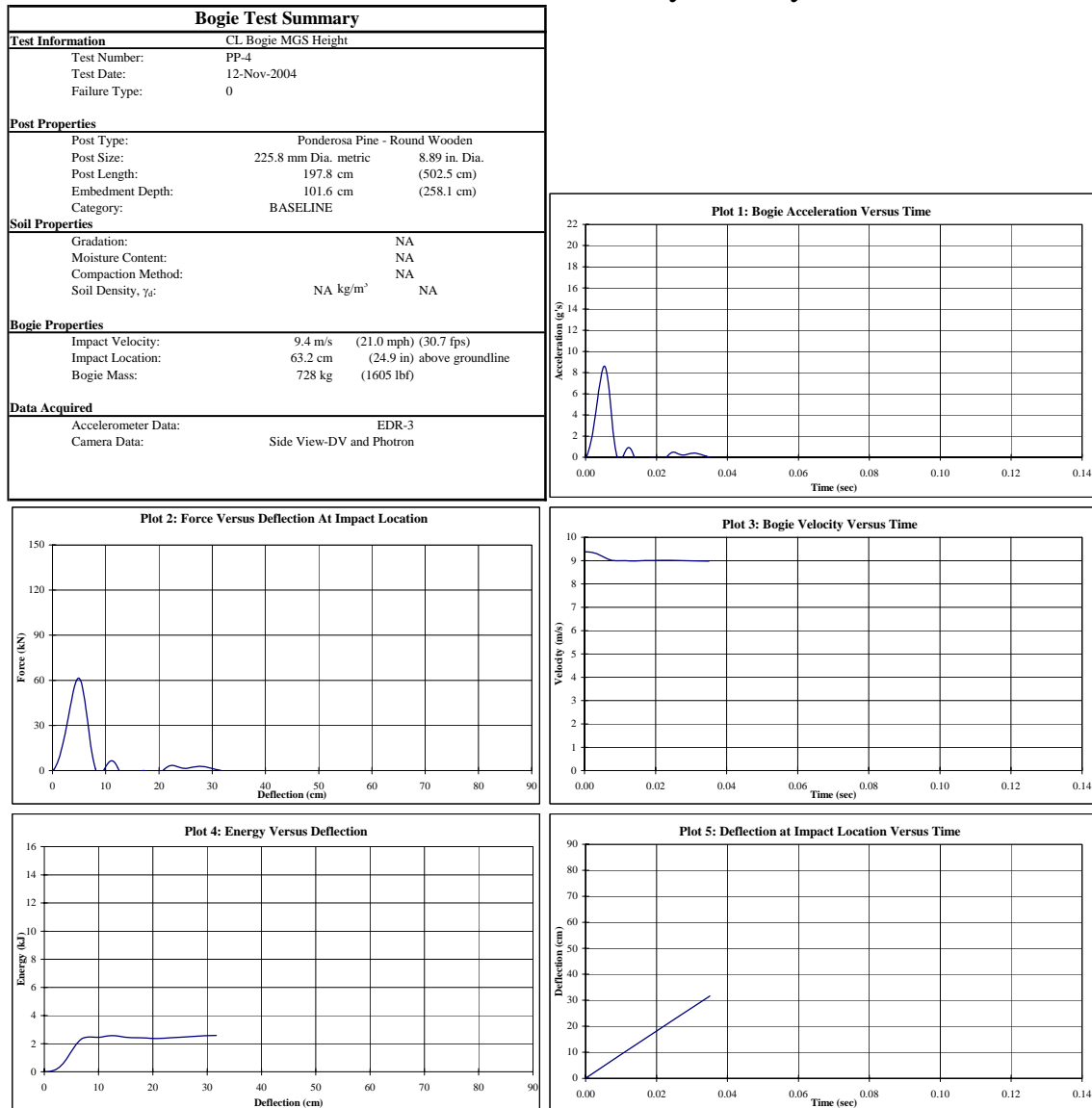


Figure B-19. Results of Test No. PP-4

Midwest Roadside Safety Facility

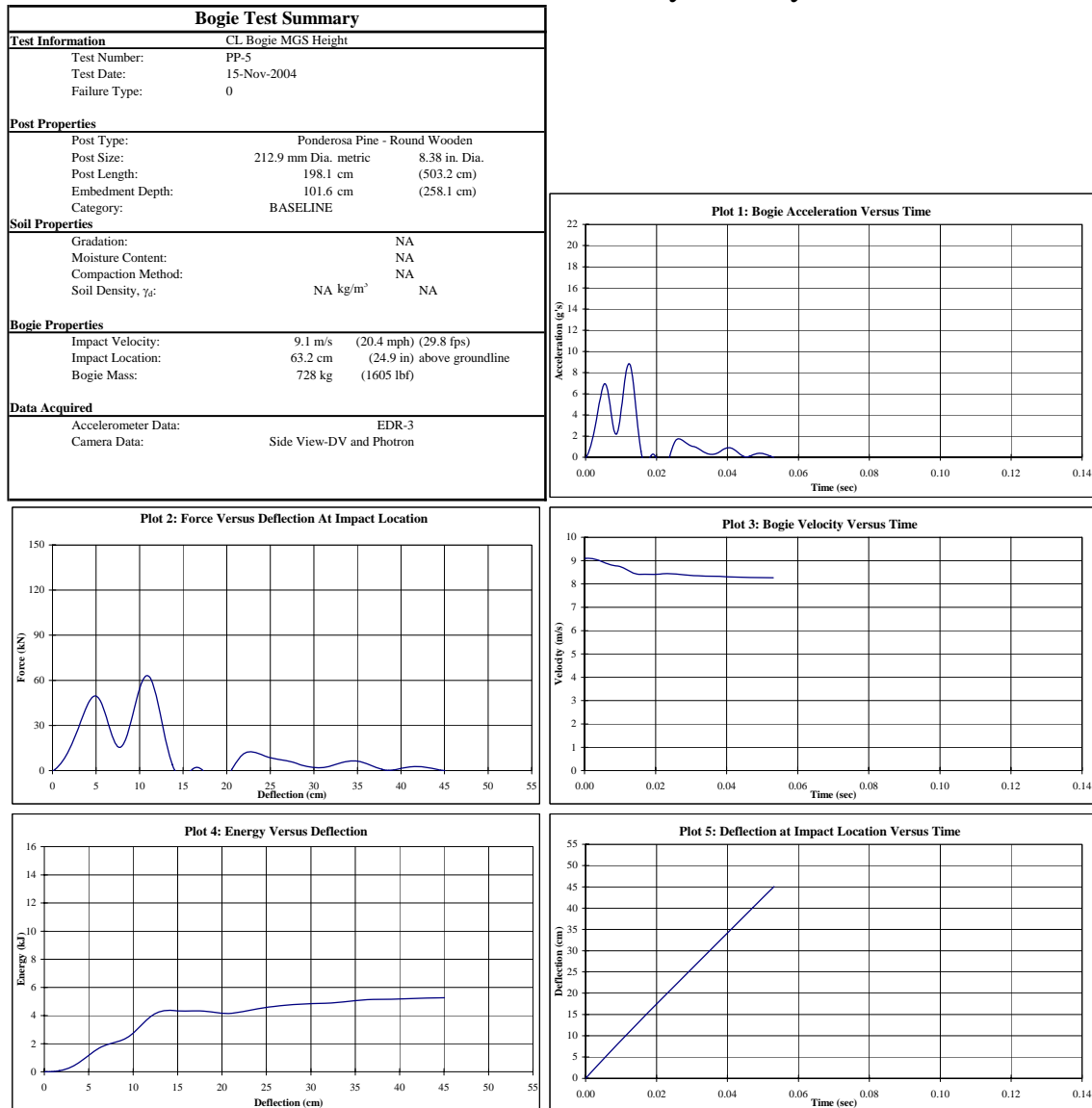


Figure B-20. Results of Test No. PP-5

Midwest Roadside Safety Facility

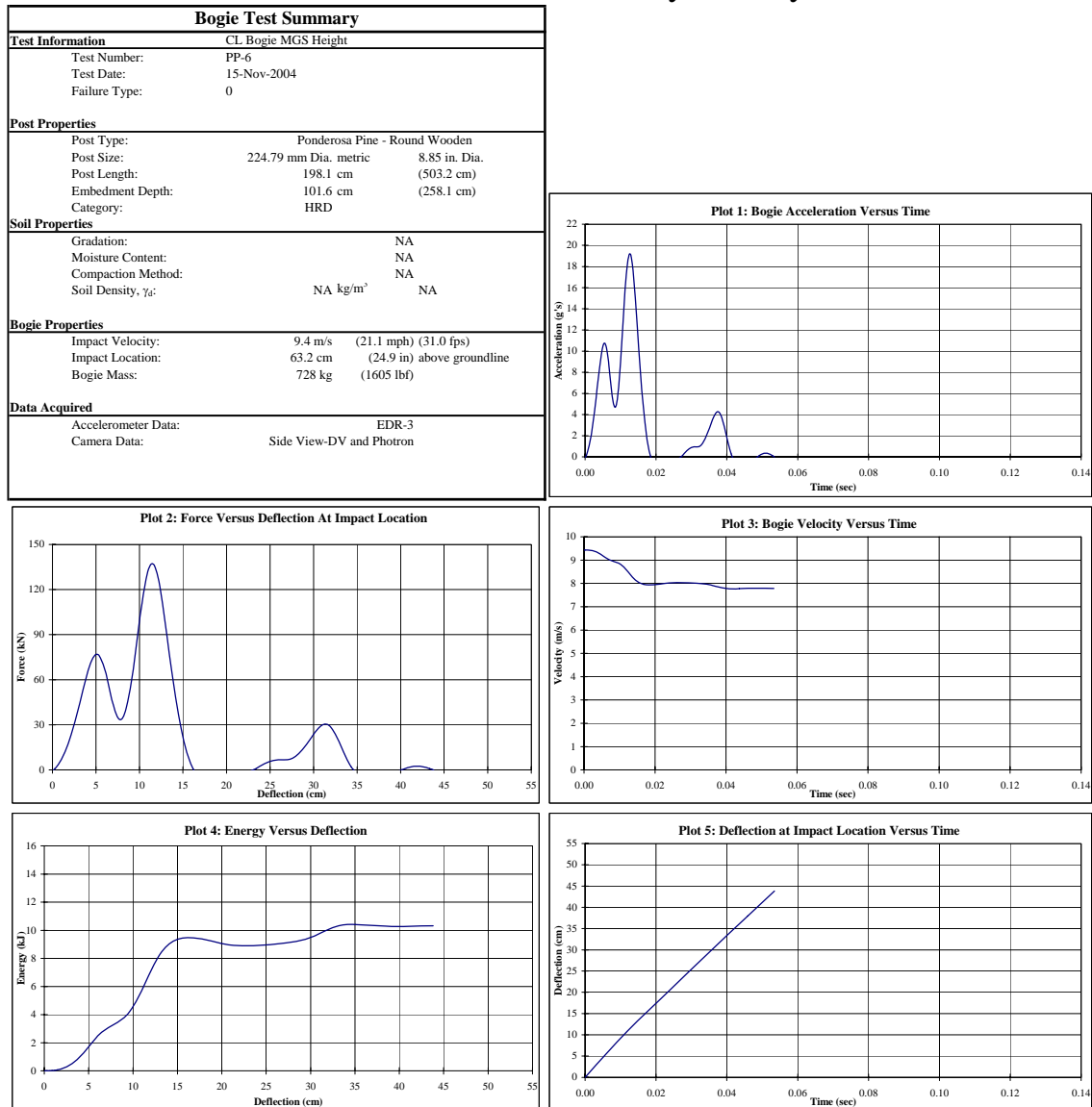


Figure B-21. Results of Test No. PP-6

Midwest Roadside Safety Facility

Bogie Test Summary			
Test Information		CL Bogie MGS Height	
Test Number:		PP-7	
Test Date:		15-Nov-2004	
Failure Type:		0	
Post Properties			
Post Type:		Ponderosa Pine - Round Wooden	
Post Size:		227.08 mm Dia. metric	8.94 in. Dia.
Post Length:		198.1 cm	(503.2 cm)
Embedment Depth:		101.6 cm	(258.1 cm)
Category:		HRD	
Soil Properties			
Gradation:		NA	
Moisture Content:		NA	
Compaction Method:		NA	
Soil Density, γ_d :		NA kg/m ³	NA
Bogie Properties			
Impact Velocity:		9.2 m/s	(20.7 mph) (30.3 fps)
Impact Location:		63.2 cm	(24.9 in) above groundline
Bogie Mass:		728 kg	(1605 lbf)
Data Acquired			
Accelerometer Data:		EDR-3	
Camera Data:		Side View-DV and Photon	

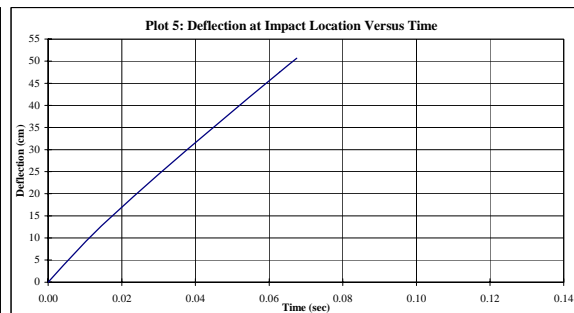
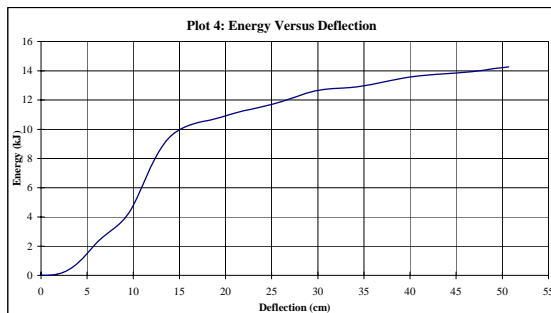
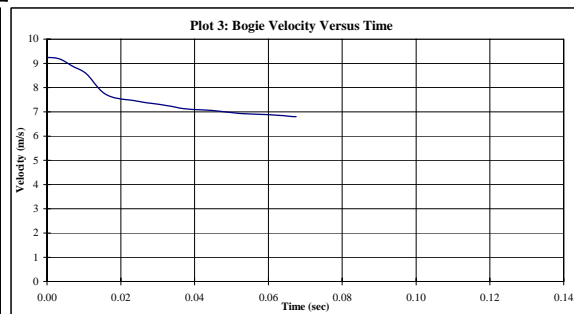
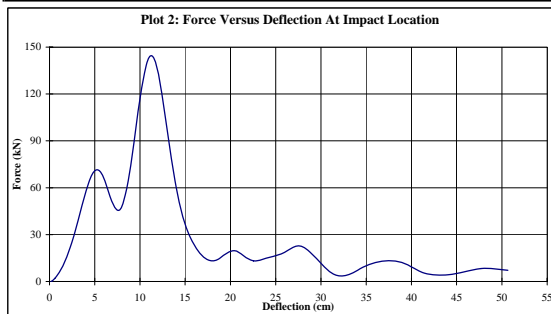
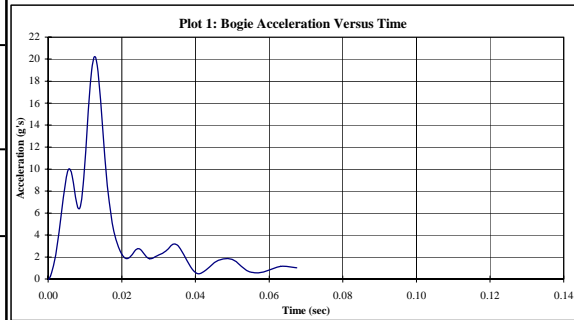


Figure B-22. Results of Test No. PP-7

Midwest Roadside Safety Facility

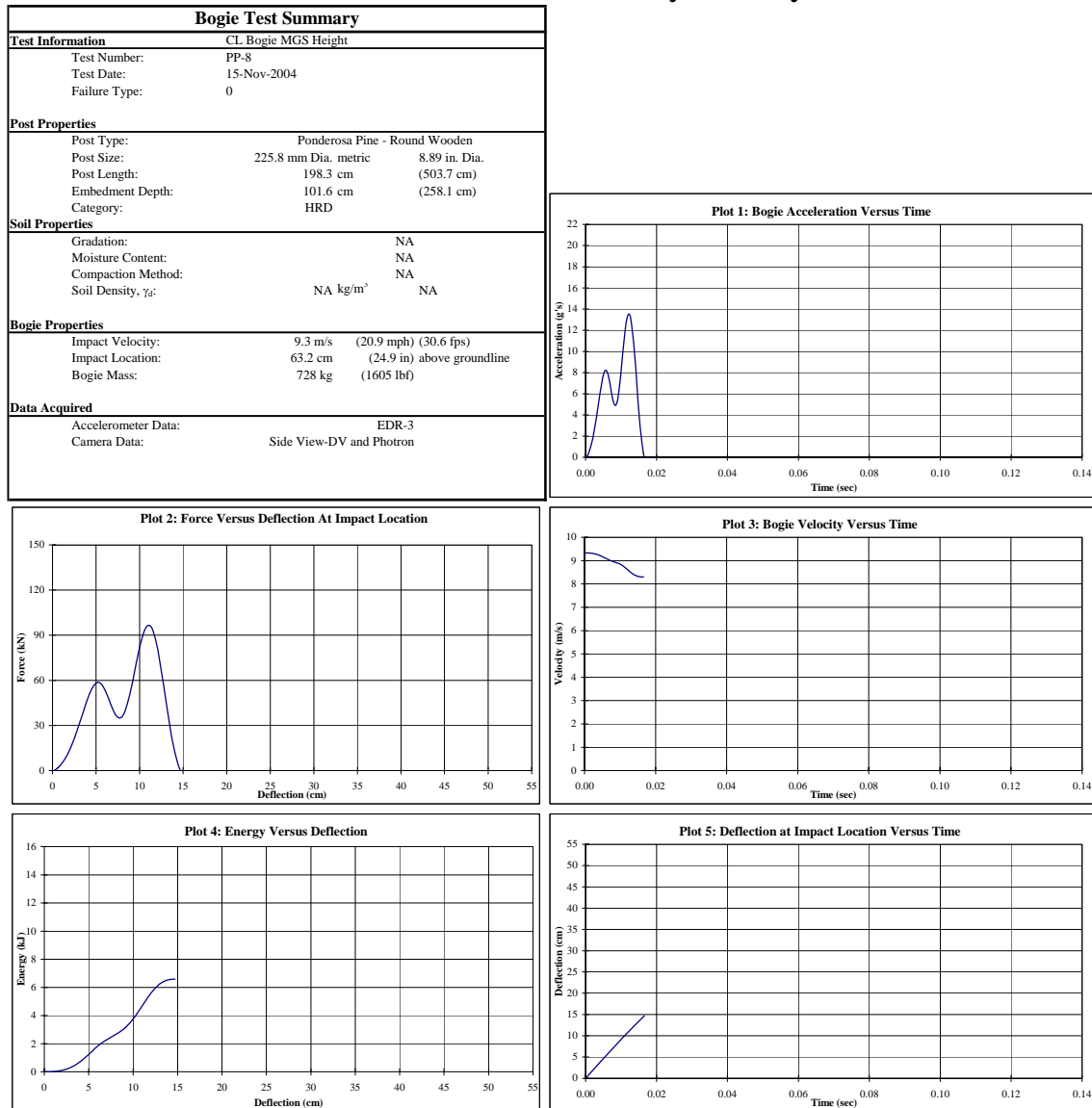


Figure B-23. Results of Test No. PP-8

Midwest Roadside Safety Facility

Bogie Test Summary			
Test Information		CL Bogie MGS Height	
Test Number:		PP-9	
Test Date:		15-Nov-2004	
Failure Type:		0	
Post Properties			
Post Type:		Ponderosa Pine - Round Wooden	
Post Size:		227.3 mm Dia. metric	8.95 in. Dia.
Post Length:		198.0 cm	(502.8 cm)
Embedment Depth:		101.6 cm	(258.1 cm)
Category:		HRD	
Soil Properties			
Gradation:		NA	
Moisture Content:		NA	
Compaction Method:		NA	
Soil Density, γ_d :		NA kg/m ³	NA
Bogie Properties			
Impact Velocity:		9.3 m/s	(20.8 mph) (30.5 fps)
Impact Location:		63.2 cm	(24.9 in) above groundline
Bogie Mass:		728 kg	(1605 lbf)
Data Acquired			
Accelerometer Data:		EDR-3	
Camera Data:		Side View-DV and Photon	

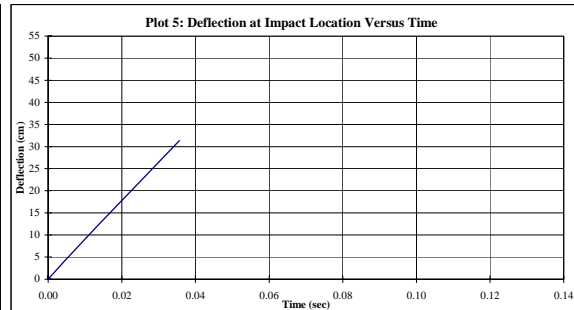
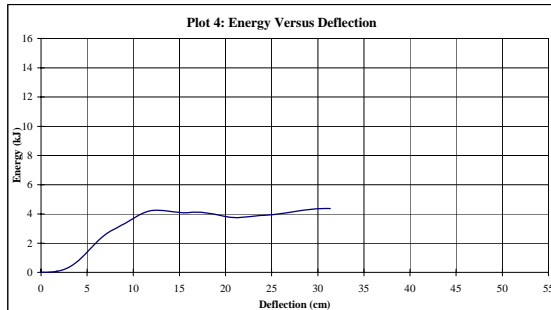
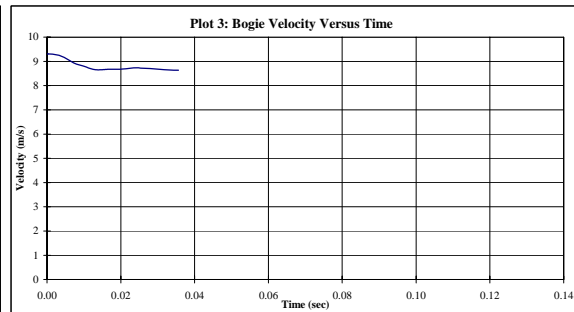
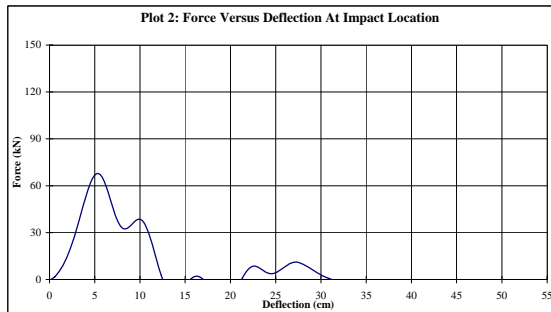
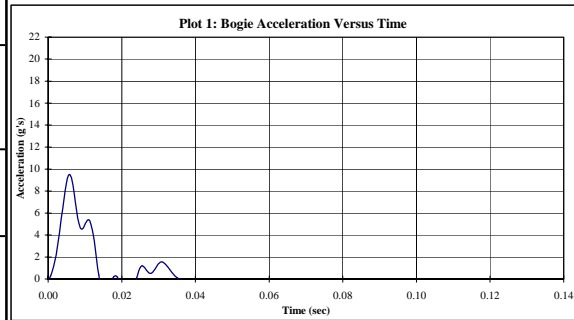


Figure B-24. Results of Test No. PP-9

Midwest Roadside Safety Facility

Bogie Test Summary			
Test Information		CL Bogie MGS Height	
Test Number:		PP-10	
Test Date:		15-Nov-2004	
Failure Type:		0	
Post Properties			
Post Type:		Ponderosa Pine - Round Wooden	
Post Size:		224.0 mm Dia. metric	8.82 in. Dia.
Post Length:		198.2 cm	(503.4 cm)
Embedment Depth:		101.6 cm	(258.1 cm)
Category:		HRD	
Soil Properties			
Gradation:		NA	
Moisture Content:		NA	
Compaction Method:		NA	
Soil Density, γ_d :		NA kg/m ³	NA
Bogie Properties			
Impact Velocity:		9.0 m/s	(20.2 mph) (29.6 fps)
Impact Location:		63.2 cm	(24.9 in) above groundline
Bogie Mass:		728 kg	(1605 lbf)
Data Acquired			
Accelerometer Data:		EDR-3	
Camera Data:		Side View-DV and Photon	

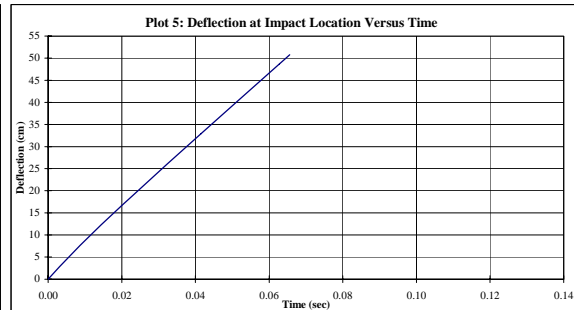
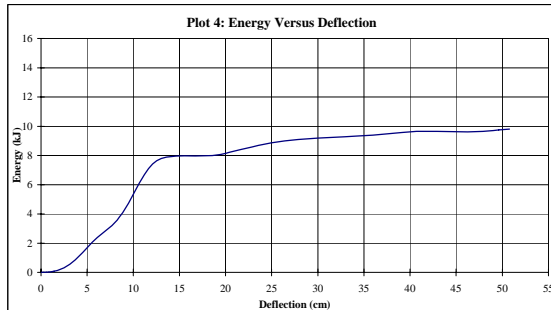
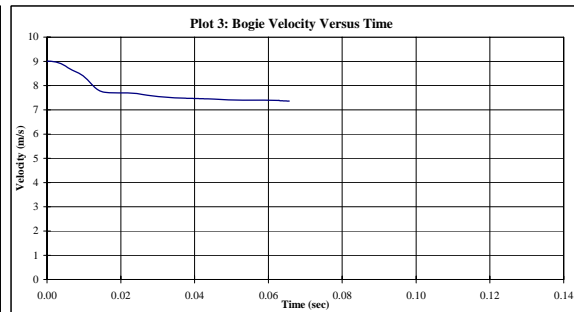
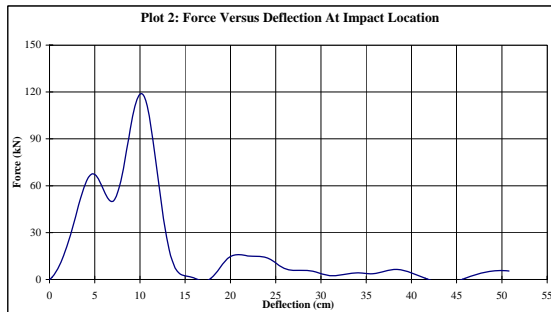
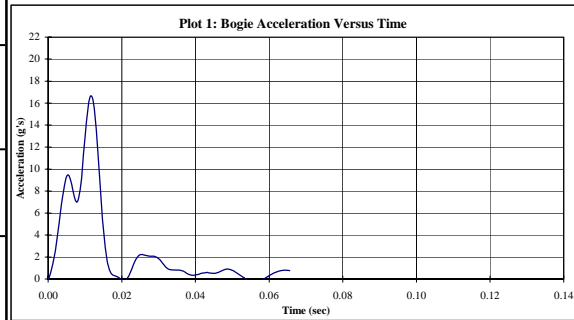


Figure B-25. Results of Test No. PP-10

Midwest Roadside Safety Facility

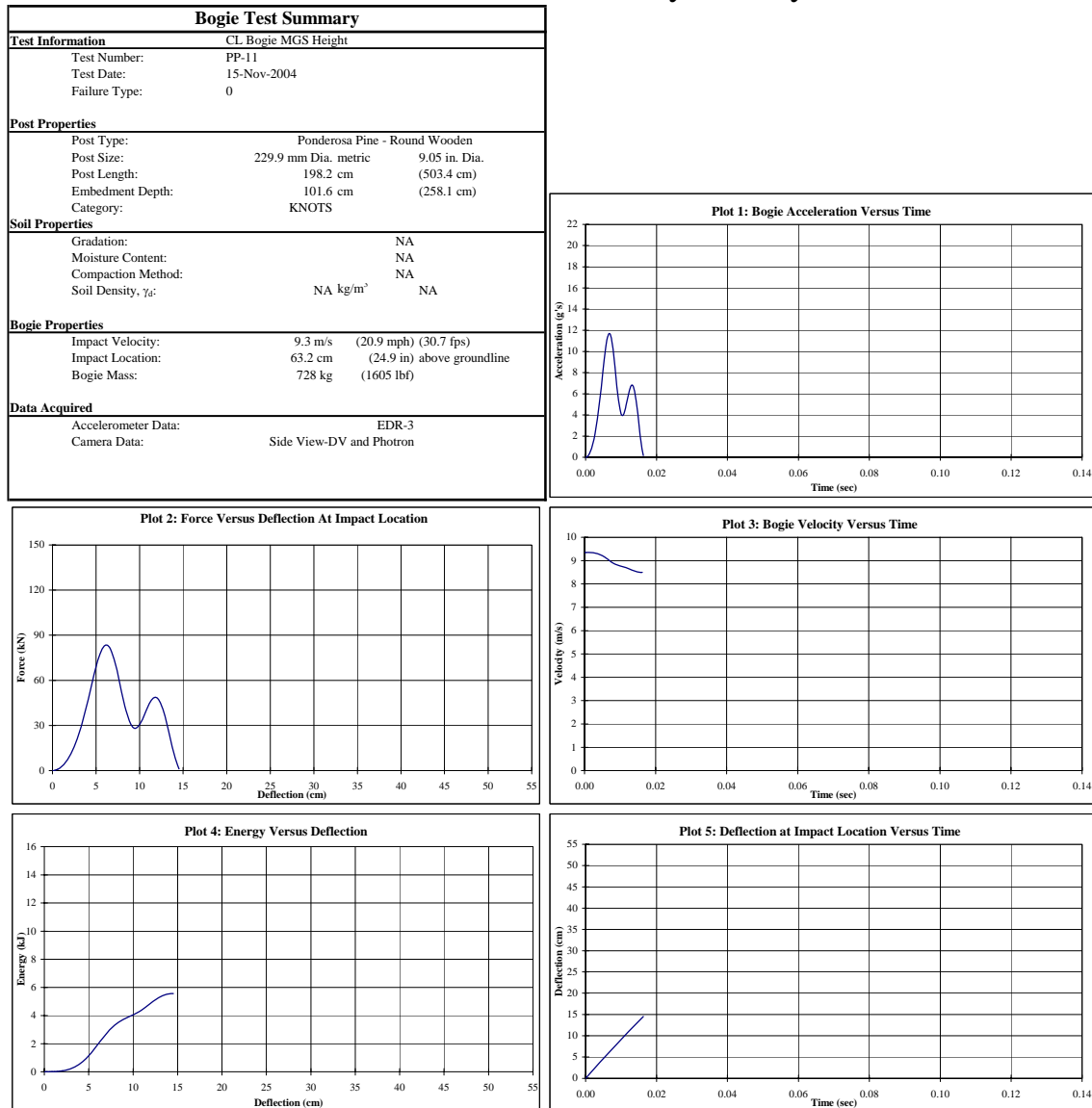


Figure B-26. Results of Test No. PP-11

Midwest Roadside Safety Facility

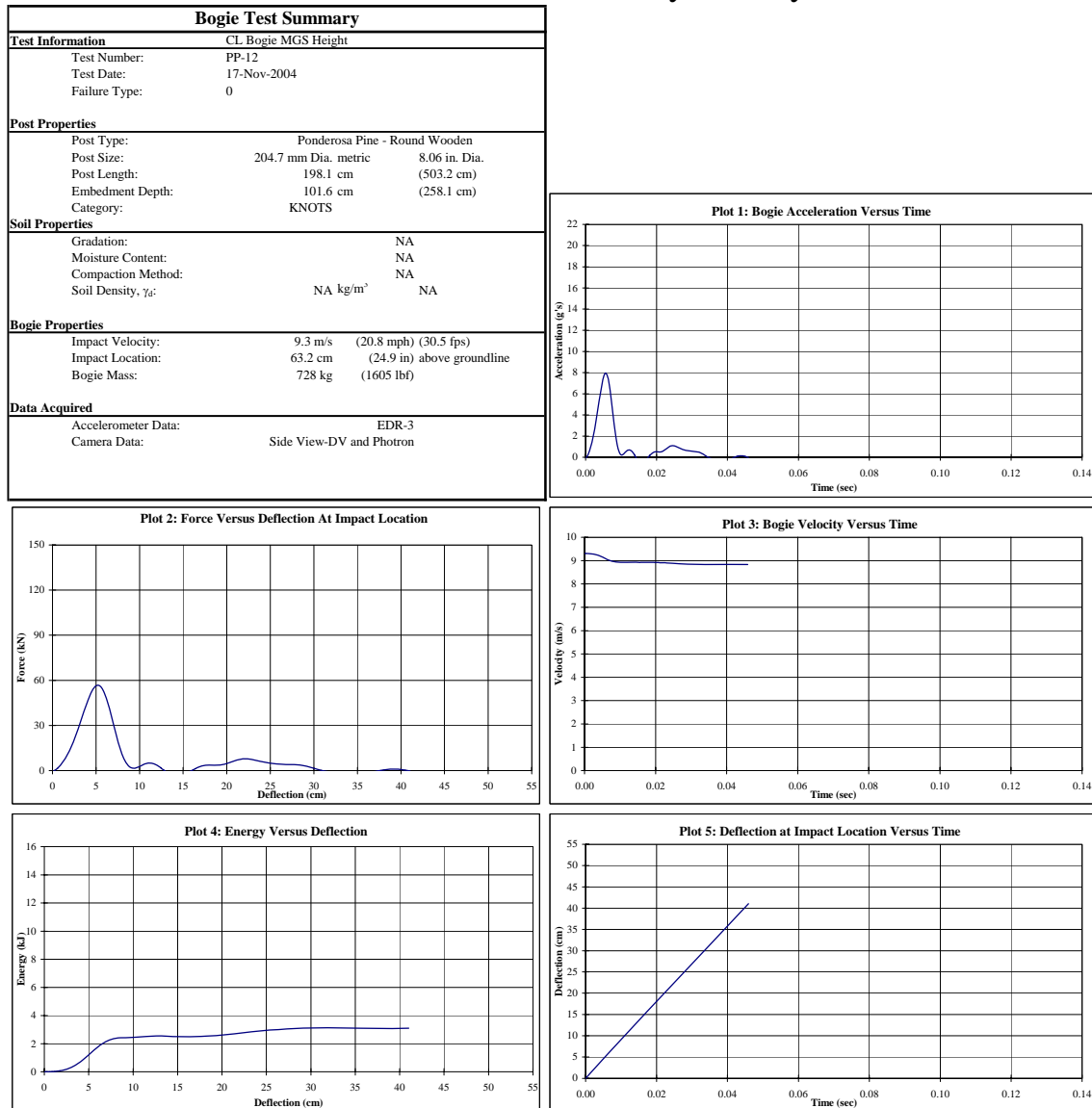


Figure B-27. Results of Test No. PP-12

Midwest Roadside Safety Facility

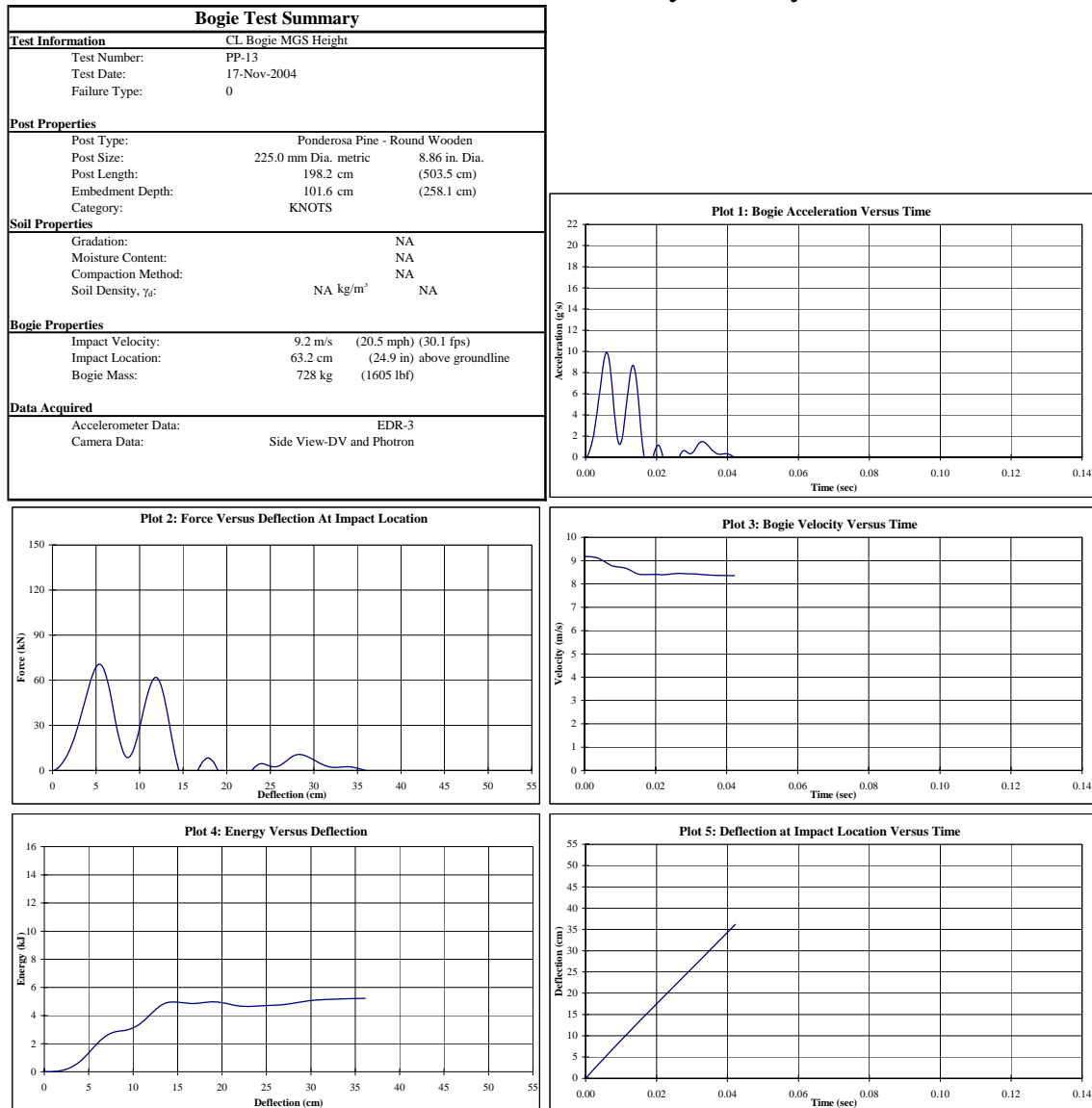


Figure B-28. Results of Test No. PP-13

Midwest Roadside Safety Facility

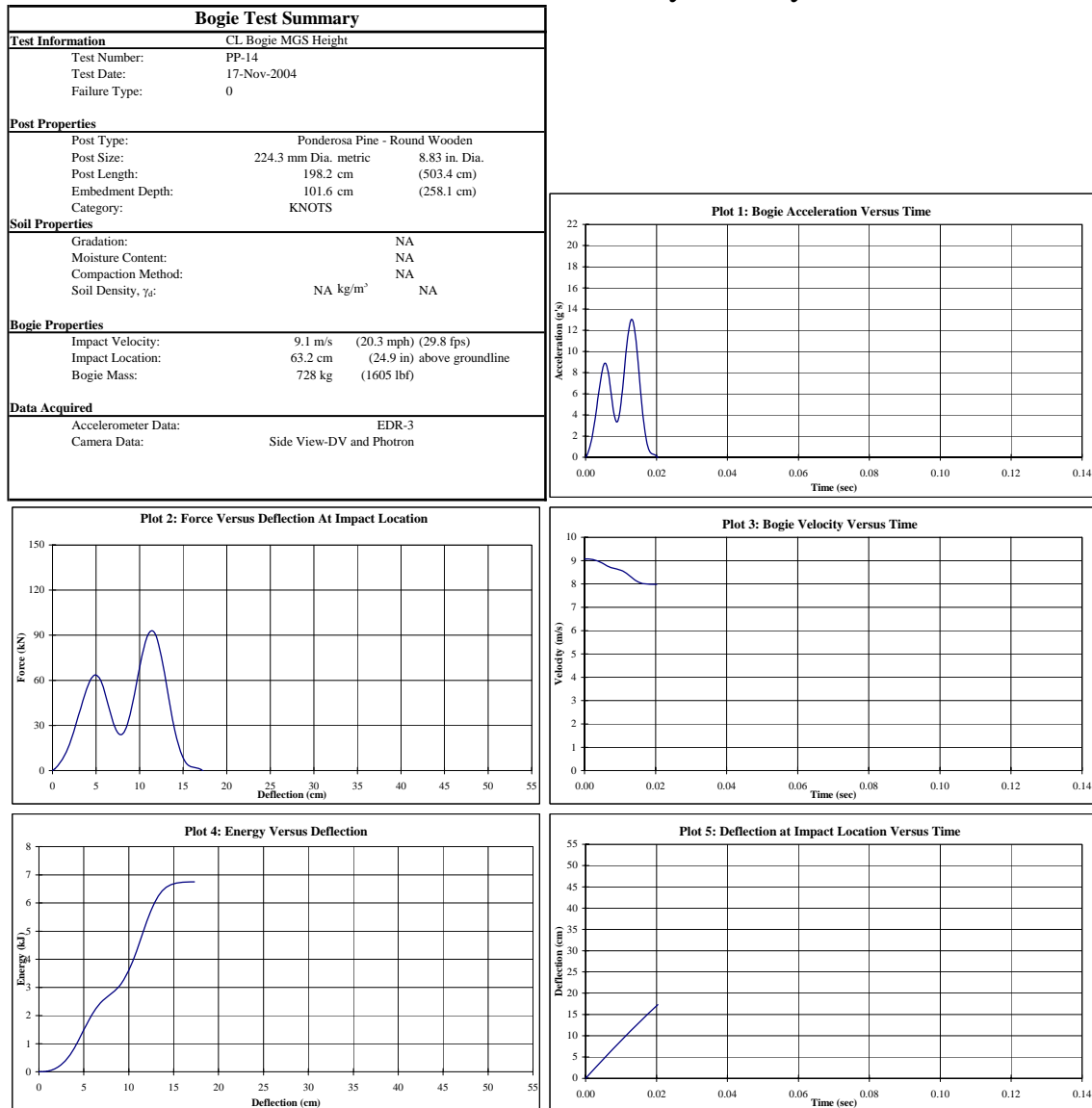


Figure B-29. Results of Test No. PP-14

Midwest Roadside Safety Facility

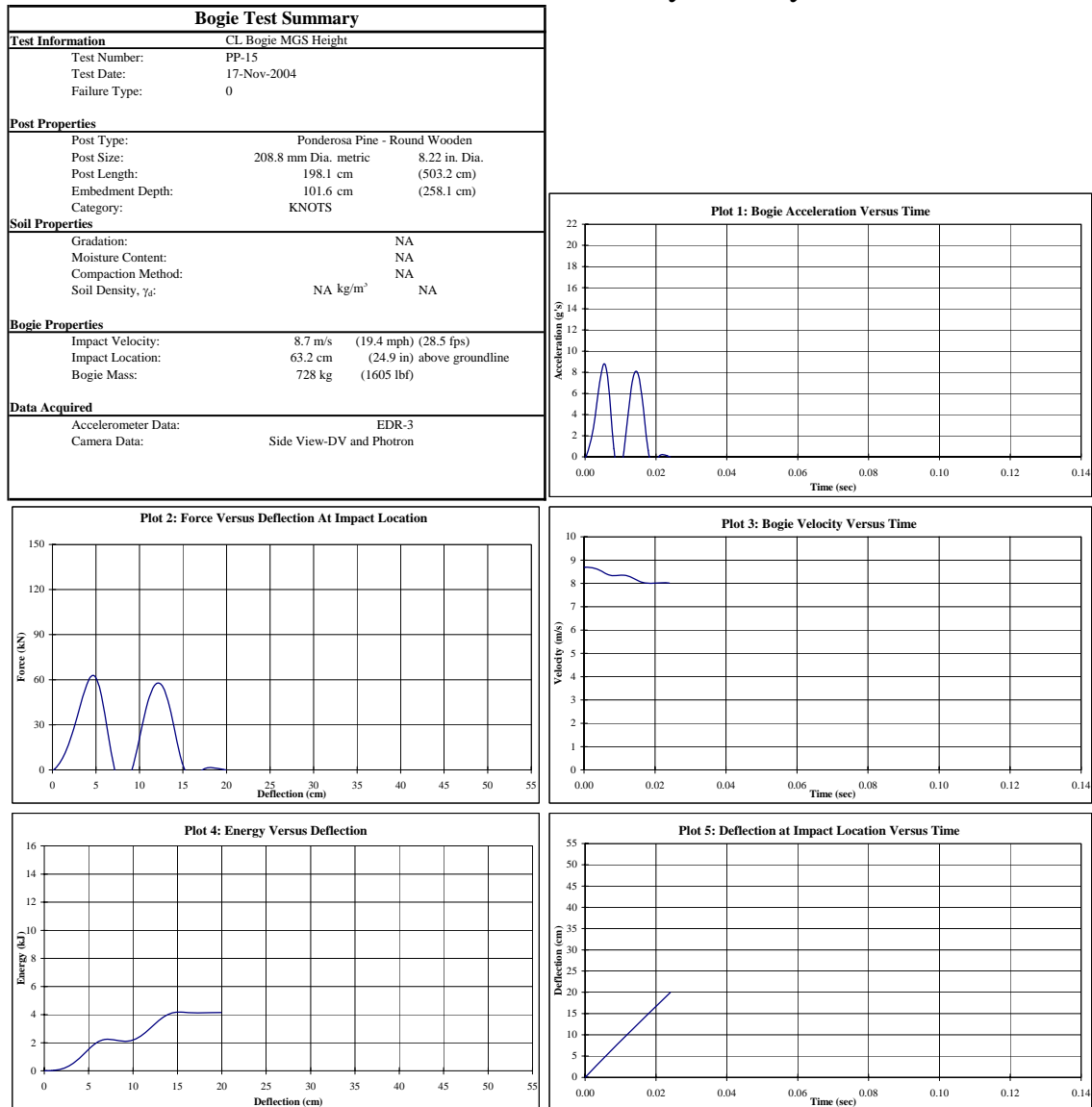


Figure B-30. Results of Test No. PP-15

Midwest Roadside Safety Facility

Bogie Test Summary		
Test Information		
Test Number:	CL Bogie MGS Height	
Test Date:	SY-1	
Failure Type:	17-Nov-2004	
	0	
Post Properties		
Post Type:	Southern Yellow Pine - Round Wooden	
Post Size:	186.7 mm Dia. metric	7.44 in. Dia.
Post Length:	196.0 cm	(497.7 cm)
Embedment Depth:	101.6 cm	(258.1 cm)
Category:	KNOTS	
Soil Properties		
Gradation:	NA	
Moisture Content:	NA	
Compaction Method:	NA	
Soil Density, γ_d :	NA kg/m ³	NA
Bogie Properties		
Impact Velocity:	8.4 m/s	(18.9 mph) (27.7 fps)
Impact Location:	63.2 cm	(24.9 in) above groundline
Bogie Mass:	728 kg	(1605 lbf)
Data Acquired		
Accelerometer Data:	EDR-3	
Camera Data:	Side View-DV and Photon	

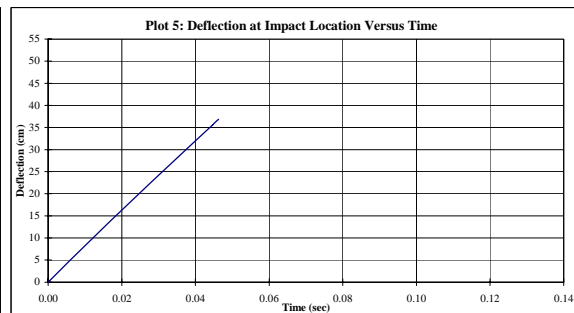
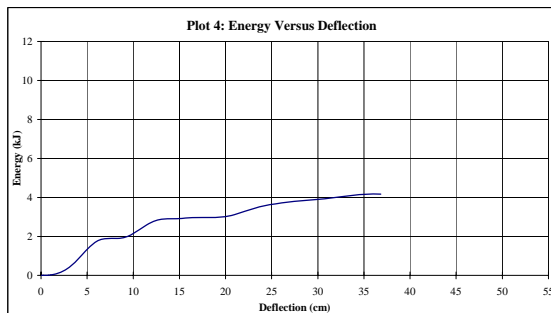
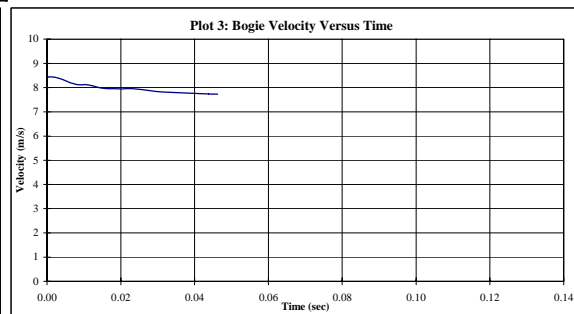
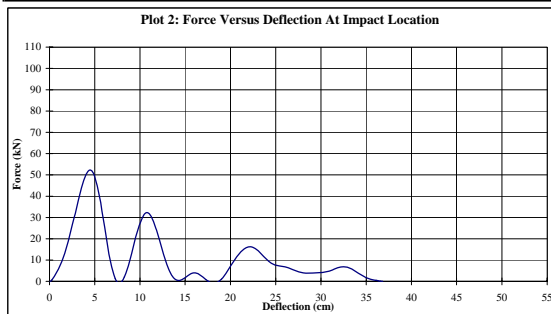
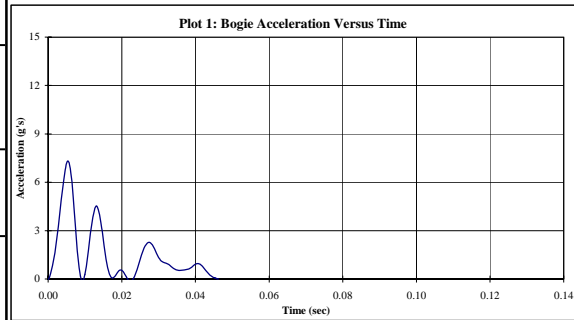


Figure B-31. Results of Test No. SY-1

Midwest Roadside Safety Facility

Bogie Test Summary		
Test Information		
Test Number:	CL Bogie MGS Height	
Test Date:	SY-2	
Failure Type:	17-Nov-2004	
	0	
Post Properties		
Post Type:	Southern Yellow Pine - Round Wooden	
Post Size:	186.7 mm Dia. metric	7.10 in. Dia.
Post Length:	196.2 cm	(498.4 cm)
Embedment Depth:	101.6 cm	(258.1 cm)
Category:	KNOTS	
Soil Properties		
Gradation:	NA	
Moisture Content:	NA	
Compaction Method:	NA	
Soil Density, γ_d :	NA kg/m ³	NA
Bogie Properties		
Impact Velocity:	9.2 m/s	(20.5 mph) (30.1 fps)
Impact Location:	63.2 cm	(24.9 in) above groundline
Bogie Mass:	728 kg	(1605 lbf)
Data Acquired		
Accelerometer Data:	EDR-3	
Camera Data:	Side View-DV and Photon	

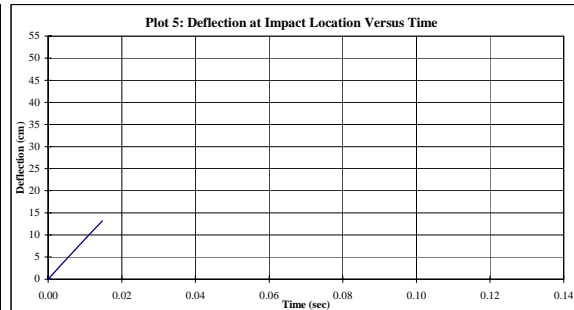
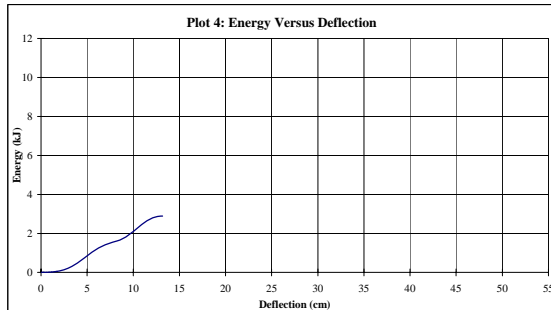
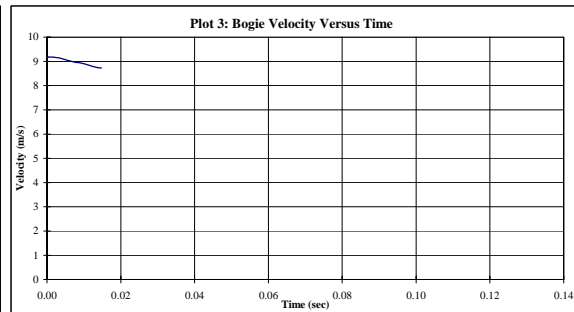
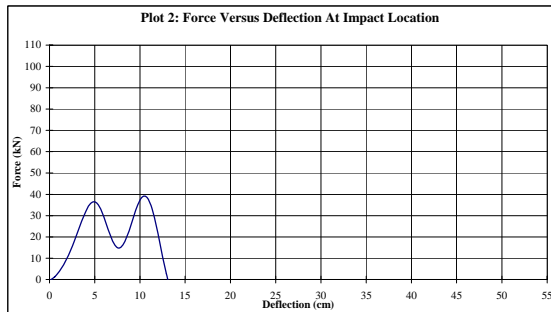
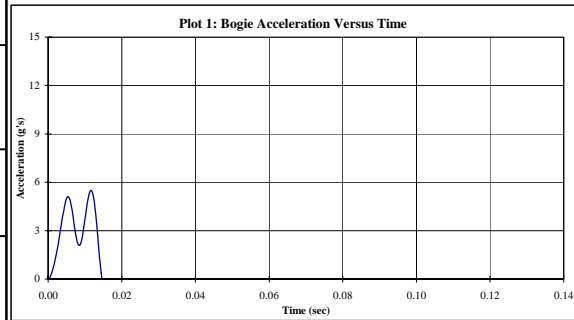


Figure B-32. Results of Test No. SY-2

Midwest Roadside Safety Facility

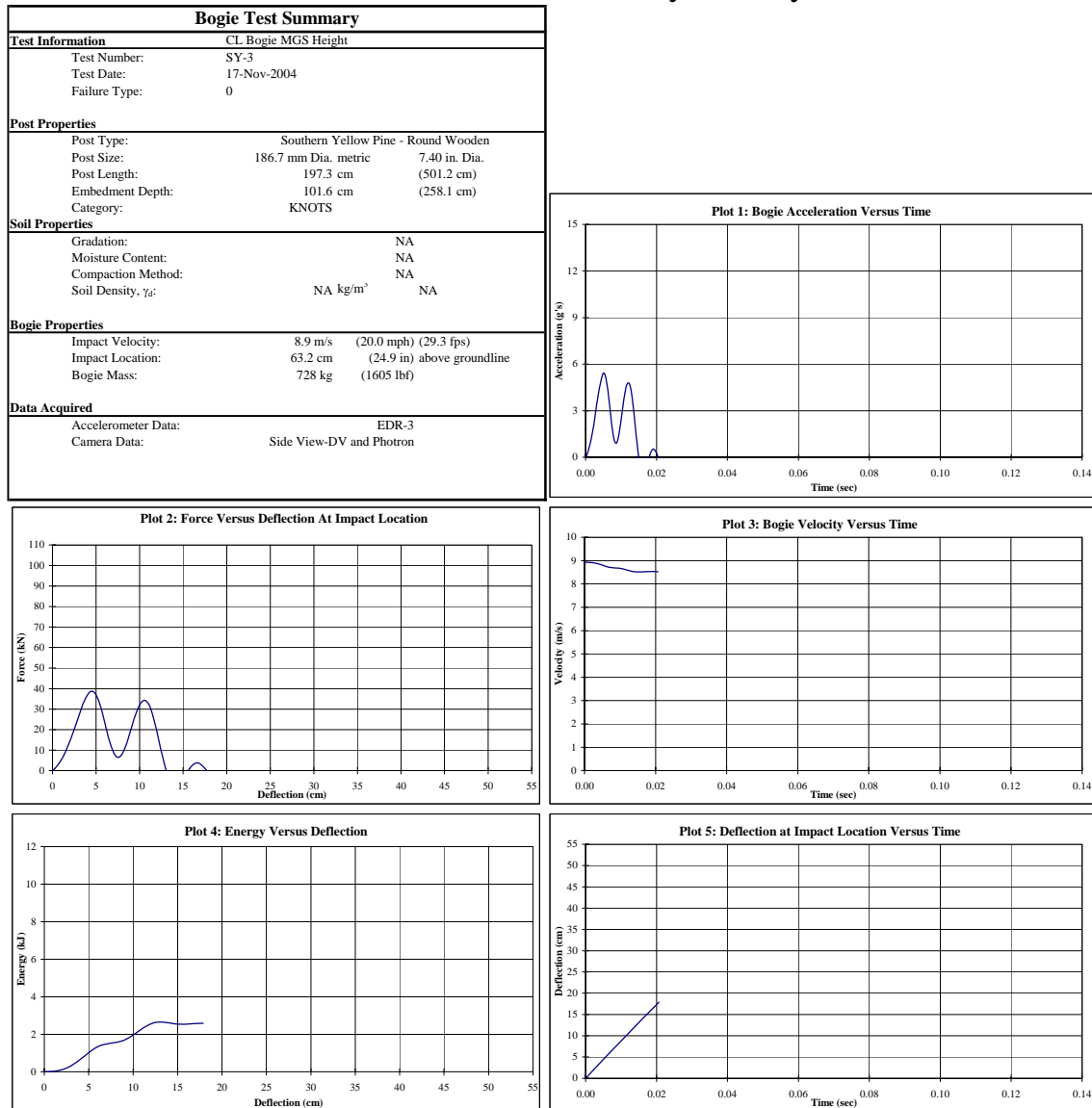


Figure B-33. Results of Test No. SY-3

Midwest Roadside Safety Facility

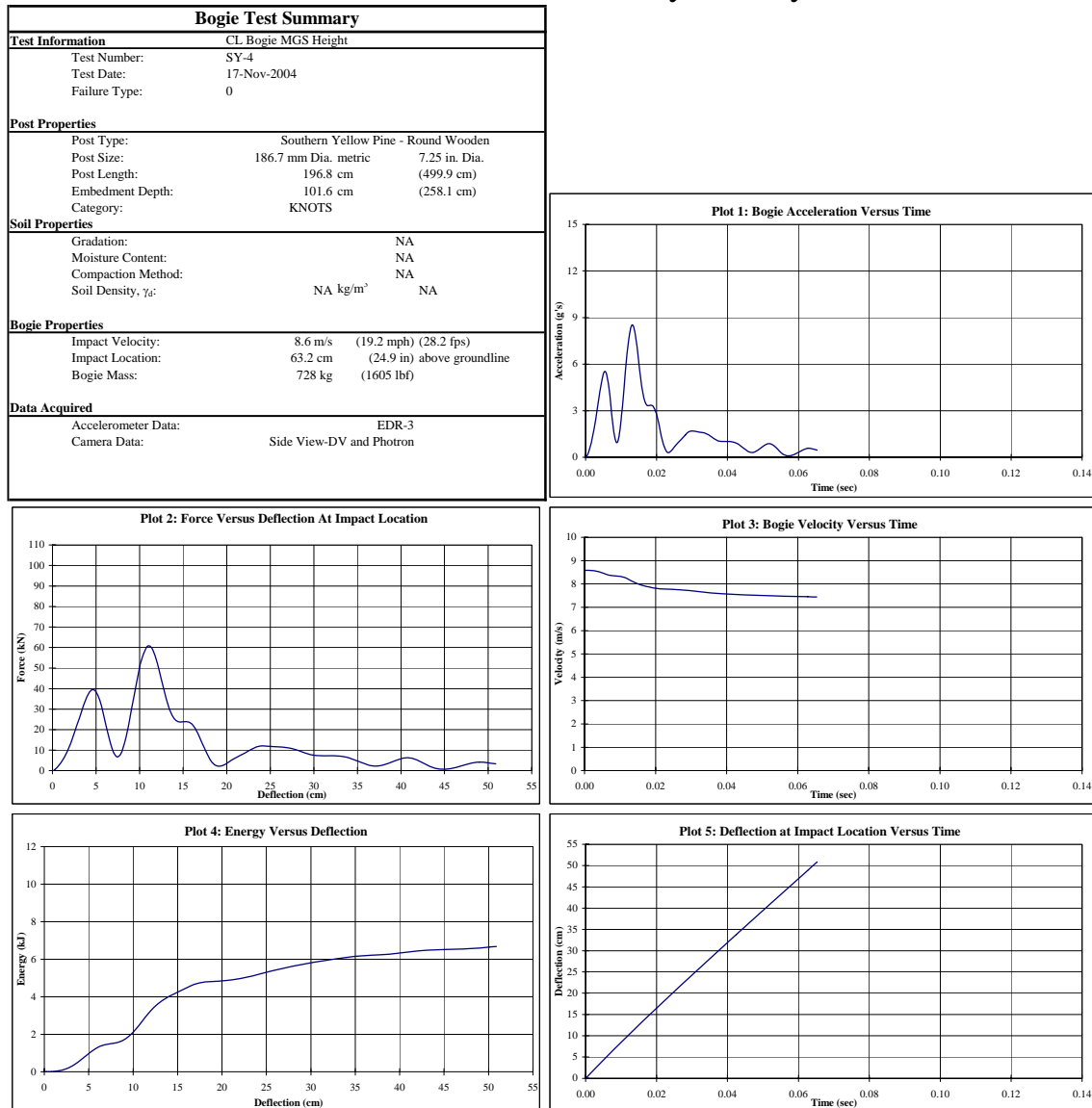


Figure B-34. Results of Test No. SY-4

Midwest Roadside Safety Facility

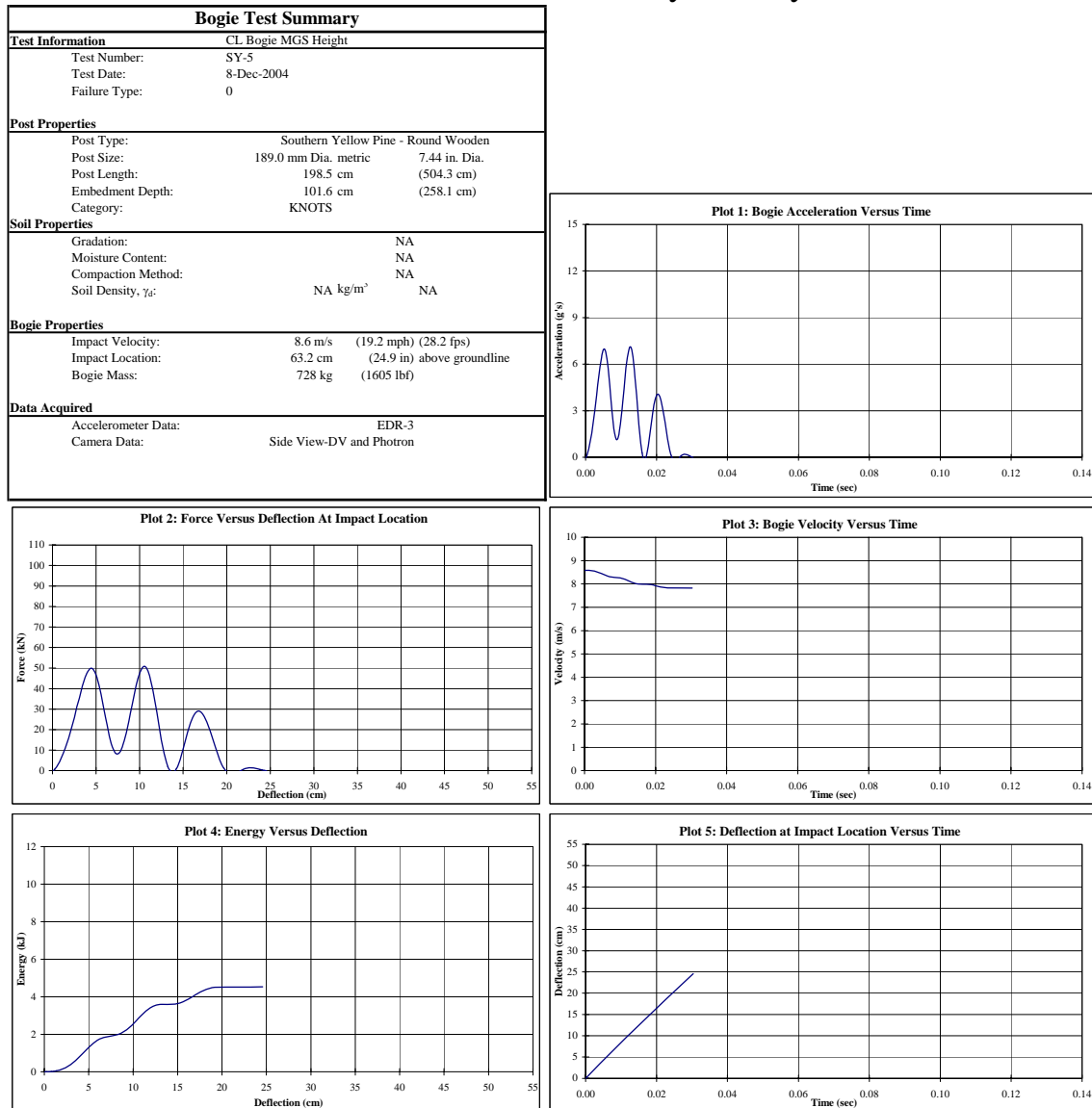


Figure B-35. Results of Test No. SY-5

Midwest Roadside Safety Facility

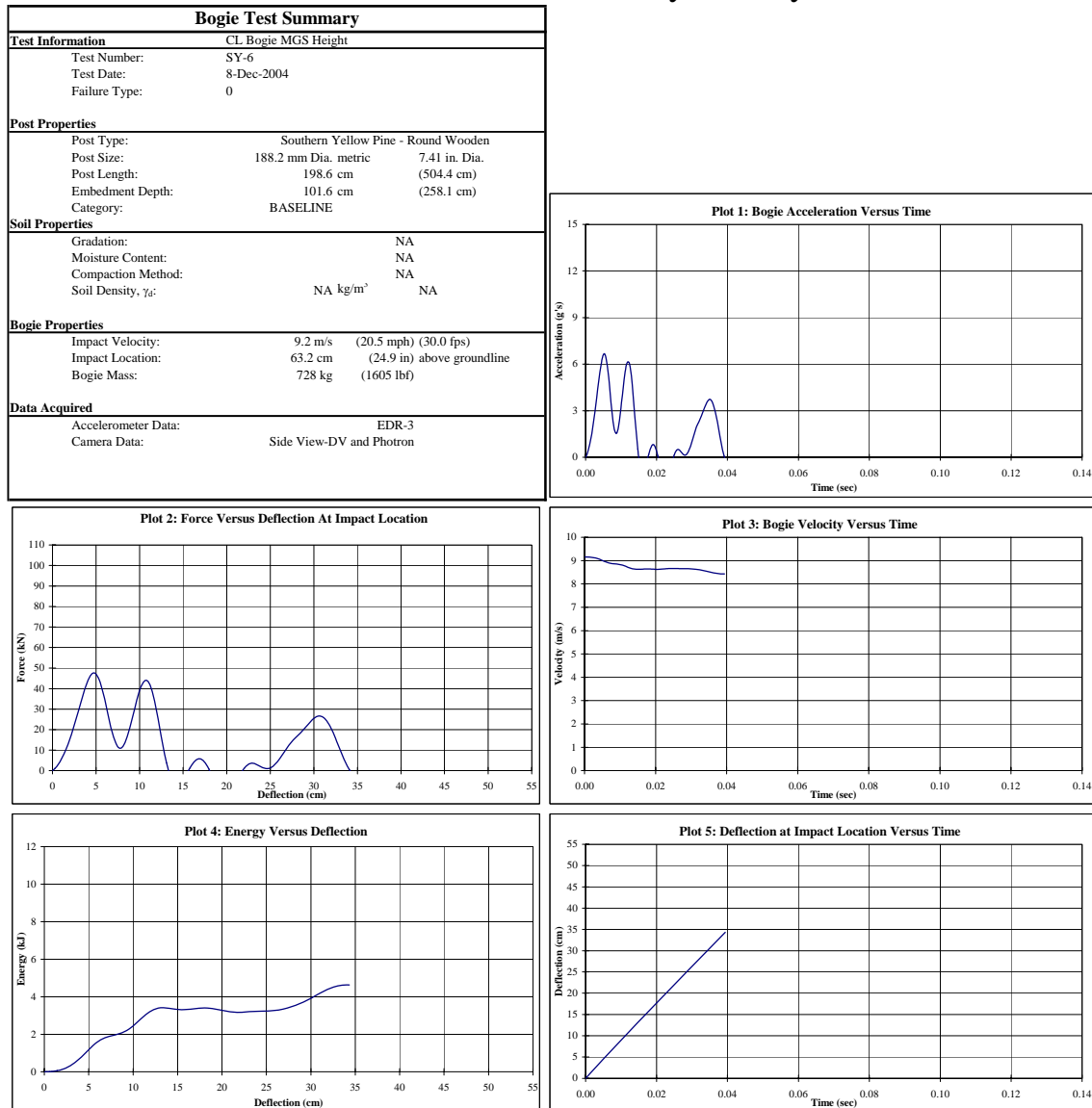


Figure B-36. Results of Test No. SY-6

Midwest Roadside Safety Facility

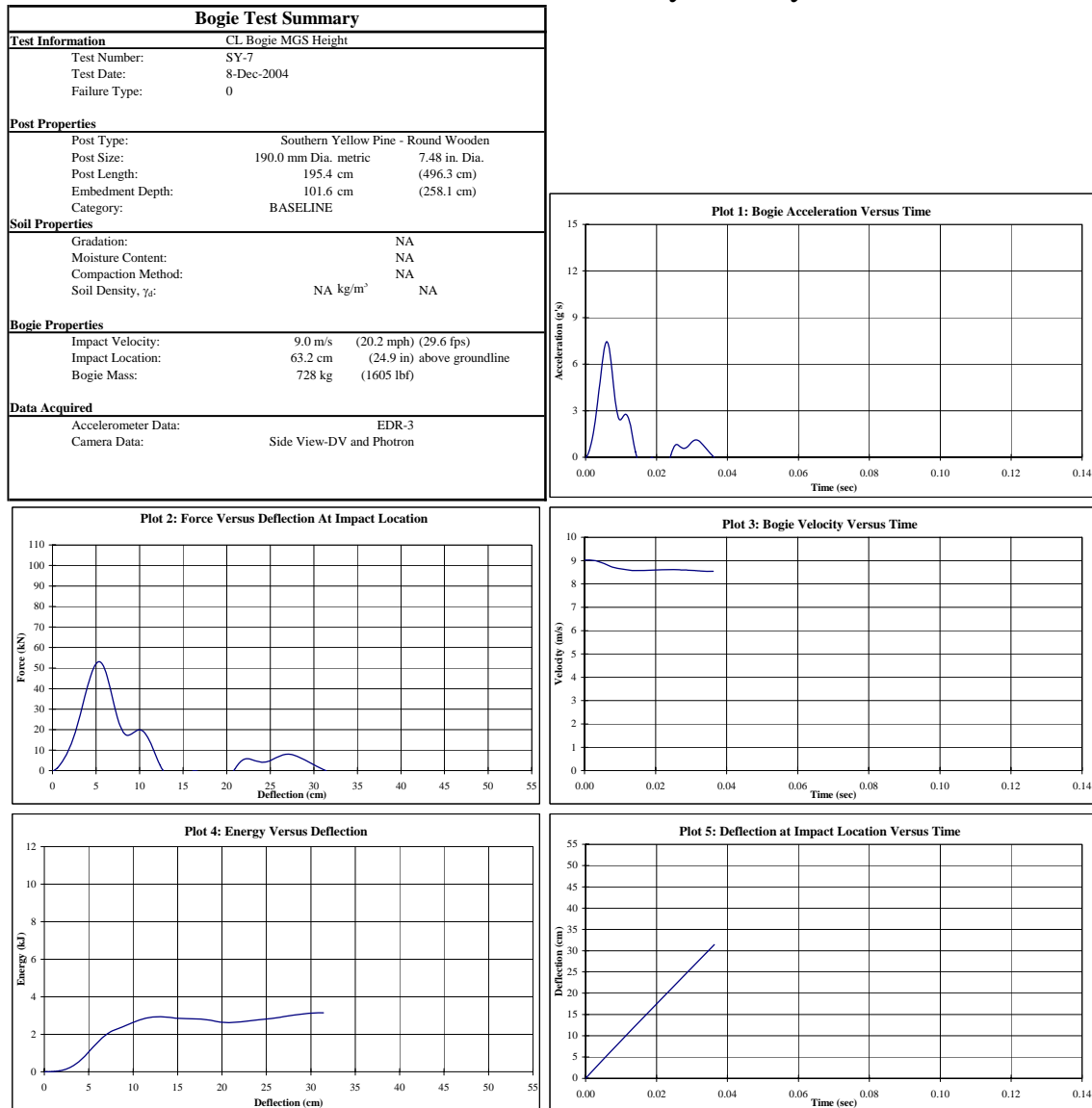


Figure B-37. Results of Test No. SY-7

Midwest Roadside Safety Facility

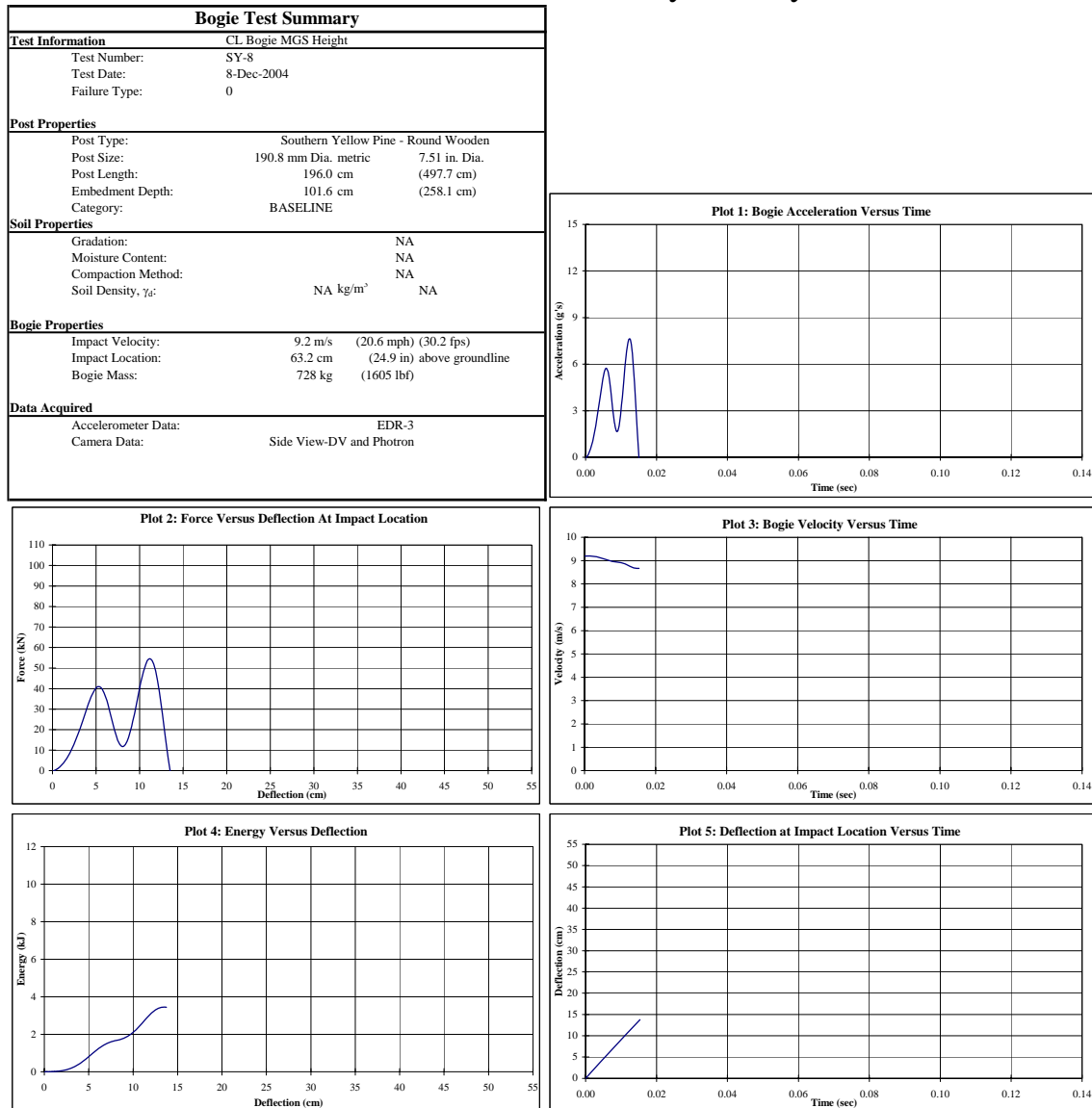


Figure B-38. Results of Test No. SY-8

Midwest Roadside Safety Facility

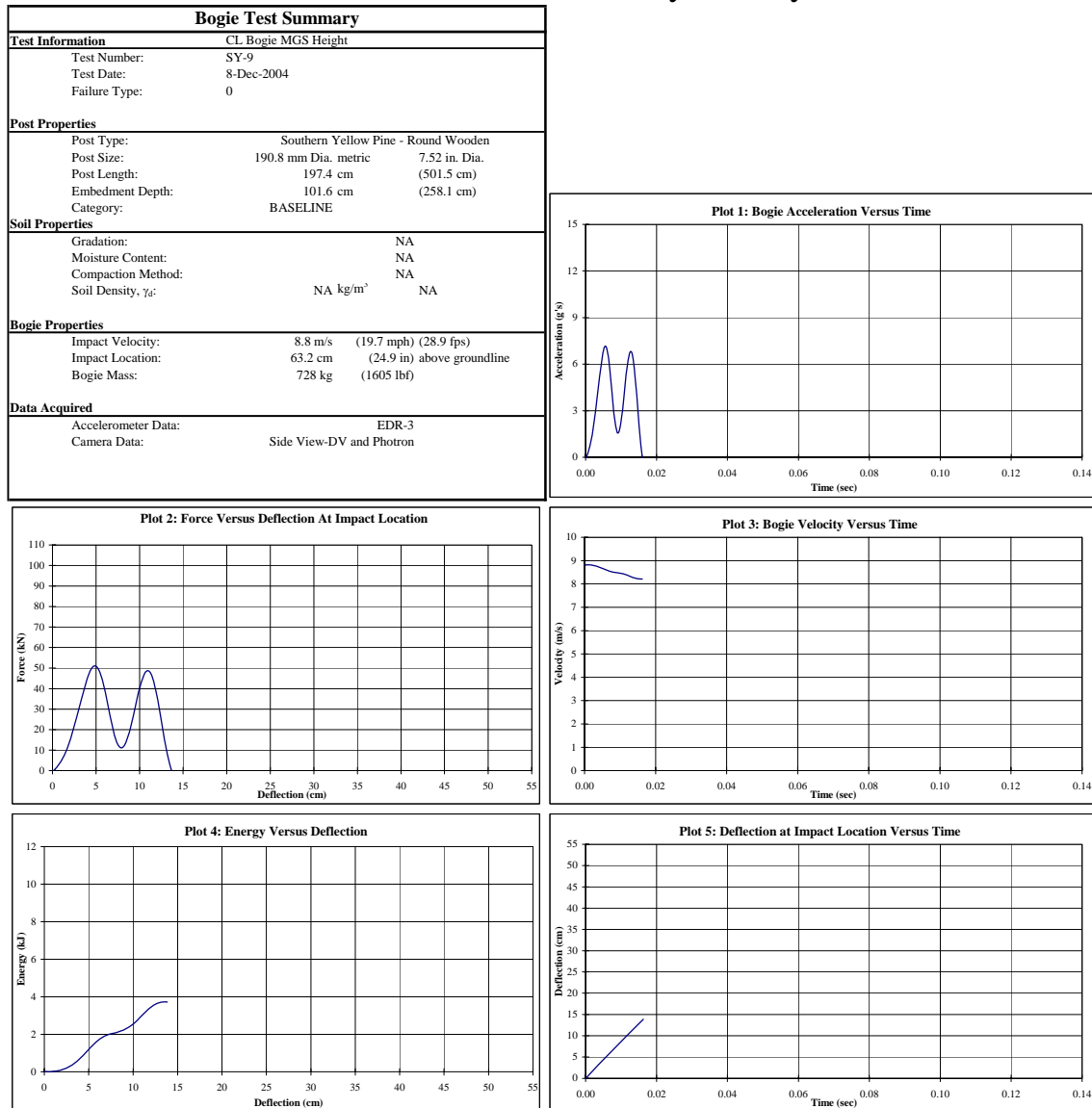


Figure B-39. Results of Test No. SY-9

Midwest Roadside Safety Facility

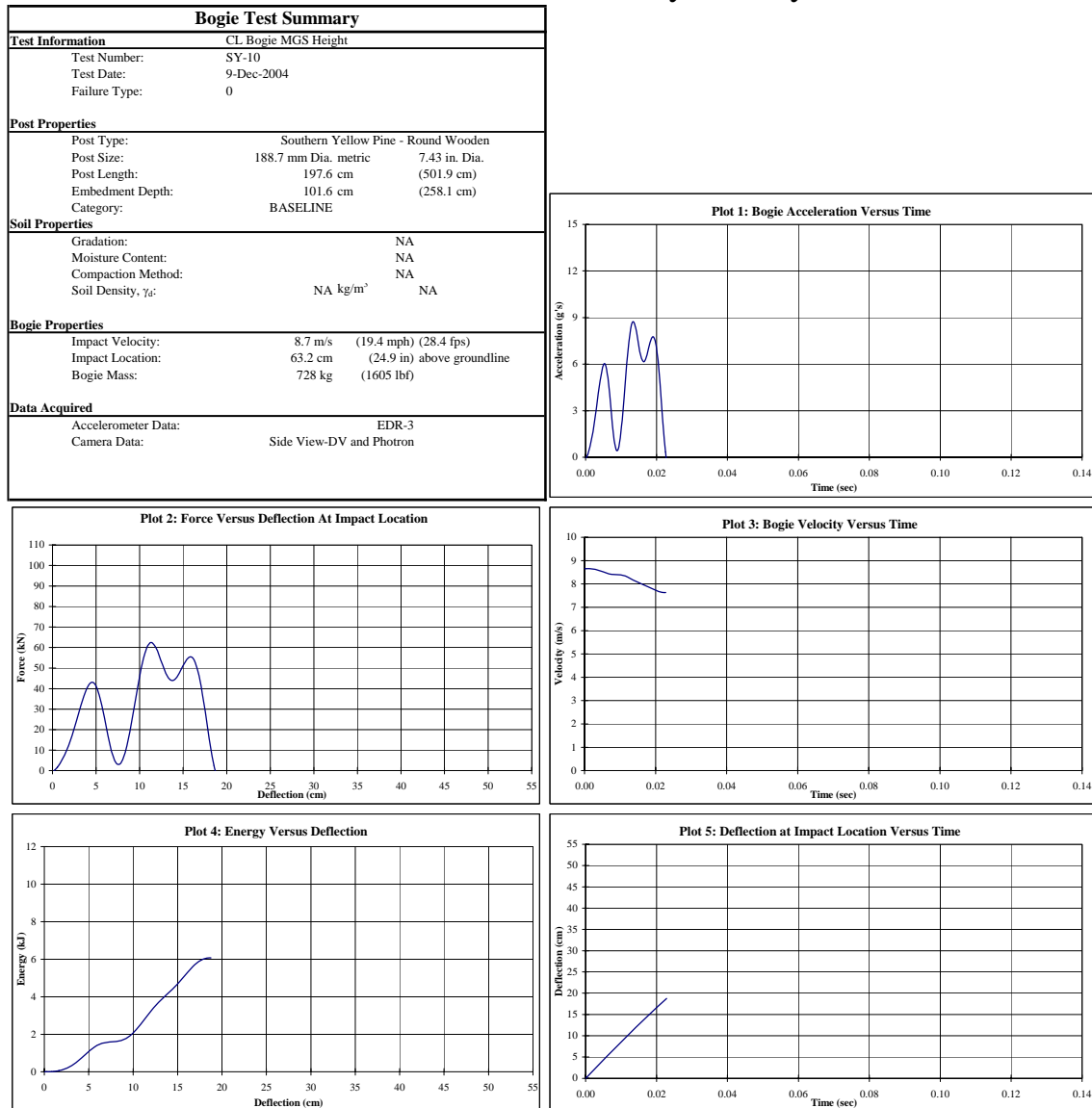


Figure B-40. Results of Test No. SY-10

Midwest Roadside Safety Facility

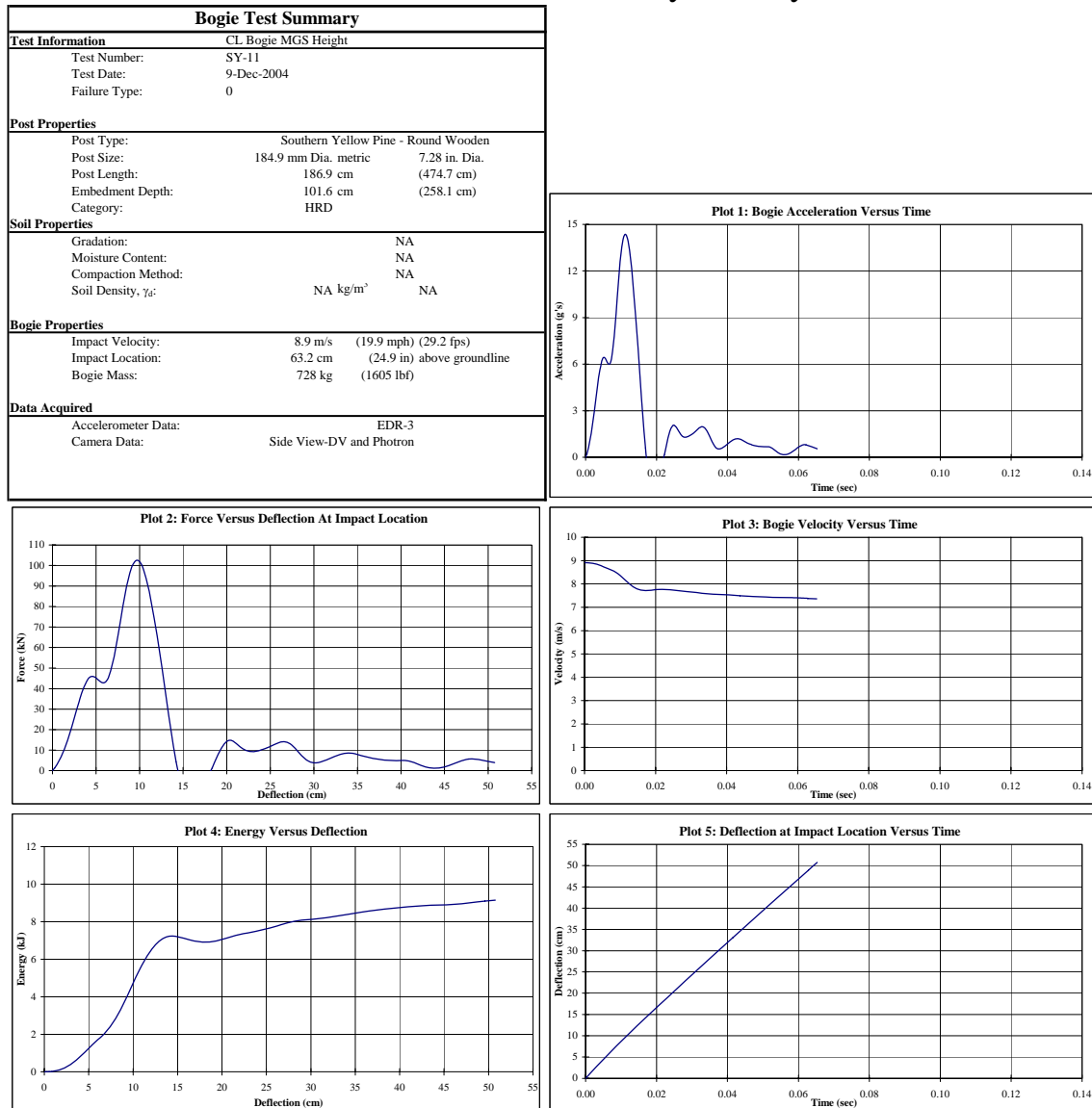


Figure B-41. Results of Test No. SY-11

Midwest Roadside Safety Facility

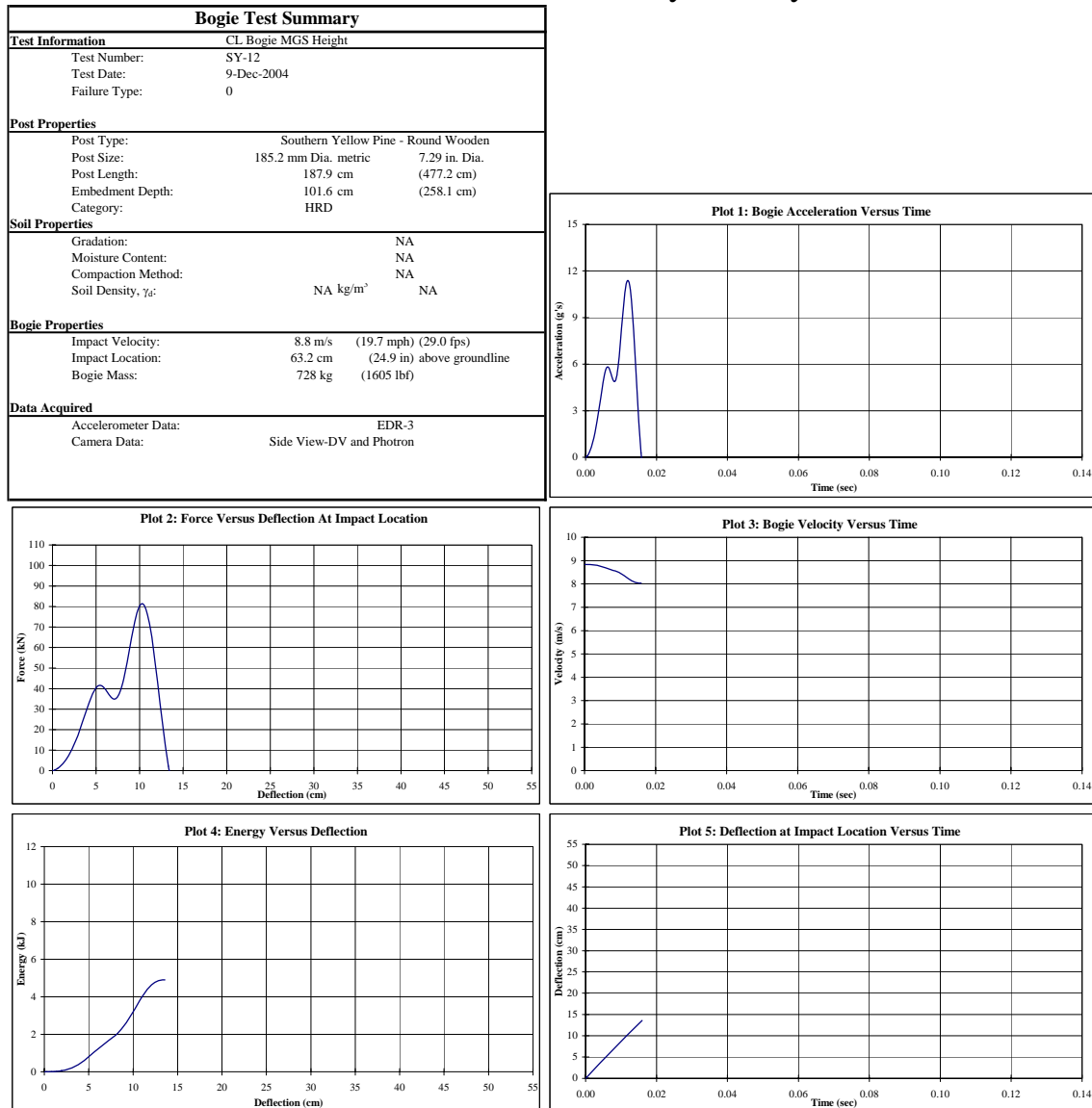


Figure B-42. Results of Test No. SY-12

Midwest Roadside Safety Facility

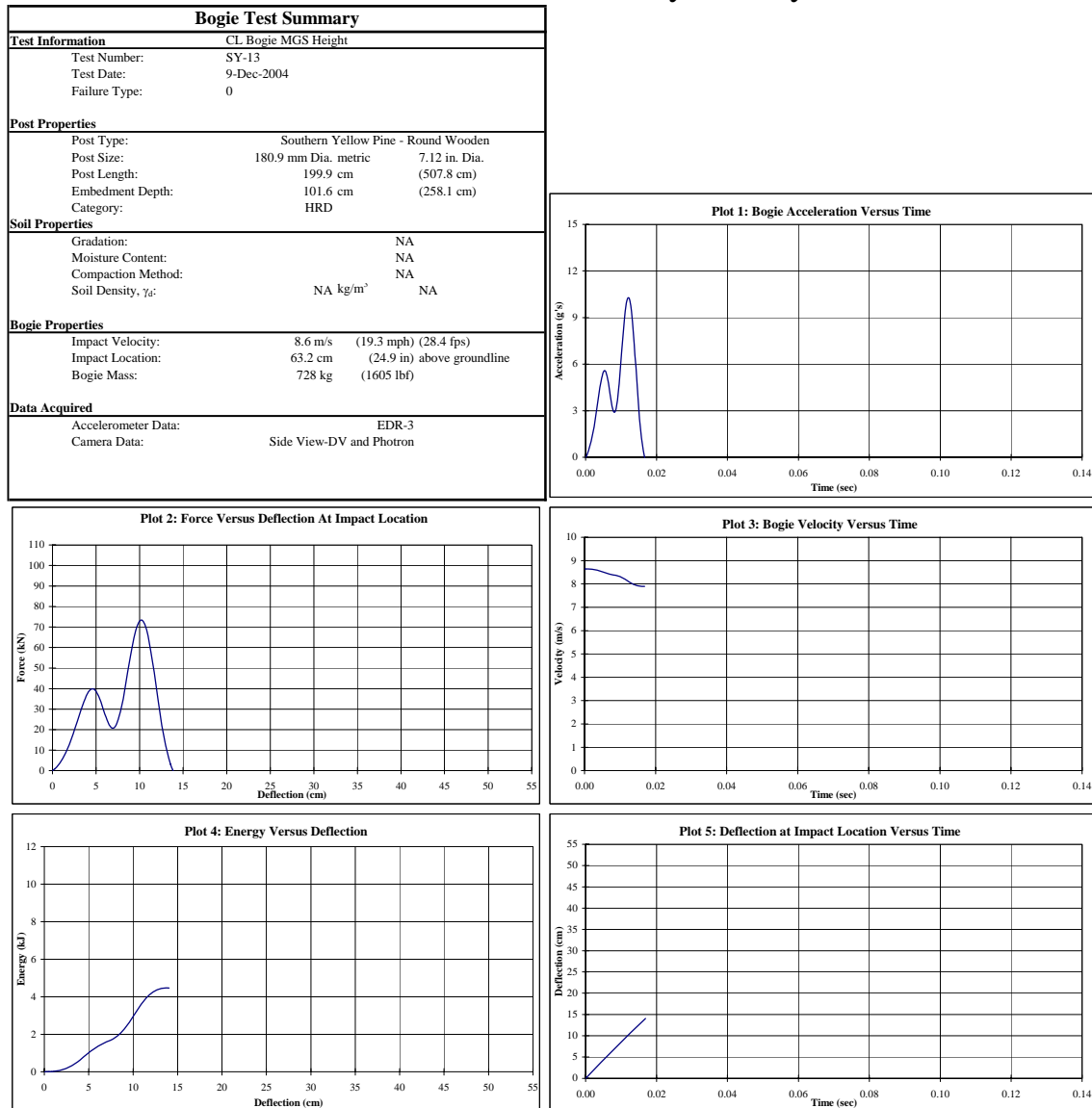


Figure B-43. Results of Test No. SY-13

Midwest Roadside Safety Facility

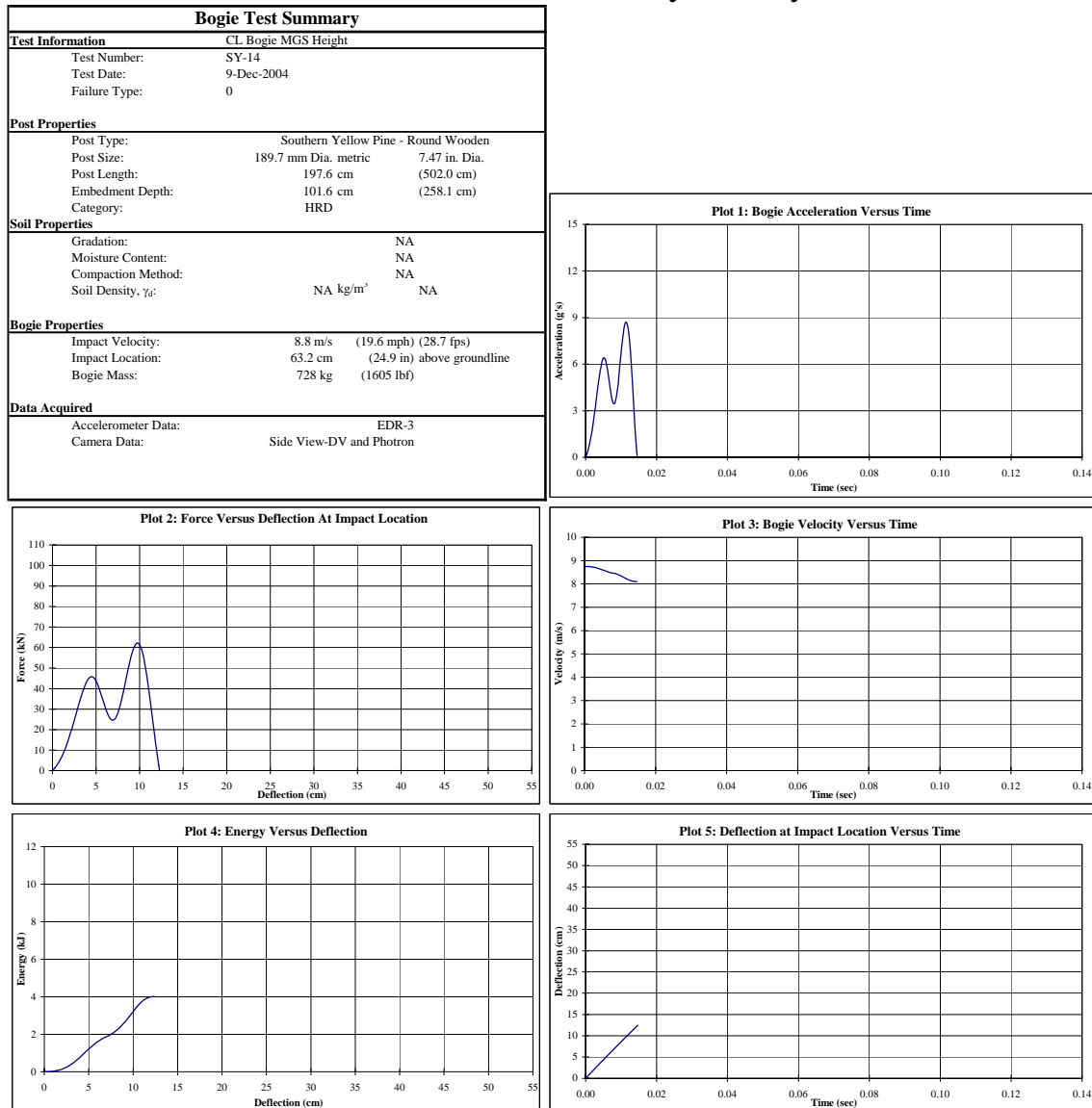


Figure B-44. Results of Test No. SY-14

Midwest Roadside Safety Facility

Bogie Test Summary	
Test Information	
Test Number:	SY-15
Test Date:	9-Dec-2004
Failure Type:	0
Post Properties	
Post Type:	Southern Yellow Pine - Round Wooden
Post Size:	183.6 mm Dia. metric 7.23 in. Dia.
Post Length:	197.3 cm (501.2 cm)
Embedment Depth:	101.6 cm (258.1 cm)
Category:	HRD
Soil Properties	
Gradation:	NA
Moisture Content:	NA
Compaction Method:	NA
Soil Density, γ_d :	NA kg/m ³ NA
Bogie Properties	
Impact Velocity:	8.9 m/s (19.9 mph) (29.2 fps)
Impact Location:	63.2 cm (24.9 in) above groundline
Bogie Mass:	728 kg (1605 lbf)
Data Acquired	
Accelerometer Data:	EDR-3
Camera Data:	Side View-DV and Photon

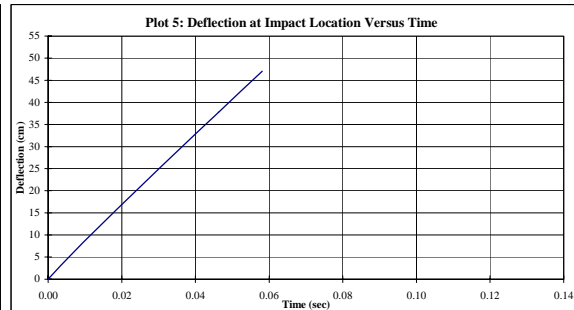
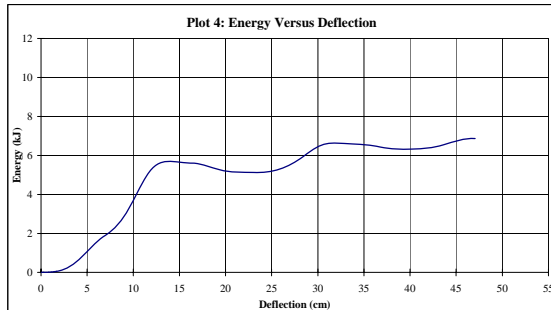
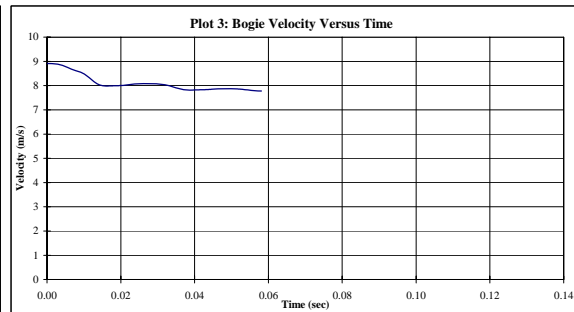
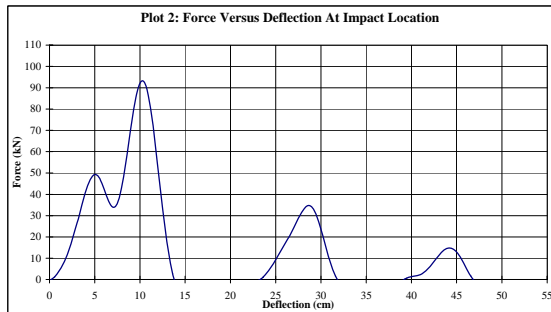
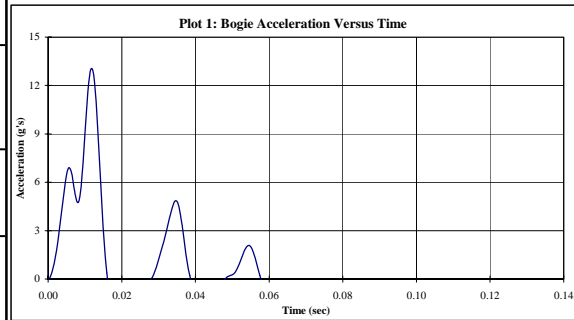
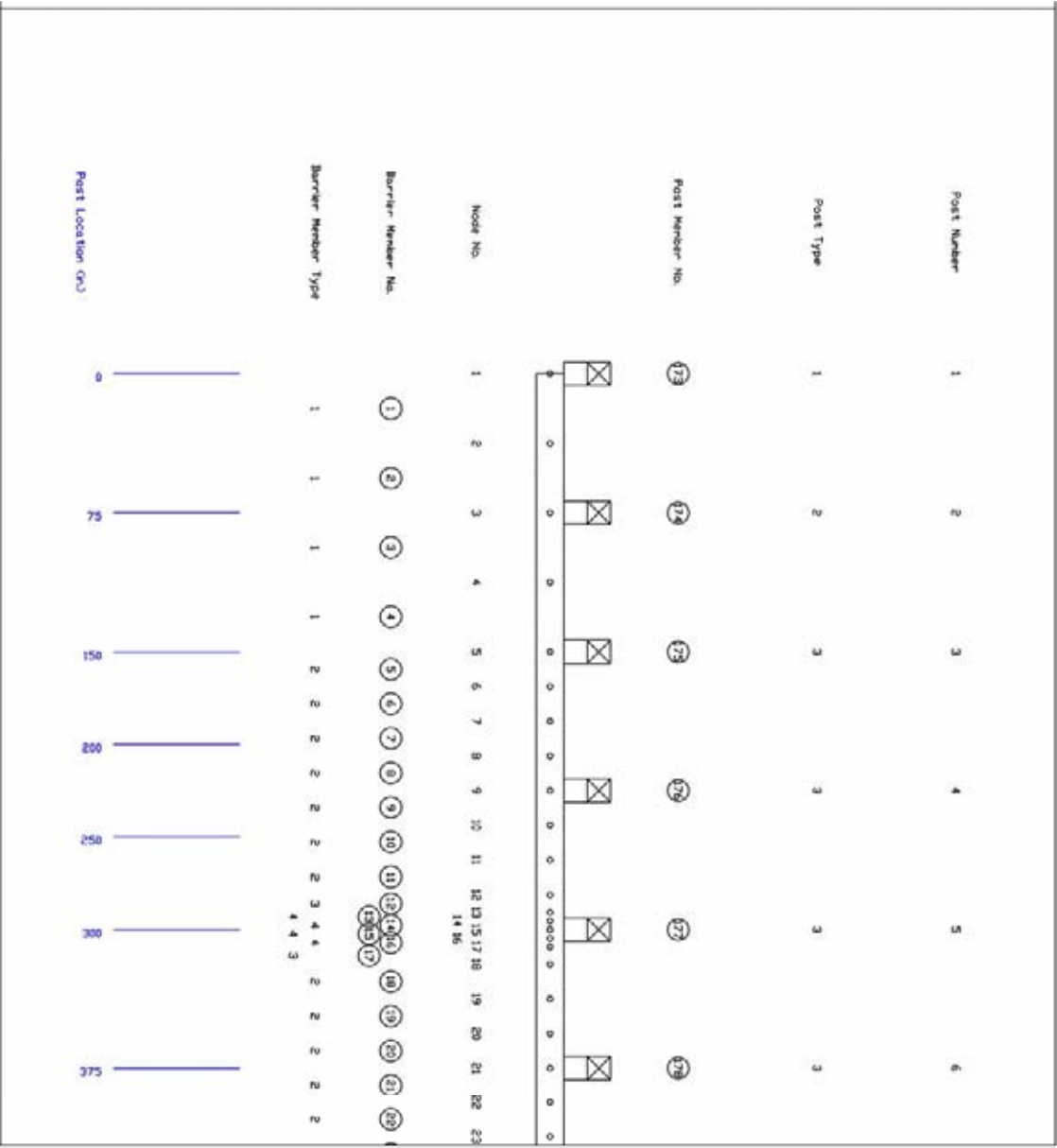


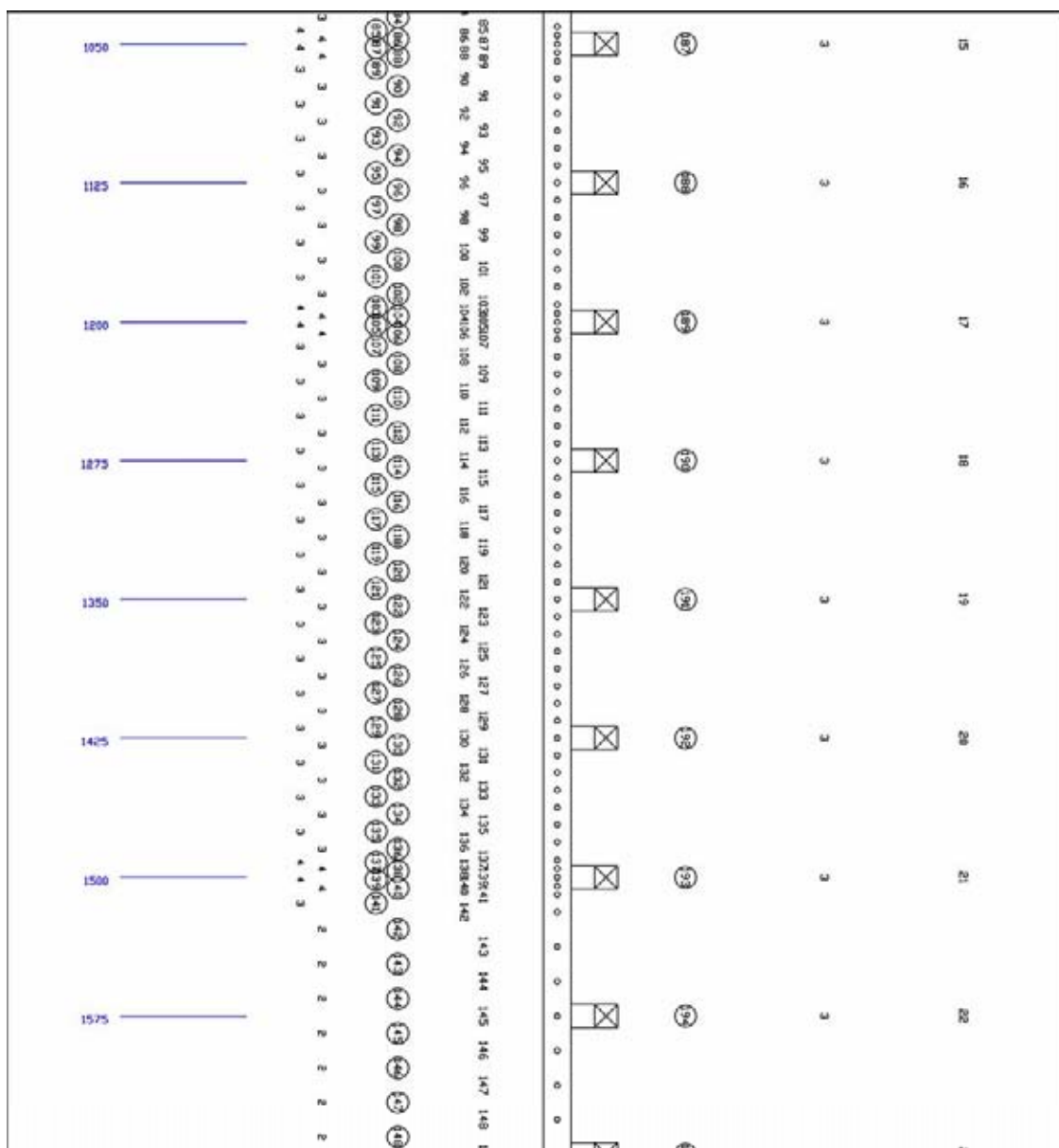
Figure B-45. Results of Test No. SY-15

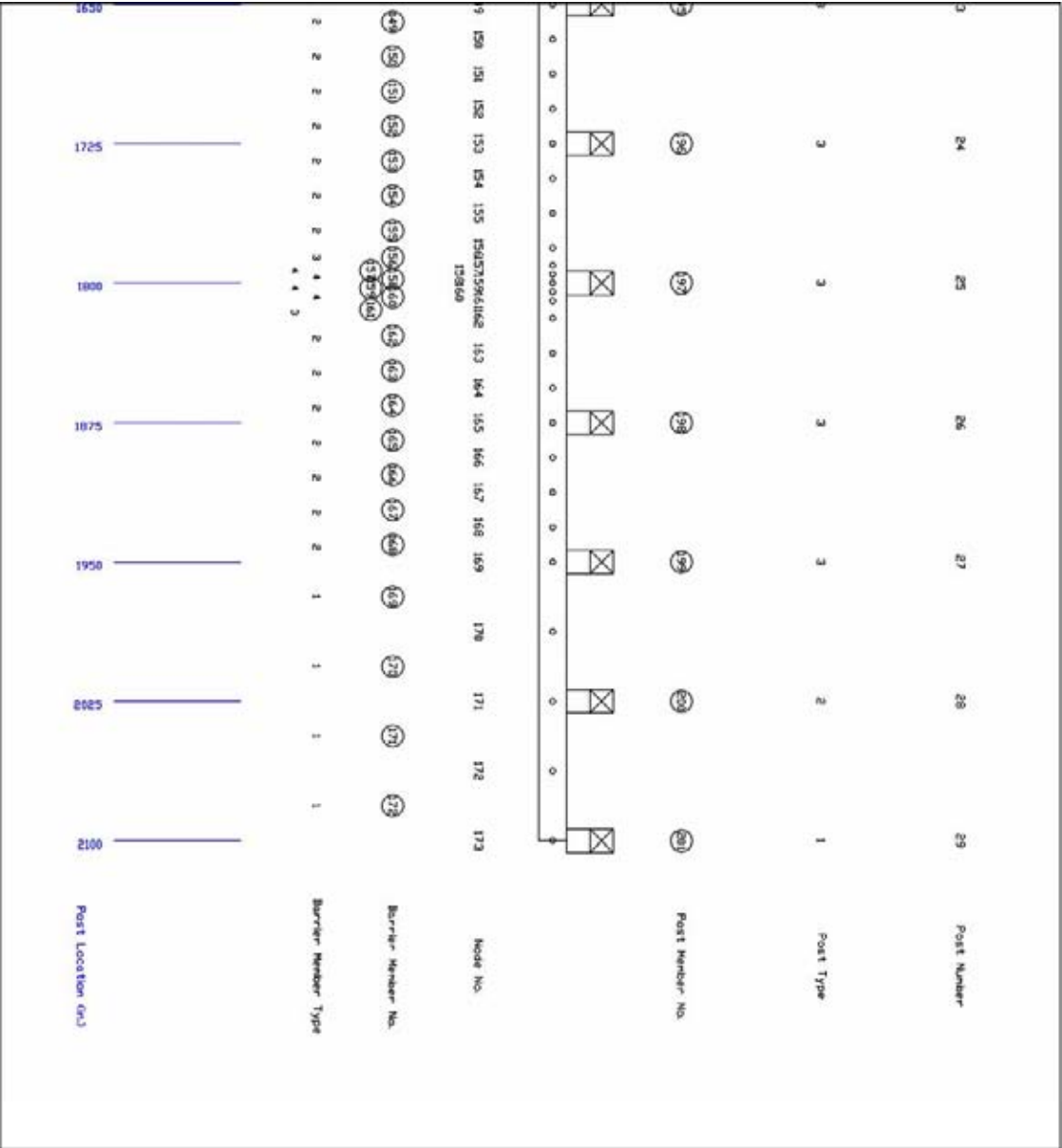
APPENDIX C - Barrier VII Simulation Deck

BARRIER VII – Model Schematic



7	8	9	10	11	12	13	14																											
3	3	3	3	3	3	3	3																											
175	180	185	185	185	184	185	184																											
<input checked="" type="checkbox"/>	<input checked="" type="checkbox"/>	<input checked="" type="checkbox"/>	<input checked="" type="checkbox"/>	<input checked="" type="checkbox"/>	<input checked="" type="checkbox"/>	<input checked="" type="checkbox"/>	<input checked="" type="checkbox"/>																											
0	0	0	0	0	0	0	0																											
24	25	26	27	28	29	30	31	32	33	35	37	39	41	43	45	47	49	51	53	55	57	59	61	63	65	67	69	71	73	75	77	79	81	83
								34	36	38	40	42	44	46	48	50	52	54	56	58	60	62	64	66	68	70	72	74	76	78	80	82	84	
25	26	27	28	29	30	31	32	33	35	37	39	41	43	45	47	49	51	53	55	57	59	61	63	65	67	69	71	73	75	77	79	81	83	
25	26	27	28	29	30	31	32	33	35	37	39	41	43	45	47	49	51	53	55	57	59	61	63	65	67	69	71	73	75	77	79	81	83	
2	2	2	2	2	2	2	2	2	2	2	2	2	2	2	2	2	2	2	2	2	2	2	2	2	2	2	2	2	2	2	2	2	2	
450	525	600	675	750	825	900	975																											





BARRIER VII – Input Deck – Approximated Round Post

FPL-MGS Baseline Model With Approx. Round Posts FPL-B-1.b7

173	71	28	1	201	73	2	0		
	0.0001		0.0001		2.000	2000	0	1.0	1
2	10	10	10	10	500	1			
1		0.0		0.0					
3		75.00		0.0					
5		150.00		0.0					
9		225.00		0.0					
12		281.25		0.0					
13		290.625		0.0					
14		295.3125		0.0					
15		300.00		0.0					
16		304.6875		0.0					
17		309.375		0.0					
18		318.75		0.0					
21		375.00		0.0					
25		450.00		0.0					
29		525.00		0.0					
32		581.25		0.0					
33		590.625		0.0					
34		595.3125		0.0					
35		600.00		0.0					
36		604.6875		0.0					
37		609.375		0.0					
38		618.75		0.0					
44		675.00		0.0					
52		750.00		0.0					
60		825.00		0.0					
66		881.25		0.0					
67		890.625		0.0					
68		895.3125		0.0					
69		900.00		0.0					
70		904.6875		0.0					
71		909.375		0.0					
72		918.75		0.0					
78		975.00		0.0					
84		1031.25		0.0					
85		1040.625		0.0					
86		1045.3125		0.0					
87		1050.00		0.0					
88		1054.6875		0.0					
89		1059.375		0.0					
90		1068.75		0.0					
96		1125.00		0.0					
102		1181.25		0.0					
103		1190.625		0.0					
104		1195.3125		0.0					
105		1200.00		0.0					
106		1204.6875		0.0					
107		1209.375		0.0					
108		1218.75		0.0					
114		1275.00		0.0					
122		1350.00		0.0					
130		1425.00		0.0					
136		1481.25		0.0					
137		1490.625		0.0					
138		1495.3125		0.0					
139		1500.00		0.0					
140		1504.6875		0.0					
141		1509.375		0.0					
142		1518.75		0.0					
145		1575.00		0.0					
149		1650.00		0.0					
153		1725.00		0.0					
156		1781.25		0.0					
157		1790.625		0.0					
158		1795.3125		0.0					
159		1800.00		0.0					

15.0			15.0		15.0		15.0													
4			24.875		0.0		1.34		6.75		60.0		92.88		143.65		0.05		FPL	
Weak Round Post			Overall																	
7.0			7.0		2.4		2.4													
1	1	2	4	1	101	0.0	0.0	0.0	0.0											
5	5	6	11	1	102	0.0	0.0	0.0	0.0											
12	12	13			103	0.0	0.0	0.0	0.0											
13	13	14			104	0.0	0.0	0.0	0.0											
14	14	15			104	0.0	0.0	0.0	0.0											
15	15	16			104	0.0	0.0	0.0	0.0											
16	16	17			104	0.0	0.0	0.0	0.0											
17	17	18			103	0.0	0.0	0.0	0.0											
18	18	19	31	1	102	0.0	0.0	0.0	0.0											
32	32	33			103	0.0	0.0	0.0	0.0											
33	33	34			104	0.0	0.0	0.0	0.0											
34	34	35			104	0.0	0.0	0.0	0.0											
35	35	36			104	0.0	0.0	0.0	0.0											
36	36	37			104	0.0	0.0	0.0	0.0											
37	37	38	66	1	103	0.0	0.0	0.0	0.0											
67	67	68			104	0.0	0.0	0.0	0.0											
68	68	69			104	0.0	0.0	0.0	0.0											
69	69	70			104	0.0	0.0	0.0	0.0											
70	70	71			104	0.0	0.0	0.0	0.0											
71	71	72	84	1	103	0.0	0.0	0.0	0.0											
85	85	86			104	0.0	0.0	0.0	0.0											
86	86	87			104	0.0	0.0	0.0	0.0											
87	87	88			104	0.0	0.0	0.0	0.0											
88	88	89			104	0.0	0.0	0.0	0.0											
89	89	90	102	1	103	0.0	0.0	0.0	0.0											
103	103	104			104	0.0	0.0	0.0	0.0											
104	104	105			104	0.0	0.0	0.0	0.0											
105	105	106			104	0.0	0.0	0.0	0.0											
106	106	107			104	0.0	0.0	0.0	0.0											
107	107	108	136	1	103	0.0	0.0	0.0	0.0											
137	137	138			104	0.0	0.0	0.0	0.0											
138	138	139			104	0.0	0.0	0.0	0.0											
139	139	140			104	0.0	0.0	0.0	0.0											
140	140	141			104	0.0	0.0	0.0	0.0											
141	141	142			103	0.0	0.0	0.0	0.0											
142	142	143	155	1	102	0.0	0.0	0.0	0.0											
156	156	157			103	0.0	0.0	0.0	0.0											
157	157	158			104	0.0	0.0	0.0	0.0											
158	158	159			104	0.0	0.0	0.0	0.0											
159	159	160			104	0.0	0.0	0.0	0.0											
160	160	161			104	0.0	0.0	0.0	0.0											
161	161	162			103	0.0	0.0	0.0	0.0											
162	162	163	168	1	102	0.0	0.0	0.0	0.0											
169	169	170	172	1	101	0.0	0.0	0.0	0.0											
173	1				301	0.0	0.0	0.0	0.0				0.0					0.0		
174	3				302	0.0	0.0	0.0	0.0				0.0					0.0		
175	5				303	0.0	0.0	0.0	0.0				0.0					0.0		
176	9				303	0.0	0.0	0.0	0.0				0.0					0.0		
177	15				303	0.0	0.0	0.0	0.0				0.0					0.0		
178	21				303	0.0	0.0	0.0	0.0				0.0					0.0		
179	25				303	0.0	0.0	0.0	0.0				0.0					0.0		
180	29				303	0.0	0.0	0.0	0.0				0.0					0.0		
181	35				303	0.0	0.0	0.0	0.0				0.0					0.0		
182	44				303	0.0	0.0	0.0	0.0				0.0					0.0		
183	52				303	0.0	0.0	0.0	0.0				0.0					0.0		
184	60				303	0.0	0.0	0.0	0.0				0.0					0.0		
185	69				303	0.0	0.0	0.0	0.0				0.0					0.0		
186	78				303	0.0	0.0	0.0	0.0				0.0					0.0		
187	87				303	0.0	0.0	0.0	0.0				0.0					0.0		
188	96				303	0.0	0.0	0.0	0.0				0.0					0.0		
189	105				303	0.0	0.0	0.0	0.0				0.0					0.0		
190	114				303	0.0	0.0	0.0	0.0				0.0					0.0		
191	122				303	0.0	0.0	0.0	0.0				0.0					0.0		
192	130				303	0.0	0.0	0.0	0.0				0.0					0.0		
193	139				303	0.0	0.0	0.0	0.0				0.0					0.0		
194	145				303	0.0	0.0	0.0	0.0				0.0					0.0		
195	149				303	0.0	0.0	0.0	0.0				0.0					0.0		
196	153				303	0.0	0.0	0.0	0.0				0.0					0.0		

197	159		303	0.0	0.0	0.0	0.0	0.0
198	165		303	0.0	0.0	0.0	0.0	0.0
199	169		303	0.0	0.0	0.0	0.0	0.0
200	171		302	0.0	0.0	0.0	0.0	0.0
201	173		301	0.0	0.0	0.0	0.0	0.0
	4400.0	47400.0	20	6	4	0	25	
1	0.055	0.12		6.00			17.0	
2	0.057	0.15		7.00			18.0	
3	0.062	0.18		10.00			12.0	
4	0.110	0.35		12.00			6.0	
5	0.35	0.45		6.00			5.0	
6	1.45	1.50		15.00			1.0	
1	100.75	15.875	1	12.0	1	1	0	0
2	100.75	27.875	1	12.0	1	1	0	0
3	100.75	39.875	2	12.0	1	1	0	0
4	88.75	39.875	2	12.0	1	1	0	0
5	76.75	39.875	2	12.0	1	1	0	0
6	64.75	39.875	2	12.0	1	1	0	0
7	52.75	39.875	2	12.0	1	1	0	0
8	40.75	39.875	2	12.0	1	1	0	0
9	28.75	39.875	2	12.0	1	1	0	0
10	16.75	39.875	2	12.0	1	1	0	0
11	-13.25	39.875	3	12.0	1	1	0	0
12	-33.25	39.875	3	12.0	1	1	0	0
13	-53.25	39.875	3	12.0	1	1	0	0
14	-73.25	39.875	3	12.0	1	1	0	0
15	-93.25	39.875	3	12.0	1	1	0	0
16	-113.25	39.875	4	12.0	1	1	0	0
17	-113.25	-39.875	4	12.0	0	0	0	0
18	100.75	-39.875	1	12.0	0	0	0	0
19	69.25	37.75	5	1.0	1	1	0	0
20	-62.75	37.75	6	1.0	1	1	0	0
1	69.25	32.75		0.0			608.	
2	69.25	-32.75		0.0			608.	
3	-62.75	32.75		0.0			492.	
4	-62.75	-32.75		0.0			492.	
1	100.75	39.88						
2	-113.25	39.88						
3	-113.25	-39.88						
4	100.75	-39.88						
5	5.00	2.50						
6	5.00	-2.50						
7	-5.00	-2.50						
8	-5.00	2.50						
9	83.75	37.75						
10	83.75	27.75						
11	54.75	27.75						
12	54.75	37.75						
13	83.75	-27.75						
14	83.75	-37.75						
15	54.75	-37.75						
16	54.75	-27.75						
17	-48.25	37.75						
18	-48.25	27.75						
19	-77.25	27.75						
20	-77.25	37.75						
21	-48.25	-27.75						
22	-48.25	-37.75						
23	-77.25	-37.75						
24	-77.25	-27.75						
25	0.00	0.00						
3	787.50	0.0	25.0	62.14	0.0	0.0	1.0	

BARRIER VII – Input Deck – Average Round Post

FPL-MGS Baseline Model With Overall Approx. Round Posts FPL-B-1.b7

173	71	28	1	201	73	2	0		
0.0001		0.0001		2.000	2000		0	1.0	1
2	10	10	10	10	500	1			
1		0.0		0.0					
3		75.00		0.0					
5		150.00		0.0					
9		225.00		0.0					
12		281.25		0.0					
13		290.625		0.0					
14		295.3125		0.0					
15		300.00		0.0					
16		304.6875		0.0					
17		309.375		0.0					
18		318.75		0.0					
21		375.00		0.0					
25		450.00		0.0					
29		525.00		0.0					
32		581.25		0.0					
33		590.625		0.0					
34		595.3125		0.0					
35		600.00		0.0					
36		604.6875		0.0					
37		609.375		0.0					
38		618.75		0.0					
44		675.00		0.0					
52		750.00		0.0					
60		825.00		0.0					
66		881.25		0.0					
67		890.625		0.0					
68		895.3125		0.0					
69		900.00		0.0					
70		904.6875		0.0					
71		909.375		0.0					
72		918.75		0.0					
78		975.00		0.0					
84		1031.25		0.0					
85		1040.625		0.0					
86		1045.3125		0.0					
87		1050.00		0.0					
88		1054.6875		0.0					
89		1059.375		0.0					
90		1068.75		0.0					
96		1125.00		0.0					
102		1181.25		0.0					
103		1190.625		0.0					
104		1195.3125		0.0					
105		1200.00		0.0					
106		1204.6875		0.0					
107		1209.375		0.0					
108		1218.75		0.0					
114		1275.00		0.0					
122		1350.00		0.0					
130		1425.00		0.0					
136		1481.25		0.0					
137		1490.625		0.0					
138		1495.3125		0.0					
139		1500.00		0.0					
140		1504.6875		0.0					
141		1509.375		0.0					
142		1518.75		0.0					
145		1575.00		0.0					
149		1650.00		0.0					
153		1725.00		0.0					
156		1781.25		0.0					
157		1790.625		0.0					
158		1795.3125		0.0					
159		1800.00		0.0					

	15.0		15.0		15.0	15.0							
4	24.875		0.0		1.34	6.75		60.0	92.00	161.50	0.05	FPL	
Weak Round Post	Overall												
	7.0		7.0		2.4	2.4							
1	1	2	4	1	101	0.0	0.0	0.0					
5	5	6	11	1	102	0.0	0.0	0.0					
12	12	13			103	0.0	0.0	0.0					
13	13	14			104	0.0	0.0	0.0					
14	14	15			104	0.0	0.0	0.0					
15	15	16			104	0.0	0.0	0.0					
16	16	17			104	0.0	0.0	0.0					
17	17	18			103	0.0	0.0	0.0					
18	18	19	31	1	102	0.0	0.0	0.0					
32	32	33			103	0.0	0.0	0.0					
33	33	34			104	0.0	0.0	0.0					
34	34	35			104	0.0	0.0	0.0					
35	35	36			104	0.0	0.0	0.0					
36	36	37			104	0.0	0.0	0.0					
37	37	38	66	1	103	0.0	0.0	0.0					
67	67	68			104	0.0	0.0	0.0					
68	68	69			104	0.0	0.0	0.0					
69	69	70			104	0.0	0.0	0.0					
70	70	71			104	0.0	0.0	0.0					
71	71	72	84	1	103	0.0	0.0	0.0					
85	85	86			104	0.0	0.0	0.0					
86	86	87			104	0.0	0.0	0.0					
87	87	88			104	0.0	0.0	0.0					
88	88	89			104	0.0	0.0	0.0					
89	89	90	102	1	103	0.0	0.0	0.0					
103	103	104			104	0.0	0.0	0.0					
104	104	105			104	0.0	0.0	0.0					
105	105	106			104	0.0	0.0	0.0					
106	106	107			104	0.0	0.0	0.0					
107	107	108	136	1	103	0.0	0.0	0.0					
137	137	138			104	0.0	0.0	0.0					
138	138	139			104	0.0	0.0	0.0					
139	139	140			104	0.0	0.0	0.0					
140	140	141			104	0.0	0.0	0.0					
141	141	142			103	0.0	0.0	0.0					
142	142	143	155	1	102	0.0	0.0	0.0					
156	156	157			103	0.0	0.0	0.0					
157	157	158			104	0.0	0.0	0.0					
158	158	159			104	0.0	0.0	0.0					
159	159	160			104	0.0	0.0	0.0					
160	160	161			104	0.0	0.0	0.0					
161	161	162			103	0.0	0.0	0.0					
162	162	163	168	1	102	0.0	0.0	0.0					
169	169	170	172	1	101	0.0	0.0	0.0					
173	1				301	0.0	0.0	0.0	0.0	0.0			
174	3				302	0.0	0.0	0.0	0.0	0.0			
175	5				303	0.0	0.0	0.0	0.0	0.0			
176	9				303	0.0	0.0	0.0	0.0	0.0			
177	15				303	0.0	0.0	0.0	0.0	0.0			
178	21				303	0.0	0.0	0.0	0.0	0.0			
179	25				303	0.0	0.0	0.0	0.0	0.0			
180	29				303	0.0	0.0	0.0	0.0	0.0			
181	35				303	0.0	0.0	0.0	0.0	0.0			
182	44				303	0.0	0.0	0.0	0.0	0.0			
183	52				303	0.0	0.0	0.0	0.0	0.0			
184	60				303	0.0	0.0	0.0	0.0	0.0			
185	69				303	0.0	0.0	0.0	0.0	0.0			
186	78				303	0.0	0.0	0.0	0.0	0.0			
187	87				303	0.0	0.0	0.0	0.0	0.0			
188	96				303	0.0	0.0	0.0	0.0	0.0			
189	105				303	0.0	0.0	0.0	0.0	0.0			
190	114				303	0.0	0.0	0.0	0.0	0.0			
191	122				303	0.0	0.0	0.0	0.0	0.0			
192	130				303	0.0	0.0	0.0	0.0	0.0			
193	139				303	0.0	0.0	0.0	0.0	0.0			
194	145				303	0.0	0.0	0.0	0.0	0.0			
195	149				303	0.0	0.0	0.0	0.0	0.0			
196	153				303	0.0	0.0	0.0	0.0	0.0			

197	159		303	0.0	0.0	0.0	0.0	0.0
198	165		303	0.0	0.0	0.0	0.0	0.0
199	169		303	0.0	0.0	0.0	0.0	0.0
200	171		302	0.0	0.0	0.0	0.0	0.0
201	173		301	0.0	0.0	0.0	0.0	0.0
4400.0	47400.0	20	6	4	0	25		
1	0.055	0.12		6.00		17.0		
2	0.057	0.15		7.00		18.0		
3	0.062	0.18		10.00		12.0		
4	0.110	0.35		12.00		6.0		
5	0.35	0.45		6.00		5.0		
6	1.45	1.50		15.00		1.0		
1	100.75	15.875	1	12.0	1	1	0	0
2	100.75	27.875	1	12.0	1	1	0	0
3	100.75	39.875	2	12.0	1	1	0	0
4	88.75	39.875	2	12.0	1	1	0	0
5	76.75	39.875	2	12.0	1	1	0	0
6	64.75	39.875	2	12.0	1	1	0	0
7	52.75	39.875	2	12.0	1	1	0	0
8	40.75	39.875	2	12.0	1	1	0	0
9	28.75	39.875	2	12.0	1	1	0	0
10	16.75	39.875	2	12.0	1	1	0	0
11	-13.25	39.875	3	12.0	1	1	0	0
12	-33.25	39.875	3	12.0	1	1	0	0
13	-53.25	39.875	3	12.0	1	1	0	0
14	-73.25	39.875	3	12.0	1	1	0	0
15	-93.25	39.875	3	12.0	1	1	0	0
16	-113.25	39.875	4	12.0	1	1	0	0
17	-113.25	-39.875	4	12.0	0	0	0	0
18	100.75	-39.875	1	12.0	0	0	0	0
19	69.25	37.75	5	1.0	1	1	0	0
20	-62.75	37.75	6	1.0	1	1	0	0
1	69.25	32.75		0.0		608.		
2	69.25	-32.75		0.0		608.		
3	-62.75	32.75		0.0		492.		
4	-62.75	-32.75		0.0		492.		
1	100.75	39.88						
2	-113.25	39.88						
3	-113.25	-39.88						
4	100.75	-39.88						
5	5.00	2.50						
6	5.00	-2.50						
7	-5.00	-2.50						
8	-5.00	2.50						
9	83.75	37.75						
10	83.75	27.75						
11	54.75	27.75						
12	54.75	37.75						
13	83.75	-27.75						
14	83.75	-37.75						
15	54.75	-37.75						
16	54.75	-27.75						
17	-48.25	37.75						
18	-48.25	27.75						
19	-77.25	27.75						
20	-77.25	37.75						
21	-48.25	-27.75						
22	-48.25	-37.75						
23	-77.25	-37.75						
24	-77.25	-27.75						
25	0.00	0.00						
3	787.50	0.0	25.0	62.14	0.0	0.0	1.0	

APPENDIX D - Supplemental Inertia Cantilever Bogie Test Results

Figure D-1. Results of Test No. SYPI-1	336
Figure D-2. Results of Test No. SYPI-2	337
Figure D-3. Results of Test No. SYPI-3	338

Midwest Roadside Safety Facility

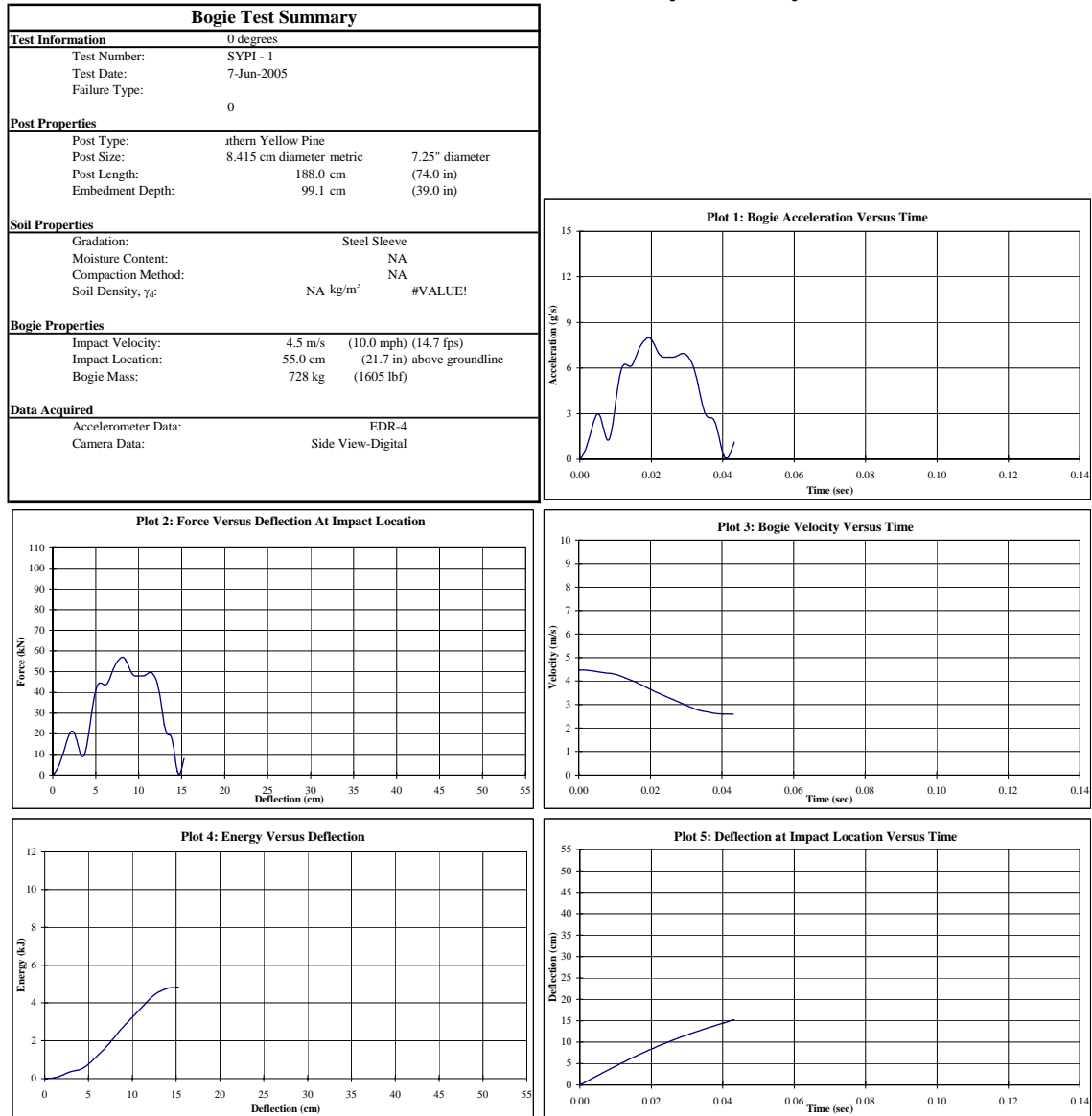


Figure D-1. Results of Test No. SYPI-1

Midwest Roadside Safety Facility

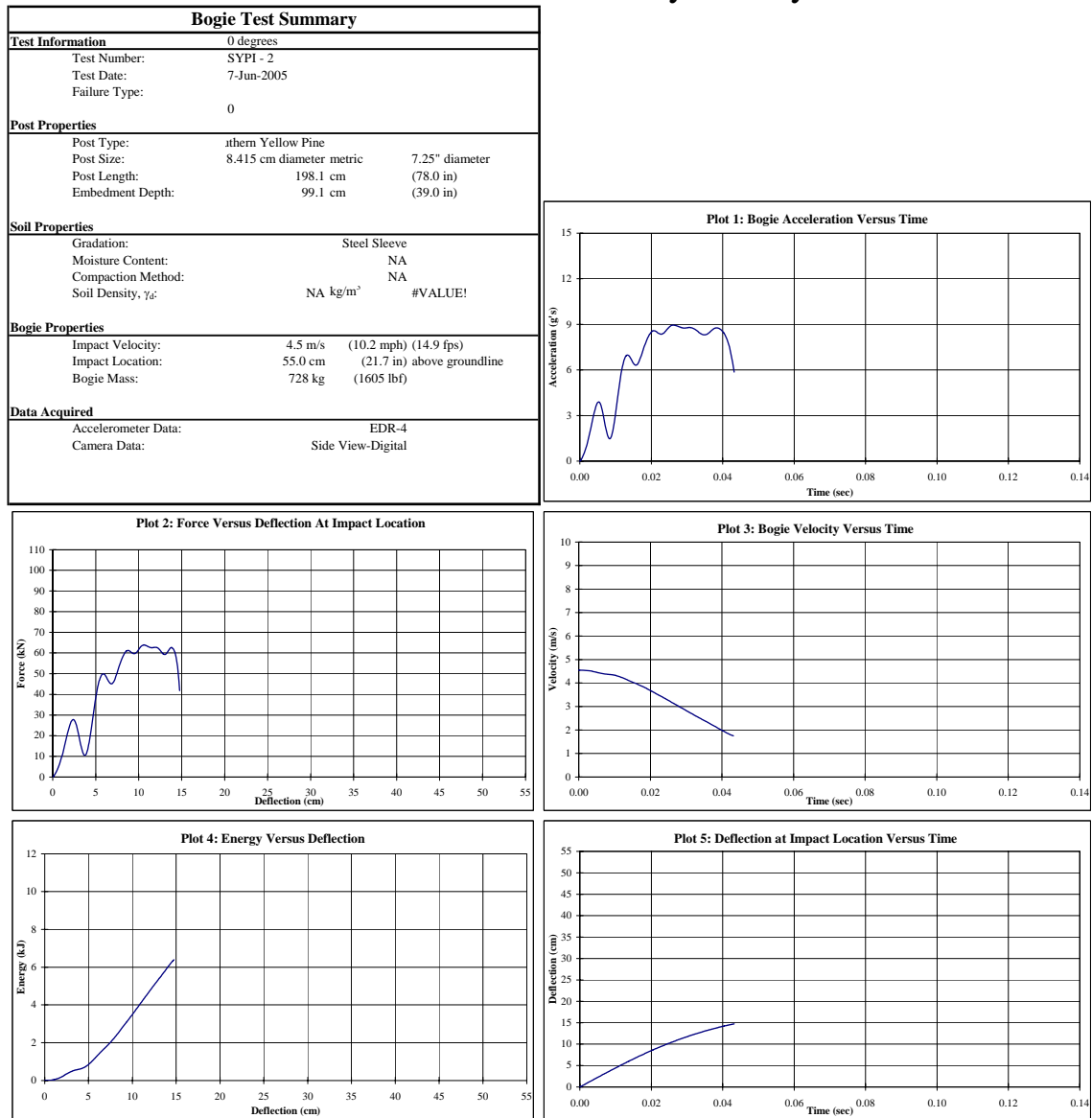


Figure D-2. Results of Test No. SYPI-2

Midwest Roadside Safety Facility

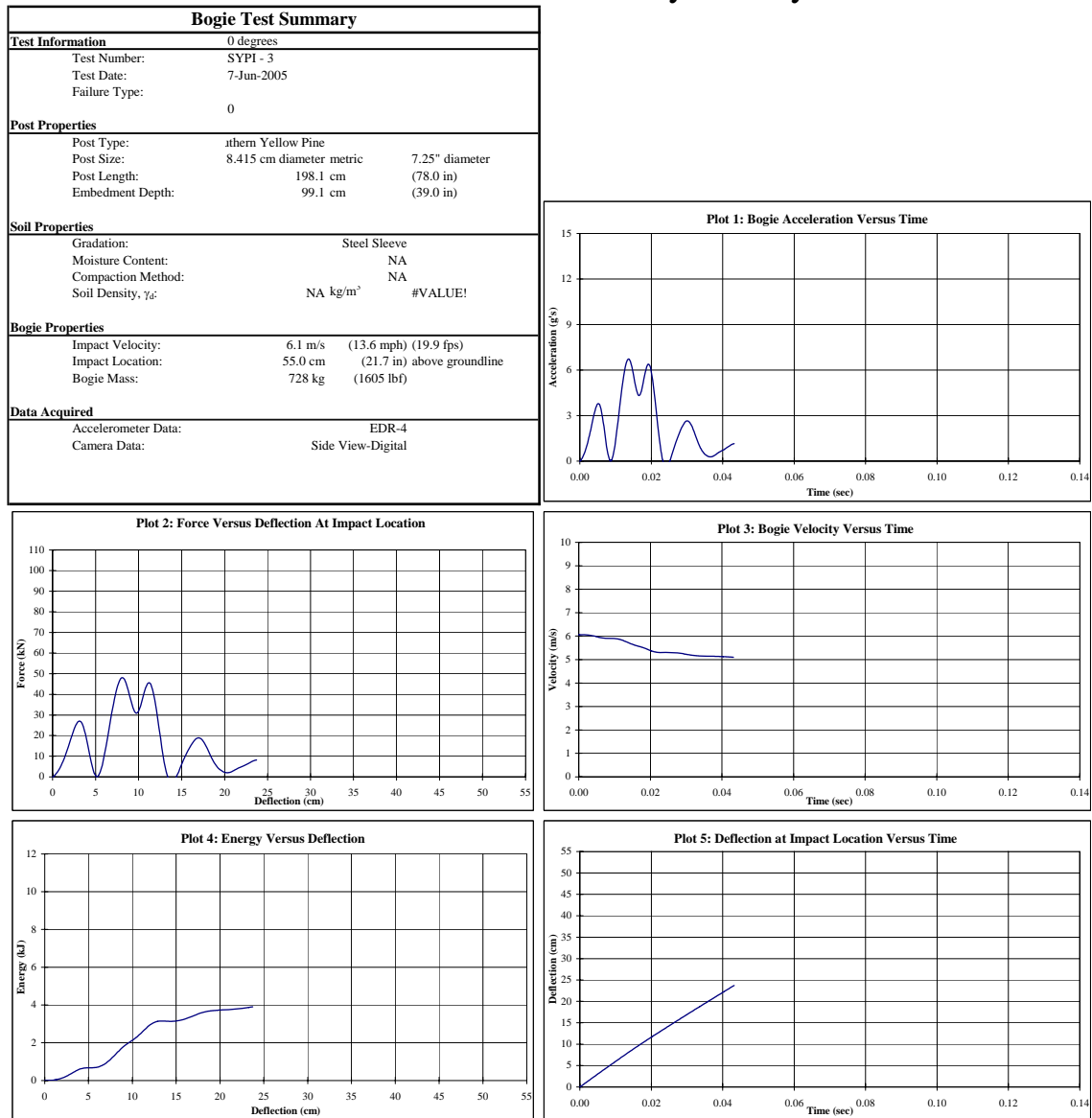


Figure D-3. Results of Test No. SYPI-3

APPENDIX E - Round 2 Cantilever Bogie Test Results

Figure E-1. Results of Test No. DF-16.....	341
Figure E-2. Results of Test No. DF-17.....	342
Figure E-3. Results of Test No. DF-18.....	343
Figure E-4. Results of Test No. DF-19.....	344
Figure E-5. Results of Test No. DF-20.....	345
Figure E-6. Results of Test No. DF-21.....	346
Figure E-7. Results of Test No. DF-22.....	347
Figure E-8. Results of Test No. DF-23.....	348
Figure E-9. Results of Test No. DF-24.....	349
Figure E-10. Results of Test No. DF-25.....	350
Figure E-11. Results of Test No. DF-26.....	351
Figure E-12. Results of Test No. DF-27.....	352
Figure E-13. Results of Test No. DF-28.....	353
Figure E-14. Results of Test No. DF-29.....	354
Figure E-15. Results of Test No. DF-30.....	355
Figure E-16. Results of Test No. PP-16.....	356
Figure E-17. Results of Test No. PP-17.....	357
Figure E-18. Results of Test No. PP-18.....	358
Figure E-19. Results of Test No. PP-19.....	359
Figure E-20. Results of Test No. PP-20.....	360
Figure E-21. Results of Test No. PP-21.....	361
Figure E-22. Results of Test No. PP-22.....	362
Figure E-23. Results of Test No. PP-23.....	363
Figure E-24. Results of Test No. PP-24.....	364
Figure E-25. Results of Test No. PP-25.....	365
Figure E-26. Results of Test No. PP-26.....	366
Figure E-27. Results of Test No. PP-27.....	367
Figure E-28. Results of Test No. PP-28.....	368
Figure E-29. Results of Test No. PP-29.....	369
Figure E-30. Results of Test No. PP-30.....	370
Figure E-31. Results of Test No. SY-16.....	371
Figure E-32. Results of Test No. SY-17.....	372
Figure E-33. Results of Test No. SY-18.....	373
Figure E-34. Results of Test No. SY-19.....	374
Figure E-35. Results of Test No. SY-20.....	375
Figure E-36. Results of Test No. SY-21.....	376
Figure E-37. Results of Test No. SY-22.....	377
Figure E-38. Results of Test No. SY-23.....	378
Figure E-39. Results of Test No. SY-24.....	379
Figure E-40. Results of Test No. SY-25.....	380
Figure E-41. Results of Test No. SY-26.....	381
Figure E-42. Results of Test No. SY-27.....	382
Figure E-43. Results of Test No. SY-28.....	383
Figure E-44. Results of Test No. SY-29.....	384
Figure E-45. Results of Test No. SY-30.....	385

Midwest Roadside Safety Facility

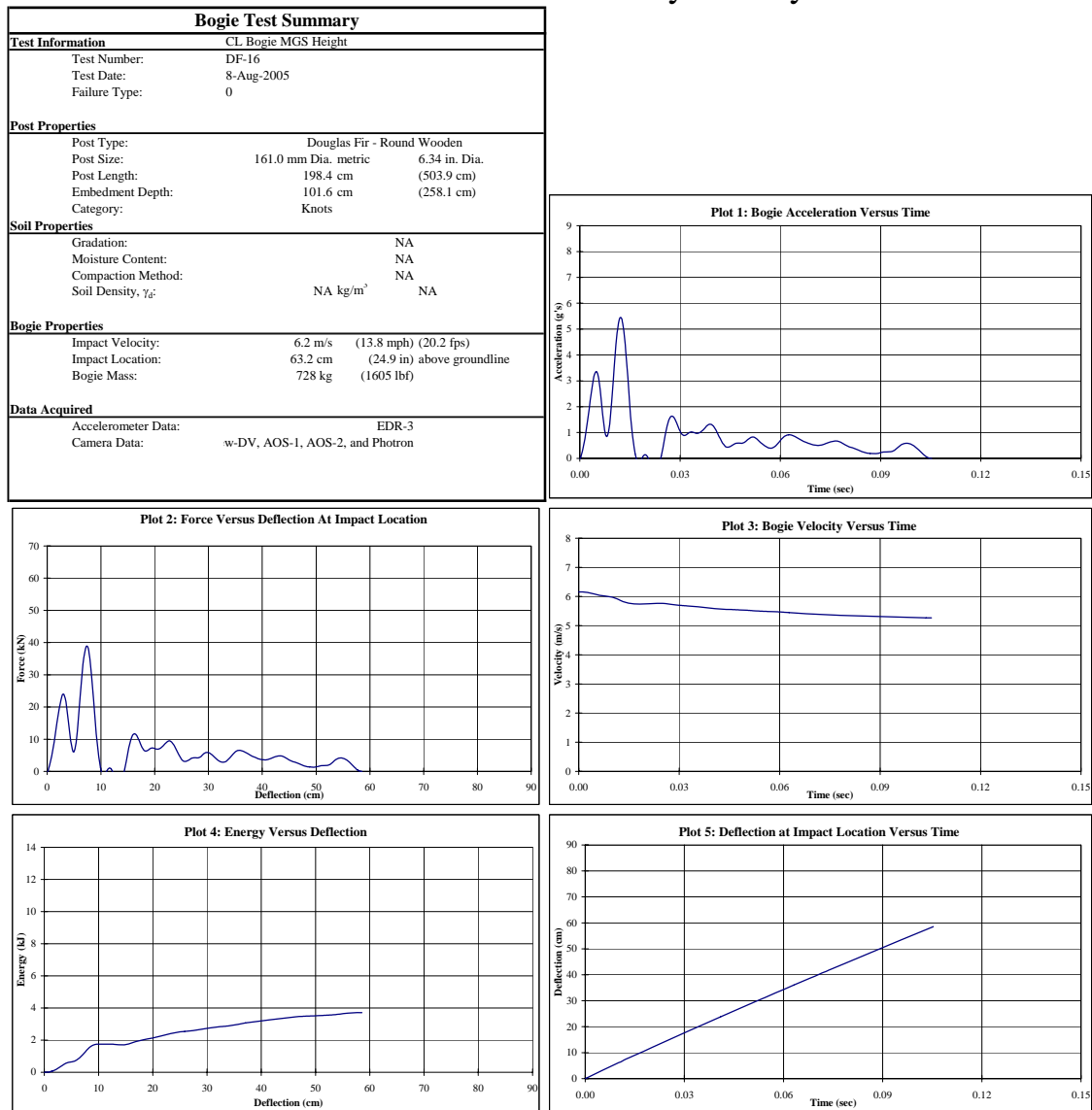


Figure E-1. Results of Test No. DF-16

Midwest Roadside Safety Facility

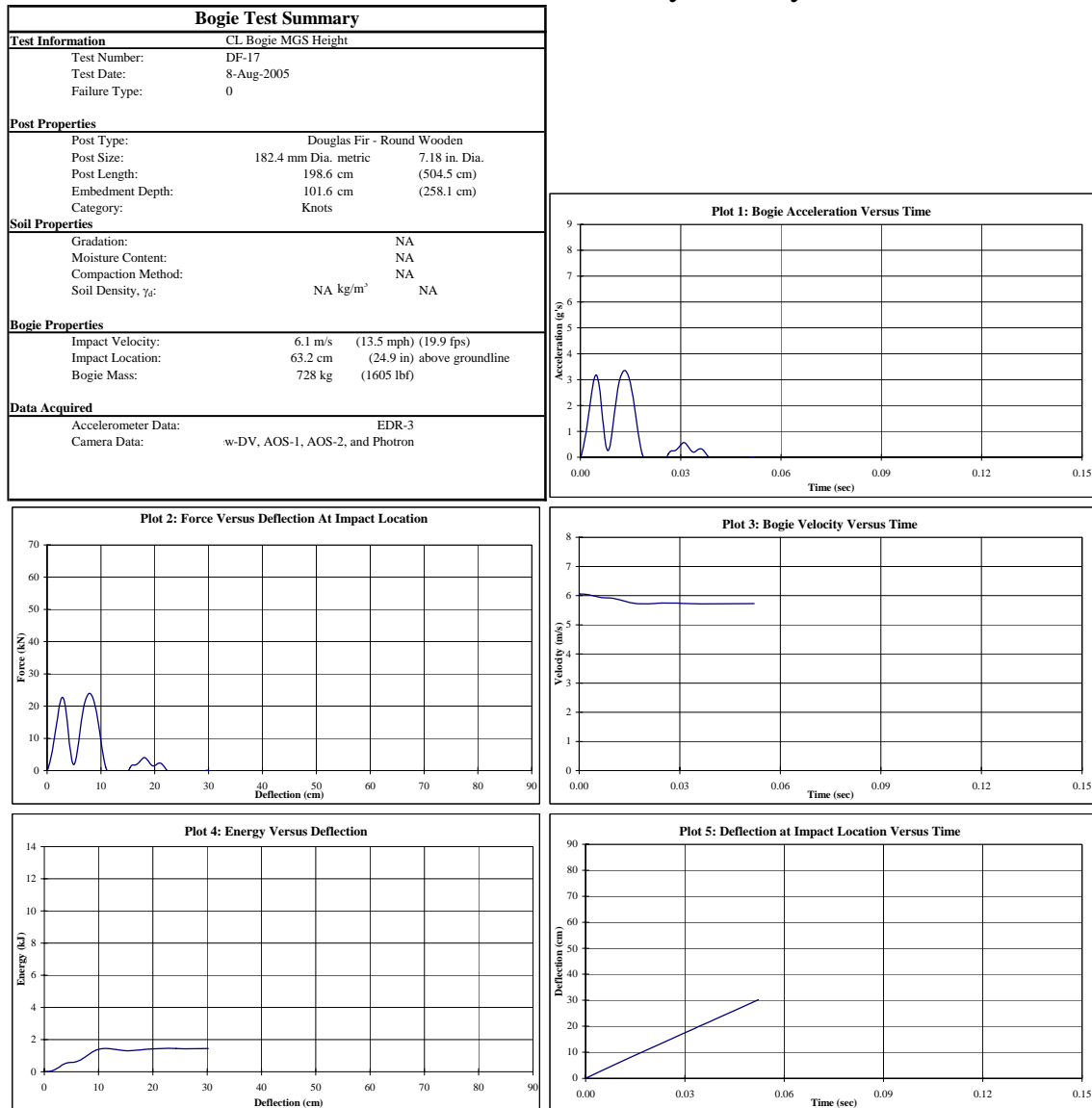


Figure E-2. Results of Test No. DF-17

Midwest Roadside Safety Facility

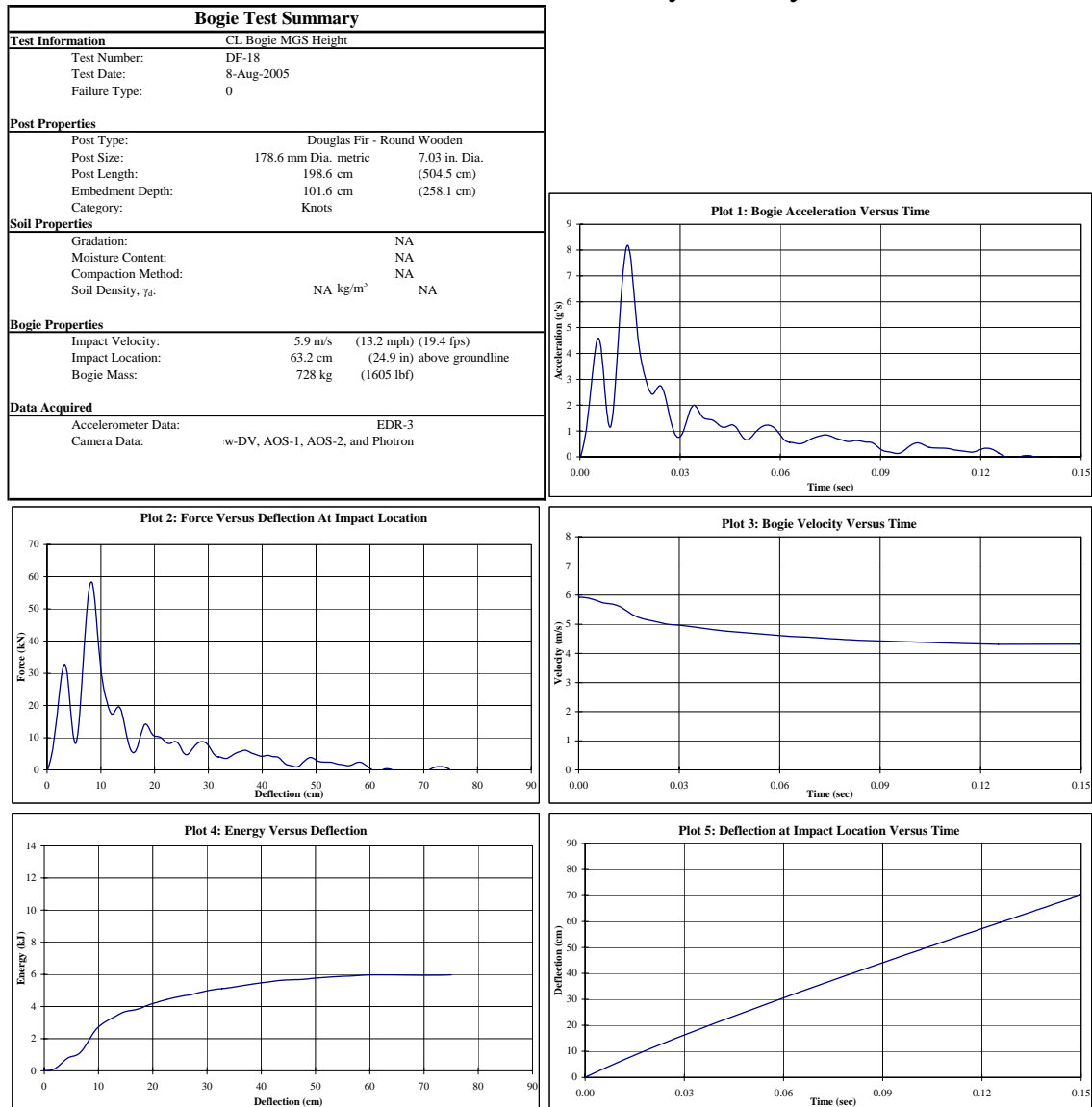


Figure E-3. Results of Test No. DF-18

Midwest Roadside Safety Facility

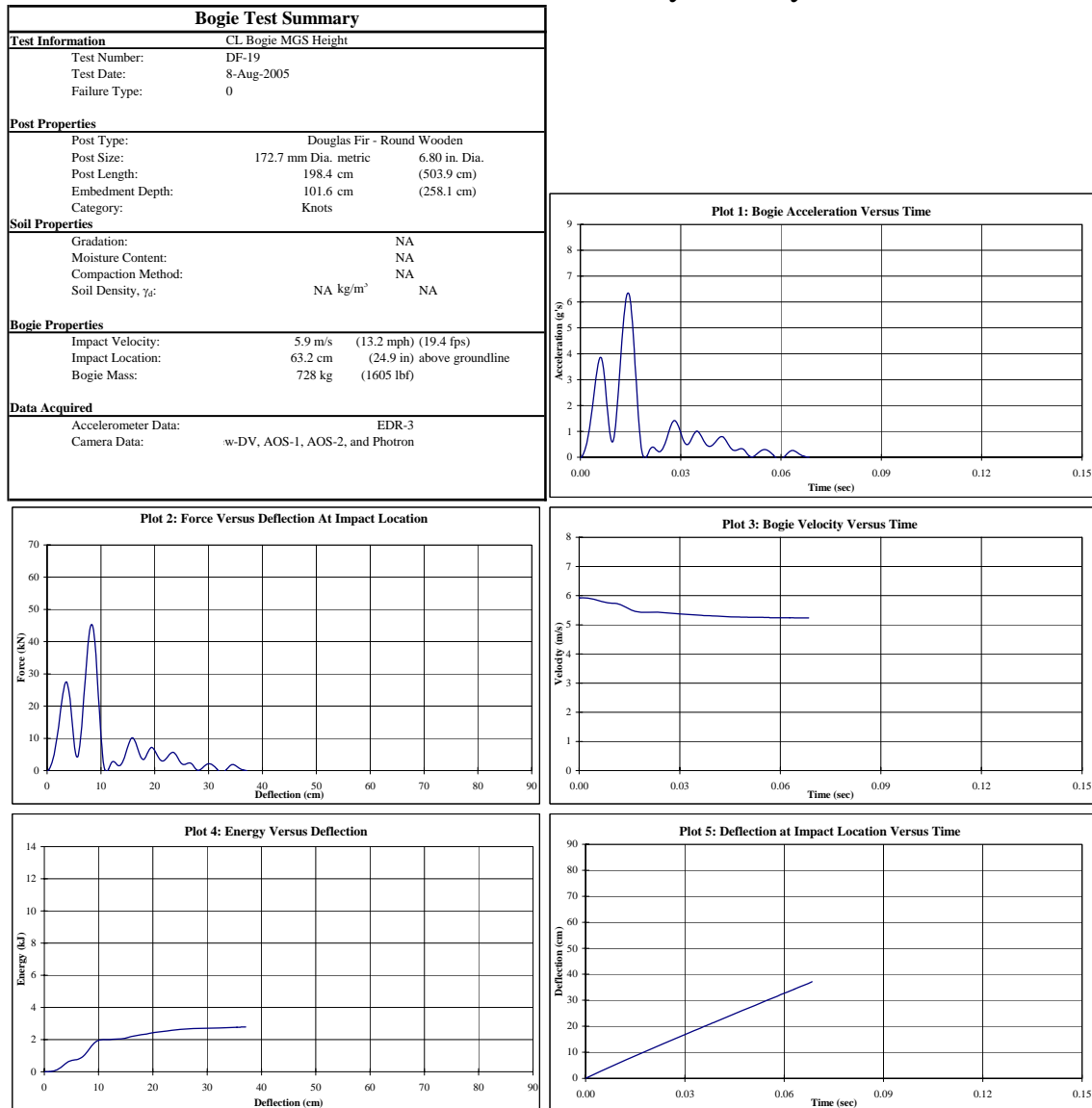


Figure E-4. Results of Test No. DF-19

Midwest Roadside Safety Facility

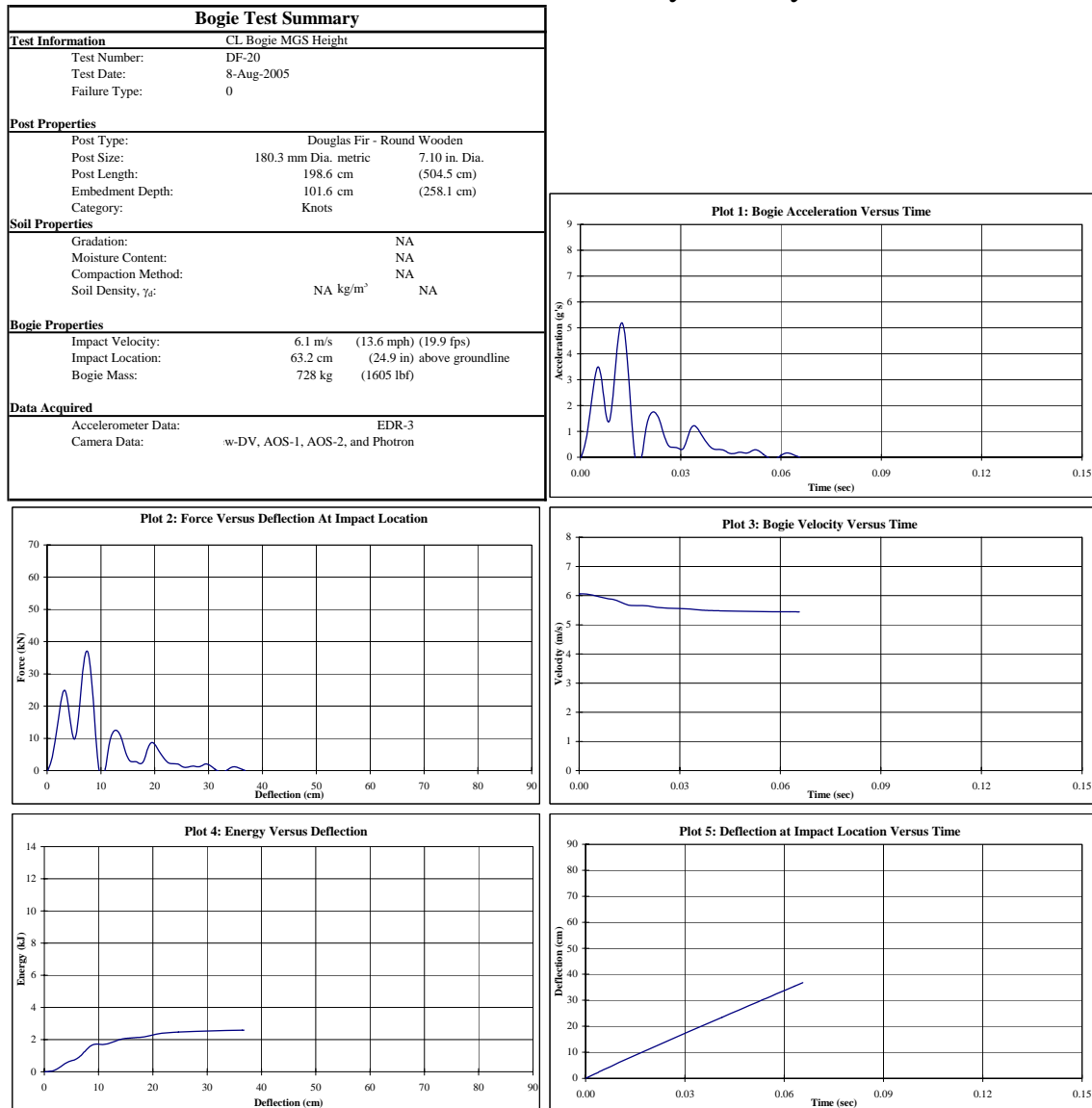


Figure E-5. Results of Test No. DF-20

Midwest Roadside Safety Facility

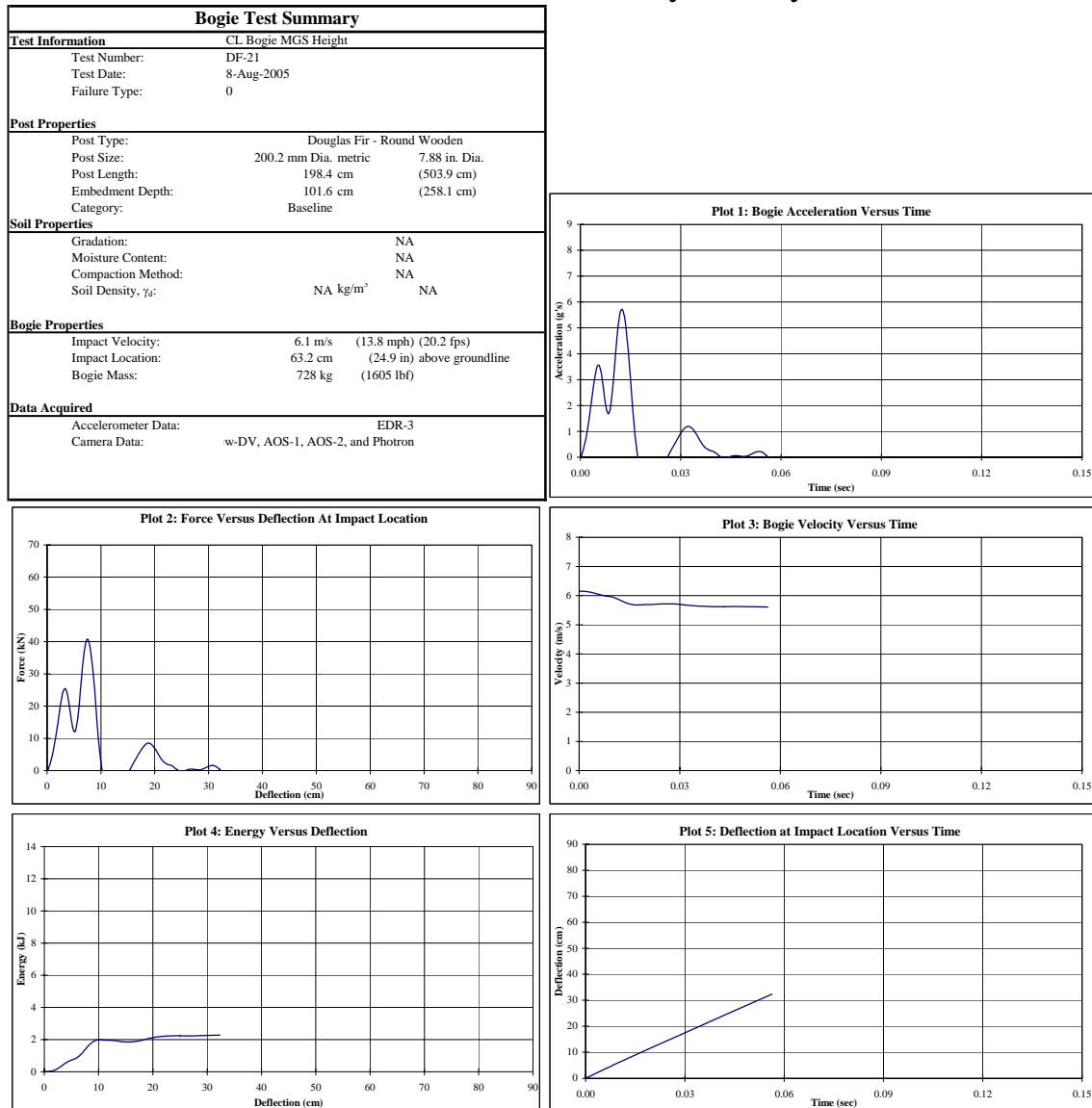


Figure E-6. Results of Test No. DF-21

Midwest Roadside Safety Facility

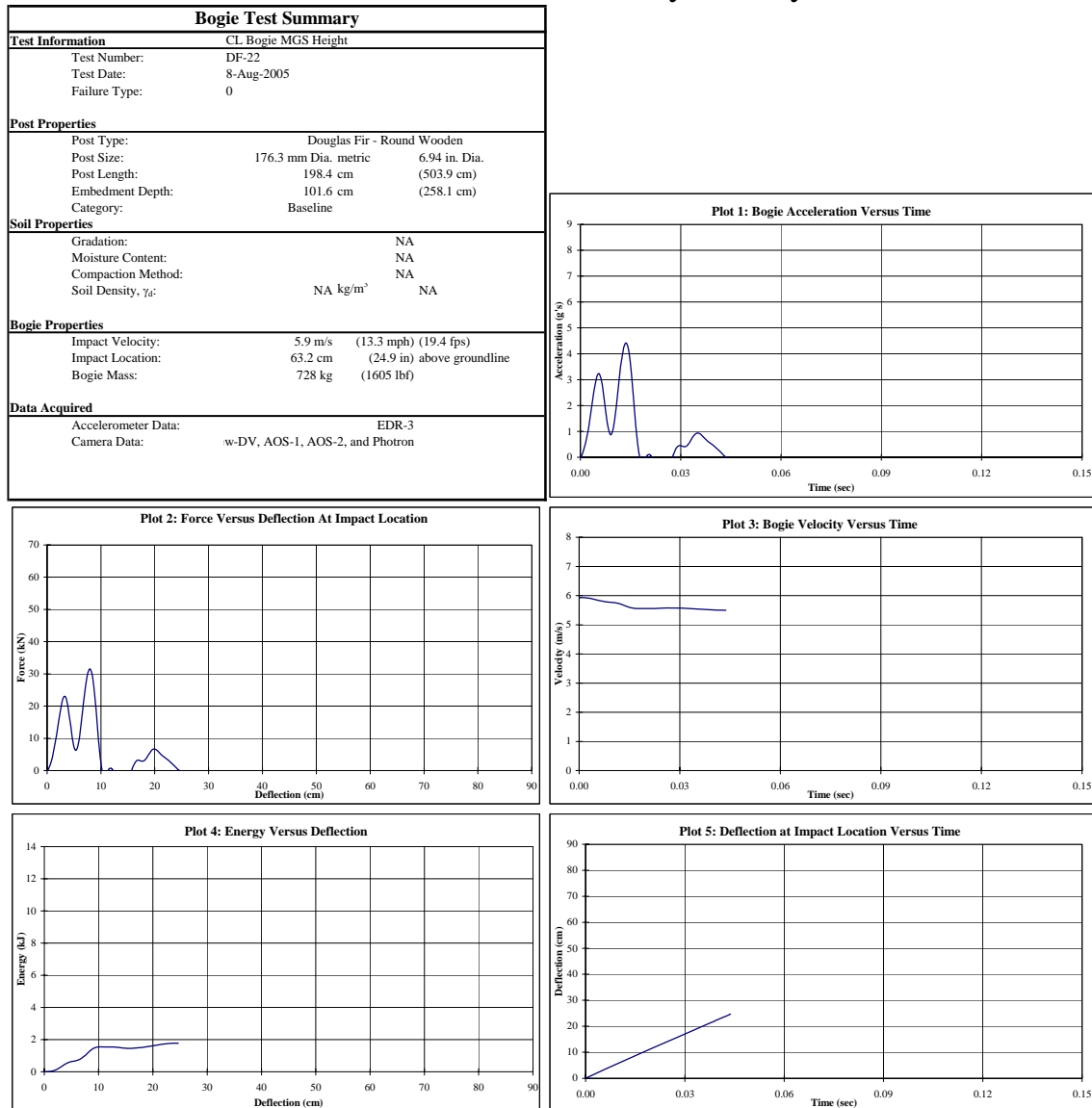


Figure E-7. Results of Test No. DF-22

Midwest Roadside Safety Facility

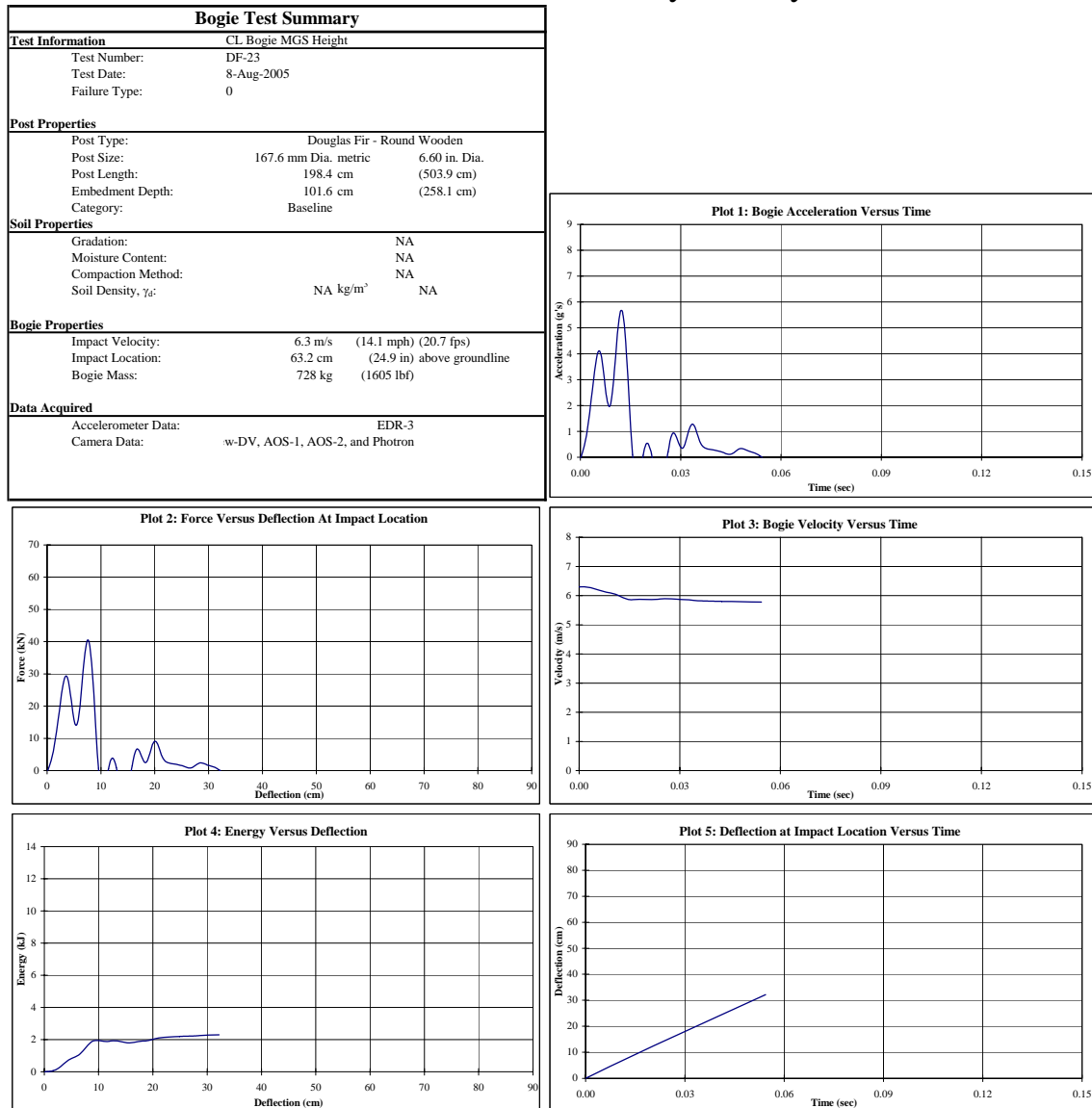


Figure E-8. Results of Test No. DF-23

Midwest Roadside Safety Facility

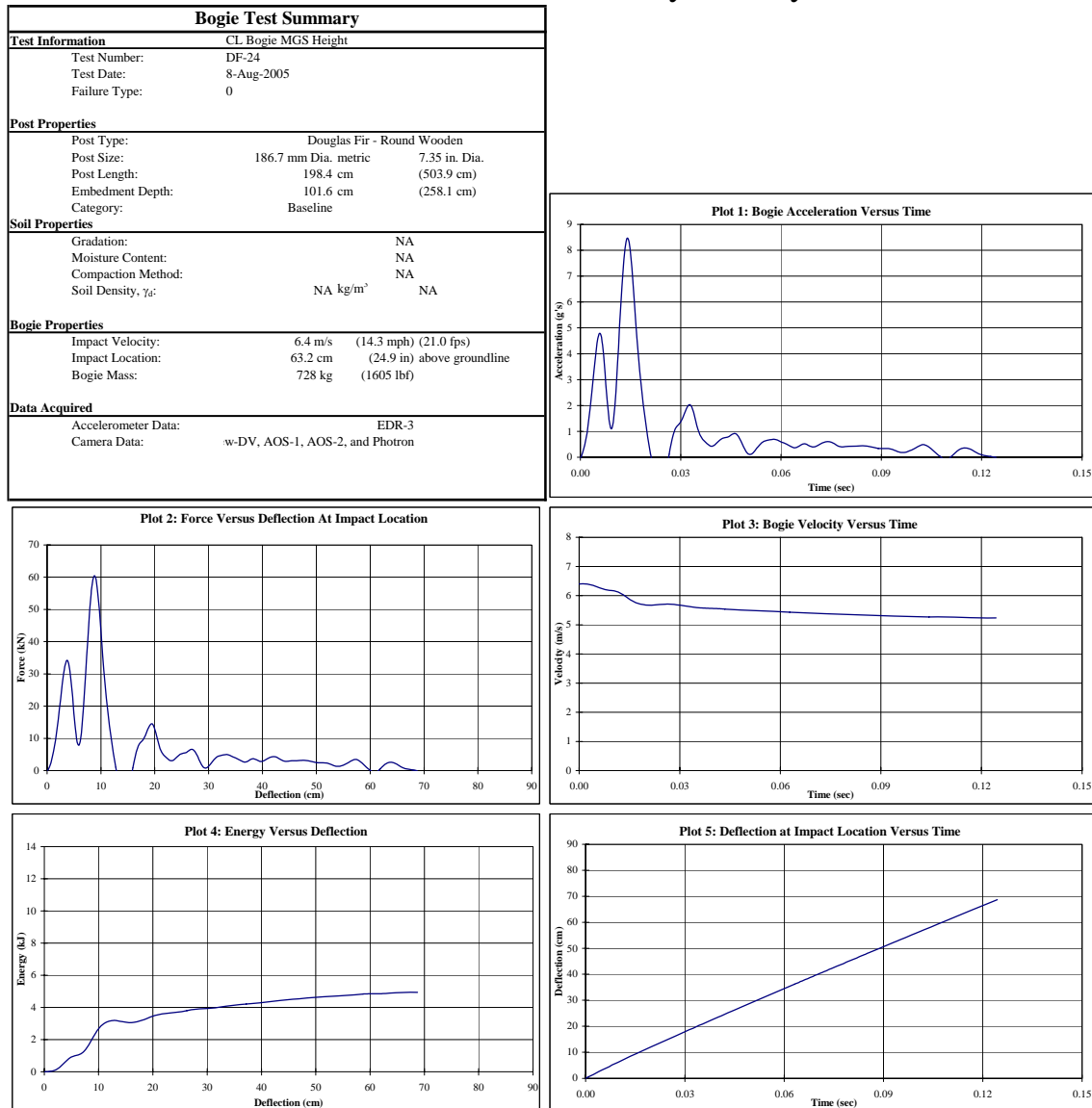


Figure E-9. Results of Test No. DF-24

Midwest Roadside Safety Facility

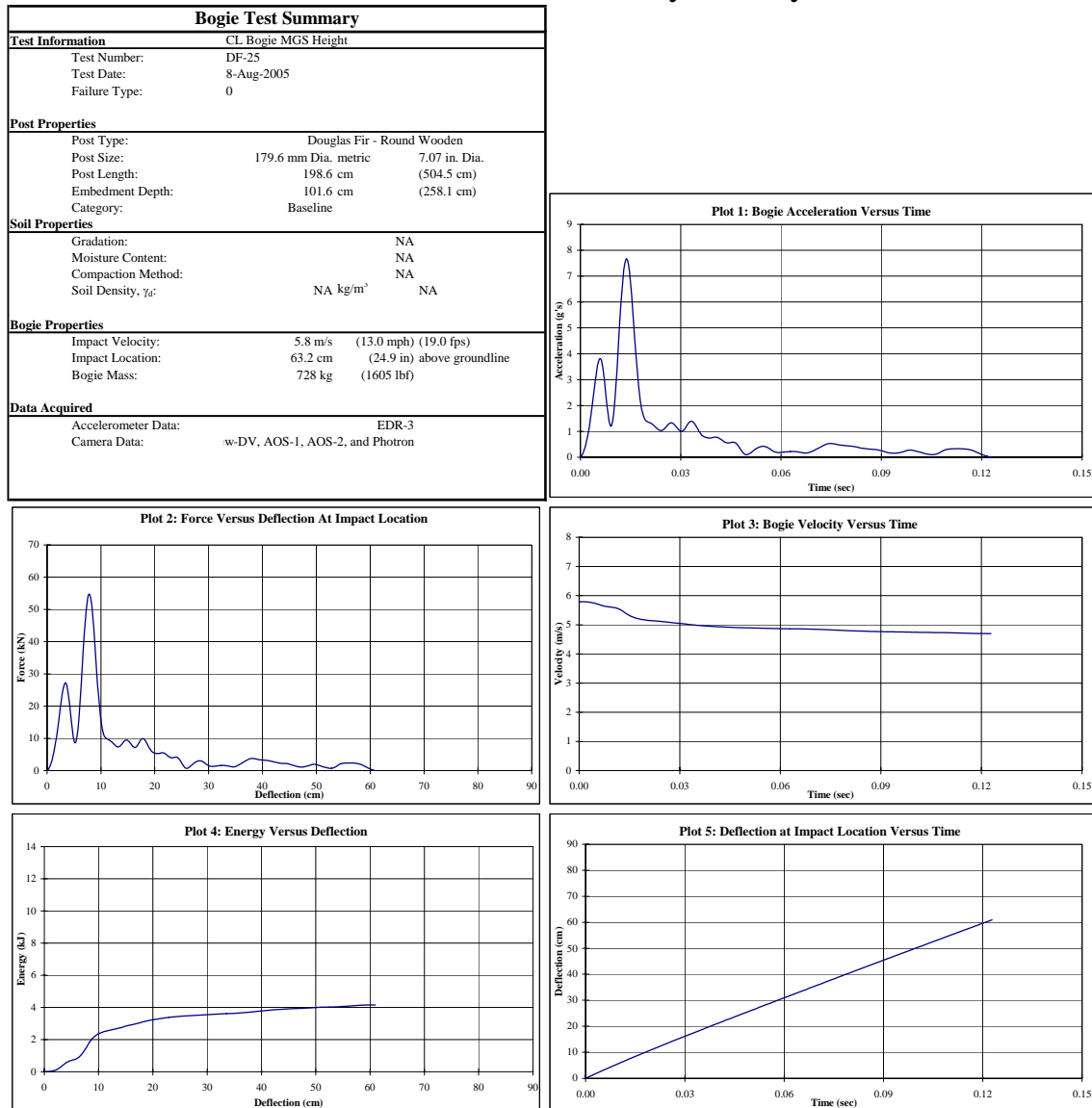


Figure E-10. Results of Test No. DF-25

Midwest Roadside Safety Facility

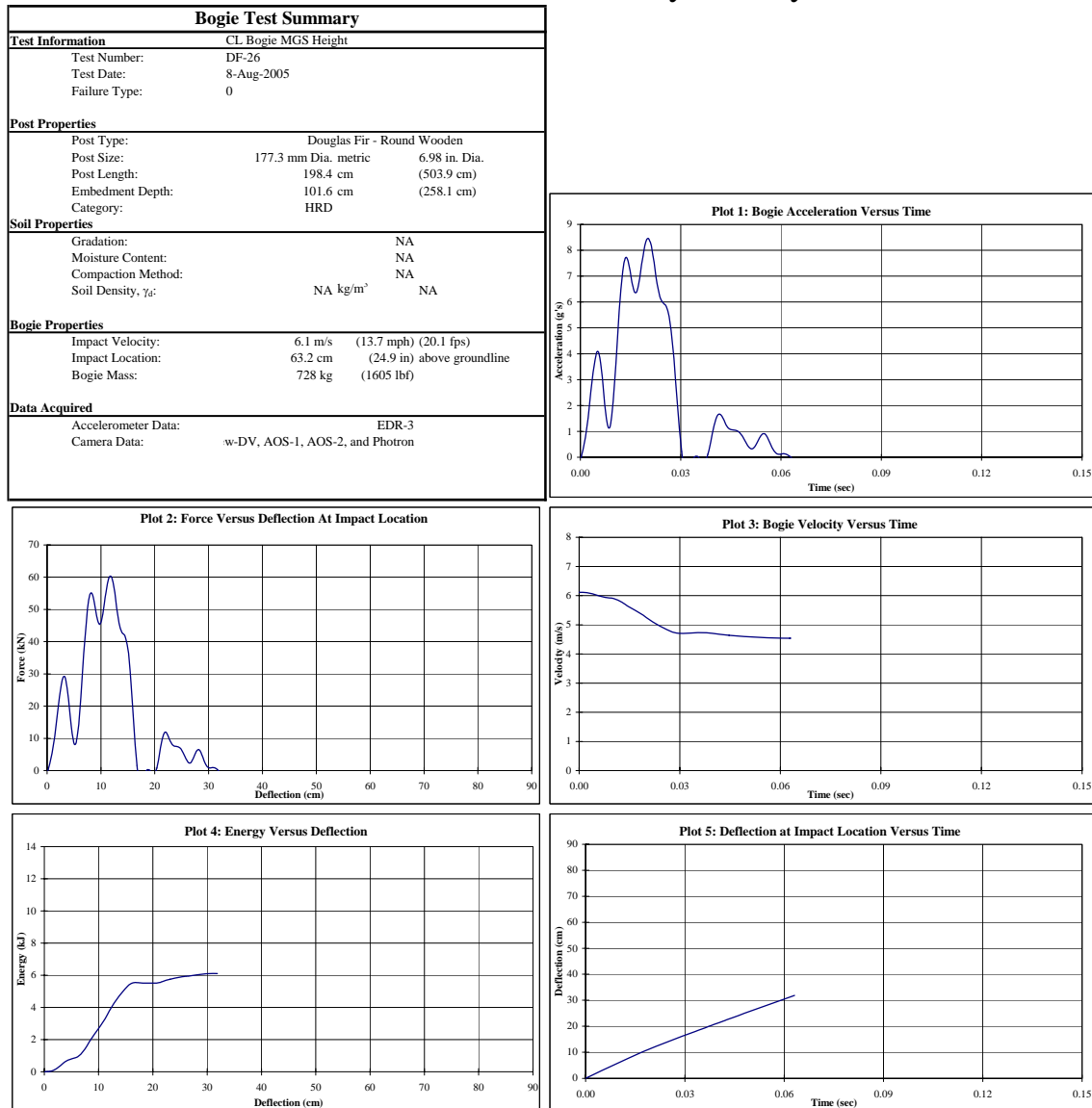


Figure E-11. Results of Test No. DF-26

Midwest Roadside Safety Facility

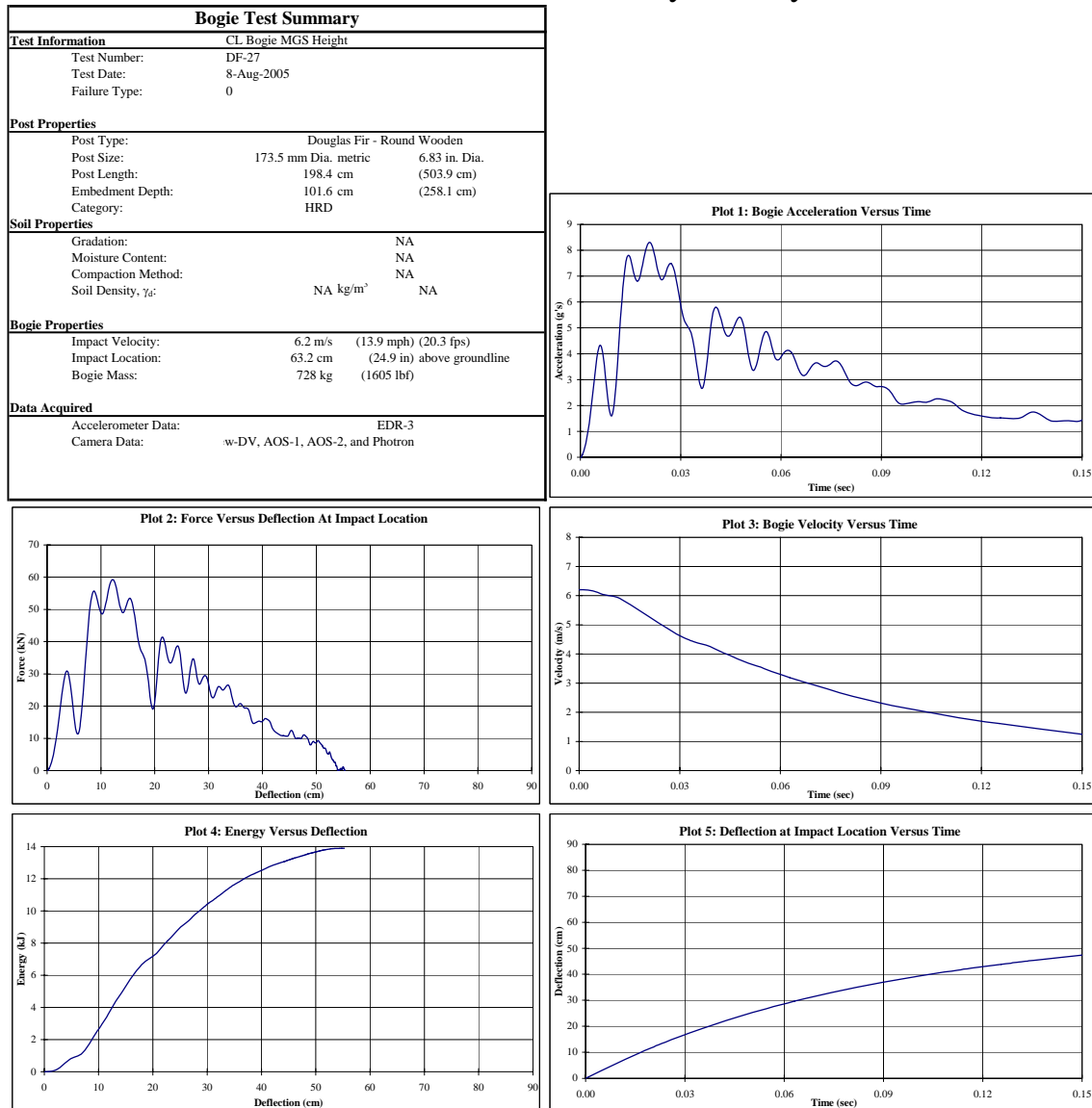


Figure E-12. Results of Test No. DF-27

Midwest Roadside Safety Facility

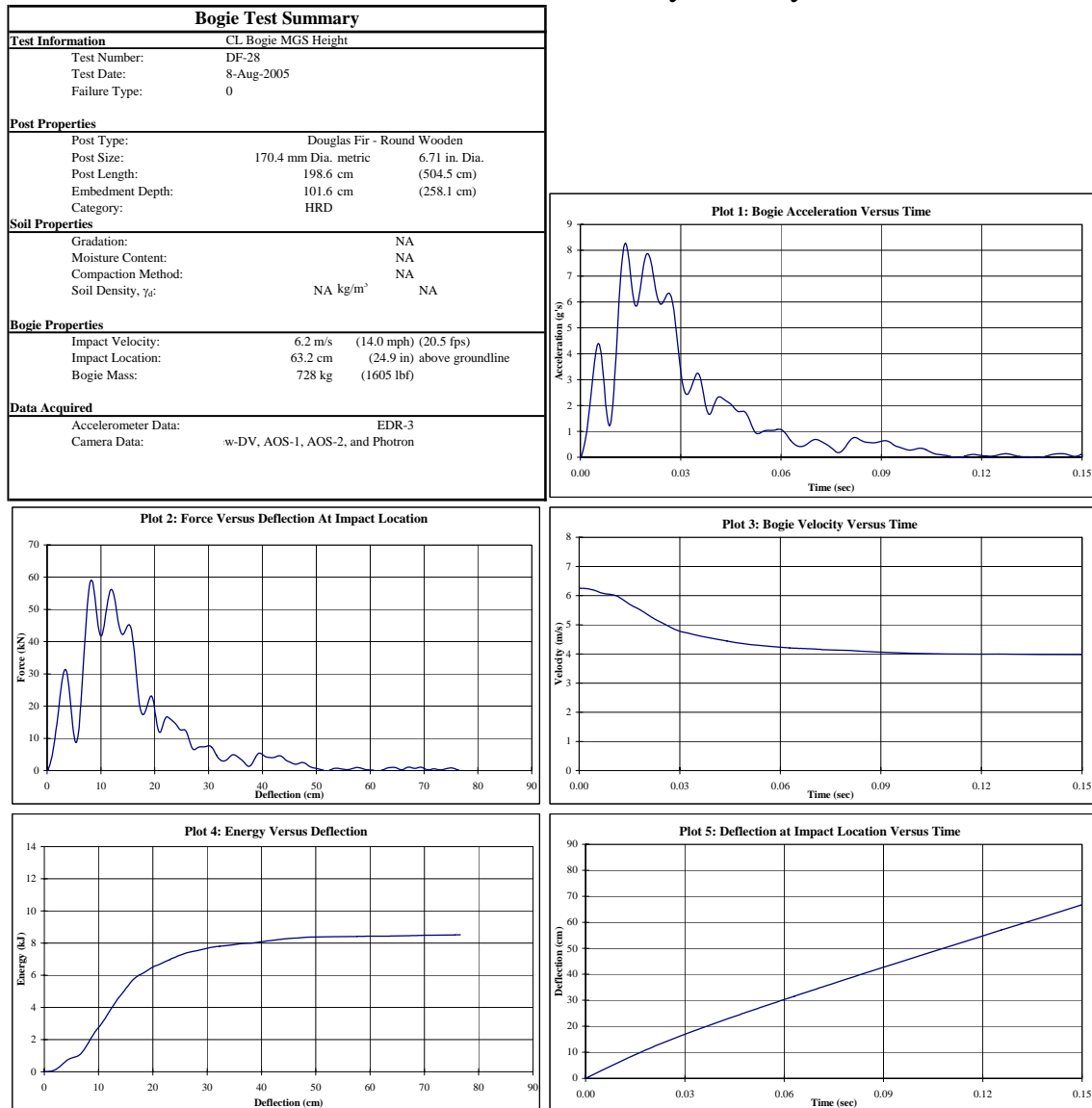


Figure E-13. Results of Test No. DF-28

Midwest Roadside Safety Facility

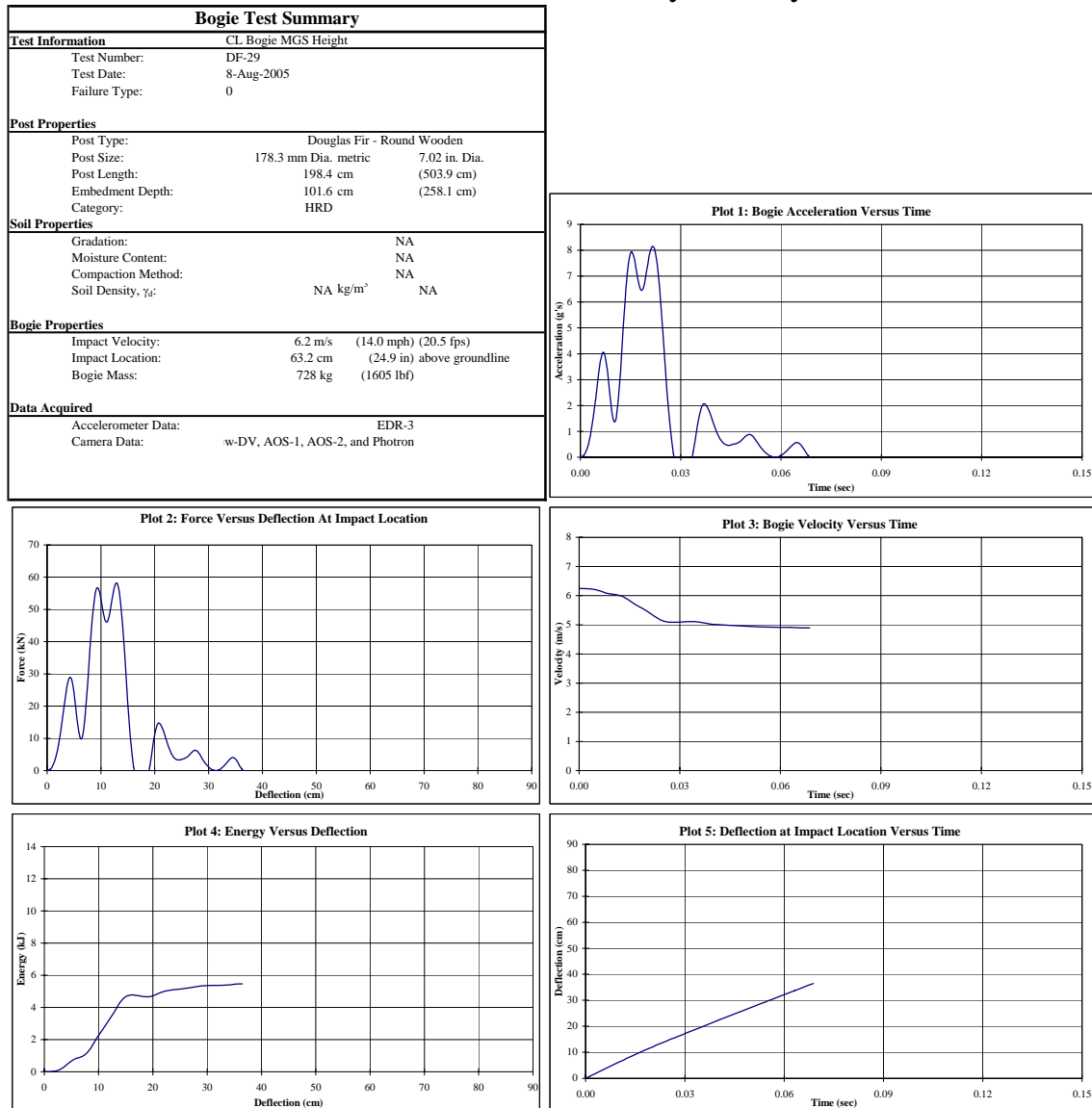


Figure E-14. Results of Test No. DF-29

Midwest Roadside Safety Facility

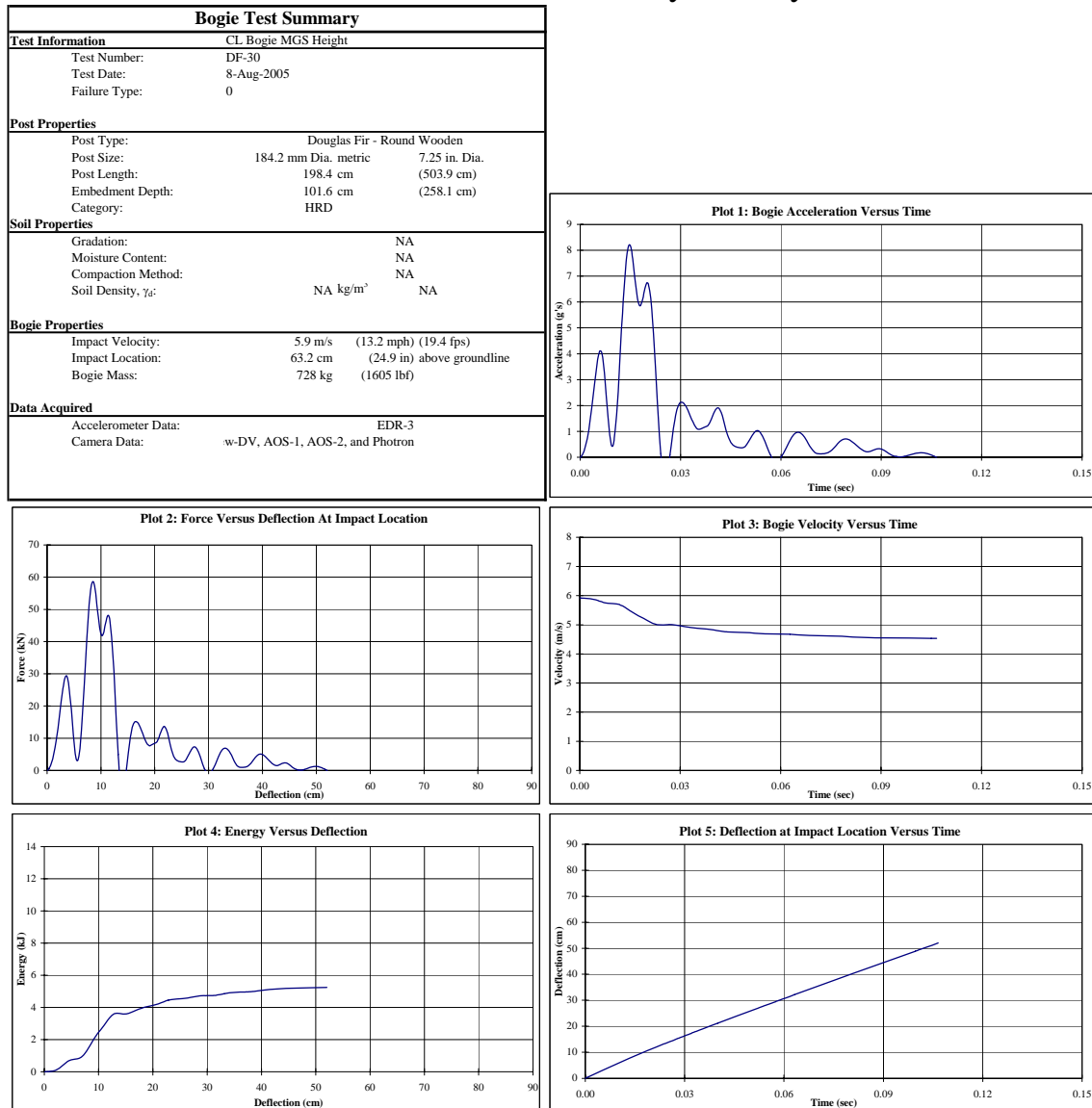


Figure E-15. Results of Test No. DF-30

Midwest Roadside Safety Facility

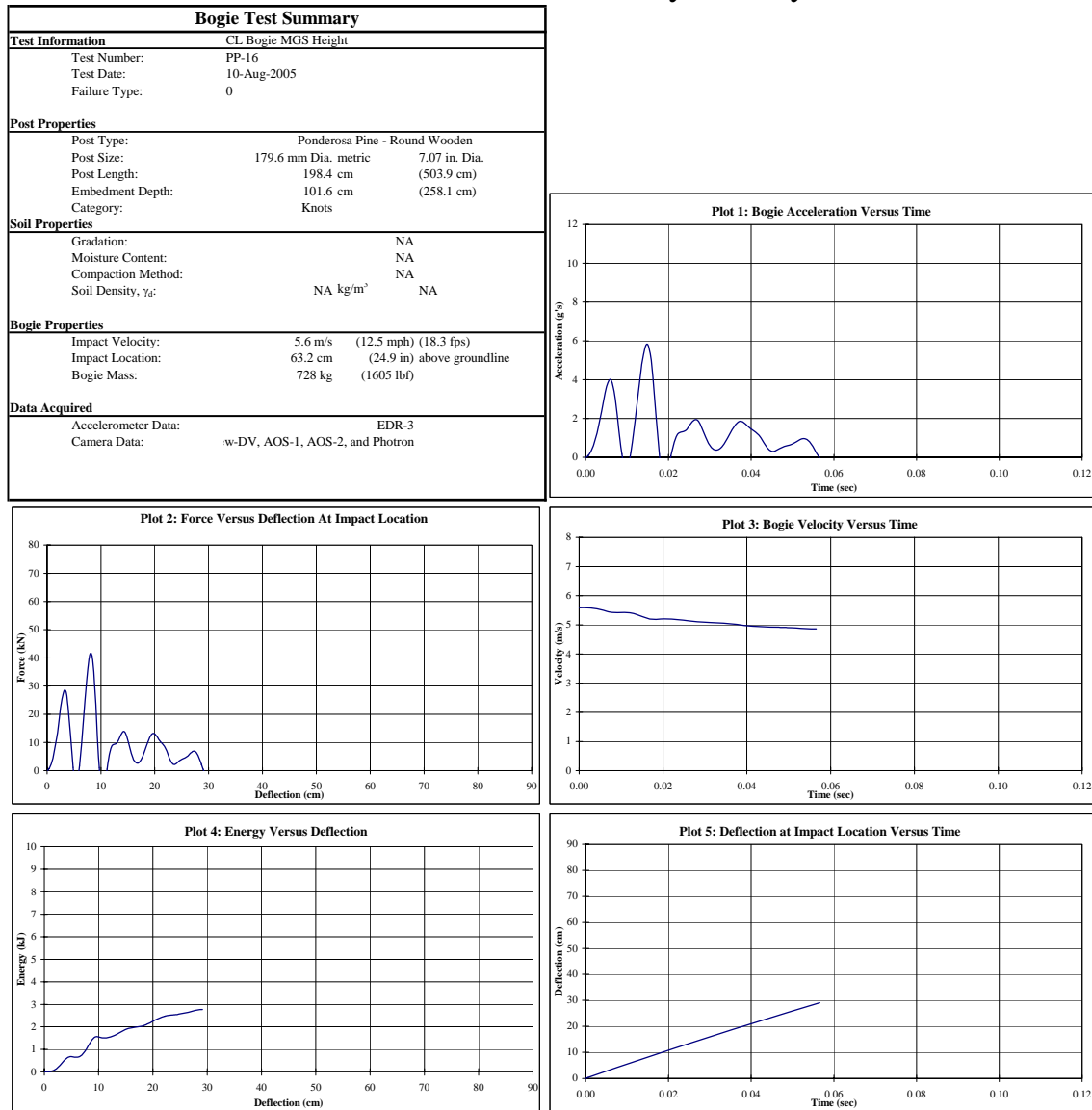


Figure E-16. Results of Test No. PP-16

Midwest Roadside Safety Facility

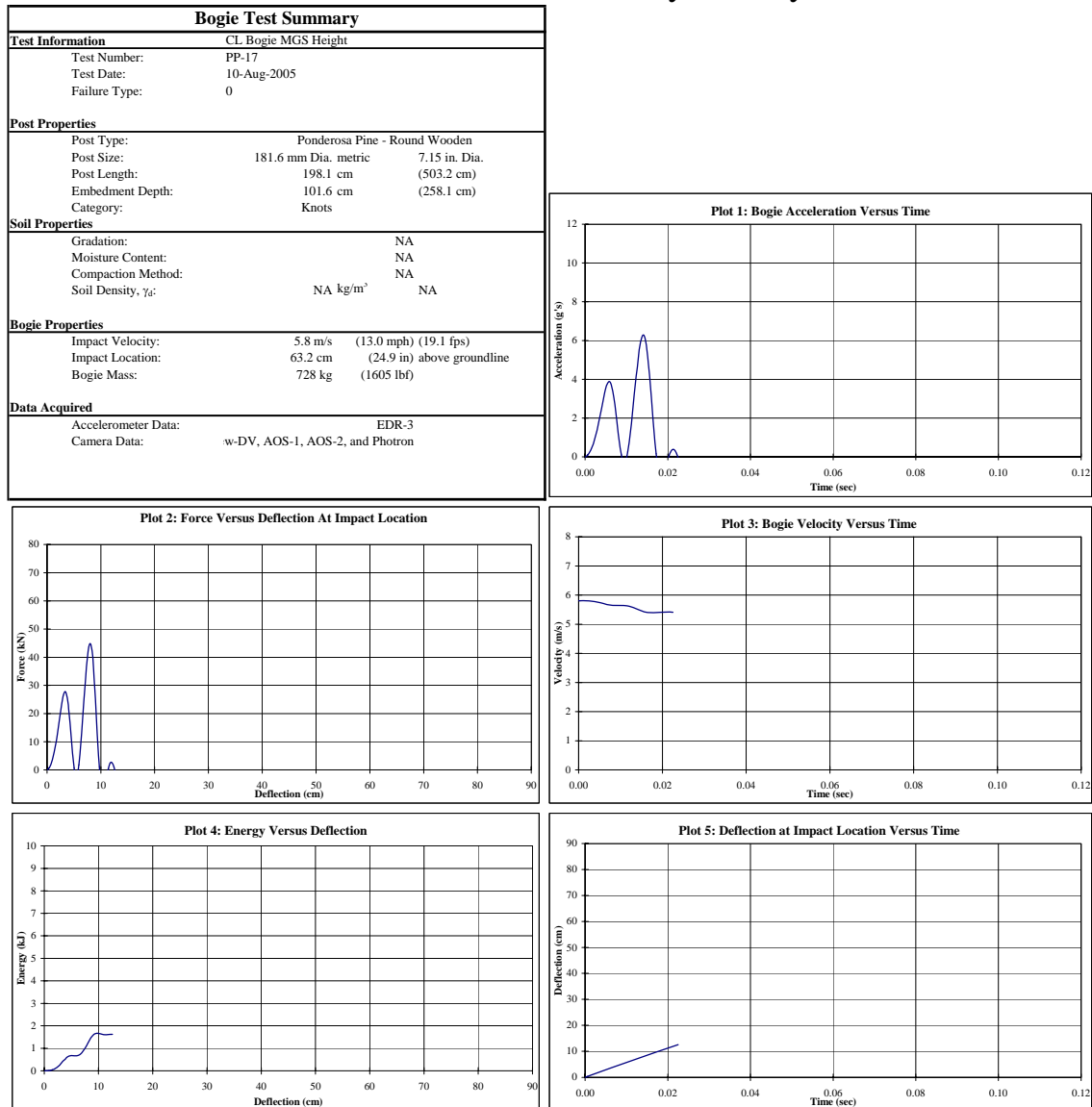


Figure E-17. Results of Test No. PP-17

Midwest Roadside Safety Facility

Bogie Test Summary	
Test Information	
Test Number:	PP-18
Test Date:	10-Aug-2005
Failure Type:	0
Post Properties	
Post Type:	Ponderosa Pine - Round Wooden
Post Size:	179.6 mm Dia. metric 7.07 in. Dia.
Post Length:	198.4 cm (503.9 cm)
Embedment Depth:	101.6 cm (258.1 cm)
Category:	Knots
Soil Properties	
Gradation:	NA
Moisture Content:	NA
Compaction Method:	NA
Soil Density, γ_d :	NA kg/m ³ NA
Bogie Properties	
Impact Velocity:	6.2 m/s (13.9 mph) (20.4 fps)
Impact Location:	63.2 cm (24.9 in) above groundline
Bogie Mass:	728 kg (1605 lbf)
Data Acquired	
Accelerometer Data:	EDR-3
Camera Data:	w-DV, AOS-1, AOS-2, and Photon

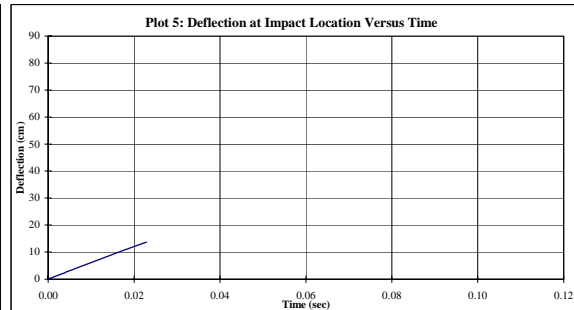
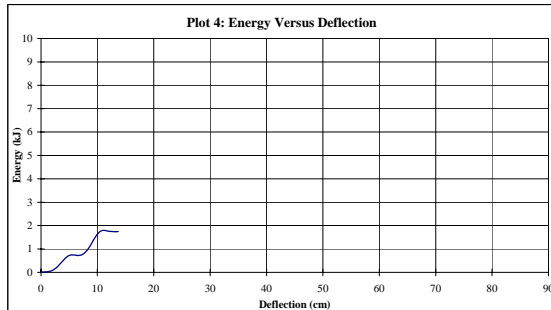
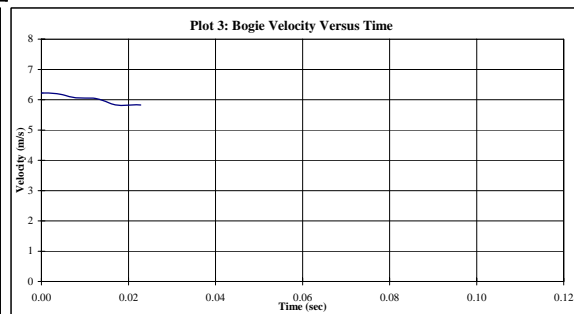
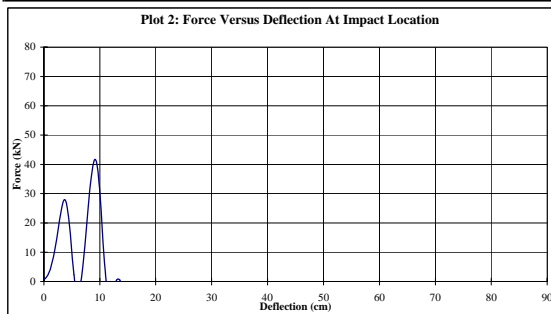
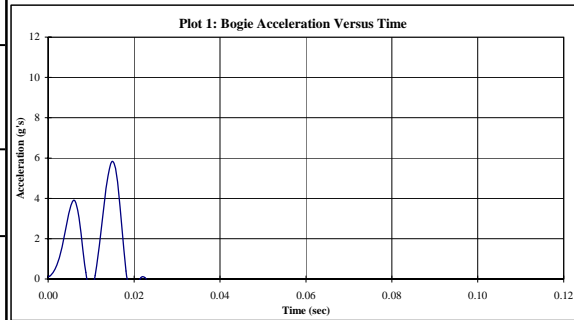


Figure E-18. Results of Test No. PP-18

Midwest Roadside Safety Facility

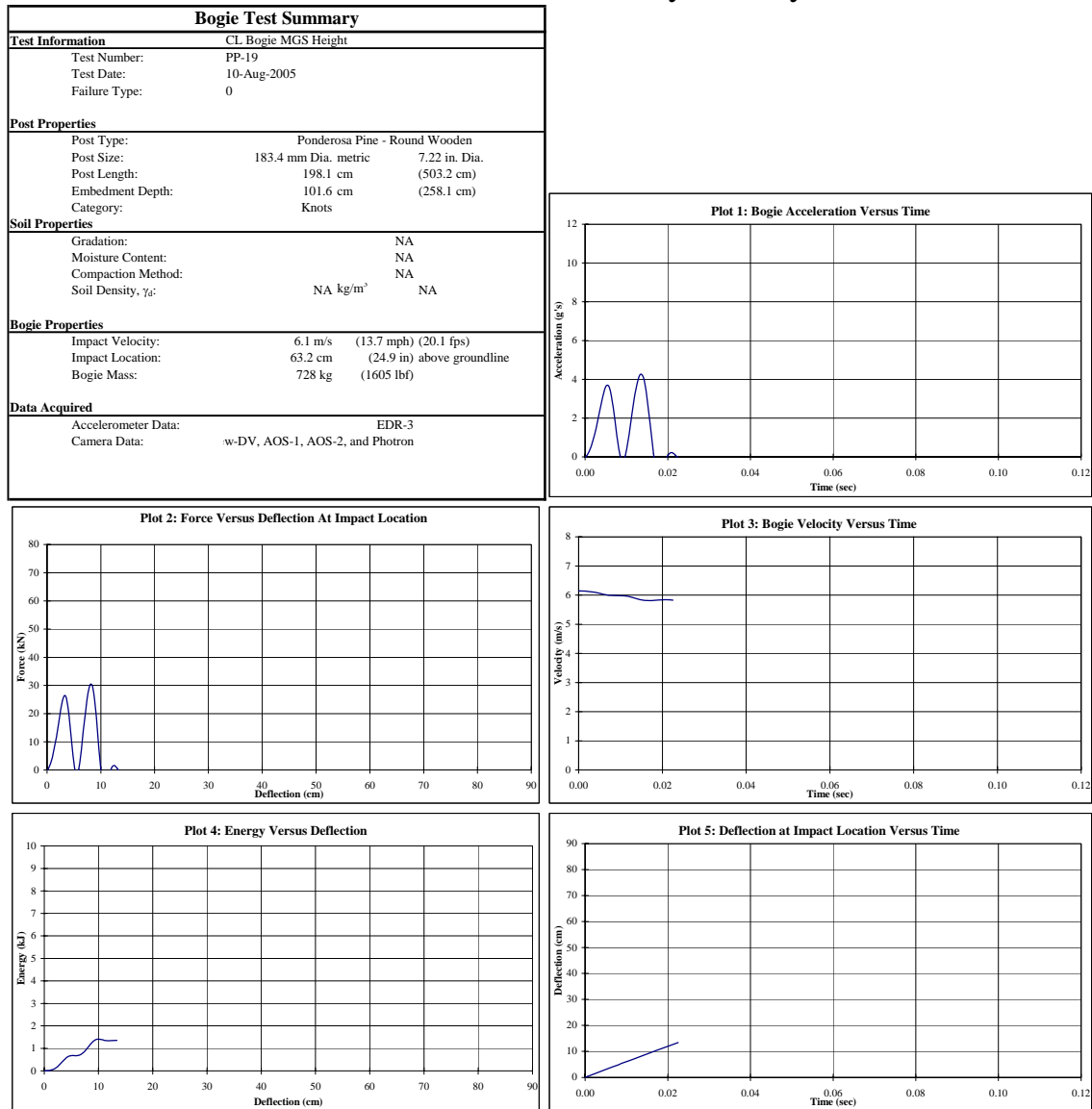


Figure E-19. Results of Test No. PP-19

Midwest Roadside Safety Facility

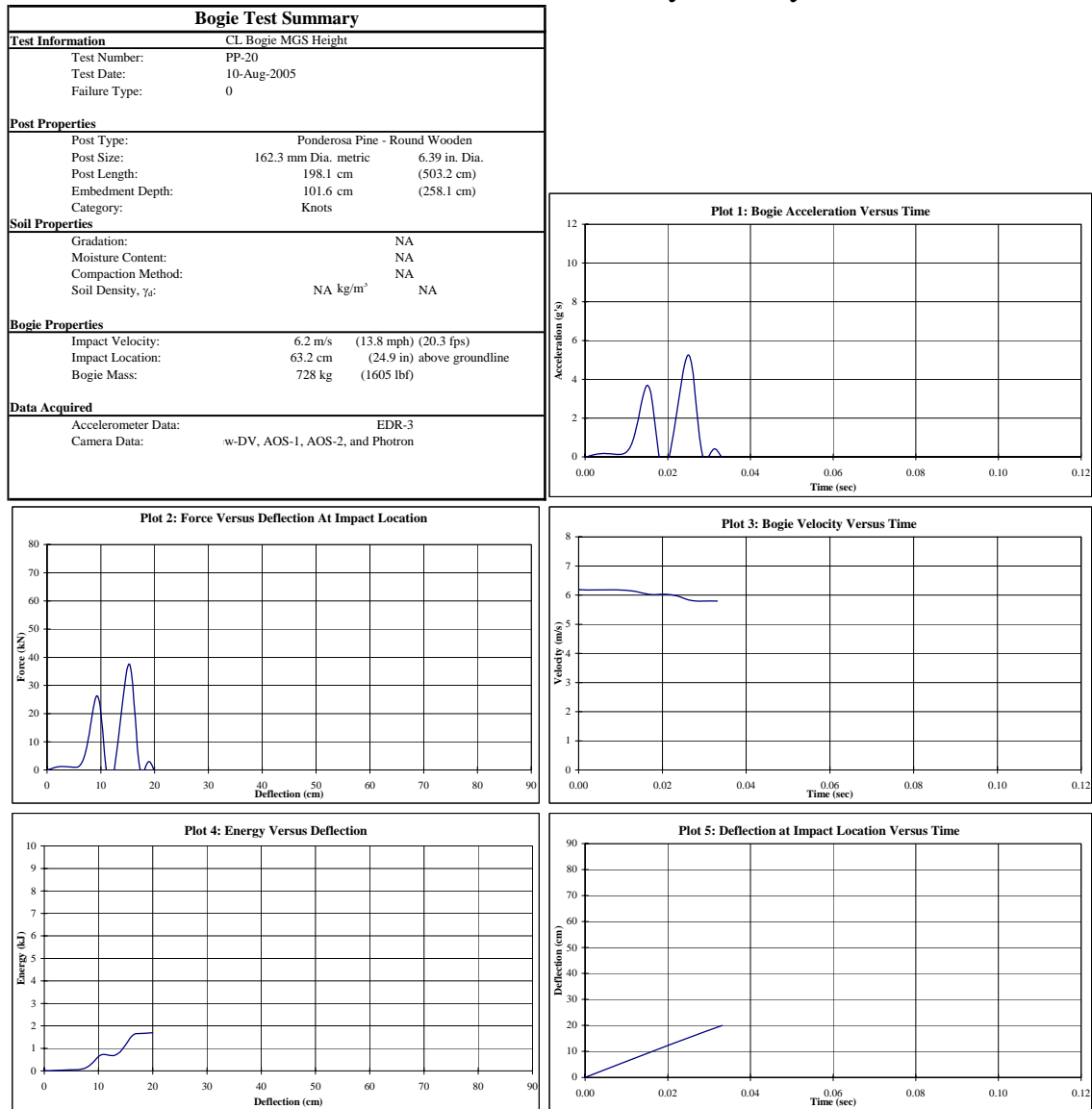


Figure E-20. Results of Test No. PP-20

Midwest Roadside Safety Facility

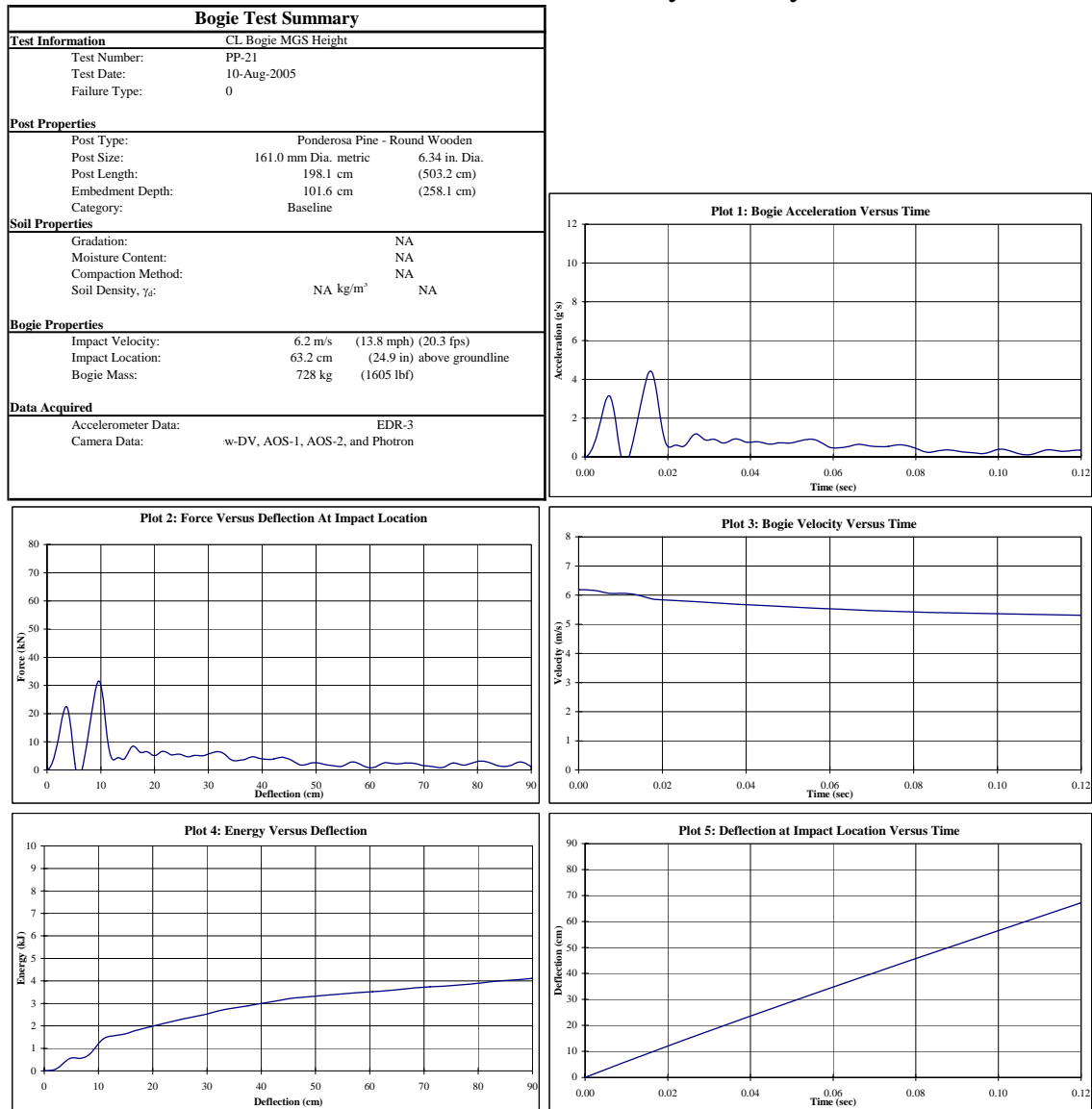


Figure E-21. Results of Test No. PP-21

Midwest Roadside Safety Facility

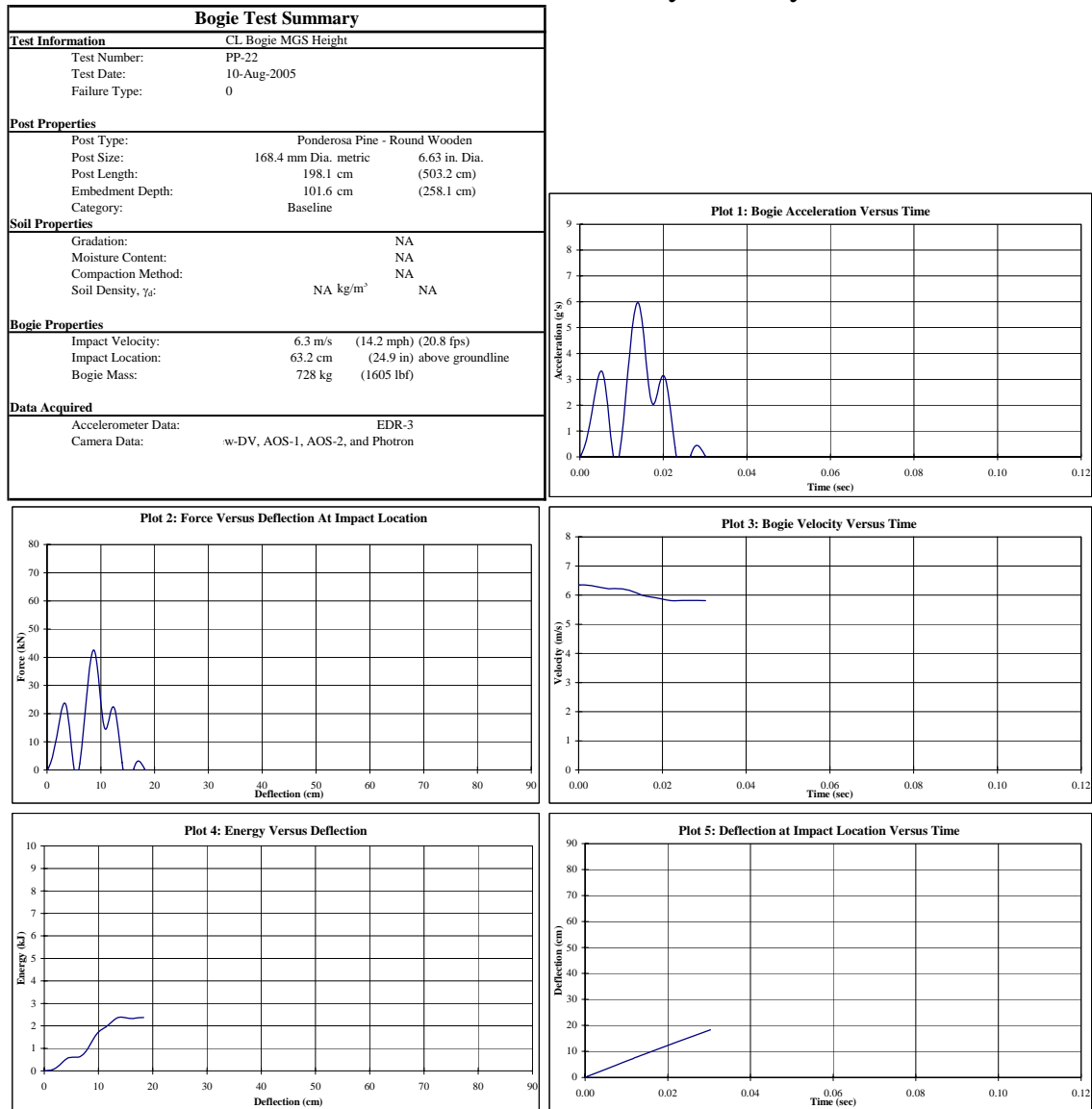


Figure E-22. Results of Test No. PP-22

Midwest Roadside Safety Facility

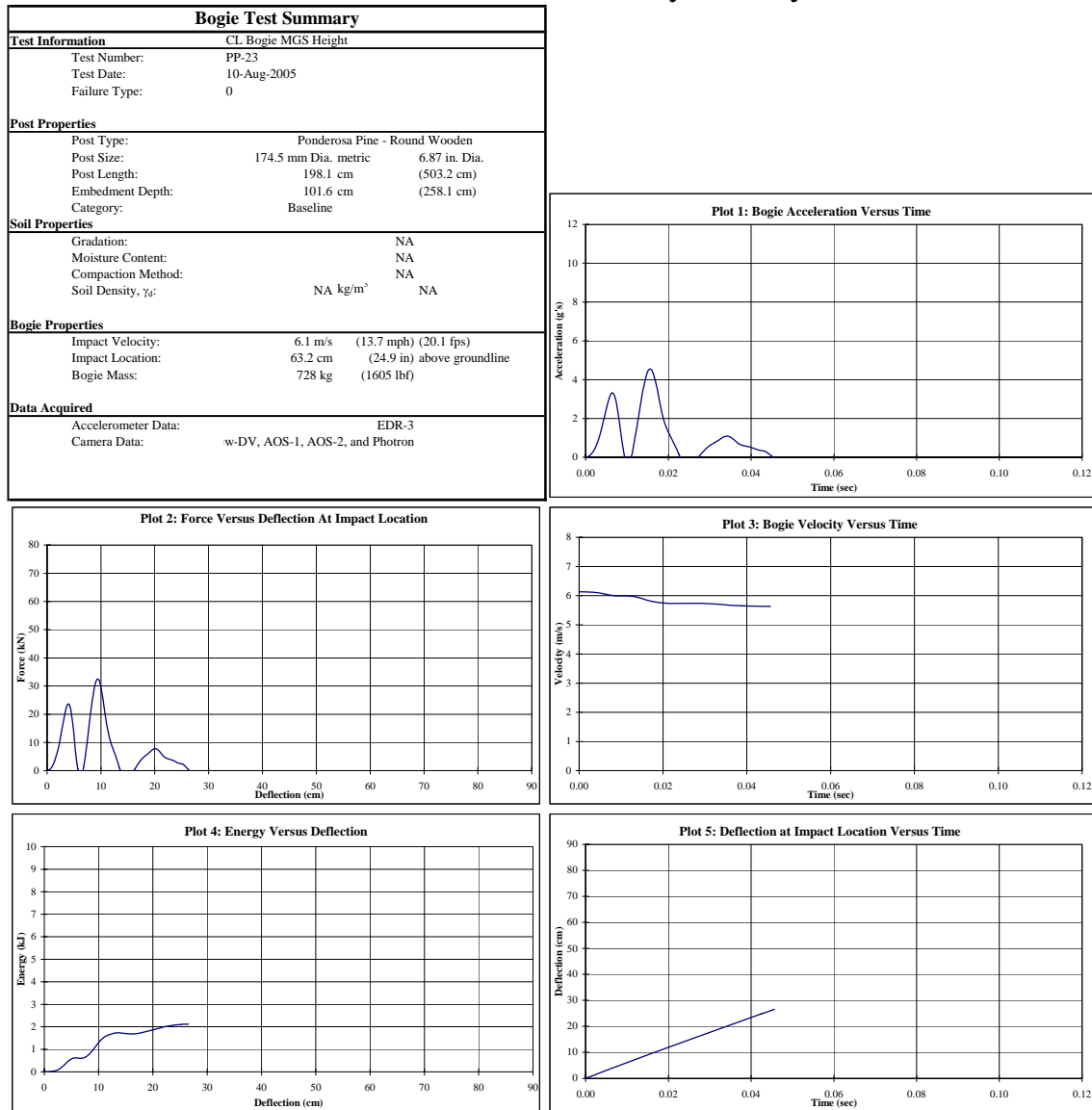


Figure E-23. Results of Test No. PP-23

Midwest Roadside Safety Facility

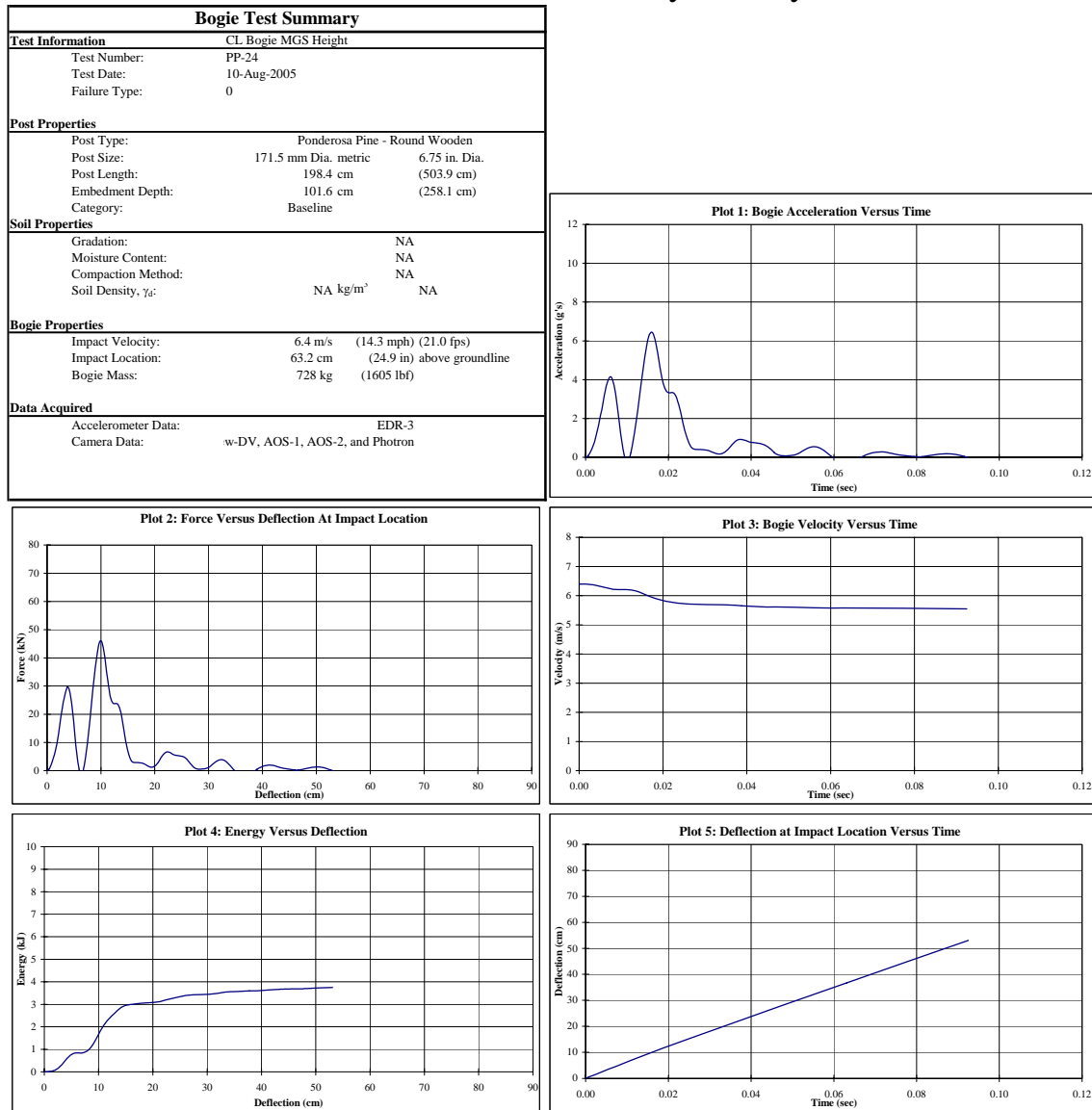


Figure E-24. Results of Test No. PP-24

Midwest Roadside Safety Facility

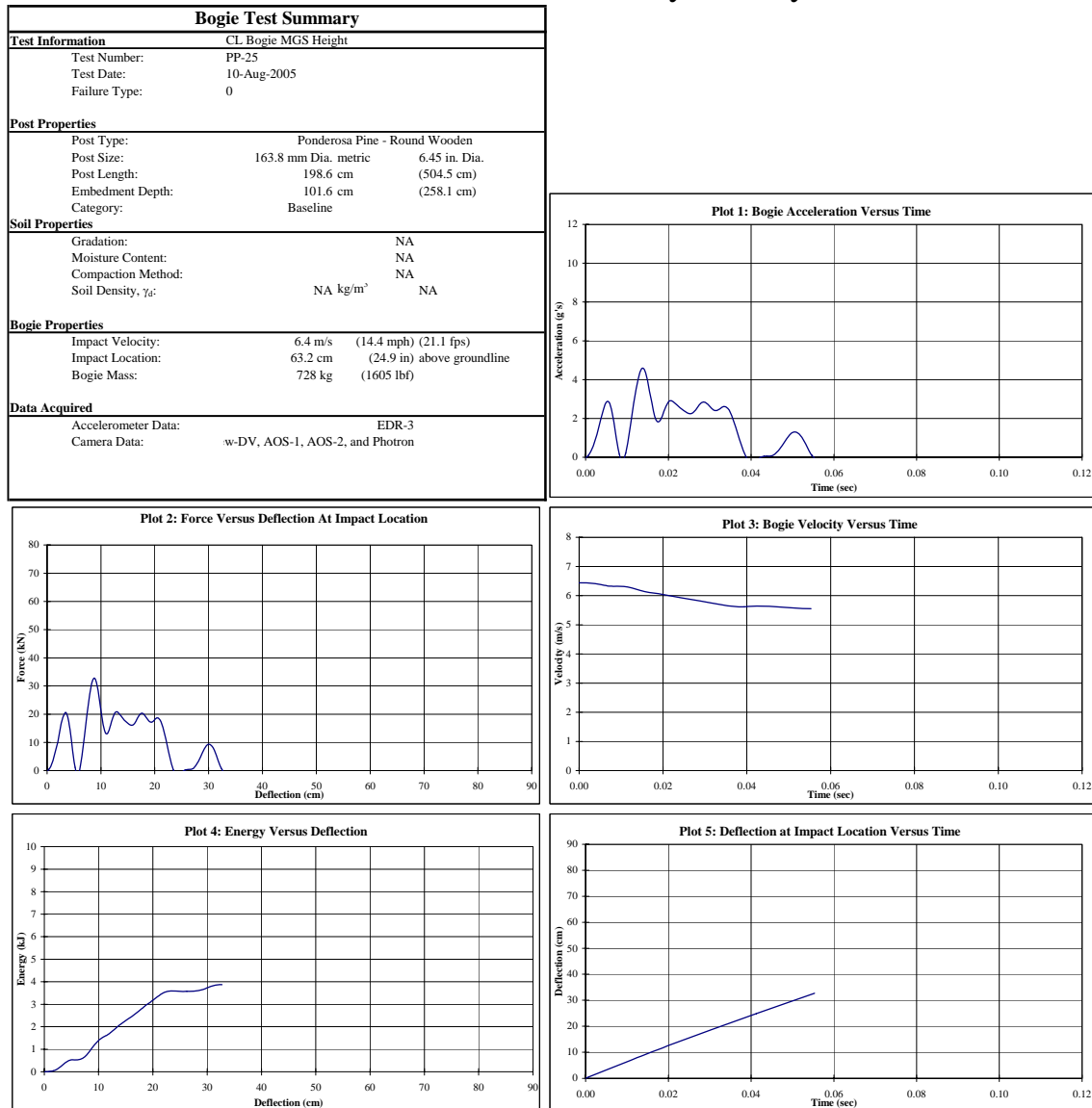


Figure E-25. Results of Test No. PP-25

Midwest Roadside Safety Facility

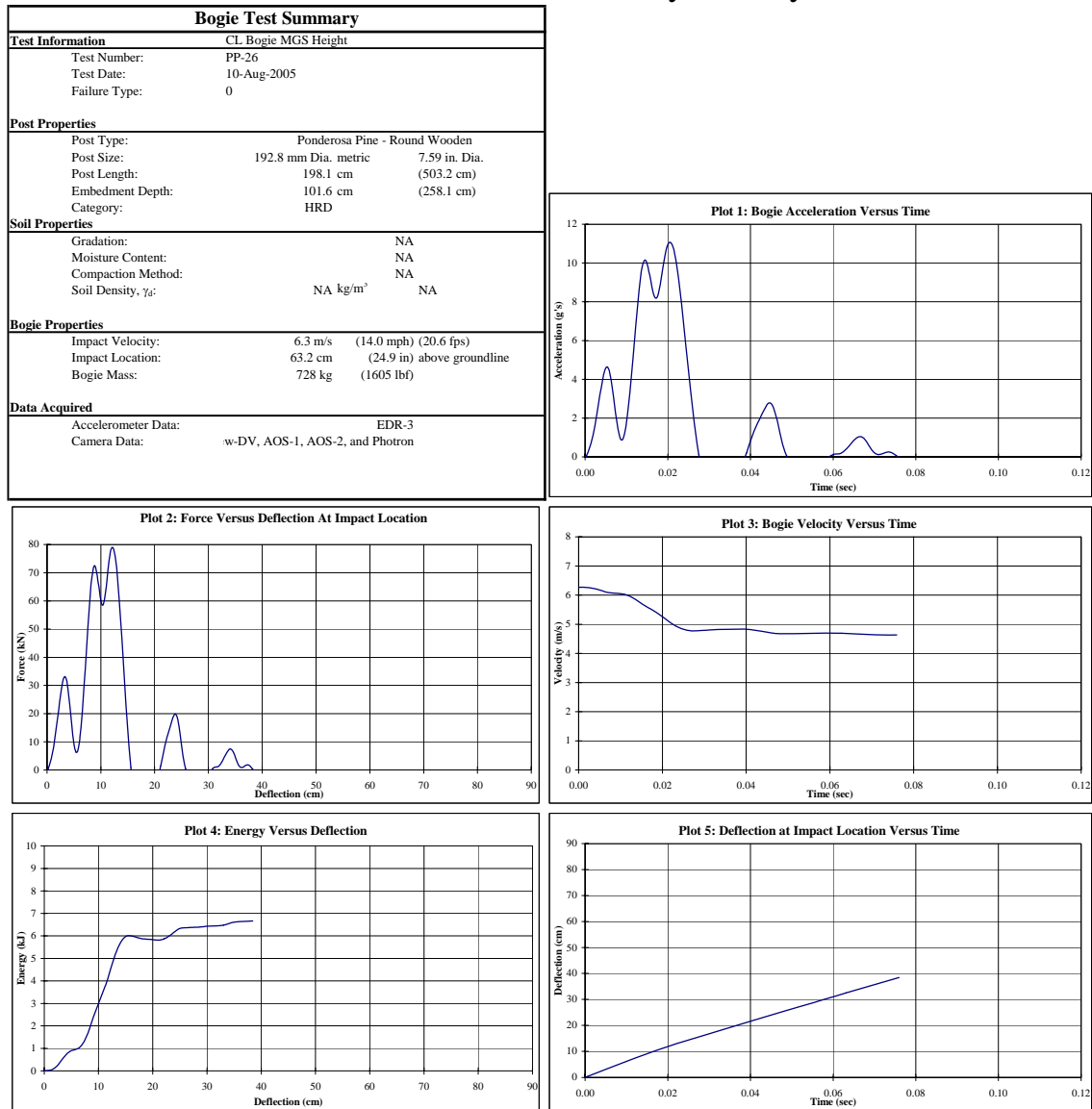


Figure E-26. Results of Test No. PP-26

Midwest Roadside Safety Facility

Bogie Test Summary	
Test Information	
Test Number:	PP-27
Test Date:	11-Aug-2005
Failure Type:	0
Post Properties	
Post Type:	Ponderosa Pine - Round Wooden
Post Size:	191.8 mm Dia. metric 7.55 in. Dia.
Post Length:	198.4 cm (503.9 cm)
Embedment Depth:	101.6 cm (258.1 cm)
Category:	HRD
Soil Properties	
Gradation:	NA
Moisture Content:	NA
Compaction Method:	NA
Soil Density, γ_d :	NA kg/m ³ NA
Bogie Properties	
Impact Velocity:	5.8 m/s (13.0 mph) (19.0 fps)
Impact Location:	63.2 cm (24.9 in) above groundline
Bogie Mass:	728 kg (1605 lbf)
Data Acquired	
Accelerometer Data:	EDR-3
Camera Data:	w-DV, AOS-1, AOS-2, and Photon

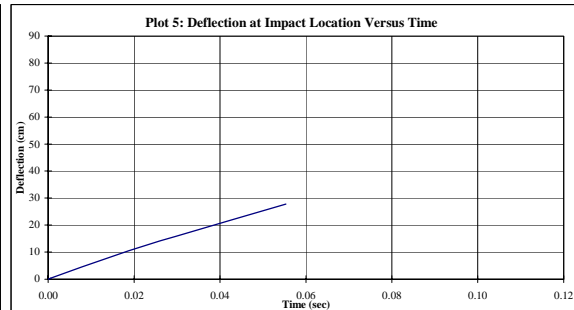
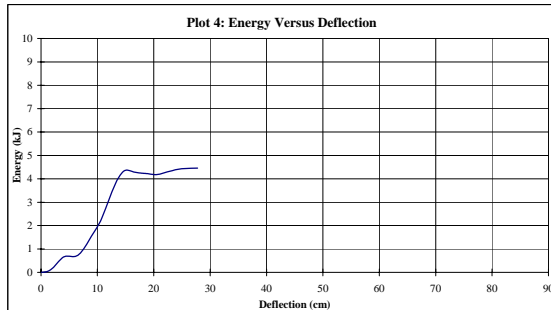
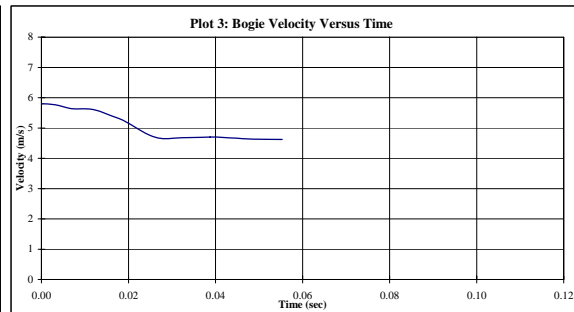
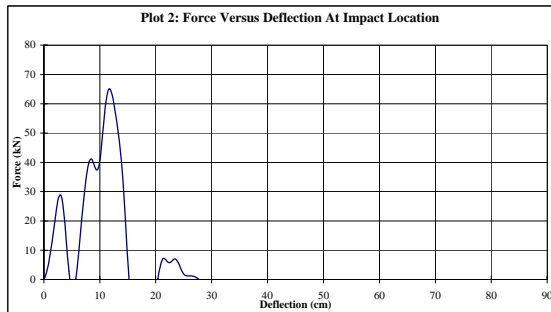
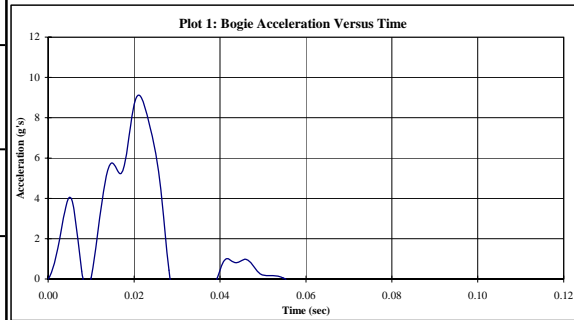


Figure E-27. Results of Test No. PP-27

Midwest Roadside Safety Facility

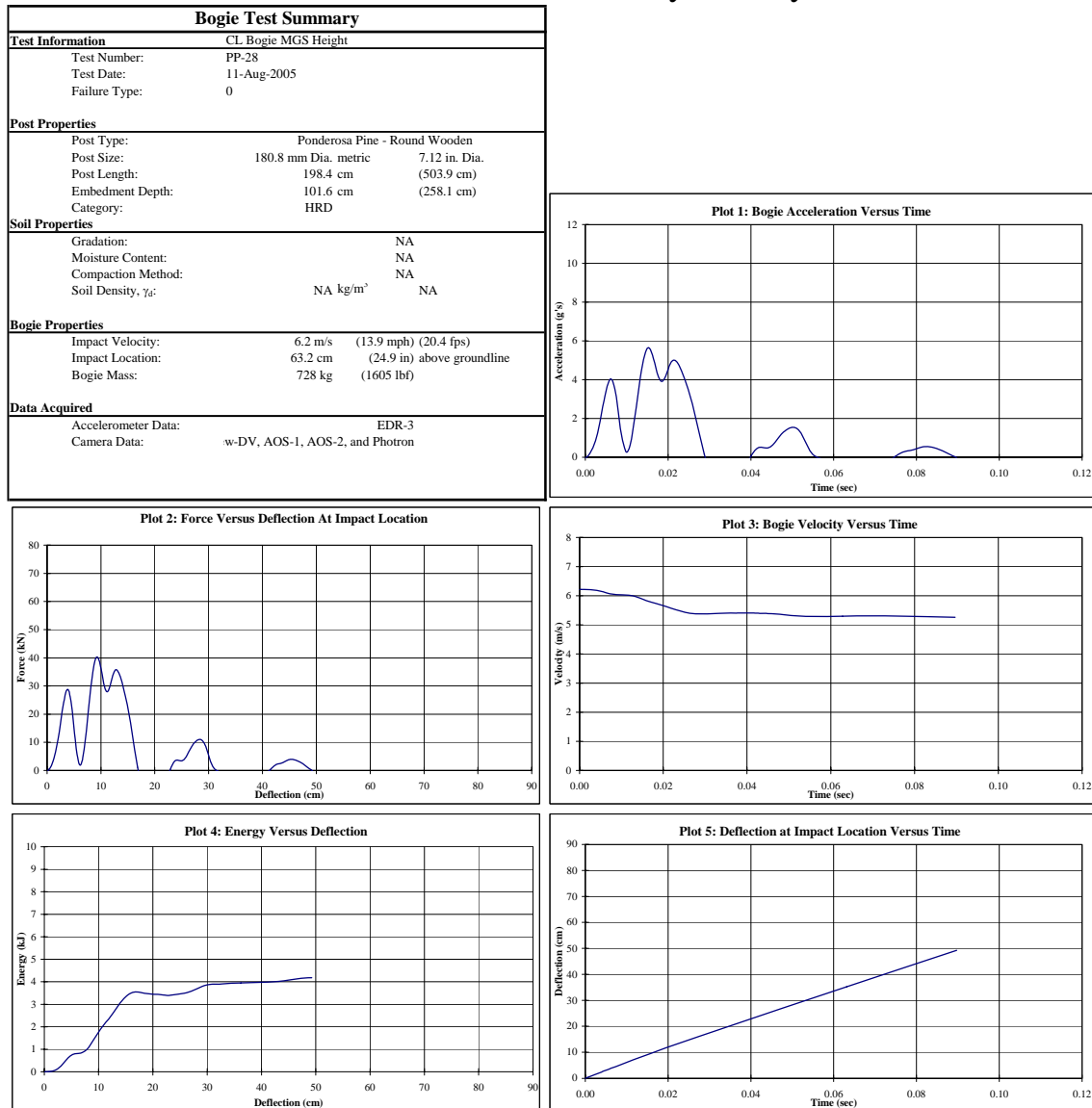


Figure E-28. Results of Test No. PP-28

Midwest Roadside Safety Facility

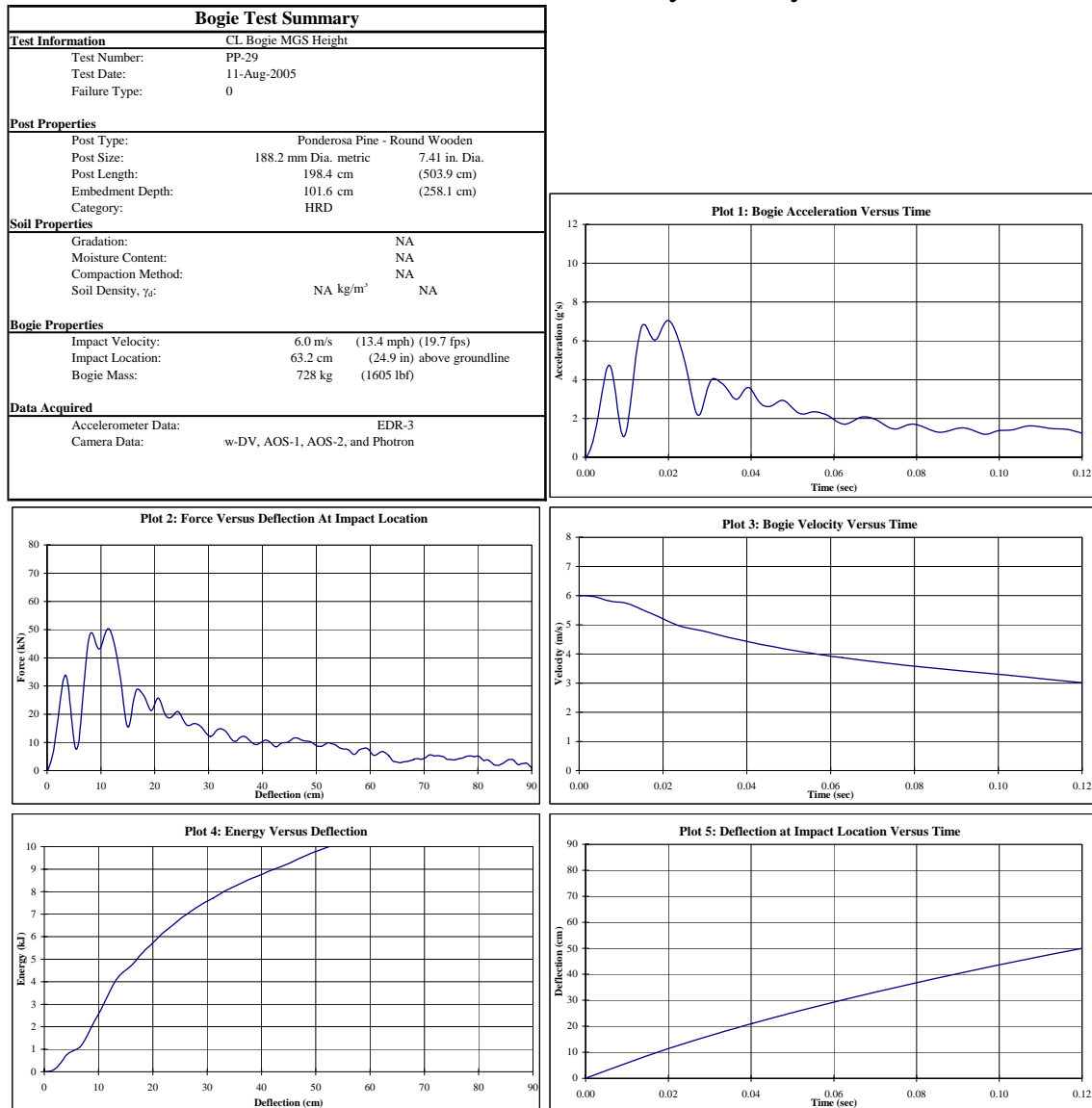


Figure E-29. Results of Test No. PP-29

Midwest Roadside Safety Facility

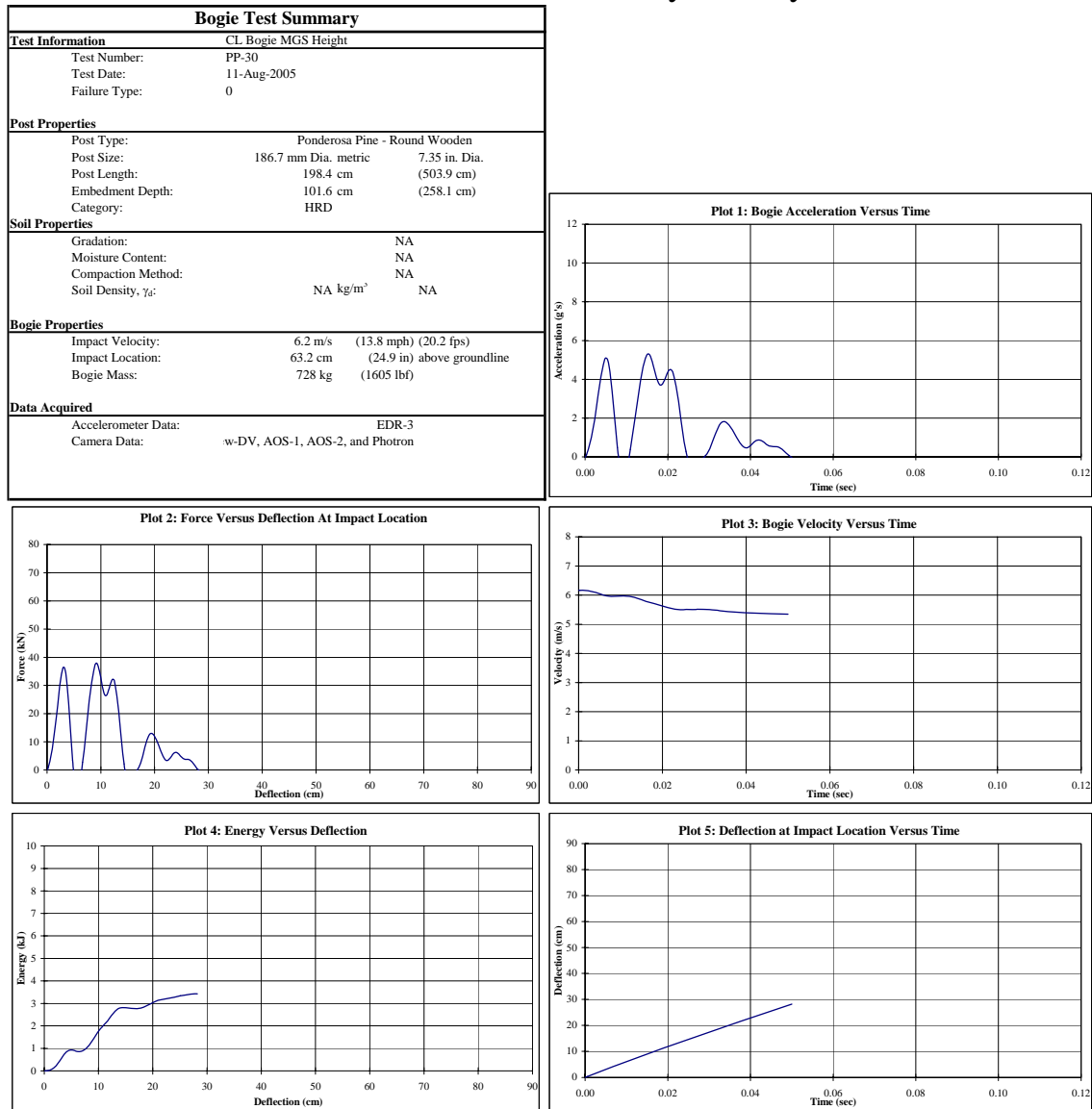


Figure E-30. Results of Test No. PP-30

Midwest Roadside Safety Facility

Bogie Test Summary		
Test Information		
Test Number:	CL Bogie MGS Height	
Test Date:	SY-16	
Failure Type:	10-Aug-2005	
	0	
Post Properties		
Post Type:	Southern Yellow Pine - Round Wooden	
Post Size:	181.9 mm Dia. metric	7.16 in. Dia.
Post Length:	188.0 cm	(477.4 cm)
Embedment Depth:	101.6 cm	(258.1 cm)
Category:	Knots	
Soil Properties		
Gradation:	NA	
Moisture Content:	NA	
Compaction Method:	NA	
Soil Density, γ_d :	NA kg/m ³	NA
Bogie Properties		
Impact Velocity:	5.9 m/s	(13.2 mph) (19.4 fps)
Impact Location:	63.2 cm	(24.9 in) above groundline
Bogie Mass:	728 kg	(1605 lbf)
Data Acquired		
Accelerometer Data:	EDR-3	
Camera Data:	w-DV, AOS-1, AOS-2, and Photron	

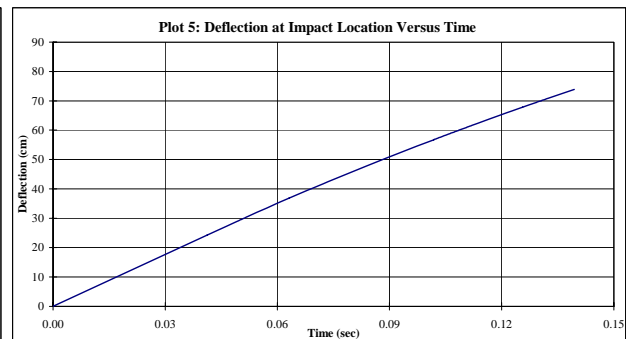
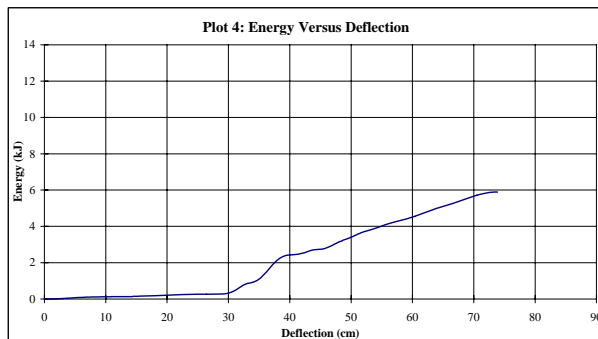
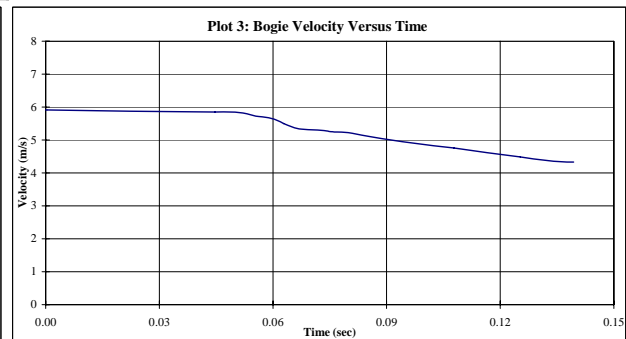
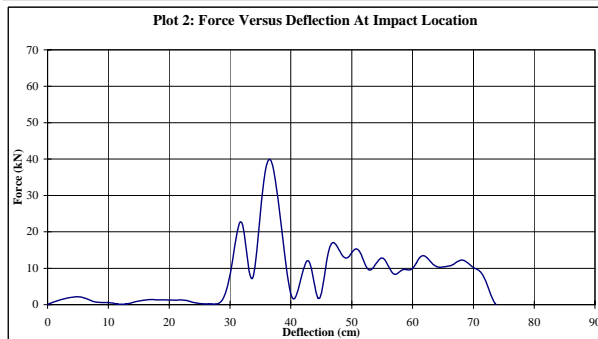
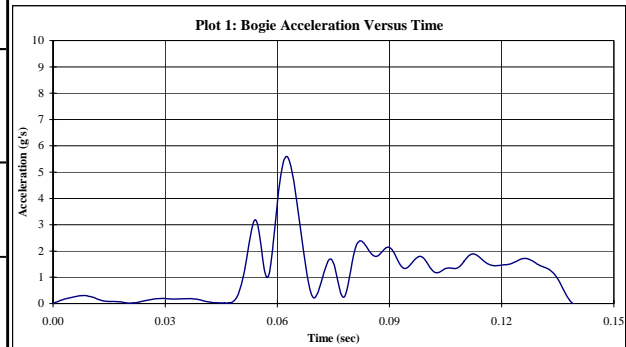


Figure E-31. Results of Test No. SY-16

Midwest Roadside Safety Facility

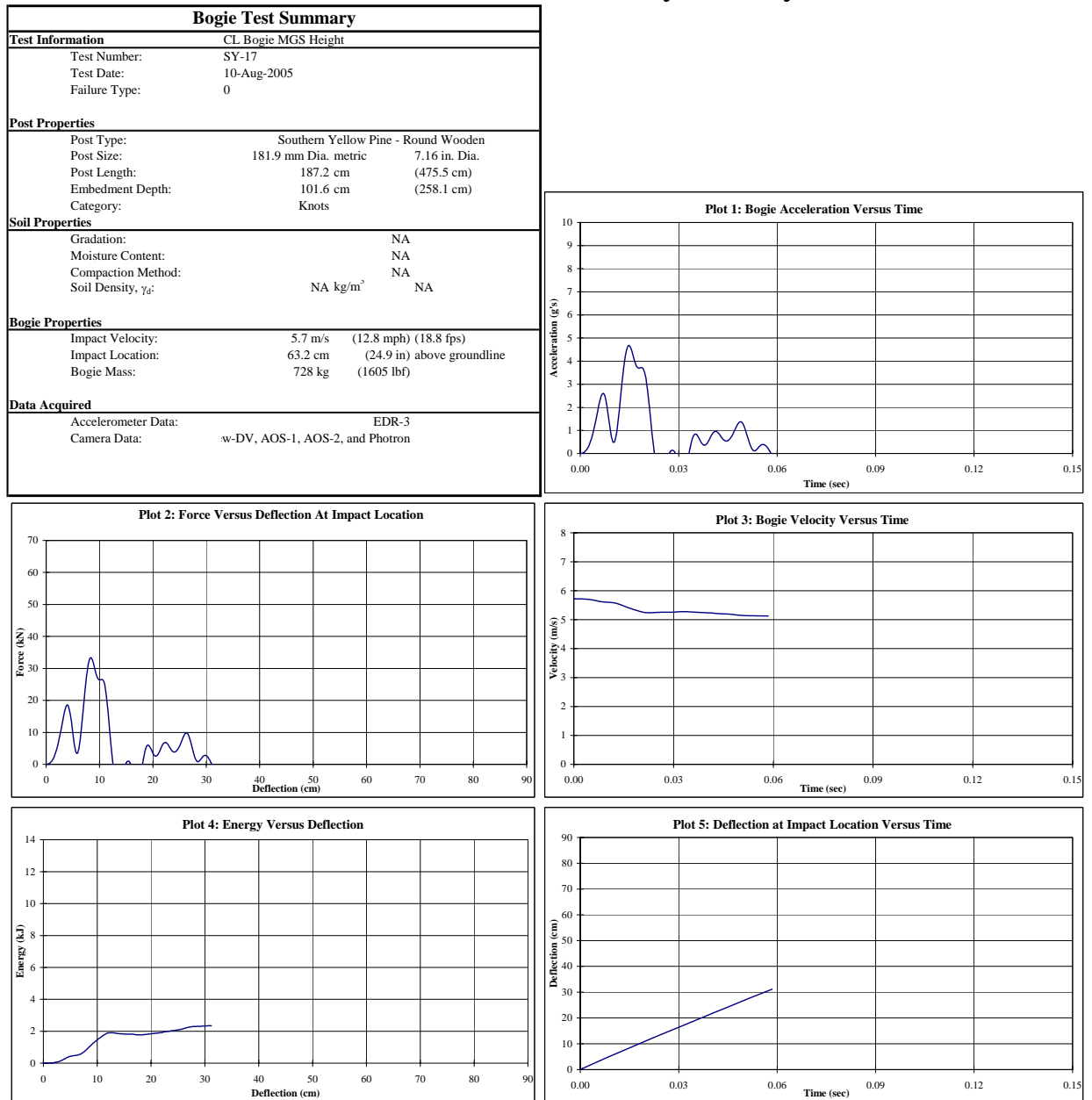


Figure E-32. Results of Test No. SY-17

Midwest Roadside Safety Facility

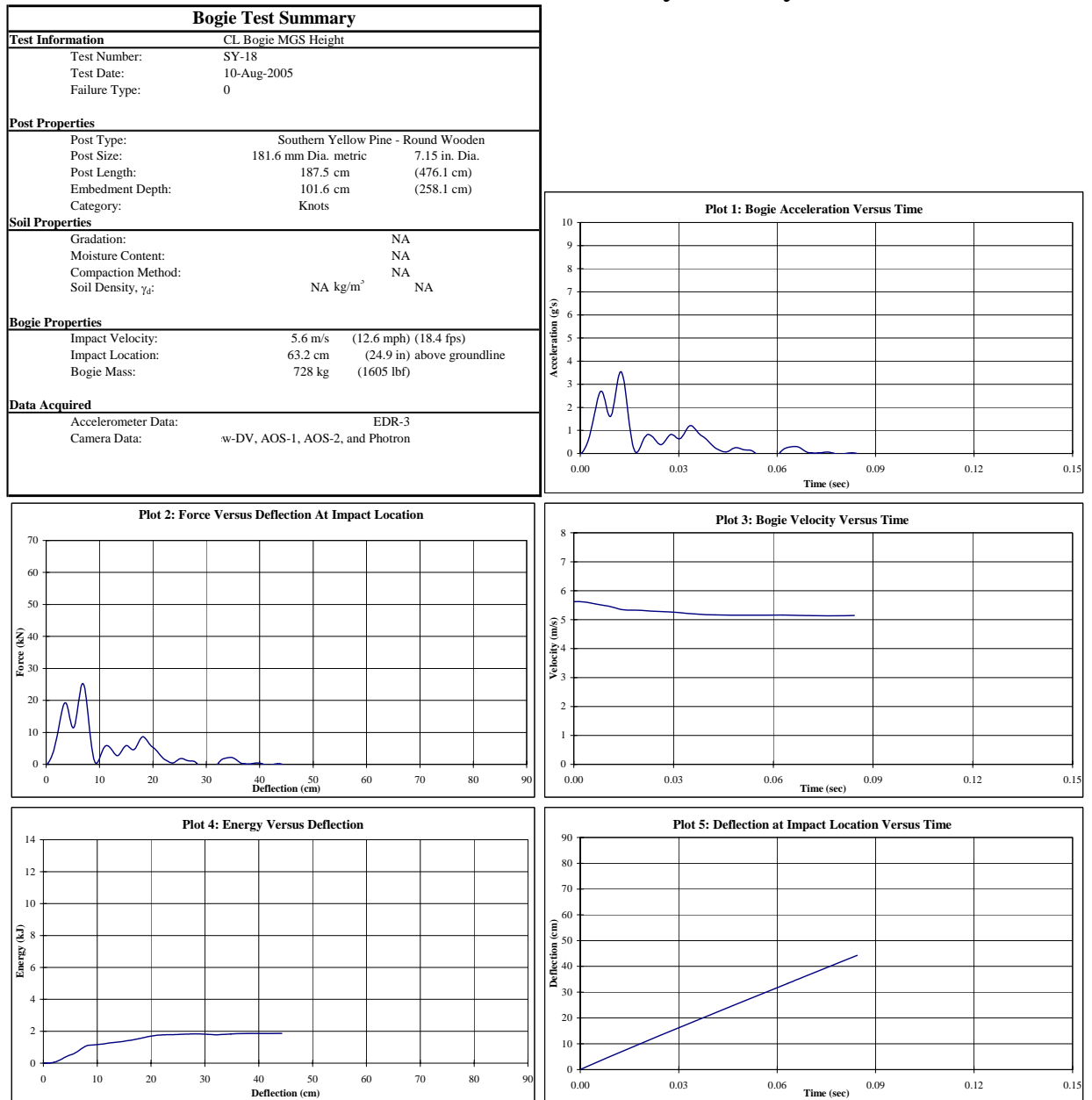


Figure E-33. Results of Test No. SY-18

Midwest Roadside Safety Facility

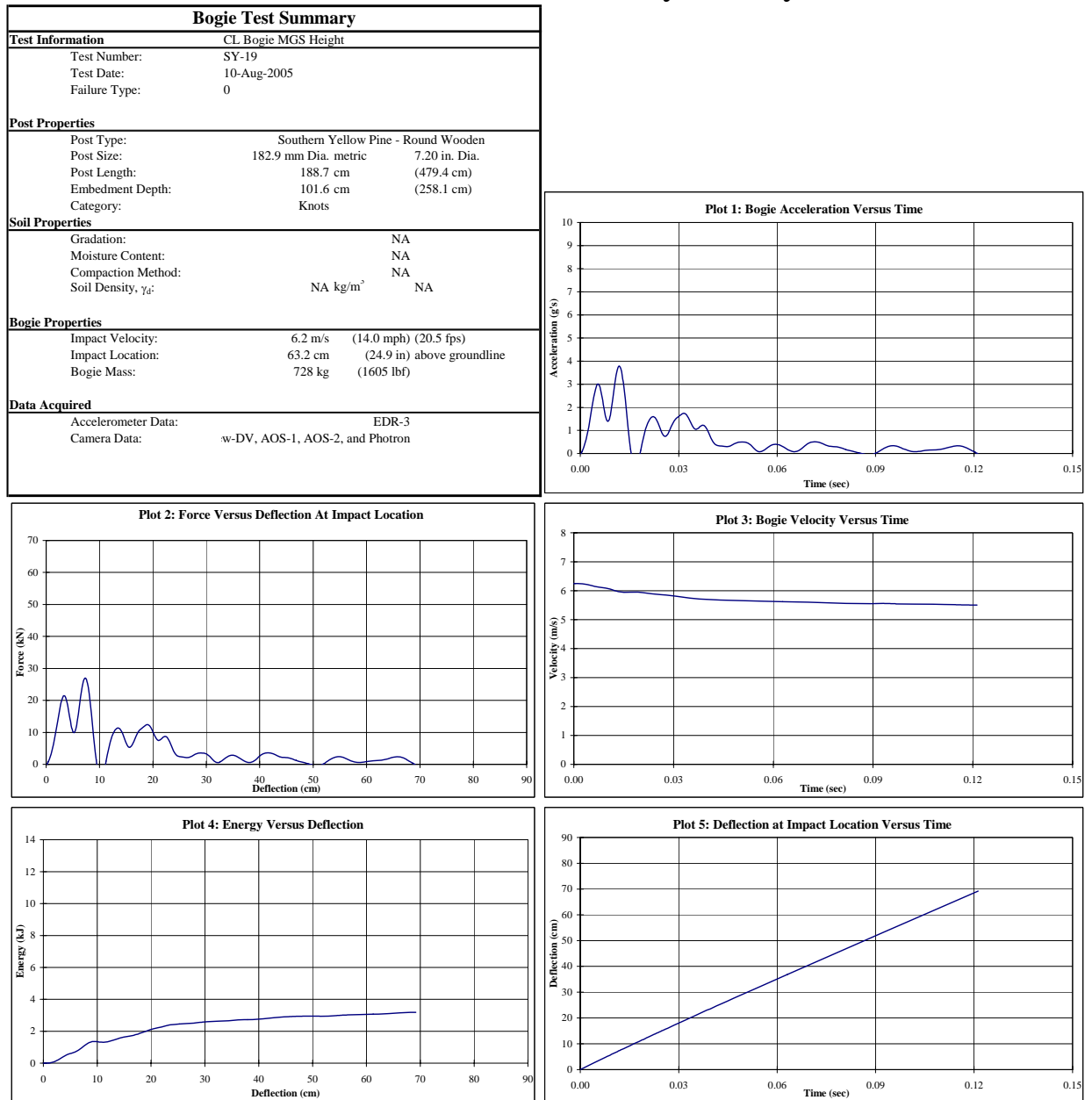


Figure E-34. Results of Test No. SY-19

Midwest Roadside Safety Facility

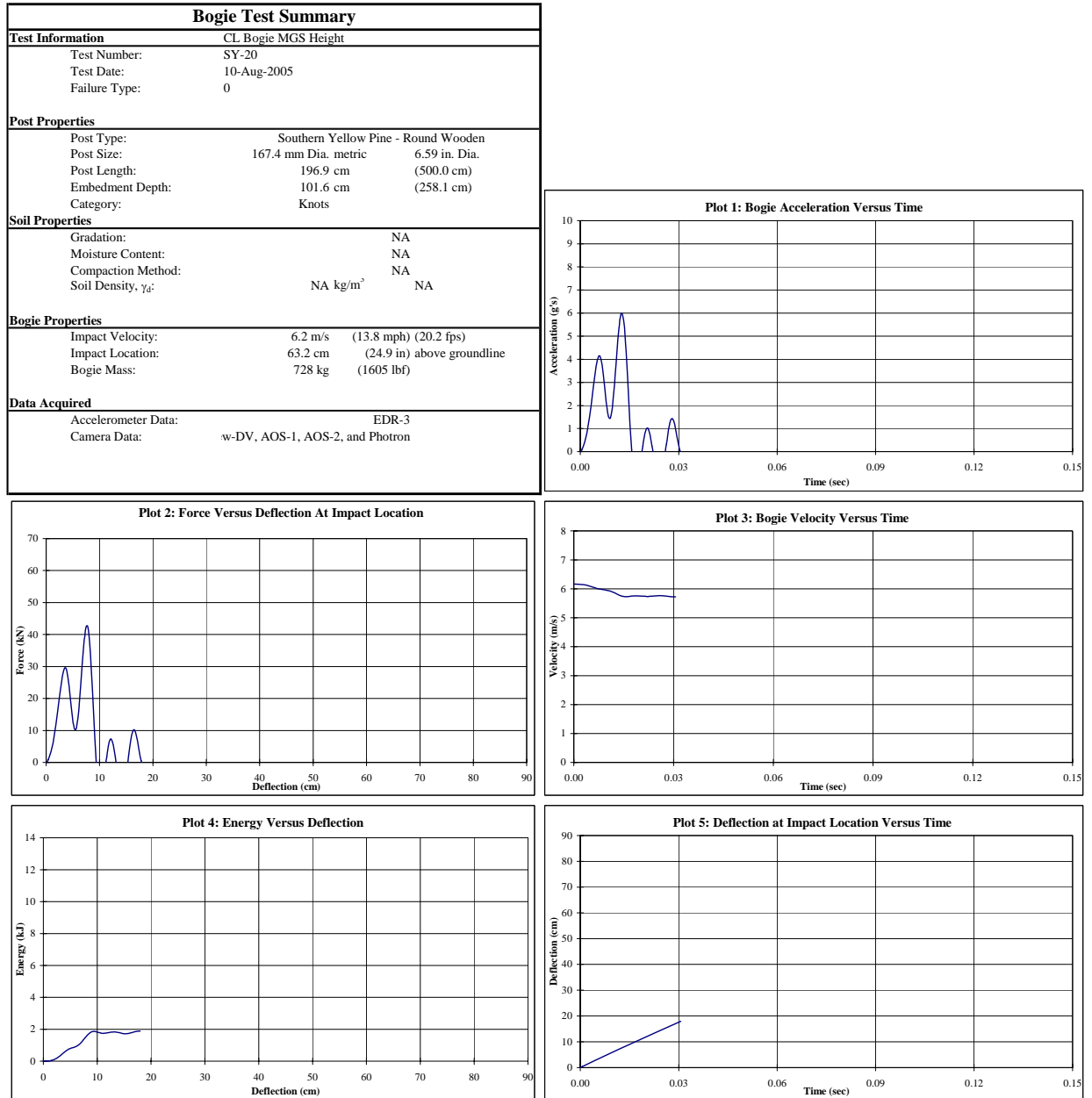


Figure E-35. Results of Test No. SY-20

Midwest Roadside Safety Facility

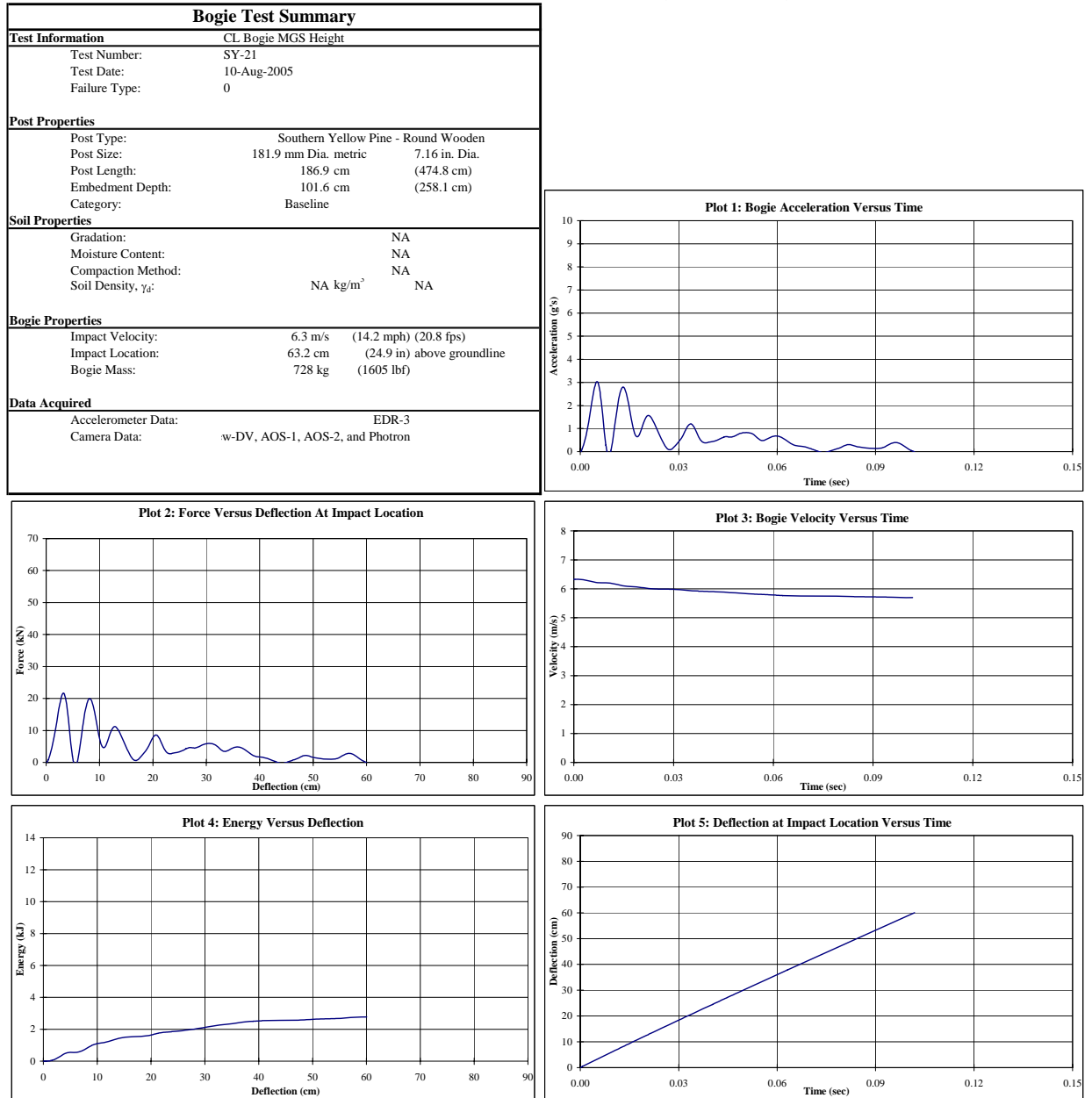


Figure E-36. Results of Test No. SY-21

Midwest Roadside Safety Facility

Bogie Test Summary		
Test Information		
Test Number:	CL Bogie MGS Height	
Test Date:	SY-22	
Failure Type:	10-Aug-2005	
	0	
Post Properties		
Post Type:	Southern Yellow Pine - Round Wooden	
Post Size:	181.9 mm Dia. metric	7.16 in. Dia.
Post Length:	188.0 cm	(477.4 cm)
Embedment Depth:	101.6 cm	(258.1 cm)
Category:	Baseline	
Soil Properties		
Gradation:	NA	
Moisture Content:	NA	
Compaction Method:	NA	
Soil Density, γ_d :	NA kg/m ³	NA
Bogie Properties		
Impact Velocity:	6.4 m/s	(14.4 mph) (21.1 fps)
Impact Location:	63.2 cm	(24.9 in) above groundline
Bogie Mass:	728 kg	(1605 lbf)
Data Acquired		
Accelerometer Data:	EDR-3	
Camera Data:	w-DV, AOS-1, AOS-2, and Photron	

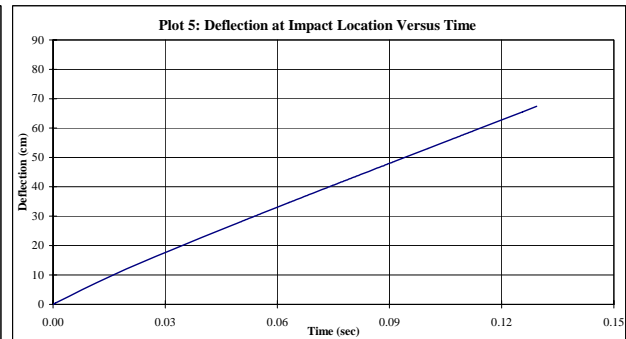
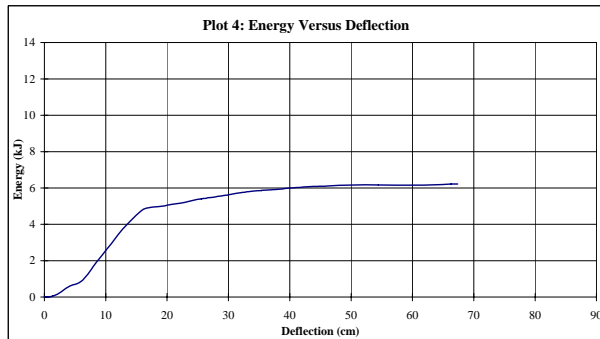
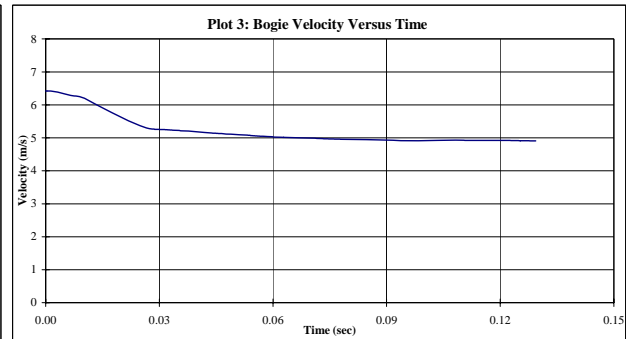
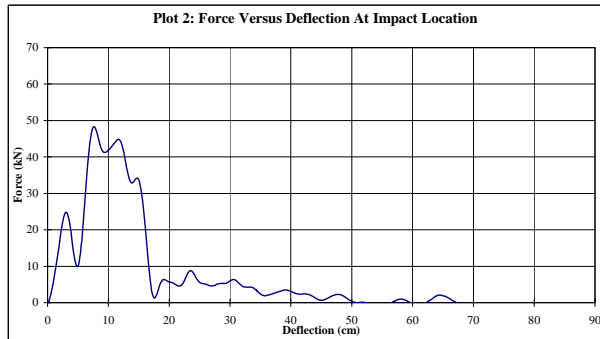
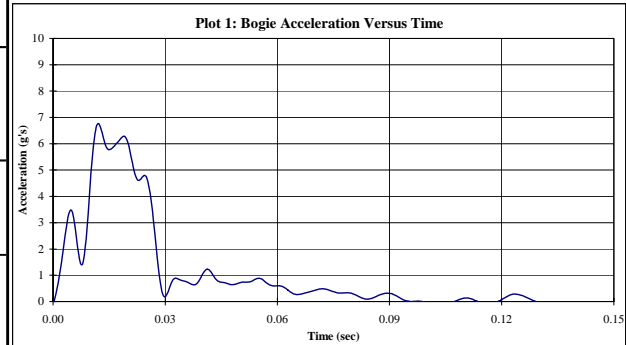


Figure E-37. Results of Test No. SY-22

Midwest Roadside Safety Facility

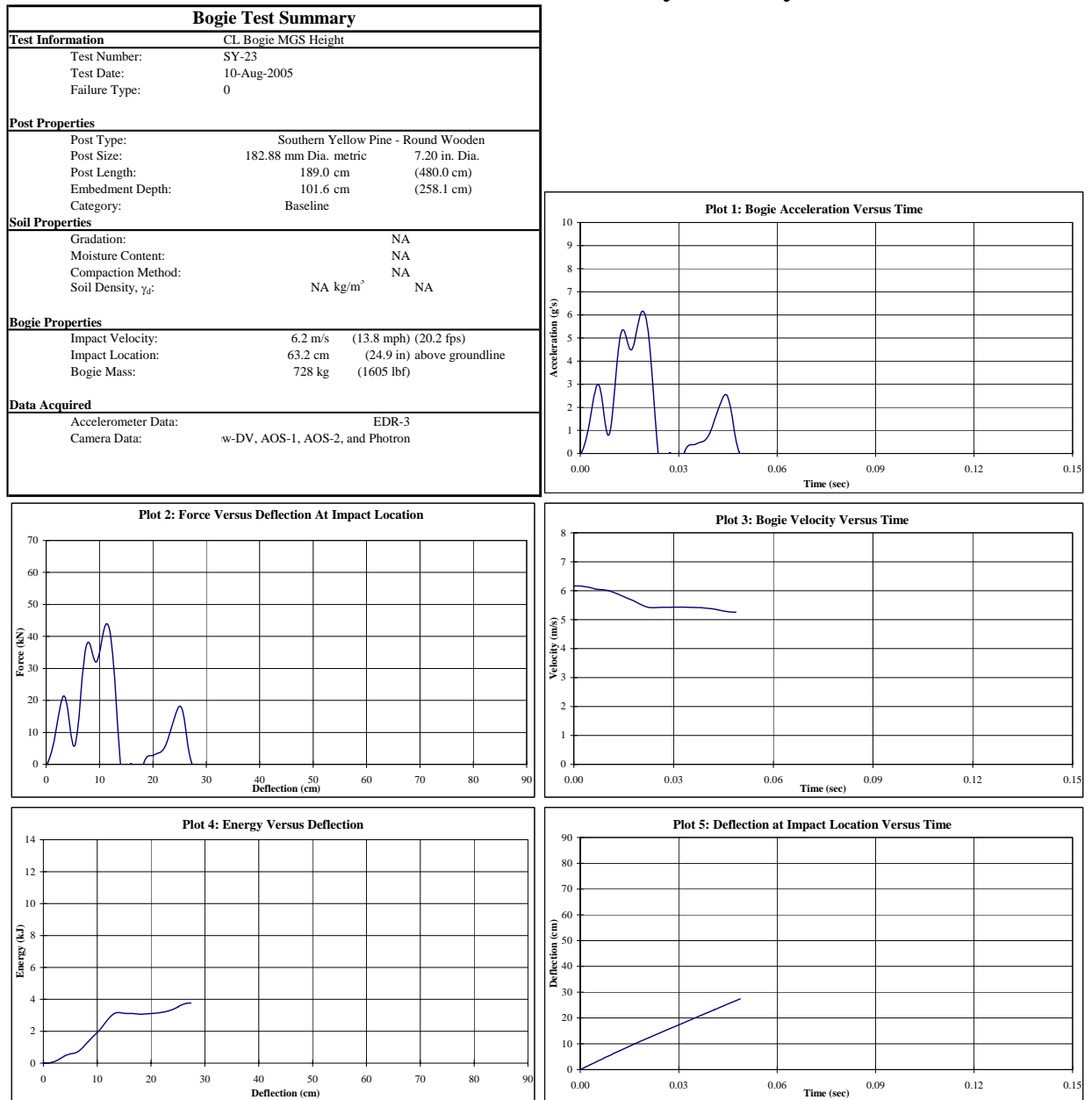


Figure E-38. Results of Test No. SY-23

Midwest Roadside Safety Facility

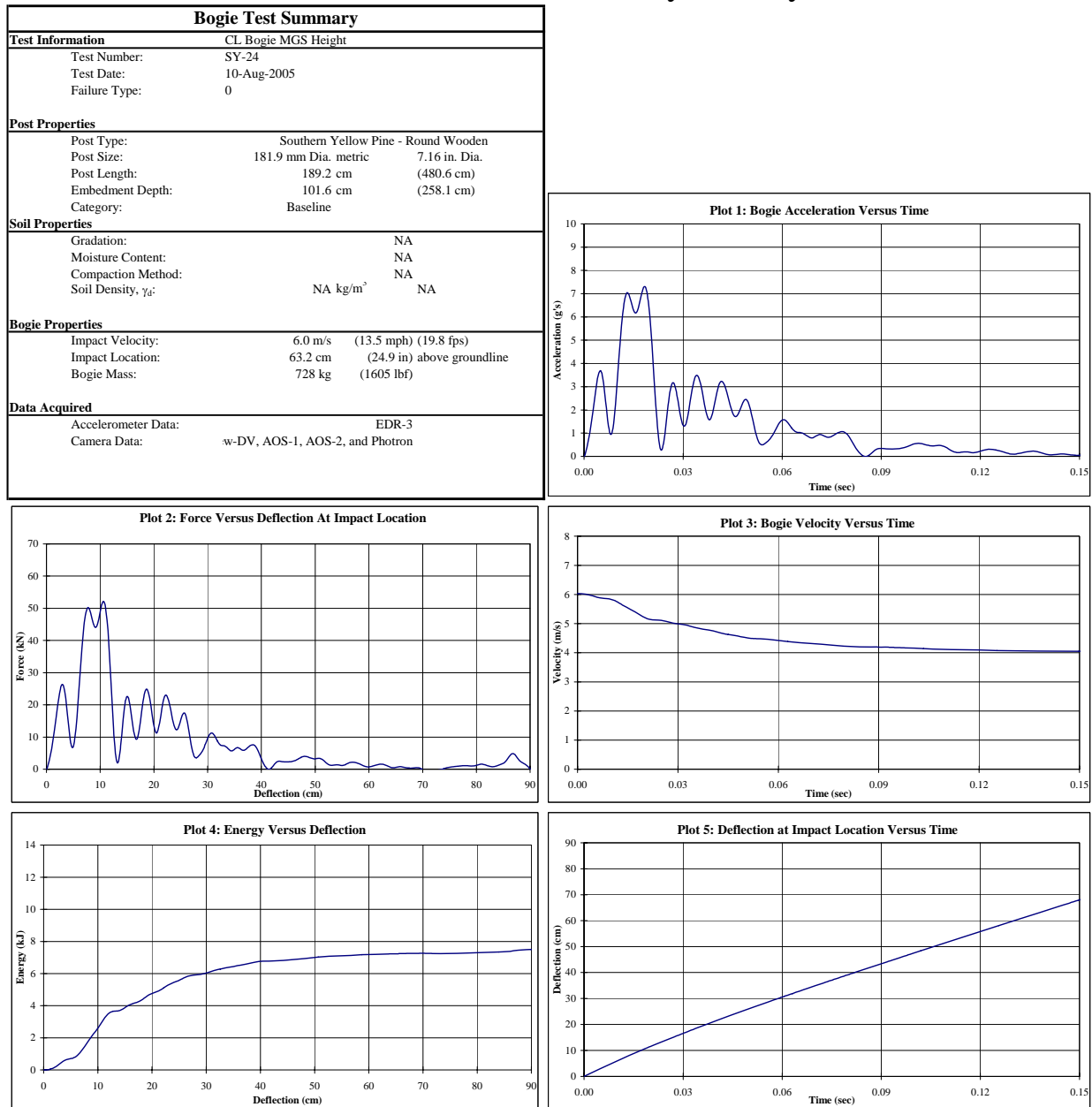


Figure E-39. Results of Test No. SY-24

Midwest Roadside Safety Facility

Bogie Test Summary		
Test Information		
Test Number:	CL Bogie MGS Height	
Test Date:	SY-25	
Failure Type:	10-Aug-2005	
	0	
Post Properties		
Post Type:	Southern Yellow Pine - Round Wooden	
Post Size:	184.9 mm Dia. metric	7.28 in. Dia.
Post Length:	186.7 cm	(474.2 cm)
Embedment Depth:	101.6 cm	(258.1 cm)
Category:	Baseline	
Soil Properties		
Gradation:	NA	
Moisture Content:	NA	
Compaction Method:	NA	
Soil Density, γ_d :	NA kg/m ³	NA
Bogie Properties		
Impact Velocity:	5.9 m/s	(13.3 mph) (19.4 fps)
Impact Location:	63.2 cm	(24.9 in) above groundline
Bogie Mass:	728 kg	(1605 lbf)
Data Acquired		
Accelerometer Data:	EDR-3	
Camera Data:	w-DV, AOS-1, AOS-2, and Photron	

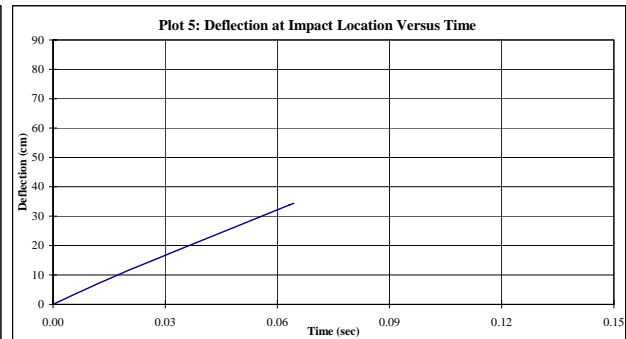
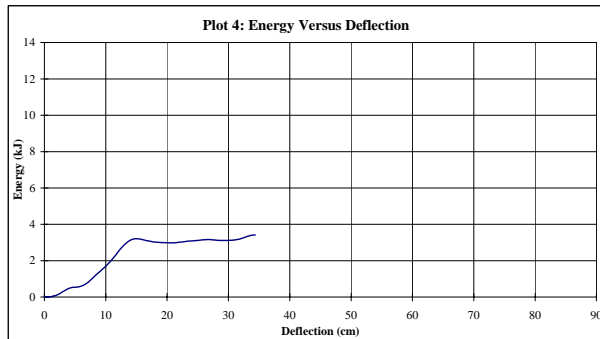
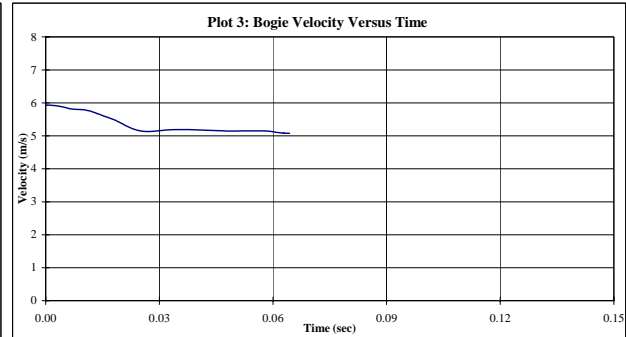
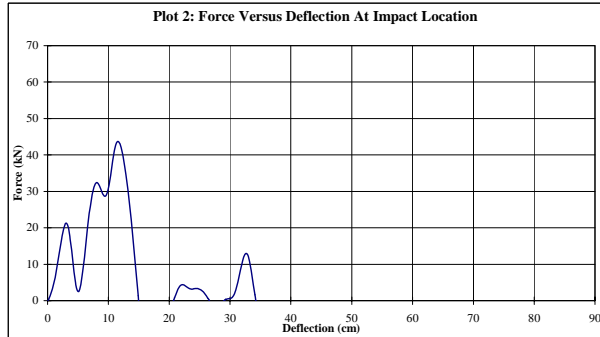
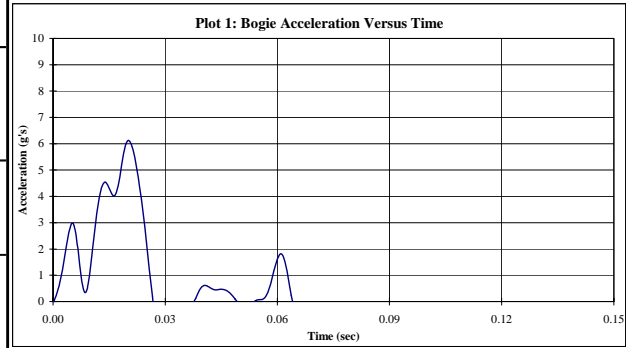


Figure E-40. Results of Test No. SY-25

Midwest Roadside Safety Facility

Bogie Test Summary		
Test Information		
Test Number:	CL Bogie MGS Height	
Test Date:	SY-26	
Failure Type:	10-Aug-2005	
	0	
Post Properties		
Post Type:	Southern Yellow Pine - Round Wooden	
Post Size:	180.8 mm Dia. metric	7.12 in. Dia.
Post Length:	198.9 cm	(505.2 cm)
Embedment Depth:	101.6 cm	(258.1 cm)
Category:	HRD	
Soil Properties		
Gradation:	NA	
Moisture Content:	NA	
Compaction Method:	NA	
Soil Density, γ_d :	NA kg/m ³	NA
Bogie Properties		
Impact Velocity:	6.1 m/s	(13.6 mph) (20.0 fps)
Impact Location:	63.2 cm	(24.9 in) above groundline
Bogie Mass:	728 kg	(1605 lbf)
Data Acquired		
Accelerometer Data:	EDR-3	
Camera Data:	w-DV, AOS-1, AOS-2, and Photron	

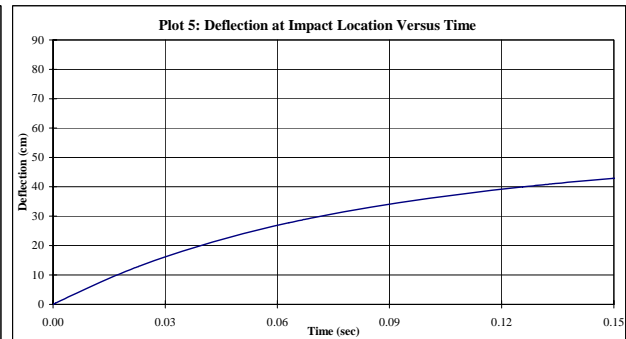
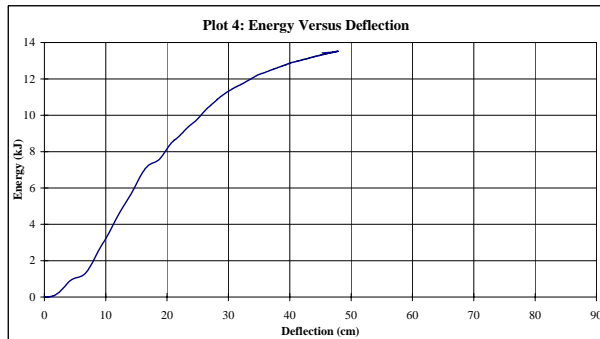
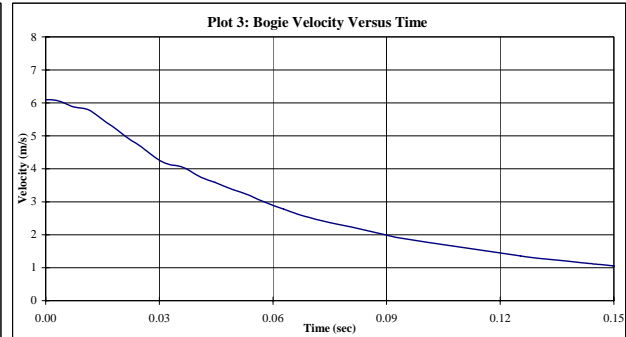
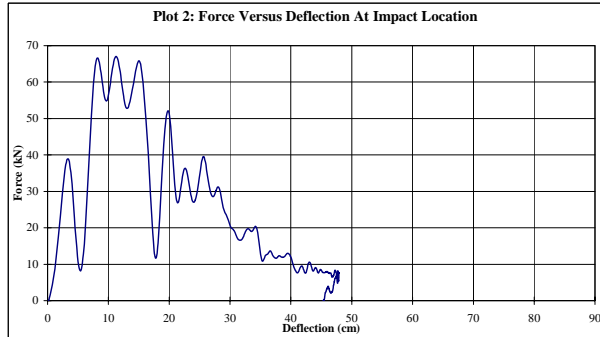
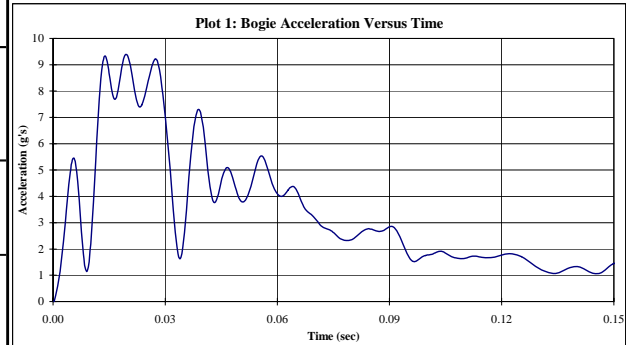


Figure E-41. Results of Test No. SY-26

Midwest Roadside Safety Facility

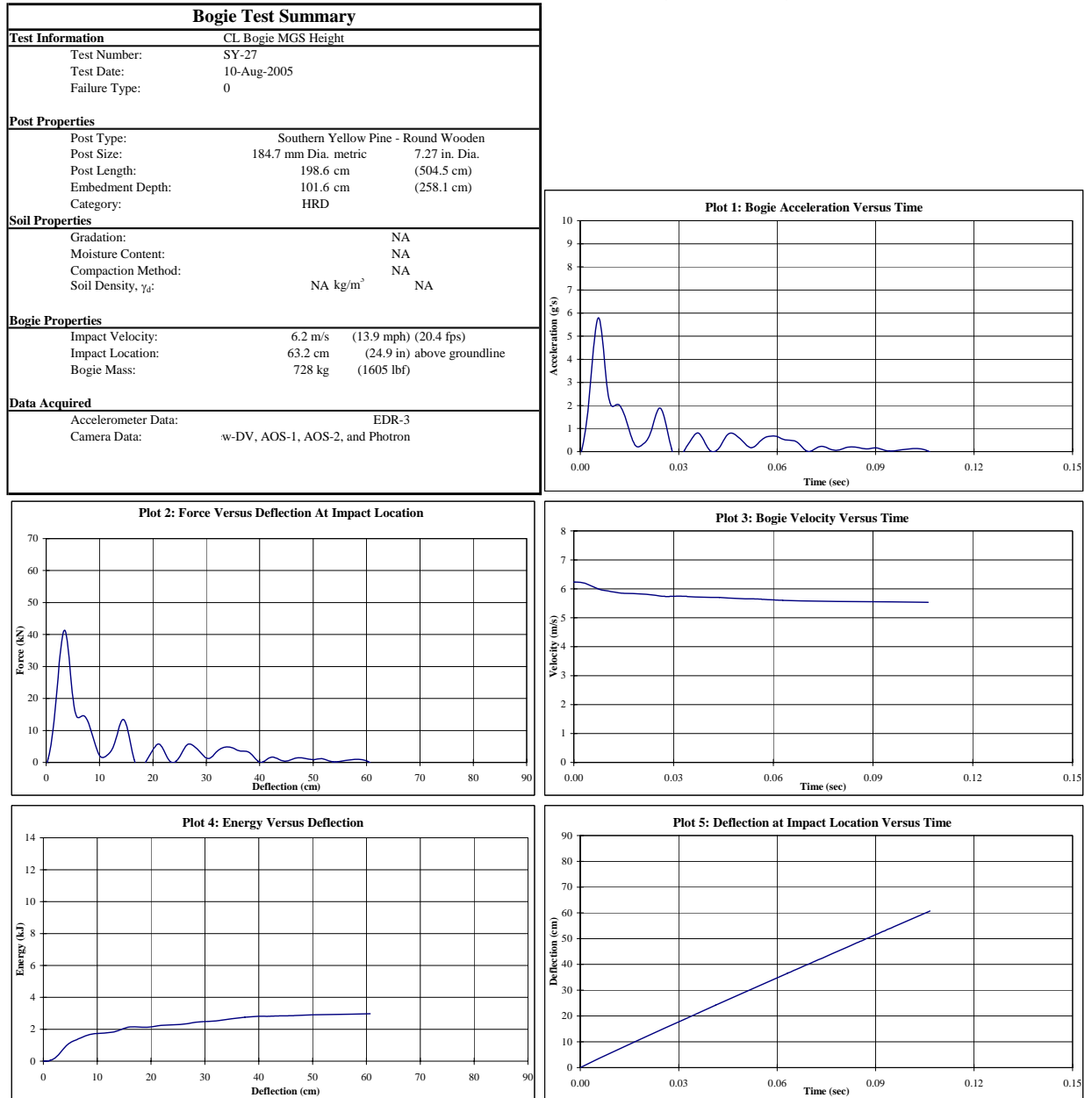


Figure E-42. Results of Test No. SY-27

Midwest Roadside Safety Facility

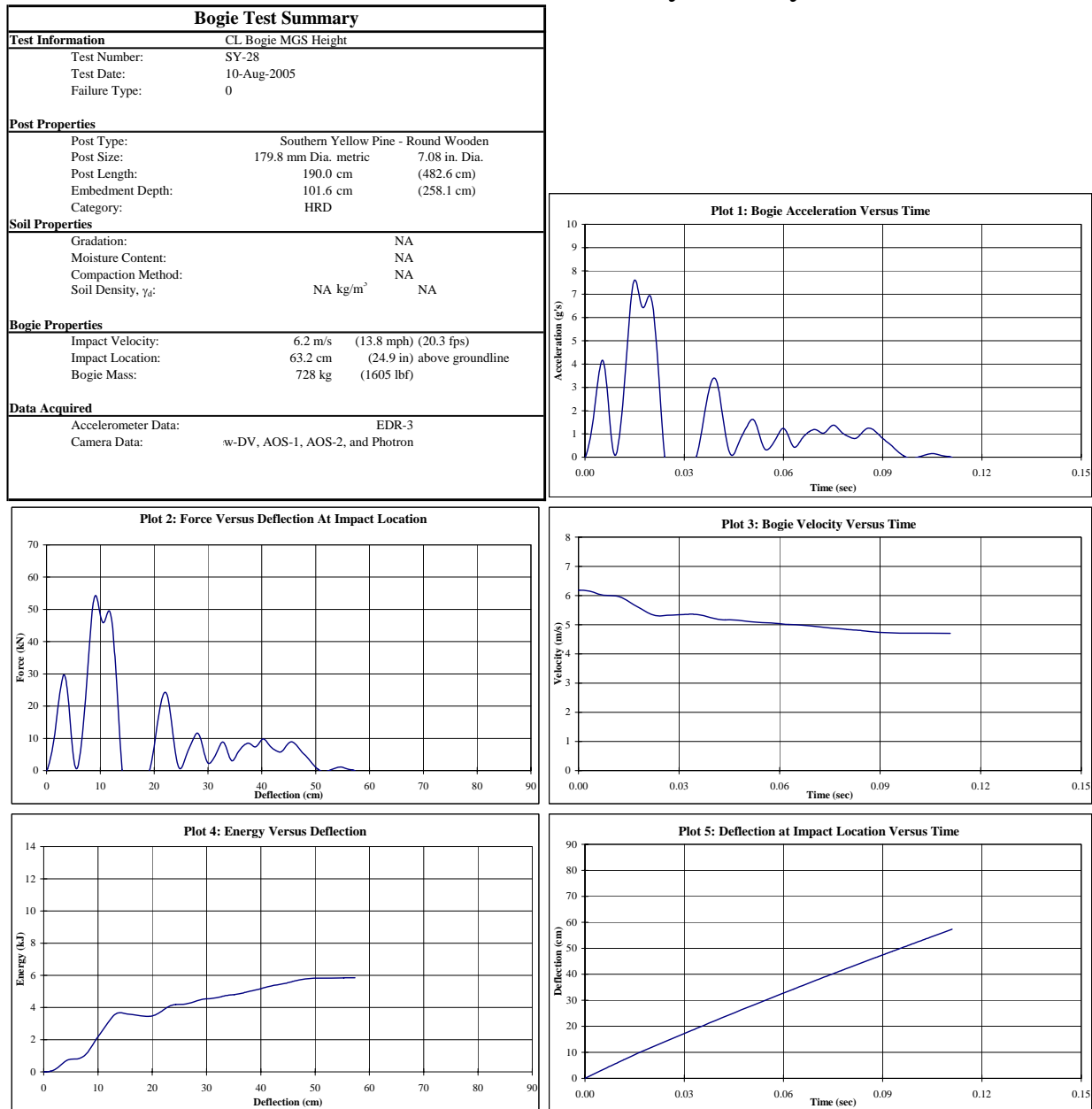


Figure E-43. Results of Test No. SY-28

Midwest Roadside Safety Facility

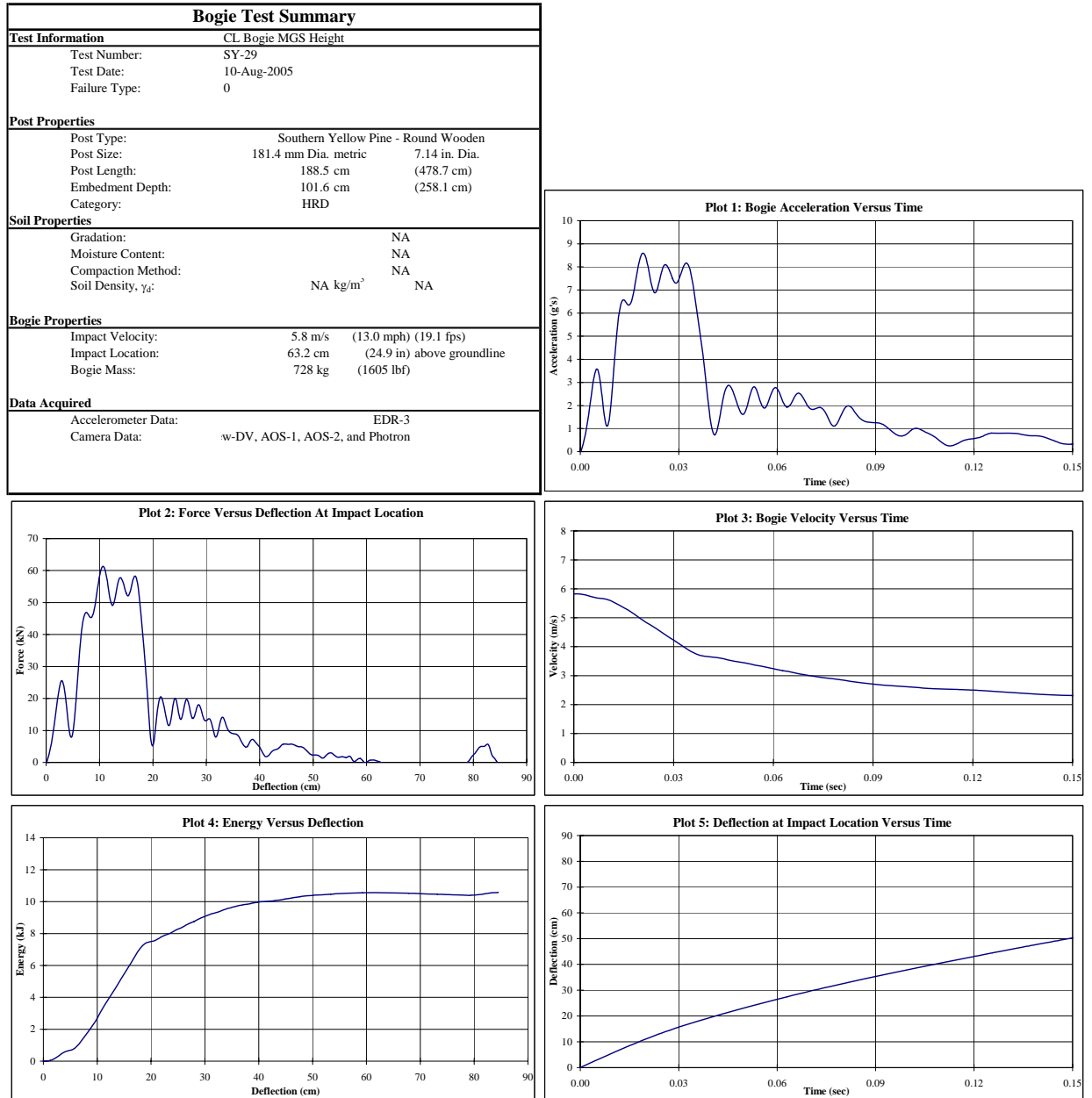


Figure E-44. Results of Test No. SY-29

Midwest Roadside Safety Facility

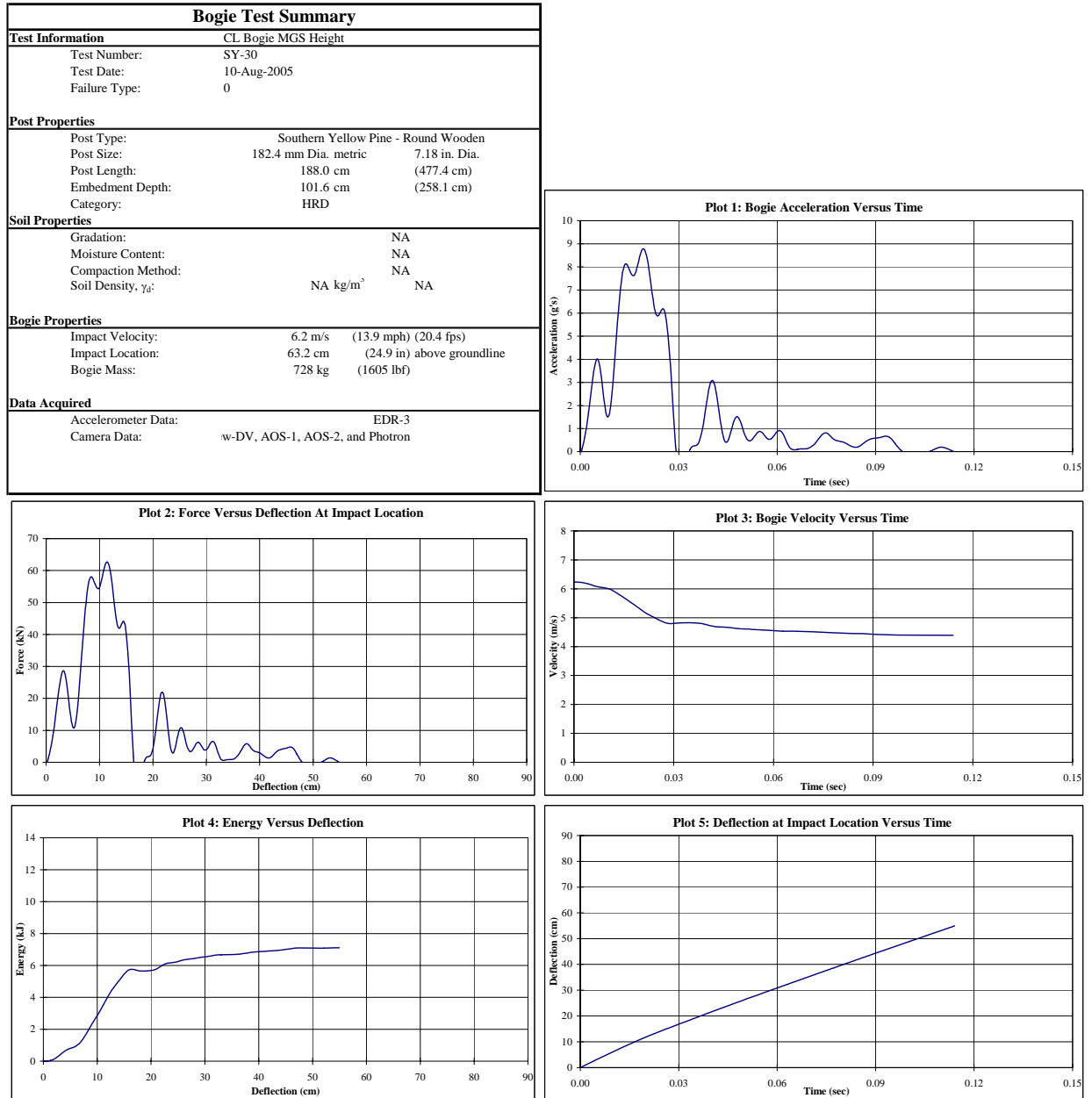
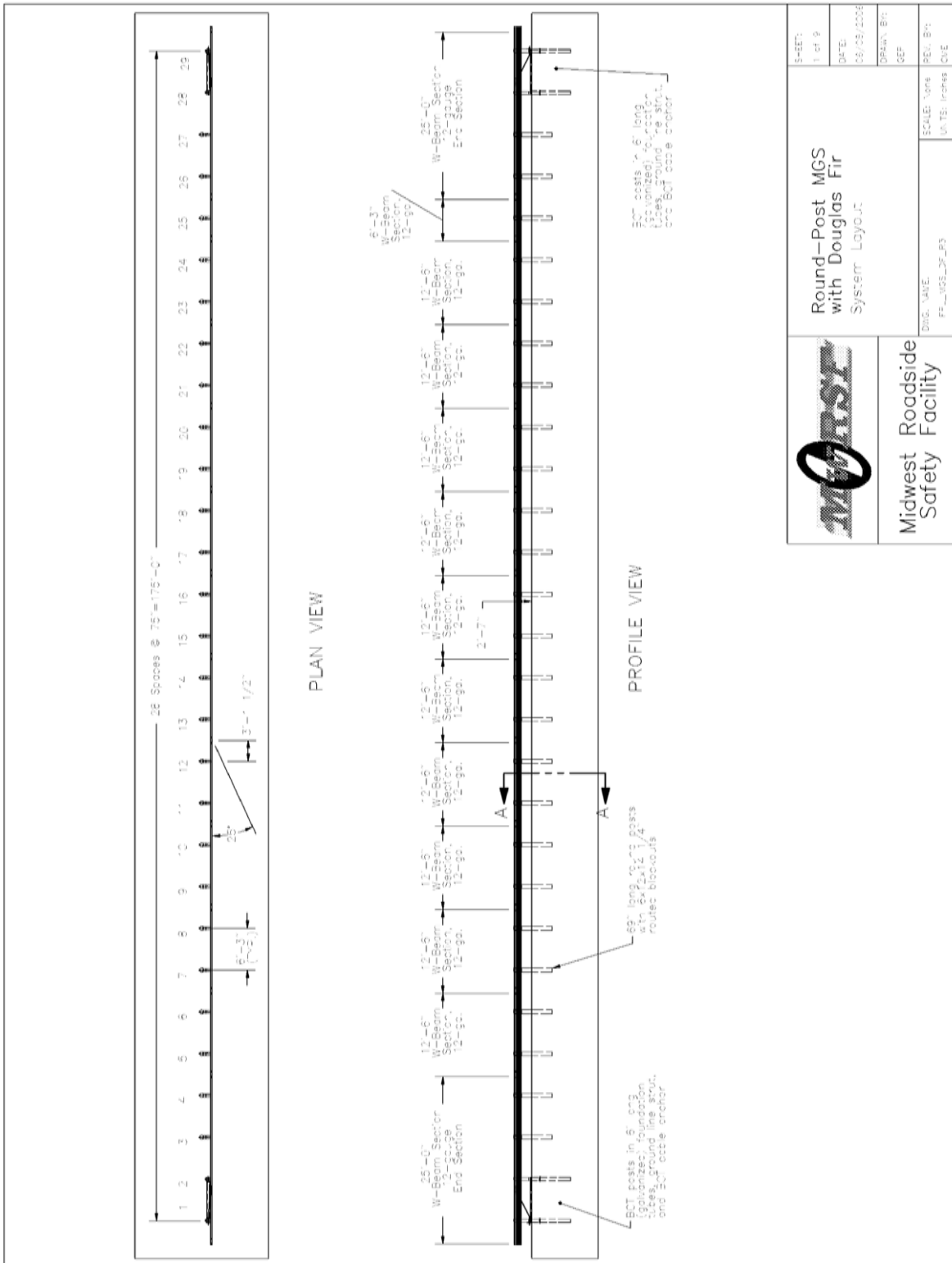


Figure E-45. Results of Test No. SY-30

APPENDIX F - MGSDF System Details – English Units

Figure F-1. MGS Round Post Douglas Fir English Details – System Layout.....	387
Figure F-2. MGS Round Post Douglas Fir English Details – End Rail and Splice Detail	388
Figure F-3. MGS Round Post Douglas Fir English Details – Post Detail	389
Figure F-4. MGS Round Post Douglas Fir English Details – Segmented Block Detail.....	390
Figure F-5. MGS Round Post Douglas Fir English Details – Anchor Post Detail	391
Figure F-6. MGS Round Post Douglas Fir English Details – BCT Anchor Cable Detail.....	392
Figure F-7. MGS Round Post Douglas Fir English Details – Ground Strut and Anchor Bracket Detail.....	393
Figure F-8. MGS Round Post Douglas Fir English Details – Rail Section Detail	394
Figure F-9. MGS Round Post Douglas Fir English Details – Grading Specifications	395



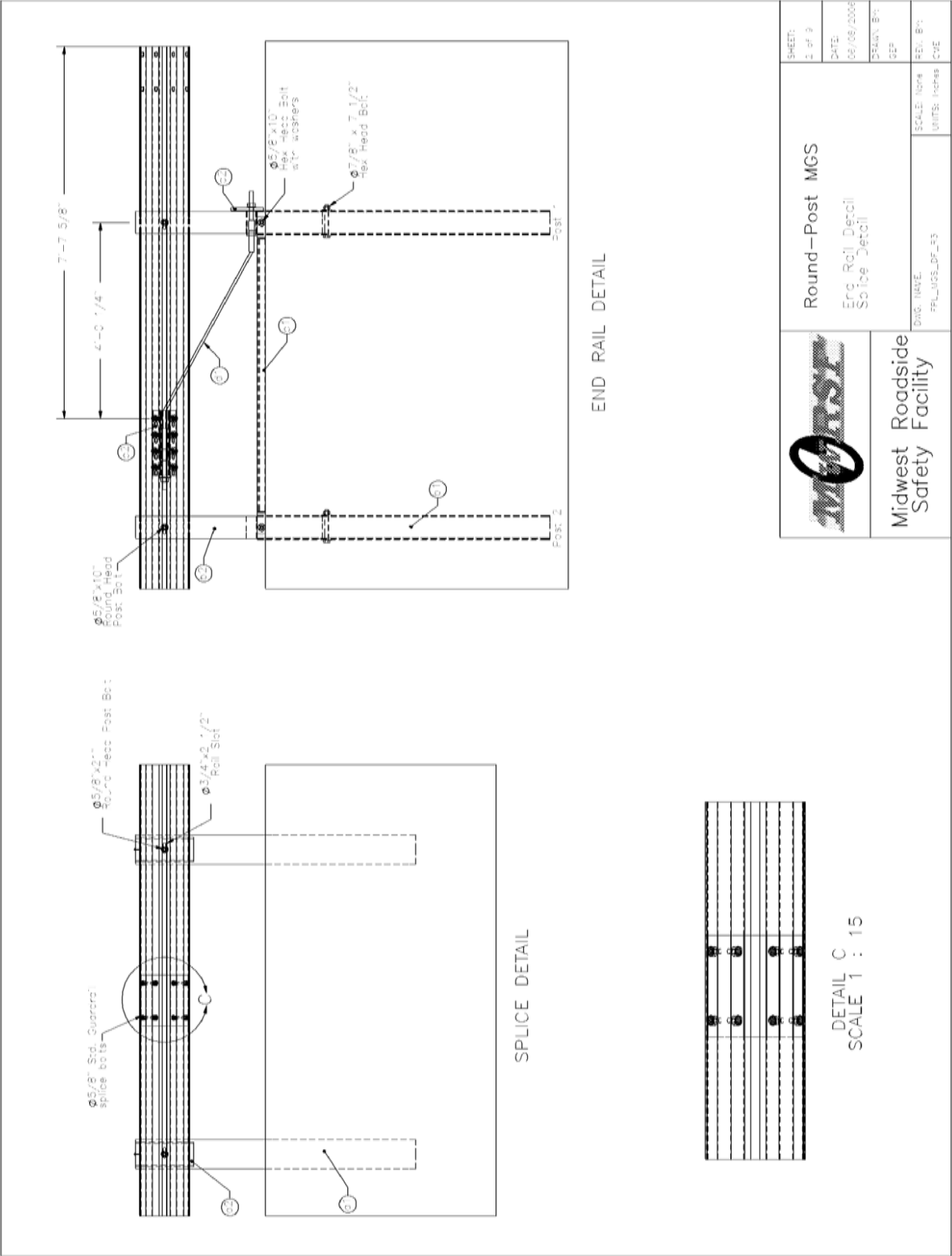
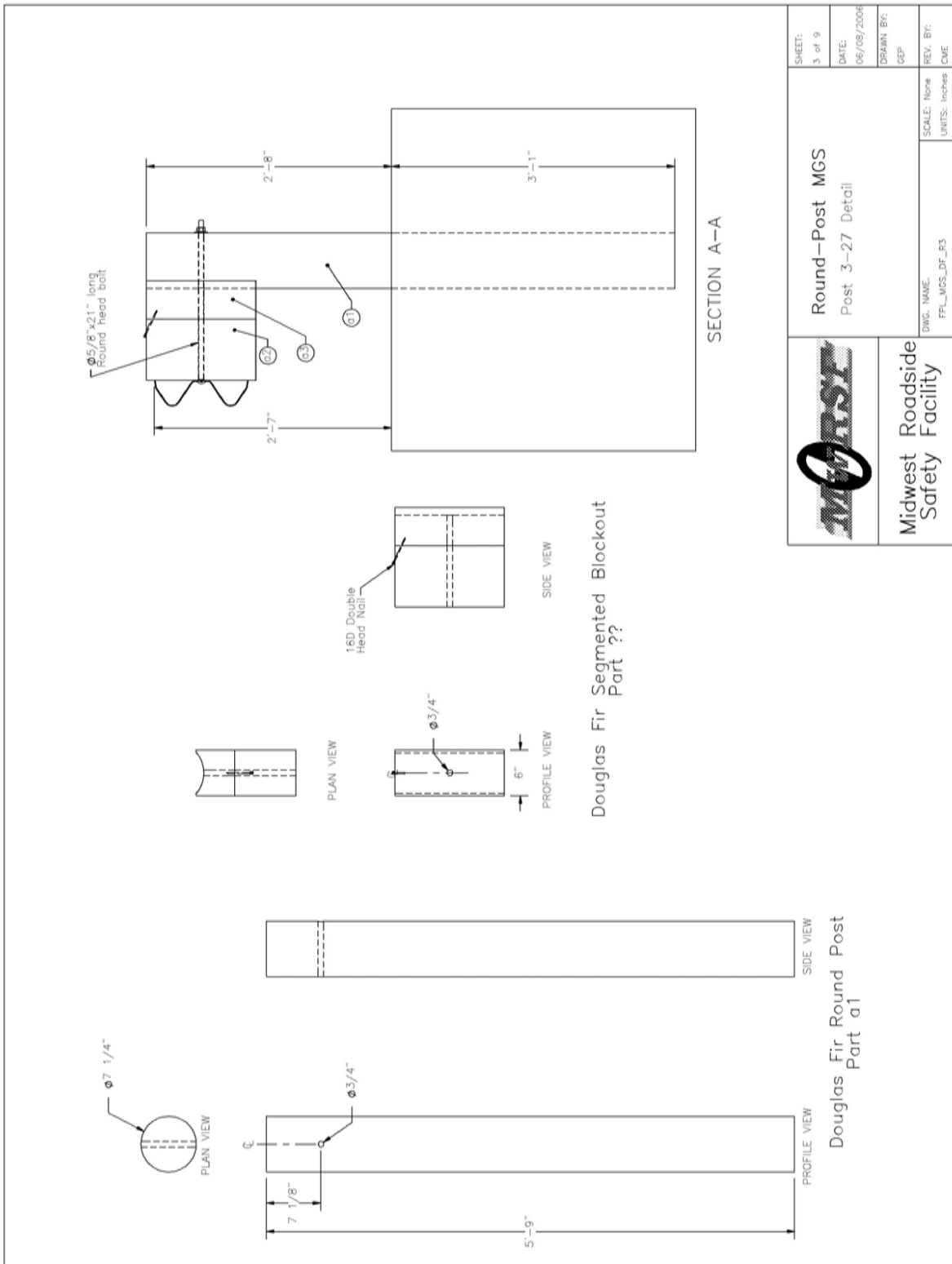


Figure F-2. MGS Round Post Douglas Fir English Details – End Rail and Splice Detail



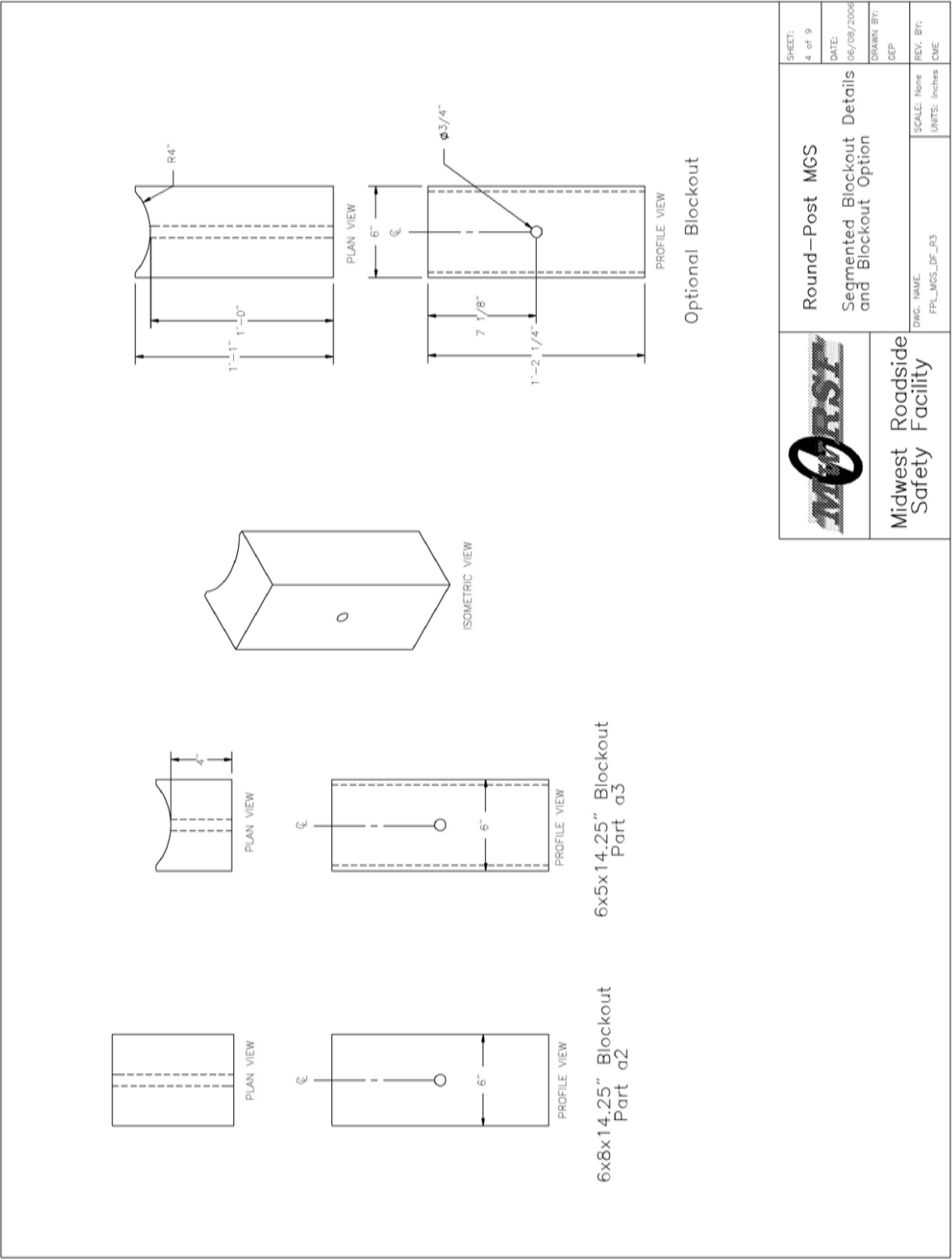


Figure F-4. MGS Round Post Douglas Fir English Details – Segmented Block Detail

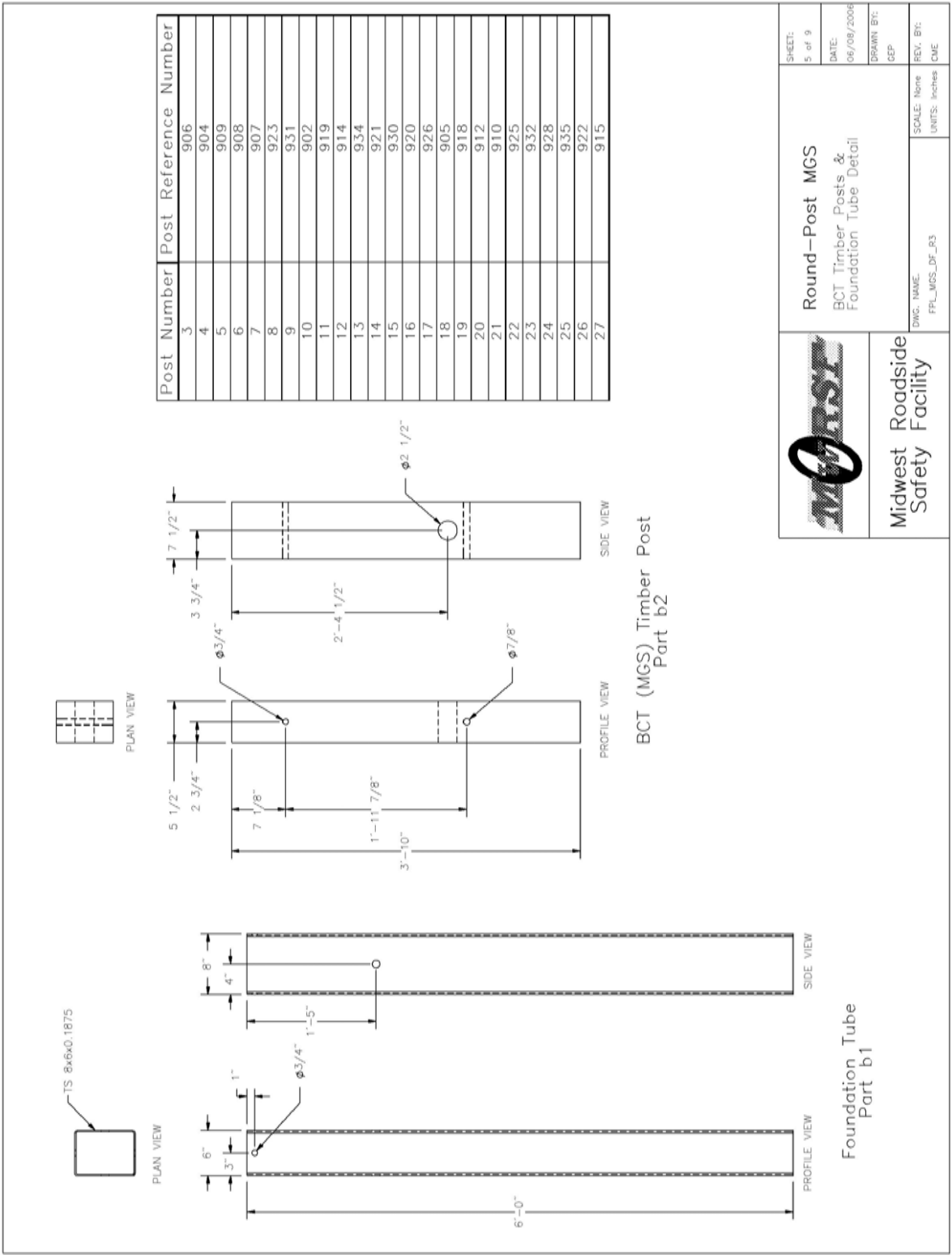


Figure F-5. MGS Round Post Douglas Fir English Details – Anchor Post Detail

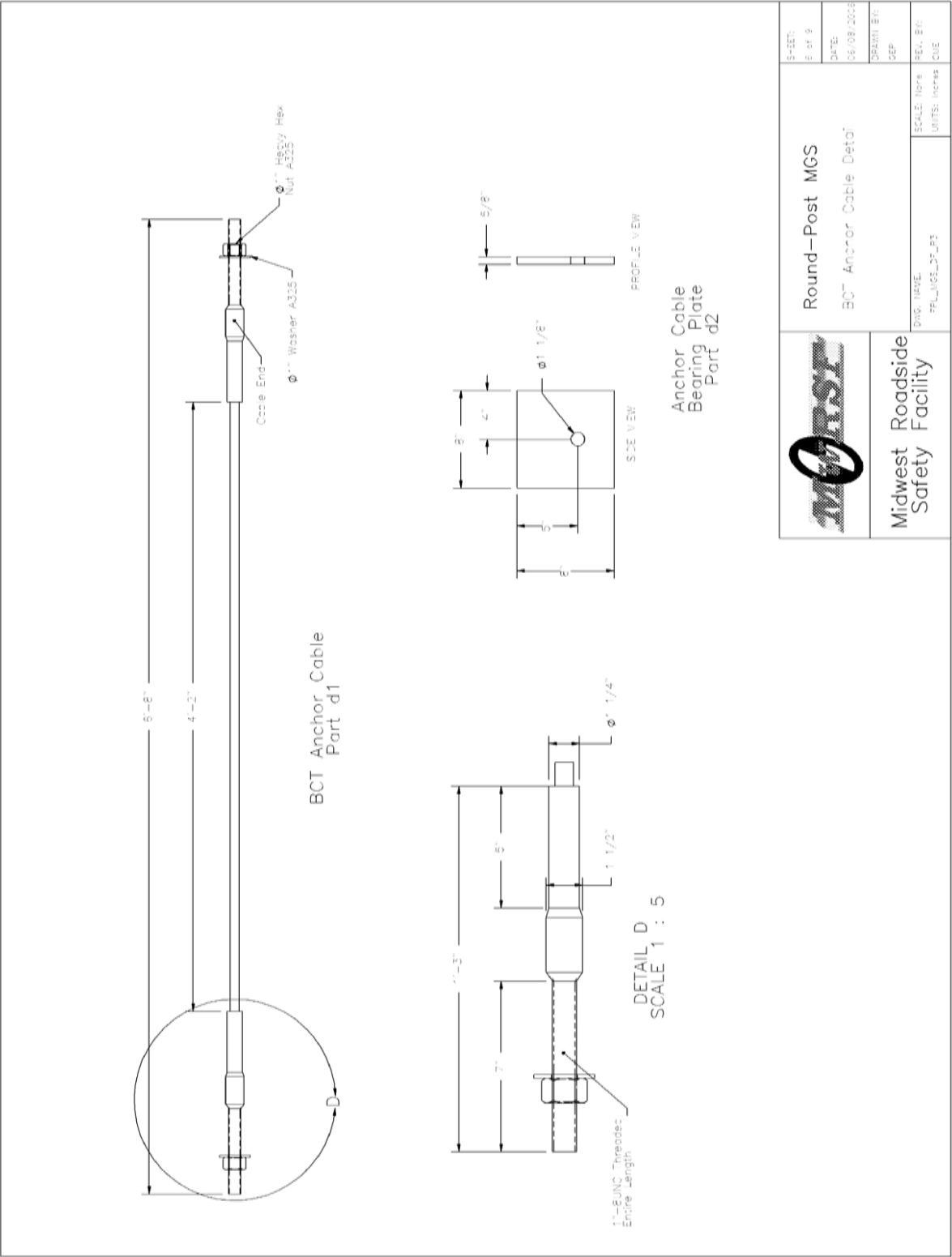
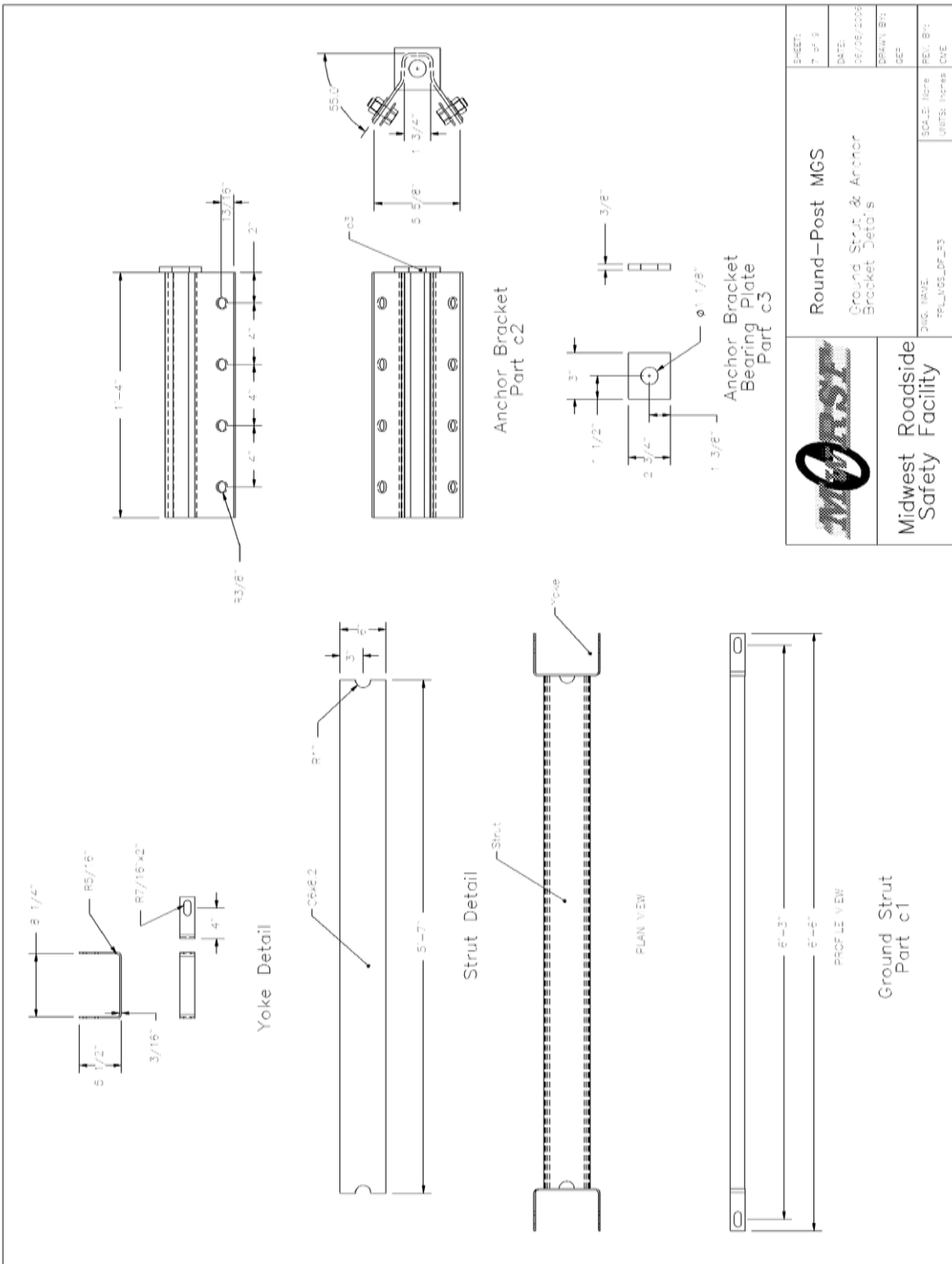


Figure F-6. MGS Round Post Douglas Fir English Details – BCT Anchor Cable Detail



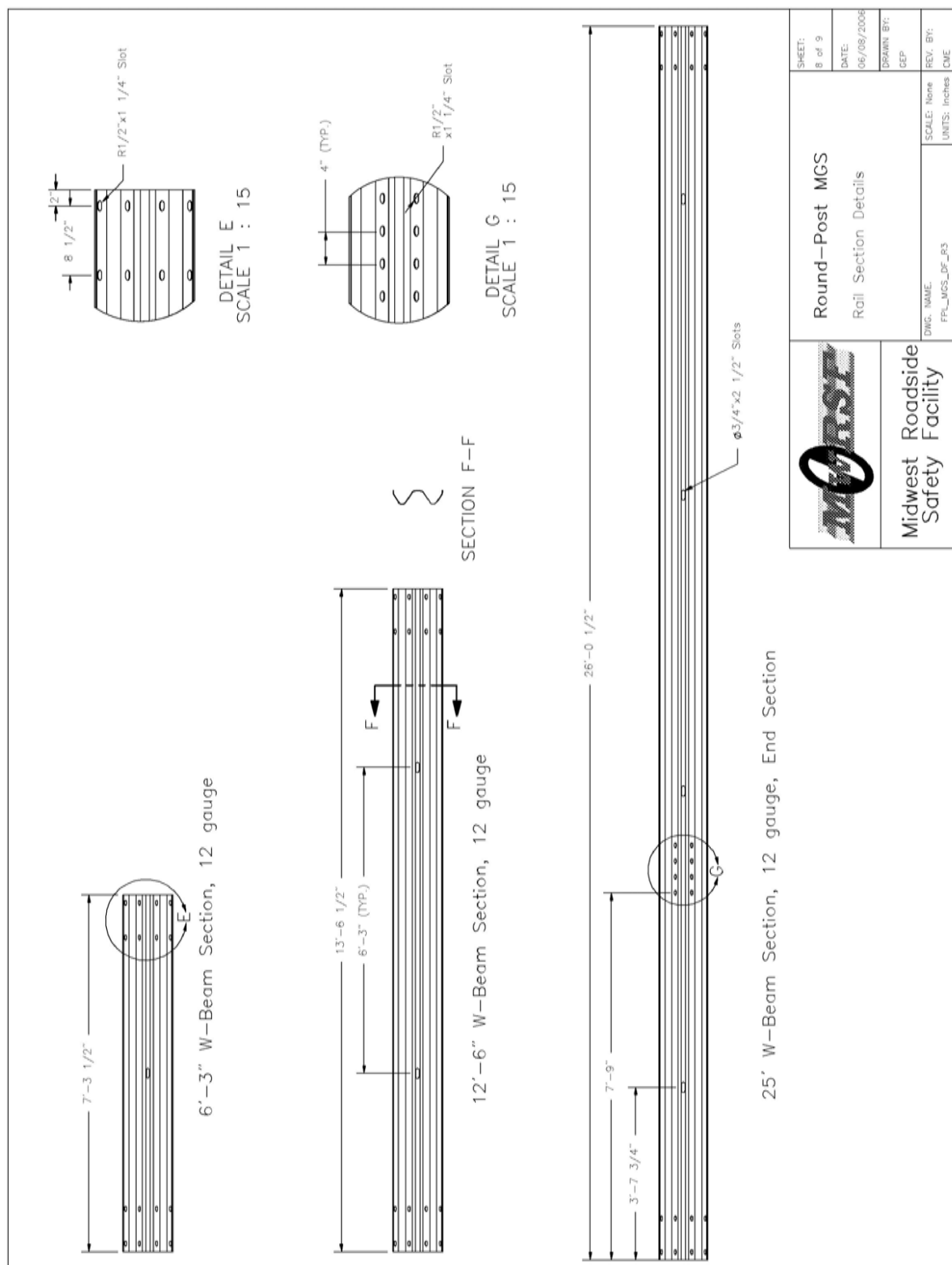


Figure F-8. MGS Round Post Douglas Fir English Details – Rail Section Detail

General	Guardrail Post Grading Criteria			Midwest Safety Facility	Round—Post MGS	SHEET: 9 of 9
					Grading Specifications	DATE: 06/08/2008
					DRAWN BY: GEP	REV. BY: CUE
					SCALE: None	UNITS: inches
					FILE: MGS_05-PS	

All posts shall meet the current quality requirements of the American National Standards Institute (ANSI) Q361, "Wood Posts" except as supplemented herein:	
Manufacture: All posts shall be smooth shored by machine. No "ringing" of the posts, as caused by improperly adjusted peeling machine, is permitted. All outer and inner bark shall be removed during the shoring process. A knots and knots shall be trimmed smooth and flush with the surface of the posts. The guardrail posts will be a minimum of 1.75 m (66 in.) long. The use of peeler cores is prohibited.	
Ground-line: The ground-line, for the purpose of applying these restrictions of ANSI Q361 that reference the ground-line, shall be defined as being located 9' 4 mm (36 in.) from the butt end of each post.	
Size: The size of the posts shall be classified based on their diameter at the ground-line and their length and will be species specific. The ground-line diameter shall be specified by diameter in 6 mm (3/4 in.) breaks. The length shall be specified in 300 mm (1' 0 in.) breaks. Dimension shall apply to fully seasoned posts. When measured between their extreme ends, the post shall be no shorter than the specified length but may be up to 75 mm (3 in.) longer.	
Scars: Scars are permitted in the middle third as defined in ANSI Q361 provided that the depth of the trimmed scar is not more than (1 %).	
Shape and Straightness: All timber posts shall be nominally round in cross section. A straight line drawn from the centerline of the top to the center of the butt of any post shall not deviate from the centerline of the post more than 32 mm (1 1/4 in.) at any point. Posts shall be free from reverse bends.	
Splits and Shakes: Splits or ring shakes are not permitted in the top two thirds of the post. Splits not to exceed the diameter in length are permitted in the bottom third of the post. A single shake is permitted in the bottom third, provided it is not wider than one-half the butt diameter.	
Decay: Allowed in knots only.	
Holes: Posts shall have 1 mm (1/16 in.) or less are not restricted.	
Slope of Grain: 1 in 10.	
Compression Wood: Not allowed, in the outer 25 mm (1 in.) or if exceeding 1/4 of the radius.	
Timber Spacers: When timber spacers are required, the timber species shall be the same as those furnished for the timber posts. The size and use location shall be as shown on the plans, with a tolerance of 6 mm (1/4 in.). Spacers shall be of medium grain, at least four (4) rings per inch on one end, and free from splits, shakes, compression wood or decay in any form. Individual knots, knot clusters or knots in the same cross section of a face are permitted, provided they are sound or firm, and are limited in cumulative width (when measured between lines parallel to the edges) to no more than one-half the width of the face. Where the absence of wood is limited to one-third of the face or no more than 10 percent of the lot. Slope of grain deviation is limited to one in six. The material may be rough scar or surfaced, full size, kiln or miss, with a tolerance of 6 mm (1/4 in.) for all dimensions.	
Treatment: Treating — American Wood-Preservers' Association (AWPA) — Book of Standards (BOS) U1—05 Use category system UCS: user specification for treated wood; commodity specification B: posts; Wood for Highway Construction must be met using the methods outlined in AWPA BOS T1—05 Section 8.2. Each post treated shall have a minimum stacked depth of 19 mm (3/4 in.) as determined by examination of the tops and butts of each post. Material that has been air dried or in case shall be inspected for moisture content in accordance with AWPA standard M2 prior to treatment. Tests of representative pieces shall be conducted. The lot shall be considered acceptable when the average moisture content does not exceed 25 percent. Pieces exceeding 25 percent moisture content shall be rejected and removed from the lot.	

Species Specific Criteria	Douglas Fir: Knot diameter for posts of Douglas Fir shall not exceed 51 mm (2 in.). Ring density for the species shall be at least 6 rings-per-inch as measured over a 76 mm (3 in.) distance. The diameter of the Douglas fir posts shall be 64 mm (2 1/2 in.) at the ground line with a taper not of 253 mm (10 in.).
---------------------------	--

Figure F-9. MGS Round Post Douglas Fir English Details – Grading Specifications

APPENDIX G - MGSPP System Details – English Units

Figure G-1. MGS Round Post Ponderosa Pine English Details – System Layout	397
Figure G-2. MGS Round Post Ponderosa Pine English Details – End Rail and Splice Detail..	398
Figure G-3. MGS Round Post Ponderosa Pine English Details – Post Detail.....	399
Figure G-4. MGS Round Post Ponderosa Pine English Details – Segmented Blockout Detail	400
Figure G-5. MGS Round Post Ponderosa Pine English Details – Anchor Post Detail.....	401
Figure G-6. MGS Round Post Ponderosa Pine English Details – BCT Anchor Cable Detail ..	402
Figure G-7. MGS Round Post Ponderosa Pine English Details – Ground Strut and Anchor Bracket Detail	403
Figure G-8. MGS Round Post Ponderosa Pine English Details – Rail Section Detail.....	404
Figure G-9. MGS Round Post Ponderosa Pine English Details – Grading Specifications.....	405



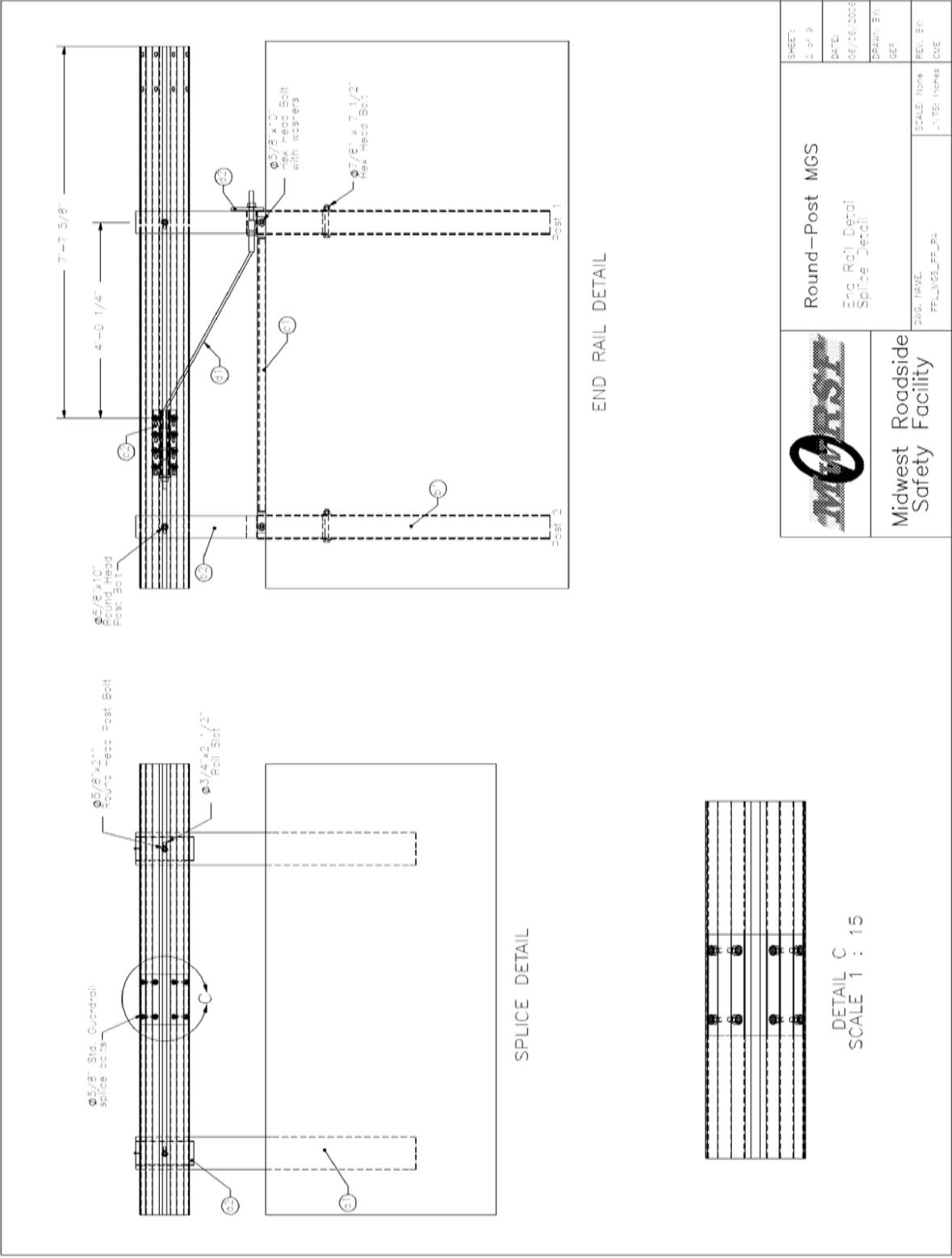
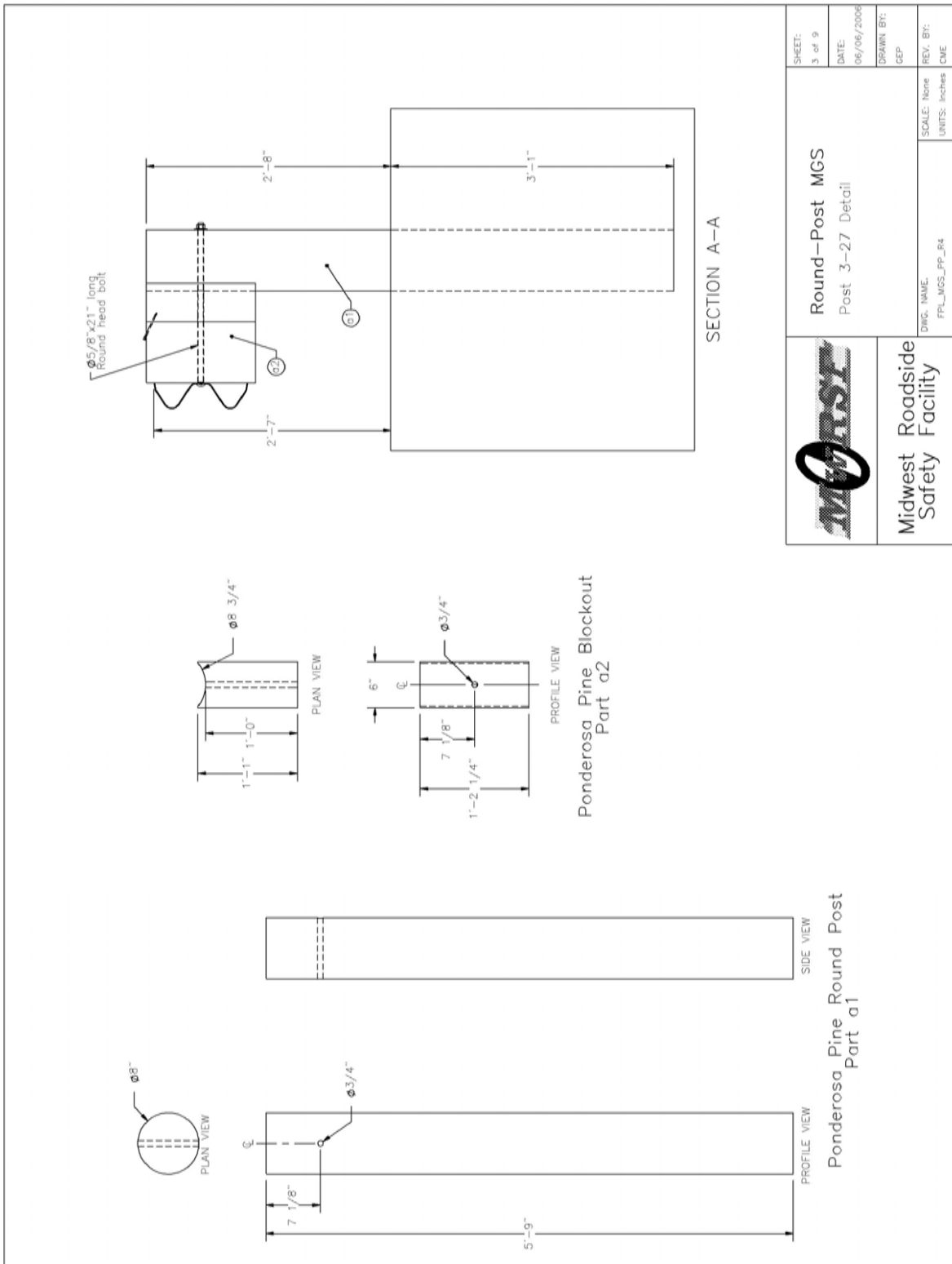
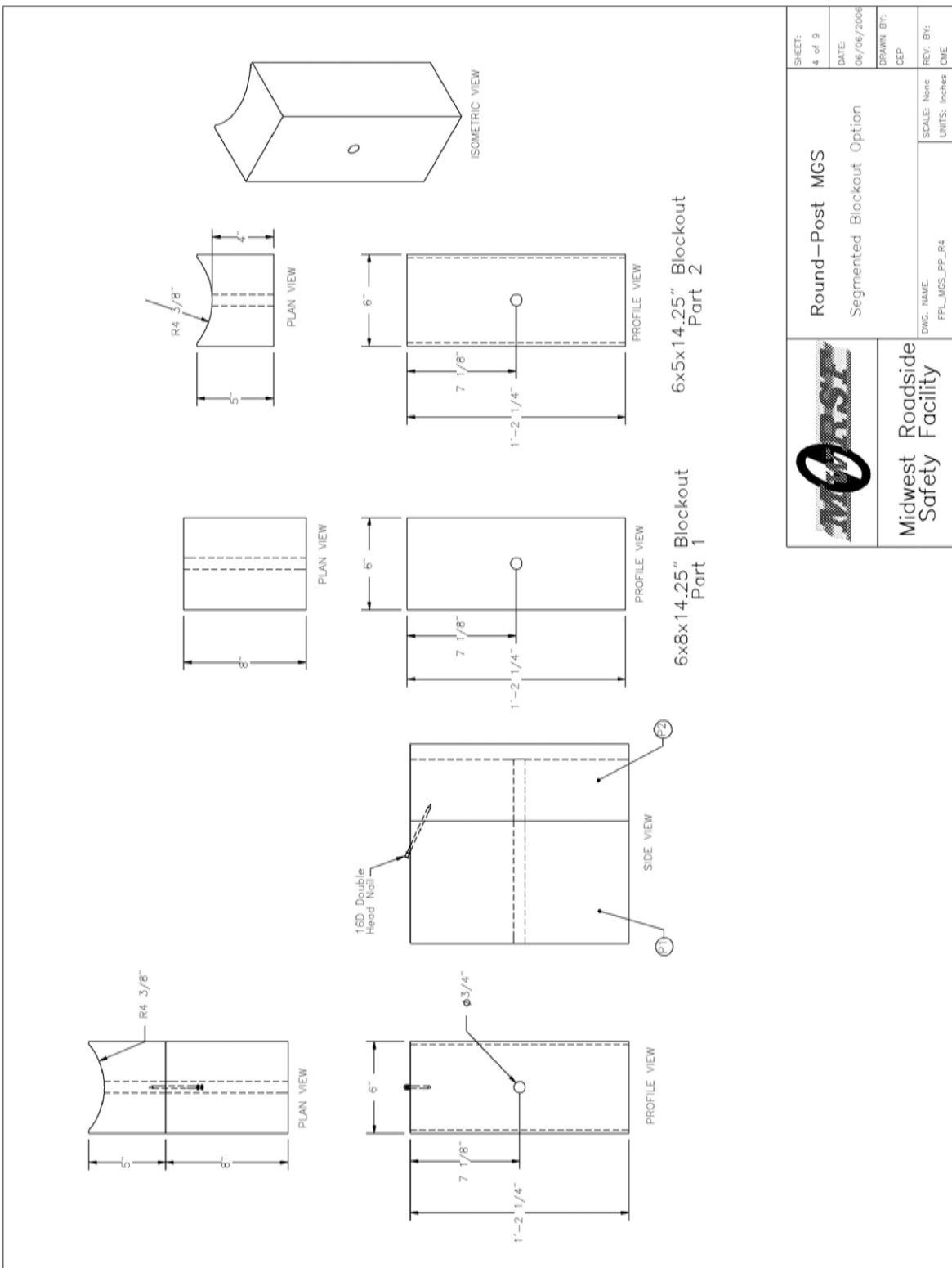


Figure G-2. MGS Round Post Ponderosa Pine English Details – End Rail and Splice Detail





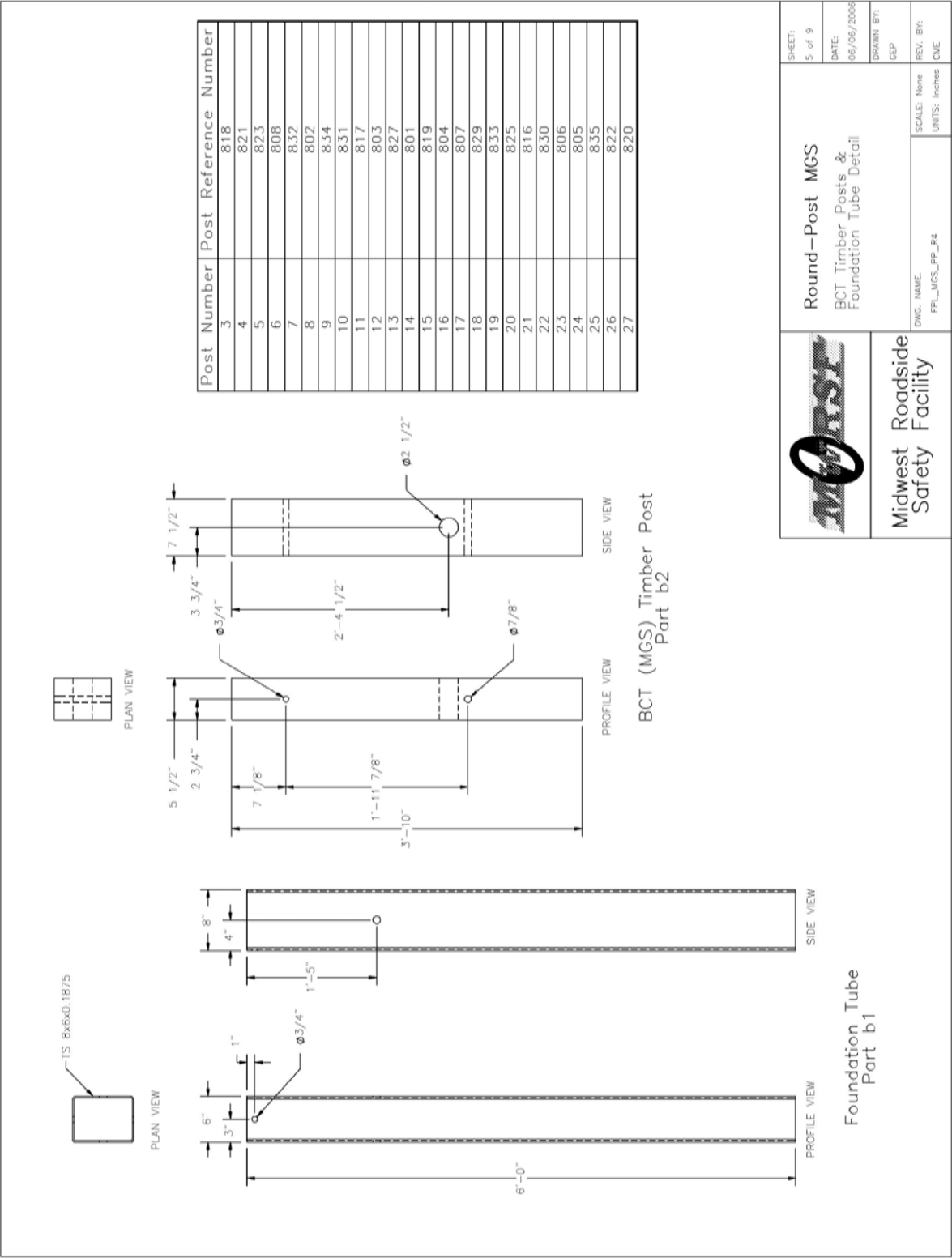


Figure G-5. MGS Round Post Ponderosa Pine English Details – Anchor Post Detail

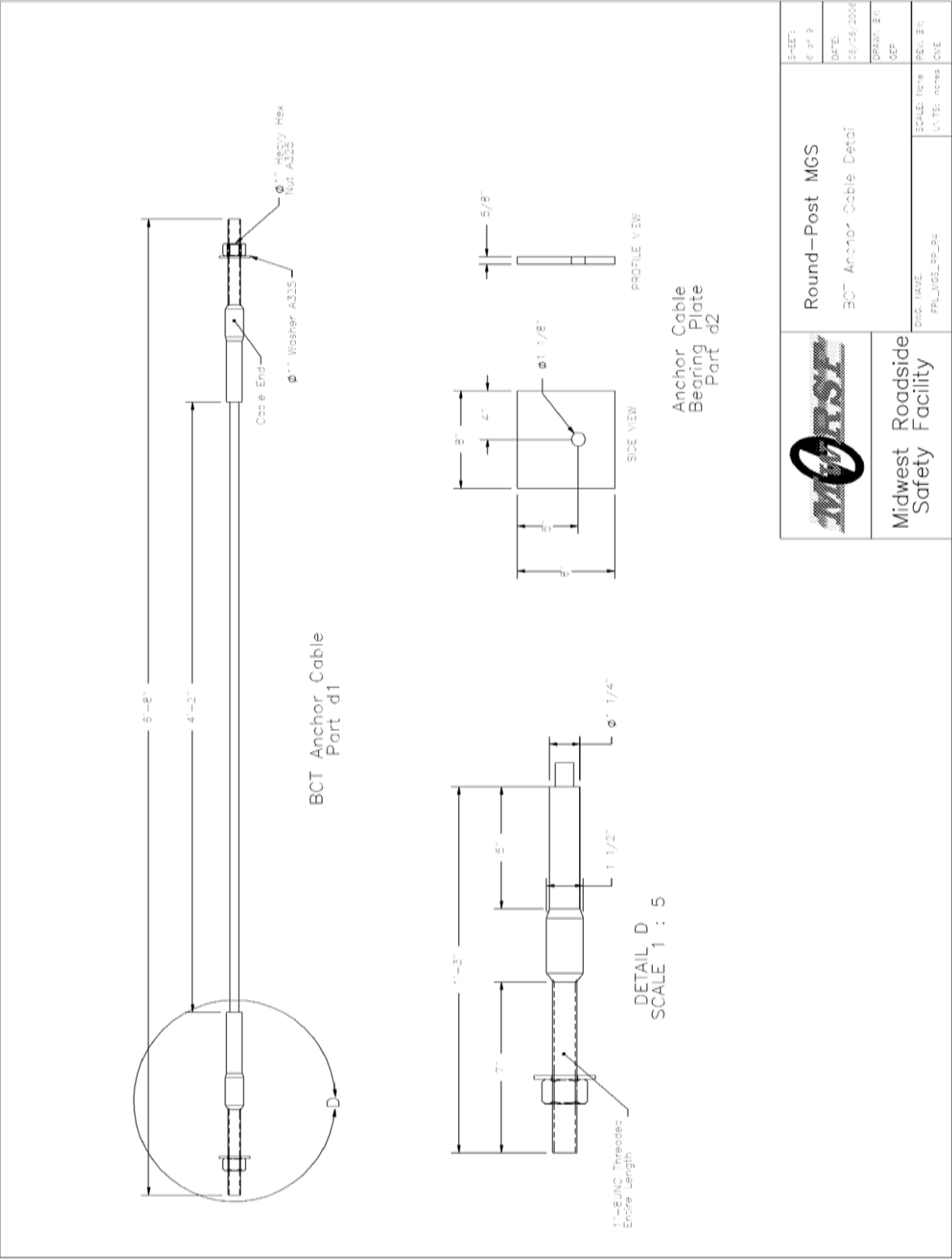
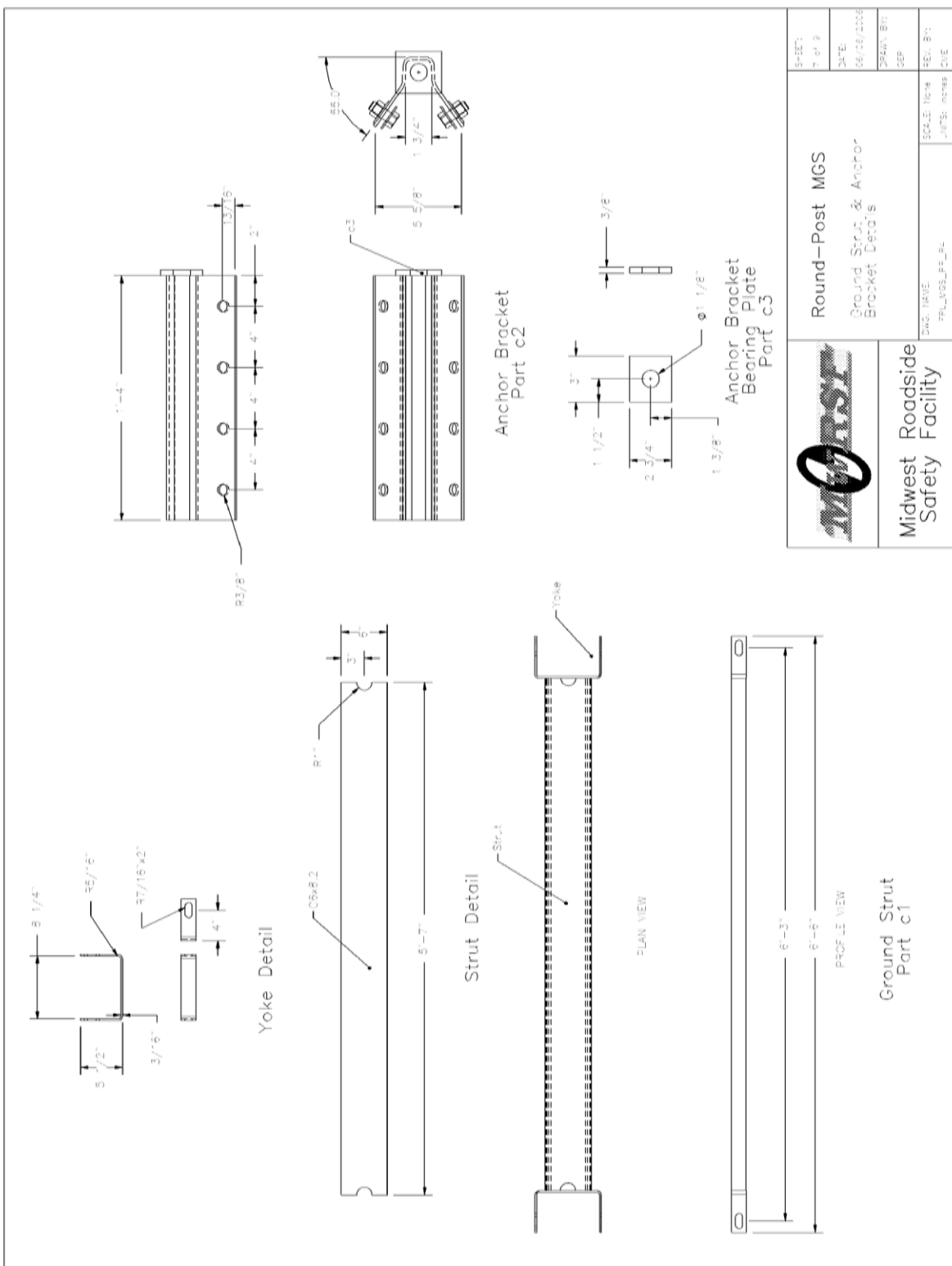


Figure G-6. MGS Round Post Ponderosa Pine English Details – BCT Anchor Cable Detail



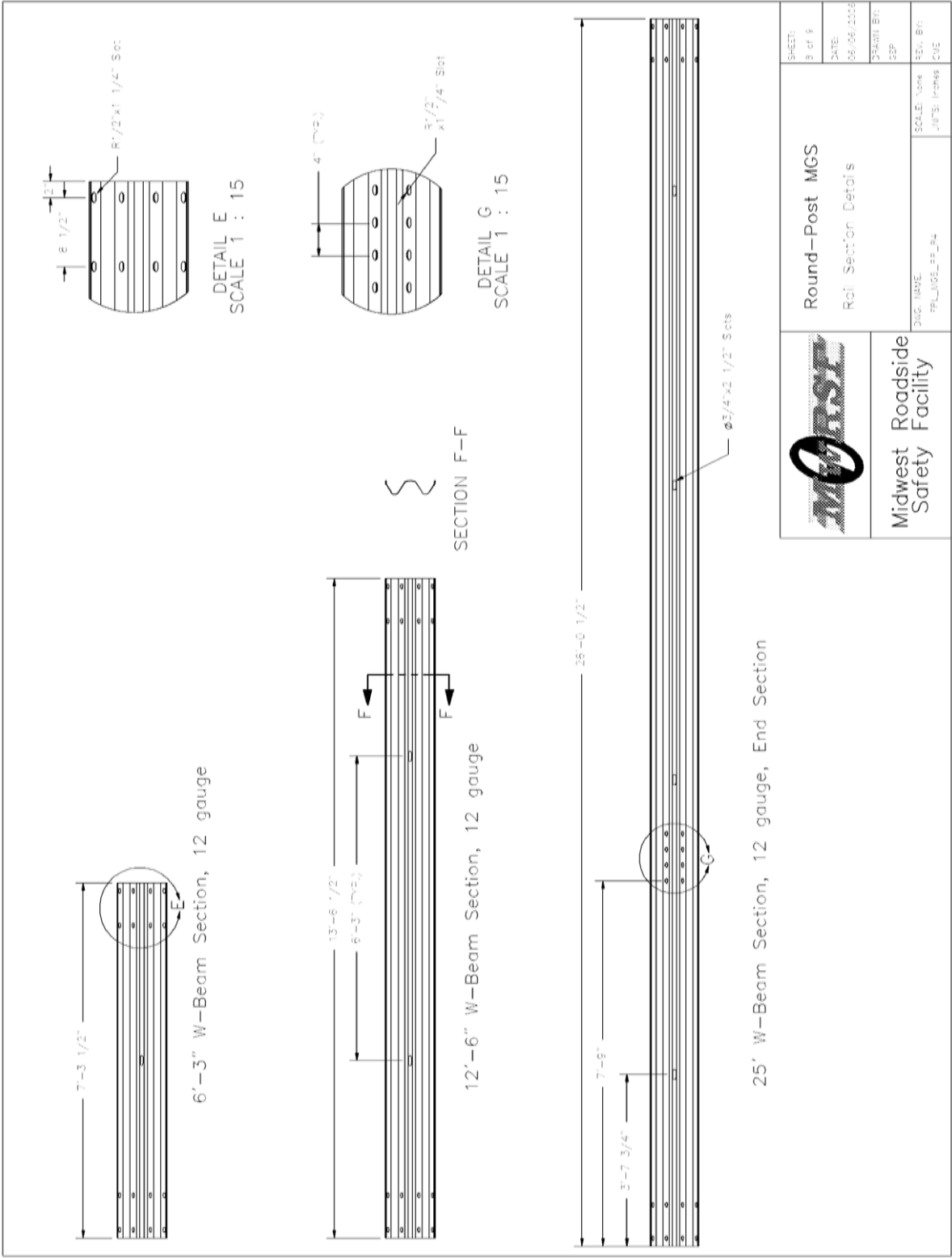


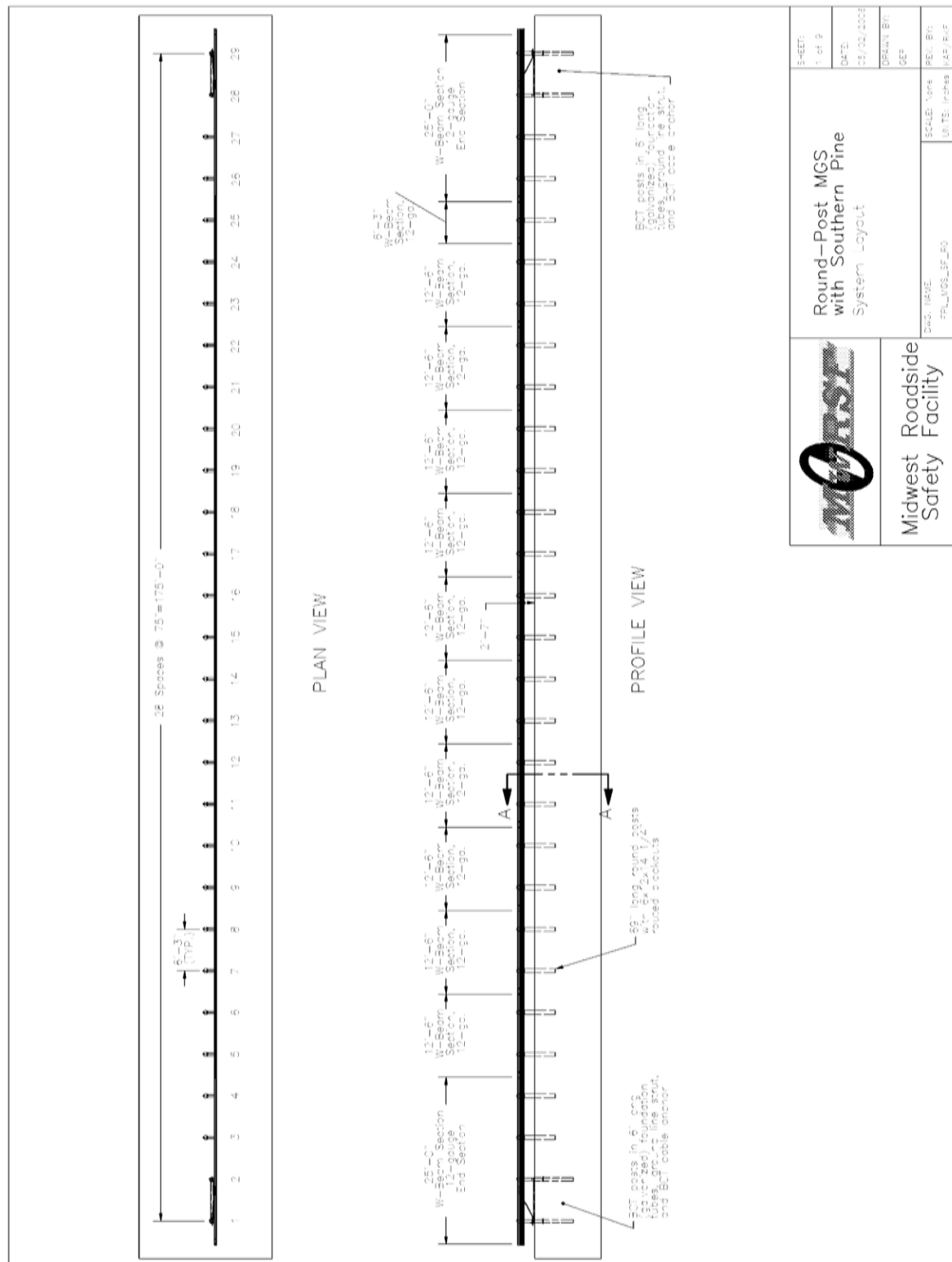
Figure G-8. MGS Round Post Ponderosa Pine English Details – Rail Section Detail

<p><i>General</i></p> <p>Guardrail Post Grading Criteria</p> <p>All posts shall meet the current quality requirements of the American National Standards Institute (ANSI) 05.1, "Wood Poles" except as supplemented herein:</p> <p>Manufacture: All posts shall be smooth shored by machine. No "ringing" of the posts, as caused by improperly adjusted peeling machine, is permitted. All outer and inner bark shall be removed during the shoring process. All knots and knobs shall be trimmed smooth and flush with the surface of the posts. The guardrail posts will be a minimum of 1.75 m (69 in.) long. The use of peeler cores is prohibited.</p> <p>Ground-line: The ground-line, for the purpose of applying these restrictions of ANSI 05.1 that reference the ground-line, shall be defined as being located 914 mm (36 in.) from the butt end of each post.</p> <p>Size: The size of the posts shall be classified based on their diameter at the ground-line and their length and will be species specific. The ground-line diameter shall be specified by diameter in 6 mm ($\frac{1}{4}$ in.) breaks. The length shall be specified in 300 mm (1 ft) breaks. Dimension shall apply to fully seasoned posts. When measured between their extreme ends, the post shall be no shorter than the specified lengths but may be up to 75 mm (3 in.) longer.</p> <p>Scars: Scars are permitted in the middle third as defined in ANSI 05.1 provided that the depth of the trimmed scar is not more than (1 in.).</p> <p>Shape and Straightness: All timber posts shall be nominally round in cross section. A straight line drawn from the centerline of the top to the center of the butt of any post shall not deviate from the centerline of the post more than 32 mm (1$\frac{1}{4}$ in.) at any point. Posts shall be free from reverse bends.</p> <p>Splits and Shakes: Splits or ring shakes are not permitted in the top two thirds of the post. Splits not to exceed the diameter in length are permitted in the bottom third of the post. A single shake is permitted in the bottom third, provided it is not wider than one-half the butt diameter.</p> <p>Decay: Allowed in knots only.</p> <p>Holes: Pin holes 1 mm (1/16 in.) or less are not restricted.</p> <p>Slope of Grain: 1 in 10.</p> <p>Compression Wood: Not allowed, in the outer 25 mm (1 in.) or if exceeding $\frac{1}{4}$ of the radius.</p> <p>Timber Spacers: When timber spacers are required, the timber species shall be the same as those furnished for the timber posts. The size and hole location shall be as shown on the plans, with a tolerance of 6 mm ($\frac{1}{4}$ in.). Spacers shall be of medium grain, at least four (4) rings per inch on one end, and free from splits, shakes, compression wood or decay in any form. Individual knots, knot clusters or knots in the same cross section of a face are permitted, provided they are sound or firm, and are limited in cumulative width (when measured between lines parallel to the edges) to no more than one-half the width of the face. Where or the absence of wood is limited to one-third of the face on no more than 10 percent of the lot. Slope of grain deviation is limited to one in six. The material may be rough sawn or surfaced, full size, fit or miss, with a tolerance of 6 mm ($\frac{1}{4}$ in.) for all dimensions.</p> <p>Treatment: Treating – American Wood-Preservers' Association (AWPA) – Book of Standards (BOS) U1-05 use category system UCS: user specification for treated wood; commodity specification B; Posts; Wood for Highway Construction must be met using the methods outlined in AWPA BOS T1-05 Section 8.2. Each post treated shall have a minimum sapwood depth of 19 mm ($\frac{3}{4}$ in.) as determined by examination of the tops and butts of each post. Material that has been air dried or kiln dried shall be inspected for moisture content in accordance with AWPA standard M2 prior to treatment. Tests of representative pieces shall be conducted. The lot shall be considered acceptable when the average moisture content does not exceed 25 percent. Pieces exceeding 29 percent moisture content shall be rejected and removed from the lot.</p>		<p>Species Specific Criteria</p> <p>Ponderosa Pine: Knot diameter for posts of Ponderosa Pine shall not exceed 102 mm (4 in.). Ring density for the species shall be at least 6 rings-per-inch as measured over a 76 mm (3 in.) distance. The diameter of the Ponderosa Pine posts shall be 203 mm (8 in.) at the ground line with an upper limit of 222 mm (8$\frac{3}{4}$ in.).</p>		<p></p> <p>Midwest Roadside Safety Facility</p> <p>Round-Post MGS Grading Specifications</p> <p>DWG. NAME: FPL_MGS_PP_B4 SCALE: None UNITS: Inches</p> <p>SHEET: 9 of 9 DATE: 06/06/2008 DRAWN BY: CEP REV. BY: CME</p>	
--	--	--	--	--	--

Figure G-9. MGS Round Post Ponderosa Pine English Details – Grading Specifications

APPENDIX H - MGSSYP System Details – English Units

Figure H-1. MGS Round Post Southern Pine English Details – System Layout	407
Figure H-2. MGS Round Post Southern Pine English Details – End Rail and Splice Detail	408
Figure H-3. MGS Round Post Southern Pine English Details – Post Detail	409
Figure H-4. MGS Round Post Southern Pine English Details – Segmented Blockout Detail ..	410
Figure H-5. MGS Round Post Southern Pine English Details – Anchor Post Detail	411
Figure H-6. MGS Round Post Southern Pine English Details – BCT Anchor Cable Detail	412
Figure H-7. MGS Round Post Southern Pine English Details – Ground Strut and Anchor Bracket Detail	413
Figure H-8. MGS Round Post Southern Pine English Details – Rail Section Detail	414
Figure H-9. MGS Round Post Southern Pine English Details – Grading Specifications	415



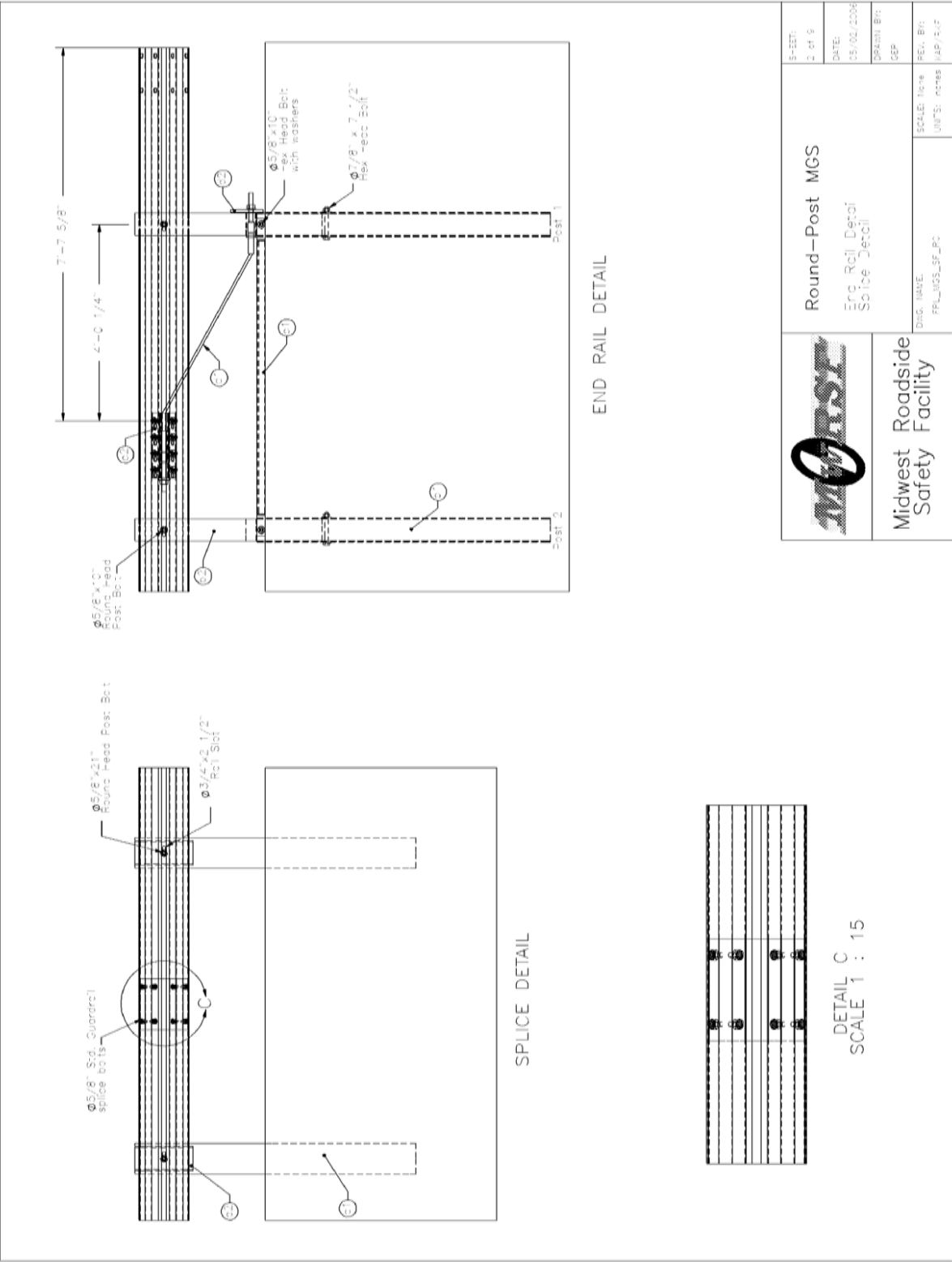


Figure H-2. MGS Round Post Southern Pine English Details – End Rail and Splice Detail

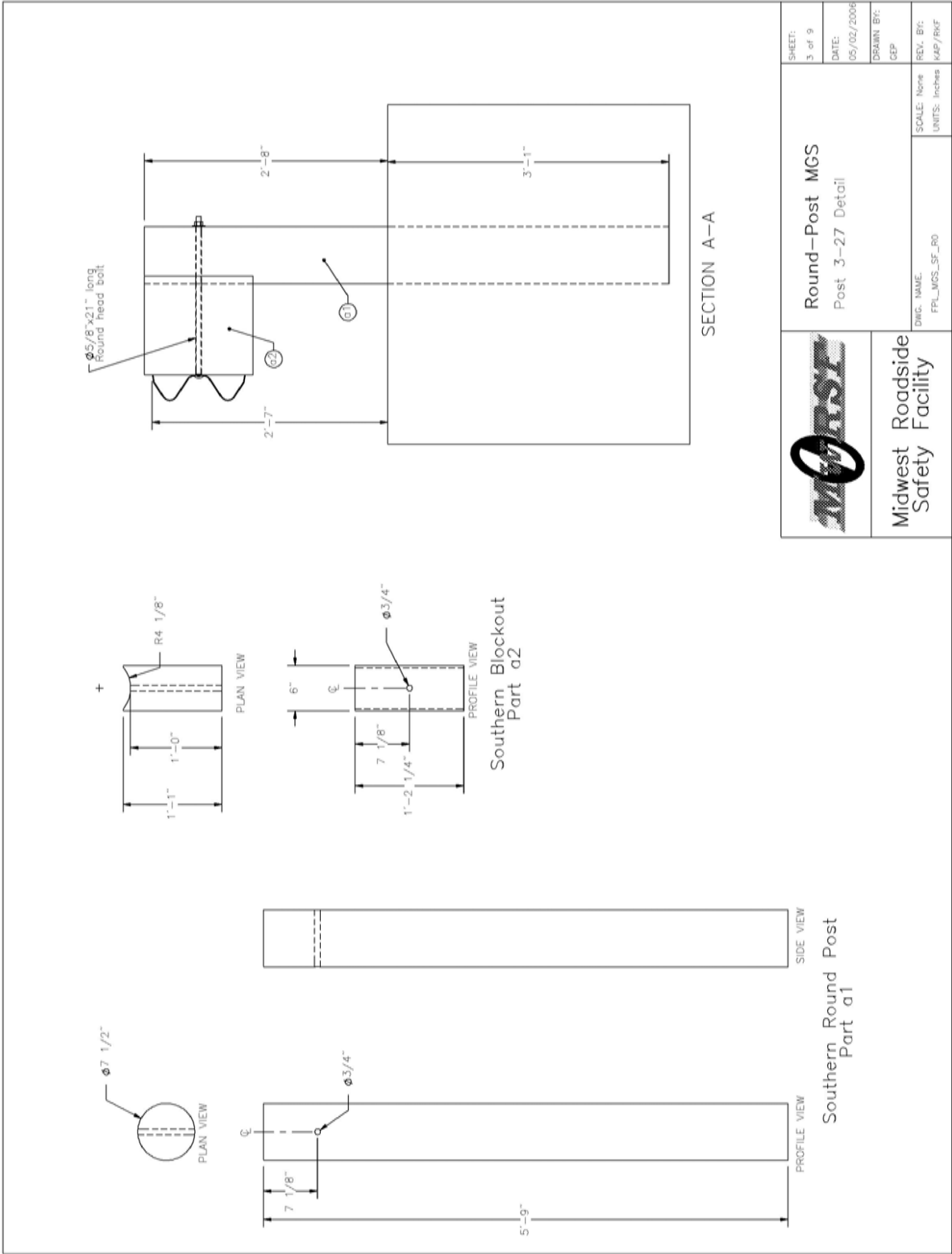


Figure H-3. MGS Round Post Southern Pine English Details – Post Detail

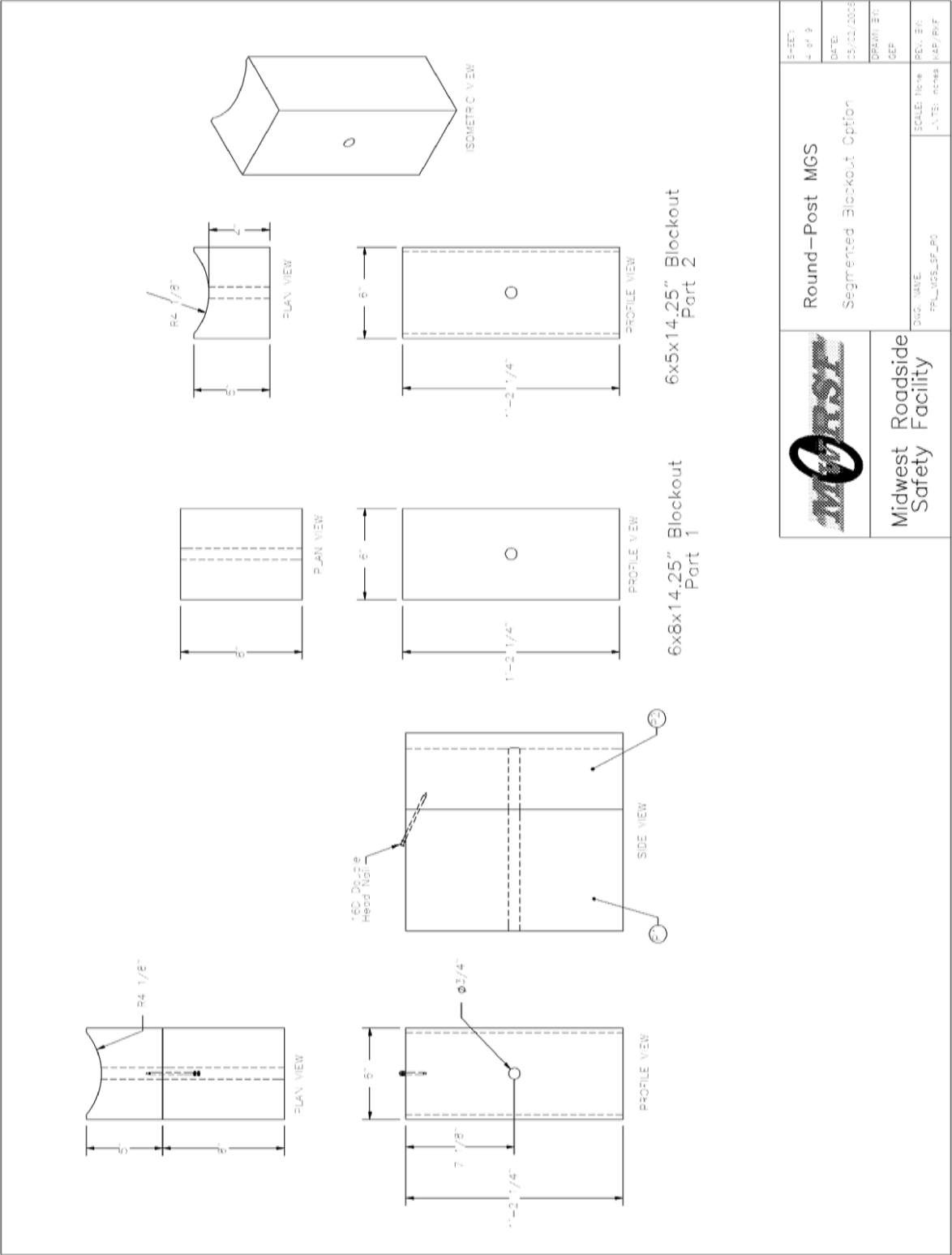


Figure H-4. MGS Round Post Southern Pine English Details – Segmented Blockout Detail

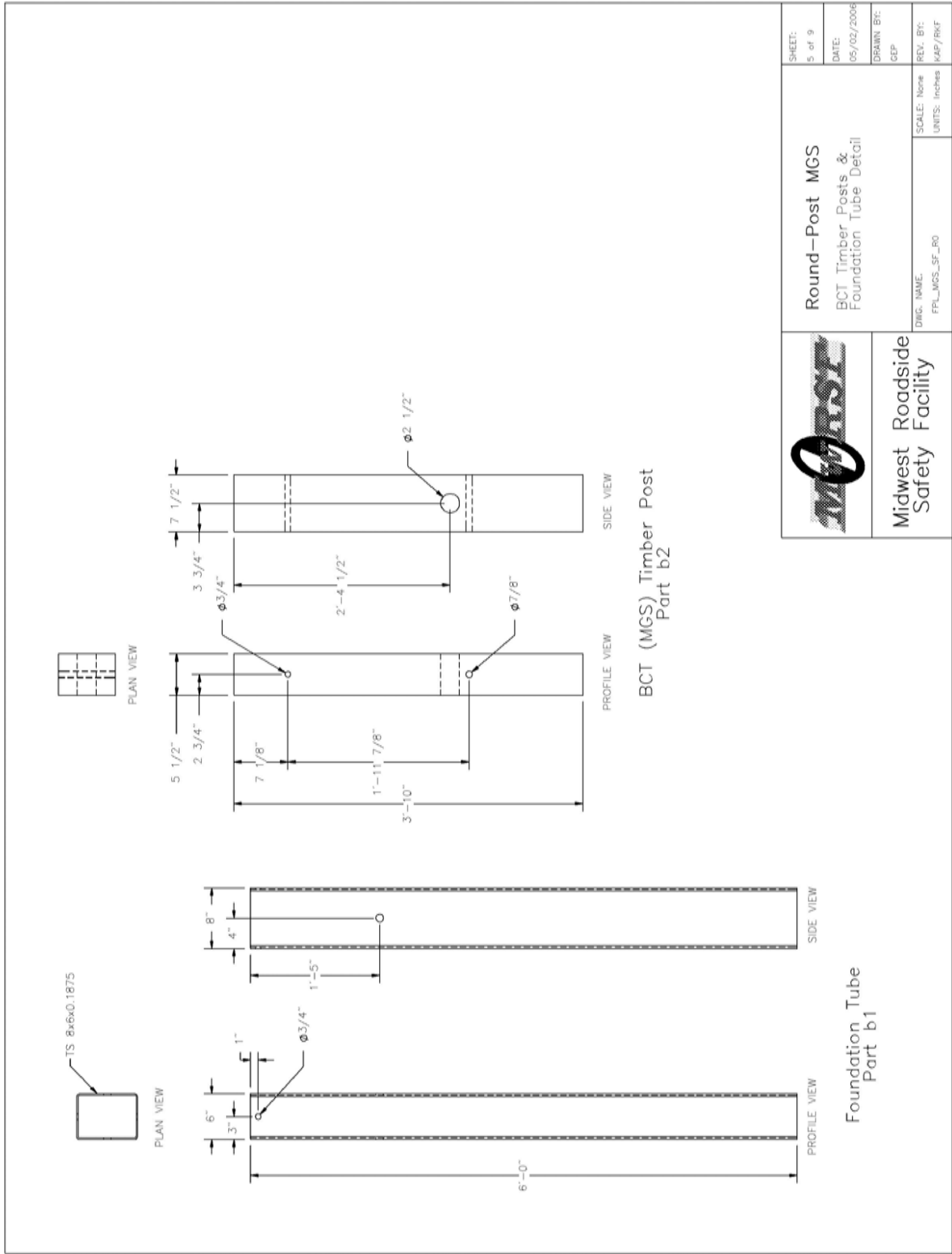


Figure H-5. MGS Round Post Southern Pine English Details – Anchor Post Detail

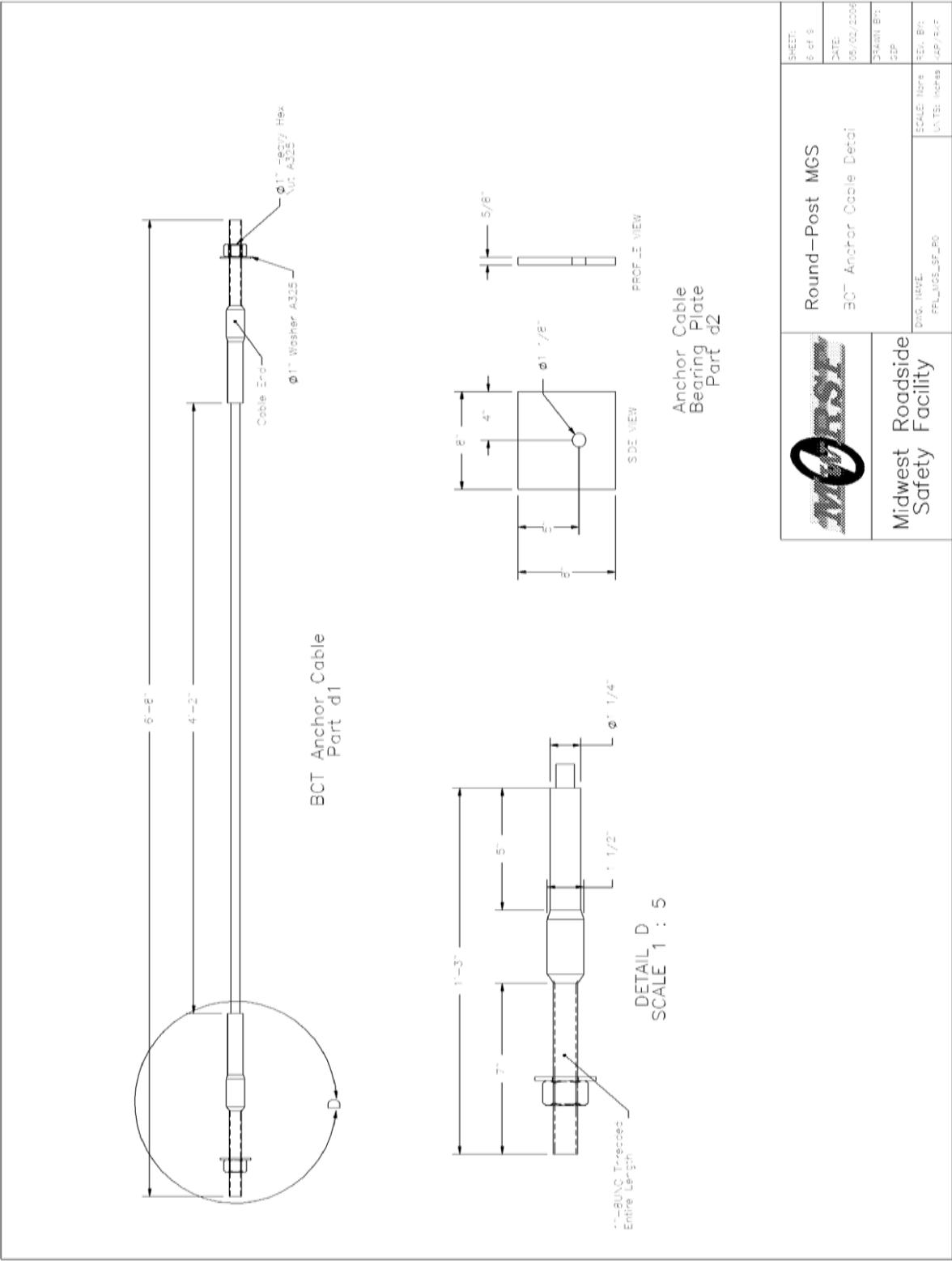
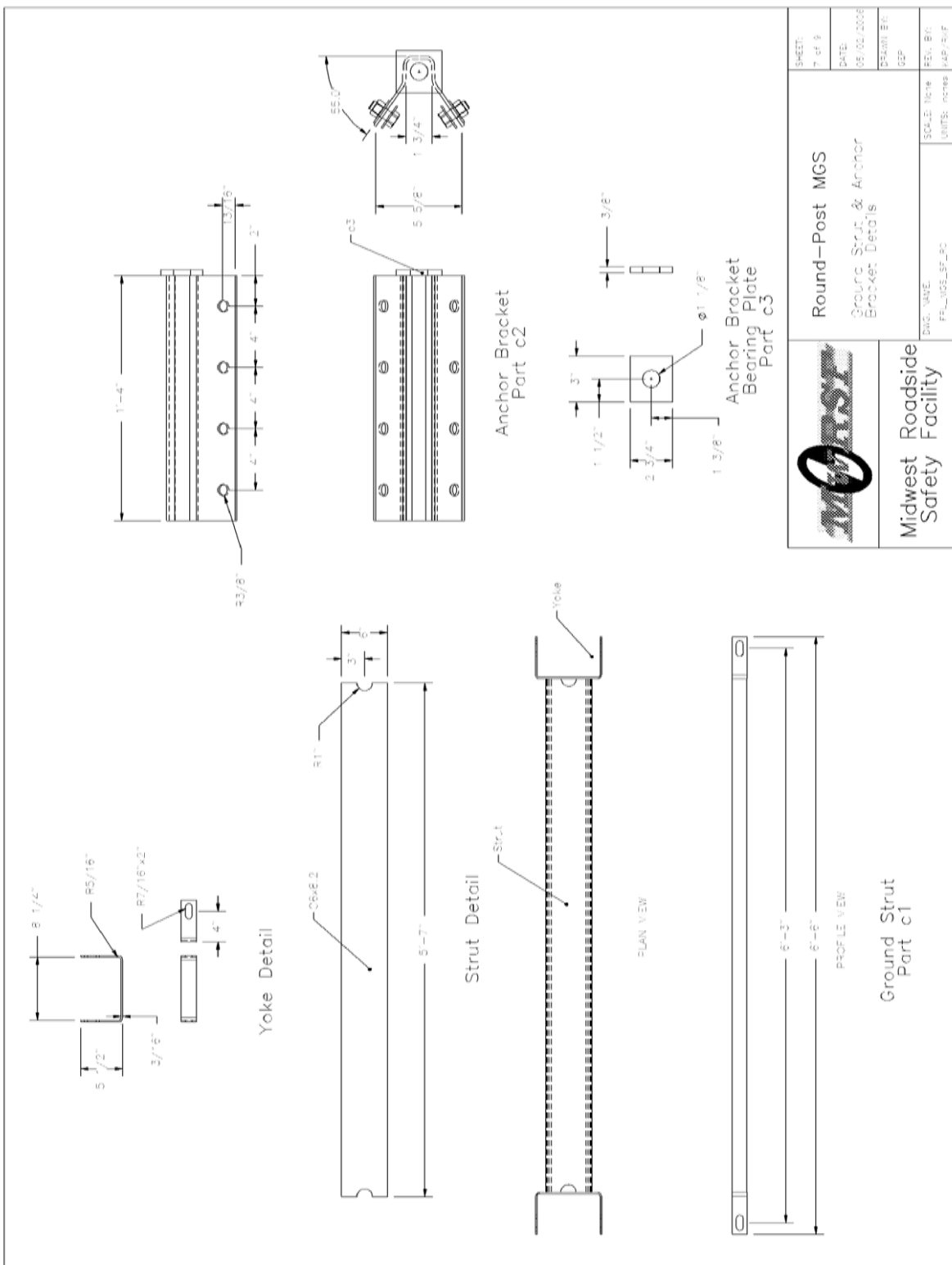


Figure H-6. MGS Round Post Southern Pine English Details – BCT Anchor Cable Detail



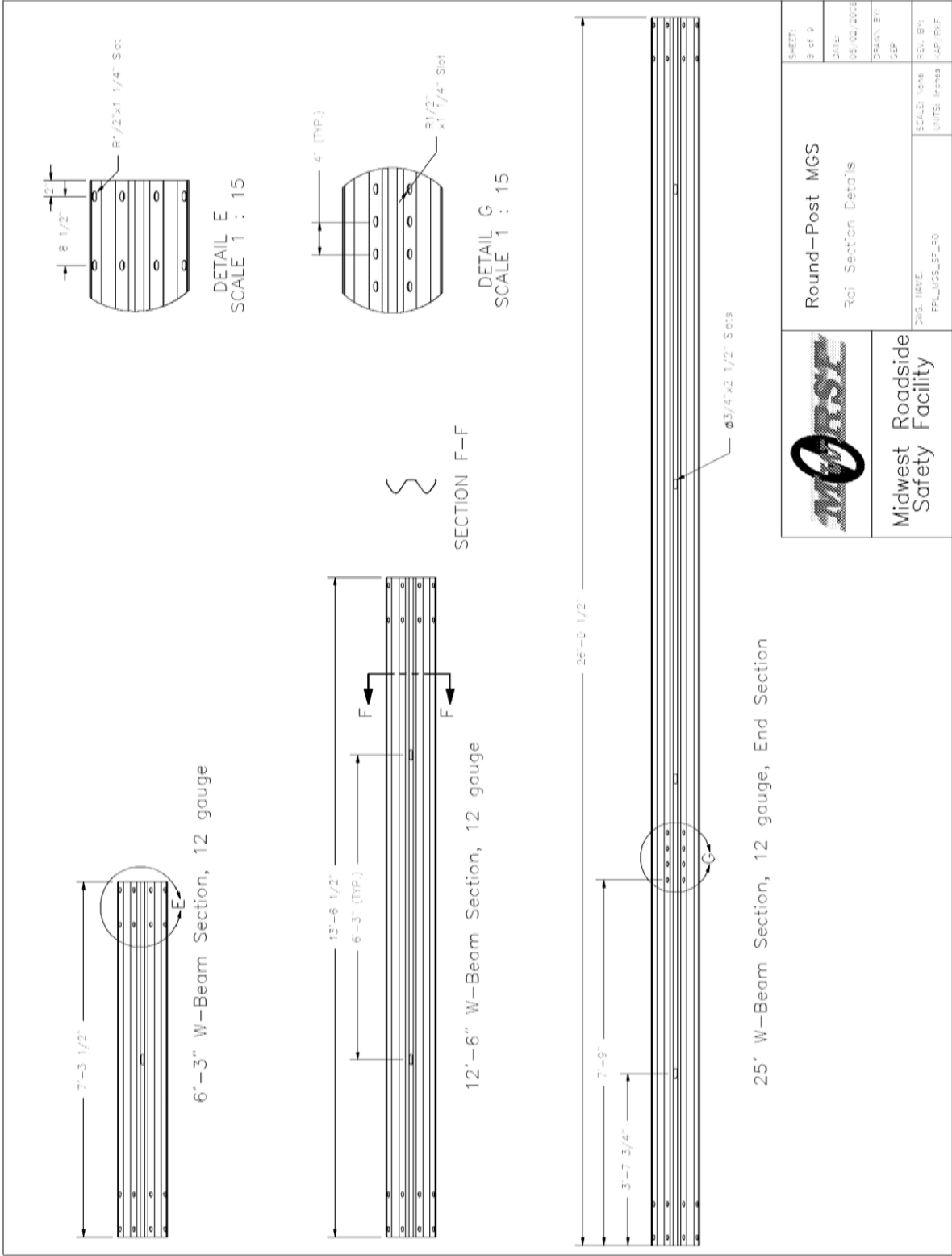


Figure H-8. MGS Round Post Southern Pine English Details – Rail Section Detail

General		Guardrail Post Grading Criteria	
All posts shall meet the current quality requirements of the American National Standards Institute (ANSI) D5.1, "Wood Poles" except as supplemented herein.			
Manufacture: All posts shall be smooth shored by machine. No "ringing" of the posts, as caused by improperly adjusted shearing machine, is permitted. All outer and inner bark shall be removed during the shoring process. All knots and knobs shall be trimmed smooth and flush with the surface of the posts. The guardrail posts shall be a minimum of 1.75 m (58 in.) long. The use of peeler cores is prohibited.			
Ground-line: The ground-line, for the purpose of applying these restrictions of ANSI D5.1 that reference the ground-line, shall be defined as being located 914 mm (36 in.) from the butt end of each post.			
Size: The size of the posts shall be classified based on their diameter at the ground-line and their length and shall be species specific. The ground-line diameter shall be specified by diameter in 6 mm (3/8 in.) breaks. The length shall be specified in 300 mm (1 ft) breaks. Dimensions shall apply to fully seasoned posts. When measured between their extreme ends, the post shall be no shorter than the specified lengths but may be up to 75 mm (3 in.) longer.			
Scars: Scars are permitted in the middle third as defined in ANSI D5.1 provided that the depth of the trimmed scar is not more than (1 in.).			
Shape and Straightness: All timber posts shall be nominally round in cross section. A straight line drawn from the centerline of the top to the center of the butt of any post shall not deviate from the centerline of the post more than 32 mm (1 1/4 in.) at any point. Posts shall be free from reverse bends.			
Splits and Shakes: Splits or ring shakes are not permitted in the top two thirds of the post. Splits not to exceed the diameter in length are permitted in the bottom third of the post. A single shake is permitted in the bottom third, provided it is not wider than one-half the butt diameter.			
Decay: Allowed in knots only.			
Holes: Pin holes 1 mm (1/16 in.) or less are not restricted.			
Slope of Grain: 1 in 10.			
Compression Wood: Not allowed, in the outer 25 mm (1 in.) or if exceeding 1/4 of the radius.			
Timber Spacers: When timber spacers are required, the timber species shall be the same as those specified for the timber posts. The size and use section shall be as shown on the plans, with a tolerance of 6 mm (1/4 in.). Spacers shall be of medium grain, at least two (2) rings per inch on one end, and free from splits, shakes, compression wood or decay in dry form. Individual knots, knot clusters or knots in the same cross section of a piece are permitted, provided they are sound or firm, and are limited in cumulative width (when measured between lines parallel to the edges) to no more than one-half the width of the face. Wane or the absence of wood is limited to one-third of the face on no more than 10 percent of the lot. Slope of grain deviation is limited to one in six. The material may be rough sawn or surfaced, full size, kiln or air dried, with a tolerance of 6 mm (1/4 in.) for all dimensions.			
Treatment: Treating – American Wood-Preservers' Association (AWPA) – Book of Standards (BOS) U1–05, use category system UCS; user specification for treated wood; commodity specification B; Posts; Wood for Highway Construction must be met using the methods outlined in AWPA BOS U1–05 Section 8.2. Each post treated shall have a minimum spaced depth of 19 mm (3/4 in.) as determined by examination of the tops and cuts of each post. Material that has been air dried or kiln dried shall be inspected for moisture content in accordance with AWPA standard U2 prior to treatment. Tests of representative pieces shall be conducted. The lot shall be considered acceptable when the average moisture content does not exceed 25 percent. Pieces exceeding 25 percent moisture content shall be rejected and removed from the lot.			
Species Specific Criteria			
Species: Southern Pine: Knot diameter for posts of Southern Pine shall not exceed 64 mm (2 1/2 in.). Ring density for the species shall be at least 4 rings-per-inch as measured over a 16 mm (3/4 in.) distance. The diameter of the Southern Pine posts shall be 150 mm (6 in.) at the ground line with a upper limit of 210 mm (8 1/4 in.).		Round—Post MGS Grading Specifications	
			
		Midwest Roadside Safety Facility	
		DWG. NAME: FE_MGS_SF_P0 SCALE: N/A UNITS: mm/ft	
		SHEET: 6 of 6 DATE: 02/02/2006 DRAWN BY: GEF REV. BY: N/A DATE: N/A	

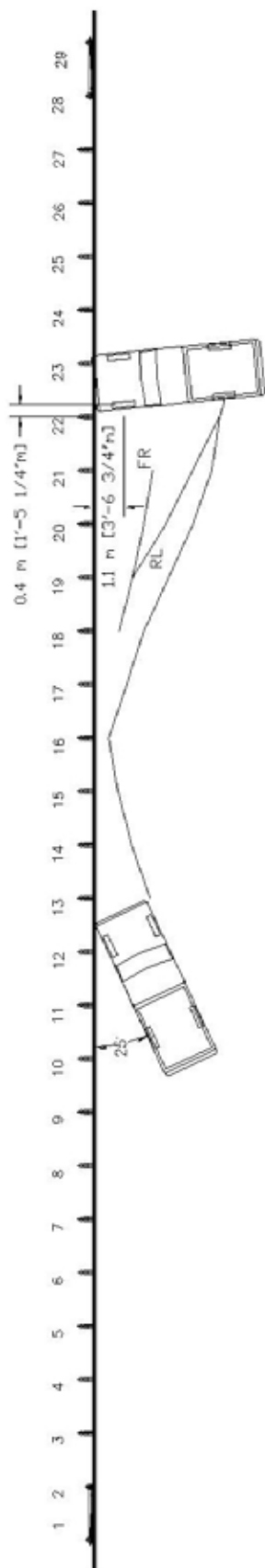
Figure H-9. MGS Round Post Southern Pine English Details – Grading Specifications

APPENDIX I - Test Nos. MGSDF-1 and MGSPP-1 Summary Sheets – English Units

Figure I-1. Summary of Test Results and Sequential Photographs, Test MGSDF-1	417
Figure I-2. Summary of Test Results and Sequential Photographs, Test MGSPP-1	418

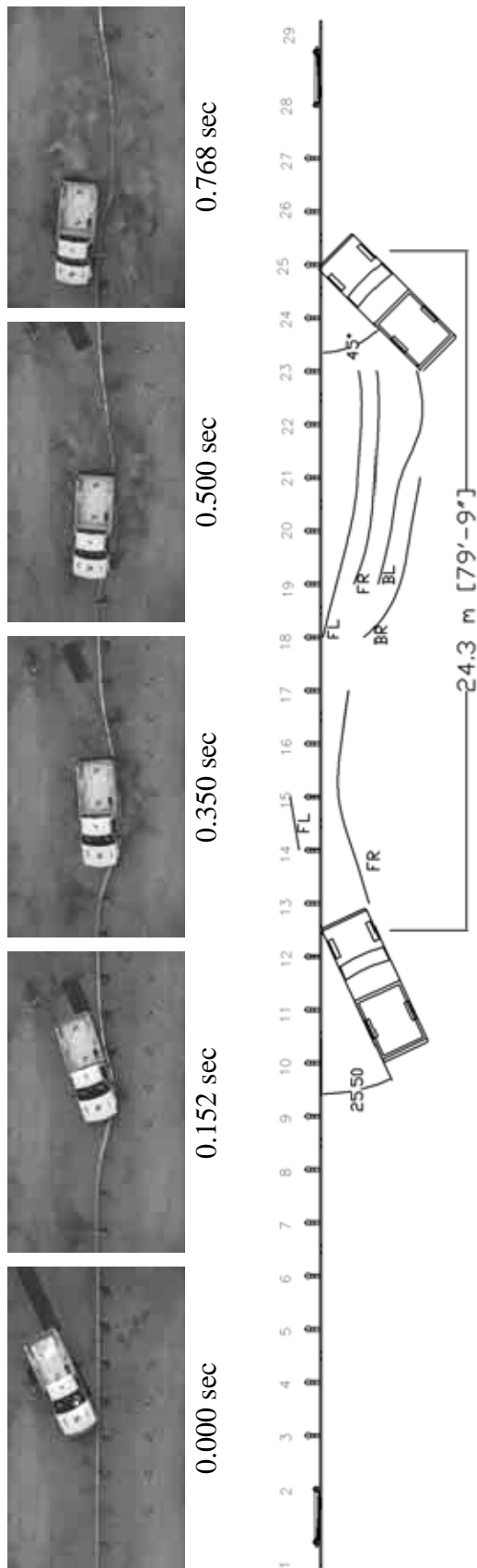


0.000 sec 0.134 sec 0.204 sec 0.372 sec 0.596 sec



- Test Number..... MGSDF-1 (3-11)
- Date 6/16/06
- Test Article..... Midwest Guardrail System
 - Key Elements..... Round Douglas Fir Posts
- Impact Location 37.5 in. Downstream of Post 12
- Soil Type Grading B AASHTO M147-65 (1990)
- Vehicle Model..... 2000 GMC C2500
 - Curb 4,581 lb
 - Test Inertial..... 4,451 lb
 - Gross Static..... 4,451 lb
- Vehicle Speed
 - Impact 62.1 mph
 - Exit NA
- Vehicle Angle
 - Impact (trajectory) 25.5 deg
 - Exit (trajectory)..... NA
- Vehicle Stability Satisfactory
- Vehicle Snagging Minor
- Occupant Ridedown Deceleration (10 msec avg.)
 - Longitudinal 8.76 g's < 20 g's
 - Lateral 5.69 g's < 20 g's
- Occupant Impact Velocity
 - Longitudinal 13.22 ft/s < 39.37 ft/s
 - Lateral 13.22 ft/s < 39.37 ft/s
- THIV 22.4 ft/s < 39.37 ft/s (not req.)
- PHD 8.87 g's < 20 g's (not req.)
- Vehicle Damage..... Moderate
 - TAD 11-LFQ-4
 - SAE 10LFEW5
 - OCDI LF000000000
- Vehicle Stopping Distance..... 63.0 ft downstream of impact
- Test Article Damage Moderate
- Maximum Deflection
 - Permanent Set..... 35.5 in.
 - Dynamic 60.2 in.
 - Working Width 60.3 in.

Figure I-1. Summary of Test Results and Sequential Photographs, Test MGSDF-1



• Test Number.....	MGSP-1 (3-11)	• Occupant Ridedown Deceleration (10 msec avg.)	
• Date	6/1/06	Longitudinal	5.90 g's < 20 g's
• Test Article.....	Midwest Guardrail System	Lateral	4.09 g's < 20 g's
• Key Elements.....	Round Ponderosa Pine Posts	• Occupant Impact Velocity	
• Impact Location.....	37.5 in. Downstream of Post 12	Longitudinal	22.47 ft/s < 39.37 m/s
• Soil Type	Grading B AASHTO M147-65 (1990)	Lateral	23.56 ft/s < 39.37 m/s
• Vehicle Model.....	2000 GMC C2500	• THIV	20.1 ft/s < 39.37 ft/s (not req.)
• Curb	4,319 lb	• PHD	8.47 g's < 20 g's (not req.)
• Test Inertial.....	4,464 lb	• Vehicle Damage.....	Moderate
• Gross Static.....	4,464 lb	TAD	11-LQF-4
• Vehicle Speed		SAE.....	10LFEW5
Impact	62.3 mph	OCDI.....	LF000000000
Exit	23.2 mph	• Vehicle Stopping Distance.....	79.7 ft downstream of impact
• Vehicle Angle		• Test Article Damage	Moderate
Impact (trajectory)	25.5 deg	• Maximum Deflection	
Exit (trajectory).....	19.9 deg	Permanent Set.....	27.8 in.
• Vehicle Stability	Satisfactory	Dynamic.....	37.6 in.
• Vehicle Snagging	Minor	• Working Width	48.6 in.

Figure I-2. Summary of Test Results and Sequential Photographs, Test MGSPPP-1

APPENDIX J - Occupant Compartment Deformation, Test Nos. MGSDF-1 and MGSPP-1

Figure J-1. Occupant Compartment Deformation Data, Test MGSDF-1	420
Figure J-2. Occupant Compartment Deformation Index (OCDI), Test MGSDF-1	421
Figure J-3. Occupant Compartment Deformation Data, Test MGSPP-1.....	422
Figure J-4. Occupant Compartment Deformation Index (OCDI), Test MGSPP-1.....	423

VEHICLE PRE/POST CRUSH INFO
Set-2

TEST: MGSDF-1
VEHICLE: 2000 Chevy C2500

Note: If impact is on driver side need to enter negative number for Y

POINT	X	Y	Z	X'	Y'	Z'	DEL X	DEL Y	DEL Z
1	50.75	-20	-1.5	50.75	-20	-1.5	0	0	0
2	51.25	-14	-3.5	51.5	-14	-3.5	0.25	0	0
3	50.75	-6.5	-4.25	51	-6.25	-4.25	0.25	0.25	0
4	48	3.25	-1.5	48	3.25	-1.25	0	0	0.25
5	46.75	7	-0.5	46.75	7	0	0	0	0.5
6	47.25	-20.5	-5.5	47.25	-20	-5.5	0	0.5	0
7	47	-13	-6.5	47	-12.75	-6.75	0	0.25	-0.25
8	46.75	-5.75	-7.25	46.75	-5.5	-7.25	0	0.25	0
9	43.75	1.25	-6	44	1.25	-5.75	0.25	0	0.25
10	42	6.5	-3	41.75	6.5	-2.75	-0.25	0	0.25
11	41.25	-20.75	-7.5	41.25	-20.5	-7.75	0	0.25	-0.25
12	40.75	-13.25	-8.25	40.75	-13.25	-8.5	0	0	-0.25
13	40.5	-6	-9	40.5	-5.75	-8.75	0	0.25	0.25
14	39.75	3	-9	39.75	3	-8.75	0	0	0.25
15	37.75	3.25	-4	37.75	3.25	-3.75	0	0	0.25
16	36	-20.5	-8.25	36	-20.5	-8.5	0	0	-0.25
17	35.5	-12	-8.75	35.5	-12	-8.75	0	0	0
18	35	-5.25	-9.5	35	-5	-9.5	0	0.25	0
19	34	0.5	-9	34	0.75	-8.75	0	0.25	0.25
20	33	5.5	-4.25	33	5.5	-4	0	0	0.25
21	29.75	-19.75	-8.75	29.75	-19.5	-8.75	0	0.25	0
22	29.5	-12.5	-9	29.75	-12.25	-9.25	0.25	0.25	-0.25
23	30	-4.25	-9.75	30	-4	-9.75	0	0.25	0
24	29.25	1	-9	29.25	1	-8.75	0	0	0.25
25	27.25	6.25	-5	27.25	6.25	-4.75	0	0	0.25
26	19.75	-19	-8.75	20	-18.75	-8.75	0.25	0.25	0
27	20.25	-10.75	-8.75	20.25	-10.75	-8.75	0	0	0
28	20.5	-1.5	-9.25	20.5	-1.75	-9	0	-0.25	0.25
29									
30									

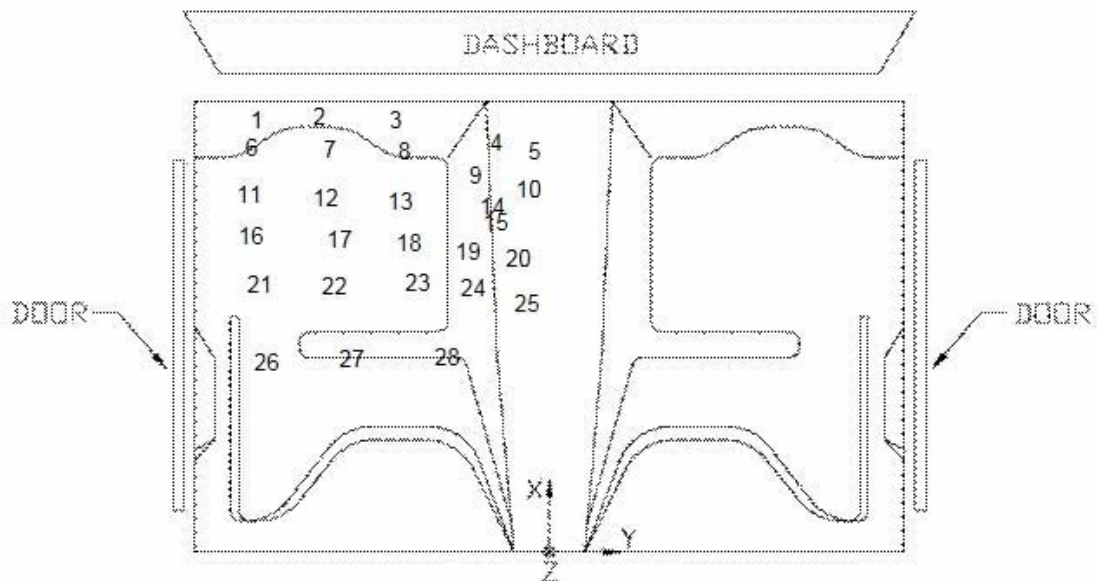


Figure J-1. Occupant Compartment Deformation Data, Test MGSDF-1

Occupant Compartment Deformation Index (OCDI)

Test No. MGSDF-1
Vehicle Type: 2000Chevy C2500

OCDI = XXABCDEFGHI

XX = location of occupant compartment deformation

A = distance between the dashboard and a reference point at the rear of the occupant compartment, such as the top of the rear seat or the rear of the cab on a pickup

B = distance between the roof and the floor panel

C = distance between a reference point at the rear of the occupant compartment and the motor panel

D = distance between the lower dashboard and the floor panel

E = interior width

F = distance between the lower edge of right window and the upper edge of left window

G = distance between the lower edge of left window and the upper edge of right window

H = distance between bottom front corner and top rear corner of the passenger side window

I = distance between bottom front corner and top rear corner of the driver side window

Severity Indices

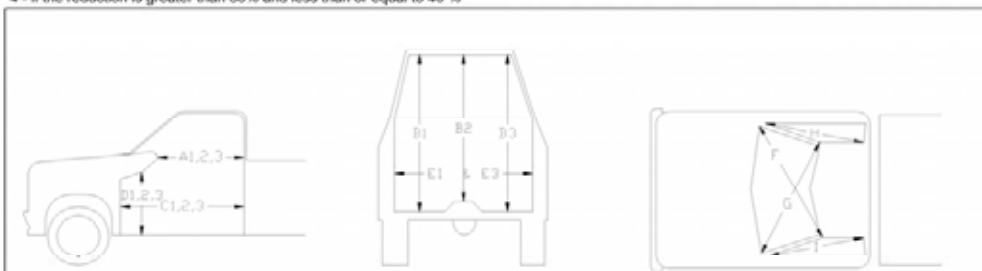
0 - if the reduction is less than 3%

1 - if the reduction is greater than 3% and less than or equal to 10 %

2 - if the reduction is greater than 10% and less than or equal to 20 %

3 - if the reduction is greater than 20% and less than or equal to 30 %

4 - if the reduction is greater than 30% and less than or equal to 40 %



where,
1 = Passenger Side
2 = Middle
3 = Driver Side

Location:

Measurement	Pre-Test (in.)	Post-Test (in.)	Change (in.)	% Difference	Severity Index
A1	41.25	41.25	0.00	0.00	0
A2	42.25	42.25	0.00	0.00	0
A3	40.00	40.00	0.00	0.00	0
B1	46.75	46.75	0.00	0.00	0
B2	43.00	42.75	-0.25	-0.58	0
B3	46.75	47.00	0.25	0.53	0
C1	57.50	57.75	0.25	0.43	0
C2	52.50	52.25	-0.25	-0.48	0
C3	57.00	57.00	0.00	0.00	0
D1	16.50	16.75	0.25	1.52	0
D2	10.50	10.25	-0.25	-2.38	0
D3	15.75	15.75	0.00	0.00	0
E1	62.25	61.50	-0.75	-1.20	0
E2	64.00	64.25	0.25	0.39	0
F	56.75	56.50	-0.25	-0.44	0
G	56.50	56.50	0.00	0.00	0
H	41.75	41.75	0.00	0.00	0
I	41.75	41.75	0.00	0.00	0

Note: Maximum severity index for each variable (A-I) is used for determination of final OCDI value

Final OCDI: XXABCDEFGHI
LF 0 0 0 0 0 0 0 0 0

Figure J-2. Occupant Compartment Deformation Index (OCDI), Test MGSDF-1

VEHICLE PRE/POST CRUSH INFO

Set-2

TEST: MGSPP-1
VEHICLE: 2000 Chevy C2500

Note: If impact is on driver side need to enter negative number for Y

POINT	X	Y	Z	X'	Y'	Z'	DEL X	DEL Y	DEL Z
1	47.75	-36.25	-4.75	48	-36	-4.5	0.25	0.25	0.25
2	48.25	-30	-5	48	-29.75	-4.5	-0.25	0.25	0.5
3	48	-23.75	-5	48	-24	-4.5	0	-0.25	0.5
4	46	-15	-2.5	45.75	-14.75	-2	-0.25	0.25	0.5
5	44.75	-10.5	-0.25	44.75	-10.5	0	0	0	0.25
6	41.75	-36.5	-7	42.25	-36	-6.75	0.5	0.5	0.25
7	42.5	-28.25	-7.25	42.5	-28	-7	0	0.25	0.25
8	41.75	-21.25	-7	41.75	-21	-6.75	0	0.25	0.25
9	40.25	-15.75	-5.5	40.25	-15.75	-5	0	0	0.5
10	39	-11.75	-1.5	39.25	-11.5	-1	0.25	0.25	0.5
11	36.25	-36.25	-7.25	36.75	-36.5	-7.25	0.5	-0.25	0
12	37	-31.25	-7.25	36.75	-31.25	-7	-0.25	0	0.25
13	36.5	-22.75	-7.75	36.25	-22.75	-7.5	-0.25	0	0.25
14	35.25	-16.5	-6.75	35.25	-16.25	-6.25	0	0.25	0.5
15	35	-11.5	-2	35	-11.5	-1.5	0	0	0.5
16	31.5	-33.75	-7.25	31.5	-33.5	-7	0	0.25	0.25
17	32	-27	-7.75	31.75	-26.75	-7.5	-0.25	0.25	0.25
18	32	-20.75	-7.75	31.75	-20.75	-7.5	-0.25	0	0.25
19	30.5	-15	-5	30.25	-15	-4.25	-0.25	0	0.75
20	30.25	-11.5	-2.5	30	-11.5	-1.75	-0.25	0	0.75
21	27	-35.5	-7.5	27	-35	-7.25	0	0.5	0.25
22	27.75	-28.5	-7.5	28	-28.5	-7.25	0.25	0	0.25
23	27.5	-23.25	-7.75	27.5	-23.25	-7.5	0	0	0.25
24	26.25	-15.25	-5.25	26.25	-15.5	-4.75	0	-0.25	0.5
25	25.75	-10.75	-2.75	25.75	-10.75	-2.25	0	0	0.5
26	23.25	-28.25	-7.5	23.25	-28	-7.25	0	0.25	0.25
27	23.5	-22.25	-7.5	23.25	-22	-7.25	-0.25	0.25	0.25
28	21.5	-12.75	-3	21.5	-12.75	-2.5	0	0	0.5
29									
30									

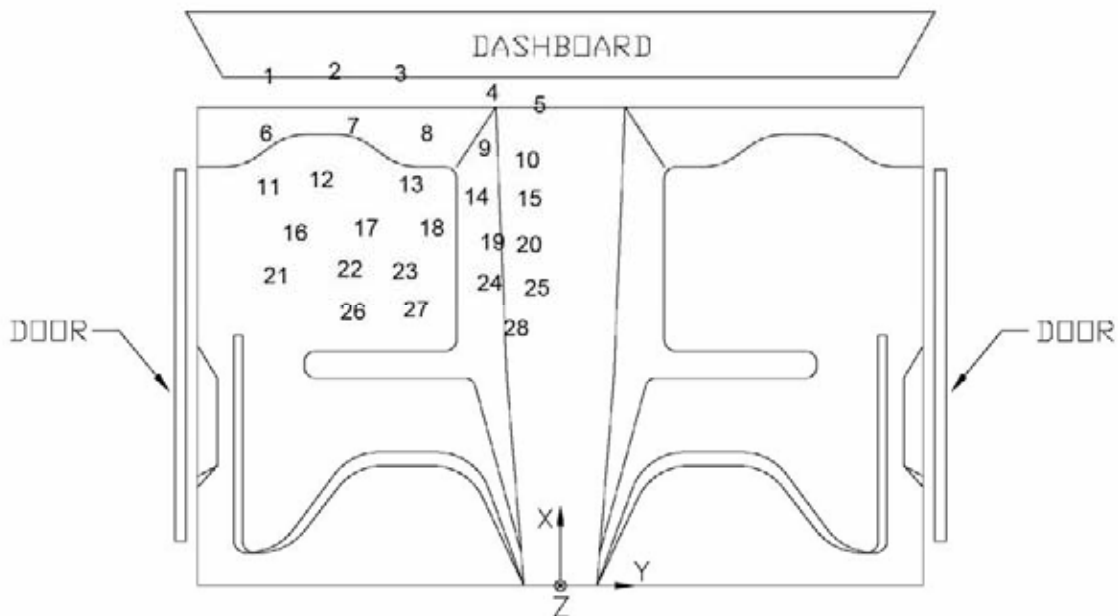


Figure J-3. Occupant Compartment Deformation Data, Test MGSPP-1

Occupant Compartment Deformation Index (OCDI)

Test No. MGSP-1
Vehicle Type: 2000Chevy C2500

OCDI = XXABCDEFGHI

XX = location of occupant compartment deformation

A = distance between the dashboard and a reference point at the rear of the occupant compartment, such as the top of the rear seat or the rear of the cab on a pickup

B = distance between the roof and the floor panel

C = distance between a reference point at the rear of the occupant compartment and the motor panel

D = distance between the lower dashboard and the floor panel

E = interior width

F = distance between the lower edge of right window and the upper edge of left window

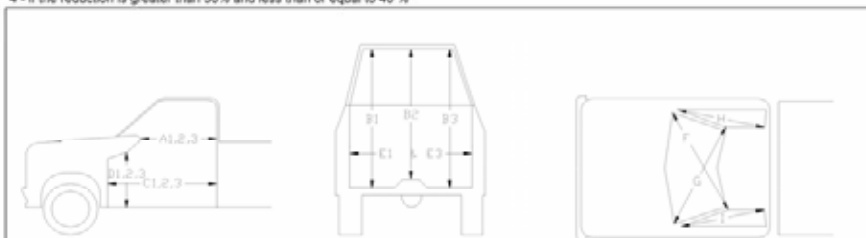
G = distance between the lower edge of left window and the upper edge of right window

H = distance between bottom front corner and top rear corner of the passenger side window

I = distance between bottom front corner and top rear corner of the driver side window

Severity Indices

- 0 - if the reduction is less than 3%
- 1 - if the reduction is greater than 3% and less than or equal to 10 %
- 2 - if the reduction is greater than 10% and less than or equal to 20 %
- 3 - if the reduction is greater than 20% and less than or equal to 30 %
- 4 - if the reduction is greater than 30% and less than or equal to 40 %



where,
1 = Passenger Side
2 = Middle
3 = Driver Side

Location:

Measurement	Pre-Test (in.)	Post-Test (in.)	Change (in.)	% Difference	Severity Index
A1	40.25	40.00	-0.25	-0.62	0
A2	40.75	41.00	0.25	0.61	0
A3	40.25	40.25	0.00	0.00	0
B1	47.25	46.75	-0.50	-1.06	0
B2	44.25	43.75	-0.50	-1.13	0
B3	47.75	47.75	0.00	0.00	0
C1	57.50	57.25	-0.25	-0.43	0
C2	52.50	52.50	0.00	0.00	0
C3	57.75	57.50	-0.25	-0.43	0
D1	15.50	15.50	0.00	0.00	0
D2	9.25	9.00	-0.25	-2.70	0
D3	15.75	16.50	0.75	4.76	0
E1	62.50	61.75	-0.75	-1.20	0
E3	64.25	64.13	-0.13	-0.19	0
F	56.50	56.50	0.00	0.00	0
G	57.00	56.75	-0.25	-0.44	0
H	42.75	42.50	-0.25	-0.58	0
I	42.75	42.00	-0.75	-1.75	0

[Note: Maximum severity index for each variable (A-I) is used for determination of final OCDI value]

Final OCDI: XXABCDEFGHI
LF 0 0 0 0 0 0 0 0 0

Figure J-4. Occupant Compartment Deformation Index (OCDI), Test MGSP-1

APPENDIX K - Accelerometer and Rate Transducer Data Analysis

Test Nos. MGSDF-1 and MGSPP-1

Figure K-1. Graph of Longitudinal Deceleration – Filtered Data, Test MGSDF-1	425
Figure K-2. Graph of Longitudinal Occupant Impact Velocity – Filtered Data, Test MGSDF-1	426
Figure K-3. Graph of Longitudinal Occupant Displacement – Filtered Data, Test MGSDF-1 ..	427
Figure K-4. Graph of Lateral Deceleration – Filtered Data, Test MGSDF-1	428
Figure K-5. Graph of Lateral Occupant Impact Velocity – Filtered Data, Test MGSDF-1	429
Figure K-6. Graph of Lateral Occupant Displacement – Filtered Data, Test MGSDF-1	430
Figure K-7. Graph of Longitudinal Deceleration – Filtered Data, Test MGSPP-1	431
Figure K-8. Graph of Longitudinal Occupant Impact Velocity – Filtered Data, Test MGSPP-1	432
Figure K-9. Graph of Longitudinal Occupant Displacement – Filtered Data, Test MGSPP-1 ..	433
Figure K-10. Graph of Lateral Deceleration – Filtered Data, Test MGSPP-1	434
Figure K-11. Graph of Lateral Occupant Impact Velocity – Filtered Data, Test MGSPP-1	435
Figure K-12. Graph of Lateral Occupant Displacement – Filtered Data, Test MGSPP-.....	436

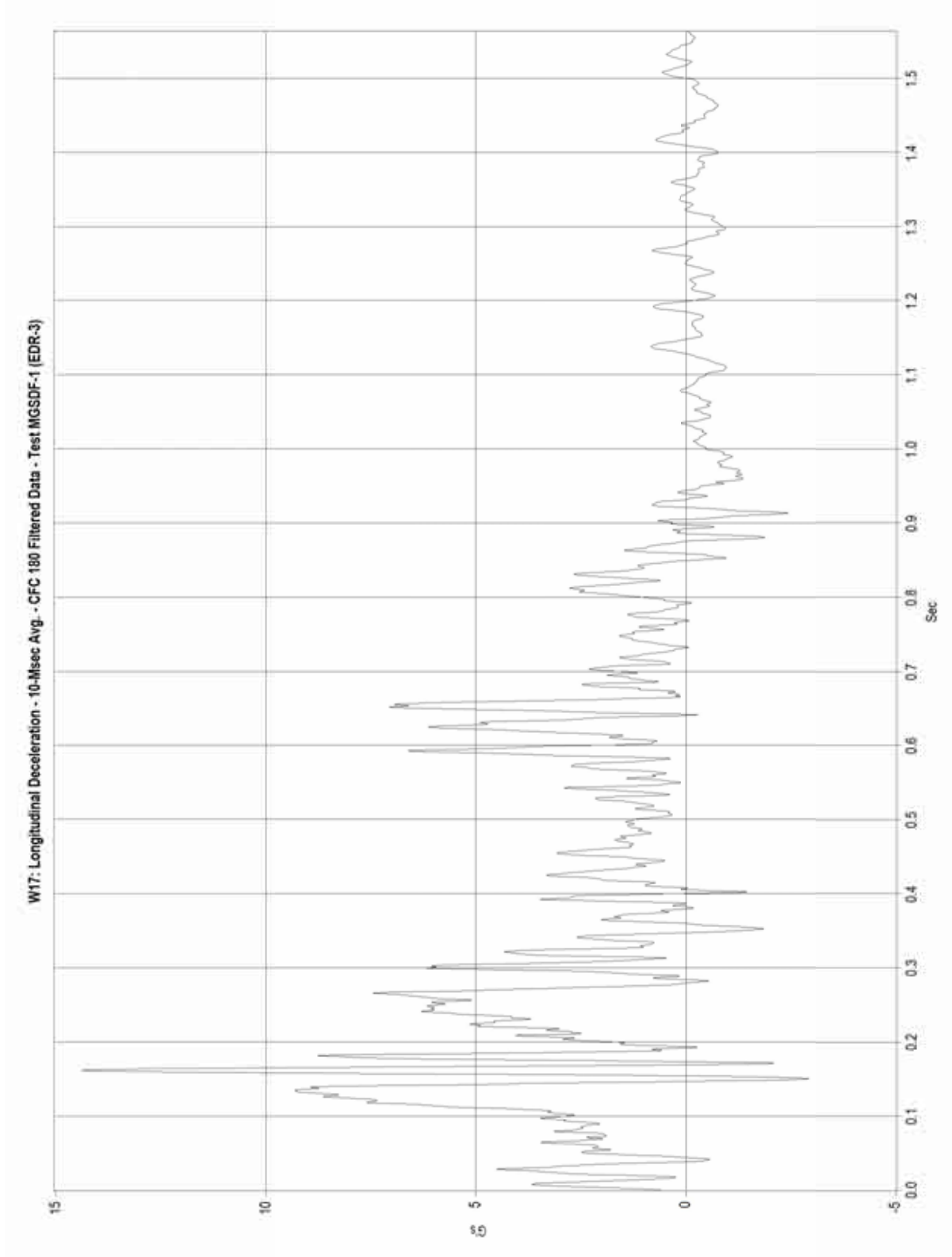


Figure K-1. Graph of Longitudinal Deceleration – Filtered Data, Test MGSDF-1

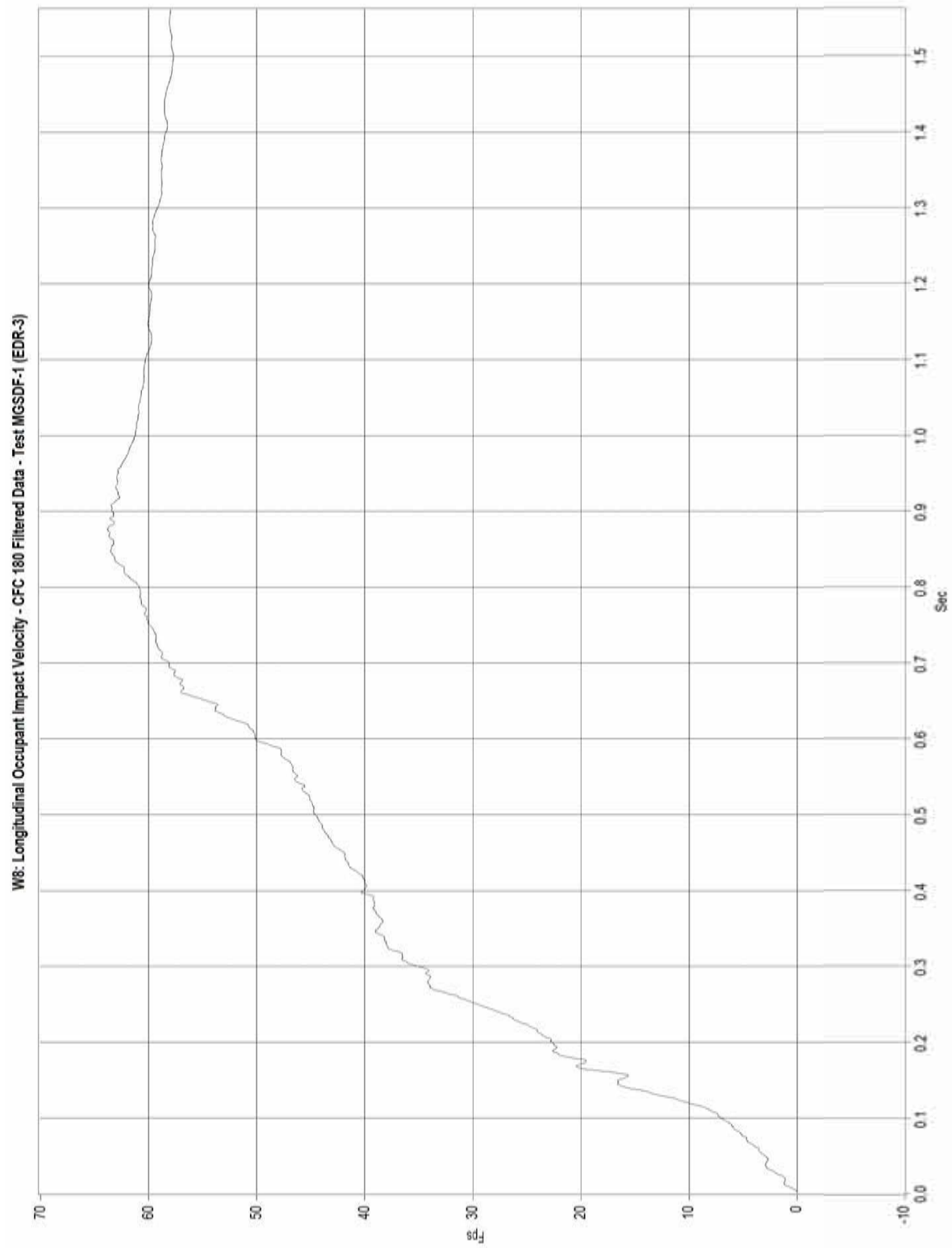


Figure K-2. Graph of Longitudinal Occupant Impact Velocity – Filtered Data, Test MGSDF-1

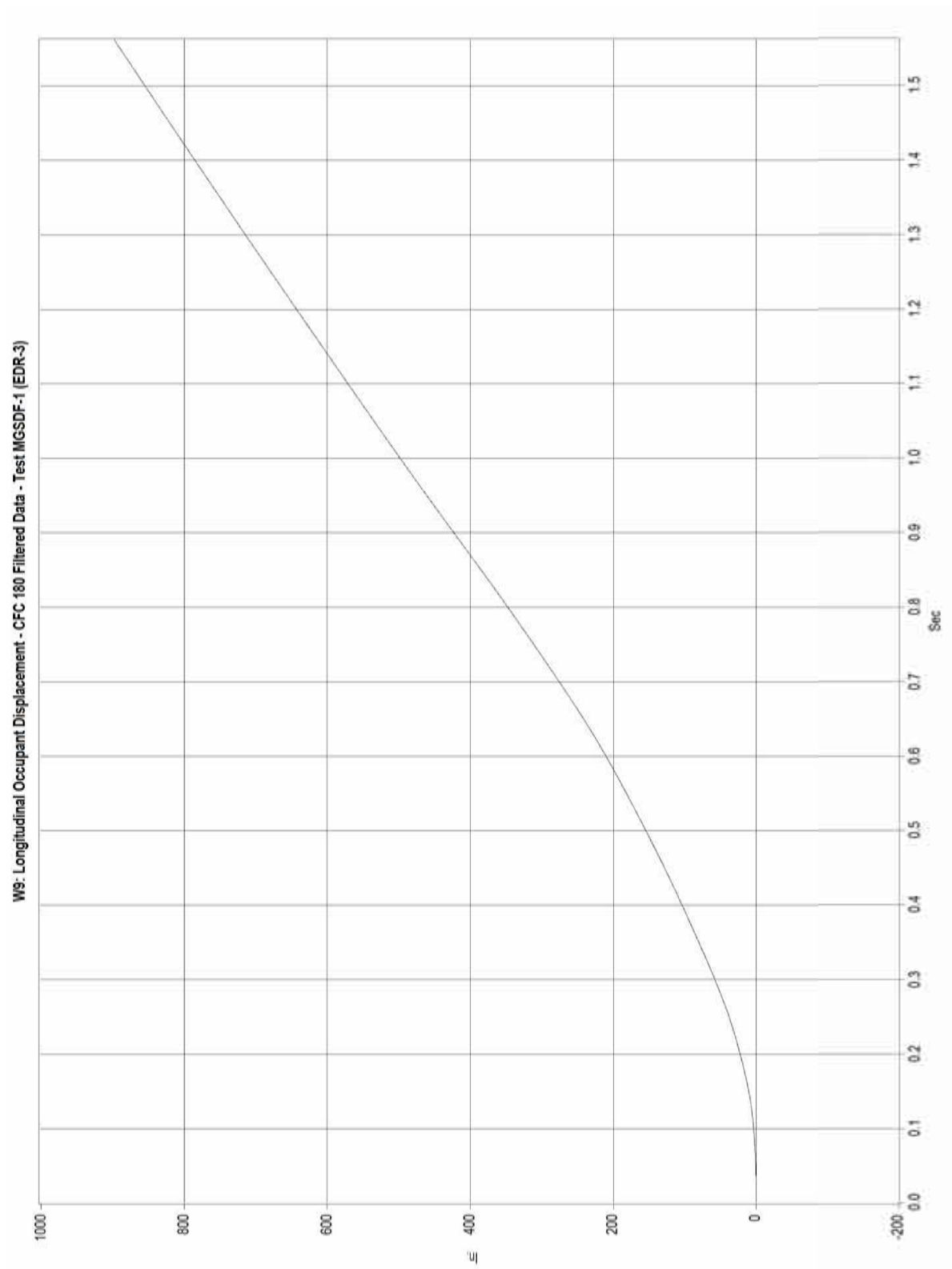


Figure K-3. Graph of Longitudinal Occupant Displacement – Filtered Data, Test MGSDF-1

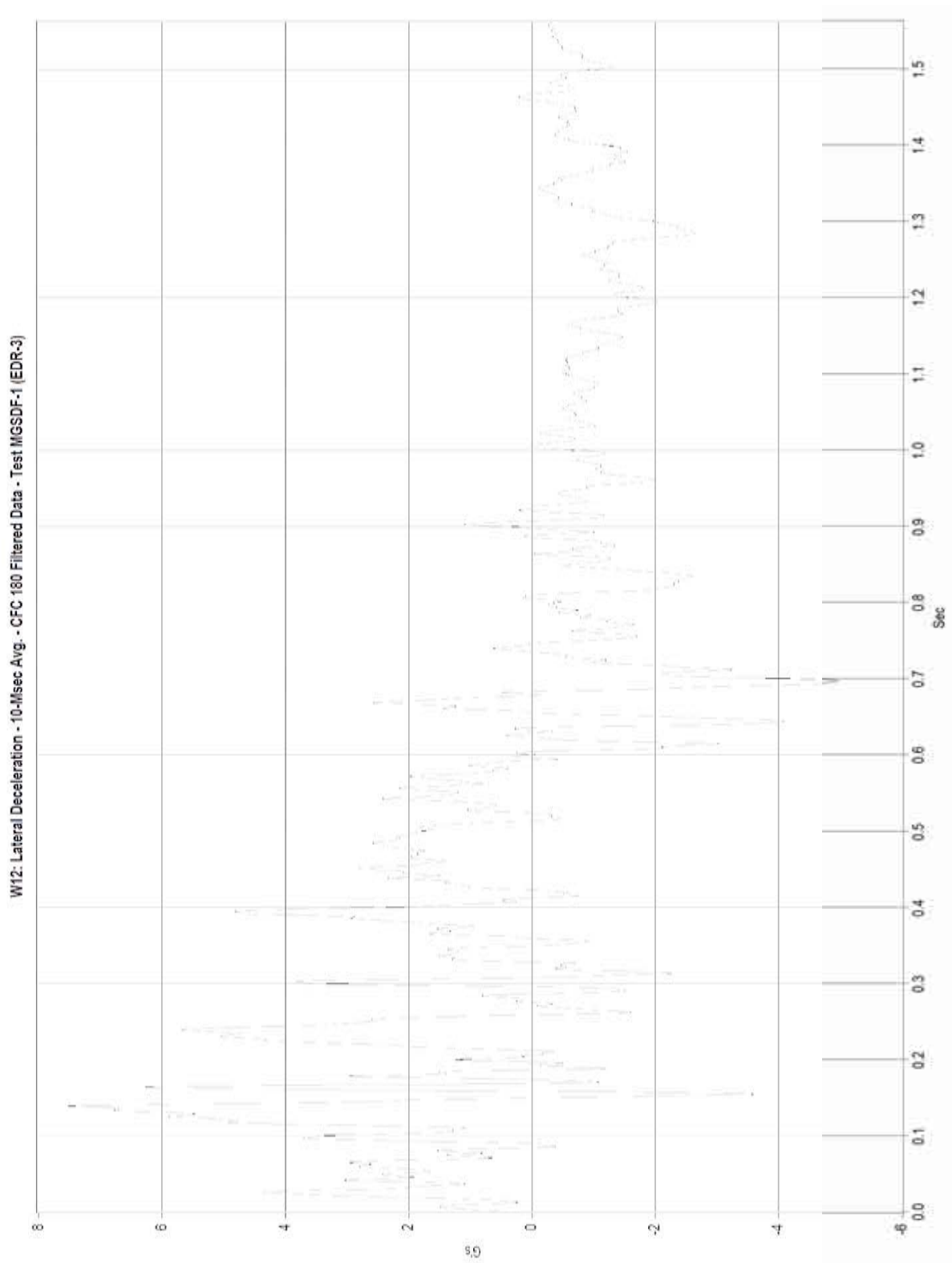


Figure K-4. Graph of Lateral Deceleration – Filtered Data, Test MGSDF-1

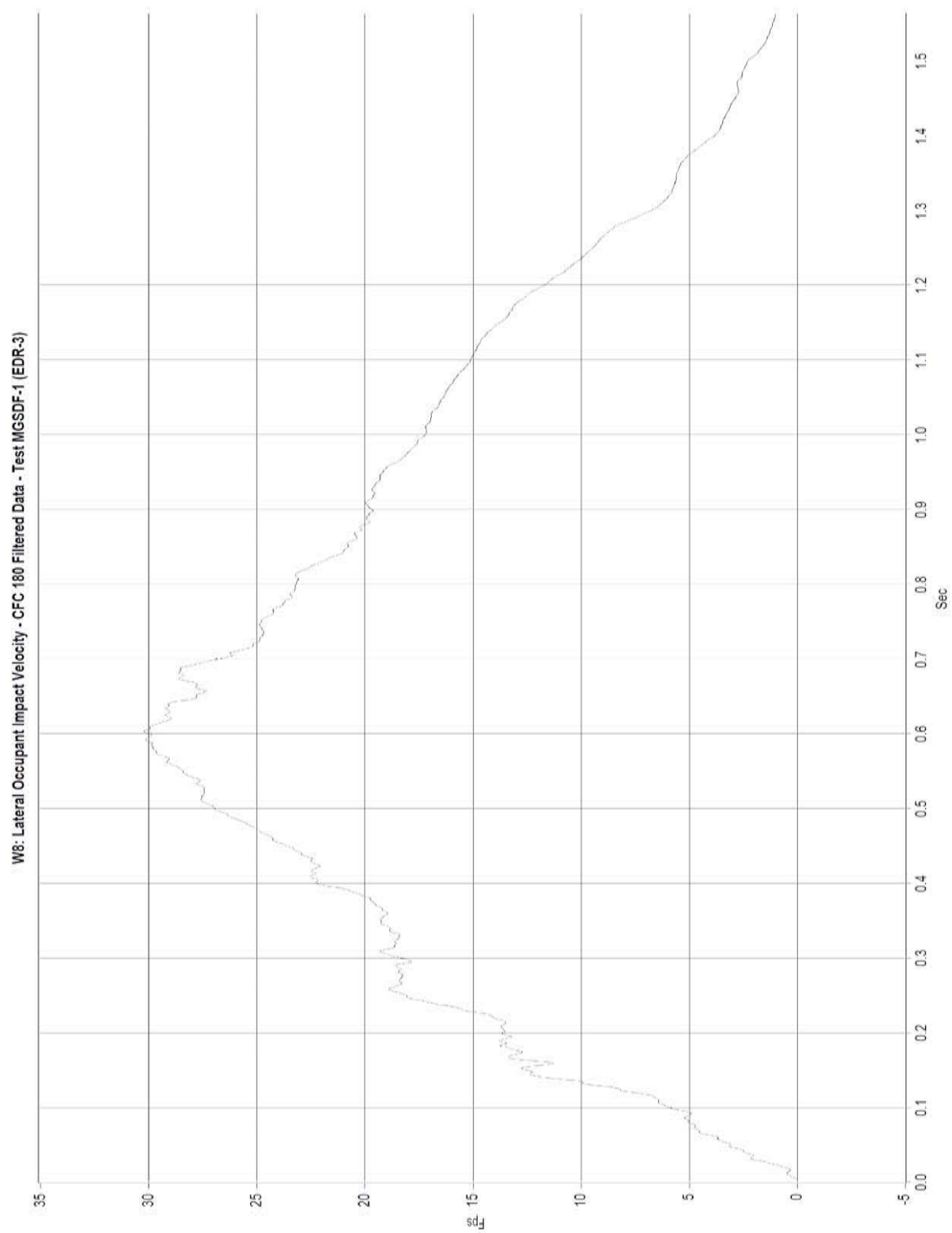


Figure K-5. Graph of Lateral Occupant Impact Velocity – Filtered Data, Test MGSDF-1

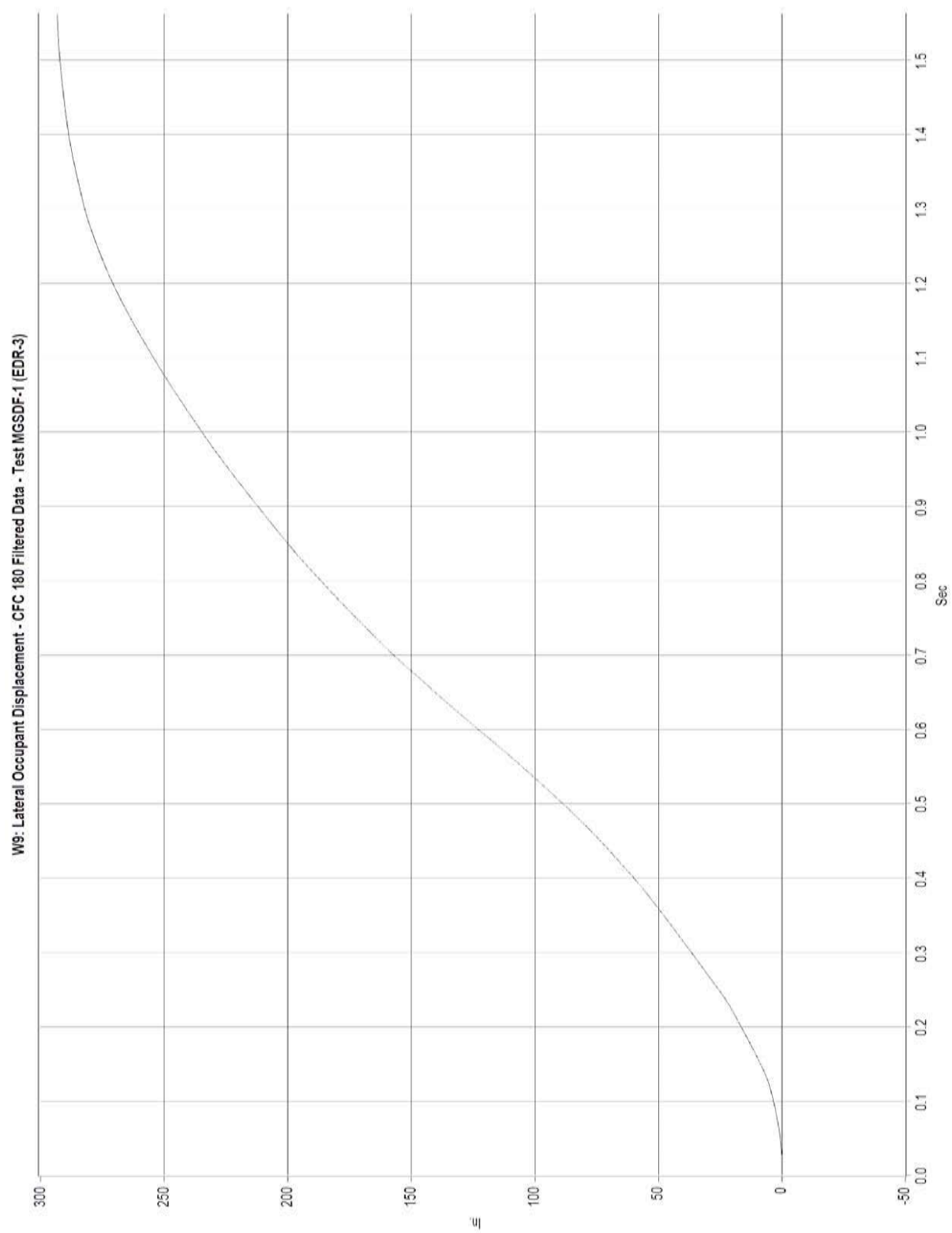


Figure K-6. Graph of Lateral Occupant Displacement – Filtered Data, Test MGSDF-1

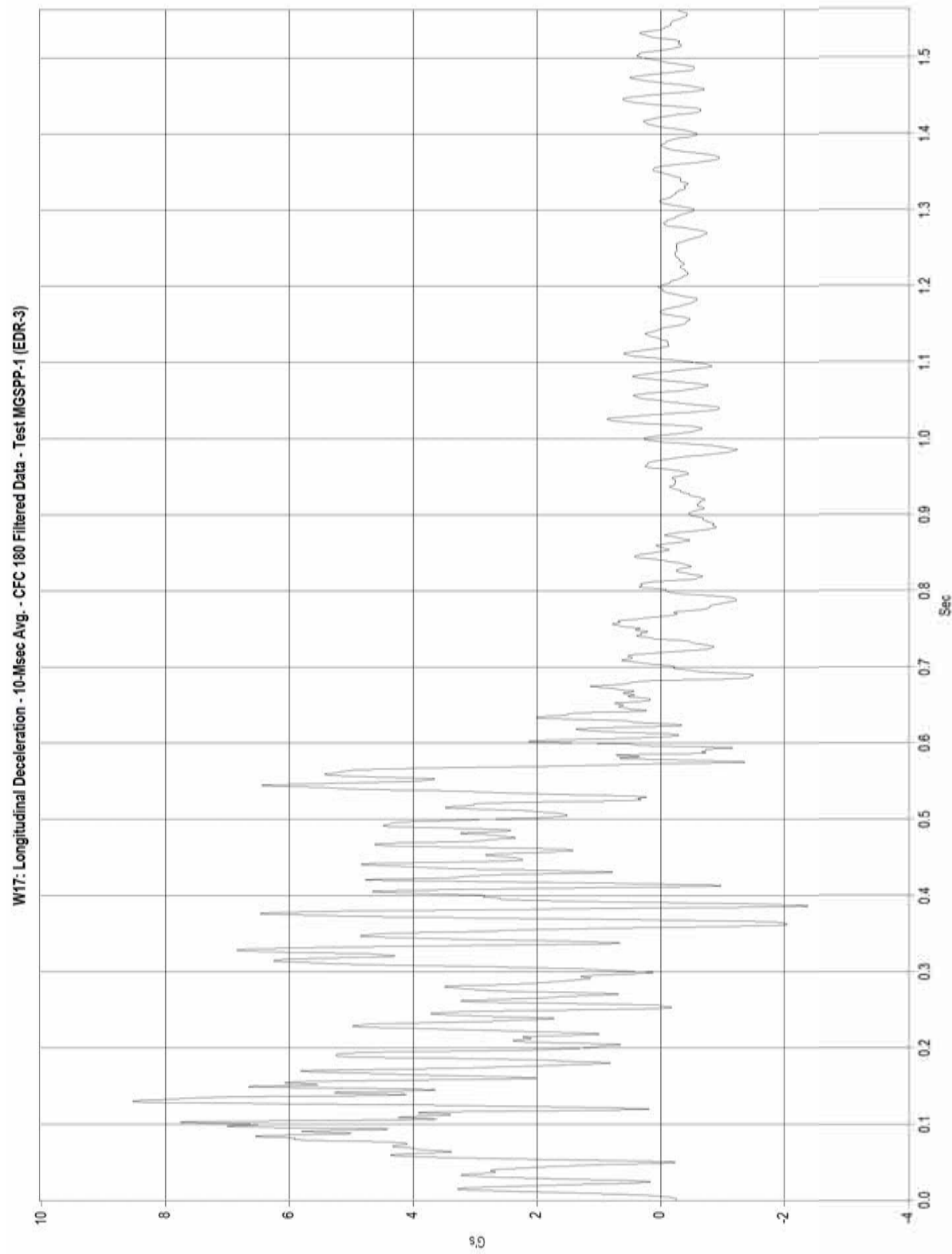


Figure K-7. Graph of Longitudinal Deceleration – Filtered Data, Test MGSPP-1

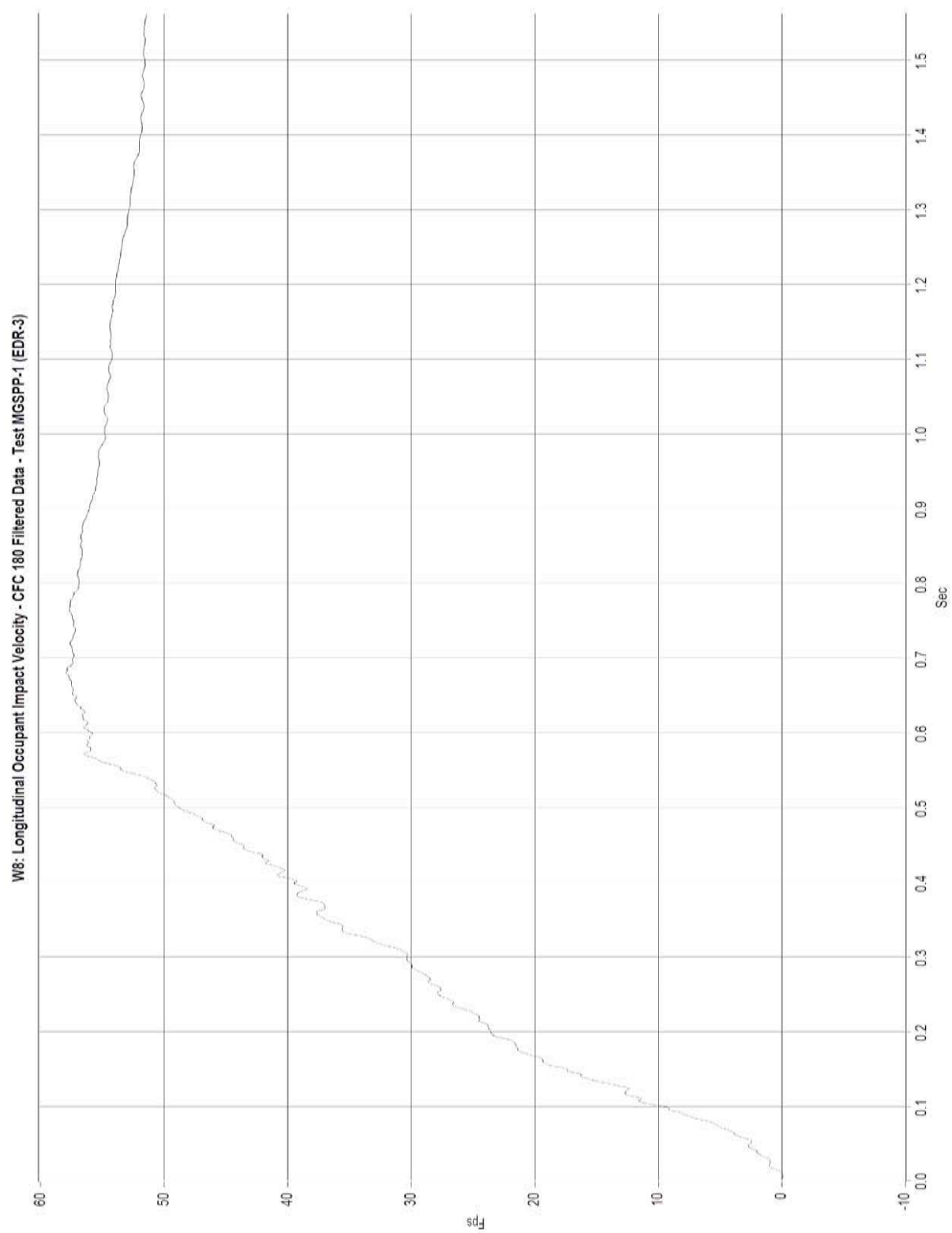


Figure K-8. Graph of Longitudinal Occupant Impact Velocity – Filtered Data, Test MGSPP-1

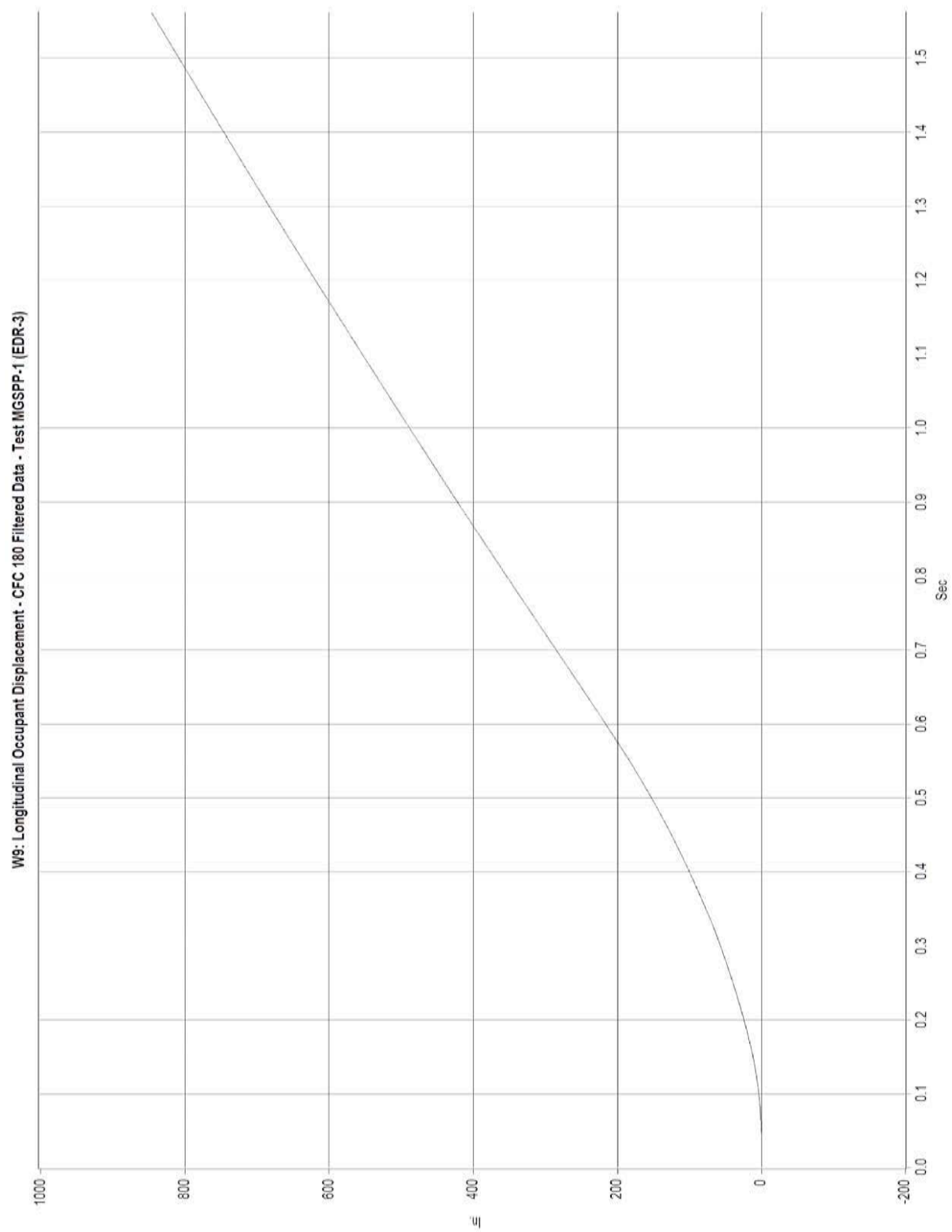


Figure K-9. Graph of Longitudinal Occupant Displacement – Filtered Data, Test MGSPP-1

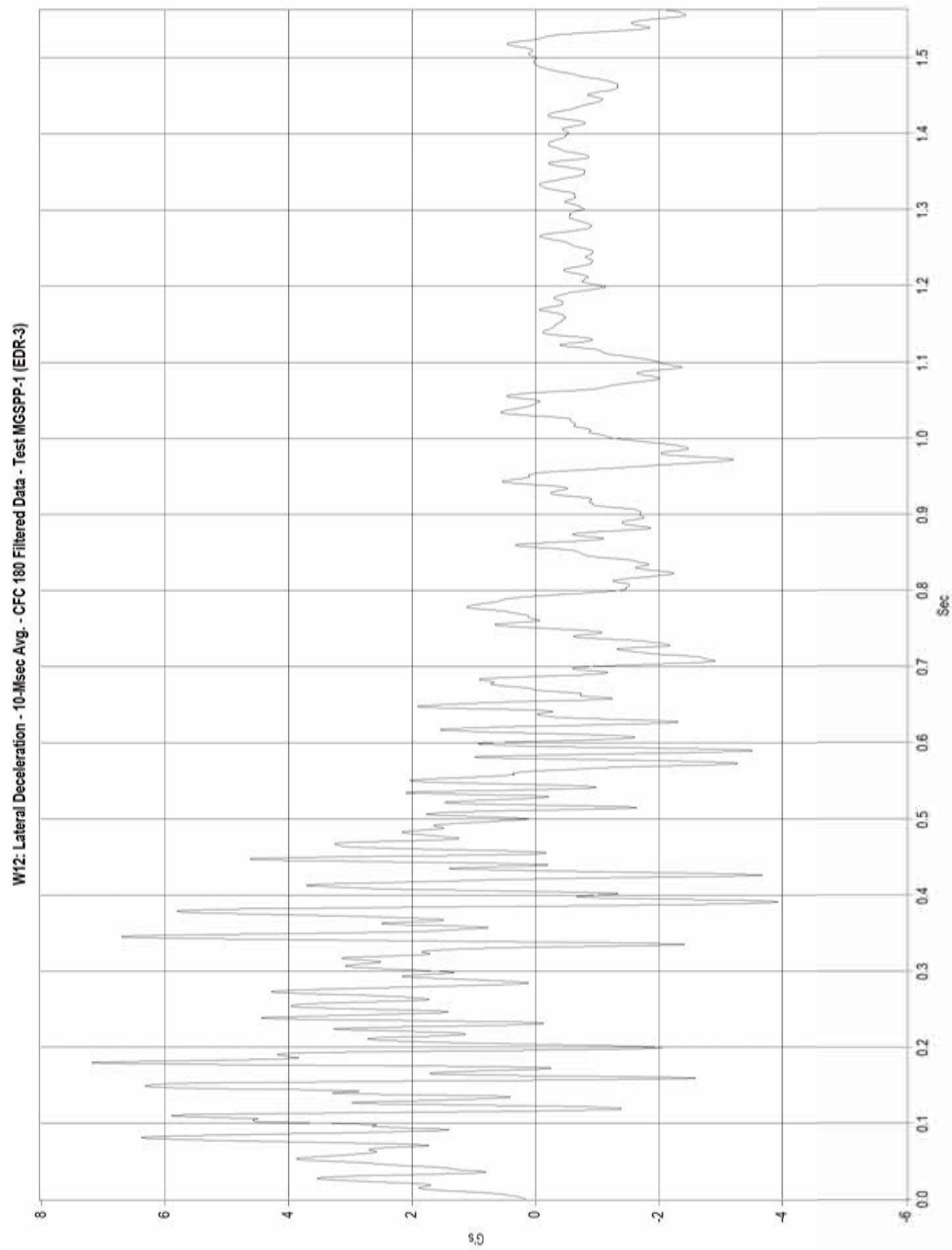


Figure K-10. Graph of Lateral Deceleration – Filtered Data, Test MGSPP-1

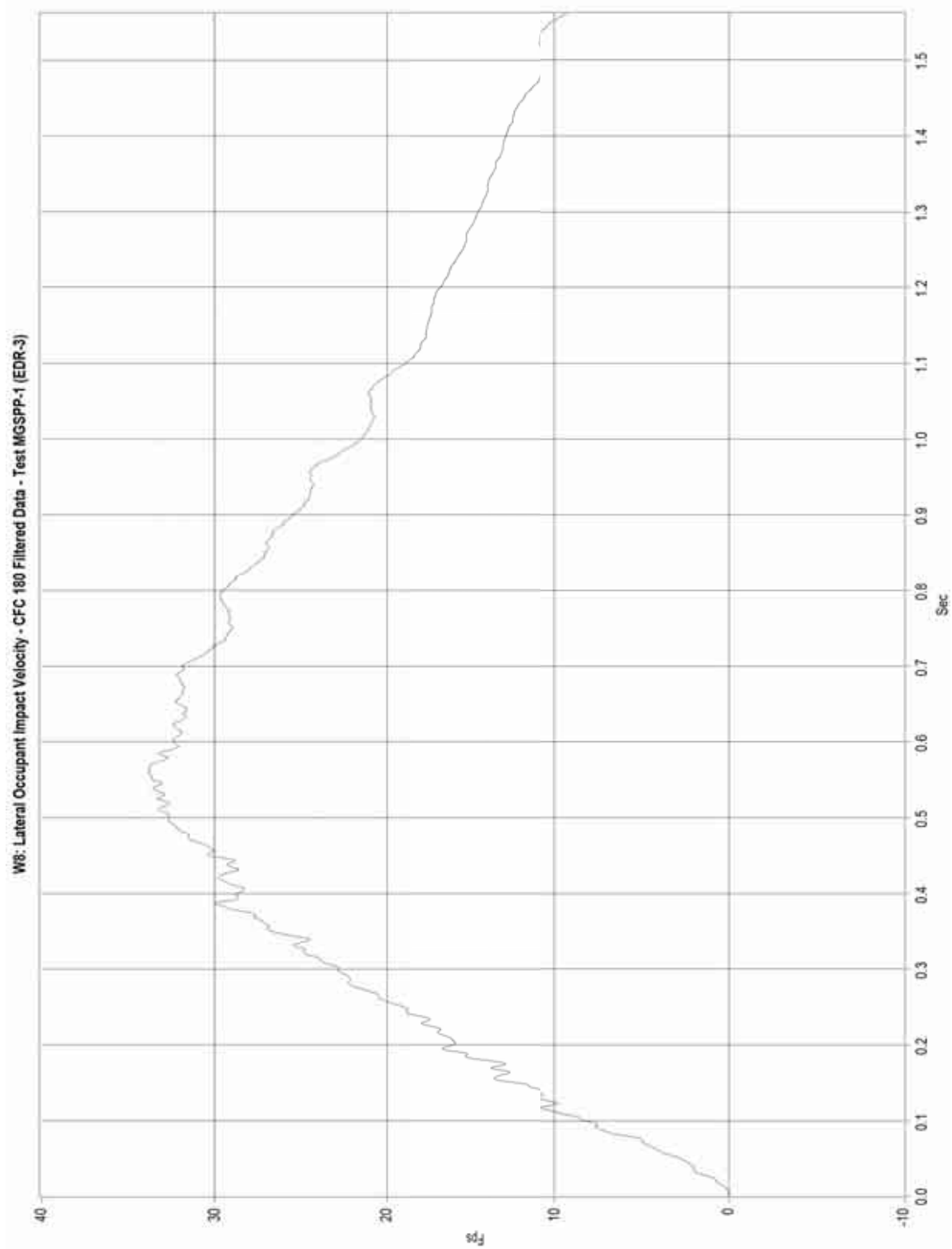


Figure K-11. Graph of Lateral Occupant Impact Velocity – Filtered Data, Test MGSPP-1

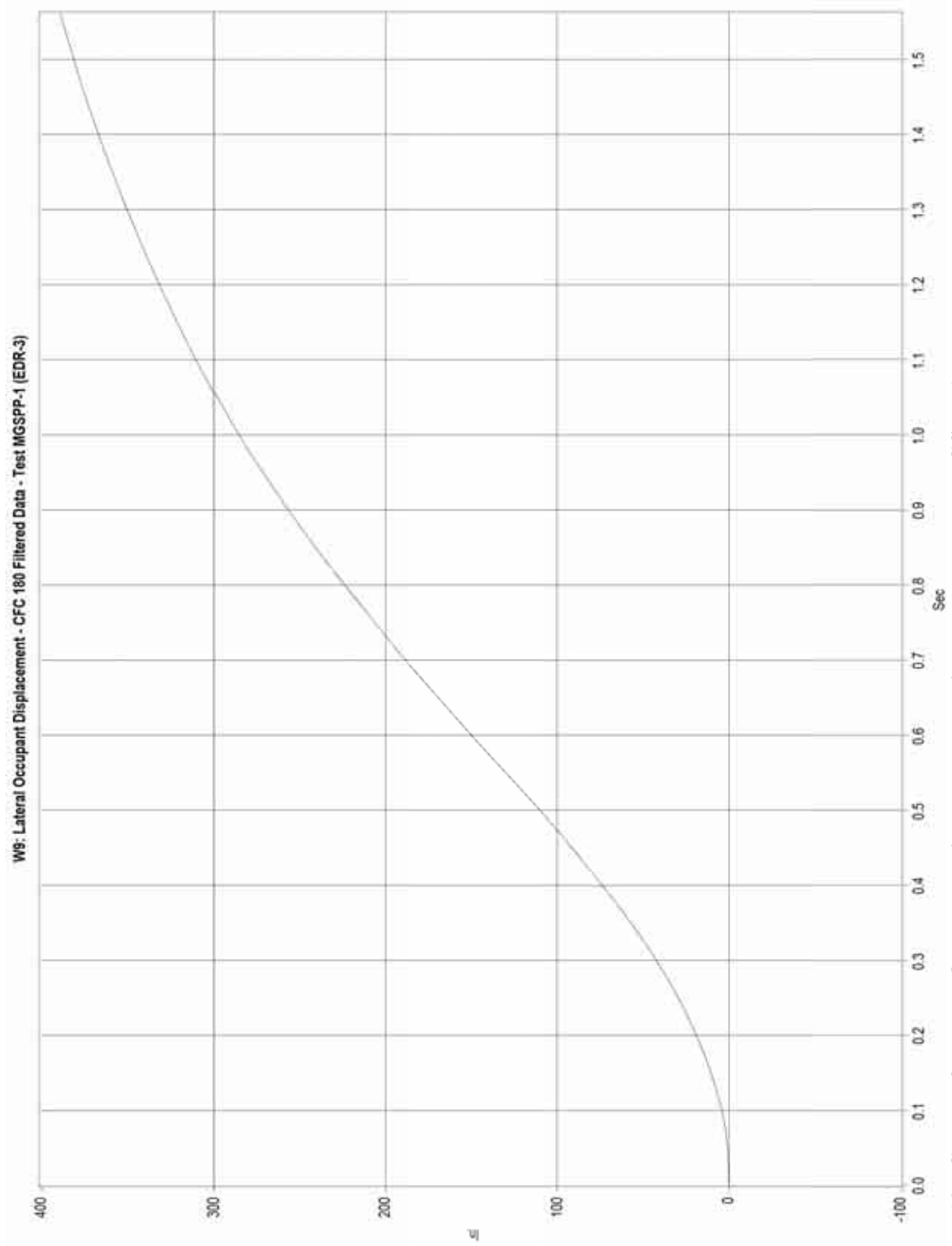


Figure K-12. Graph of Lateral Occupant Displacement – Filtered Data, Test MGSPP-1